U.S. Army
Coastal Engineering
Research Center

SHORE PROTECTION
MANUAL

Volume I

DEPARTMENT OF THE ARMY
CORPS OF ENGINEERS
1975

U.S. Army Coastal Engineering Research Center
Kingman Building
Fort Belvoir, Virginia 22060

SONOMA COAST, CALIFORNIA (GOAT ROCK) — 10 December 1958

SHORE PROTECTION MANUAL

VOLUME I

(Chapters 1 Through 4)

U.S. ARMY COASTAL ENGINEERING RESEARCH CENTER

1975

Second Edition
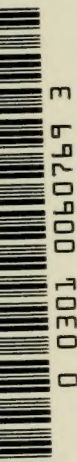
PREFACE

The U.S. Army Coastal Engineering Research Center, (CERC) formerly the Beach Erosion Board, has, since 1930, conducted studies on shore processes and methods of shore protection. CERC continues an extensive research and development program to improve both shore protection and offshore engineering techniques. The scientific and engineering aspects of coastal processes and offshore structures are in the developmental stage and the requirement for improved techniques for use in design and engineering of coastal structures is evident. This need was met in 1954, to the extent of available knowledge, by publication of Technical Report Number 4, "Shore Protection, Planning and Design" (TR 4); revised editions thereof appeared in 1957, 1961, and 1966.

Significant advances in knowledge and capability have been made since the 1966 revision. This Shore Protection Manual (SPM) incorporates new material with appropriate information extracted from TR 4, and expands coverage within the shore protection field. This SPM is a replacement volume covering guidelines and techniques for functional and structural design for shore protection works. Accordingly, further editions of TR 4 are not planned.

The Shore Protection Manual is in three volumes. Volume I describes the physical environment in the coastal zone starting with an introduction of coastal engineering, continuing with discussions of mechanics of wave motion, wave and water level predicitons, and finally littoral processes.

Volume II translates the interaction of the physical environment and coastal structures into design parameters for use in the solution of coastal engineering problems. It discusses planning, analysis, structural features, and structural design as related to physical factors, and shows an example of a coastal engineering problem which utilizes the technical content of material presented in all three volumes.

Volume III contains four appendixes including a glossary of coastal engineering terms, a list of symbols, tables and plates, and a subject index.

R. A. Jachowski, Chief, Design Branch, Engineering Development Division, was the project engineer responsible for preparation and assemblage of the text, under the general supervision of G. M. Watts, Chief, Engineering Development Division. At the time of approval for publication by the Coastal Engineering Research Board, LTC Don S. McCoy was Commander and Director and Thorndike Saville, Jr. was Technical Director. Members of the Coastal Engineering Research Board were: MG John W. Morris (President), MG Daniel A. Raymond, MG Ernest Graves, Jr., BG George B. Fink, Dean Morrough P. O'Brien, Dr. Arthur T. Ippen, and Prof. Robert G. Dean. The board members were intimately involved in both the planning and review of this manual.

Preparation of this manual includes the contribution, review and suggestions of numerous engineers, scientists, technical and support personnel. Present members of the CERC staff who made significant technical contributions to this manual are: R. H. Allen, B. R. Bodine, M. T. Czerniak, A. E. DeWall, D. B. Duane, C. J. Galvin, R. J. Hallermeier, D. L. Harris, R. A. Jachowski, W. R. James, O. M. Madsen, P. C. Pritchett, A. C. Rayner, R. L. Rector, R. P. Savage, T. Saville, Jr., P. N. Stoa, P. G. Teleki, G. M. Watts, J. R. Weggel and D. W. Woodard. Technical editor for this manuscript was R. H. Allen. Typing and composing were done by M. L. Vrooman and C. M. Lowe; and drafting by H. J. Bruder and J. S. Rivas. LCDR K. E. Fusch was responsible for the completion of the final manuscript.

The manual format and binding were selected to optimize its use by scientists and engineers as a learning text as well as a field and office engineering reference. Chapters include a bibliography. The binding facilitates text and chart removal for separate use or rebinding in loose leaf form.

Comments or suggestions on material in this manual are invited.

This report is published under authority of Public Law 166, 79th Congress, approved July 31, 1945, as supplemented by Public Law 172, 88th Congress, approved November 7, 1963.

TABLE OF CONTENTS

VOLUME II

VOLUME III

TABLE OF CONTENTS

VOLUME I

CHAPTER 1 - INTRODUCTION TO COASTAL ENGINEERING

CHAPTER 2 - MECHANICS OF WAVE MOTION

CHAPTER 3 - WAVE AND WATER LEVEL PREDICTIONS

CHAPTER 4 - LITTORAL PROCESSES

LIST OF FIGURES

LIST OF TABLES

CHAPTER 1

INTRODUCTION
TO
COASTAL ENGINEERING

HALEIWA BEACH, OAHU, HAWAII — 23 August 1970

CHAPTER 1

INTRODUCTION TO COASTAL ENGINEERING

1.1 INTRODUCTION TO THE SHORE PROTECTION MANUAL

This Shore Protection Manual has been prepared to assemble in a single three-volume publication coastal-engineering practices for shore protection. "Coastal Engineering" is defined as the application of the physical and engineering sciences to the planning, design, and construction of works to modify or control the interaction of the air, sea, and land in the coastal zone for the benefit of man and for the enhancement of natural shoreline resources. "Shore protection," as used in this Manual, applies to works designed to stabilize the shores of large bodies of water where wave action is the principal cause of erosion. Much of the material is applicable to the protection of navigation channels and harbors.

The nature and degree of required shore-protection measures vary widely at different localities. Proper solution of any specific problem requires systematic and thorough study. The first requisite for such study is a clear definition of the problem and the objectives sought. The first factor to be determined is the cause of the problem. Ordinarily there will be more than one method of obtaining the immediate objective. Therefore, the long-term effects of each method should be studied. The immediate and long-term effects of each method should be evaluated not only within the problem area, but also in adjacent shore areas. All physical and environmental effects, advantageous and detrimental, should be considered in comparing annual costs and benefits to determine the justification of protection methods.

Detailed summaries of applicable methods, techniques, and useful data pertinent to the solution of shore protection problems have been included in this Manual.

By replacing *Shore Protection, Planning and Design* with the *Shore Protection Manual*, CERC is providing coastal engineers with an improved tool for solving shore-protection problems. The Manual is designed as an advanced text, but contains sufficient introductory material to allow a person with an engineering background to obtain an understanding of coastal phenomena and to solve related engineering problems.

Chapter 1 presents a basic introduction to the subject. Chapter 2, "Mechanics of Wave Motion," treats wave theories, wave refraction and diffraction, wave reflection, and breaking waves. Chapter 3, "Wave and Water Level Predictions," discusses wave forecasting, hurricane waves, storm surge, and water level fluctuations. Chapter 4, "Littoral Processes," treats the characteristics and sources of littoral material nearshore currents, littoral transport, and sand budget techniques. Chapter 5, "Planning Analyses," treats the functional planning of shore-protection measures. Chapter 6, "Structural Features," illustrates the

functional design of various structures. Chapter 7, "Structural Design--Physical Factors," treats the effects of environmental forces on the design of protective works. Chapter 8, "Engineering Analysis--Case Study," presents a series of calculations for the preliminary design of an offshore island facility in the mouth of the Delaware Bay.

Each chapter contains its own bibliography. This Manual concludes with four appendixes. Because the meanings of coastal engineering terms differ from place to place, the reader is urged to use Appendix A, Glossary of Terms, that defines the terms used in this Manual. Appendix B lists the symbols used. Appendix C is a collection of miscellaneous tables and plates that supplement the material in the chapters. Appendix D is the subject index.

1.2 THE SHORE ZONE

Table 1-1 summarizes regional shoreline characteristics. The information obtained from the "Report on the National Shoreline Study," by the Department of the Army, Corps of Engineers (1971), indicates that of the total 84,240 miles of U.S. shoreline, there are 34,520 miles (41 percent) of exposed shoreline and 49,720 miles (59 percent) of sheltered shoreline (i.e., in bays, estuaries and lagoons). About 20,500 miles of the shoreline (or 24 percent of the total) are eroding. Of the total length of shoreline, exclusive of Alaska (36,940 miles), about 12,150 miles (33 percent) have beaches; the remaining 24,790 miles have no beach.

1.21 NATURAL BEACH PROTECTION

Where the land meets the ocean at a sandy beach, the shore has natural defenses against attack by waves, currents and storms. First of these defenses is the sloping nearshore bottom that causes waves to break offshore, dissipating their energy over the surf zone. The process of breaking often creates an offshore bar in front of the beach that helps to trip following waves. The broken waves re-form to break again, and may do this several times before finally rushing up the beach foreshore. At the top of wave uprush a ridge of sand is formed. Beyond this ridge, or crest of the berm, lies the flat beach berm that is reached only by higher storm waves. A beach profile and its related terminology are shown in Figure 1-1.

1.22 NATURAL PROTECTIVE DUNES

Winds blowing inland over the foreshore and berm move sand behind the beach to form dunes. (See Figures 1-2 and 1-3.) Grass, and sometimes bushes and trees, grow on the dunes, and the dunes become a natural levee against sea attack. Dunes are the final natural protection line against wave attack, and are also a reservoir for storage of sand against storm waves.

Table 1-1. Shoreline Characteristics

Region	Shoreline Total (miles)	Shoreline Exposed (miles)	Shoreline Sheltered (miles)	Shore Change Eroding (miles)	Shore Change Non-Eroding (miles)	Shoreline With Beach (miles)	Shoreline Without Beach (miles)
North Atlantic	8,620	4,730	3,890	7,460	1,160	2,320	6,300
South Atlantic-Gulf	14,620	2,470	12,150,	2,820	11,800	3,600	11,020
Lower Mississippi	1,940	810	1,130	1,580	360	830	1,110
Texas Gulf	2,500	370	2,130	360	2,140	380	2,120
Great Lakes	3,680	3,020	660	1,260	2,420	2,110	1,570
California	1,810	1,320	490	1,550	260	680	1,130
North Pacific	2,840	650	2,190	260	2,580	2,050	790
Hawaii	930	900	30	110	820	180	750
Total	36,940	14,270	22,670	15,400	21,540	12,150	24,790
Alaska	47,300	20,250	27,050	5,100	42,200	Unknown	Unknown
Total National	84,240	34,520	49,720	20,500	63,740	12,150	24,790

From: Report on National Shoreline Study, Department of the Army, Corps of Engineers, August 1971.
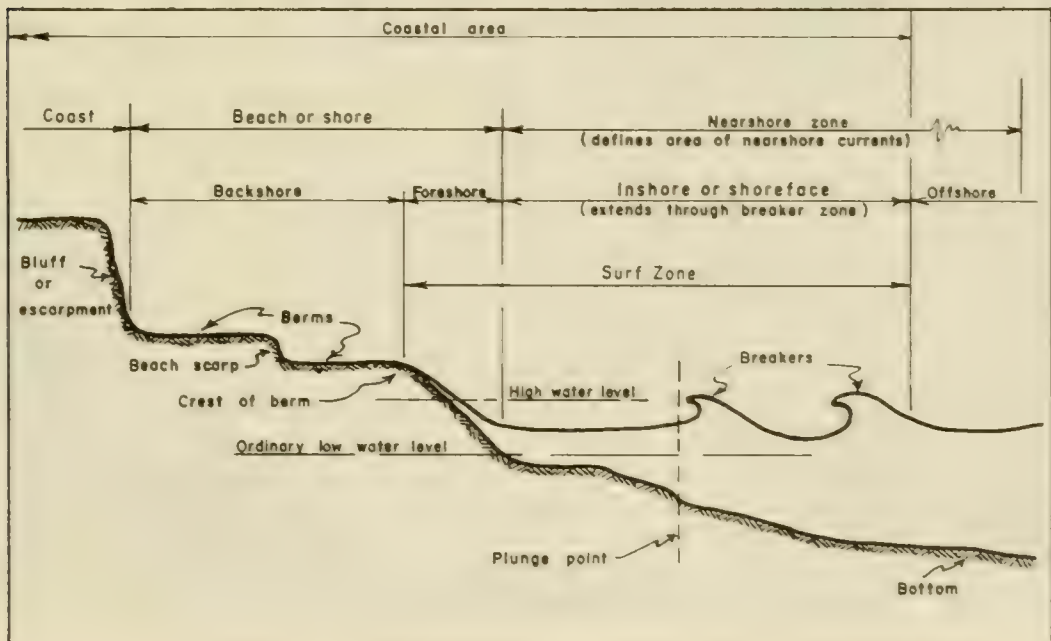
Figure 1-1. Beach Profile - Related Terms

Figure 1-2. Sand Dunes along the South Shore of Lake Michigan

Figure 1-3. Sand Dune, Honeyman State Park, Oregon

1.23 BARRIER BEACHES, LAGOONS AND INLETS

In some areas, an additional natural protection for the mainland is provided in the form of barrier beaches. (See Figure 1-4.) Nearly all of the U.S. east coast from Long Island to Mexico is comprised of barrier beaches. These are long narrow islands or spits lying parallel to the shoreline. Barrier beaches generally enclose shallow lagoons that separate the mainland from the ocean. During severe storms these barrier beaches absorb the brunt of the wave attack. When barrier-beach dunes are breached, the result may be the cutting of an inlet. The inlet permits sand to enter the lagoon and settle to the bottom, removing sand from the beach.

1.24 STORM ATTACK

During storms, strong winds generate high waves. Storm surge and waves may raise the water level near the shore. If storm surge does occur, large waves can then pass over the offshore bar formation without breaking. If the storm occurs at high tide, storm surge super-elevates the water, and some waves may break on the beach or even at the base of the dunes. After a storm or storm season, natural defenses may again be re-formed by normal wave and wind action.

1.25 ORIGIN AND MOVEMENT OF BEACH SANDS

Most of the sands of the beaches and nearshore slopes are normally small, resistant rock particles that have traveled many miles from inland mountains. When the sand reaches the shore, it is moved alongshore by waves and littoral currents. This alongshore transport is a constant process, and great volumes may be transported. In most coastal segments the direction of movement changes as direction of wave attack changes.

1.3 THE SEA IN MOTION

1.31 TIDES AND WINDS

The motions of the sea originate in the gravitational effects of the sun, the moon, and earth; and from air movements or winds caused by differential heating of the earth.

The moon, and to a lesser extent the sun, creates ocean tides by gravitational forces. These forces of attraction, and the fact that the sun, moon, and earth are always in motion with relation to each other, cause waters of ocean basins to be set in motion. These tidal motions of water masses are a form of very long period wave motion, resulting in a rise and fall of the water surface at a point. There are normally two tides per day, but some localities have only one per day.

1.32 WAVES

The familiar waves of the ocean are *wind waves* generated by winds blowing over water. They may vary in size from ripples on a pond to

Figure 1-4. Barrier Beach Island Developed as Recreational Park – Jones Beach State Park, Long Island, New York

3 July 1955

ATLANTIC OCEAN

large ocean waves as high as 100 feet. (See Figure 1-5.) Wind waves cause most of the damage to the ocean coasts. Another type of wave, the tsunami, is created by earthquakes or other tectonic disturbances on the ocean bottom. Tsunamis have caused spectacular damage at times, but fortunately, major tsunamis do not occur frequently.

Wind waves are of the type known as oscillatory waves, and are usually defined by their height, length, and period. (See Figure 1-6.) Wave height is the vertical distance from the top of the crest to the bottom of the trough. Wavelength is the horizontal distance between successive crests. Wave period is the time between successive crests passing a given point.

As waves propagate in water, only the form and part of the energy of the waves move forward; the water particles remain.

The height, length, and period of wind waves are determined by the *fetch* (the distance the wind blows over the sea in generating the waves), the wind speed, the length of time the wind blows, and the *decay distance* (the distance the wave travels after leaving the generating area). Generally, the longer the fetch, the stronger the wind; and the longer the time the wind blows, the larger the waves. The water depth, if shallow enough, will also affect the size of wave generated. The wind simultaneously generates waves of many heights, lengths, and periods as it blows over the sea.

If winds of a local storm blow toward the shore, the generated waves will reach the beach in nearly the form in which they are generated. Under these conditions, the waves are steep; that is, the wavelength is 10 to 20 times the wave height. Such waves are called *seas*. If waves are generated by a distant storm, they may travel through hundreds or even thousands of miles of calm areas before reaching the shore. Under these conditions, waves *decay* - short, steep waves are eliminated, and only relatively long, low waves reach the shore. Such waves have lengths from 30 to more than 500 times the wave height, and are called *swell*.

1.33 CURRENTS AND SURGES

Currents are created in oceans and adjacent bays and lagoons when water in one area becomes higher than water in another area. Water in the higher area flows toward the lower area, creating a current. Some causes of differences in the elevation of the water surface in the oceans are tides, wind, waves breaking on a beach, and streams. Changes in water temperature or salinity cause changes in water density that may also produce currents.

Wind creates currents because, as it blows over the water surface, it creates a stress on surface water particles, and starts these particles moving in the direction in which the wind is blowing. Thus, a surface current is created. When such a current reaches a barrier, such as coastline, water tends to pile up against the land. In this way, *wind*

(Portland Cement Association)

Figure 1-5. Large Waves Breaking over a Breakwater
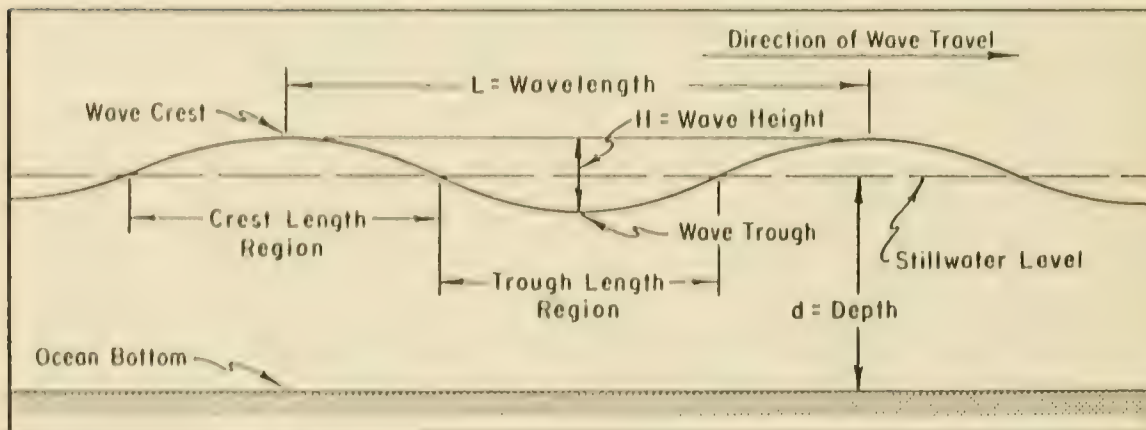
Figure 1-6. Wave Characteristics

setup or *storm surges* are created by strong winds. The height of storm surge depends on wind velocity and direction, fetch, water depth, and nearshore slope. In violent storms, storm surge may raise sea level at the shore as much as 20 feet. In the United States, larger surges occur on the Gulf coast because of the shallower and broader shelf off that coast compared to the shelves off the Atlantic and Pacific coasts. Storm surges may also be increased by a funneling effect in converging estuaries.

When waves approach the beach at an angle, they create a current in shallow water parallel to the shore, known as the *longshore current*. This current, under certain conditions, may turn and run out to sea in what is known as a *rip current*.

1.34 TIDAL CURRENTS

If water level rises and falls at an area, then water must flow into and out of the area. Significant currents generated by tides occur at inlets to lagoons and bays or at entrances to harbors. At such constricted places, tidal currents generally flow in when the tide is rising (flood tide) and flow out as the tide falls (ebb tide). Exceptions can occur at times of high river discharge or strong winds, or when density currents are an important part of the current system.

In addition to creating currents, tides constantly change the level at which waves attack the beach.

1.4 THE BEHAVIOR OF BEACHES

1.41 BEACH COMPOSITION

The size and character of sediments on a beach are related to forces to which the beach is exposed and the type of material available at the shore. Most beaches are composed of fine or coarse sand and, in some areas, of small stones called *shingle* or *gravel*. This material is supplied to the beach zone by streams, by erosion of the shores caused by waves and currents and, in some cases, by onshore movement of material from deeper water. Clay and silt do not usually remain on ocean beaches because the waves create such turbulence in the water along the shore that these fine materials are kept in suspension. It is only after moving away from the beaches into quieter or deeper water that these fine particles settle out and deposit on the bottom.

1.42 BEACH CHARACTERISTICS

Characteristics of a beach are usually described in terms of average size of the sand particles that make up the beach, range and distribution of sizes of those particles, sand composition, elevation and width of berm, slope or steepness of the foreshore, the existence (or lack) of a bar, and the general slope of the inshore zone fronting the beach. Generally, the larger the sand particles the steeper the beach slope. Beaches with gently sloping foreshores and inshore zones usually have a preponderance

of the finer sizes of sand. Daytona Beach, Florida, is a good example
of a gently sloping beach composed of fine sand.

1.43 BREAKERS

As a wave moves toward shore, it reaches a depth of water so shallow
that the wave collapses or breaks. This depth is equal to about 1.3 times
the wave height. Thus a wave 3 feet high will break in a depth of about
4 feet. Breaking can occur in several different ways (plunging, spilling,
surging, or collapsing). Breaking results in a dissipation of the energy
of the wave and is manifested by turbulence in the water. This turbulence
stirs up the bottom materials. For most waves, the water travels forward
after breaking as a foaming, turbulent mass, expending most of its remain-
ing energy in a rush up the beach slope.

1.44 EFFECTS OF WIND WAVES

Wind waves affect beaches in two major ways. Short steep waves,
which usually occur during a storm near the coast, tend to tear the
beach down. (See Figure 1-7.) Long swells, which originate from dis-
tant storms, tend to rebuild the beaches. On most beaches, there is a
constant change caused by the tearing away of the beach by local storms
followed by gradual rebuilding by swells. A series of violent local
storms in a short time can result in severe erosion of the shore if
there is not enough time between storms for swells to rebuild the
beaches. Alternate erosion and accretion of beaches may be seasonal
on some beaches; the winter storms tear the beach away, and the summer
swells rebuild it. Beaches may also follow long-term cyclic patterns.
They may erode for several years, and then accrete for several years.

1.45 LITTORAL TRANSPORT

Littoral transport is defined as the movement of sediments in the
nearshore zone by waves and currents and is divided into two general
classes: transport parallel to the shore (longshore transport) and
transport perpendicular to the shore (onshore-offshore transport). This
transport is distinguished from the material moved, which is called
littoral drift.

Onshore-offshore transport is determined primarily by wave steepness,
sediment size, and beach slope. In general, high steep waves move material
offshore, and low waves of long period (low steepness waves) move material
onshore. This onshore-offshore process associated with storm waves is
illustrated in Figure 1-7.

Longshore transport results from the stirring up of sediment by the
breaking wave, and the movement of this sediment by the component of the
wave in an alongshore direction, and by the longshore current generated
by the breaking wave. The direction of longshore transport is directly
related to the direction of wave approach, and the angle of the wave to
the shore. Thus, due to the variability of wave approach, longshore
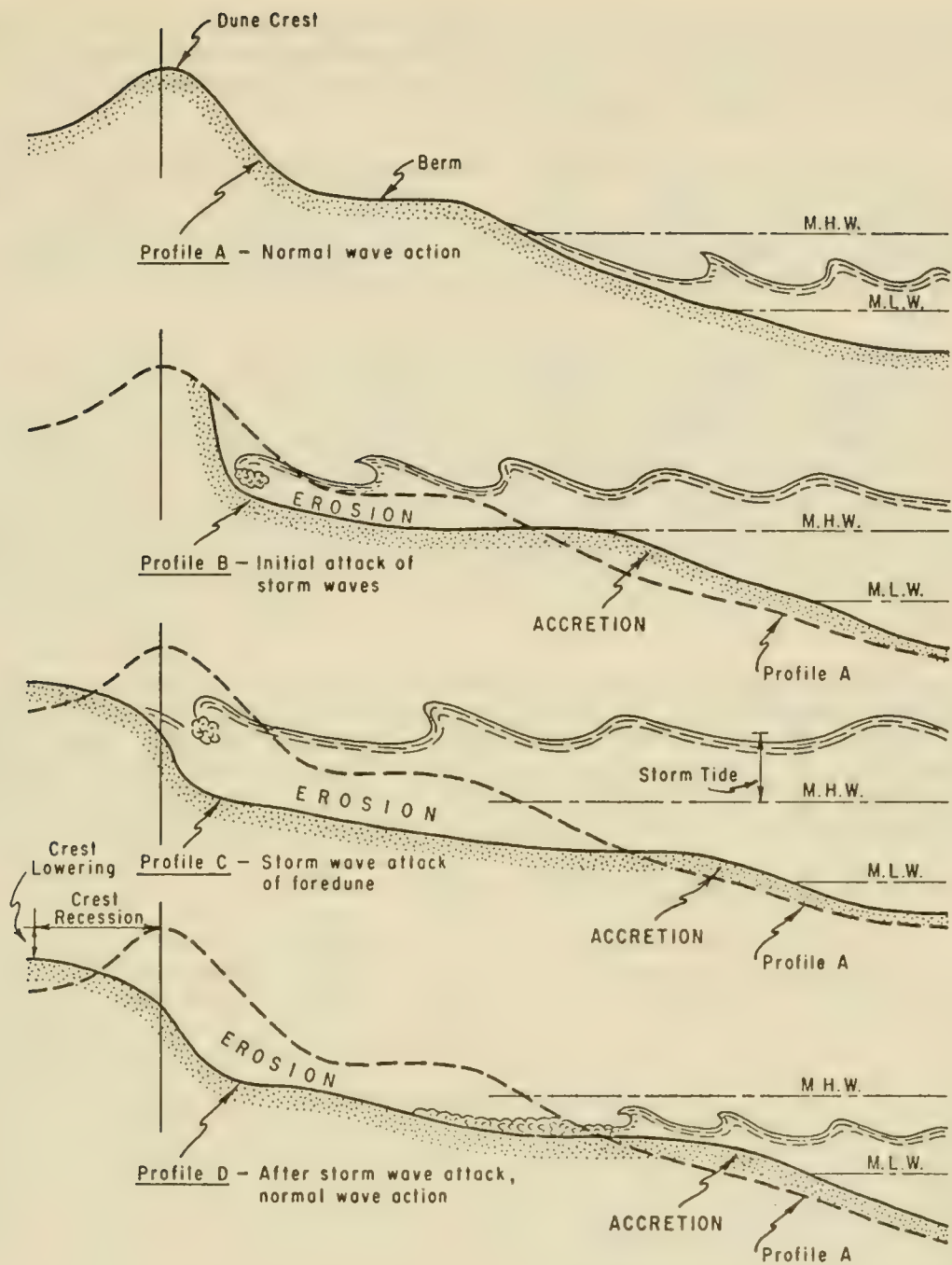
Figure 1-7. Schematic Diagram of Storm Wave Attack on Beach and Dune

transport direction can vary from season to season, day to day or hour to hour. These reversals of transport direction are quite common for most United States shores. Direction may vary at random, but in most areas the net effect is seasonal.

The rate of longshore transport is dependent on both angle of wave approach, and wave energy. Thus, high storm waves will generally move more material per unit time than low waves. However, if low waves exist for a much longer time than do high waves, the low waves may be more significant in moving sand than the high waves.

Because reversals in transport direction occur, and because different types of waves transport material at different rates, two components of the longshore transport rate become important. The first is the net rate, the net amount of material passing a particular point in the predominant direction during an average year. The second component is the gross rate, the total of all material moving past a given point in a year regardless of direction. Most shores consistently have a net annual longshore transport in one direction. Determining the direction and average net and gross annual amount of longshore transport is important in developing shore protection plans.

In landlocked water of limited extent, such as the Great Lakes, a longshore transport rate in one direction can normally be expected to be no more than about 150,000 cubic yards per year. For open ocean coasts, the net rate of transport may vary from 100,000 to more than 2 million cubic yards per year. The rate depends on the local shore conditions and shore alignment as well as the energy and direction of wave action.

1.46 EFFECT OF INLETS ON BARRIER BEACHES

Inlets may have significant effects on adjacent shores by interrupting the longshore transport and trapping onshore-offshore moving sand. On ebb current, sand moved to the inlet by waves is carried a short distance out to sea and deposited on an outer bar. When this bar becomes large enough, the waves begin to break on it, and sand again begins to move over the bar back toward the beach. On the flood tide, when water flows through the inlet into the lagoon, sand in the inlet is carried a short distance into the lagoon and deposited. This process creates shoals in the landward end of the inlet known as *middleground shoals* or *inner bars*. Later, ebb flows may bring some of the material in these shoals back to the ocean, but some is always lost from the stream of littoral drift and thus from the downdrift beaches. In this way, tidal inlets may store sand and reduce the supply of sand to adjacent shorelines.

1.47 IMPACT OF STORMS

Hurricanes or severe storms moving over the ocean near the shore may greatly change beaches. Strong winds of a storm often create a storm surge. This surge raises the water level and exposes to wave attack higher parts of the beach not ordinarily vulnerable to waves. Such storms also generate

large, steep waves. These waves carry large quantities of sand from the
beach to the nearshore bottom. Land structures, inadequately protected
and located too close to the water, are then subjected to the forces of
waves and may be damaged or destroyed. Low-lying areas next to the ocean,
lagoons, and bays are often flooded by storm surge. Storm surges are
especially damaging if they occur concurrently with astronomical high tide.

Beach berms are built naturally by waves to about the highest eleva-
tion reached by normal storm waves. Berms tend to absorb the wave energy;
however, overtopping permits waves to reach the dunes or bluffs in back of
the beach and damage unprotected upland features.

When storm waves erode the berm and carry the sand offshore, the pro-
tective value of the berm is reduced and large waves can overtop the beach.
The width of the berm at the time of a storm is thus an important factor
in the amount of upland damage a storm can inflict.

Notwithstanding changes in the beach that result from storm-wave
attack, a gently sloping beach of adequate width and height is the most
effective method known for dissipating wave energy.

1.48 BEACH STABILITY

Although a beach may be temporarily eroded by storm waves and later
partly or wholly restored by swells, and erosion and accretion patterns
may occur seasonally, the long-range condition of the beach - whether
eroding, stable or accreting - depends on the rates of supply and loss
of littoral material. The shore accretes or progrades when the rate of
supply exceeds the rate of loss. The shore is considered stable (even
though subject to storm and seasonal changes) when the long-term rates
of supply and loss are equal.

1.5 EFFECTS OF MAN ON THE SHORE

1.51 ENCROACHMENT ON THE SEA

During the early days of the United States, natural beach processes
continued to mold the shore as in ages past. As the country developed,
activity in the shore area was confined principally to harbor areas.
Between harbor areas, development along the shore progressed slowly as
small, isolated, fishing villages. As the national economy grew, im-
provements in transportation brought more people to the beaches. Gradu-
ally, extensive housing, commercial, recreational and resort developments
replaced fishing villages as the predominant coastal manmade features.
Examples of this development are Atlantic City and Miami Beach.

Numerous factors control the growth of development at beach areas,
but undoubtedly the beach environment is the development's basic asset.
The desire of visitors, residents, and industries to find accommodations
as close to the ocean as possible has resulted in man's encroachment on
the sea.

There are places where the beach has been gradually widened, as well as narrowed, by natural processes over the years. This is evidenced by lighthouses and other structures that once stood on the beach, but now stand hundreds of feet inland.

In their eagerness to be as close as possible to the water, developers and property owners often forget that land comes and goes, and that land which nature provides at one time may later be reclaimed by the sea. Yet once the seaward limit of a development is established, this line must be held if large investments are to be preserved. This type of encroachment has resulted in great monetary losses due to storm damage, and in ever-increasing costs of shore protection.

1.52 NATURAL PROTECTION

While the sloping beach and beach berm are the outer line of defense to absorb most of the wave energy, dunes are the last zone of defense in absorbing the energy of storm waves that overtop the berm. Although dunes erode during severe storms, they are often substantial enough to afford complete protection to the land behind them. Even when breached by waves of a severe storm, dunes may gradually rebuild naturally to provide protection during future storms. Continuing encroachment on the sea with manmade development has often taken place without proper regard for the protection provided by dunes. Large dune areas have been leveled to make way for real estate developments, or have been lowered to permit easy access to the beach. Where there is inadequate dune or similar protection against storm waves, the storm waters may wash over low-lying land, moving or destroying everything in their path, as illustrated by Figure 1-8.

1.53 SHORE PROTECTION METHODS

Where beaches and dunes protect shore developments, additional protective works may not be required. However, when natural forces do create erosion, storm waves may overtop the beach and damage backshore structures. Manmade structures must then provide protection. In general, measures designed to stabilize the shore fall into two classes: structures to prevent waves from reaching erodible material (seawalls, bulkheads, revetments); and an artificial supply of beach sand to make up for a deficiency in sand supply through natural processes. Other manmade structures, such as groins and jetties, are used to retard the longshore transport of littoral drift. These may be used in conjunction with seawalls or beachfills or both.

Separate protection for short reaches of eroding shores (as an individual lot frontage) within a larger zone of eroding shore, is difficult and costly. Such protection often fails at its flanks as the adjacent unprotected shores continue to recede. Partial or inadequate protective measures may even accelerate erosion of adjacent shores. Coordinated action under a comprehensive plan that considers erosion processes over the full length of the regional shore compartment is much more effective and economical.

Figure 1-8. Backshore Damage at Sea Isle City, New Jersey

March 1962 Storm

1.54 BULKHEADS, SEAWALLS AND REVETMENTS

Protection on the upper part of the beach which fronts backshore development is required as a partial substitute for the natural protection that is lost when the dunes are destroyed. Shorefront owners have resorted to shore armoring by wave-resistant walls of various types. A vertical wall in this location is known as a bulkhead, and serves as a secondary line of defense in major storms. Bulkheads are constructed of steel, timber, or concrete piling. For ocean-exposed locations, bulkheads do not provide a long-term solution, because a more substantial wall is required as the beach continues to recede and larger waves reach the structure. Unless combined with other types of protection, the bulkhead must be enlarged into a massive seawall capable of withstanding the direct onslaught of the waves. Seawalls may have vertical, curved or stepped faces. While seawalls may protect the upland, they can create a local problem. Downward forces of water created by waves striking the wall, can rapidly remove sand from in front of the wall. A stone apron is often necessary to prevent excessive scouring and undermining.

A revetment armors the slope face of a dune or bluff. It is usually composed of one or more layers of stone or is of concrete construction. This sloping protection dissipates wave energy with less damaging effect on the beach than waves striking vertical walls.

1.55 BREAKWATERS

Beaches and bluffs or dunes can be protected by an offshore breakwater that reduces the wave energy reaching the shore. However, offshore breakwaters are usually more costly than onshore structures, and are seldom built solely for shore protection. Offshore breakwaters are constructed mainly for navigation purposes. A breakwater protecting a harbor area provides shelter for boats. Breakwaters have both beneficial and detrimental effects on the shore. All breakwaters reduce or eliminate wave action and thus protect the shore immediately behind them. Whether offshore or shore-connected, the elimination of wave action reduces longshore transport, obstructing the movement of sand along the shore and starving the downdrift beaches.

At a harbor breakwater, the sand stream generally can be restored by pumping sand through a pipeline from the side where sand accumulates to the eroded downdrift side. This type of operation has been in use for many years at Santa Barbara, California.

Even without a shore arm, an offshore breakwater reduces wave action and creates quiet water between it and the shore. In the absence of wave action to move sand, it is deposited and builds the shore seaward toward the breakwater. The buildup serves as a barrier which also blocks the movement of littoral materials. If the offshore breakwater is placed immediately updrift from a navigation opening, the structure impounds sand, prevents it from entering the navigation channel, and affords

shelter for a floating dredge to pump the impounded material across the navigation opening back onto the downdrift beach. This method is used at Channel Island Harbor near Port Hueneme, California.

1.56 GROINS

The groin is a barrier-type structure that extends from the backshore into the littoral zone. The basic purposes of a groin are to interrupt longshore sand movement, to accumulate sand on the shore, or to retard sand losses. Trapping of sand by a groin is done at the expense of the adjacent downdrift shore unless the groin or groin system is artificially filled with sand to its entrapment capacity from other sources. To reduce the potential for damage to property downdrift of a groin, some limitation must be imposed on the amount of sand permitted to be impounded on the updrift side. Since more and more shores are being protected, and less and less sand is available as natural supply, it is now desirable, and frequently necessary, to place sand artificially to fill the area between the groins, thereby ensuring a more or less uninterrupted passage of the sand to the downdrift shores.

Groins have been constructed in various configurations using timber, steel, concrete or rock. Groins can be classified as high or low, long or short, permeable or impermeable, and fixed or adjustable.

A high groin, extending through the breaking zone for ordinary or moderate storm waves, initially entraps nearly all of the longshore moving sand within that intercepted area until the areal pattern or surface profile of the accumulated sand mass allows sand to pass around the seaward end of the groin to downdrift shores. Low groins (top profile no higher than that of desired beach dimensions) function like high groins, except that sand also passes over the top of the structure. Permeable groins permit some of the wave energy and moving sand to pass through the structure.

1.57 JETTIES

Jetties are generally employed at inlets in connection with navigation improvements. When sand being transported along the coast by waves and currents arrives at an inlet, it flows inward on the flood tide to form an inner bar, and outward on the ebb tide to form an outer bar. Both formations are harmful to navigation through the inlet, and must be controlled to maintain an adequate navigation channel. The jetty is similar to the groin in that it traps sand moving along the beach. Jetties are usually constructed of steel, concrete, or rock. The jetty type depends on foundation conditions, wave climate, and economic considerations. Jetties are much larger than groins, since jetties sometimes extend from the shoreline seaward to a depth equivalent to the channel depth desired for navigation purposes. To be efficient in maintaining the channel, the jetty must be high enough to completely obstruct sand movement.

Jetties aid navigation by reducing movement of sand into the channel, by stabilizing the location of the channel, and by shielding vessels from waves. Sand is impounded at the updrift jetty, and the supply of sand to the shore downdrift from the inlet is reduced, thus causing erosion of that shore. Before the installation of a jetty, nature supplied sand by transporting it across the inlet intermittently along the outer bar to the downdrift shore.

To eliminate undesirable downdrift erosion, some projects provide for dredging the sand impounded by the updrift jetty and pumping it through a pipeline (bypassing the inlet) to the eroding beach. This provides an intermittent flow of sand to nourish the downdrift beach, and also prevents shoaling of the entrance channel.

A more recent development for sand bypassing provides a low section or weir in the updrift jetty over which sand moves into a sheltered pre-dredged, deposition basin. By dredging the basin periodically, deposition in the channel is reduced or eliminated. The dredged material is normally pumped across the inlet to provide nourishment for the downdrift shore. A *weir jetty* of this type at Masonboro Inlet, North Carolina, is shown in Figure 1-9.

1.58 BEACH RESTORATION AND NOURISHMENT

As previously stated, beaches are very effective in dissipating wave energy. When maintained to adequate dimensions, they afford protection for the adjoining backshore. Therefore, a protective beach is classed as a shore-protection structure. When studying an erosion problem, it is generally advisable to investigate the feasibility of mechanically or hydraulically placing borrow material on the shore to form and maintain an adequate protective beach. The method of placing beach fill to ensure sand supply at the required replenishment rate is important. Where stabilization of an eroding beach is the problem, suitable beach material may be stockpiled at the updrift sector of the problem area. The establishment and periodic replenishment of such a stockpile is termed *artificial beach nourishment*. To restore an eroded beach and stabilize it at the restored position, fill is placed directly along the eroded sector, and then the beach is artificially nourished by the stockpiling method.

When conditions are suitable for artificial nourishment, long reaches of shore may be protected by this method at a relatively low cost per linear foot of protected shore. An equally important advantage is that artificial nourishment directly remedies the basic cause of most erosion problems - a deficiency in natural sand supply - and benefits rather than damages the adjacent shore. An added consideration is that the widened beach has value as a recreation feature. A project for beach restoration with an artificial dune for protection against hurricane wave action, completed in 1965 at Wrightsville Beach, North Carolina, is shown in Figure 1-10.

February 1966

Figure 1-9. Weir Jetty at Masonboro Inlet, North Carolina
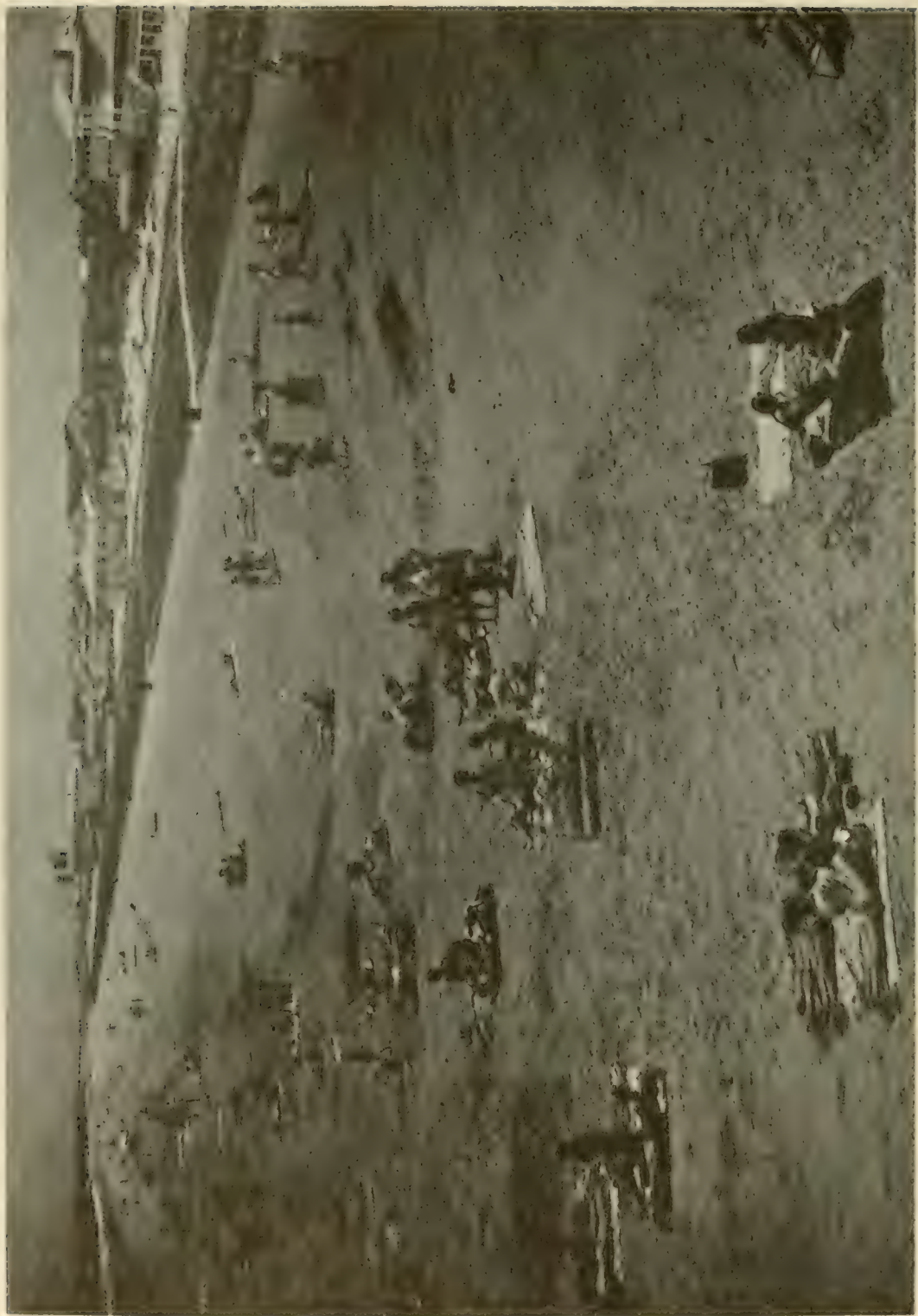
Figure 1-10. Wrightsville Beach, North Carolina, after Completion of Beach Restoration and Hurricane Protection Project

Sometimes structures must be provided to protect dunes, to maintain a specific beach dimension, or to reduce nourishment requirements. In each case, the cost of such structures must be weighed against the benefits they would provide. Thus, measures to provide and keep a wider protective and recreational beach for a short section of an eroding shore would require excessive nourishment without supplemental structures such as groins to reduce the rate of loss of material from the widened beach. A long, high terminal groin or jetty is frequently justified at the downdrift end of a beach restoration project to reduce losses of fill into an inlet and to stabilize the lip of the inlet.

1.6 CONSERVATION OF SAND

Experience and study have demonstrated that sand from dunes, beaches, and nearshore areas is the best material available naturally in suitable form to protect shores. Where sand is available in abundant quantities, protective measures are greatly simplified and reduced in cost. When dunes and broad, gently sloping beaches can no longer be provided, it is necessary to resort to alternative structures, and the recreational attraction of the seashore is lost or greatly diminished.

Sand is a diminishing natural resource. Sand was once available to our shores in adequate supply from streams, rivers and glaciers, and by coastal erosion. Now cultural development in the watershed areas and along previously eroding shores has progressed to a stage where large areas of our coast now receive little or no sand through natural geological processes. Continued cultural development in both inland and shore areas tends to further reduce coastal erosion with resulting reduction in sand supply to the shore. It thus becomes apparent that sand must be conserved. This does not mean local hoarding of beach sand at the expense of adjoining areas, but rather the elimination of wasteful practices and the prevention of losses from the shore zone whenever feasible.

Fortunately, nature has provided extensive stores of beach sand in bays, lagoons, estuaries and offshore areas that can be used as a source of beach and dune replenishment where the ecological balance will not be disrupted. Massive dune deposits are also available at some locations, though these must be used with caution to avoid exposing the area to flood hazard. These sources are not always located in the proper places for economic utilization, nor will they last forever. When they are gone, we must face increasing costs for the preservation of our shores. Offshore sand deposits will probably become the most important source in the future.

Mechanical bypassing of sand at coastal inlets is one means of conservation that will come into increasing practice. Mining of beach sand for commercial purposes, formerly a common procedure, is rapidly being reduced as coastal communities learn the need for regulating this practice. Modern hopper dredges, used for channel maintenance in coastal inlets, are being equipped with a pump-out capability so their loads can be discharged near the shore instead of being dumped at sea. On the California coast, where large volumes of sand are lost into deep submarine canyons near the shore,

facilities are being considered that will trap the sand before it reaches the canyon and transport it mechanically to a point where it can resume normal longshore transport. Dune planting with appropriate grasses and shrubs reduces landward windborne losses and aids in dune preservation.

Sand conservation is an important factor in the preservation of our seacoasts, and must be included in long-range planning. Protection of our seacoasts is not a simple problem; neither is it insurmountable. It is a task and a responsibility that has increased tremendously in importance in the past 50 years, and is destined to become a necessity in future years. While the cost will mount as time passes, it will be possible through careful planning, adequate management, and sound engineering to do the job properly and economically.

MECHANICS

OF
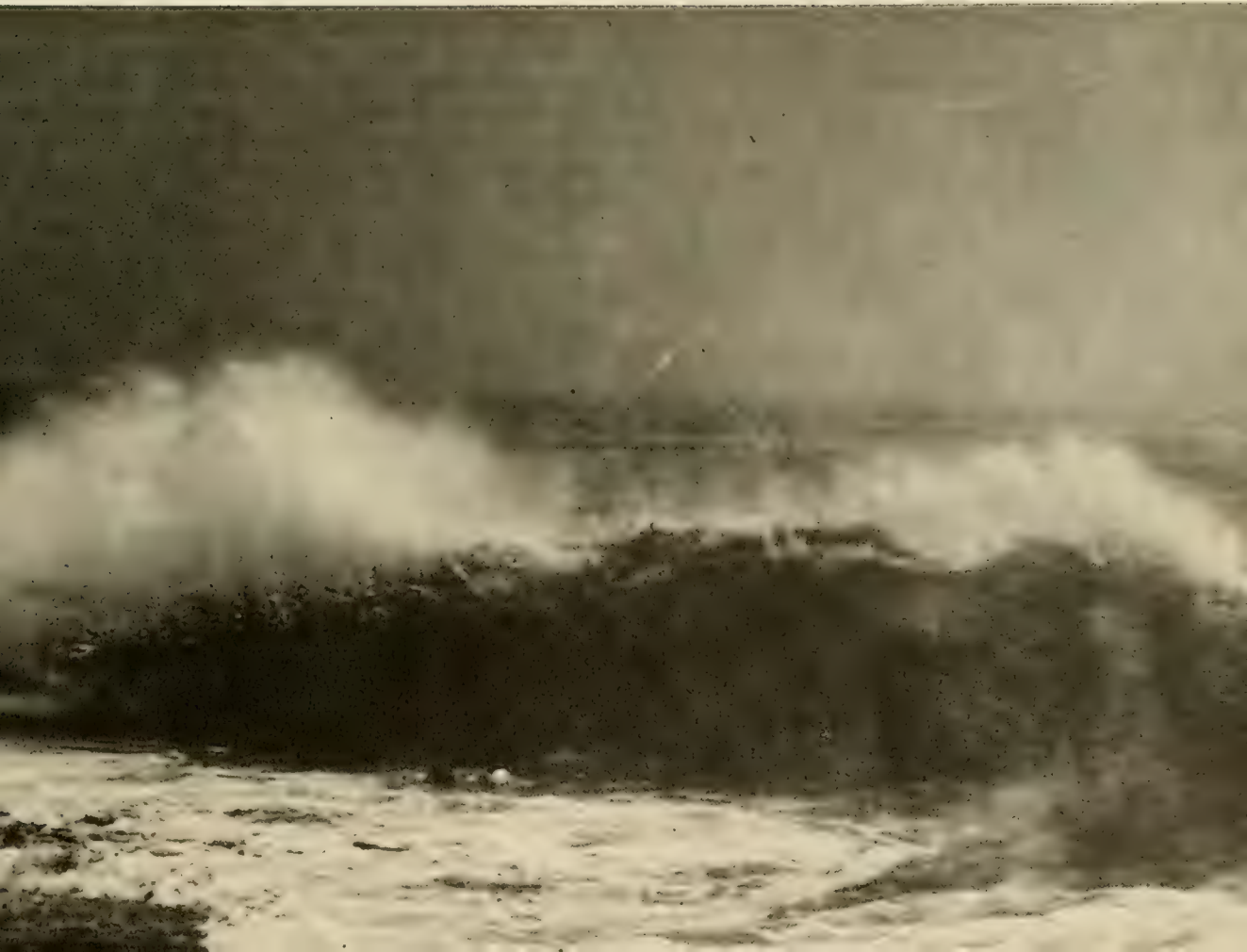
WAVE MOTION

LEO CARRILLO STATE BEACH, CALIFORNIA – July 1968

CHAPTER 2

MECHANICS OF WAVE MOTION

2.1 INTRODUCTION

The effects of water waves are of paramount importance in the field of coastal engineering. Waves are the major factor in determining the geometry and composition of beaches, and significantly influence planning and design of harbors, waterways, shore protection measures, coastal structures, and other coastal works. Surface waves generally derive their energy from the winds. A significant amount of this wave energy is finally dissipated in the nearshore region and on the beaches.

Waves provide an important energy source for forming beaches; assorting bottom sediments on the shoreface; transporting bottom materials onshore, offshore, and alongshore; and for causing many of the forces to which coastal structures are subjected. An adequate understanding of the fundamental physical processes in surface wave generation and propagation must precede any attempt to understand complex water motion in the nearshore areas of large bodies of water. Consequently, an understanding of the mechanics of wave motion is essential in the planning and design of coastal works.

This chapter presents an introduction to surface wave theories. Surface and water particle motion, wave energy, and theories used in describing wave transformation due to interaction with the bottom and with structures are described. The purpose is to provide an elementary physical and mathematical understanding of wave motion, and to indicate limitations of selected theories. A number of wave theories have been omitted. References are cited to provide information on theories not discussed and to supplement the theories presented.

The reader is cautioned that man's ability to describe wave phenomena is limited, especially when the region under consideration is the coastal zone. Thus, the results obtained from the wave theories presented should be carefully interpreted for application to actual design of coastal structures or description of the coastal environment.

2.2 WAVE MECHANICS

2.21 GENERAL

Waves in the ocean often appear as a confused and constantly changing sea of crests and troughs on the water surface because of the irregularity of wave shape and the variability in the direction of propagation. This is particularly true while the waves are under the influence of the wind. The direction of wave propagation can be assessed as an average of the directions of individual waves. A description of the sea surface is difficult because of the interaction between individual waves. Faster waves overtake and pass through slower ones from various directions. Waves sometimes reinforce or cancel each other by this interaction, and often collide with each other and are transformed into turbulence, and

spray. When waves move out of the area where they are directly affected by the wind, they assume a more ordered state with the appearance of definite crests and troughs and with a more rhythmic rise and fall. These waves may travel hundreds or thousands of miles after leaving the area in which they were generated. Wave energy is dissipated internally within the fluid by interaction with the air above, by turbulence on breaking, and at the bottom in shallow depths.

Waves which reach coastal regions expend a large part of their energy in the nearshore region. As the wave nears the shore, wave energy may be dissipated as heat through turbulent fluid motion induced by breaking and through bottom friction and percolation. While the heat is of little concern to the coastal engineer, breaking is important since it affects both beaches and manmade shore structures. Thus, shore protection measures and coastal structure designs are dependent on the ability to predict wave forms and fluid motion beneath waves, and on the reliability of such predictions. Prediction methods generally have been based on simple waves where elementary mathematical functions can be used to describe wave motion. For some situations, simple mathematical formulas predict wave conditions well, but for other situations predictions may be unsatisfactory for engineering applications. Many theoretical concepts have evolved in the past two centuries for describing complex sea waves; however, complete agreement between theory and observation is not always found.

In general, actual water-wave phenomena are complex and difficult to describe mathematically because of nonlinearities, three-dimensional characteristics and apparent random behavior. However, there are two classical theories, one developed by Airy (1845) and the other by Stokes (1880), that describe simple waves. The Airy and Stokes theories generally predict wave behavior better where water depth relative to wavelength is not too small. For shallow water, a cnoidal wave theory often provides an acceptable approximation of simple waves. For very shallow water near the breaker zone, solitary wave theory satisfactorily predicts certain features of the wave behavior. These theories will be described according to their fundamental characteristics together with the mathematical equations which describe wave behavior. Many other wave theories have been presented in the literature which, for some specific situations, may predict wave behavior more satisfactorily than the theories presented here. These other theories are not included, since it is beyond the scope of this Manual to cover all theories.

The most elementary wave theory, referred to as small-amplitude or linear wave theory, was developed by Airy (1845). It is of fundamental importance since it not only is easy to apply, but is reliable over a large segment of the whole wave regime. Mathematically, the Airy theory can be considered a first approximation of a complete theoretical description of wave behavior. A more complete theoretical description of waves may be obtained as the sum of an infinite number of successive approximations, where each additional term in the series is a correction to preceding terms. For some situations, waves are better described by these higher order theories which are usually referred to as finite amplitude

theories. The first finite amplitude theory, known as the trochoidal theory, was developed by Gerstner (1802). It is so called because the free surface or wave profile is a trochoid. This theory is mentioned only because of its classical interest. It is not recommended for application, since the water particle motion predicted is not that observed in nature. The trochoidal theory does, however, predict wave profiles quite accurately. Stokes (1880) developed a finite-amplitude theory which is more satisfactory than the trochodial theory. Only the second-order Stokes' equations will be presented, but the use of higher order approximations is sometimes justified for the solution of practical problems.

For shallow-water regions, cnoidal wave theory, originally developed by Korteweg and De Vries (1895), predicts rather well the waveform and associated motions for some conditions. However, cnoidal wave theory has received little attention with respect to actual application in the solution of engineering problems. This may be due to the difficulties in making computations. Recently, the work involved in using cnoidal wave theory has been substantially reduced by introduction of graphical and tabular forms of functions. (Wiegel, 1960), (Masch and Wiegel, 1961.) Application of the theory is still quite involved. At the limit of cnoidal wave theory, certain aspects of wave behavior may be described satisfactorily by solitary wave theory. Unlike cnoidal wave theory, the solitary wave theory is easy to use since it reduces to functions which may be evaluated without recourse to special tables.

Development of individual wave theories is omitted, and only the results are presented since the purpose is to present only that information which may be useful for the solution of practical engineering problems. Many publications are available such as Wiegel (1964), Kinsman (1965), and Ippen (1966a), which cover in detail the development of some of the theories mentioned above as well as others. The mathematics used here generally will be restricted to elementary arithmetic and algebraic operations. Emphasis is placed on selection of an appropriate theory in accordance with its application and limitations.

Numerous example problems are provided to illustrate the theory involved and to provide some practice in using the appropriate equations or graphical and tabular functions. Some of the sample computations give more significant digits than are warranted for practical applications. For instance, a wave height could be determined to be 10.243 feet for certain conditions based on purely theoretical considerations. This accuracy is unwarranted because of the uncertainty in the basic data used and the assumption that the theory is representative of real waves. A practical estimate of the wave height given above would be 10 feet. When calculating real waves, the final answer should be rounded off.

2.22 WAVE FUNDAMENTALS AND CLASSIFICATION OF WAVES

Any adequate physical description of a water wave involves both its surface form and the fluid motion beneath the wave. A wave which can be described in simple mathematical terms is called a *simple wave*. Waves

which are difficult to describe in form or motion, and which may be comprised of several components are termed *complex waves*. *Sinusoidal* or *simple harmonic waves* are examples of *simple waves* since their surface profile can be described by a single sine or cosine function. A wave is *periodic* if its motion and surface profile recur in equal intervals of time. A wave form which moves relative to a fluid is called a *progressive wave*; the direction in which it moves is termed the *direction of wave propagation*. If a wave form merely moves up and down at a fixed position, it is called a *complete standing wave* or a *clapotis*. A progressive wave is said to be a wave of *permanent form* if it is propagated without experiencing any changes in free surface configuration.

Water waves are considered *oscillatory* or *nearly oscillatory* if the water particle motion is described by orbits, which are closed or nearly-closed for each wave period. Linear, or Airy, theory describes pure oscillatory waves. Most finite amplitude wave theories describe nearly oscillatory waves since the fluid is moved a small amount in the direction of wave advance by each successive wave. This motion is termed *mass transport* of the waves. When water particles advance with the wave, and do not return to their original position, the wave is called a *wave of translation*. A solitary wave is an example of a wave of translation.

It is important to distinguish between various types of water waves that may be generated and propagated. One way to classify waves is by wave period T (the time for a wave to travel a distance of one wave length), or by the reciprocal of T, the wave frequency f. One illustration of classification by period or frequency is given by Kinsman (1965) and shown in Figure 2-1. The figure shows the relative amount of energy contained in ocean waves having a particular frequency. Of primary concern are those waves referred to as gravity waves in Figure 2-1, having periods from 1 to 30 seconds. A narrower range of wave periods, from 5 to 15 seconds, is usually more important in coastal engineering problems. Waves in this range are referred to as *gravity waves* since gravity is the principal restoring force; that is, the force due to gravity attempts to bring the fluid back to its equilibrium position. Figure 2-1 also shows that a large amount of the total wave energy is associated with waves classified as gravity waves; hence gravity waves are extremely important in dealing with the design of coastal and offshore structures.

Gravity waves can be further separated into two states:

(a) seas, when the waves are under the influence of wind in a generating area, and

(b) swell, when the waves move out of the generating area and are no longer subjected to significant wind action.

Seas are usually made up of steeper waves with shorter periods and lengths, and the surface appears much more confused than for swell. Swell behaves much like a free wave, i.e., free from the disturbing force that caused it, while seas consist to some extent of forced waves, i.e., waves on which the disturbing force is applied continuously.
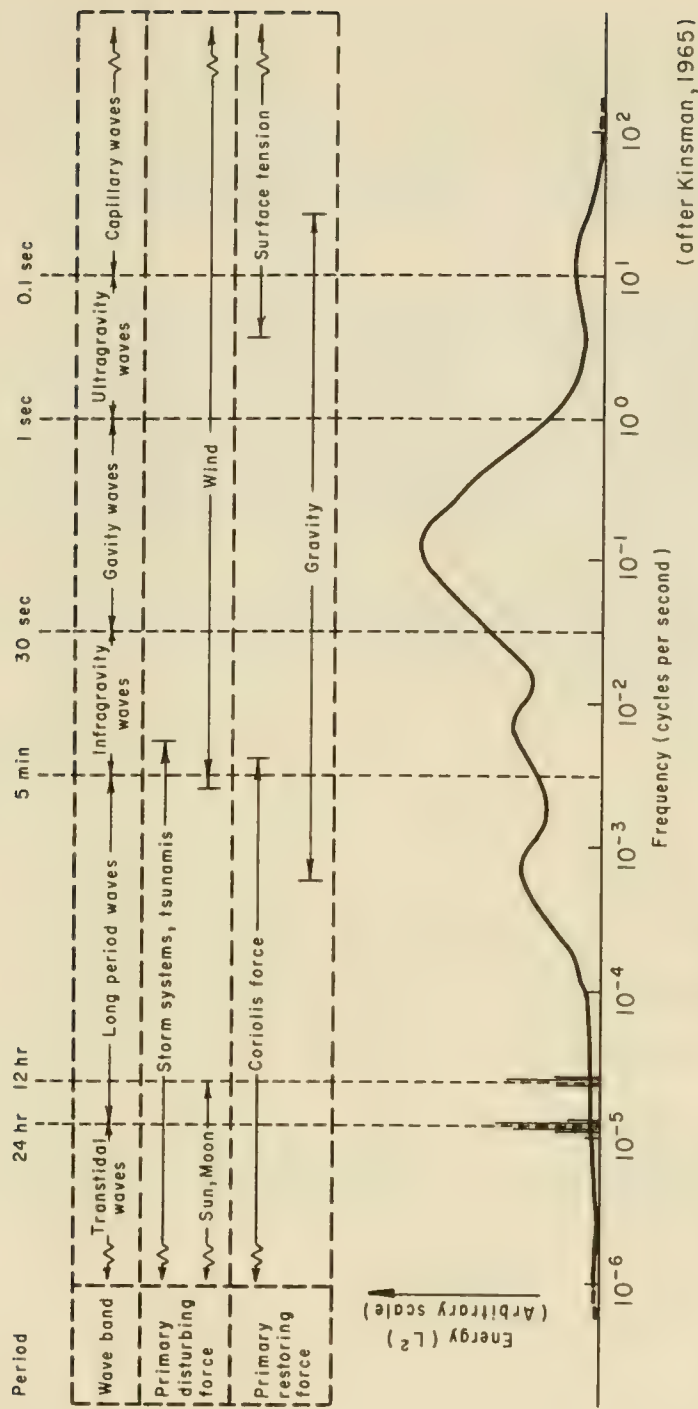
Figure 2-1. Approximate Distribution of Ocean Surface Wave Energy Illustrating the Classification of Surface Waves by Wave Band, Primary Disturbing Force and Primary Restoring Force.

2-5

Ocean waves are complex. Many aspects of fluid mechanics necessary to a complete discussion have only a minor influence on solving most coastal engineering problems. Thus, a simplified theory which omits most of the complicating factors is useful. The assumptions made in developing the simple theory should be understood, because not all of the assumptions are justified in all problems. When an assumption is not valid in a particular problem, a more complete theory should be employed.

The most restrictive of common assumptions is that waves are small perturbations on the surface of a fluid which is otherwise at rest. This leads to a wave theory which is variously called, small-amplitude theory, linear theory, or Airy theory. The small-amplitude theory provides insight for all periodic wave behavior and a description of the periodic flow adequate for most practical problems. This theory is unable to account for mass transport due to waves (Section 2.253 Mass Transport Velocity), or the fact that wave crests depart further from the mean water level than do the troughs. A more general theory, usually called the *finite amplitude*, or *nonlinear wave theory* is required to account for these phenomena as well as most interactions between waves and other flows. The nonlinear wave theory also permits a more accurate evaluation of some wave properties than can be obtained with linear theory.

Several assumptions, commonly made in developing a simple wave theory are listed below.

(a) The fluid is homogeneous and incompressible; therefore, the density ρ is a constant.

(b) Surface tension can be neglected.

(c) Coriolis effect can be neglected.

(d) Pressure at the free surface is uniform and constant.

(e) The fluid is ideal or inviscid (lacks viscosity).

(f) The particular wave being considered does not interact with any other water motions.

(g) The bed is a horizontal, fixed, impermeable boundary which implies that the vertical velocity at the bed is zero.

(h) The wave amplitude is small and wave form is invariant in time and space.

(i) Waves are plane or long crested (two-dimensional).

The first three are acceptable for virtually all coastal engineering problems. It will be necessary to relax assumptions (d), (e), and (f) for some specialized problems not considered in this Manual. Relaxing the three final assumptions is essential in many problems, and is considered later in this chapter.

In applying assumption (g) to waves in water of varying depth encountered when waves approach a beach the local depth is usually used. This can be rigorously justified, but not without difficulty, for most practical cases in which the bottom slope is flatter than about 1 on 10. A progressive wave moving into shallow water will change its shape significantly. Effects due to viscosity and vertical velocity on a permeable bottom may be measurable in some situations, but these effects can be neglected in most engineering problems.

2.23 ELEMENTARY PROGRESSIVE WAVE THEORY (Small-Amplitude Wave Theory)

The most fundamental description of a simple sinusoidal oscillatory wave is by its length L (the horizontal distance between corresponding points on two successive waves); height H (the vertical distance to its crest from the preceding trough); period T (the time for two successive crests to pass a given point); and depth d (the distance from the bed to the stillwater level). (See Appendix B for a list of common symbols.)

Figure 2-2 shows a two-dimensional simple progressive wave propagating in the positive x-direction. The symbols used here are presented in the figure. The symbol η denotes the displacement of the water surface relative to the stillwater level (SWL) and is a function of x and time. At the wave crest, η is equal to the amplitude of the wave a, or one-half of the wave height.

Small-amplitude wave theory and some finite-amplitude wave theories can be developed by introduction of a velocity potential $\phi(x, z, t)$. Horizontal and vertical components of the water particle velocities are defined at a point (x, z) in the fluid as $u = \partial\phi/\partial x$ and $w = \partial\phi/\partial z$. The velocity potential, Laplace's equation, and Bernoulli's dynamic equation together with the appropriate boundary conditions provide the necessary information needed in deriving the small-amplitude wave formulas. Such a development has been shown by Lamb (1932), Eagleson and Dean (See Ippen 1966b), and others.

2.231 Wave Celerity, Length and Period. The speed at which a wave form propagates is termed the phase velocity or wave celerity, C. Since the distance traveled by a wave during one wave period is equal to one wavelength, the wave celerity can be related to the wave period and length by

$$C = \frac{L}{T} \qquad\qquad (2\text{-}1)$$

An expression relating the wave celerity to the wavelength and water depth is given by

$$C = \sqrt{\frac{gL}{2\pi} \tanh\left(\frac{2\pi d}{L}\right)} \qquad\qquad (2\text{-}2)$$
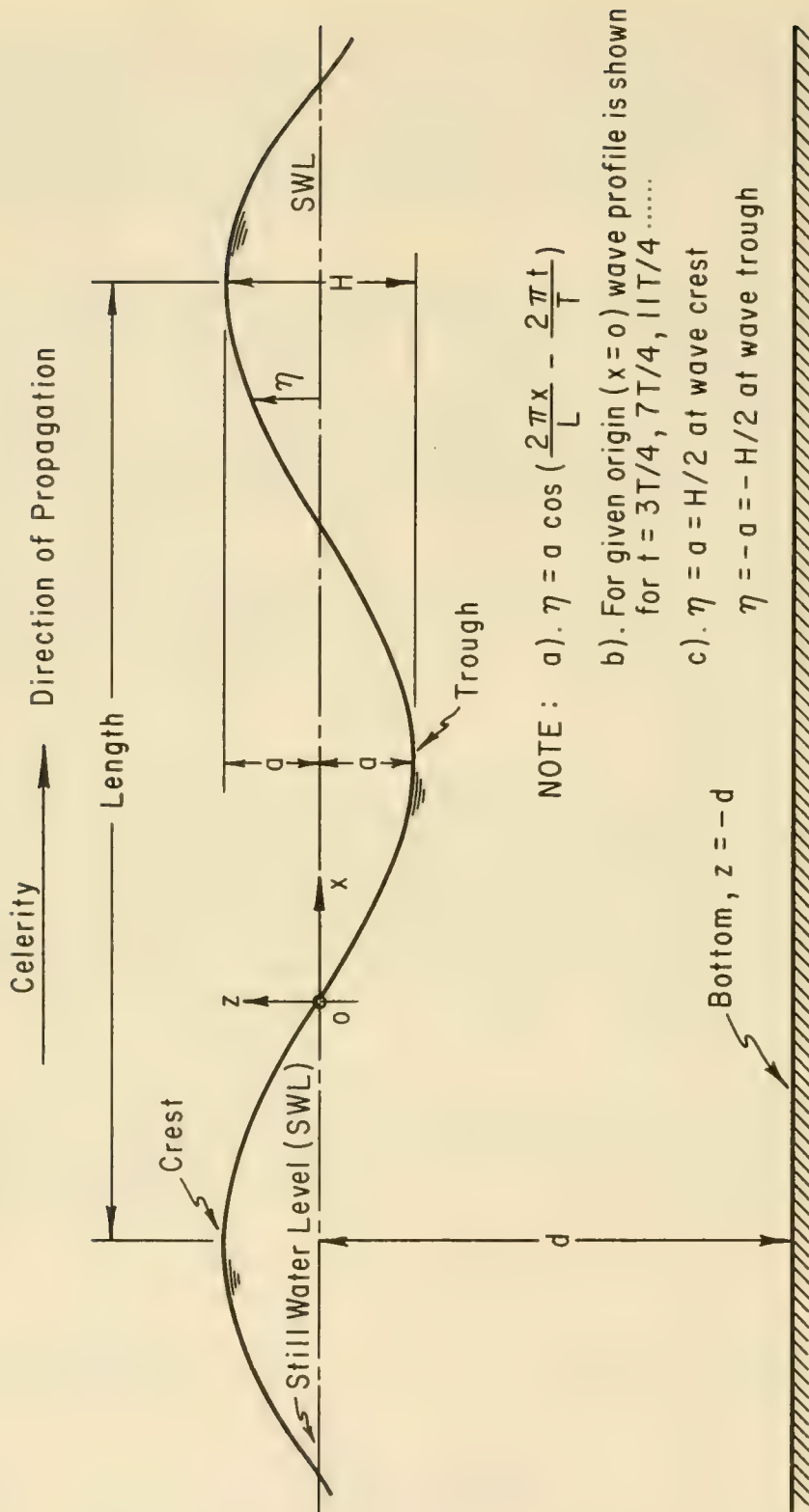
Figure 2-2. Definition of Terms - Elementary, Sinusoidal, Progressive Wave

NOTE : a). $\eta = a \cos \left(\dfrac{2\pi x}{L} - \dfrac{2\pi t}{T} \right)$

b). For given origin (x = 0) wave profile is shown
   for t = 3T/4, 7T/4, 11T/4 ......

c). $\eta = a = H/2$ at wave crest

   $\eta = -a = -H/2$ at wave trough

Direction of Propagation

Celerity

Length

Crest

Still Water Level (SWL)

SWL

Trough

Bottom, z = -d

2-8

From Equation 2-1, it is seen that 2-2 can be written as

$$C = \frac{gT}{2\pi} \tanh\left(\frac{2\pi d}{L}\right)$$

(2-3)

The values $2\pi/L$ and $2\pi/T$ are called the wave number k and wave angular frequency ω, respectively. From Equations 2-1 and 2-3 an expression for wavelength as a function of depth and wave period may be obtained.

$$L = \frac{gT^2}{2\pi} \tanh\left(\frac{2\pi d}{L}\right)$$

(2-4)

Use of Equation 2-4 involves some difficulty since the unknown L, appears on both sides of the equation. Tabulated values in Appendix C may be used to simplify the solution of Equation 2-4.

Gravity waves may also be classified by the depth of water in which they travel. Classification is made according to the magnitude of d/L and the resulting limiting values taken by the function $\tanh(2\pi d/L)$. Classifications are:

Classification	d/L	$2\pi d/L$	$\tanh(2\pi d/L)$
Deep Water	> 1/2	> π	≈ 1
Transitional	1/25 to 1/2	1/4 to π	$\tanh(2\pi d/L)$
Shallow Water	< 1/25	< 1/4	$\approx 2\pi d/L$

In deep water, $\tanh(2\pi d/L)$ approaches unity and Equations 2-2 and 2-3 reduce to

$$C_o = \sqrt{\frac{gL_o}{2\pi}} = \frac{L_o}{T}$$

(2-5)

and

$$C_o = \frac{gT}{2\pi}$$

(2-6)

Although *deep water* actually occurs at infinite depth, $\tanh(2\pi d/L)$, for most practical purposes, approaches unity at a much smaller d/L. For a relative depth of 1/2 (that is, when the depth is one-half the wavelength), $\tanh(2\pi d/L) = 0.9964$.

Thus, when the relative depth d/L, is greater than 1/2, the wave characteristics are virtually independent of depth. Deepwater conditions are indicated by the subscript o as in L_o and C_o. The period T, remains constant and independent of depth for oscillatory waves; hence the

2-9

subscript is omitted. (Ippen, 1966b, pp 21-24.) If units of feet and seconds are specified, the constant $g/2\pi$ is equal to 5.12 ft/sec^2 and

$$C_o = \frac{gT}{2\pi} = 5.12\ T\ (\text{ft/sec}),\qquad(2\text{-}7)$$

and

$$L_o = \frac{gT^2}{2\pi} = 5.12\ T^2\ (\text{ft}).\qquad(2\text{-}8)$$

If Equation 2-7 is used to compute wave celerity when the relative depth is $d/L = 0.25$, the resulting error will be about 9 percent. It is evident that a relative depth of 0.5 is a satisfactory boundary separating deepwater waves from waves in water of transitional depth. If a wave is traveling in *transitional* depths, Equations 2-2 and 2-3 must be used without simplification. Care should be exercised to use Equations 2-2 and 2-3 when necessary, that is, when the relative depth is between 1/2 and 1/25.

When the relative water depth becomes shallow, i.e., $2\pi d/L < 1/4$ or $d/L < 1/25$, Equation 2-2 can be simplified to

$$C = \sqrt{gd}.\qquad(2\text{-}9)$$

This relation, attributed to Lagrange, is of importance when dealing with long-period waves, often referred to as long waves. Thus, when a wave travels in shallow water, wave celerity depends only on water depth.

2.232 <u>The Sinusoidal Wave Profile</u>. The equation describing the free surface as a function of time t, and horizontal distance x, for a simple sinusoidal wave can be shown to be

$$\eta = a\ \cos\left(\frac{2\pi x}{L} - \frac{2\pi t}{T}\right) = \frac{H}{2}\ \cos\left(\frac{2\pi x}{L} - \frac{2\pi t}{T}\right),\qquad(2\text{-}10)$$

where η is the elevation of the water surface relative to stillwater level, and H/2 is one-half the wave height equal to the wave amplitude a. This expression represents a periodic, sinusoidal, progressive wave traveling in the positive x-direction. For a wave moving in the negative x-direction, one need only replace the minus sign before $2\pi t/T$ with a plus sign. When $(2\pi x/L - 2\pi t/T)$ equals 0, $\pi/2$, π, $3\pi/2$, the corresponding values of η are H/2, 0, - H/2, and 0, respectively.

2.233 <u>Some Useful Functions</u>. It can be shown by dividing Equation 2-3 by Equation 2-6, and by dividing Equation 2-4 by Equation 2-8 that

$$\frac{C}{C_o} = \frac{L}{L_o} = \tanh\left(\frac{2\pi d}{L}\right).\qquad(2\text{-}11)$$

If both sides of Equation 2-11 are multiplied by d/L, it becomes:

$$\frac{d}{L_o} = \frac{d}{L} \tanh \left(\frac{2\pi d}{L} \right). \tag{2-12}$$

The term d/L_O has been tabulated as a function of d/L by Wiegel (1954), and is presented in Appendix C on Table C-1. Table C-2 includes d/L as a function of d/L_O in addition to other useful functions such as $2\pi d/L$ and $\tanh(2\pi d/L)$. These functions simplify the solution of wave problems described by the linear theory.

An example problem illustrating the use of linear wave theory and the tables in Appendix C follows:

* * * * * * * * * * * * *   EXAMPLE PROBLEM * * * * * * * * * * * * * * *

GIVEN: A wave with a period of $T = 10$ seconds is propagated shoreward over a uniformly sloping shelf from a depth of $d = 600$ feet to a depth of $d = 10$ feet.

FIND: The wave celerities C and lengths L corresponding to depths of $d = 600$ feet and $d = 10$ feet.

SOLUTION:

  Using Equation 2-8,

$$L_o = 5.12 \, T^2 = 5.12 \, (10)^2 = 512 \text{ feet.}$$

  For $d = 600$ feet

$$\frac{d}{L_o} = \frac{600}{512} = 1.1719.$$

  From Table C-1 it is seen that for values of

$$\frac{d}{L_o} > 1.0$$

$$\frac{d}{L_o} = \frac{d}{L},$$

  therefore

$$L = L_o = 512 \text{ feet} \left(\text{deepwater wave, since } \frac{d}{L} > \frac{1}{2} \right).$$

$$C = \frac{L}{T} = \frac{512}{T},$$

$$C = \frac{512}{10} = 51.2 \text{ ft/sec.}$$

For d = 10 feet

$$\frac{d}{L_o} = \frac{10}{512} = 0.0195.$$

Entering Table C-1 with d/L_o it is found that,

$$\frac{d}{L} = 0.05692,$$

hence

$$L = \frac{10}{0.05692} = 176 \text{ feet} \left(\text{transitional depth, since } \frac{1}{25} < \frac{d}{L} < \frac{1}{2} \right),$$

$$C = \frac{L}{T} = \frac{176}{10} = 17.6 \text{ ft/sec.}$$

* *

2.234 Local Fluid Velocities and Accelerations. In wave force studies, it is often desirable to know the local fluid velocities and accelerations for various values of z and t during the passage of a wave. The horizontal component u, and the vertical component w, of the local fluid velocity are given by:

$$u = \frac{H}{2} \frac{gT}{L} \frac{\cosh\left[2\pi(z+d)/L\right]}{\cosh\left(2\pi d/L\right)} \cos\left(\frac{2\pi x}{L} - \frac{2\pi t}{T}\right), \qquad (2\text{-}13)$$

$$w = \frac{H}{2} \frac{gT}{L} \frac{\sinh\left[2\pi(z+d)/L\right]}{\cosh\left(2\pi d/L\right)} \sin\left(\frac{2\pi x}{L} - \frac{2\pi t}{T}\right). \qquad (2\text{-}14)$$

These equations express the local fluid velocity components any distance (z + d) above the bottom. The velocities are harmonic in both x and t. For a given value of the phase angle $\theta = (2\pi x/L - 2\pi t/T)$, the hyperbolic functions, *cosh* and *sinh,* as functions of z result in an approximate exponential decay of the magnitude of velocity components with increasing distance below the free surface. The maximum positive horizontal velocity

occurs when $\theta = 0, 2\pi$, etc., while the maximum horizontal velocity in the negative direction occurs when $\theta = \pi, 3\pi$, etc. On the other hand the maximum positive vertical velocity occurs when $\theta = \pi/2, 5\pi/2$, etc., and the maximum vertical velocity in the negative direction occurs when $\theta = 3\pi/2, 7\pi/2$, etc. (See Figure 2-3.)

The local fluid particle accelerations are obtained from Equations 2-13 and 2-14 by differentiating each equation with respect to t. Thus,

$$\alpha_x = + \frac{g\pi H}{L} \frac{\cosh [2\pi(z+d)/L]}{\cosh (2\pi d/L)} \sin \left(\frac{2\pi x}{L} - \frac{2\pi t}{T} \right), \qquad (2\text{-}15)$$

$$\alpha_z = - \frac{g\pi H}{L} \frac{\sinh [2\pi(z+d)/L]}{\cosh (2\pi d/L)} \cos \left(\frac{2\pi x}{L} - \frac{2\pi t}{T} \right). \qquad (2\text{-}16)$$

Positive and negative values of the horizontal and vertical fluid accelerations for various values of $\theta = 2\pi x/L - 2\pi t/T$ are shown in Figure 2-3.

The following problem will illustrate the computations required to determine local fluid velocities and accelerations resulting from wave motions.

* * * * * * * * * * * * * *   EXAMPLE PROBLEM   * * * * * * * * * * * * * * *

GIVEN: A wave with a period of T = 8 seconds, in a water depth of
   d = 50 feet, and a height of H = 18 feet.

FIND: The local horizontal and vertical velocities, u and w, and
   accelerations α_x and α_z at a depth d = 15 feet below the SWL
   when $\theta = 2\pi x/L - 2\pi t/T = \pi/3$ (60 degrees).

SOLUTION: Calculate

$$L_o = 5.12\, T^2 = 5.12\, (8)^2 = 328 \text{ feet} ,$$

$$\frac{d}{L_o} = \frac{50}{328} = 0.1526 .$$

From Table C-1 in Appendix C for a value of

$$\frac{d}{L_o} = 0.1526 ,$$

$$\frac{d}{L} \approx 0.1854; \cosh \frac{2\pi d}{L} = 1.759 ,$$

2-13

Figure 2-3. Local Fluid Velocities and Accelerations

hence

$$L = \frac{50}{0.1854} = 270 \text{ feet} .$$

Evaluation of the constant terms in Equations 2-13 through 2-16 gives

$$\frac{HgT}{2L} \frac{1}{\cosh (2\pi d/L)} = \frac{18 \, (32.2) \, (8)}{2(270) \, (1.758)} = 4.88 ,$$

$$\frac{g\pi H}{L} \frac{1}{\cosh (2\pi d/L)} = \frac{18 \, (32.2) \, (\pi)}{(270) \, (1.758)} = 3.84 .$$

Substitution into Equation 2-13 gives

$$u = 4.88 \cosh \left[\frac{2\pi(50 - 15)}{270}\right] [\cos 60°] = 4.88 \, [\cosh (0.8145)] \, (0.500) .$$

From Table C-1 find

$$\frac{2\pi d}{L} = 0.8145 ,$$

and by interpolation

$$\cosh (0.8145) = 1.3503 ,$$

and

$$\sinh (0.8145) = 0.9074 .$$

Therefore

$$u = 4.88 \, (1.3503) \, (0.500) = 3.29 \text{ ft/sec} ,$$

$$w = 4.88 \, (0.9074) \, (0.866) = 3.83 \text{ ft/sec} ,$$

$$\alpha_x = 3.84 \, (1.3503) \, (0.866) = 4.49 \text{ ft/sec}^2 ,$$

$$\alpha_z = -3.84 \, (0.9074) \, (0.500) = -1.74 \text{ ft/sec}^2 .$$

Figure 2-3, a sketch of the local fluid motion, indicates that the fluid under the crest moves in the direction of wave propagation and returns during passage of the trough. Linear theory does not predict any mass transport; hence the sketch shows only an oscillatory fluid motion.

* *

2.235 Water Particle Displacements. Another important aspect of linear wave mechanics deals with the displacements of individual water particles within the wave. Water particles generally move in elliptical paths in shallow or transitional water and in circular paths in deep water. If the

mean particle position is considered to be at the center of the ellipse or circle, then vertical particle displacement with respect to the mean position cannot exceed one-half the wave height. Thus, since the wave height is assumed to be small, the displacement of any fluid particle from its mean position is small. Integration of Equations 2-13 and 2-14 gives the horizontal and vertical particle displacement from the mean position, respectively. (See Figure 2-4.)

Thus,

$$\xi = - \frac{HgT^2}{4\pi L} \frac{\cosh [2\pi(z+d)/L]}{\cosh (2\pi d/L)} \sin \left(\frac{2\pi x}{L} - \frac{2\pi t}{T} \right), \tag{2-17}$$

$$\zeta = + \frac{HgT^2}{4\pi L} \frac{\sinh [2\pi(z+d)/L]}{\cosh (2\pi d/L)} \cos \left(\frac{2\pi x}{L} - \frac{2\pi t}{T} \right). \tag{2-18}$$

The above equations can be simplified by using the relationship

$$\left(\frac{2\pi}{T} \right)^2 = \frac{2\pi g}{L} \tanh \frac{2\pi d}{L}.$$

Thus,

$$\xi = - \frac{H}{2} \frac{\cosh [2\pi(z + d)/L]}{\sinh (2\pi d/L)} \sin \left(\frac{2\pi x}{L} - \frac{2\pi t}{T} \right), \tag{2-19}$$

$$\zeta = + \frac{H}{2} \frac{\sinh [2\pi(z + d)/L]}{\sinh (2\pi d/L)} \cos \left(\frac{2\pi x}{L} - \frac{2\pi t}{T} \right). \tag{2-20}$$

Writing Equations 2-19 and 2-20 in the following forms:

$$\sin^2 \left(\frac{2\pi x}{L} - \frac{2\pi t}{T} \right) = \left[\frac{\xi}{a} \frac{\sinh (2\pi d/L)}{\cosh [2\pi(z+d)/L]} \right]^2,$$

$$\cos^2 \left(\frac{2\pi x}{L} - \frac{2\pi t}{T} \right) = \left[\frac{\zeta}{a} \frac{\sinh (2\pi d/L)}{\sinh [2\pi(z+d)/L]} \right]^2.$$

and adding, gives:

$$\frac{\xi^2}{A^2} + \frac{\zeta^2}{B^2} = 1, \tag{2-21}$$

in which

$$A = \frac{H}{2} \frac{\cosh [2\pi(z+d)/L]}{\sinh (2\pi d/L)}, \tag{2-22}$$

$$B = \frac{H}{2} \frac{\sinh [2\pi(z+d)/L]}{\sinh (2\pi d/L)}. \tag{2-23}$$

2-16
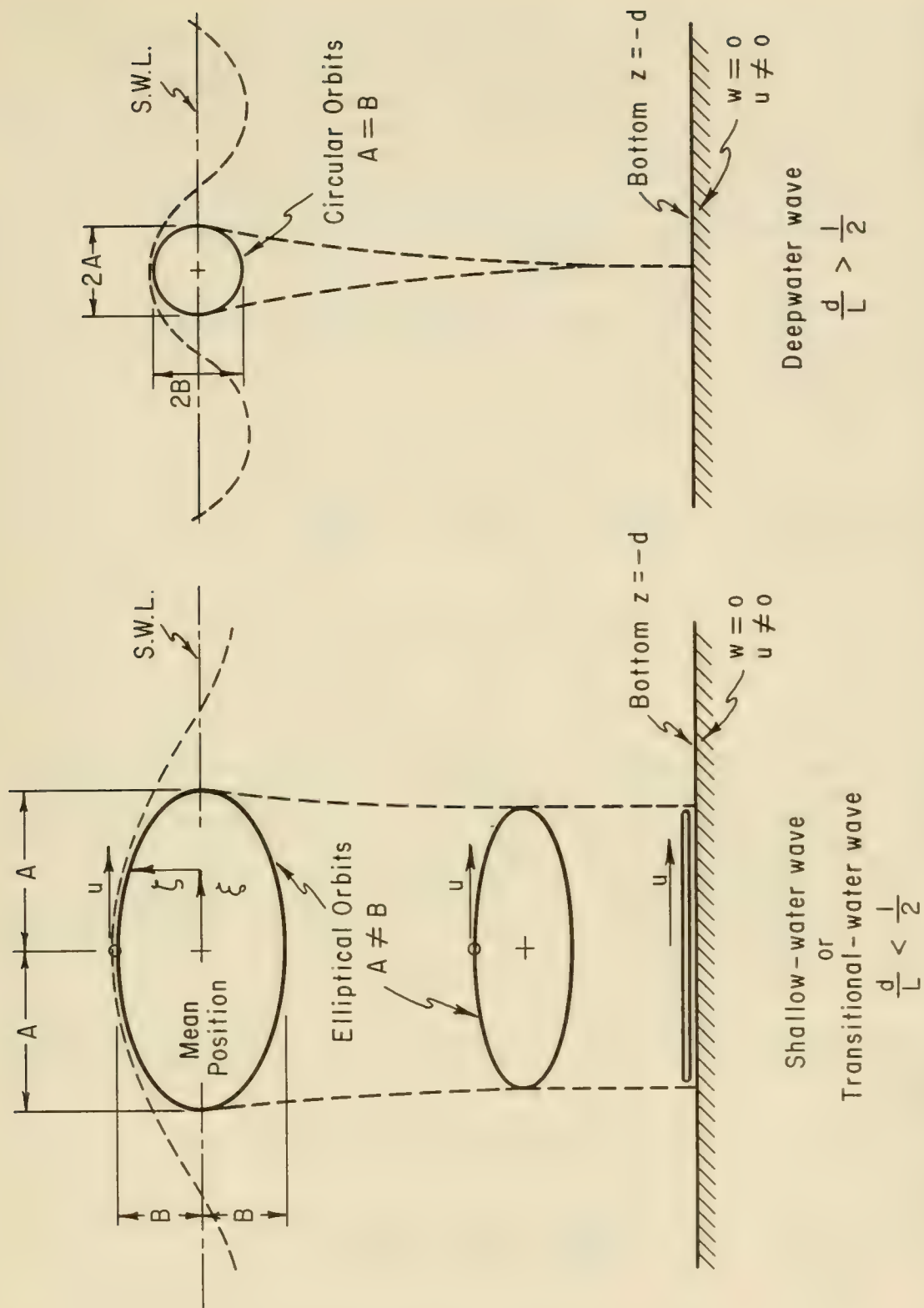
Figure 2-4. Water Particle Displacements from Mean Position for Shallow-Water and Deepwater Waves

Equation 2-21 is the equation of an ellipse with a major (horizontal) semiaxis equal to A, and a minor (vertical) semiaxis equal to B. The lengths of A and B are measures of the horizontal and vertical displacements of the water particles. Thus, the water particles are predicted to move in closed orbits by linear wave theory: i.e., each particle returns to its initial position after each wave cycle. Morison and Crooke (1953), compared laboratory measurements of particle orbits with wave theory and found, as had others, that particle orbits were not completely closed. This difference between linear theory and observations is due to the mass transport phenomenon which is discussed in a subsequent section.

Examination of Equations 2-22 and 2-23 shows that for deepwater conditions A and B are equal and particle paths are circular. The equations become

$$A = B = \frac{H}{2} e^{2\pi z/L} \quad \text{for } \frac{d}{L} > \frac{1}{2}. \qquad (2\text{-}24)$$

For shallow-water conditions, the equations become

$$A = \frac{H}{2} \frac{L}{2\pi d}$$
$$\qquad\qquad \text{for } \frac{d}{L} < \frac{1}{25} \qquad (2\text{-}25)$$
$$B = \frac{H}{2} \frac{z+d}{d}$$

Thus, in deep water, the water particle orbits are circular. The more shallow the water, the flatter the ellipse. The amplitude of the water particle displacement decreases exponentially with depth and in deepwater regions becomes small relative to the wave height at a depth equal to one-half the wavelength below the free surface, i.e., when $z = -L_O/2$. This is illustrated in Figure 2-4. For shallow regions, horizontal particle displacement near the bottom can be large. In fact, this is apparent in offshore regions seaward of the breaker zone where wave action and turbulence lift bottom sediments into suspension.

The vertical displacement of water particles varies from a minimum of zero at the bottom to a maximum equal to one-half the wave height at the surface.

* * * * * * * * * * * * * *   EXAMPLE PROBLEM   * * * * * * * * * * * * * *

PROVE:

(a)
$$\left(\frac{2\pi}{T}\right)^2 = \frac{2\pi g}{L} \tanh\left(\frac{2\pi d}{L}\right).$$

(b)
$$u = \frac{\pi H}{T} \frac{\cosh\,[2\pi(z+d)/L]}{\sinh\,(2\pi d/L)} \cos\left(\frac{2\pi x}{L} - \frac{2\pi t}{T}\right).$$

2-18

SOLUTION:

(a) Equation 2-3,

$$C = \frac{gT}{2\pi} \tanh \left(\frac{2\pi d}{L}\right).$$

Equation 2-1,

$$C = \frac{L}{T}.$$

Therefore, equating 2-1 and 2-3,

$$\frac{L}{T} = \frac{gT}{2\pi} \tanh \left(\frac{2\pi d}{L}\right),$$

and multiplying both sides by $(2\pi)^2/LT$

$$\frac{(2\pi)^2}{LT} \frac{L}{T} = \frac{(2\pi)^2}{LT} \frac{gT}{2\pi} \tanh \left(\frac{2\pi d}{L}\right).$$

Hence,

$$\left(\frac{2\pi}{T}\right)^2 = \frac{2\pi g}{L} \tanh \left(\frac{2\pi d}{L}\right).$$

(b) Equation 2-13 may be written

$$u = \frac{gTH}{2L} \frac{\cosh\left[2\pi(z+d)/L\right]}{\cosh\left(2\pi d/L\right)} \cos \left(\frac{2\pi x}{L} - \frac{2\pi t}{T}\right),$$

$$= \frac{1}{C} \frac{gH}{2} \frac{\cosh\left[2\pi(z+d)/L\right]}{\cosh\left(2\pi d/L\right)} \cos \left(\frac{2\pi x}{L} - \frac{2\pi t}{T}\right),$$

since

$$\frac{T}{L} = \frac{1}{C}.$$

Since

$$C = \frac{gT}{2\pi} \tanh \left(\frac{2\pi d}{L}\right),$$

$$u = \frac{\pi H}{T} \frac{1}{\tanh\left(2\pi d/L\right)} \frac{\cosh\left[2\pi(z+d)/L\right]}{\cosh\left(2\pi d/L\right)} \cos \left(\frac{2\pi x}{L} - \frac{2\pi t}{T}\right).$$

2-19

and since,

$$\tanh\left(\frac{2\pi d}{L}\right) = \frac{\sinh{(2\pi d/L)}}{\cosh{(2\pi d/L)}} \; ,$$

therefore,

$$u = \frac{\pi H}{T} \; \frac{\cosh{[2\pi(z+d)/L]}}{\sinh{(2\pi d/L)}} \cos\left(\frac{2\pi x}{L} - \frac{2\pi t}{T}\right).$$

* *

* * * * * * * * * * * * * * EXAMPLE PROBLEM * * * * * * * * * * * * * *

GIVEN: A wave in a depth of d = 40 feet, height of H = 10 feet, and a period of T = 10 seconds. The corresponding deepwater wave height is H_o = 10.45 feet.

FIND:

(a) The horizontal and vertical displacement of a water particle from its mean position when z = 0, and when z = - d.

(b) The maximum water particle displacement at a depth d = 25 feet when the wave is in infinitely deep water.

(c) For the deepwater conditions of (b) above, show that the particle displacements are small relative to the wave height when z = - $L_o/2$.

SOLUTION:

(a) $$L_o = 5.12 \, T^2 = 5.12 \, (10)^2 = 512 \text{ feet} \, ,$$

$$\frac{d}{L_o} = \frac{40}{512} = 0.0781 \; .$$

From Appendix C, Table C-1

$$\sinh\left(\frac{2\pi d}{L}\right) = 0.8394 \; ,$$

$$\tanh\left(\frac{2\pi d}{L}\right) = 0.6430 \; .$$

When z = 0, Equation 2-22 reduces to

$$A = \frac{H}{2} \; \frac{1}{\tanh{(2\pi d/L)}} \; ,$$

2-20

and Equation 2-23 reduces to

$$B = \frac{H}{2} .$$

Thus,

$$A = \frac{10}{2} \frac{1}{(0.6430)} = 7.78 \text{ feet} ,$$

$$B = \frac{H}{2} = \frac{10}{2} = 5.0 \text{ feet} .$$

When $z = -d$,

$$A = \frac{H}{2 \sinh (2\pi d/L)} = \frac{10}{2 (0.8394)} = 5.96 \text{ feet} ,$$

and, $B = 0$.

(b) With $H_O = 10.45$ feet, and $z = -25$, evaluate the exponent of e for use in Equation 2-24, noting that $L = L_O$,

$$\left(\frac{2\pi z}{L}\right) = \frac{2\pi(-25)}{512} = -0.307 ,$$

thus

$$e^{-0.307} = 0.736 .$$

Therefore,

$$A = B = \frac{H_o}{2} e^{2\pi z/L} = \frac{10.45}{2} (0.736) = 3.85 \text{ feet} .$$

The maximum displacement or diameter of the orbit circle would be $2(3.85) = 7.70$ feet.

(c)

$$z = -\frac{L_o}{2} = \frac{-512}{2} = -256 \text{ feet} ,$$

$$\frac{2\pi z}{L} = \frac{2\pi(-256)}{512} = -3.142 .$$

Using Table C-4 of Appendix C,

$$e^{-3.142} = 0.043 .$$

$$A = B = \frac{H_o}{2} e^{2\pi z/L} = \frac{10.45}{2} (0.043) = 0.225 \text{ feet} .$$

Thus the maximum displacement of the particle is 0.45 feet which is small when compared with the deepwater height, H_O = 10.45 feet.

* *

2.236 Subsurface Pressure. Subsurface pressure under a wave is the summation of two contributing components, dynamic and static pressures, and is given by

$$p' = \rho g \; \frac{\cosh \left[2\pi(z+d)/L \right]}{\cosh (2\pi d/L)} \; \frac{H}{2} \cos \left(\frac{2\pi x}{L} - \frac{2\pi t}{T} \right) \; - \; \rho g z + p_a \, , \qquad (2\text{-}26)$$

where p' is the total or absolute pressure, p_a is the atmospheric pressure and $\rho = w/g$ is the mass density of water (for saltwater, ρ = 2.0 lbs sec^2/ft^4 = 2.0 slugs/ft^3; for fresh water, ρ = 1.94 slugs/ft^3). The first term of Equation 2-26 represents a dynamic component due to acceleration, while the second term is the static component of pressure. For convenience, the pressure is usually taken as the gage pressure defined as

$$p = p' - p_a = \rho g \; \frac{\cosh \left[2\pi(z+d)/L \right]}{\cosh (2\pi d/L)} \; \frac{H}{2} \cos \left(\frac{2\pi x}{L} - \frac{2\pi t}{T} \right) - \rho g z \; . \qquad (2\text{-}27)$$

Equation 2-27 can be written as

$$p = \rho g \eta \; \frac{\cosh \left[2\pi(z+d)/L \right]}{\cosh (2\pi d/L)} - \rho g z \, , \qquad (2\text{-}28)$$

since

$$\eta = \frac{H}{2} \cos \left(\frac{2\pi x}{L} - \frac{2\pi t}{T} \right) .$$

The ratio

$$K_z = \frac{\cosh \left[2\pi(z+d)/L \right]}{\cosh (2\pi d/L)} \, , \qquad (2\text{-}29)$$

is termed the pressure response factor. Hence, Equation 2-28 can be written as

$$p = \rho g \left(\eta K_z - z \right) . \qquad (2\text{-}30)$$

2-22

The pressure response factor K, for the pressure at the bottom when $z = -d$,

$$K_z = K = \frac{1}{\cosh (2\pi d/L)} , \qquad\qquad (2\text{-}31)$$

is tabulated as a function of d/L_o and d/L in Tables C-1 and C-2 of Appendix C.

It is often necessary to determine the height of surface waves based on subsurface measurements of pressure. For this purpose it is convenient to rewrite Equation 2-30 as,

$$\eta = \frac{N(p+\rho gz)}{\rho g K_z} , \qquad\qquad (2\text{-}32)$$

where z is the depth below the SWL of the pressure gage, and N is a correction factor equal to unity if the linear theory applies. Several empirical studies have found N to be a function of period, depth, wave amplitude and other factors. In general, N decreases with decreasing period, being greater than 1.0 for long-period waves and less than 1.0 for short-period waves.

A complete discussion of the interpretation of pressure gage wave records is beyond the scope of this Manual. For a more detailed discussion of the variation of N with wave parameters, the reader is referred to Draper (1957), Grace (1970), and Esteva and Harris (1971).

* * * * * * * * * * * * * *   EXAMPLE PROBLEM   * * * * * * * * * * * * * *

GIVEN: An average maximum pressure of p = 2590 lbs/ft^2 is measured by a subsurface pressure gage located 2 feet above the bed in water at d = 40 feet. The average frequency f = 0.0666 cycles per second.

FIND: The height of the wave H assuming that linear theory applies and the average frequency corresponds to the average wave amplitude.

SOLUTION:

$$T = \frac{1}{f} = \frac{1}{(0.0666)} \approx 15 \text{ seconds} ,$$

$$L_o = 5.12\, T^2 = 5.12\,(15)^2 = 1152 \text{ feet} ,$$

$$\frac{d}{L_o} = \frac{40}{1152} \approx 0.0347 .$$

2-23

From Table C-1 of Appendix C, entering with d/L_O,

$$\frac{d}{L} = 0.07712 \; ,$$

hence

$$L = \frac{40}{(0.07712)} = 519 \text{ feet} \; ,$$

and

$$\cosh\left(\frac{2\pi d}{L}\right) = 1.1197 \; .$$

Therefore, from Equation 2-29

$$K_z = \frac{\cosh\left[2\pi(z+d)/L\right]}{\cosh(2\pi d/L)} = \frac{\cosh\left[2\pi(-38+40)/519\right]}{1.1197} = \frac{1.0003}{1.1197} = 0.8934 \; .$$

Since $\eta = a = H/2$ when the pressure is maximum (under the wave crest), and $N = 1.0$ since linear theory is assumed valid,

$$\frac{H}{2} = \frac{N(p + \rho gz)}{\rho g K_z} = \frac{1.0\left[2590 + (64.4)(-38)\right]}{(64.4)(0.8934)} = 2.47 \text{ feet}$$

Therefore,

$$H = 2(2.47) \approx 5 \text{ feet} \; .$$

Note that the tabulated value of K in Appendix C, Table C-1, could not be used since the pressure was not measured at the bottom.

* *

2.237 <u>Velocity of a Wave Group</u>. The speed with which a group of waves or a wave train travels is generally not identical to the speed with which individual waves within the group travel. The group speed is termed the group velocity, C_g; the individual wave speed is the phase velocity or wave celerity given by Equations 2-2 or 2-3. For waves propagating in deep or transitional water with gravity as the primary restoring force, the group velocity will be less than the phase velocity. (For those waves propagated primarily under the influence of surface tension, i.e., capillary waves, the group velocity may exceed the velocity of an individual wave.)

The concept of group velocity can be described by considering the interaction of two sinusoidal wave trains moving in the same direction

with slightly different wavelengths and periods. The equation of the water surface is given by:

$$\eta = \eta_1 + \eta_2 = \frac{H}{2} \cos\left(\frac{2\pi x}{L_1} - \frac{2\pi t}{T_1}\right) + \frac{H}{2} \cos\left(\frac{2\pi x}{L_2} - \frac{2\pi t}{T_2}\right), \qquad (2\text{-}33)$$

where η_1 and η_2 are the contributions of each of the two components. They may be summed since superposition of solutions is permissible when linear wave theory is used. For simplicity, the heights of both wave components have been assumed equal. Since the wavelengths of the two component waves, L_1 and L_2, have been assumed slightly different, for some values of x at a given time, the two components will be in phase and the wave height observed will be $2H$; for some other values of x, the two waves will be completely out of phase and the resultant wave height will be zero. The surface profile made up of the sum of the two sinusoidal waves is given by Equation 2-33 and is shown in Figure 2-5. The waves shown on Figure 2-5 appear to be traveling in groups described by the equation of the envelope curves:

$$\eta_{envelope} = \pm H \cos\left[\pi\left(\frac{L_2 - L_1}{L_1 \, L_2}\right) x - \pi\left(\frac{T_2 - T_1}{T_1 \, T_2}\right) t\right]. \qquad (2\text{-}34)$$

It is the speed of these groups, i.e. the velocity of propagation of the envelope curves, that represents the group velocity. The limiting speed of the wave groups as they become large, i.e., as the wavelength, L_1, approaches L_2 and consequently the wave period T_1 approaches T_2 is the group velocity and can be shown to be equal to:

$$C_g = \frac{1}{2} \frac{L}{T} \left[1 + \frac{4\pi d/L}{\sinh\left(4\pi d/L\right)}\right] = nC \,, \qquad (2\text{-}35)$$

where

$$n = \frac{1}{2} \left[1 + \frac{4\pi d/L}{\sinh\left(4\pi d/L\right)}\right].$$

In deep water, the term $(4\pi d/L)/\sinh(4\pi d/L)$ is approximately zero and,

$$C_g = \frac{1}{2} \frac{L_o}{T} = \frac{1}{2} C_o \text{ (deep water)}, \qquad (2\text{-}36)$$

or the group velocity is one-half the phase velocity. In shallow water, $\sinh(4\pi d/L) \approx 4\pi d/L$ and,

$$C_g = \frac{L}{T} = C \approx \sqrt{gd} \text{ (shallow water)}, \qquad (2\text{-}37)$$
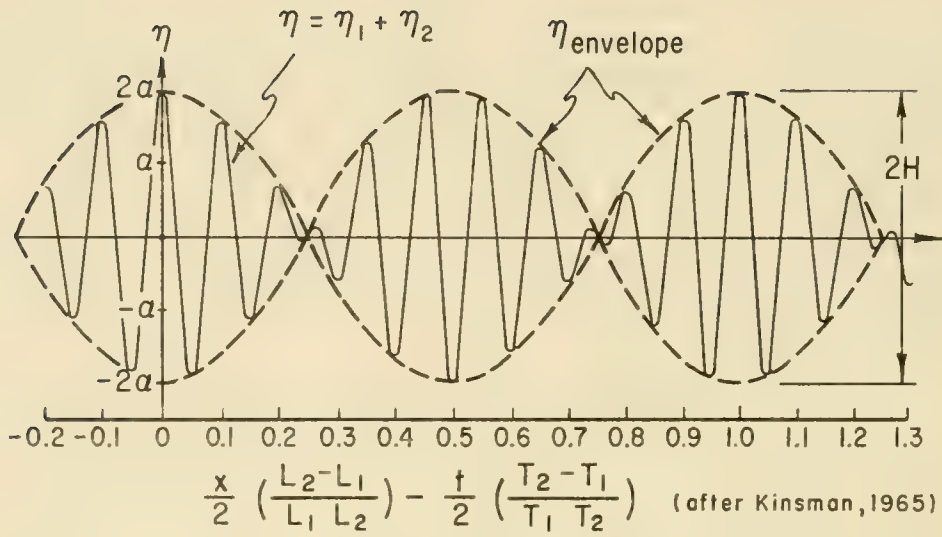
Figure 2-5. Formation of Wave Groups by the Addition of Two Sinusoids Having Different Periods

hence the group and phase velocities are equal. Thus in shallow water, because wave celerity is fully determined by the depth, all component waves in a wave train will travel at the same speed precluding the alternate reinforcing and cancelling of components. In deep and transitional water, wave celerity depends on the wavelength; hence slightly longer waves travel slightly faster, and produce the small phase differences resulting in wave groups. These waves are said to be *dispersive* or propagating in a *dispersive medium*, i.e. in a medium where their celerity is dependent on wavelength.

Outside of shallow water, the phase velocity of gravity waves is greater than the group velocity, and an observer moving along with a group of waves at the group velocity will see waves that originate at the rear of the group move forward through the group traveling at the phase velocity, and disappear at the front of the wave group.

Group velocity is important because it is with this velocity that wave energy is propagated.

Although mathematically, the group velocity can be shown rigorously from the interference of two or more waves (Lamb, 1932), the physical significance is not as obvious as it is in the method based on the consideration of wave energy. Therefore an additional explanation of group velocity is provided on wave energy and energy transmission.

2.238 Wave Energy and Power. The total energy of a wave system is the sum of its kinetic energy and its potential energy. The kinetic energy is that part of the total energy due to water particle velocities associated with wave motion. Potential energy is that part of the energy resulting from part of the fluid mass being above the trough - the wave crest. According to the Airy theory, if the potential energy is determined relative to mean water level, and all waves are propagated in the same direction, potential and kinetic energy components are equal, and the total wave energy in one wavelength per unit crest width is given by

$$E = E_k + E_p = \frac{\rho g H^2 L}{16} + \frac{\rho g H^2 L}{16} = \frac{\rho g H^2 L}{8} . \qquad (2\text{-}38)$$

Subscripts k and p refer to kinetic and potential energies. Total average wave energy per unit surface area, termed the *specific energy* or *energy density*, is given by

$$\bar{E} = \frac{E}{L} = \frac{\rho g H^2}{8} . \qquad (2\text{-}39)$$

Wave energy flux is the rate at which energy is transmitted in the direction of wave propagation across a vertical plane perpendicular to the direction of wave advance and extending down the entire depth. The average

energy flux per unit wave crest width transmitted across a plane perpendicular to wave advance is

$$\overline{P} = \overline{E}nC = \overline{E}C_g .$$

(2-40)

Energy flux $\overline{P}$ is frequently called *wave power* and

$$n = \frac{1}{2}\left[1 + \frac{4\pi d/L}{\sinh{(4\pi d/L)}}\right].$$

If a plane is taken other than perpendicular to the direction of wave advance, $\overline{P} = \overline{E} C_g \sin \phi$, where ϕ is the angle between the plane across which the energy is being transmitted and the direction of wave advance.

For deep and shallow water, Equation 2-40 becomes

$$\overline{P}_o = \frac{1}{2} \overline{E}_o C_o \text{ (deep water)} .$$

(2-41)

$$\overline{P} = \overline{E}C_g = \overline{E}C \text{ (shallow water)} .$$

(2-42)

An energy balance for a region through which waves are passing will reveal, that for steady state, the amount of energy entering the region will equal the amount leaving the region provided no energy is added or removed from the system. Therefore, when the waves are moving so that their crests are parallel to the bottom contours,

$$\overline{E}_o n_o C_o = \overline{E}nC ,$$

or, since

$$n_o = \frac{1}{2} ,$$

$$\frac{1}{2} \overline{E}_o C_o = \overline{E}nC .$$

(2-43)

When the wave crests are not parallel to the bottom contours, some parts of the wave will be traveling at different speeds, the wave will be refracted and Equation 2-43 does not apply. (See Section 2.3. WAVE REFRACTION.)

The following problem illustrates some basic principles of wave energy and energy flux.

GIVEN: A deepwater oscillatory wave with a wavelength of $L_O = 512$ feet, a height of $H_O = 5$ feet and a celerity of $C_O = 51.2$ ft/sec, moving shoreward with its crest parallel to the depth contours. Any effects due to reflection from the beach are negligible.

FIND:

(a) Derive a relationship between the wave height in any depth of water and the wave height in deep water, assuming that wave energy per unit crest width is conserved as a wave moves from deep water into shoaling water.

(b) Calculate the wave height for the given wave when the depth is 10 feet.

(c) Determine the rate at which energy per unit crest width is transported toward the shoreline and the total energy per unit width delivered to the shore in 1 hour by the given waves.

SOLUTION:

(a) Since the wave crests are parallel to the bottom contours, refraction does not occur, therefore $H_O = H_O'$. (See Section 2.3. WAVE REFRACTION.)

From Equation 2-43,

$$\frac{1}{2}\, \overline{E}_o C_o = n\overline{E}C \ .$$

The expressions for $\overline{E}_O$ and $\overline{E}$ are,

$$\overline{E}_o = \frac{\rho g H_o'^2}{8} \ ,$$

and

$$\overline{E} = \frac{\rho g H^2}{8} \ ,$$

where H_O' represents the wave height in deep water if the wave were not refracted.

Substituting into the above equation gives,

$$\frac{1}{2}\, C_o\, \frac{\rho g H_o'^2}{8} = nC\, \frac{\rho g H^2}{8} \ .$$

2-29

Therefore,

$$\left(\frac{H}{H'_o}\right)^2 = \frac{1}{2}\frac{1}{n}\frac{C_o}{C} \quad ,$$

and since from Equations 2-3 and 2-6

$$\frac{C}{C_o} = \tanh\left(\frac{2\pi d}{L}\right) \quad ,$$

and from Equation 2-35 where

$$n = \frac{1}{2}\left[1 + \frac{4\pi d/L}{\sinh(4\pi d/L)}\right] \quad ,$$

$$\frac{H}{H'_o} = \sqrt{\frac{1}{\tanh(2\pi d/L)} \cdot \frac{1}{\left[1 + \frac{(4\pi d/L)}{\sinh(4\pi d/L)}\right]}} = K_s \ , \qquad (2\text{-}44)$$

where K_s or H/H'_o is termed the *shoaling coefficient*. Values of H/H'_o as a function of d/L_o and d/L have been tabulated in Tables C-1 and C-2 of Appendix C.

(b) For the given wave, $d/L_o = 10/512 = 0.01953$. Either from Table C-1 or from an evaluation of Equation 2-44 above,

$$\frac{H}{H'_o} = 1.233 \ .$$

Therefore,

$$H = 1.233\,(5) = 6.165 \text{ ft.}$$

(c) The rate at which energy is being transported toward shore is the wave energy flux.

$$\bar{P} = \frac{1}{2}\,\bar{E}_o C_o = n\bar{E}C \ .$$

Since it is easier to evaluate the energy flux in deep water, the left side of the above equation will be used.

$$\bar{P} = \frac{1}{2}\,\bar{E}_o C_o = \frac{1}{2}\frac{\rho g\,(H'_o)^2}{8}\,51.2 = \frac{1}{2}\frac{64\,(5)^2}{8}\,51.2 \ .$$

$$\bar{P} = 5120\,\frac{\text{ft-lb}}{\text{sec}} \text{ per ft. of wave crest} \ ,$$

$$\bar{P} = \frac{5120}{550} = 9.31 \text{ horsepower per ft. of wave crest} \ .$$

2-30

This represents the expenditure of

$$5120 \; \frac{\text{ft-lb}}{\text{sec}} \times 3600 \; \frac{\text{sec}}{\text{hr}} = 18.55 \times 10^6 \; \text{ft-lbs},$$

of energy each hour on each foot of beach.

* *

The mean rate of energy transmission associated with waves propagating into an area of calm water provides a better physical description of the concept of group velocity. An excellent treatment of this subject is given by Sverdrup and Munk (1947) and is repeated here.

Quoting from the Beach Erosion Board Technical Report No. 2, (1942): "As the first wave in the group advances one wave length, its form induces corresponding velocities in the previously undisturbed water and the kinetic energy corresponding to those velocities must be drawn from the energy flowing ahead with the form. If there is equipartition of energy in the wave, half of the potential energy which advanced with the wave must be given over to the kinetic form and the wave loses height. Advancing another wave length another half of the potential energy is used to supply kinetic energy to the undisturbed liquid. The process continues until the first wave is too small to identify. The second, third, and subsequent waves move into water already disturbed and the rate at which they lose height is less than for the first wave. At the rear of the group, the potential energy might be imagined as moving ahead, leaving a flat surface and half of the total energy behind as kinetic energy. But the velocity pattern is such that flow converges toward one section thus developing a crest and diverges from another section forming a trough. Thus the kinetic energy is converted into potential and a wave develops in the rear of the group."

This concept can be interpreted in a quantitative manner, by taking the following example from R. Gatewood (Gaillard 1904, p. 50). Suppose that in a very long trough containing water originally at rest, a plunger at one end is suddenly set into harmonic motion and starts generating waves by periodically imparting an energy $E/2$ to the water. After a time interval of n periods there are n waves present. Let m be the position of a particular wave in this group such that $m=1$ refers to the wave which has just been generated by the plunger, $m=(n+1)/2$ to the center wave, and $m=n$ to the wave furthest advanced. Let the waves travel with constant velocity C, and neglect friction.

After the first complete stroke one wave will be present and its energy is $E/2$. One period later this wave has advanced one wave length but has left one-half of its energy or $E/4$ behind. It now occupies a previously undisturbed area to which it has brought energy $E/4$. In the meantime, a second wave has been generated, occupying the position next to the plunger where $E/4$ was left behind by the first wave. The energy of this second wave equals $E/4 + E/2 = 3E/4$. Repeated applications of this reasoning lead to the results shown in Table 2-1.

The series number n gives the total number of waves present and equals the time in periods since the first wave entered the area of calm; the wave number m gives the position of the wave measured from the plunger and equals the distance from the plunger expressed in wave lengths. In any series, n, the deviation of the energy from the value $E/2$ is symmetrical about the center wave. Relative to the center wave all waves nearer the plunger show an excess of energy and all waves beyond the center wave show a deficit. For any two waves at equal distances from the center wave the excess equals the deficiency. In every series, n, the energy first decreases slowly with increasing distance from the plunger, but in the vicinity of the center wave it decreases rapidly. Thus, there develops an "energy front" which advances with the speed of the central part of the wave system, that is, with half the wave velocity.

According to the last line in Table 2-1 a definite pattern develops after a few strokes: the wave closest to the plunger has an energy $E(2^n-1)/2^n$ which approaches the full amount E, the center wave has an energy $E/2$, and the wave which has traveled the greatest distance has very little energy $(E/2^n)$.

Table 2-1. Distribution of Wave Heights in a Short Train of Waves

Series number n	Wave number, m							Total energy of group
	1	2	3	4	5	6	7	
1	1/2E	————	————	————	————	————	————	1/2E
2	3/4	1/4E	————	————	————	————	————	2/2
3	7/8	4/8	1/8E	————	————	————	————	3/2
4	15/16	11/16	5/16	1/16E	————	————	————	4/2
5	31/32	26/32	16/32	6/32	1/32E	————	————	5/2
6	63/64	57/64	42/64	22/64	7/64	1/64E		6/2

With a large number of waves (a large n), energy decreases with increasing m, and the leading wave will eventually lose its identity. At the group center, energy increases and decreases rapidly - to nearly maximum and to nearly zero. Consequently, an energy front is located at the center wave group for deepwater conditions. If waves had been examined for shallow rather than deep water, the energy front would have been found at the leading edge of the group. For any depth, the ratio of group to phase velocity (C_g/C) generally defines the energy front. Also, wave energy is transported in the direction of phase propagation, but moves with the group velocity rather than phase velocity.

2.239 <u>Summary - Linear Wave Theory</u>. Equations describing water surface profile particle velocities, particle accelerations, and particle displacements for linear (Airy) theory are summarized in Figure 2-6.

2.24 HIGHER ORDER WAVE THEORIES

Solution of the hydroynamic equations for gravity-wave phenomena can be improved. Each extension of the theories usually produces better agreement between theoretical and observed wave behavior. The extended theories can explain phenomena such as mass transport that cannot be explained by linear theory. If amplitude and period are known precisely, the extended theories can provide more accurate estimates of such derived quantities as the velocity and pressure fields due to waves than can linear theory. In shallow water, the maximum wave height is determined by depth, and can be estimated without wave records.

When concern is primarily with the oscillating character of waves, estimates of amplitude and period must be determined from empirical data. In such problems, the uncertainty about the accurate wave height and period leads to a greater uncertainty about the ultimate answer than does neglecting the effect of nonlinear processes. Thus it is unlikely that the extra work involved in using nonlinear theories is justified.

The engineer must define regions where various wave theories are valid. Since investigators differ on the limiting conditions for the several theories, some overlap must be permitted in defining the regions. Le Mehaute (1969) presented Figure 2-7 to illustrate approximate limits of validity for several wave theories. Theories discussed here are indicated as are Stokes' third- and fourth-order theories. Dean (1973), after considering three analytic theories, presents a slightly different analysis. Dean (1973) and Le Mehaute (1969) agree in recommending cnoidal theory for shallow-water waves of low steepness, and Stokes' higher order theories for steep waves in deep water, but differ in regions assigned to Airy theory. Dean indicates that tabulated stream function theory is most internally consistent over most of the domain considered. For the limit of low steepness waves in transitional and deep water, the difference between stream function theory and Airy theory is small. Additional wave theories not presented in Figure 2-7 may also be useful in studying

RELATIVE DEPTH	SHALLOW WATER $\frac{d}{L} < \frac{1}{25}$	TRANSITIONAL WATER $\frac{1}{25} < \frac{d}{L} < \frac{1}{2}$	DEEP WATER $\frac{d}{L} > \frac{1}{2}$
1. Wave Profile	Same As →	$\eta = \frac{H}{2}\cos\left[\frac{2\pi x}{L} - \frac{2\pi t}{T}\right] = \frac{H}{2}\cos\theta$	← Same As
2. Wave Celerity	$C = \frac{L}{T} = \sqrt{gd}$	$C = \frac{L}{T} = \frac{gT}{2\pi}\tanh\left(\frac{2\pi d}{L}\right)$	$C = C_0 = \frac{L}{T} = \frac{gT}{2\pi}$
3. Wave Length	$L = T\sqrt{gd} = CT$	$L = \frac{gT^2}{2\pi}\tanh\left(\frac{2\pi d}{L}\right)$	$L = L_0 = \frac{gT^2}{2\pi} = C_0 T$
4. Group Velocity	$Cg = C = \sqrt{gd}$	$Cg = nC = \frac{1}{2}\left[1 + \frac{4\pi d/L}{\sinh(4\pi d/L)}\right]\cdot C$	$Cg = \frac{1}{2}C = \frac{gT}{4\pi}$
5. Water Particle Velocity a) Horizontal	$u = \frac{H}{2}\sqrt{\frac{g}{d}}\cos\theta$	$u = \frac{H}{2}\frac{gT}{L}\frac{\cosh[2\pi(z+d)/L]}{\cosh(2\pi d/L)}\cos\theta$	$u = \frac{\pi H}{T}e^{\frac{2\pi z}{L}}\cos\theta$
b) Vertical	$w = \frac{H\pi}{T}\left(1+\frac{z}{d}\right)\sin\theta$	$w = \frac{H}{2}\frac{gT}{L}\frac{\sinh[2\pi(z+d)/L]}{\cosh(2\pi d/L)}\sin\theta$	$w = \frac{\pi H}{T}e^{\frac{2\pi z}{L}}\sin\theta$
6. Water Particle Accelerations a) Horizontal	$a_x = \frac{H\pi}{T}\sqrt{\frac{g}{d}}\sin\theta$	$a_x = \frac{g\pi H}{L}\frac{\cosh[2\pi(z+d)/L]}{\cosh(2\pi d/L)}\sin\theta$	$a_x = 2H\left(\frac{\pi}{T}\right)^2 e^{\frac{2\pi z}{L}}\sin\theta$
b) Vertical	$a_z = -2H\left(\frac{\pi}{T}\right)^2\left(1+\frac{z}{d}\right)\cos\theta$	$a_z = -\frac{g\pi H}{L}\frac{\sinh[2\pi(z+d)/L]}{\cosh(2\pi d/L)}\cos\theta$	$a_z = -2H\left(\frac{\pi}{T}\right)^2 e^{\frac{2\pi z}{L}}\cos\theta$
7. Water Particle Displacements a) Horizontal	$\xi = -\frac{HT}{4\pi}\sqrt{\frac{g}{d}}\sin\theta$	$\xi = -\frac{H}{2}\frac{\cosh[2\pi(z+d)/L]}{\sinh(2\pi d/L)}\sin\theta$	$\xi = -\frac{H}{2}e^{\frac{2\pi z}{L}}\sin\theta$
b) Vertical	$\zeta = \frac{H}{2}\left(1+\frac{z}{d}\right)\cos\theta$	$\zeta = \frac{H}{2}\frac{\sinh[2\pi(z+d)/L]}{\sinh(2\pi d/L)}\cos\theta$	$\zeta = \frac{H}{2}e^{\frac{2\pi z}{L}}\cos\theta$
8. Subsurface Pressure	$p = \rho g(\eta - z)$	$p = \rho g\eta\frac{\cosh[2\pi(z+d)/L]}{\cosh(2\pi d/L)} - \rho gz$	$p = \rho g\eta\, e^{\frac{2\pi z}{L}} - \rho gz$

Figure 2-6. Summary – Linear (Airy) Wave Theory – Wave Characteristics
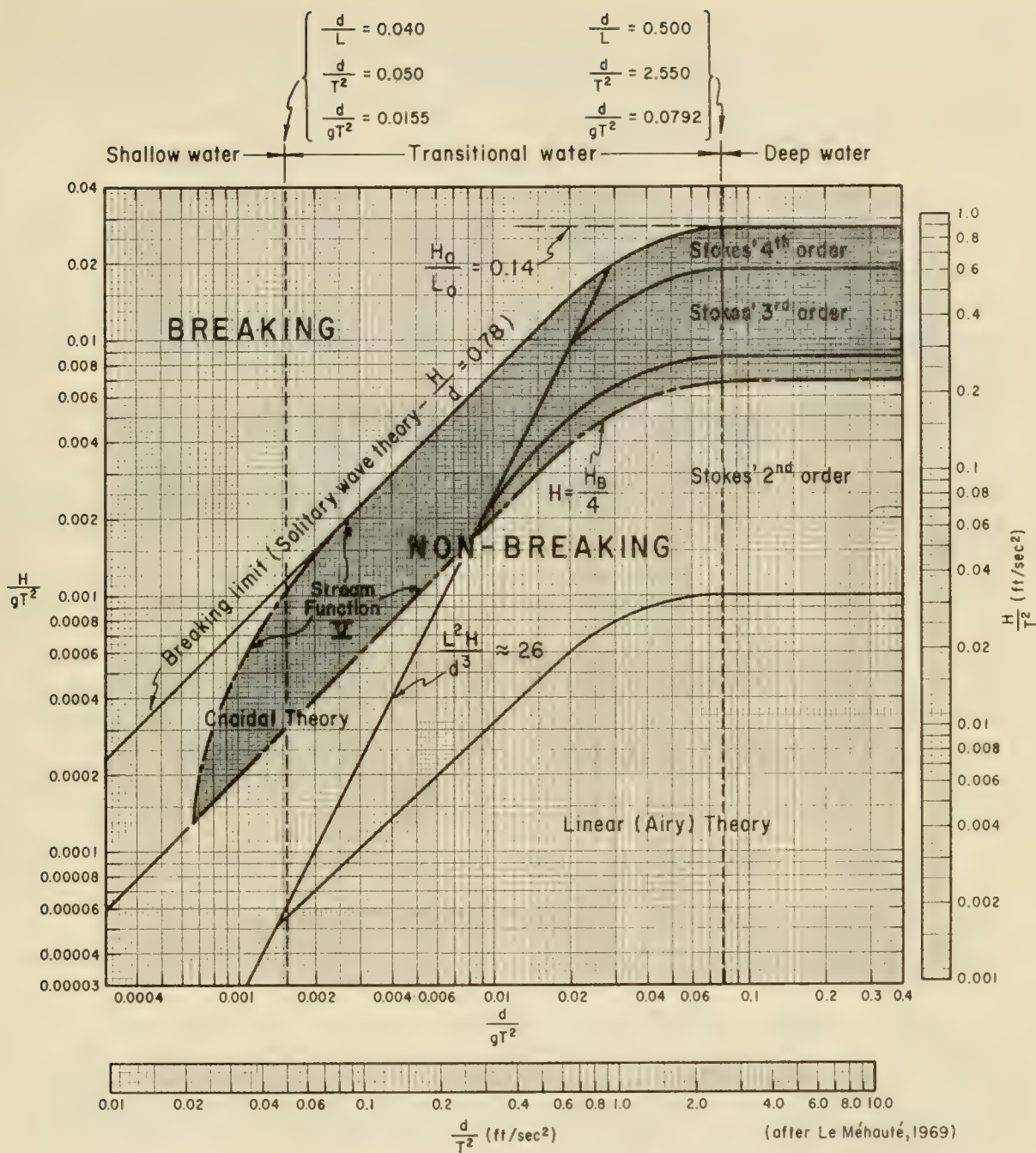
Figure 2-7. Regions of Validity for Various Wave Theories

2-35

wave phenomena. For given values of H, d and T, Figure 2-7 may be used as a guide in selecting an appropriate theory. The magnitude of the Ursell parameter U_R shown in the figure may be used to establish the boundaries of regions where a particular wave theory should be used. The Ursell parameter is defined by

$$U_R = \frac{L^2 H}{d^3} .$$

(2-45)

For linear theory to predict accurately the wave characteristics, both wave steepness, H/gT^2, and the Ursell parameter must be small as shown in Figure 2-7.

2.25 STOKES' PROGRESSIVE, SECOND-ORDER WAVE THEORY

Wave formulas presented in the preceding sections on linear wave theory are based on the assumption that the motions are so small that the free surface can be described to the first order of approximation by Equation 2-10:

$$\eta = \frac{H}{2} \cos \left(\frac{2\pi x}{L} - \frac{2\pi t}{T} \right) = \frac{H}{2} \cos \theta \text{ or a } \cos \theta .$$

More specifically, it is assumed that wave amplitude is small, and the contribution made to the solution by higher order terms is negligible. A more general expression would be:

$$\eta = a \cos (\theta) + a^2 B_2 (L, d) \cos (2\theta)$$
$$+ a^3 B_3 (L, d) \cos (3\theta) + \cdots a^n B_n (L, d) \cos (n\theta) ,$$

(2-46)

where a = H/2, for first- and second-orders, but a < H/2 for orders higher than the second, and B_2, B_3 etc. are specified functions of the wavelength L, and depth d.

Linear theory considers only the first term on the right side of Equation 2-46. To consider additional terms represents a higher order of approximation of the free surface profile. The order of the approximation is determined by the highest order term of the series considered. Thus, the ordinate of the free surface to the third order is defined by the first three terms in Equation 2-46.

When the use of a higher order theory is warranted, wave tables, such as those prepared by Skjelbreia (1959), and Skjelbreia and Hendrickson (1962), should be used to reduce the possibility of numerical errors made in using the equations. Although Stokes (1880) first developed equations for finite amplitude waves, the equations presented here are those of Miche (1944).

2-36

2.251 <u>Wave Celerity, Length, and Surface Profile</u>. It can be shown that, for second-order theories, expressions for wave celerity and wavelength are identical to those obtained by linear theory. Therefore,

$$C = \frac{gT}{2\pi} \tanh\left(\frac{2\pi d}{L}\right),$$ (2-3)

and

$$L = \frac{gT^2}{2\pi} \tanh\left(\frac{2\pi d}{L}\right).$$ (2-4)

The above equations, corrected to the third order, are given by:

$$C = \frac{gT}{2\pi} \tanh\left(\frac{2\pi d}{L}\right)\left\{1 + \left(\frac{\pi H}{L}\right)^2 \left[\frac{5 + 2\cosh(4\pi d/L) + 2\cosh^2(4\pi d/L)}{8\sinh^4(2\pi d/L)}\right]\right\},$$ (2-47)

and

$$L = \frac{gT^2}{2\pi} \tanh\left(\frac{2\pi d}{L}\right)\left\{1 + \left(\frac{\pi H}{L}\right)^2 \left[\frac{5 + 2\cosh(4\pi d/L) + 2\cosh^2(4\pi d/L)}{8\sinh^4(2\pi d/L)}\right]\right\}.$$ (2-48)

The equation of the free surface for second-order theory is

$$\eta = \frac{H}{2} \cos\left(\frac{2\pi x}{L} - \frac{2\pi t}{T}\right)$$

$$+ \left(\frac{\pi H^2}{8L}\right) \frac{\cosh(2\pi d/L)}{\sinh^3(2\pi d/L)}\left[2 + \cosh(4\pi d/L)\right] \cos\left(\frac{4\pi x}{L} - \frac{4\pi t}{T}\right).$$ (2-49)

For deep water, (d/L > 1/2) Equation 2-49 becomes,

$$\eta = \frac{H_o}{2} \cos\left(\frac{2\pi x}{L_o} - \frac{2\pi t}{T}\right) + \frac{\pi H_o^2}{4L_o} \cos\left(\frac{4\pi x}{L_o} - \frac{4\pi t}{T}\right).$$ (2-50)

2.252 <u>Water Particle Velocities and Displacements</u>. The periodic x and z components of the water particle velocities to the second order are given by

$$u = \frac{HgT}{2L} \frac{\cosh[2\pi(z+d)/L]}{\cosh(2\pi d/L)} \cos\left(\frac{2\pi x}{L} - \frac{2\pi t}{T}\right)$$

$$+ \frac{3}{4}\left(\frac{\pi H}{L}\right)^2 C \frac{\cosh[4\pi(z+d)/L]}{\sinh^4(2\pi d/L)} \cos\left(\frac{4\pi x}{L} - \frac{4\pi t}{T}\right),$$ (2-51)

$$w = \frac{\pi H}{L} C \frac{\sinh [2\pi(z + d)/L]}{\sinh (2\pi d/L)} \sin \left(\frac{2\pi x}{L} - \frac{2\pi t}{T} \right)$$

$$+ \frac{3}{4} \left(\frac{\pi H}{L} \right)^2 C \frac{\sinh [4\pi(z + d)/L]}{\sinh^4 (2\pi d/L)} \sin \left(\frac{4\pi x}{L} - \frac{4\pi t}{T} \right).$$

(2-52)

Second-order equations for water-particle displacements from their mean position for a finite amplitude wave are:

$$\xi = - \frac{HgT^2}{4\pi L} \frac{\cosh [2\pi(z + d)/L]}{\cosh (2\pi d/L)} \sin \left(\frac{2\pi x}{L} - \frac{2\pi t}{T} \right) + \frac{\pi H^2}{8L} \frac{1}{\sinh^2 (2\pi d/L)}$$

(2-53)

$$\left\{ 1 - \frac{3}{2} \frac{\cosh [4\pi(z + d)/L]}{\sinh^2 (2\pi d/L)} \right\} \sin \left(\frac{4\pi x}{L} - \frac{4\pi t}{T} \right) + \left(\frac{\pi H}{L} \right)^2 \frac{Ct}{2} \frac{\cosh [4\pi(z + d)/L]}{\sinh^2 (2\pi d/L)} ,$$

and

$$\zeta = \frac{HgT^2}{4\pi L} \frac{\sinh [2\pi(z + d)/L]}{\cosh (2\pi d/L)} \cos \left(\frac{2\pi x}{L} - \frac{2\pi t}{T} \right)$$

(2-54)

$$+ \frac{3}{16} \frac{\pi H^2}{L} \frac{\sinh [4\pi(z + d)/L]}{\sinh^4 (2\pi d/L)} \cos \left(\frac{4\pi x}{L} - \frac{4\pi t}{T} \right).$$

2.253 Mass Transport Velocity. The last term in Equation 2-53 is of particular interest; it is not periodic, but is the product of time and a constant depending on the given wave period and depth. The term predicts a continuously increasing net particle displacement in the direction of wave propagation. The distance a particle is displaced during one wave period when divided by the wave period gives a mean drift velocity, $\bar{U}(z)$, called the mass transport velocity. Thus,

$$\bar{U}(z) = \left(\frac{\pi H}{L} \right)^2 \frac{C}{2} \frac{\cosh [4\pi(z + d)/L]}{\sinh^2 (2\pi d/L)} .$$

(2-55)

Equation 2-53 indicates that there is a net transport of fluid by waves in the direction of wave propagation. If the mass transport, indicated by Equation 2-55 leads to an accumulation of mass in any region, the free surface must rise, thus generating a pressure gradient. A current, formed in response to this pressure gradient, will reestablish the distribution of mass. Studies of mass transport, theoretical and experimental, have been conducted by Longuet-Higgins (1953, 1960), Mitchim (1940), Miche (1944), Ursell (1953), and Russell and Osorio (1958). Their findings indicate that the vertical distribution of the mass transport velocity is modified so that the net transport of water across a vertical plane is zero.

2.254 Subsurface Pressure. The pressure at any distance below the fluid surface is given by

$$p = \rho g \, \frac{H}{2} \, \frac{\cosh\,[2\pi(z+d)/L]}{\cosh\,(2\pi d/L)} \, \cos\left(\frac{2\pi x}{L} - \frac{2\pi t}{T}\right) - \rho g z$$

$$+ \frac{3}{8}\,\rho g \, \frac{\pi H^2}{L} \, \frac{\tanh\,(2\pi d/L)}{\sinh^2\,(2\pi d/L)} \left[\frac{\cosh\,[4\pi(z+d)/L]}{\sinh^2\,(2\pi d/L)} - \frac{1}{3}\right] \cos\left(\frac{4\pi x}{L} - \frac{4\pi t}{T}\right) \quad (2\text{-}56)$$

$$- \frac{1}{8}\,\rho g \, \frac{\pi H^2}{L} \, \frac{\tanh\,(2\pi d/L)}{\sinh^2\,(2\pi d/L)} \left\{\cosh\,\frac{4\pi(z+d)}{L} - 1\right\}.$$

2.255 Maximum Steepness of Progressive Waves. A progressive gravity wave is physically limited in height by depth and wavelength. The upper limit, or breaking wave height in deep water is a function of the wavelength, and in shallow and transitional water is a function of both depth and wavelength.

Stokes (1880) predicted theoretically that a wave would remain stable only if the water particle velocity at the crest was less than the wave celerity or phase velocity. If the wave height were to become so large that the water particle velocity at the crest exceeded the wave celerity, the wave would become unstable and break. Stokes found that a wave having a crest angle less than 120 degrees would break (angle between two lines tangent to the surface profile at the wave crest). The possibility of existence of a wave having a crest angle equal to 120 degrees was shown by Wilton (1914). Michell (1893) found that in deep water the theoretical limit for wave steepness was

$$\left(\frac{H_o}{L_o}\right)_{max} = 0.142 \approx \frac{1}{7}. \quad (2\text{-}57)$$

Havelock (1918) confirmed Michell's findings.

Miche (1944) gives the limiting steepness for waves traveling in depths less than $L_O/2$ without a change in form as

$$\left(\frac{H}{L}\right)_{max} = \left(\frac{H_o}{L_o}\right)_{max} \tanh\left(\frac{2\pi d}{L}\right) = 0.142 \tanh\left(\frac{2\pi d}{L}\right) \quad (2\text{-}58)$$

Laboratory measurements by Danel (1952) indicate that the above equation is in close agreement with an envelope curve to laboratory observations. Additional discussion of breaking waves in deep and shoaling water is presented in Section 2.6, BREAKING WAVES.

2.256 Comparison of the First- and Second-Order Theories. A comparison of first- and second-order theories is useful to obtain insight about the

choice of a theory for a particular problem. It should be kept in mind that linear (or first-order) theory applies to a wave which is symmetrical about stillwater level and has water particles that move in closed orbits. On the other hand, Stokes' second-order theory predicts a wave form that is unsymmetrical about the stillwater level but still symmetrical about a vertical line through the crest, and has water particle orbits which are open.

* * * * * * * * * * * * * * EXAMPLE PROBLEM * * * * * * * * * * * * * * *

GIVEN: A wave traveling in water depth of d = 20 feet, with a wavelength of L = 200 feet and a height of H = 4 feet.

FIND:

(a) Compare the wave profiles given by the first- and second-order theories.

(b) What is the difference between the first- and second-order horizontal velocities at the surface under both the crest and trough?

(c) How far in the direction of wave propagation will a water particle move from its initial position during one wave period when z = 0?

(d) What is pressure at the bottom under the wave crest as predicted by both the first- and second-order theories?

(e) What is the wave energy per unit width of crest predicted by the first-order theory?

SOLUTION:

(a) The first-order profile Equation 2-10 is:

$$\eta = \frac{H}{2} \cos \theta \ ,$$

where

$$\theta = \left(\frac{2\pi x}{L} - \frac{2\pi t}{T} \right),$$

and the second-order profile Equation 2-49 is:

$$\eta = \frac{H}{2} \cos \theta + \frac{\pi H^2}{8L} \frac{\cosh (2\pi d/L)}{\sinh^3 (2\pi d/L)} \left[2 + \cosh \left(\frac{4\pi d}{L} \right) \right] \cos 2\theta$$

for

$$\frac{d}{L} = \frac{20}{200} = 0.1 \ ,$$

2-40

and from Table C-2

$$\cosh\left(\frac{2\pi d}{L}\right) = 1.2040 ,$$

$$\sinh\left(\frac{2\pi d}{L}\right) = 0.6705 ,$$

$$\cosh\left(\frac{4\pi d}{L}\right) = 1.8991 ,$$

$$\frac{\pi H^2}{8L} \frac{\cosh(2\pi d/L)}{\sinh^3(2\pi d/L)}\left[2 + \cosh\left(\frac{4\pi d}{L}\right)\right] = 0.48$$

Therefore

$$\eta = 2 \cos\theta + 0.48 \cos 2\theta ,$$

$$\eta_{c,2} = 2.48 \text{ ft.},$$

$$\eta_{t,2} = -1.52 \text{ ft.}$$

where $\eta_{c,2}$ and $\eta_{t,2}$ are the values of η at the crest (i.e. $\cos\theta = 1$, $\cos 2\theta = 1$) and trough (i.e. $\cos\theta = -1$, $\cos 2\theta = 1$) according to second-order theory.

Figure 2-8 shows the surface profile η as a function of θ. The second-order profile is more peaked at the crest and flatter at the trough than the first-order profile. The height of the crest above SWL is greater than one-half the wave height; consequently the distance below the SWL of the trough is less than one-half the height. Moreover, for linear theory, the elevation of the water surface above the SWL is equal to the elevation below the SWL; however, for second-order theory there is more height above SWL than below.

(b) For convenience, let

$u_{c,1}$ = value of u at crest according to first-order theory,

$u_{t,1}$ = value of u at a trough according to first-order theory,

$u_{c,2}$ = value of u at a crest according to second-order theory,

$u_{t,2}$ = value of u at a trough according to second-order theory.
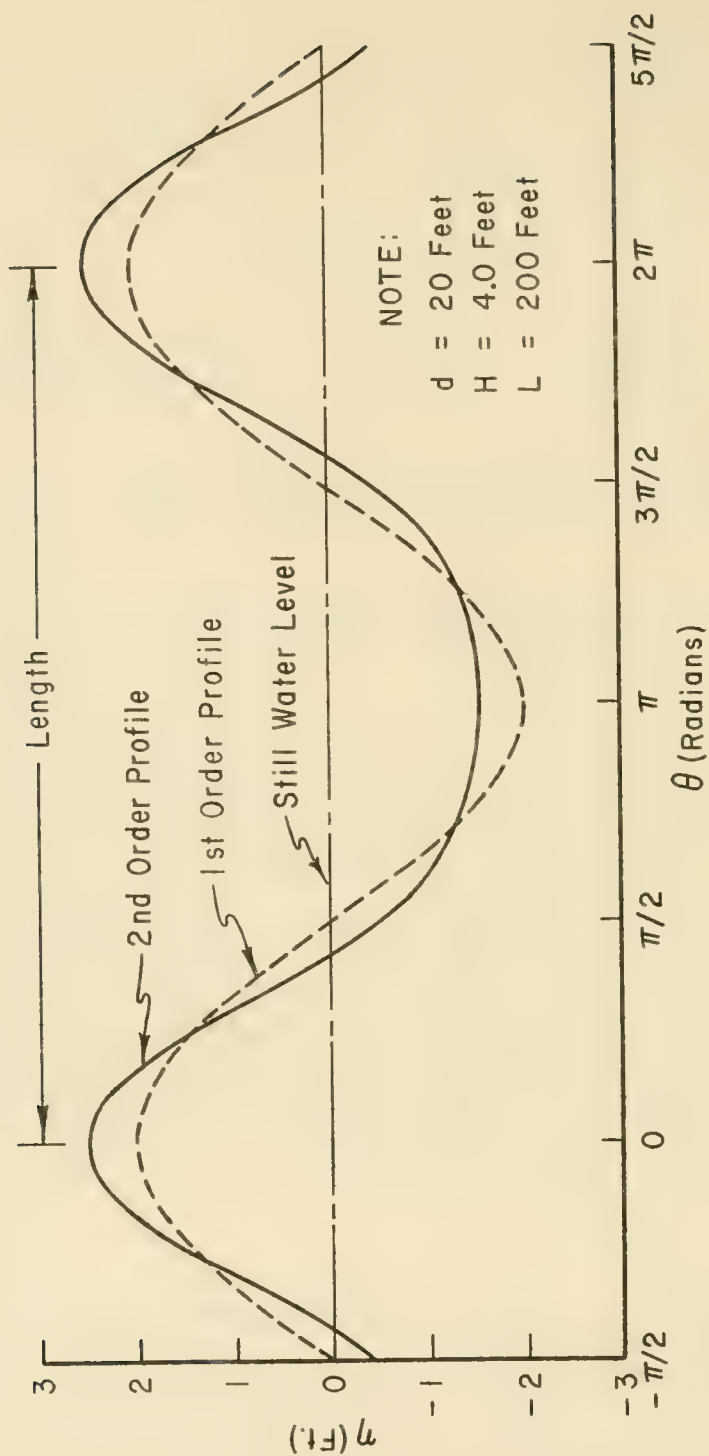
Figure 2-8. Comparison of Second Order Stokes' Profile with Linear Profile.

NOTE:

d = 20 Feet
H = 4.0 Feet
L = 200 Feet

2-42

According to first-order theory, a crest occurs at $z = H/2$, $\cos \theta = 1$ and a trough at $z = - H/2$, $\cos \theta = - 1$. Equation 2-13 therefore implies

$$u_{c,1} = \frac{Hg}{2} \frac{T}{L} \frac{\cosh [2\pi(z + d)/L]}{\cosh (2\pi d/L)} ,$$

with

$$z = \frac{H}{2}$$

and,

$$u_{t,1} = - \frac{HgT}{2L} \frac{\cosh [2\pi(z + d)/L]}{\cosh (2\pi d/L)} ,$$

with

$$z = - \frac{H}{2} .$$

According to second-order theory, a crest occurs at $z = \eta_{c,2} = 2.48$ feet, $\cos \theta = \cos 2\theta = 1$ and a trough at $z = \eta_{t,2} = - 1.52$ feet, $\cos \theta = - 1$, $\cos 2\theta = 1$. Equation 2-51 therefore implies

$$u_{c,2} = \frac{HgT}{2L} \frac{\cosh [2\pi(z + d)/L]}{\cosh (2\pi d/L)}$$

$$+ \frac{3}{4} \left(\frac{\pi H}{L}\right)^2 C \frac{\cosh [4\pi(z + d)/L]}{\sinh^4 (2\pi d/L)} ,$$

with

$$z = \eta_{c,2} = + 2.48 \text{ feet}$$

and,

$$u_{t,2} = - \frac{HgT}{2L} \frac{\cosh [2\pi(z + d)/L]}{\cosh (2\pi d/L)}$$

$$+ \frac{3}{4} \left(\frac{\pi H}{L}\right)^2 C \frac{\cosh [4\pi(z + d)/L]}{\sinh^4 (2\pi d/L)} ,$$

with

$$z = \eta_{t,2} = - 1.52 \text{ feet} .$$

2-43

Entering Table C-2 with d/L = 0.10, find tanh $(2\pi d/L)$ = 0.5569.

From Equation 2-3 which is true for both first- and second-order theories,

$$C^2 = \frac{gL}{2\pi} \ \tanh\left(\frac{2\pi d}{L}\right) = \frac{(32.2)\,(200)\,(0.5569)}{2\pi} = 571 \ (\text{ft/sec})^2 \ ,$$

or

$$C = 23.9 \ \text{ft/sec}.$$

As a consequence,

$$\frac{T}{L} = \frac{1}{C} = 0.0418 \ \text{sec/ft} \ .$$

Referring again to Table C-2, it is found that when

$$z = \frac{H}{2} \ ,$$

$$\cosh\left[\frac{2\pi(z+d)}{L}\right] = \cosh\,[2\pi(0.11)] = 1.249 \ ,$$

and when

$$z = -\frac{H}{2} \ ,$$

$$\cosh\left[\frac{2\pi(z+d)}{L}\right] = \cosh\,[2\pi(0.09)] = 1.164 \ .$$

Thus, the value of u at a crest and trough respectively according to first-order theory is

$$u_{c,1} = \frac{4}{2}\,(32.2)\,(0.0418)\,\frac{1.249}{1.2040} = 2.8 \ \text{ft/sec} \ ,$$

$$u_{t,1} = \frac{4}{2}\,(32.2)\,(0.0418)\,\frac{1.164}{1.2040} = -\,2.6 \ \text{ft/sec} \ .$$

2-44

Entering Table C-2 again, it is found that when

$$z = \eta_{c,2} = 2.48 \text{ feet},$$

$$\cosh\left[\frac{2\pi(z+d)}{L}\right] = \cosh\left[2\pi(0.1124)\right] = 1.260,$$

$$\cosh\left[\frac{4\pi(z+d)}{L}\right] = \cosh\left[4\pi(0.1124)\right] = 2.175.$$

When

$$z = \eta_{t,2} = -1.52 \text{ feet},$$

$$\cosh\left[\frac{2\pi(z+d)}{L}\right] = \cosh\left[2\pi(0.0924)\right] = 1.174,$$

$$\cosh\left[\frac{4\pi(z+d)}{L}\right] = \cosh\left[4\pi(0.0924)\right] = 1.753.$$

Thus, the value of u at a crest and trough respectively according to second-order theory is

$$u_{c,2} = \frac{4}{2}(32.2)(0.0418)\frac{1.260}{1.2040} + \frac{3}{4}\left(\frac{4\pi}{200}\right)^2 (23.9)\frac{2.175}{0.202} = 3.6 \text{ ft/sec},$$

$$u_{t,2} = -\frac{4}{2}(32.2)(0.0418)\frac{1.174}{1.2040} + \frac{3}{4}\left(\frac{4\pi}{200}\right)^2 (23.9)\frac{1.753}{0.202} = -2.0 \text{ ft/sec}.$$

(c) To find the horizontal distance that a particle moves during one wave period at $z = 0$, Equation 2-55 can be written as:

$$\bar{U}(z) = \frac{\Delta X(z)}{T} = \left(\frac{\pi H}{L}\right)^{2} \frac{C}{2} \frac{\cosh\left[4\pi(z+d)/L\right]}{\sinh^2(2\pi d/L)},$$

where $\Delta X(z)$ is the net horizontal distance traveled by a water particle, z feet below the surface, during one wave period.

For the example problem, when

$$z = 0 ,$$

$$\Delta X(0) = T \left(\frac{\pi H}{L}\right)^2 \frac{\cosh (4\pi d/L)}{\sinh^2 (2\pi d/L)} \cdot \frac{C}{2}$$

$$= \frac{(\pi H)^2}{2L} \frac{\cosh (4\pi d/L)}{\sinh^2 (2\pi d/L)} = \frac{(\pi 4)^2 (1.899)}{2(200) (0.6705)^2} = 1.67 \text{ ft.}$$

(d) The first-order approximation for pressure under a wave is:

$$p = \frac{\rho g H}{2} \frac{\cosh [2\pi(z + d)/L]}{\cosh (2\pi d/L)} \cos \theta - \rho g z ,$$

when

$$\theta = 0 \text{ (i.e. the wave crest), } \cos \theta = 1 ,$$

and when

$$z = - d, \cosh \left[\frac{2\pi(z + d)}{L}\right] = \cosh (0) = 1.0 .$$

Therefore

$$p = \frac{(2) (32.2) (4)}{2} \frac{1}{1.204} - (2) (32.2) (- 20) = 107 + 1288 = 1395 \text{ lbs/ft}^2 ,$$

at a depth of 20 feet below the SWL. The second-order terms according to Equation 2-56 are

$$\frac{3}{8} \rho g \frac{\pi H^2}{L} \frac{\tanh (2\pi d/L)}{\sinh^2 (2\pi d/L)} \left\{\frac{\cosh [4\pi(z + d)/L]}{\sinh^2 (2\pi d/L)} - \frac{1}{3}\right\} \cos 2\theta$$

$$- \frac{1}{8} \rho g \frac{\pi H^2}{L} \frac{\tanh (2\pi d/L)}{\sinh^2 (2\pi d/L)} \left\{\cosh \frac{4\pi(z + d)}{L} - 1\right\} .$$

Substituting in the equation:

$$\frac{3}{8} (2) (32.2) \frac{\pi (4)^2}{200} \frac{(0.5569)}{(0.6705)^2} \left[\frac{1}{(0.6705)^2} - \frac{1}{3}\right] (1)$$

$$- \frac{1}{8} (2) (32.2) \frac{\pi (4)^2}{200} \frac{(0.5569)}{(0.6705)^2} (0) = 14 \text{ lbs/ft}^2 .$$

2-46

Thus, second-order theory predicts a pressure,

$$p = 1395 + 14 = 1409 \text{ lbs/ft}^2 .$$

(e) Using Equation 2-38, the energy in one wavelength per unit width of crest given by the first-order theory is:

$$E = \frac{\rho g H^2 L}{8} = \frac{(2)(32.2)(4)^2(200)}{8} = 25,800 \frac{\text{ft-lbs}}{\text{ft}} .$$

Evaluation of the hydrostatic pressure component (1288 lbs/ft^2) indicates that Airy theory gives a dynamic component of 107 lbs/ft^2 while Stokes theory gives 121 lbs/ft^2. Stokes theory shows a dynamic pressure component about 13 percent greater than Airy theory.

* *

2.26 CNOIDAL WAVES

Long, finite-amplitude waves of permanent form propagating in shallow water are frequently best described by *cnoidal* wave theory. The existence in shallow water of such long waves of permanent form may have first been recognized by Boussinesq (1877). However, the theory was originally developed by Korteweg and DeVries (1895). The term *cnoidal* is used since the wave profile is given by the Jacobian elliptical cosine function usually designated cn .

In recent years, cnoidal waves have been studied by many investigators. Wiegel (1960) summarized much of the existing work on cnoidal waves, and presented the principal results of Korteweg and DeVries (1895) and Keulegan and Patterson (1940) in a more usable form. Masch and Wiegel (1961) presented such wave characteristics as length, celerity and period in tabular and graphical form, to facilitate application of cnoidal theory.

The approximate range of validity for the cnoidal wave theory as determined by Laitone (1963) and others is d/L < 1/8, and the Ursell parameter, $L^2 H/d^3 > 26$. (See Figure 2-7.) As wavelength becomes long, and approaches infinity, cnoidal wave theory reduces to the solitary wave theory which is described in the next section. Also, as the ratio of wave height to water depth becomes small (infinitesimal wave height), the wave profile approaches the sinusoidal profile predicted by the linear theory.

Description of local particle velocities, local particle accelerations, wave energy, and wave power for cnoidal waves is difficult; hence their description is not included here, but can be obtained in graphical form from Wiegel (1960, 1964) and Masch (1964).

Wave characteristics are described in parametric form in terms of the modulus k of the elliptic integrals. While k itself has no physical

significance, it is used to express the relationships between the various wave parameters. Tabular presentations of the elliptic integrals and other important functions can be obtained from the above references. The ordinate of the water surface y_s measured above the bottom is given by

$$y_s = y_t + H \, cn^2 \left[2K(k) \left(\frac{x}{L} - \frac{t}{T} \right), k \right],$$ (2-59a)

where y_t is the distance from the bottom to the wave trough, cn is the elliptic cosine function, $K(k)$ is the complete elliptic integral of the first kind, and k is the modulus of the elliptic integrals. The argument of cn^2 is frequently denoted simply by ( ), thus, Equation 2-59a above can be written as

$$y_s = y_t + H \, cn^2 \, ( ) .$$ (2-59b)

The elliptic cosine is a periodic function where $cn^2[2K(k) ((x/L) - (t/T))]$ has a maximum amplitude equal to unity. The modulus k is defined over the range between 0 and 1. When $k = 0$, the wave profile becomes a sinusoid as in the linear theory, and when $k = 1$, the wave profile becomes that of a solitary wave.

The distance from the bottom to the wave trough, y_t, as used in Equations 2-59a and b, is given by

$$\frac{y_t}{d} = \frac{y_c}{d} - \frac{H}{d} = \frac{16d^2}{3L^2} K(k) [K(k) - E(k)] + 1 - \frac{H}{d},$$ (2-60)

where y_c is the distance from the bottom to the crest and $E(k)$ is the complete elliptic integral of the second kind. Wavelength is given by

$$L = \sqrt{\frac{16d^3}{3H}} \, kK(k),$$ (2-61)

and wave period by

$$T \sqrt{\frac{g}{d}} = \sqrt{\frac{16y_t}{3H}} \frac{d}{y_t} \left[\frac{kK(k)}{1 + \dfrac{H}{y_t k^2} \left(\dfrac{1}{2} - \dfrac{E(k)}{K(k)} \right)} \right]$$ (2-62)

Cnoidal waves are periodic and of permanent form thus $L = CT$.

Pressure under a cnoidal wave at any elevation y, above the bottom depends on the local fluid velocity, and is therefore complex. However, it may be approximated in a hydrostatic form as

$$p = \rho g (y_s - y),$$ (2-63)

2-48

that is, the pressure distribution may be assumed to vary linearly from $\rho g y_s$ at the bed to zero at the surface.

Figures 2-9 and 2-10 show the dimensionless cnoidal wave surface profiles for various values of the square of the modulus of the elliptic integrals k^2, while Figures 2-11 through 2-15 present dimensionless plots of the parameters which characterize cnoidal waves. The ordinates of Figures 2-11 and 2-12 should be read with care, since values of k^2 are extremely close to 1.0 ($k^2 = 1-10^{-1} = 1-0.1 = 0.99$). It is the exponent α of $k^2 = 1-10^{-\alpha}$ that varies along the vertical axis of Figures 2-11 and 2-12.

Ideally, shoaling computations might best be performed using cnoidal wave theory since this theory best describes wave motion in relatively shallow (or shoaling) water. Simple, completely satisfactory procedures for applying cnoidal wave theory are not available. Although linear wave theory is often used, cnoidal theory may be applied by using figures such as 2-9 through 2-15.

The following problem will illustrate the use of these figures.

* * * * * * * * * * * * * * *   EXAMPLE PROBLEM   * * * * * * * * * * * * * * * *

GIVEN: A wave traveling in water depth of d = 10 feet, with a period of T = 15 seconds, and a height of H = 2.5 feet.

FIND:

(a) Using cnoidal wave theory, find the wavelength L and compare this length with the length determined using Airy theory.

(b) Determine the celerity C. Compare this celerity with the celerity determined using Airy theory.

(c) Determine the distance above the bottom of the wave crest (y_c) and wave trough (y_t).

(d) Determine the wave profile.

SOLUTION:

(a) Calculate

$$\frac{H}{d} = \frac{2.5}{10} = 0.25$$

and

$$T \sqrt{\frac{g}{d}} = 15 \sqrt{\frac{32.2}{10}} = 26.92$$

2-49
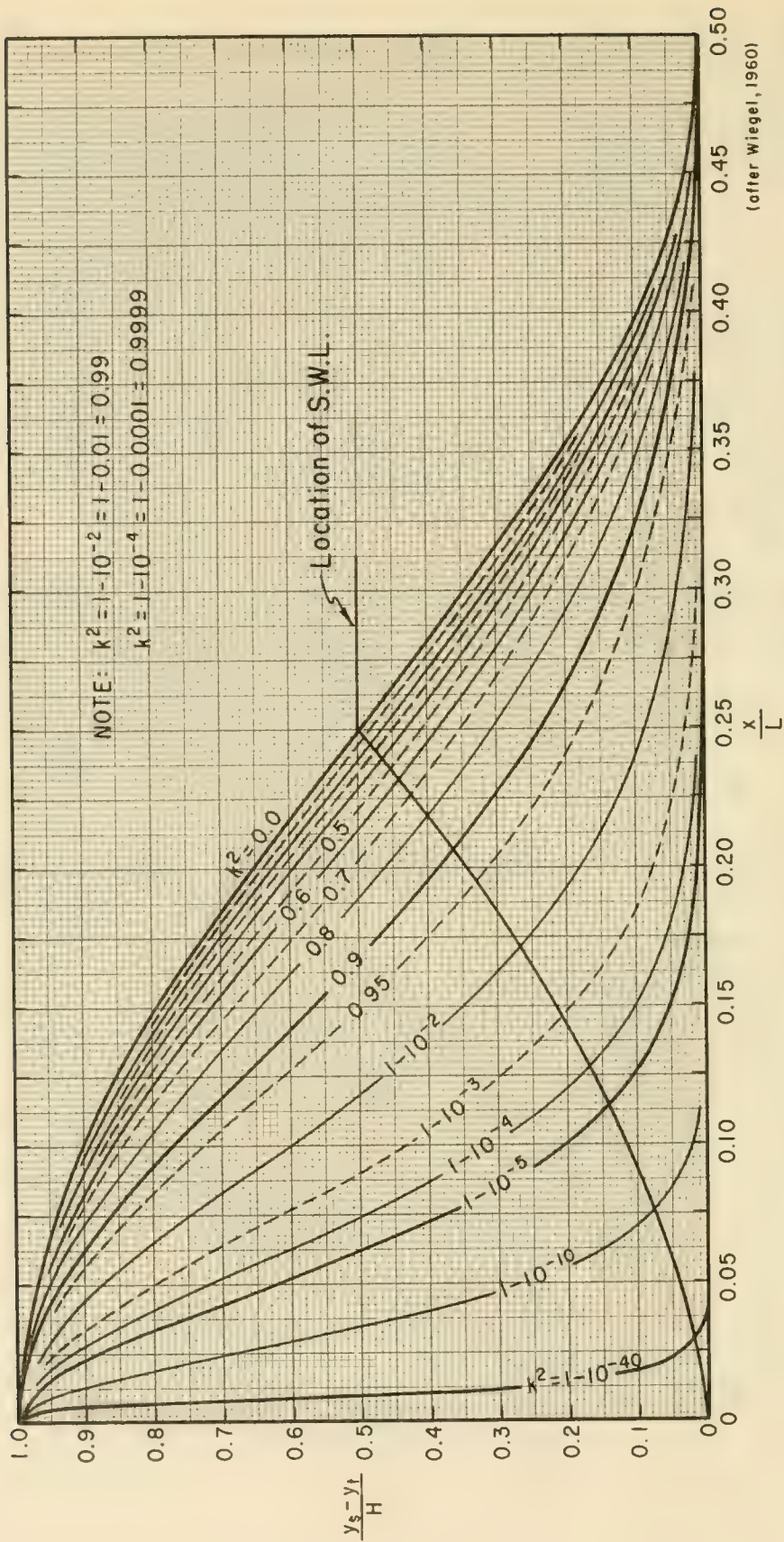
Figure 2-9. Cnoidal Wave Surface Profiles as a Function of k^2

(after Wiegel, 1960)

NOTE: $k^2 = 1 - 10^{-2} = 1 - 0.01 = 0.99$
$k^2 = 1 - 10^{-4} = 1 - 0.0001 = 0.9999$

Location of S.W.L.

$k^2 = 0.0$
0.6 0.5
0.7
0.8
0.9
0.95
$1 - 10^{-2}$
$1 - 10^{-3}$
$1 - 10^{-4}$
$1 - 10^{-5}$
$1 - 10^{-10}$
$k^2 = 1 - 10^{-40}$

$\dfrac{x}{L}$

$\dfrac{y_s - y_t}{H}$
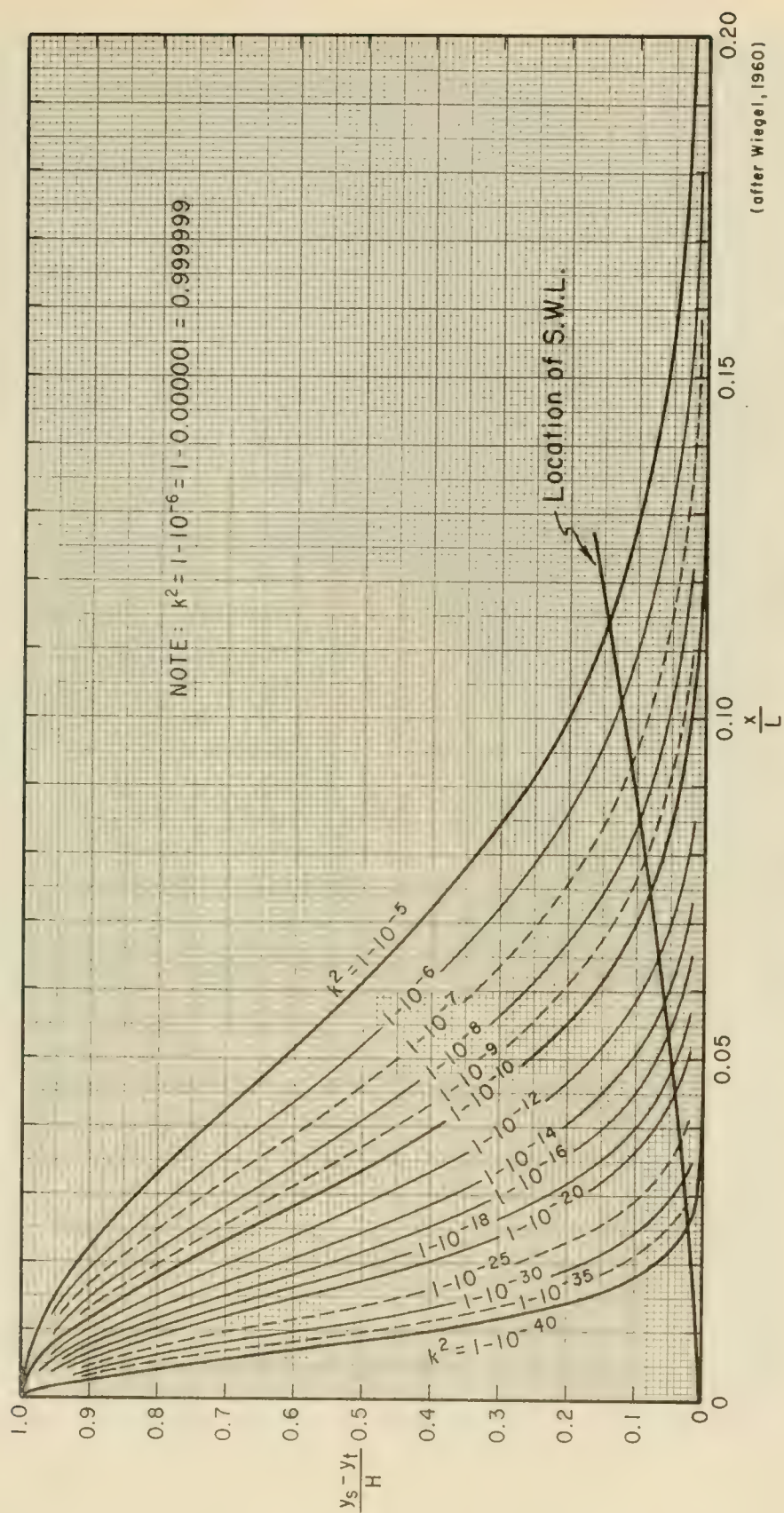
Figure 2-10. Cnoidal Wave Surface Profiles as a Function of k^2
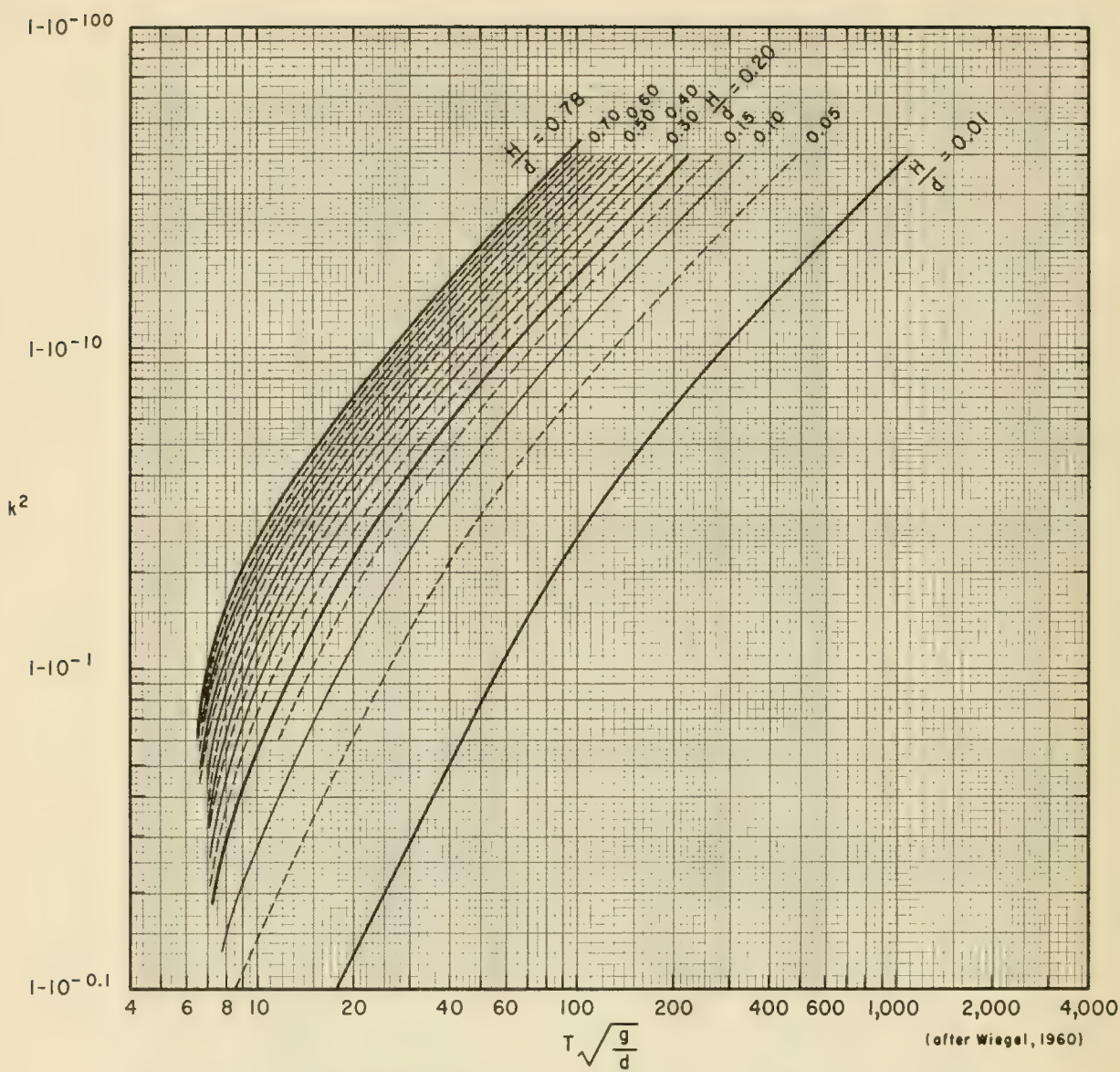
(after Wiegel, 1960)

Figure 2-11. Relationship Between k^2, H/d and $T\sqrt{g/d}$
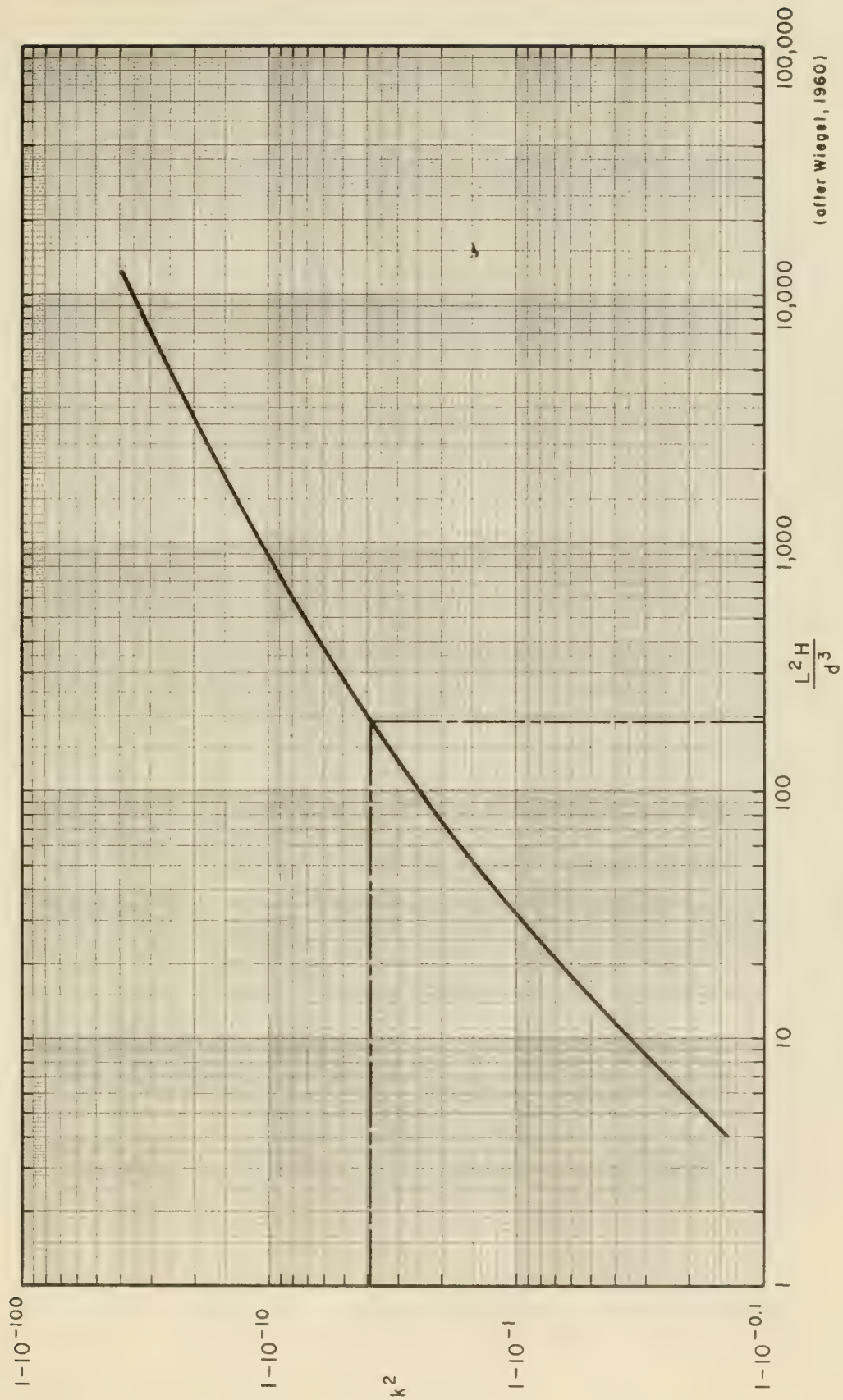
Figure 2-12. Relationships Between k^2 and $L^2 H/d^3$

(after Wiegel, 1960)

2-53
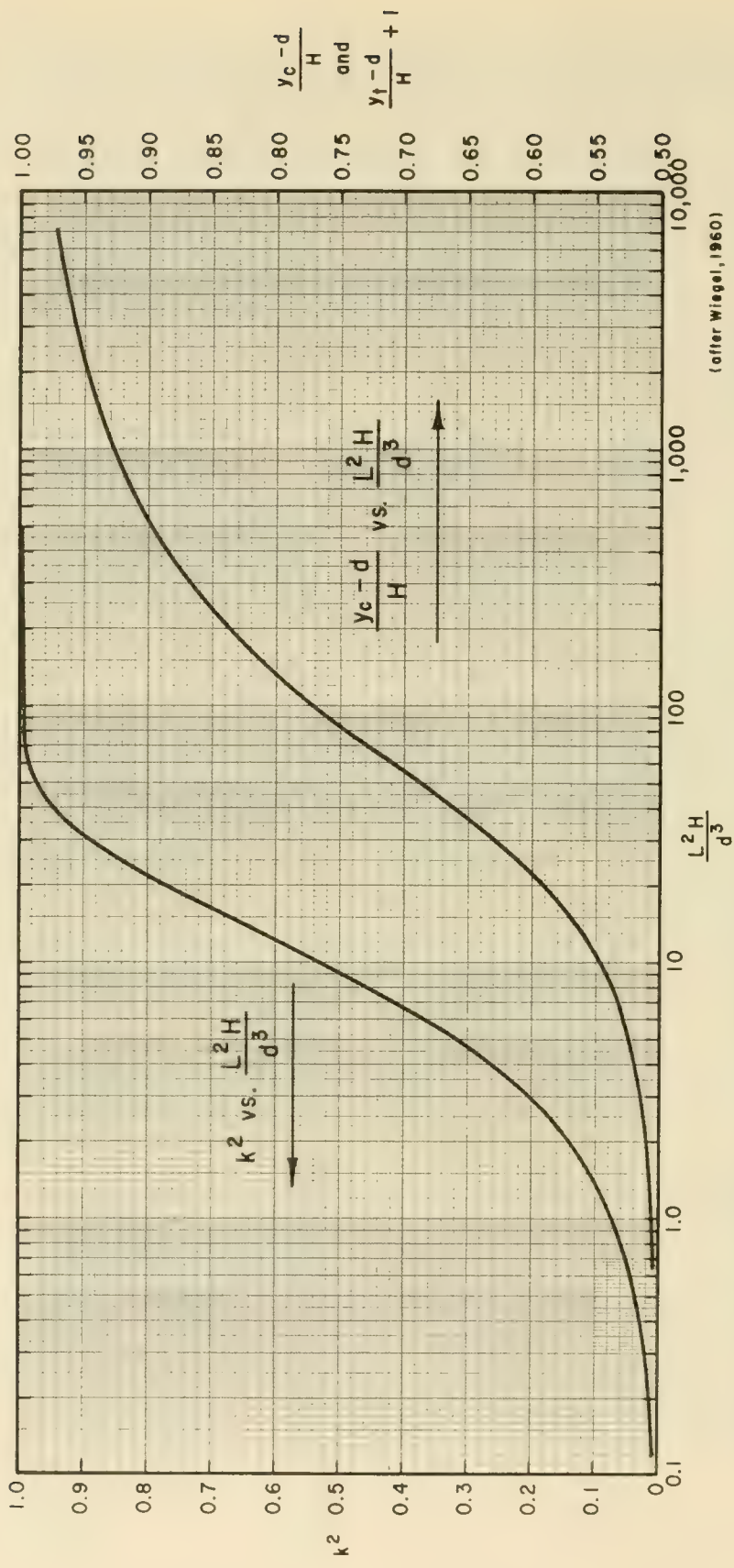
Figure 2-13. Relationships Between k^2 and L^2H/d^3 and Between $(y_c-d)/H$, $(y_t-d)/H+1$ and L^2H/d^3
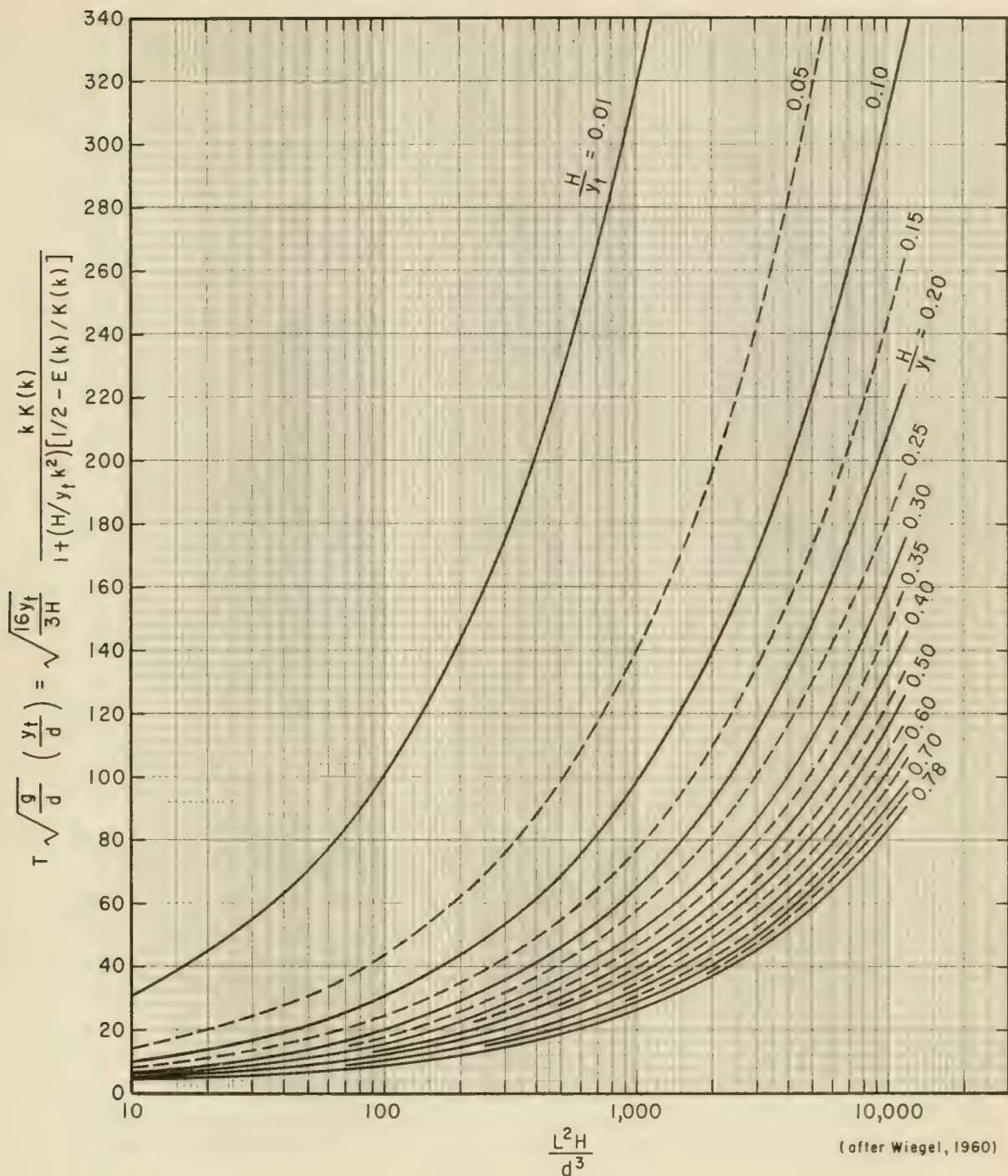
Figure 2-14. Relationship Between $T\sqrt{g/d}\ y_t/d$, H/y_t and L^2H/d^3

2-55
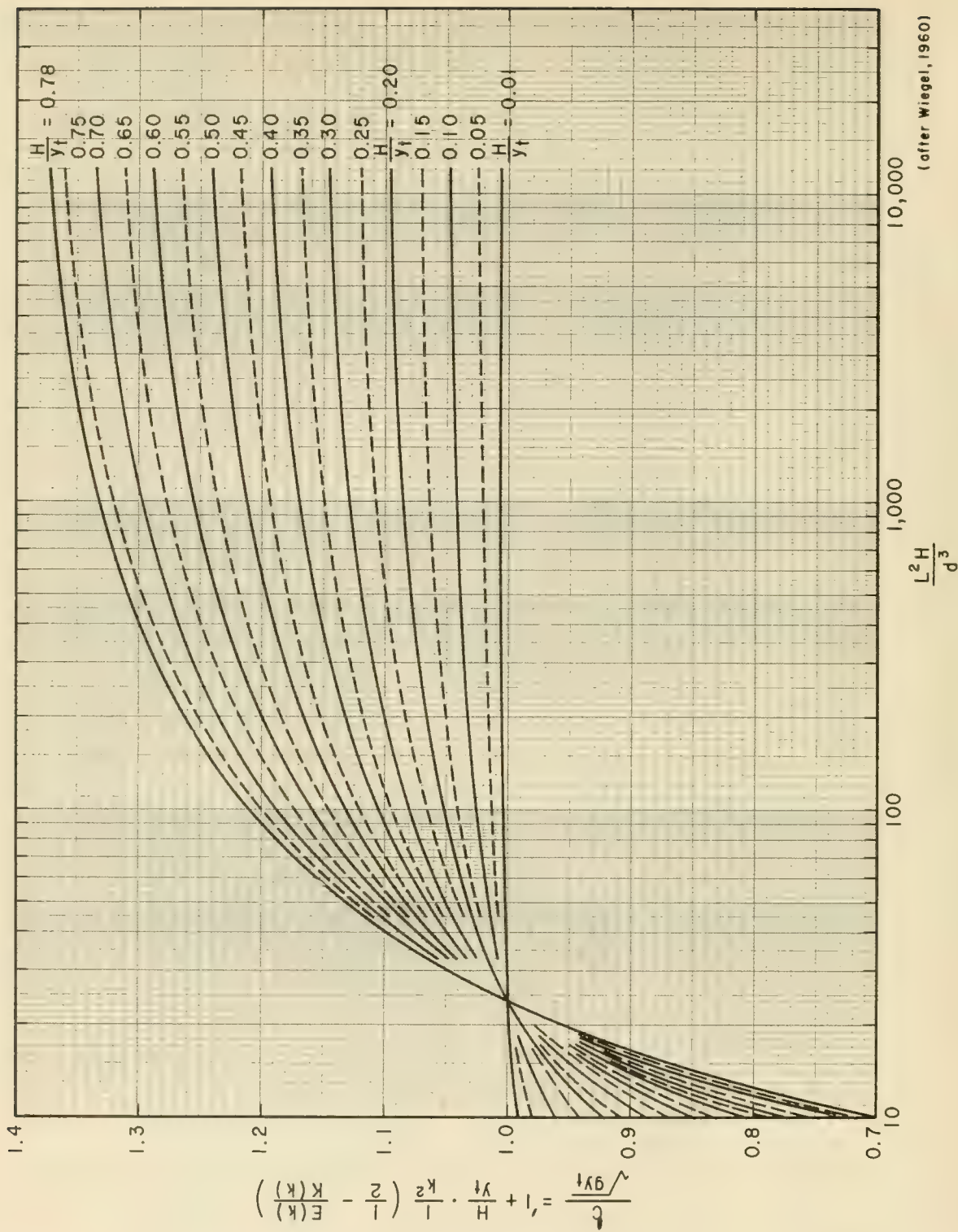
Figure 2-15. Relationship Between $C/\sqrt{gy_t}$, H/y_t and L^2H/d^3

(after Wiegel, 1960)

2-56

From Figure 2-11, entering with H/d and $T\sqrt{g/d}$, determine the square of the modulus of the complete elliptical integrals, k^2.

$$k^2 = 1 - 10^{-3.95}.$$

Entering Figure 2-12 with the value of k^2 gives

$$\frac{L^2 H}{d^3} = 190.$$

or

$$L = \sqrt{\frac{190\,d^3}{H}} = \sqrt{\frac{190(10)^3}{2.5}}$$

$$L = 275.7 \text{ ft.}$$

From Airy theory,

$$L = \frac{gT^2}{2\pi}\, \tanh\left(\frac{2\pi d}{L}\right) = 266.6 \text{ ft.}$$

To check whether the wave conditions are in the range for which cnoidal wave theory is valid, calculate d/L and the Ursell parameter, L^2H/d^3.

$$\frac{d}{L} = \frac{10}{275.7} = 0.0363 < \frac{1}{8} \text{ O.K.}$$

$$\frac{L^2 H}{d^3} = \frac{1}{(d/L)^2}\left(\frac{H}{d}\right) = 190 > 26 \text{ O.K.}$$

Therefore, cnoidal theory is applicable.

(b) Wave celerity is given by

$$C = \frac{L}{T} = \frac{275.7}{15} = 18.38 \text{ ft/sec},$$

while the Airy theory predicts

$$C = \frac{L}{T} = \frac{266.6}{15} = 17.77 \text{ ft/sec.}$$

Thus if it is assumed that the wave period is the same for Cnoidal and Airy theories then

$$\frac{C_{Cnoidal}}{C_{Airy}} = \frac{L_{Cnoidal}}{L_{Airy}} \approx 1.$$

2-57

(c) The percentage of the wave height above the SWL may be determined from Figure 2-13. Entering the figure with $L^2H/d^3 = 190$, the value of $(y_c - d)/H$ is found to be 0.833 or 83.3 percent. Therefore,

$$y_c = 0.833\,H + d.$$

$$y_c = 0.833\,(2.5) + 10 = 2.083 + 10 = 12.083 \text{ feet}.$$

Also from Figure 2-13,

$$\frac{(y_t - d)}{H} + 1 = 0.833,$$

thus

$$y_t = (0.833 - 1)\,(2.5) + 10 = 9.583 \text{ ft.}$$

(d) The dimensionless wave profile is given on Figure 2-9 and is approximately the one drawn for $k^2 = 1 - 10^{-4}$. The results obtained in (c) above can also be checked by using Figure 2-9. For the wave profile obtained with $k^2 = 1 - 10^{-4}$, it is seen that the SWL is approximately 0.17 H above the wave trough or 0.83 H below the wave crest.

The results for the wave celerity determined under (b) above can now be checked with the aid of Figure 2-15. Calculate

$$\frac{H}{y_t} = \frac{2.5}{9.583} = 0.261.$$

Entering Figure 2-15 with

$$\frac{L^2H}{d^3} = 190,$$

and

$$\frac{H}{y_t} = 0.261,$$

it is found that

$$\frac{C}{\sqrt{gy_t}} = 1.083.$$

Therefore

$$C = 1.083\,\sqrt{(32.2)\,(9.583)} = 19 \text{ ft/sec}.$$

2-58

The difference between this number and the 18.38 ft/sec calculated under (b)   above is the result of small errors in reading the curves.

* *

2.27 SOLITARY WAVE THEORY

Waves considered in the previous sections were oscillatory or nearly oscillatory waves. The water particles move backward and forward with the passage of each wave, and a distinct wave crest and wave trough are evident. A solitary wave is neither oscillatory nor does it exhibit a trough. In the pure sense, the solitary wave form lies entirely above the stillwater level. The solitary wave is a wave of translation relative to the water mass.

Russell (1838, 1845) first recognized the existence of a solitary wave. The original theoretical developments were made by Boussinesq (1872), Lord Rayleigh (1876), and McCowan (1891), and more recently by Keulegan and Patterson (1940), Keulegan (1948), and Iwasa (1955).

In nature it is difficult to form a truly solitary wave, because at the trailing edge of the wave there are usually small dispersive waves. However, long waves such as tsunamis and waves resulting from large dis-placements of water caused by such phenomena as landslides, and earthquakes sometimes behave approximately like solitary waves. When an oscillatory wave moves into shallow water, it may often be approximated by a solitary wave, (Munk, 1949). As an oscillatory wave moves into shoaling water, the wave amplitude becomes progressively higher; the crests become shorter and more pointed, and the trough becomes longer and flatter.

The solitary wave is a limiting case of the cnoidal wave. When $k^2 = 1$, $K(k) = K(1) = \infty$, and the elliptic cosine reduces to the hyperbolic secant function, $y_t = d$, and Equation 2-59 reduces to

$$y_s = d + H \operatorname{sech}^2 \left[\sqrt{\frac{3}{4} \frac{H}{d^3}} \ (x - Ct) \right],$$

or

$$\eta = H \operatorname{sech}^2 \left[\sqrt{\frac{3}{4} \frac{H}{d^3}} \ (x - Ct) \right]. \tag{2-64}$$

where the origin of x is at the wave crest. The volume of water within the wave above the still water level per unit crest width is

$$V = \left[\frac{16}{3} d^3 H \right]^{\frac{1}{2}}. \tag{2-65}$$

2-59

An equal amount of water per unit crest length is transported forward past a vertical plane that is perpendicular to the direction of wave advance. Several relations have been presented to determine the celerity of a solitary wave; these equations differ depending on the degree of approximation. Laboratory measurements by Daily and Stephan (1953) indicate that the simple expression

$$C = \sqrt{g(H+d)} \, ,$$ (2-66)

gives a reasonably accurate approximation to the celerity.

The water particle velocities for a solitary wave, as found by McCowan (1891) and given by Munk (1949), are

$$u = CN \, \frac{1 + \cos(My/d) \, \cosh(Mx/d)}{[\cos(My/d) + \cosh(Mx/d)]^2} \, ,$$ (2-67)

$$w = CN \, \frac{\sin(My/d) \, \sinh(Mx/d)}{[\cos(My/d) + \cosh(Mx/d)]^2} \, ,$$ (2-68)

where M and N are the functions of H/d shown on Figure 2-16, and y is measured from the bottom. The expression for horizontal velocity u, is often used to predict wave forces on marine structures sited in shallow water. The maximum velocity u_{max}, occurs when x and t are both equal to zero; hence,

$$u_{max} = \frac{CN}{1 + \cos(My/d)} \, .$$ (2-69)

Total energy in a solitary wave is about evenly divided between kinetic and potential energy. Total wave energy per unit crest width is,

$$E = \frac{8}{3\sqrt{3}} \, \rho g \, H^{3/2} \, d^{3/2} \, ,$$ (2-70)

and the pressure beneath a solitary wave depends upon the local fluid velocity as does the pressure under a cnoidal wave; however, it may be approximated by

$$p = \rho g \, (y_s - y) \, .$$ (2-71)

Equation 2-71 is identical to that used to approximate the pressure beneath a cnoidal wave.

As a solitary wave moves into shoaling water it eventually becomes unstable and breaks. McCowan (1891) assumed that a solitary wave breaks
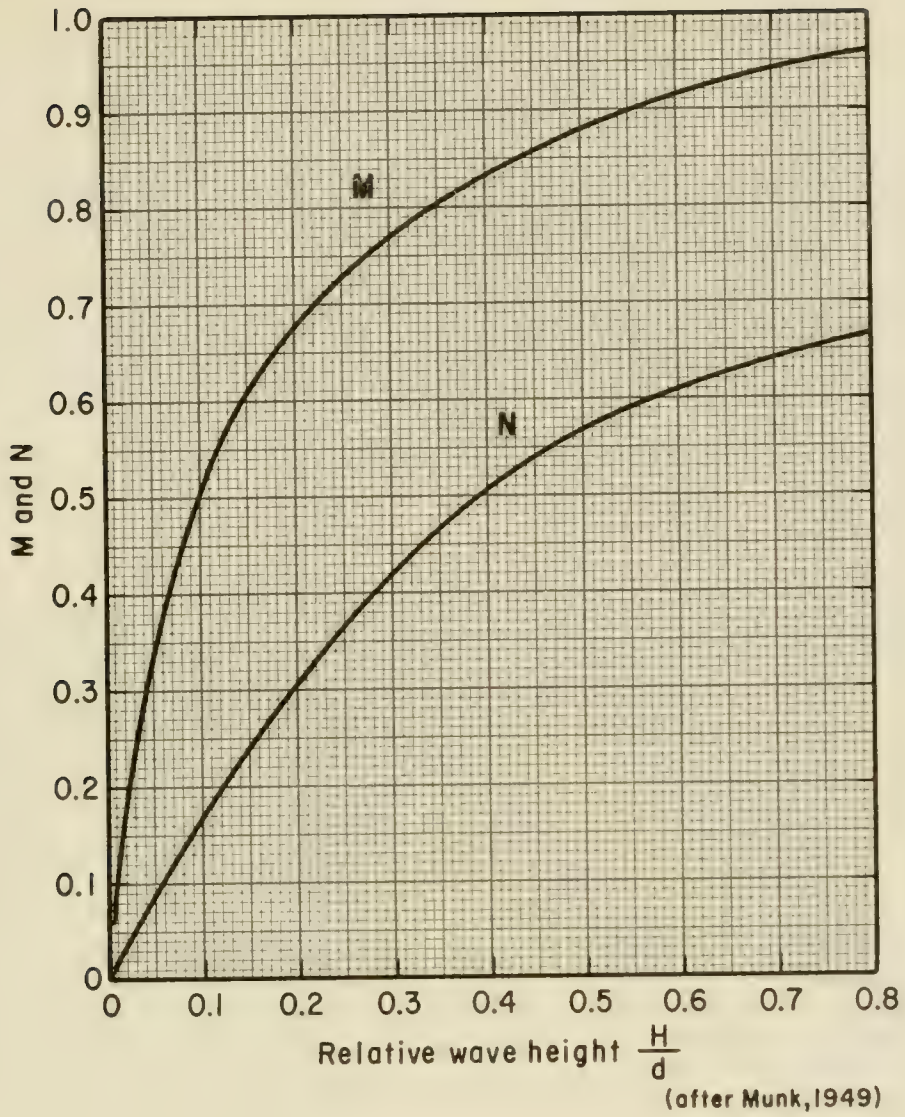
Figure 2-16. Functions M and N in Solitary Wave Theory

2-61

when the water particle velocity at the wave crest becomes equal to the wave celerity. This occurs when

$$\left(\frac{H}{d}\right)_{max} = 0.78 \, . \tag{2-72}$$

Laboratory investigations have shown that the value of $(H/d)_{max} = 0.78$ agrees better with observations for oscillatory waves than for solitary waves. Ippen and Kulin (1954) and Galvin (1969) have shown that the near-shore slope has a substantial effect on this ratio. Other factors such as bottom roughness may also be involved. For slopes of 0.0, 0.05, 0.10, and 0.20, Galvin found that H/d ratios were approximately equal to 0.83, 1.05, 1.19, and 1.32, respectively. Thus, it must be concluded that for some conditions, Equation 2-72 is unsatisfactory for predicting breaking depth. Further discussion of the breaking of waves with experimental results is in Section 2.6 - BREAKING WAVES.

2.28 STREAM FUNCTION WAVE THEORY

In recent years, numerical approximations to solutions of hydrodynamic equations describing wave motion have been proposed and developed by Dean (1965a, 1965b, 1967) and Monkmeyer (1970). The approach by Dean, termed a symmetric, stream function theory, is a nonlinear wave theory which is similar to higher order Stokes' theories. Both are constructed of sums of sine or cosine functions that satisfy the original differential equation (Laplace equation). The theory, however, determines the coefficient of each higher order term so that a best fit, in the least-squares sense, is obtained to the theoretically posed, dynamic, free-surface boundary condition. Assumptions made in the theory are identical to those made in the development of the higher-order Stokes' solutions. Consequently, some of the same limitations are inherent in the stream function theory; however, it represents a better solution to the equations used to approximate the wave phenomena. More important is that the stream function representation appears to better predict some of the wave phenomena observed in laboratory wave studies (Dean and LéMehauté, 1970), and may possibly describe naturally occurring wave phenomena better than other theories.

The long tedious computations involved in evaluating the terms of the series expansions that make up the higher-order stream function solutions, make it desirable to use tabular or graphical presentations of the solutions. These tables, their use and range of validity have been developed by Dean (1973).

2.3 WAVE REFRACTION

2.31 INTRODUCTION

Equation 2-2 shows that wave celerity depends on the depth of water in which the wave propagates. If the wave celerity decreases with depth, wavelength must decrease proportionally. Variation in wave velocity occurs

along the crest of a wave moving at an angle to underwater contours because that part of the wave in deeper water is moving faster than the part in shallower water. This variation causes the wave crest to bend toward alignment with the contours. (See Figure 2-17.) This bending effect, called **refraction**, depends on the relation of water depth to wavelength. It is analogous to refraction for other types of waves such as, light and sound.

In practice, refraction is important for several reasons such as:

(1) Refraction, coupled with shoaling, determines the wave height in any particular water depth for a given set of incident deepwater wave conditions, that is wave height, period, and direction of propagation in deep water. Refraction therefore has significant influence on the wave height and distribution of wave energy along a coast.

(2) The change of wave direction of different parts of the wave results in convergence or divergence of wave energy, and materially affects the forces exerted by waves on structures.

(3) Refraction contributes to the alteration of bottom topography by its effects on the erosion and deposition of beach sediments. Munk and Traylor (1947) confirmed earlier work by many indicating the possible interrelationships between refraction, wave energy distribution along a shore, and the erosion and deposition of beach materials.

(4) A general description of the nearshore bathymetry of an area can sometimes be obtained by analyzing aerial photography of wave refraction patterns. While the techniques for performing such analyses are not well developed, an experienced observer can obtain a general picture of simple bottom topography.

In addition to refraction caused by variations in bathymetry, waves may be refracted by currents, or any other phenomenon which causes one part of a wave to travel slower or faster than another part. At a coastal inlet, refraction may be caused by a gradient in the current. Refraction by a current occurs when waves intersect the current at an angle. The extent to which the current will refract incident waves depends on the initial angle between the wave crests and the direction of current flow, the characteristics of the incident waves, and the strength of the current. In at least two situations, wave refraction by currents may be of practical importance. At tidal entrances, ebb currents run counter to incident waves and consequently increase wave height and steepness. Also, major ocean currents such as the Gulf Stream may have some effect on the height, length and direction of approach of waves reaching the coasts. Quantitative evaluation of the effects of refraction by currents is difficult. Additional research is needed in this area. No detailed discussion of this problem will be presented here, but an introduction is presented by Johnson (1947).

The decrease in wave celerity with decreasing water depth can be considered an analog to the decrease in the speed of light with an increase in
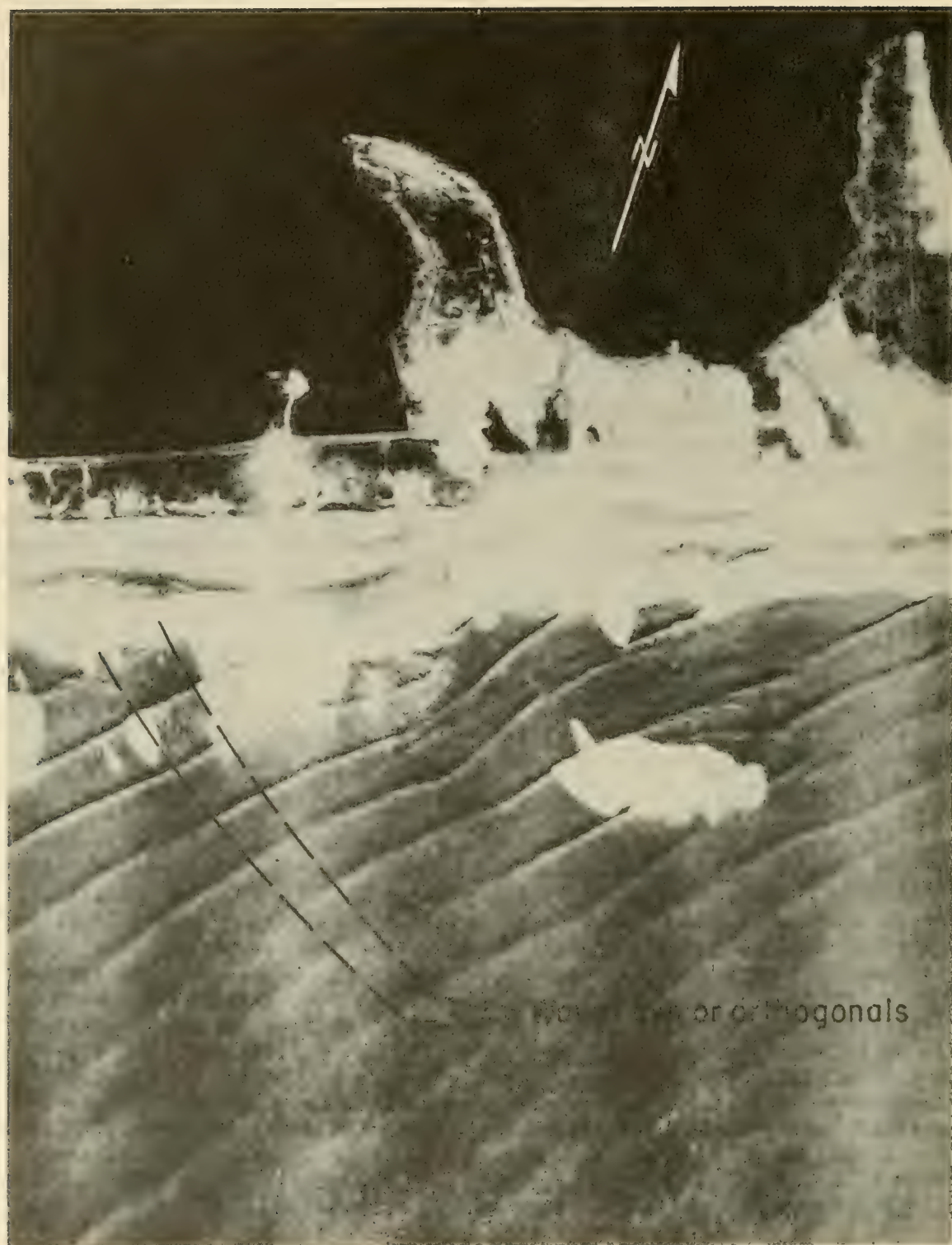
Figure 2-17. Wave Refraction at Westhampton Beach, Long Island, New York

the refractive index of the transmitting medium. Using this analogy, O'Brien (1942) suggested the use of Snell's law of geometrical optics for solving the problem of water-wave refraction by changes in depth. The validity of this approach has been verified experimentally by Chien (1954), Ralls (1956), and Wiegel and Arnold (1957). Chao (1970) showed analytically that Fermat's principle and hence Snell's law followed from the governing hydrodynamic equations, and was a valid approximation when applied to the refraction problem. Generally, two basic techniques of refraction analysis are available - graphical and numerical. Several graphical procedures are available, but fundamentally all methods of refraction analyses are based on Snell's law.

The assumptions usually made are:

(1) Wave energy between wave rays or orthogonals remains constant. (Orthogonals are lines drawn perpendicular to the wave crests, and extend in the direction of wave advance.) (See Figure 2-17.)

(2) Direction of wave advance is perpendicular to the wave crest, that is, in the direction of the orthogonals.

(3) Speed of a wave of given period at a particular location depends only on the depth at that location.

(4) Changes in bottom topography are gradual.

(5) Waves are long-crested, constant-period, small-amplitude, and monochromatic.

(6) Effects of currents, winds, and reflections from beaches, and underwater topographic variations, are considered negligible.

2.32 GENERAL - REFRACTION BY BATHYMETRY

In water deeper than one-half the wavelength, the hyperbolic tangent function in the formula

$$C^2 = \frac{gL}{2\pi} \tanh\left(\frac{2\pi d}{L}\right) \tag{2-2}$$

is nearly equal to unity, and Equation 2-2 reduces to

$$C_o^2 = \frac{gL}{2\pi}$$

In this equation, the velocity C_o, does not depend on depth; therefore in those regions deeper than one-half the wavelength (deep water), refraction by bathymetry will not be significant. Where the water depth is between 1/2 and 1/25 the wavelength (transitional water), and in the region where the water depth is less than 1/25 the wavelength (shallow water), refraction effects may be significant. In transitional water, wave velocity

must be computed from Equation 2-2; in shallow water, $\tanh(2\pi d/L)$ becomes nearly equal to $2\pi d/L$ and Equation 2-2 reduces to Equation 2-9.

$$C^2 = gd \quad \text{or} \quad C = (gd)^{1/2} . \tag{2-9}$$

Both Equations 2-2 and 2-9 show the dependence of wave velocity on depth. To a first approximation, the total energy in a wave per unit crest width may be written as

$$E = \frac{\rho g H^2 L}{8} . \tag{2-38}$$

It has been noted that not all of the wave energy E is transmitted forward with the wave; only one-half is transmitted forward in deep water. The amount of energy transmitted forward for a given wave remains nearly constant as the wave moves from deep water to the breaker line if energy dissipation due to bottom friction ($K_f = 1.0$), percolation and reflected wave energy is negligible.

In refraction analyses, it is assumed that for a wave advancing toward shore, no energy flows laterally along a wave crest; that is the transmitted energy remains constant between orthogonals. In deep water the wave energy transmitted forward across a plane between two adjacent orthogonals (the average energy flux) is

$$\bar{P}_o = \frac{1}{2} b_o \bar{E}_o C_o , \tag{2-73}$$

where b_o is the distance between the selected orthogonals in deep water. The subscript o always refers to deepwater conditions. This power may be equated to the energy transmitted forward between the same two orthogonals in shallow water

$$\bar{P} = n b \bar{E} C , \tag{2-74}$$

where b is the spacing between the orthogonals in the shallower water. Therefore, $(1/2) b_o \bar{E}_o C_o = nb \bar{E} C$, or

$$\frac{\bar{E}}{\bar{E}_o} = \frac{1}{2} \left(\frac{1}{n}\right)\left(\frac{b_o}{b}\right)\left(\frac{C_o}{C}\right). \tag{2-75}$$

From Equation 2-39,

$$\frac{H}{H_o} = \sqrt{\frac{\bar{E}}{\bar{E}_o}} . \tag{2-76}$$

2-66

and combining Equations 2-75 and 2-76,

$$\frac{H}{H_o} = \sqrt{\left(\frac{1}{2}\right)\left(\frac{1}{n}\right)\left(\frac{C_o}{C}\right)}\sqrt{\frac{b_o}{b}} \tag{2-77}$$

The term $\sqrt{(1/2)\ (1/n)\ (C_o/C)}$ is known as the *shoaling coefficient* K_S or H/H_o'. This shoaling coefficient is a function of wavelength and water depth. K_S and various other functions of d/L, such as $2\pi d/L$, $4\pi d/L$, $\tanh(2\pi d/L)$, and $\sinh(4\pi d/L)$ are tabulated in Appendix C, (Table C-1 for even increments of d/L_O, and Table C-2 for even increments of d/L).

Equation 2-77 enables determination of wave heights in transitional or shallow water, knowing the deepwater wave height when the relative spacing between orthogonals can be determined. The square root of this relative spacing, $\sqrt{b_o/b}$, is the *refraction coefficient* K_R.

Various methods may be used for constructing refraction diagrams. The earliest approaches required the drawing of successive wave crests. Later approaches permitted the immediate construction of orthogonals, and also permitted moving from the shore to deep water (Johnson, O'Brien and Isaacs, 1948), (Arthur, et al., 1952), (Kaplan, 1952) and (Saville and Kaplan, 1952).

The change of direction of an orthogonal as it passes over relatively simple hydrography may be approximated by

$$\sin \alpha_2 = \left(\frac{C_2}{C_1}\right) \sin \alpha_1 \quad \text{(Snell's law)} \tag{2-78}$$

where:

α_1 is the angle a wave crest (the perpendicular to an orthogonal) makes with the bottom contour over which the wave is passing,

α_2 is a similar angle measured as the wave crest (or orthogonal) passes over the next bottom contour,

C_1 is the wave velocity (Equation 2-2) at the depth of the first contour, and

C_2 is the wave velocity at the depth of the second contour.

From this equation, a template may be constructed which will show the angular change in α that occurs as an orthogonal passes over a particular contour interval, and construct changed-direction orthogonal. Such a template is shown in Figure 2-18. In application to wave refraction problems, it is simplest to construct this template on a transparent material.

2-67
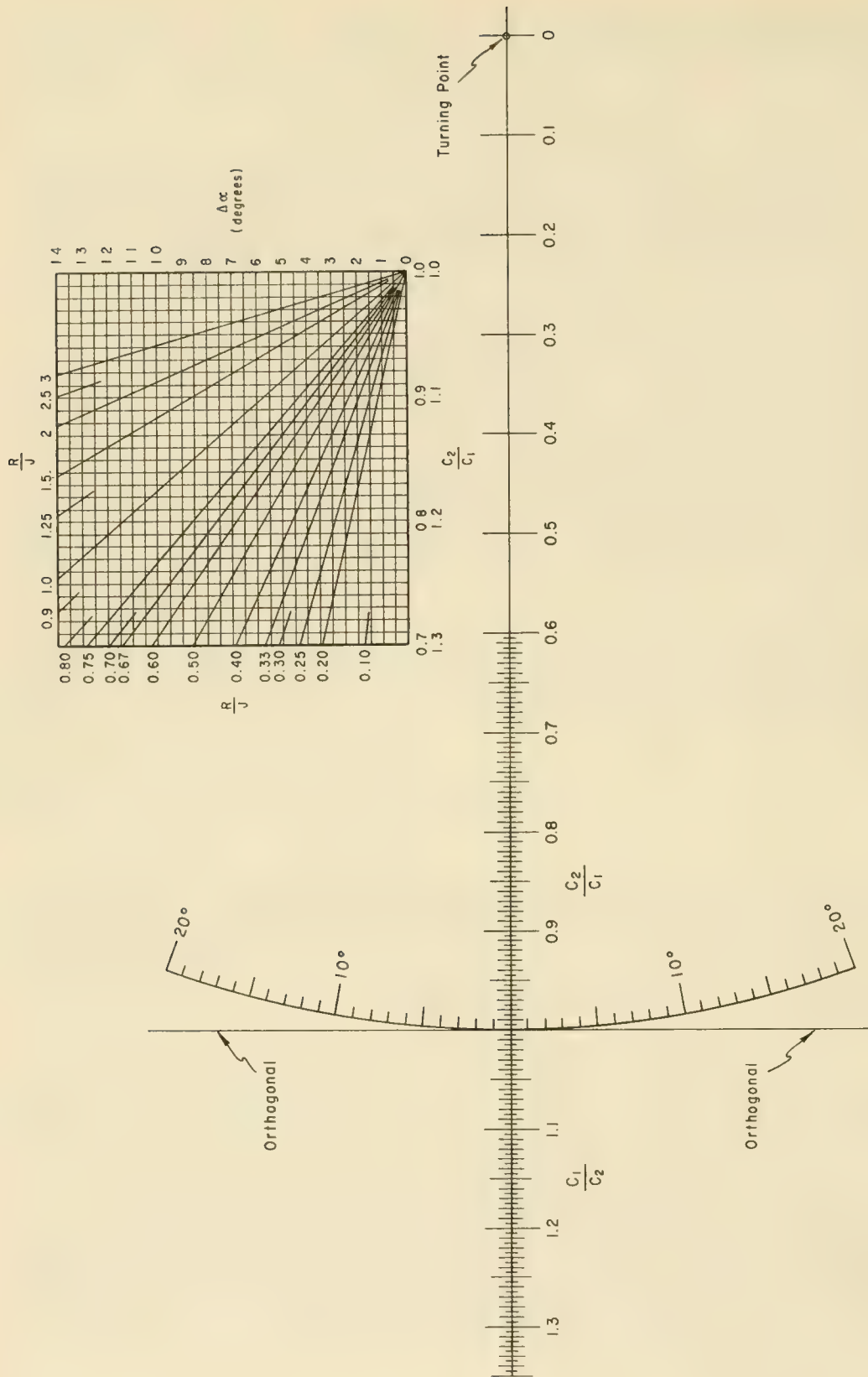
Figure 2-18. Refraction Template

2-68

Refraction may be treated analytically at a straight shoreline with parallel offshore contours, by using Snell's law directly:

$$\sin \alpha = \left(\frac{C}{C_o}\right) \sin \alpha_o \qquad (2\text{-}78a)$$

where α is the angle between the wave crest and the shoreline, and α_O is the angle between the deepwater wave crest and the shoreline.

For example, if $\alpha_O = 30^o$ and the period and depth of the wave are such that $C/C_O = 0.5$, then

$$\alpha = \sin^{-1} [0.5\,(0.5)] = 14.5 \text{ degrees}$$

$$\cos \alpha = 0.968$$

and

$$\cos \alpha_o = 0.866$$

$$K_R = \left(\frac{b_o}{b}\right)^{\frac{1}{2}} = \left(\frac{\cos \alpha_o}{\cos \alpha}\right)^{\frac{1}{2}} = \left(\frac{0.866}{0.968}\right)^{\frac{1}{2}} = 0.945$$

Figure 2-19 shows the relationships between α, α_O, period, depth, and K_R in graphical form.

2.321 Procedures in Refraction Diagram Construction - Orthogonal Method. Charts showing the bottom topography of the study area are obtained. Two or more charts of differing scale may be required, but the procedures are identical for charts of any scale. Underwater contours are drawn on the chart, or on a tracing paper overlay, for various depth intervals. The depth intervals chosen depend on the degree of accuracy desired. If overlays are used, the shoreline should be traced for reference. In tracing contours, small irregularities must be *smoothed out*, since bottom features that are comparatively small in respect to the wavelength do not affect the wave appreciably.

The range of wave periods and wave directions to be investigated is determined by a hindcasting study of historical weather charts or from other historical records relating to wave period and direction. For each wave period and direction selected, a separate diagram must be prepared. C_1/C_2 values for each contour interval may then be marked between contours. The method of computing C_1/C_2 is illustrated by Table 2-2; a tabulation of C_1/C_2 for various contour intervals and wave periods is given in Table C-4 of Appendix C.

To construct orthogonals from deep to shallow water, the deepwater direction of wave approach is first determined. A deepwater wave front (crest) is drawn as a straight line perpendicular to this wave direction,

2-69
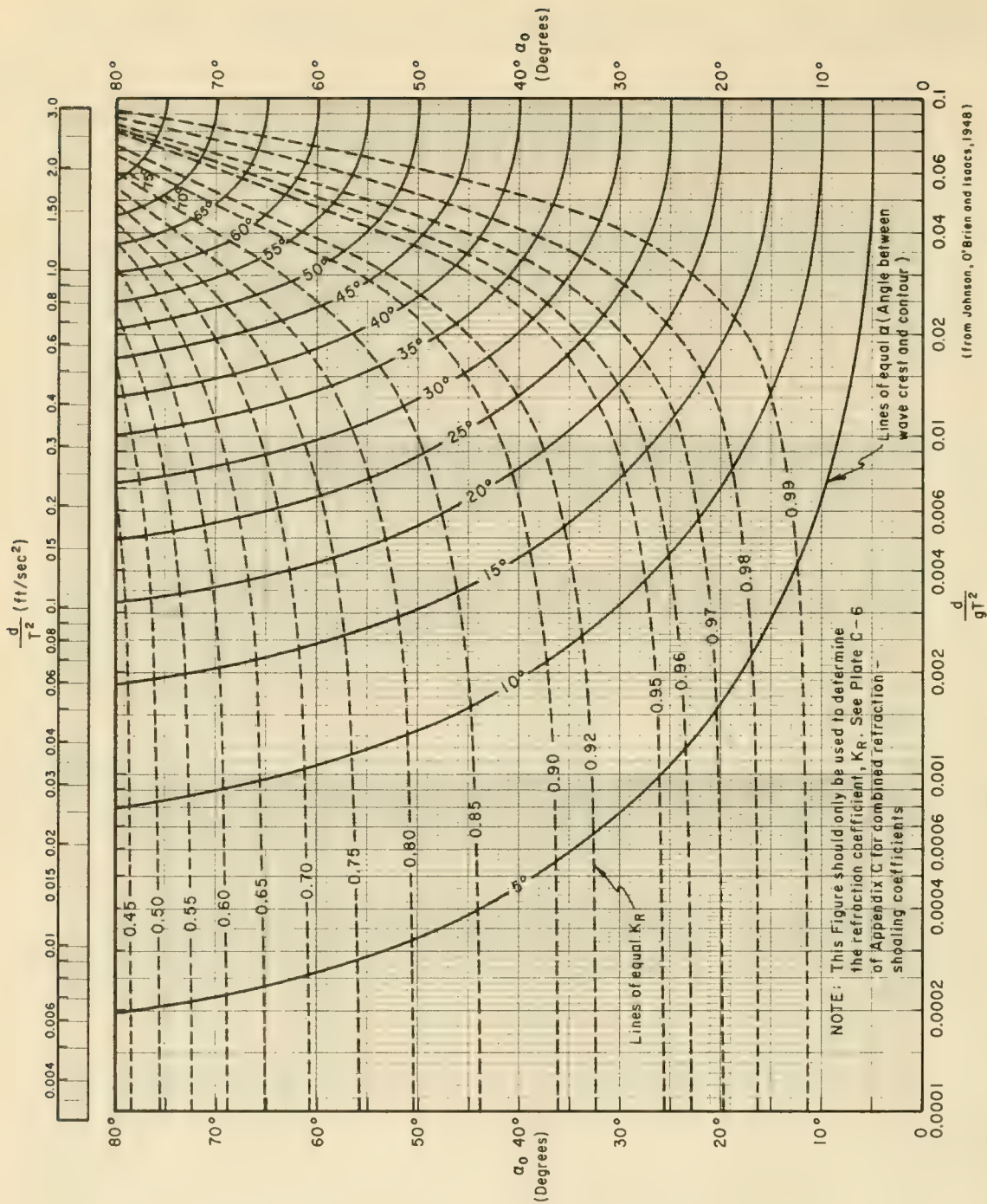
Figure 2-19. Changes in Wave Direction and Height Due to Refraction on Slopes with Straight, Parallel Depth Contours

NOTE: This Figure should only be used to determine the refraction coefficient, K_R. See Plate C-6 of Appendix C for combined refraction shoaling coefficients

Lines of equal α (Angle between wave crest and contour)

Lines of equal K_R

(from Johnson, O'Brien and Isaacs, 1948)

2-70

and suitably spaced orthogonals are drawn perpendicular to this wave front and parallel to the chosen direction of wave approach. Closely spaced orthogonals give more detailed results than widely spaced orthogonals. These lines are extended to the first depth contour shallower than $L_O/2$ where L_O (in feet) = 5.12 T^2.

TABLE 2-2   EXAMPLE COMPUTATIONS OF VALUES OF
C_1/C_2 FOR REFRACTION ANALYSIS

T = 10 seconds				
(1)	(2)	(3)	(4)	(5)
d (ft)	$\dfrac{d}{L_O}$	$\tanh \dfrac{2\pi d}{L}$	$\dfrac{C_1}{C_2}$	$\dfrac{C_2}{C_1}$
6	0.0117	0.268		
			1.40	0.72
12	0.0234	0.374		
			1.21	0.83
18	0.0352	0.453		
			1.14	0.88
24	0.0469	0.516		

Column 1 gives depths corresponding to chart contours. These would extend from 6 feet to a depth equal to $L_O/2$.

Column 2 is column 1 divided by L_O corresponding to the given period.

Column 3 is the value of tanh $2\pi d/L$ found in Table C-1 of Appendix C, corresponding to the value of d/L_O in column 2. This term is also C/C_O.

Column 4 is the quotient of successive terms in column 3.

Column 5 is the reciprocal of column 4.

2.322 Procedure when α is Less than 80 Degrees. Recall that α is the angle a wave crest makes with the bottom contour. Starting with any one orthogonal and using the refraction template in Figure 2-18, the following steps are performed in extending the orthogonal to shore:

(a) Sketch a contour midway between the first two contours to be crossed, extend the orthogonal to the midcontour, and construct a tangent to the midcontour at this point.

(b) Lay the line on the template labelled *orthogonal* along the incoming orthogonal with the point marked 1.0 at the intersection of the orthogonal and midcontour (Figure 2-20 top);

2-71

Figure 2-20. Use of the Refraction Template
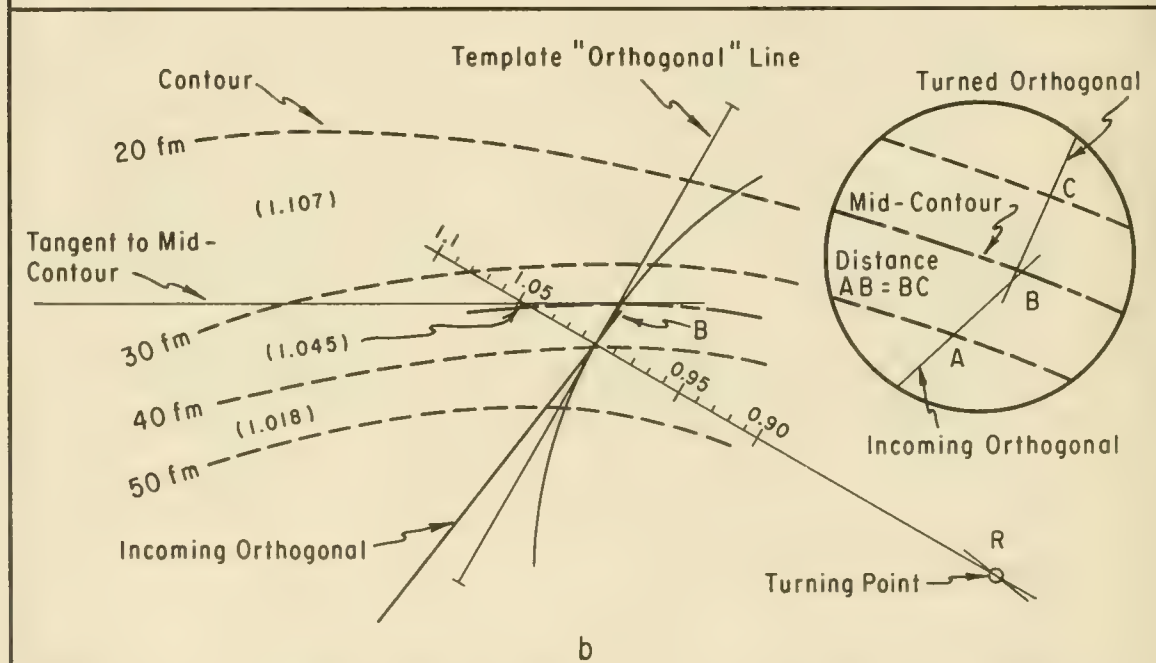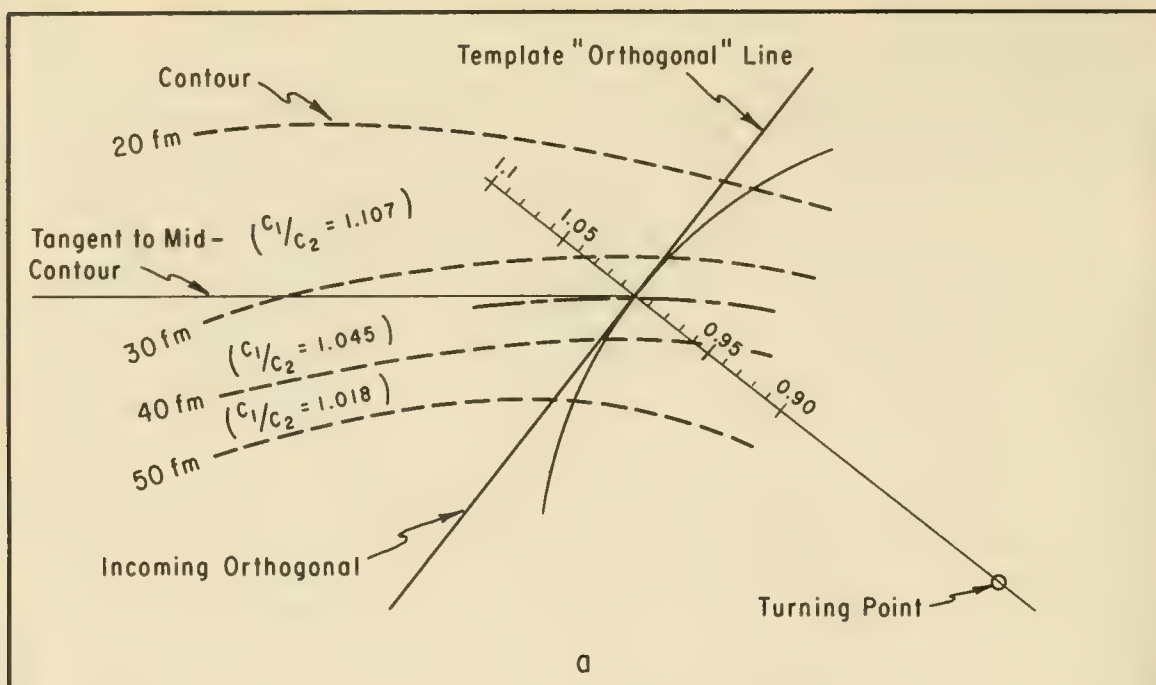
(c) Rotate the template about the *turning point* until the C_1/C_2 value corresponding to the contour interval being crossed intersects the tangent to the midcontour. The orthogonal line on the chart now lies in the direction of the turned orthogonal on the template (Figure 2-20 bottom);

(d) Place a triangle along the base of the template and construct a perpendicular to it so that the intersection of the perpendicular with the incoming orthogonal is midway between the two contours when the distances are measured along the incoming orthogonal and the perpendicular (See Point B in Figure 2-20 bottom). Note that this point is not necessarily on the midcontour line. This line represents the turned orthogonal;

(e) Repeat the above steps for successive contour intervals.

If the orthogonal is being constructed from shallow to deep water, the same procedure may be used, except that C_2/C_1 values are used instead of C_1/C_2.

A **template** suitable for attachment to a drafting machine can be made, Palmer (1957), and may make the procedure simpler if many diagrams are to be used.

2.323 Procedure when α is Greater than 80 Degrees - The R/J Method. In any depth, when α becomes greater than 80 degrees, the above procedure cannot be used. The orthogonal no longer appears to cross the contours, but tends to run almost parallel to them. In this case, the contour interval must be crossed in a series of steps. The entire interval is divided into a series of smaller intervals. At the midpoint of the individual subintervals, orthogonal-angle turnings are made.

Referring to Figure 2-21, the interval to be crossed is divided into segments or boxes by transverse lines. The spacing R, of the transverse lines is arbitrarily set as a ratio of the distance J, between the contours. For the complete interval to be crossed, C_2/C_1 is computed or **found** from Table C-4 of Appendix C. (C_2/C_1, not C_1/C_2.)

On the template (Figure 2-18), a graph showing orthogonal angle turnings $\Delta\alpha$, is plotted as a function of the C_2/C_1 value for various values of the ratio R/J. The $\Delta\alpha$ value is the angle turned by the incoming orthogonal in the center of the subinterval.

The orthogonal is extended to the middle of the box, $\Delta\alpha$ is read from the graph, and the orthogonal turned by that angle. The procedure is repeated for each box in sequence, until α at a plotted or interpolated contour becomes smaller than 80 degrees. At this point, this method of orthogonal construction must be stopped, and the preceding technique for α smaller than 80 degrees used, otherwise errors will result.

2.324 Refraction Fan Diagrams. It is often convenient, especially where sheltering land forms shield a stretch of shore from waves approaching in certain directions, to construct refraction diagrams from shallow water

J = Distance between contours at turning points, ⊙
R = Distance along orthogonal
T = 12 seconds
L_σ = 737 ft.
For contour interval from 40 fm to 30 fm C_1/C_2 = 1.045, C_2/C_1 = 0.957

30 fm
40 fm
$\Delta\alpha = 7° - 15'$
$R_5 = 3J_5$
J_5
$R_4 = 2J_4$
J_4
$R_3 = 2J_3$
J_3
$R_2 = J_2$
J_2
$R_1 = J_1$
J_1
$\Delta\alpha = 4° - 50'$
$\Delta\alpha = 4° - 50'$
$\Delta\alpha = 2° - 25'$
$\Delta\alpha = 2° - 25'$
10°
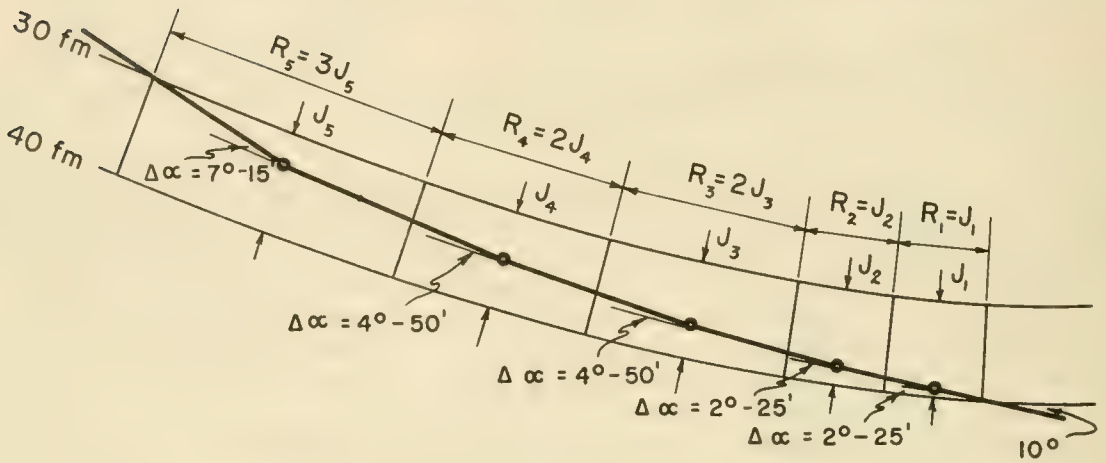
Figure 2-21.   Refraction Diagram Using R/J Method

2 - 74

toward deep water. In such cases, a sheaf or fan of orthogonals may be
projected seaward in directions some 5 or 10 degrees apart. See Figure
2-22a. With the deepwater directions thus determined by the individual
orthogonals, companion orthogonals may be projected shoreward on either
side of the seaward projected ones to determine the refraction coefficient
for the various directions of wave approach. (See Figure 2-22b.)

2.325 Other Graphical Methods of Refraction Analysis. Another graphical
method for the construction of refraction diagrams is the wave-front
method (Johnson, et al., 1948). This method is particularly applicable
to very long waves where the crest alignment is also desired. The method
is not presented here, where many diagrams are required, because, where
many diagrams are required, it is overbalanced by the advantages of the
orthogonal method. The orthogonal method permits the direct construction
of orthogonals and determination of the refraction coefficient without the
intermediate step of first constructing successive wave crests. Thus,
when the wave crests are not required, significant time is saved by using
the orthogonal method.

2.326 Computer Methods for Refraction Analysis. Harrison and Wilson (1964)
developed a method for the numerical calculation of wave refraction by use
of an electronic computer. Wilson (1966) extended the method so that, in
addition to the numerical calculation, the actual plotting of refraction
diagrams is accomplished automatically by use of a computer. Numerical
methods are a practical means of developing wave refraction diagrams when
an extensive refraction study of an area is required, and when they can
be relied upon to give accurate results. However, the interpretation of
computer output requires care, and the limitations of the particular scheme
used should be considered in the evaluation of the results. For a dis-
cussion of some of these limitations, see Coudert and Raichlen (1970).
For additional references, the reader is referred to the works of Keller
(1958), Mehr (1962), Griswold (1963), Wilson (1966), Lewis, et al., (1967),
Dobson (1967), Hardy (1968), Chao (1970), and Keulegan and Harrison (1970),
in which a number of available computer programs for calculation of refrac-
tion diagrams are presented. Most of these programs are based on an algo-
rithm derived by Munk and Arthur (1951) and, as such, are fundamentally
based on the geometrical optics approximation. (Fermat's Principle.)

2.327 Interpretation of Results and Diagram Limitations. Some general
observations of refraction phenomena are illustrated in Figures 2-23, 24,
and 25. These figures show the effects of several common bottom features
on passing waves. Figure 2-23 shows the effect of a straight beach with
parallel evenly spaced bottom contours on waves approaching from an angle.
Wave crests turn toward alignment with the bottom contours as the waves
approach shore. The refraction effects on waves normally incident on a
beach fronted by a submarine ridge or submarine depression are illustrated
in Figure 2-24a and 2-24b. The ridge tends to focus wave action toward
the section of beach where the ridge line meets the shoreline. The ortho-
gonals in this region are more closely spaced; hence $\sqrt{b_o/b}$ is greater
than 1.0 and the waves are higher than they would be if no refraction
occurred. Conversely, a submarine depression will cause orthogonals to
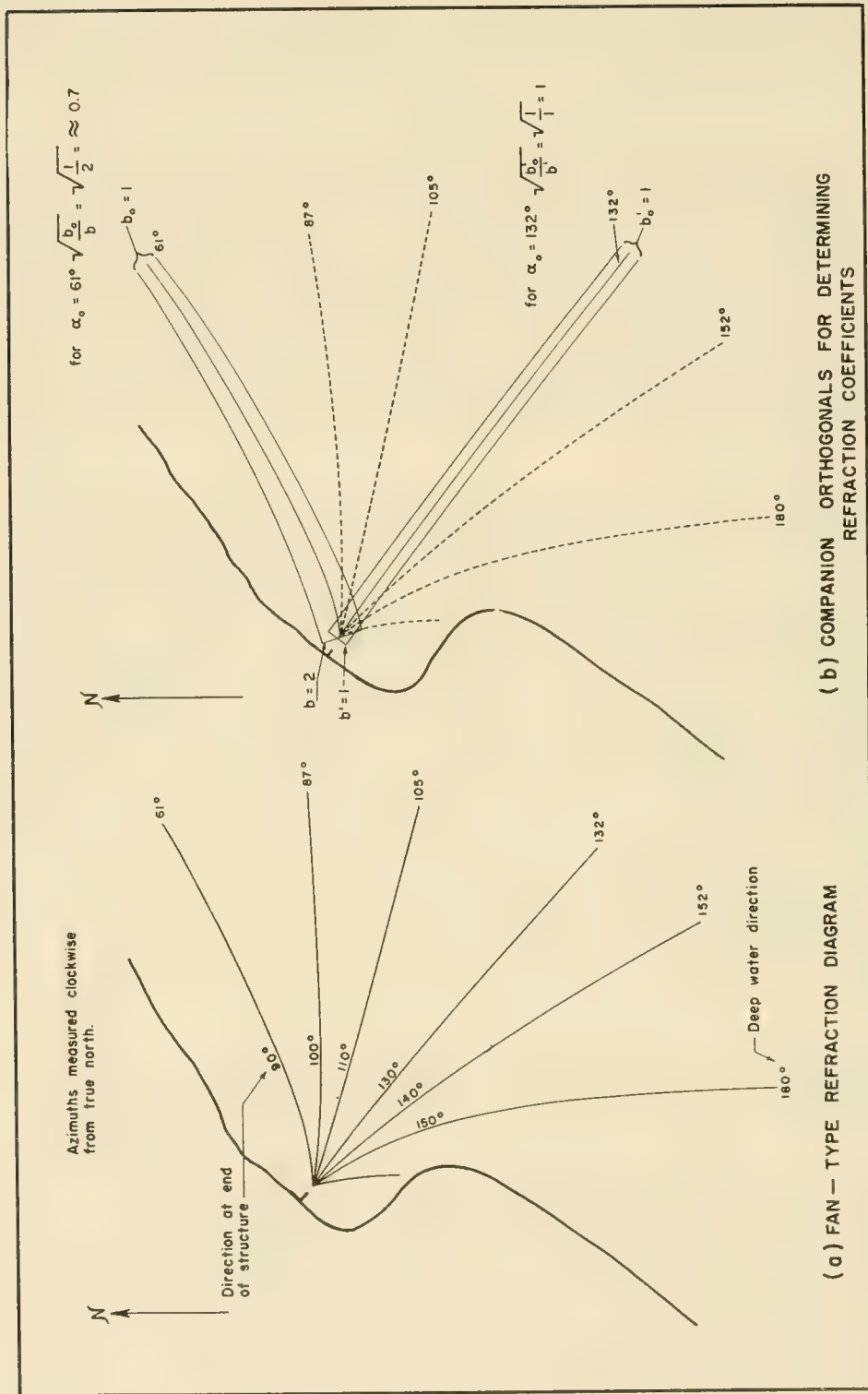
Figure 2-22. Use of Fan-Type Refraction Diagram
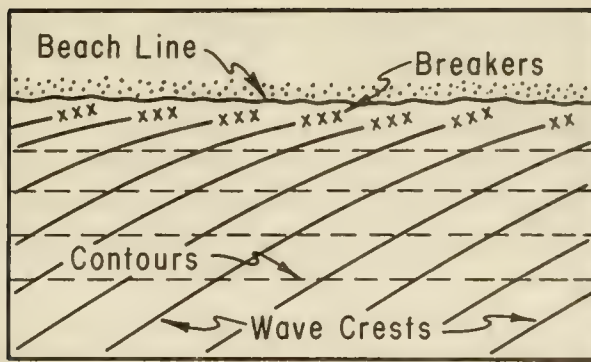
Figure 2-23. Refraction Along a Straight Beach with Parallel Bottom Contours
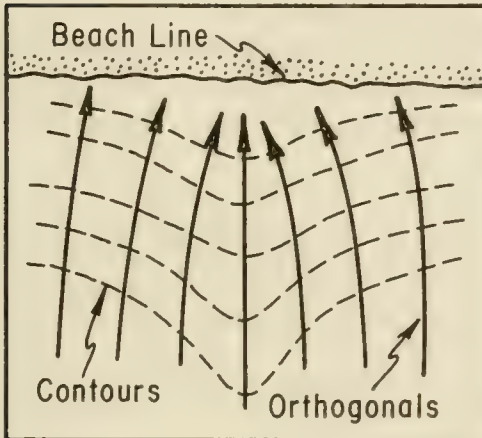
(a)
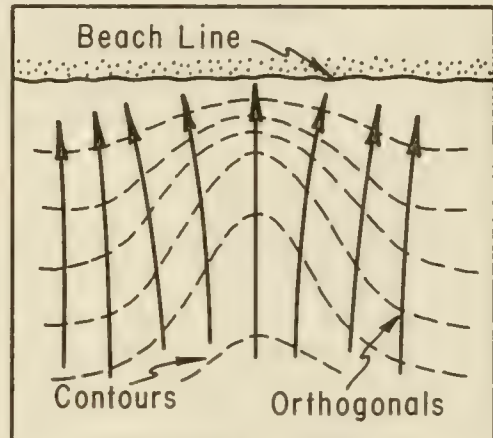
(b)

Figure 2-24. Refraction by a Submarine Ridge (a) and Submarine Canyon (b)
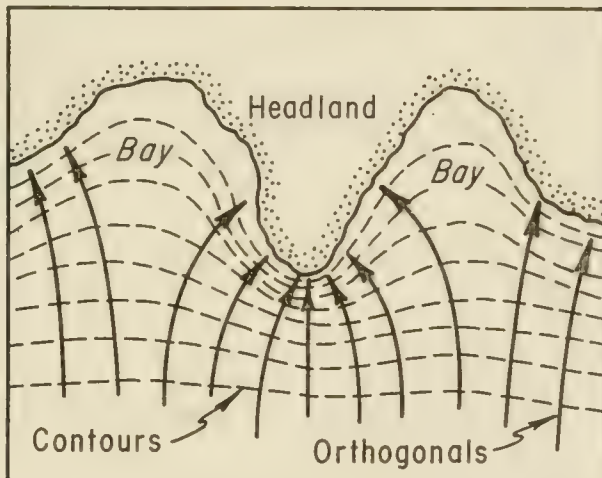
Figure 2-25. Refraction Along an Irregular Shoreline

diverge, resulting in low heights at the shore. (b_O/b less than 1.0.)
Similarly, heights will be greater at a headland than in a bay. Since
the wave energy contained between two orthogonals is constant, a larger
part of the total energy expended at the shore is focused on projections
from the shoreline; consequently, refraction straightens an irregular
coast. Bottom topography can be inferred from refraction patterns on
aerial photography. The pattern in Figure 2-17 indicates the presence
of a submarine ridge.

Refraction diagrams can provide a measure of changes in waves
approaching a shore. However, the accuracy of refraction diagrams is
limited by the validity of the theory of construction and the accuracy
of depth data. The orthogonal direction change (Equation 2-78) is
derived for straight parallel contours. It is difficult to carry an
orthogonal accurately into shore over complex bottom features (Munk and
Arthur, 1951). Moreover, the equation is derived for small waves moving
over mild slopes.

Dean (1973) considers the combined effects of refraction and shoal-
ing including nonlinearities applied to a slope with depth contours
parallel to the beach but not necessarily of constant slope. He finds
that non-linear effects can significantly increase (in comparison with
linear theory) both amplification and angular turning of waves of low
steepness in deep water.

Strict accuracy for height changes cannot be expected for slopes
steeper than 1:10, although model tests have shown that direction
changes nearly as predicted even over a vertical discontinuity (Wiegel
and Arnold, 1957). Accuracy where orthogonals bend sharply or exhibit
extreme divergence or convergence is questionable because of energy
transfer along the crest. The phenomenon has been studied by Beitinjani
and Brater (1965), Battjes (1968) and Whalin (1971). Where two ortho-
gonals meet, a caustic develops. A caustic is an envelope of ortho-
gonal crossings, caused by convergence of wave energy at the caustic
point. An analysis of wave behavior near a caustic is not available;
however, qualitative analytical results show that wave amplitude decays
exponentially away from a caustic in the shadow zone, and there is a
phase shift of $\pi/2$ across the caustic (Whalin 1971). Wave behavior
near a caustic has also been studied by Pierson (1950), Chao (1970) and
others. Little quantitative information is available for the area
beyond a caustic.

2.328 Refraction of Ocean Waves. Unlike Monochromatic waves, actual
ocean waves are more complicated. Their crest lengths are short; their
form does not remain permanent; and their speed, period, and direction
of propagation vary from wave to wave.

Pierson (1951), Longuet-Higgins (1957), and Kinsman (1965), have suggested a solution to the ocean-wave refraction problem. The sea surface waves in deep water become a number of component monochromatic waves, each with a distinct frequency and direction of propagation. The energy spectrum for each component may then be found and the conventional refraction analysis techniques applied. Near the shore, the wave energy propagated in a particular direction is approximated as the linear sum of the spectra of wave components of all frequencies refracted in the given direction from all of the deepwater directional components.

The work required for this analysis, even for a small number of individual components, is laborious and time consuming. More recent research by Borgman (1969) and Fan and Borgman (1970), has used the idea of directional spectra which may provide a technique for solving complex refraction problems more rapidly.

2.4 WAVE DIFFRACTION

2.41 INTRODUCTION

Diffraction of water waves is a phenomenon in which energy is transferred laterally along a wave crest. It is most noticeable where an otherwise regular train of waves is interrupted by a barrier such as a breakwater or an islet. If the lateral transfer of wave energy along a wave crest and across orthogonals did not occur, straight, long-crested waves passing the tip of a structure would leave a region of perfect calm in the lee of the barrier, while beyond the edge of the structure the waves would pass unchanged in form and height. The line separating two regions would be a discontinuity. A portion of the area in front of the barrier would, however, be disturbed by both the incident waves and by those waves reflected by the barrier. The three regions are shown in Figure 2-26a for the hypothetical case if diffraction did not occur, and in Figure 2-26b for the actual phenomenon as observed. The direction of the lateral energy transfer is also shown in Figure 2-26a. Energy flow across the discontinuity is from Region II into Region I. In Region III, the superposition of incident and reflected waves results in the appearance· of short-crested waves if the incident waves approach the breakwater obliquely. A partial standing wave will occur in Region III if the waves approach perpendicular to the breakwater.

This process is also similar to that for other types of waves, such as light or sound waves.

Calculation of diffraction effects is important for several reasons. Wave height distribution in a harbor or sheltered bay is determined to some degree by the diffraction characteristics of both the natural and manmade structures affording protection from incident waves. Therefore, a knowledge of the diffraction process is essential in planning such facilities. Proper design and location of harbor entrances to reduce such problems as silting and harbor resonance also require a knowledge of the effects of wave diffraction. The prediction of wave heights near
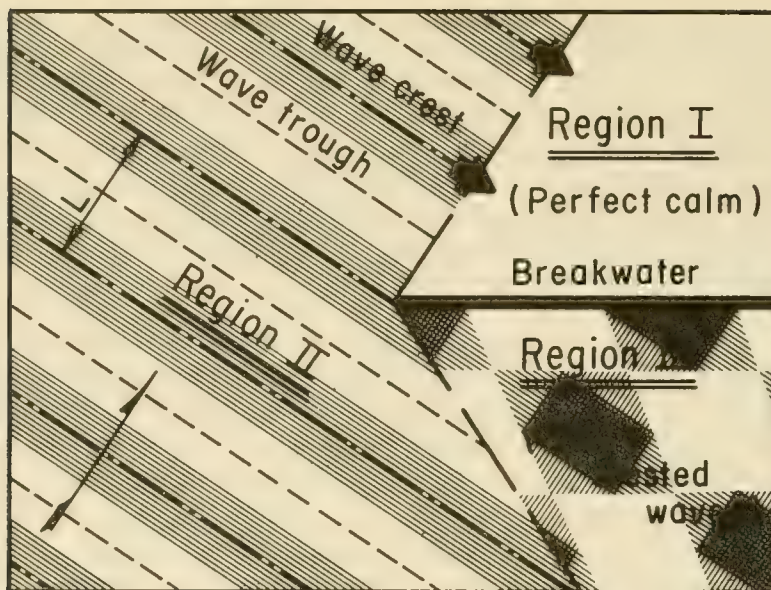
Figure 2-26a. Wave Incident on a Breakwater
No Diffraction
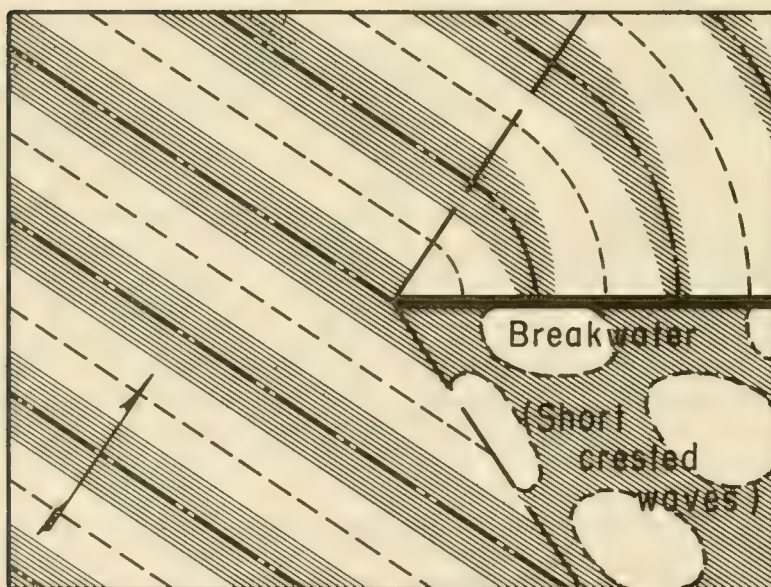
Figure 2-26b. Wave Incident on a Breakwater
Diffraction Effects

2-80

the shore is affected by diffraction caused by naturally occurring changes in hydrography. An aerial photograph illustrating the diffraction of waves by a breakwater is shown in Figure 2-27.

Putnam and Arthur (1948) presented experimental data verifying a method of solution proposed by Penny and Price (1944) for wave behavior after passing a single breakwater. Wiegel (1962) used a theoretical approach to study wave diffraction around a single breakwater. Blue and Johnson (1949) dealt with the problem of the behavior of waves after passing through a gap, as between two breakwater arms.

The assumptions usually made in the development of diffraction theories are:

(1) Water is an ideal fluid, i.e., inviscid and incompressible.

(2) Waves are of small-amplitude and can be described by linear wave theory.

(3) Flow is irrotational and conforms to a potential function which satisfies the Laplace equation.

(4) Depth shoreward of the breakwater is constant.

2.42   DIFFRACTION CALCULATIONS

2.421 Waves Passing a Single Breakwater. From a presentation by Wiegel (1962), diffraction diagrams have been prepared which, for a uniform depth adjacent to an impervious structure, show lines of equal wave height reduction. These diagrams are shown in Figures 2-28 through 2-39; the graph coordinates are in units of wavelength. Wave height reduction is given in terms of a diffraction coefficient K' which is defined as the ratio of a wave height H, in the area affected by diffraction to the incident wave height H_i, in the area unaffected by diffraction. Thus, H and H_i are determined by $H = K' H_i$.

The diffraction diagrams shown in Figures 2-28 through 2-39 are constructed in polar coordinate form with arcs and rays centered at the structure's tip. The arcs are spaced one *radius-wavelength* unit apart and rays 15° apart . In application, a given diagram must be scaled up or down so that the particular wavelength corresponds to the scale of the hydrographic chart being used. Rays and arcs on the refraction diagrams provide a coordinate system that makes it relatively easy to transfer lines of constant K' on the scaled diagrams.

When applying the diffraction diagrams to actual problems, the wavelength must first be determined based on the water depth at the tip of the structure. The wavelength L, in water depth d_s, may be found by computing $d_s/L_0 = d_s/5.12T^2$ and using Appendix C, Table C-1 to find the corresponding value of d_s/L. Dividing d_s by d_s/L will give the shallow water wave length L. It is then useful to construct a scaled diffraction

Figure 2-27.   Wave Diffraction at Channel Islands Harbor Breakwater, California
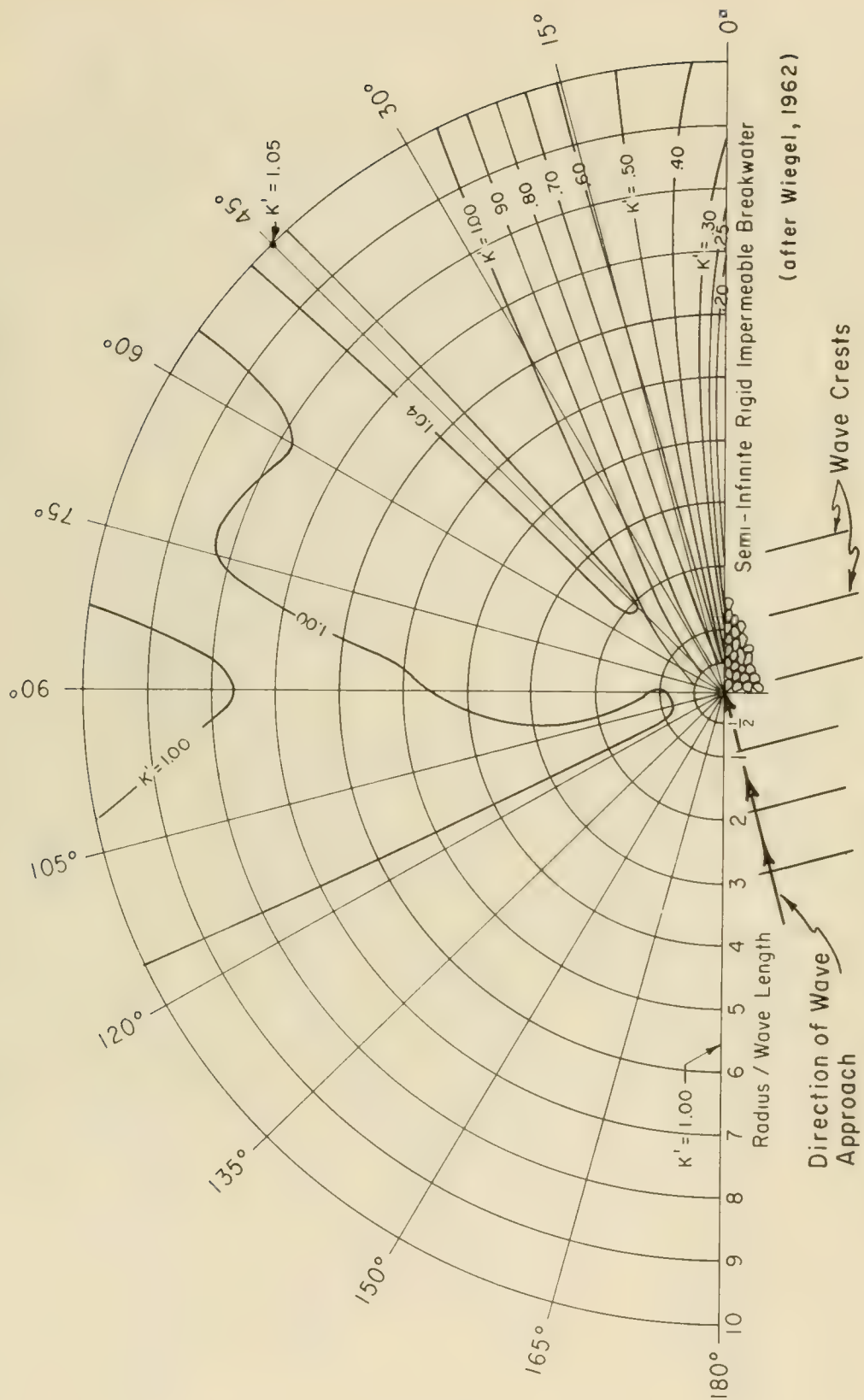
Figure 2-28. Wave Diffraction Diagram - 15° Wave Angle

Figure 2-29. Wave Diffraction Diagram - 30° Wave Angle

2-84
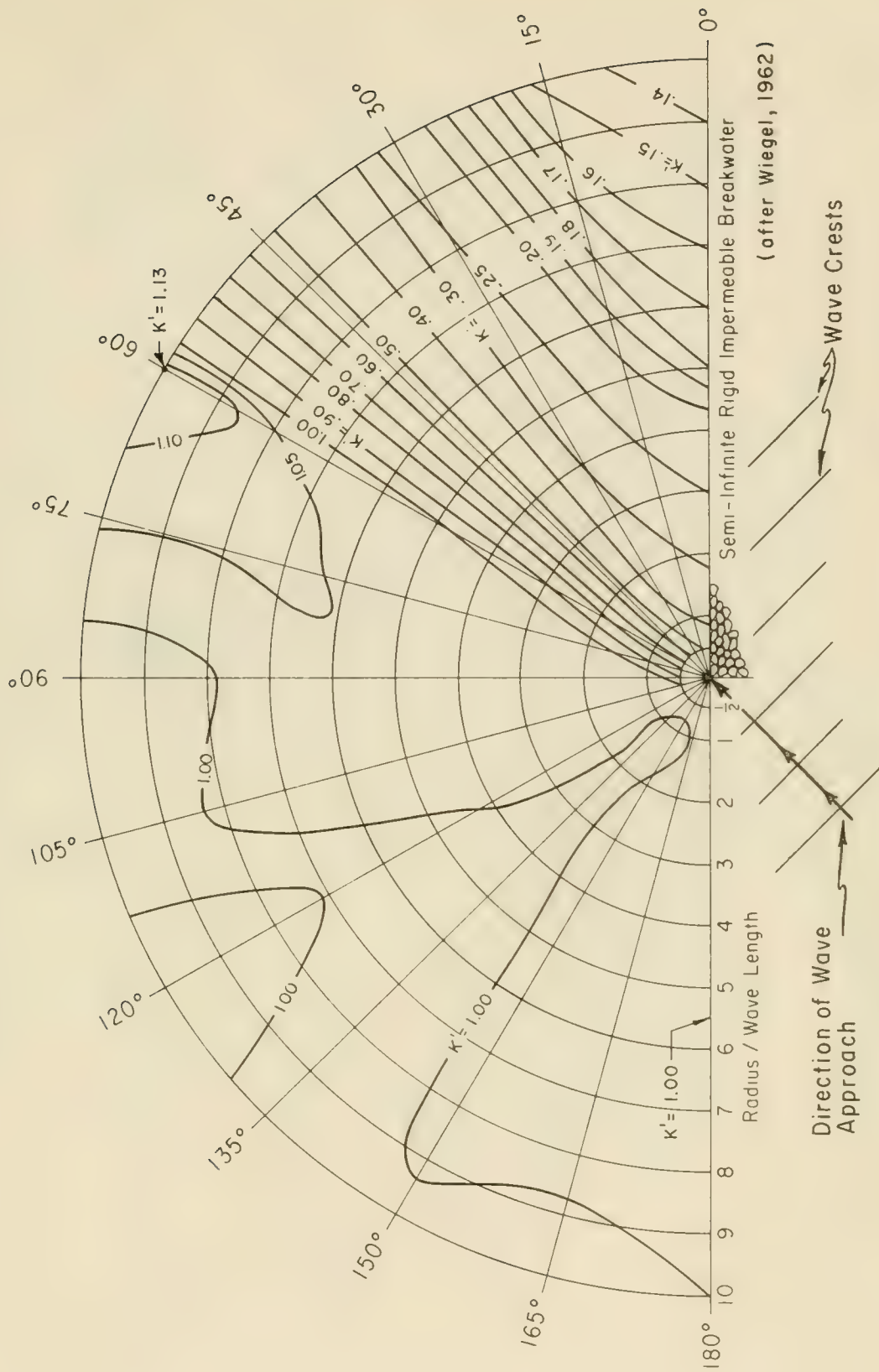
Figure 2-30. Wave Diffraction Diagram - 45° Wave Angle
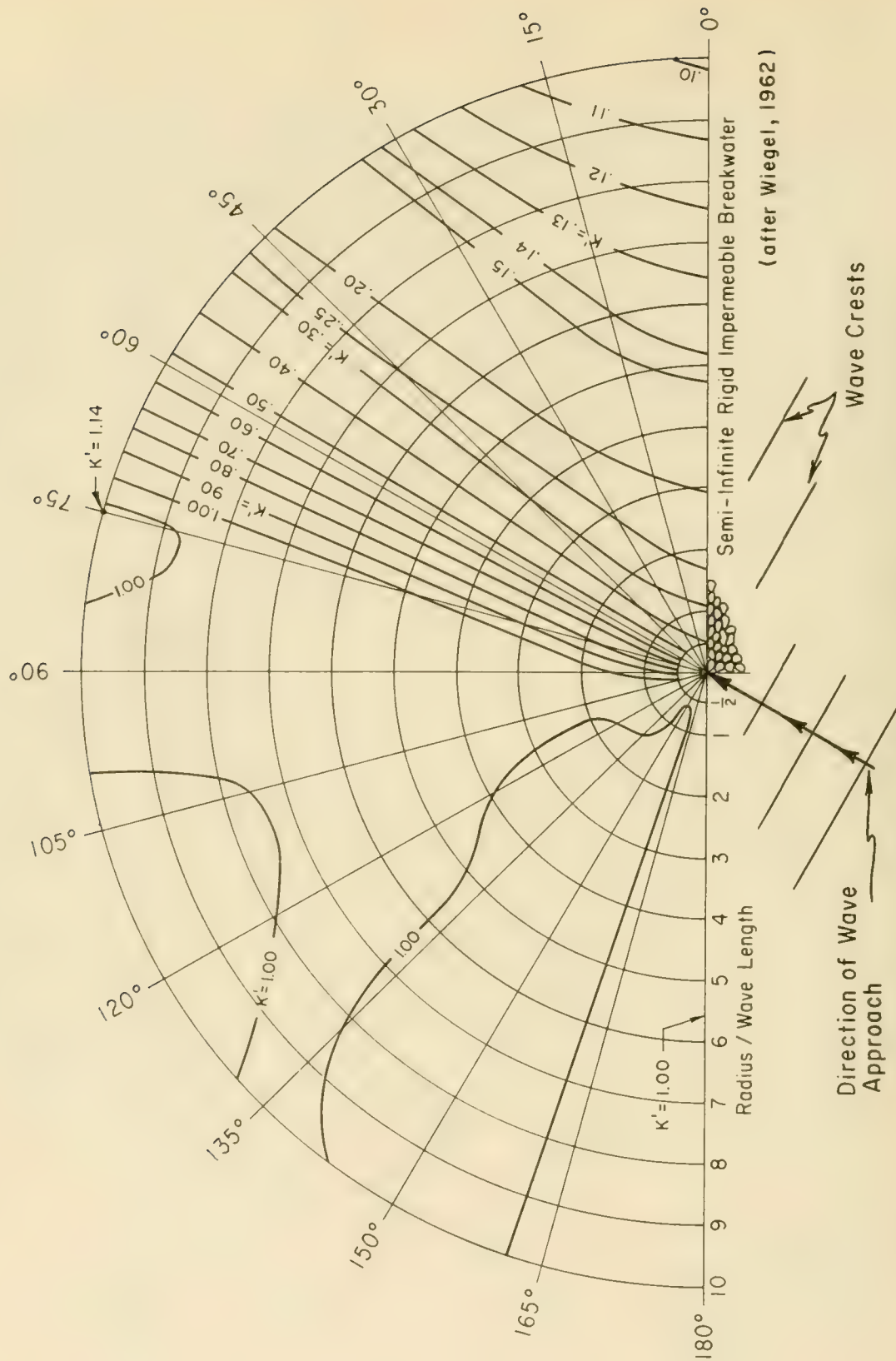
Figure 2-31. Wave Diffraction Diagram – 60° Wave Angle
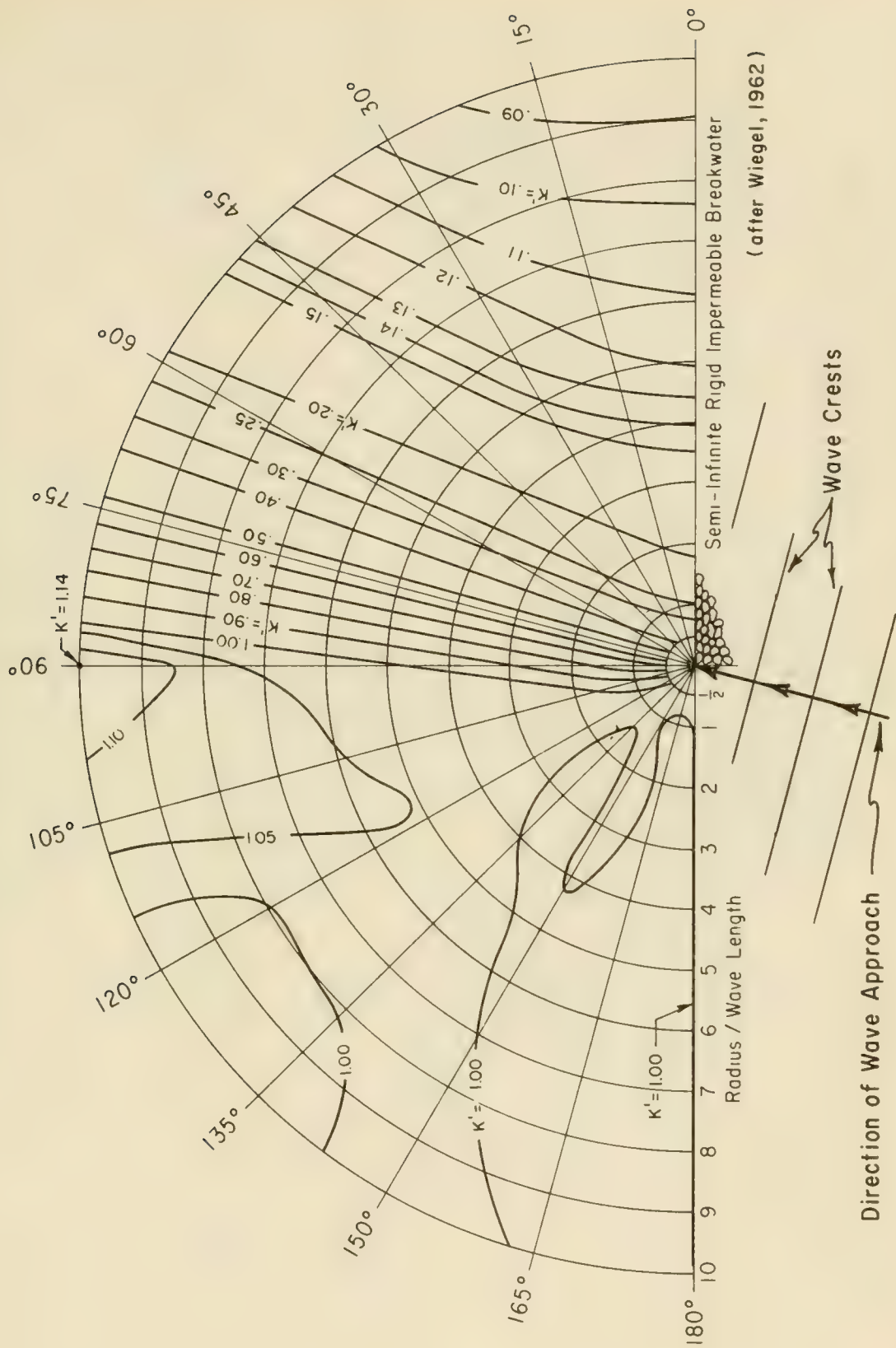
Figure 2-32. Wave Diffraction Diagram - 75° Wave Angle
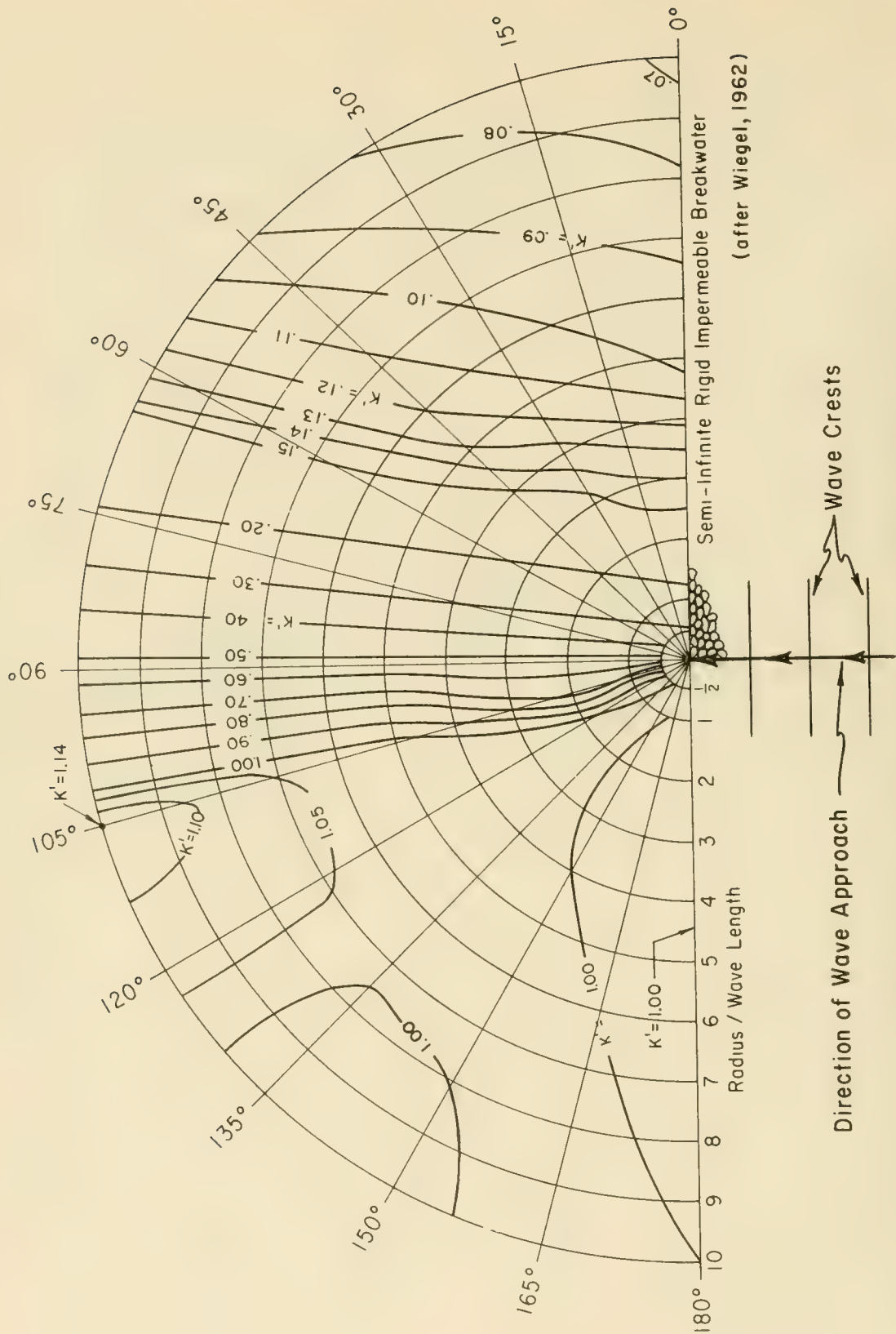
Figure 2-33. Wave Diffraction Diagram - 90° Wave Angle
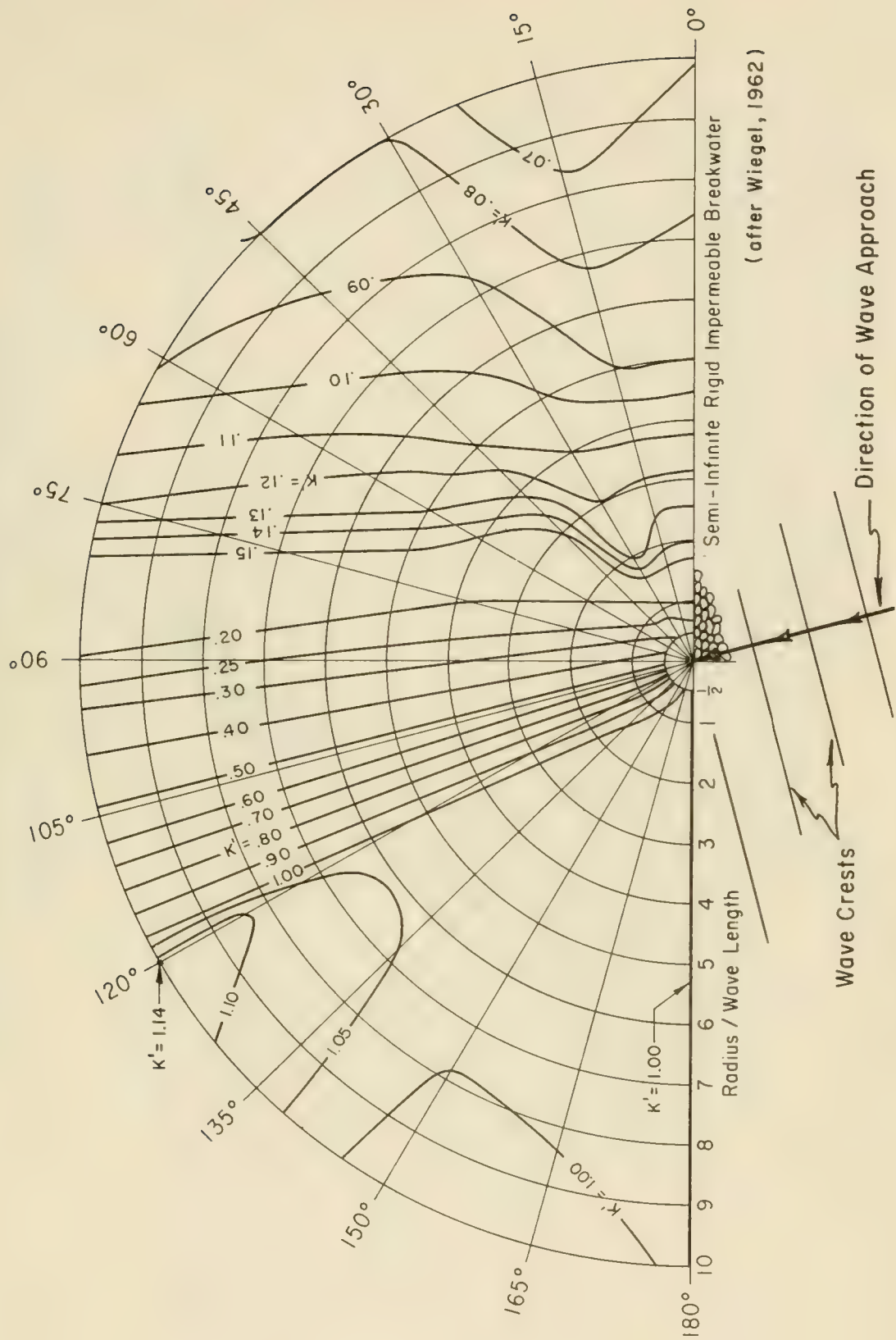
Figure 2-34. Wave Diffraction Diagram - 105° Wave Angle
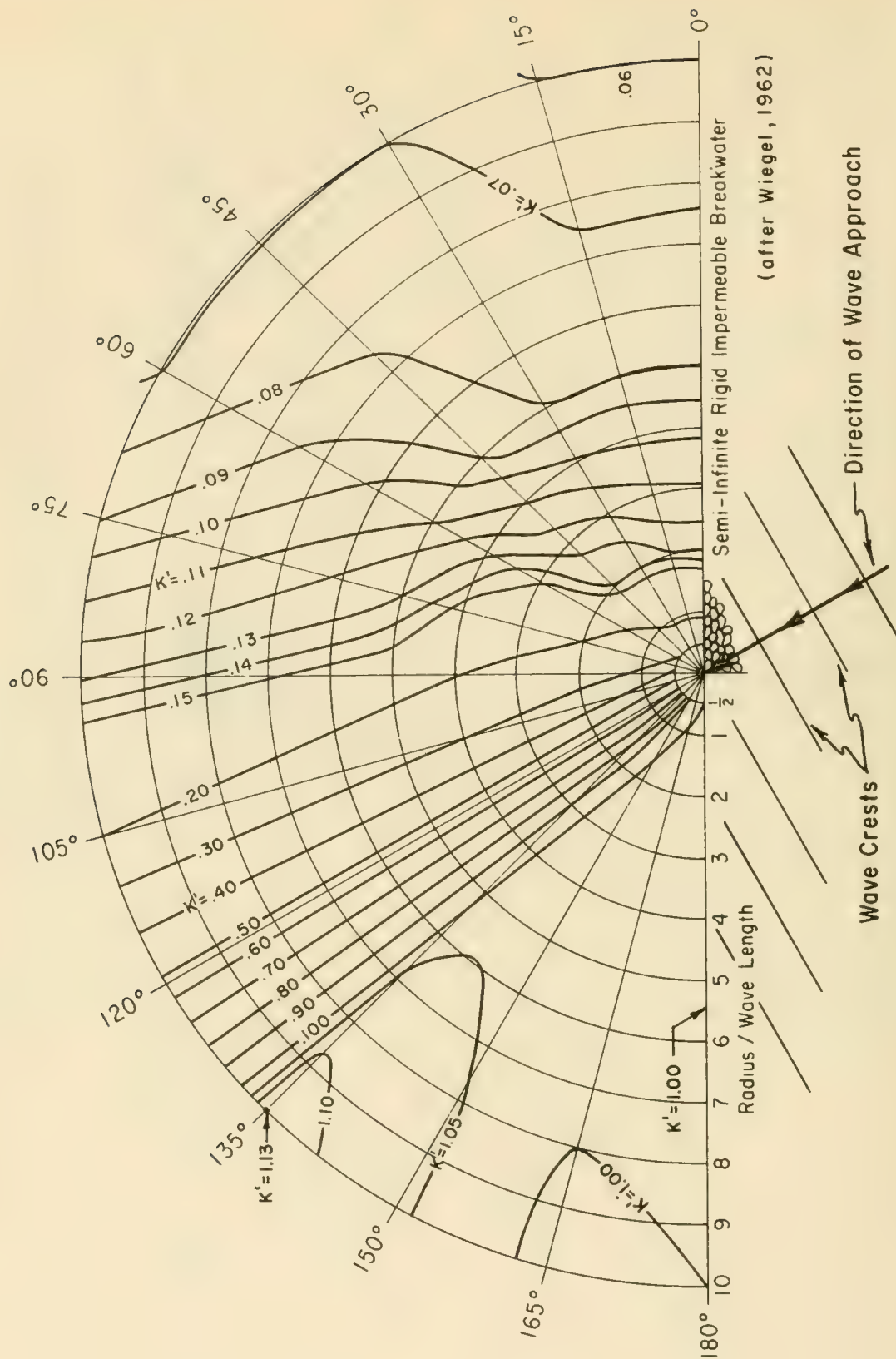
Figure 2-35. Wave Diffraction Diagram - 120° Wave Angle

2-90
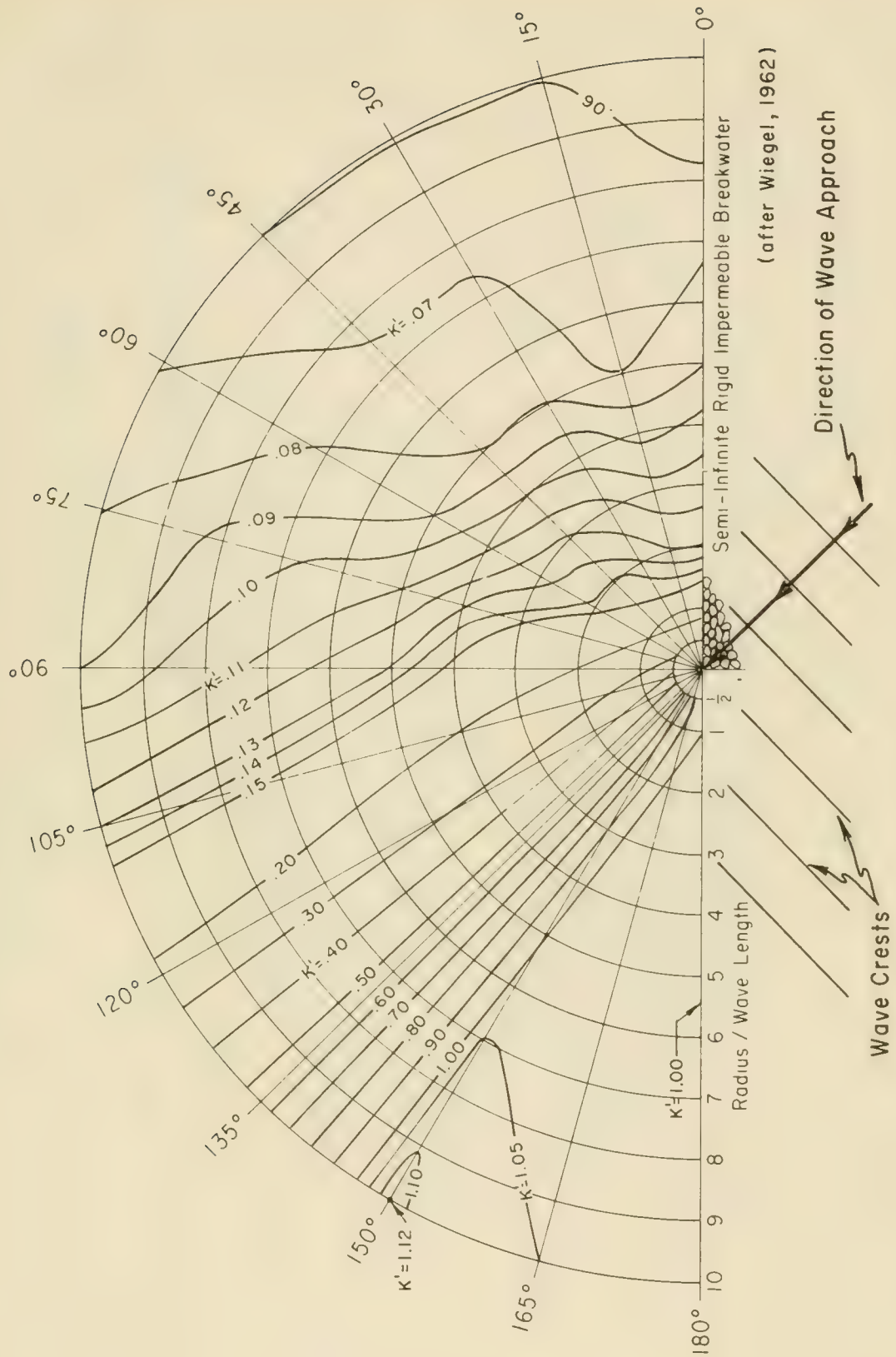
Figure 2-36. Wave Diffraction Diagram - 135° Wave Angle
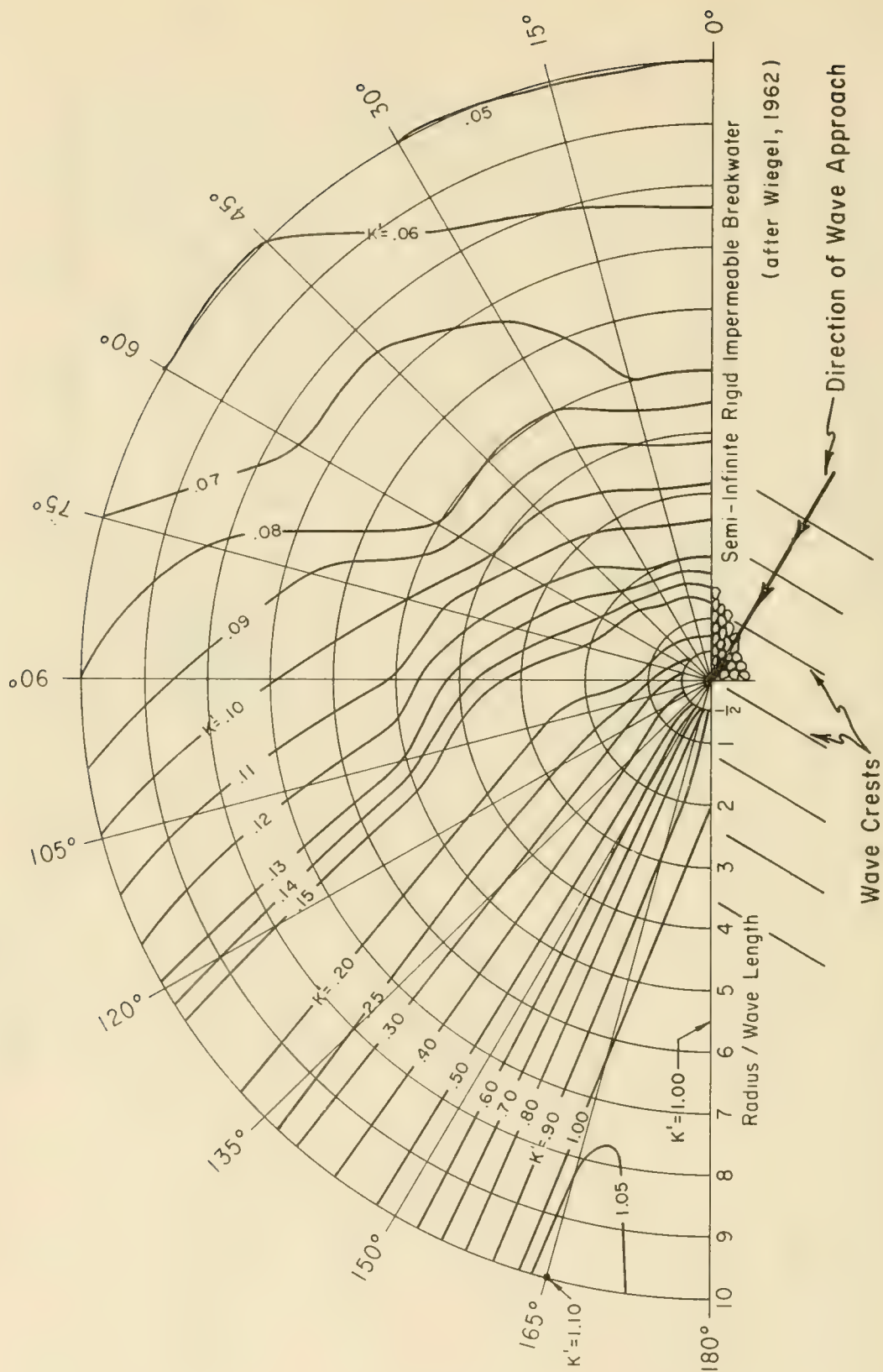
Figure 2-37. Wave Diffraction Diagram - 150° Wave Angle

2-92
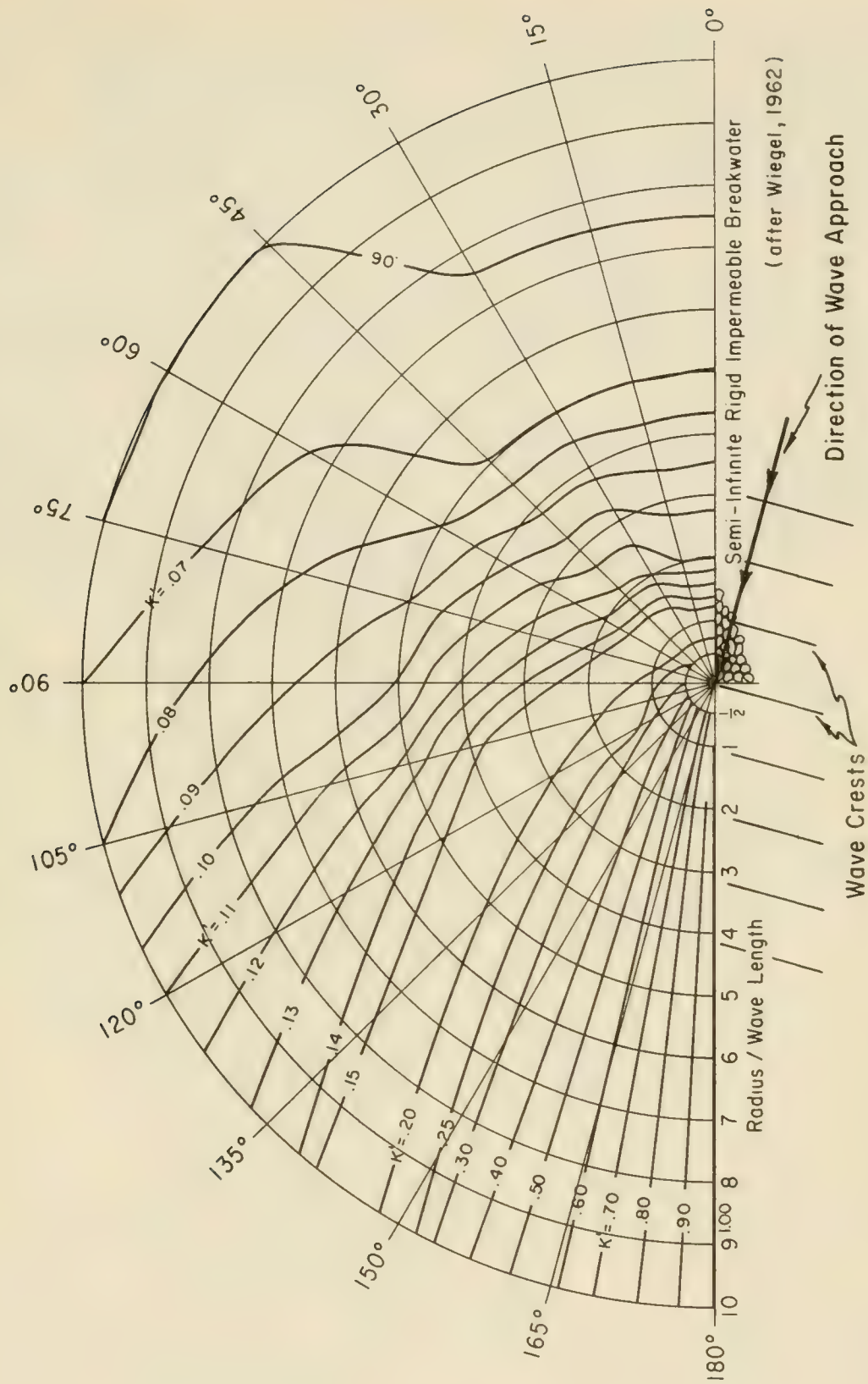
Figure 2-38. Wave Diffraction Diagram - 165° Wave Angle

2-93
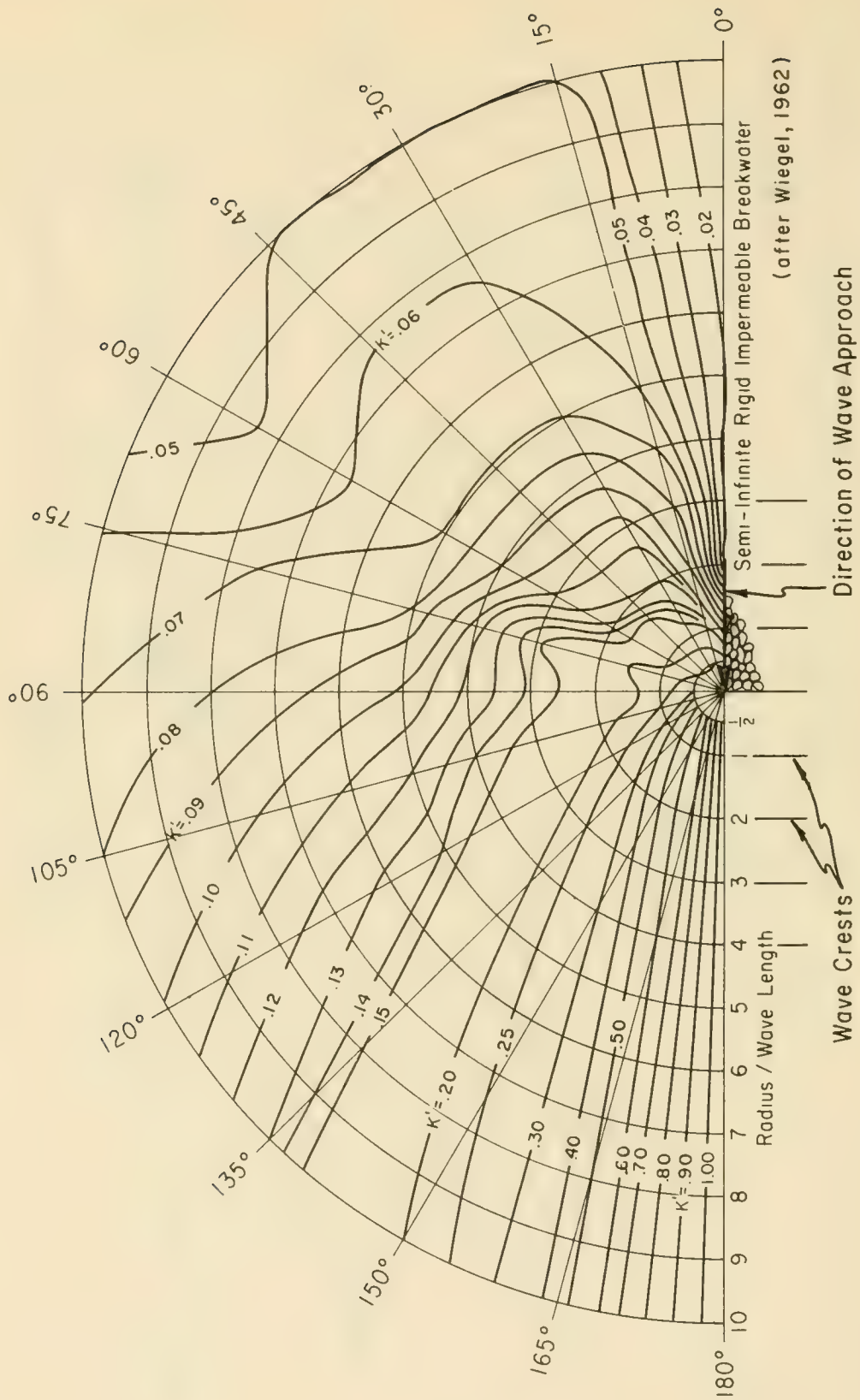
Figure 2-39. Wave Diffraction Diagram – 180° Wave Angle

2-94

diagram overlay template to correspond to the hydrographic chart being used. In constructing this overlay, first determine how long each of its *radius-wavelength* units must be. As noted previously, one radius-wavelength unit on the overlay must be identical to one wavelength on the hydrographic chart. The next step is to construct and sketch all overlay rays and arcs on clear plastic or translucent paper. This allows penciling in of the scaled lines of equal K for each angle of wave approach that may be considered pertinent to the problem. Thus, after studying the wave field for one angle of wave approach, K lines may be erased for a subsequent analysis of a different angle of wave approach.

The diffraction diagrams in Figures 2-28 through 2-39 show the breakwater extending to the right as seen looking toward the area of wave diffraction; however, for some problems the structure may extend to the left. All diffraction diagrams presented may be reversed by simply turning the transparency over to the opposite side.

Figure 2-40 illustrates the use of a template overlay. Also indicated is the angle of wave approach which is measured counterclockwise from the breakwater. This angle would be measured clockwise from the breakwater if the diagram were turned over. Figure 2-40 also shows a rectangular coordinate system with distance expressed in units of wavelength. Positive x direction is measured from the structure's tip along the breakwater and positive y direction is measured into the diffracted area.
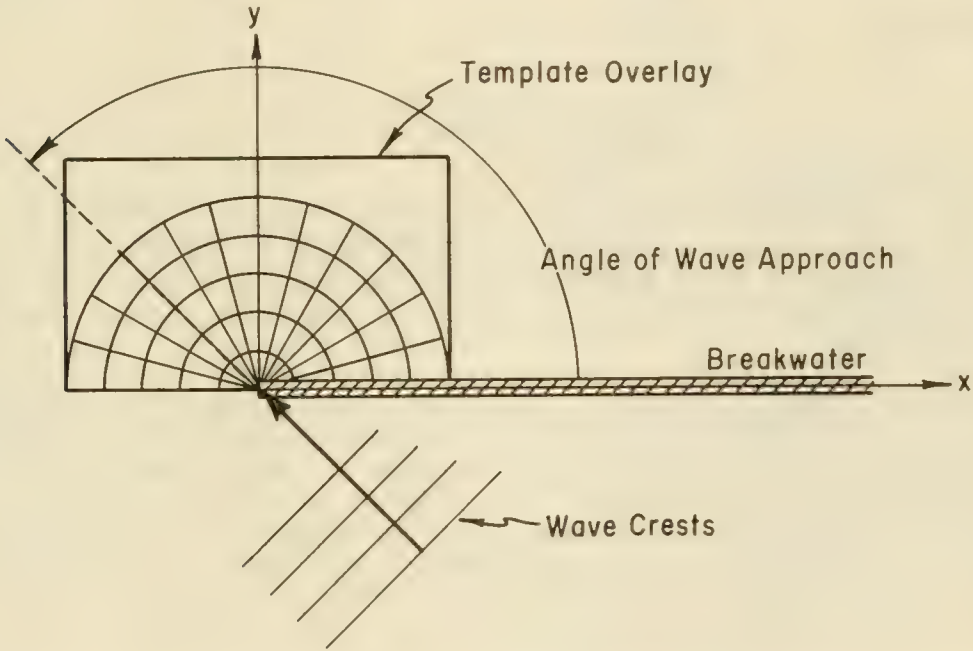
Figure 2-40. Diffraction for a Single Breakwater Normal Incidence

The following problem illustrates determination of a single wave height in the diffraction area.

* * * * * * * * * * * * * *   <u>EXAMPLE PROBLEM</u>   * * * * * * * * * * * * * *

GIVEN: Waves with a period of T = 8 seconds and height of H = 10 feet impinge upon a breakwater at an angle of 135 degrees. The water depth at the tip of the breakwater toe is d_s = 15 feet. Assume that one inch on the hydrographic chart being used is equivalent to 133 feet.

FIND: The wave height at a point P having coordinates in units of wave-length of $x = 3$ and $y = 4$. (Polar coordinates of x and y are r=5 at 53°.)

SOLUTION:

Since $d_s = 15$ feet, $T = 8$ seconds,

$$\frac{d_s}{L_o} = \frac{d_s}{5.12T^2} = \frac{15}{(5.12)(64)} = 0.0458 .$$

Using Table C-1 with

$$\frac{d}{L_o} = \frac{d_s}{L_o} = 0.0458$$

the corresponding value of

$$\frac{d}{L} \text{ or } \frac{d_s}{L} = 0.0899 ,$$

therefore,

$$L = \frac{d_s}{\left(d_s/L\right)} = \frac{15}{0.0899} = 167 \text{ feet} .$$

Because 1 inch represents 133 feet on the hydrographic chart and $L = 167$ feet, the wave-length is 1.26 inches on the chart.
This provides the necessary information for scaling Figure 2-36 to the hydrographic chart being used. Thus 1.26 inches represents a *radius/wavelength* unit.

For this example, point P and those lines of equal K' situated nearest P are shown on a schematic overlay, Figure 2-41. This over-lay is based on Figure 2-36 since the angle of wave approach is 135°. It should be noted that Figure 2-41, being a schematic rather than a true representation of the overlay, is not drawn to the hydrographic chart scale calculated in the problem. From Figure 2-41 it is seen that K' at point P is approximately 0.086. Thus the diffracted wave height at this point is

$$H = K'H_i = (0.086)(10) = 0.86 \text{ foot say } 0.9 \text{ foot} .$$

The above calculation indicates that a wave undergoes a substantial height reduction in the area considered.

* *
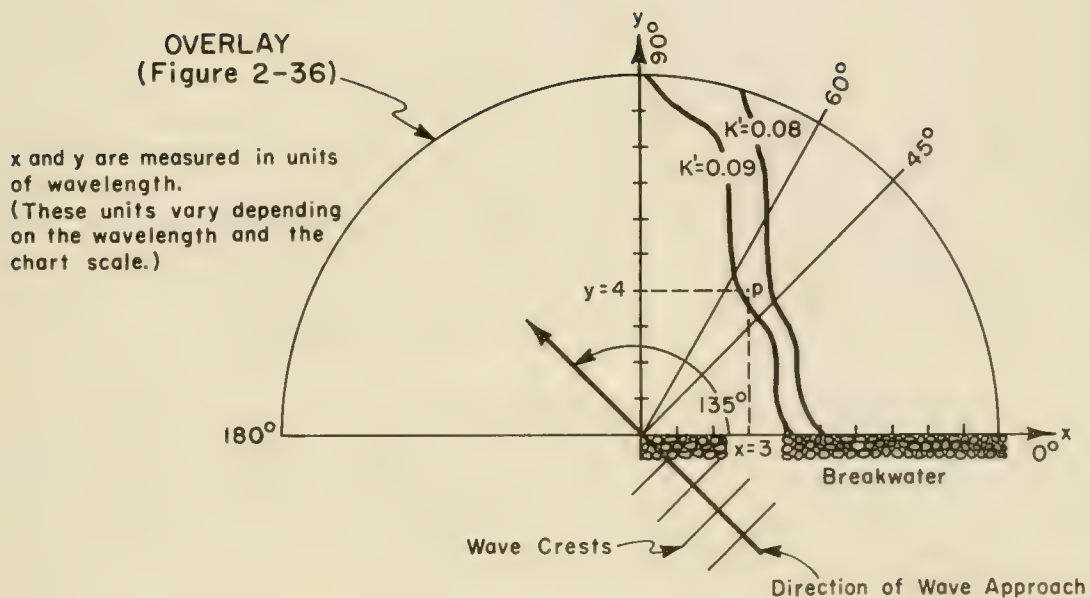
Figure 2-41.   Schematic Representation of Wave Diffraction Overlay

2.422 <u>Waves Passing a Gap of Width Less than Five Wavelengths at Normal</u>
<u>Incidence</u>. The solution of this problem is more complex than that for a
single breakwater, and it is not possible to construct a single diagram
for all conditions. A separate diagram must be drawn for each ratio of
gap width to wavelength B/L. The diagram for a B/L-ratio of 2 is shown
in Figure 2-42 which also illustrates its use. Figures 2-43 through 2-52
(Johnson, 1953) show lines of equal diffraction coefficient for B/L-ratios
of 0.50, 1.00, 1.41, 1.64, 1.78, 2.00, 2.50, 2.95, 3.82 and 5.00. A
sufficient number of diagrams have been included to represent most gap
widths encountered in practice. In all but Figure 2-48 (B/L = 2.00), the
wave ,crest lines have been omitted. Wave crest lines are usually of use
only for illustrative purposes. They are, however, required for an
accurate estimate of the combined effects of refraction and diffraction.
In such cases, wave crests may be approximated with sufficient accuracy
by circular arcs. For a single breakwater, the arcs will be centered on
the breakwater tip. That part of the wave crest extending into unprotected
water beyond the $K' = 0.5$ line may be approximated by a straight line.
For a breakwater gap, crests that are more than eight wavelengths behind
the breakwater may be approximated by an arc centered at the middle of
the gap; crests to about six wavelengths may be approximated by two arcs,
centered on the two ends of the breakwater and may be connected by a
smooth curve (approximated by a circular arc centered at the middle of
the gap). Only one-half of the diffraction diagram is presented on the
figures since the diagrams are symmetrical about the line x/L = 0.

2.423 <u>Waves Passing a Gap of Width Greater Than Five Wavelengths at</u>
<u>Normal Incidence</u>. Where the breakwater gap width is greater than five
wavelengths, the diffraction effects of each wing are nearly independent,
and the diagram (Figure 2-33) for a single breakwater with a 90° wave
approach angle may be used to define the diffraction characteristic in
the lee of both wings (See Figure 2-53.)

2.424 <u>Diffraction at a Gap-Oblique Incidence</u>. When waves approach at an
angle to the axis of a breakwater, the diffracted wave characteristics
differ from those resulting when waves approach normal to the axis. An
approximate determination of diffracted wave characteristics may be
obtained by considering the gap to be as wide as its projection in the
direction of incident wave travel as shown in Figure 2-54. Calculated
diffraction diagrams for wave approach angles of 0°, 15°, 30°, 45°, 60°
and 75° are shown in Figures 2-55, 56 and 57. Use of these diagrams will
give more accurate results than the approximate method. A comparison of
a 45° incident wave using the approximate method and the more exact diagram
method is shown in Figure 2-58.

2.43 <u>REFRACTION AND DIFFRACTION COMBINED</u>

      Usually the bottom seaward and shoreward of a breakwater is not
flat; therefore, refraction occurs in addition to diffraction. Although
a general unified theory of the two has not yet been developed, some in-
sight into the problem is presented by Battjes (1968). An approximate
picture of wave changes may be obtained by: (a) constructing a refraction
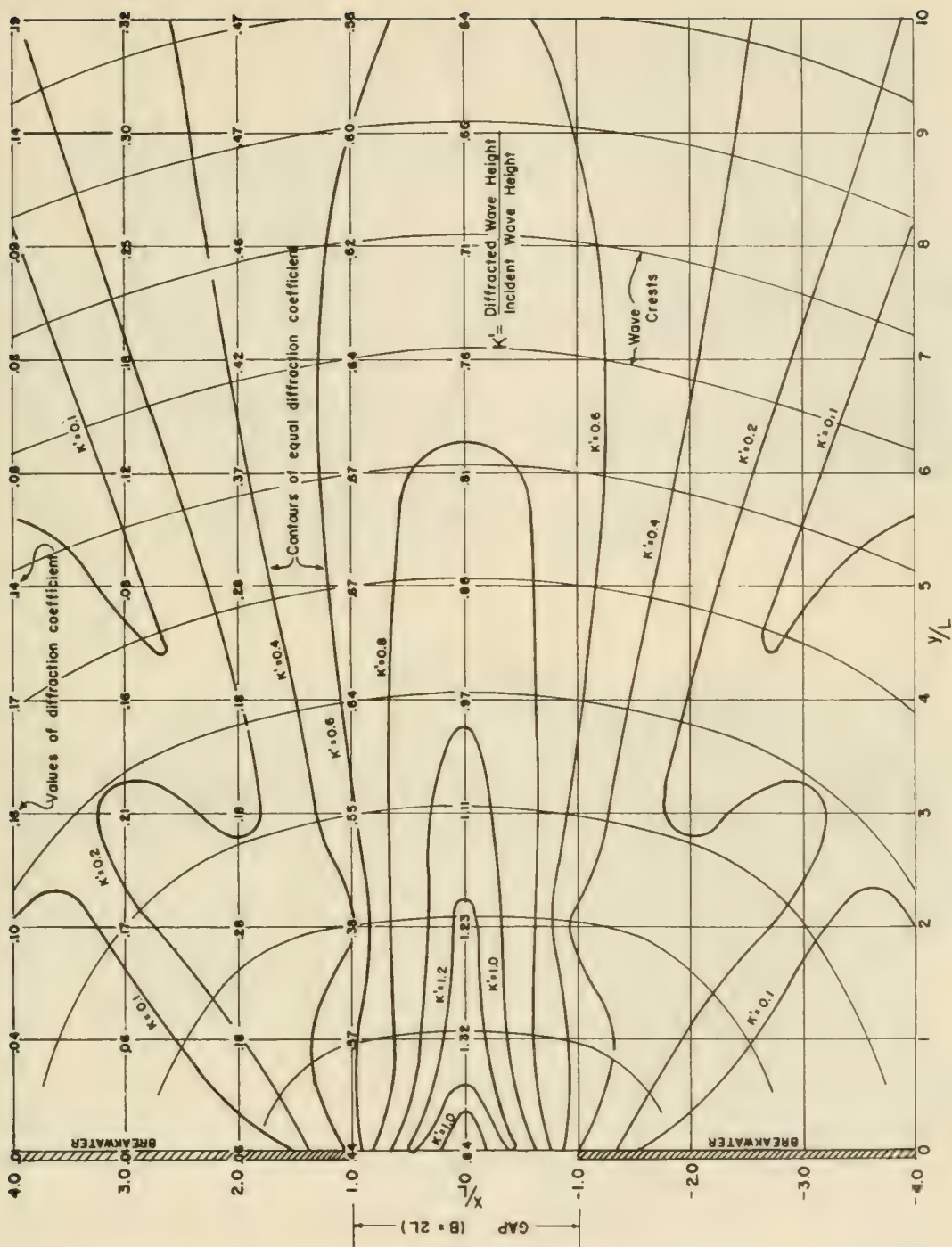
Figure 2-42. Generalized Diffraction Diagram for a Breakwater Gap Width of Two Wavelengths (B/L = 2)
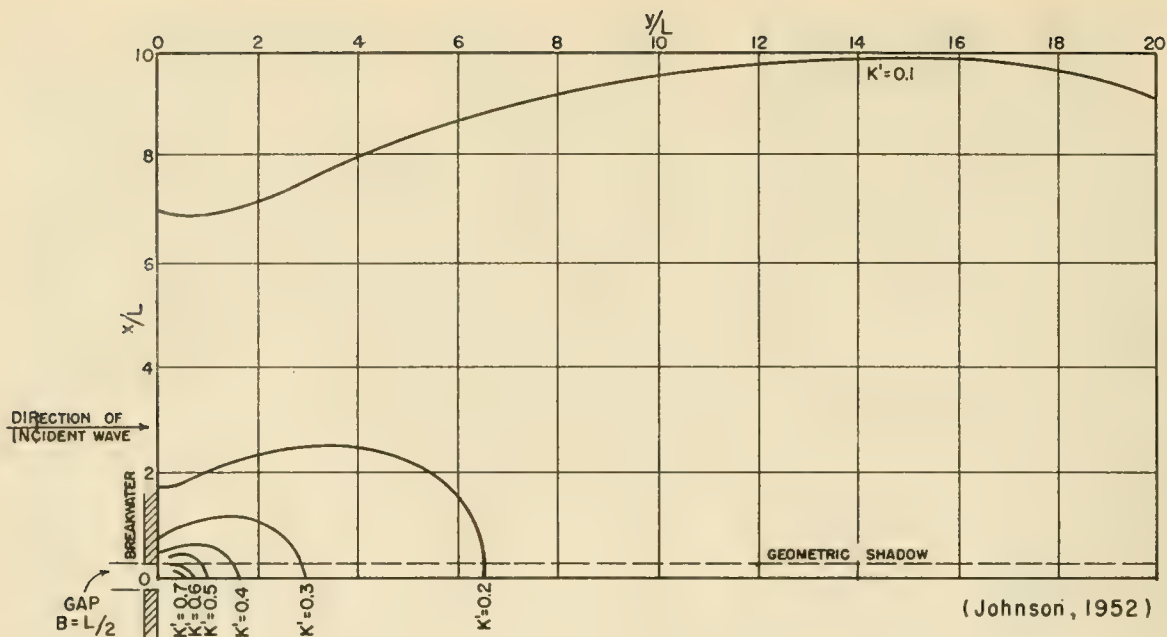
Figure 2-43. Contours of Equal Diffraction Coefficient
Gap Width = 0.5 Wave Length (B/L = 0.5)
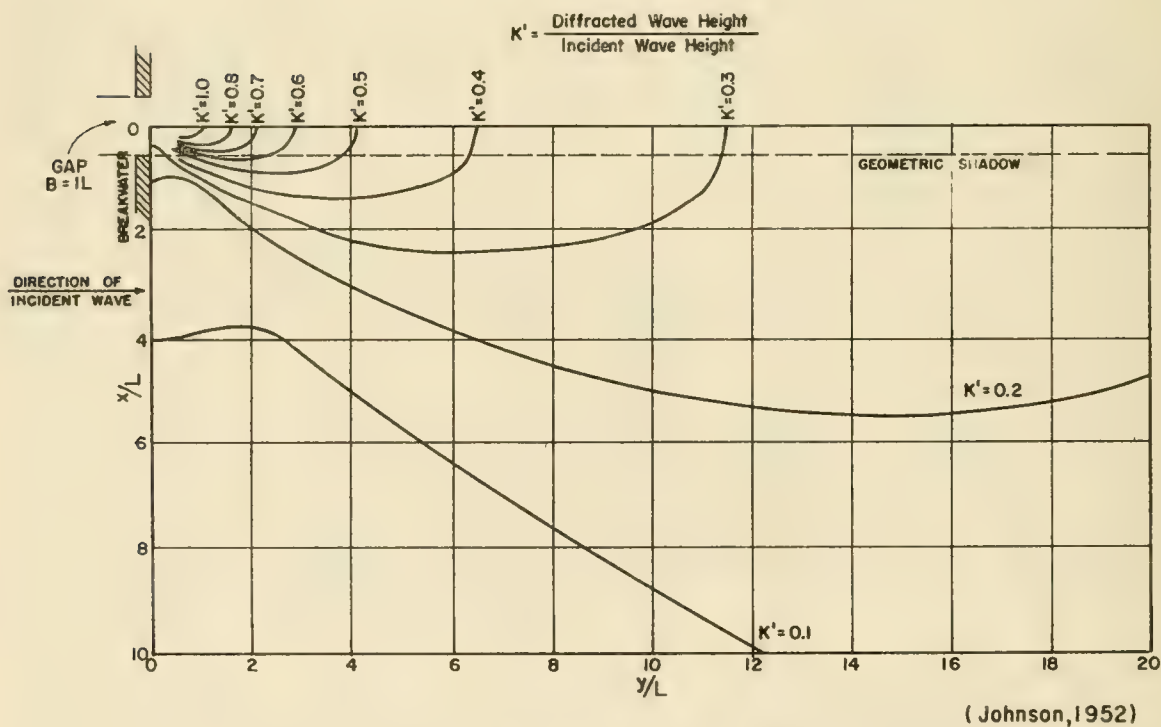
Figure 2-44. Contours of Equal Diffraction Coefficient
Gap Width = 1 Wave Length (B/L = 1)
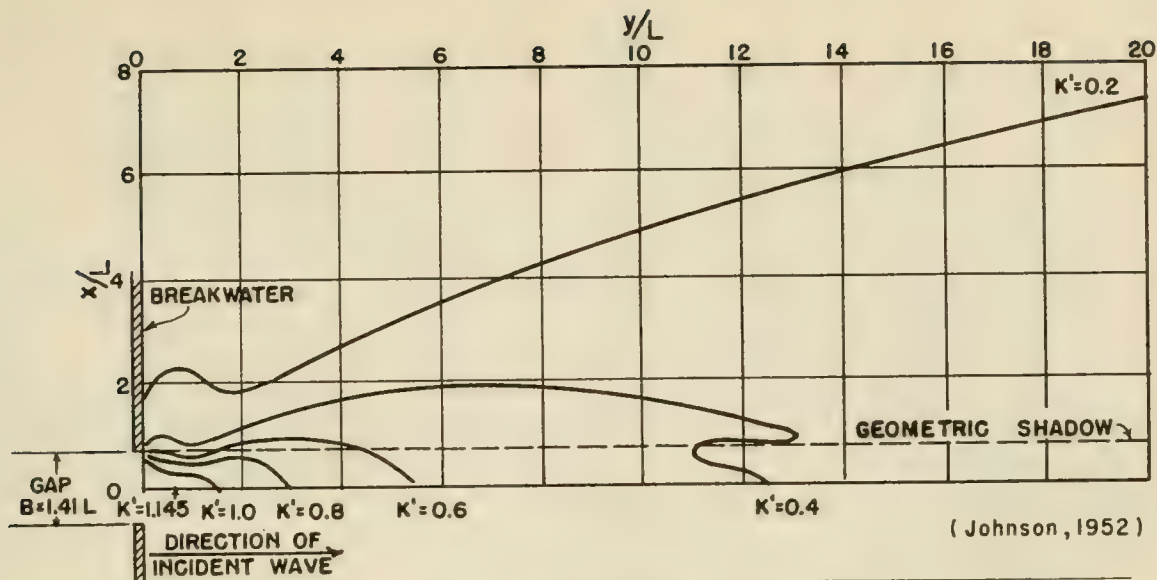
Figure 2-45. Contours of Equal Diffraction Coefficient
Gap Width = 1.41 Wave Lengths (B/L = 1.41)
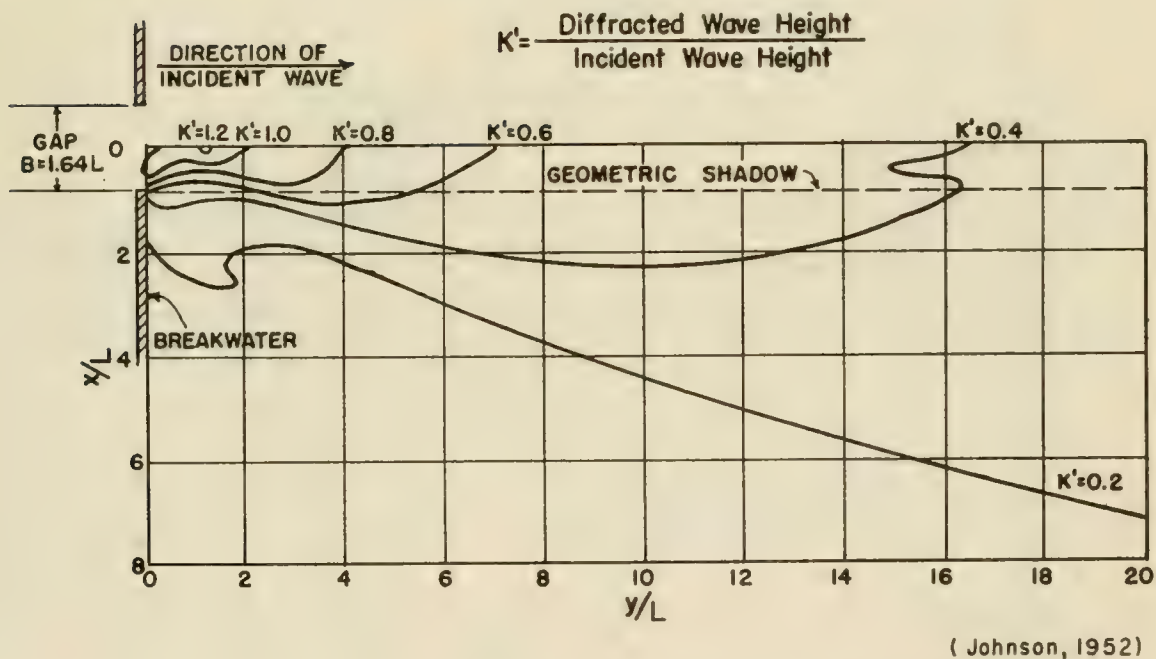
Figure 2-46. Contours of Equal Diffraction Coefficient
Gap Width = 1.64 Wave Lengths (B/L = 1.64)
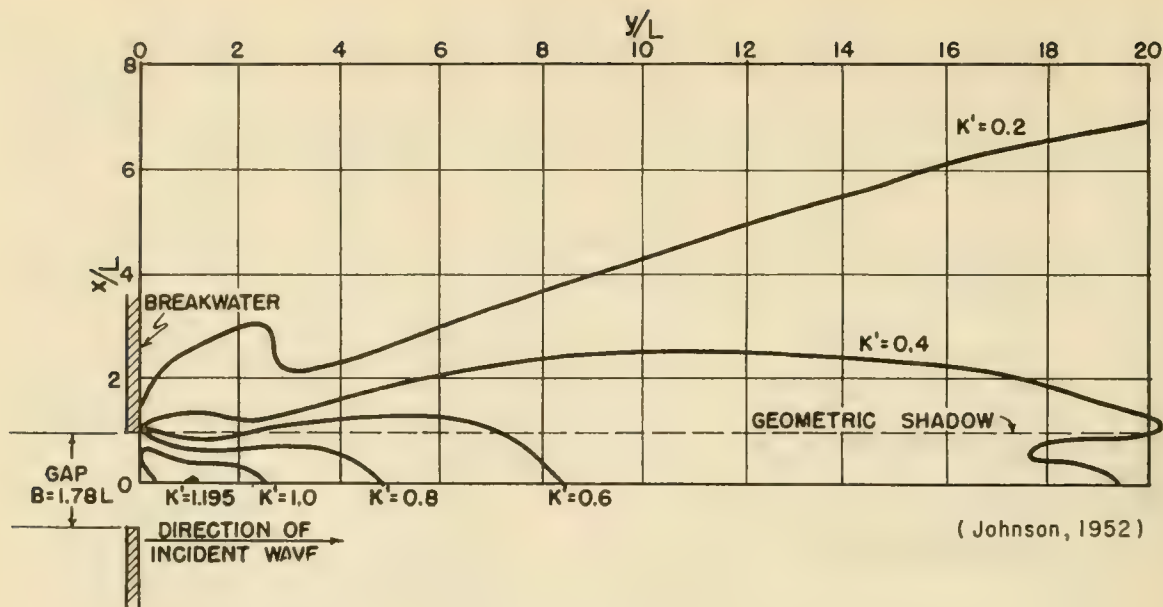
Figure 2-47.   Contours of Equal Diffraction Coefficient
              Gap Width = 1.78 Wave Lengths (B/L = 1.78)
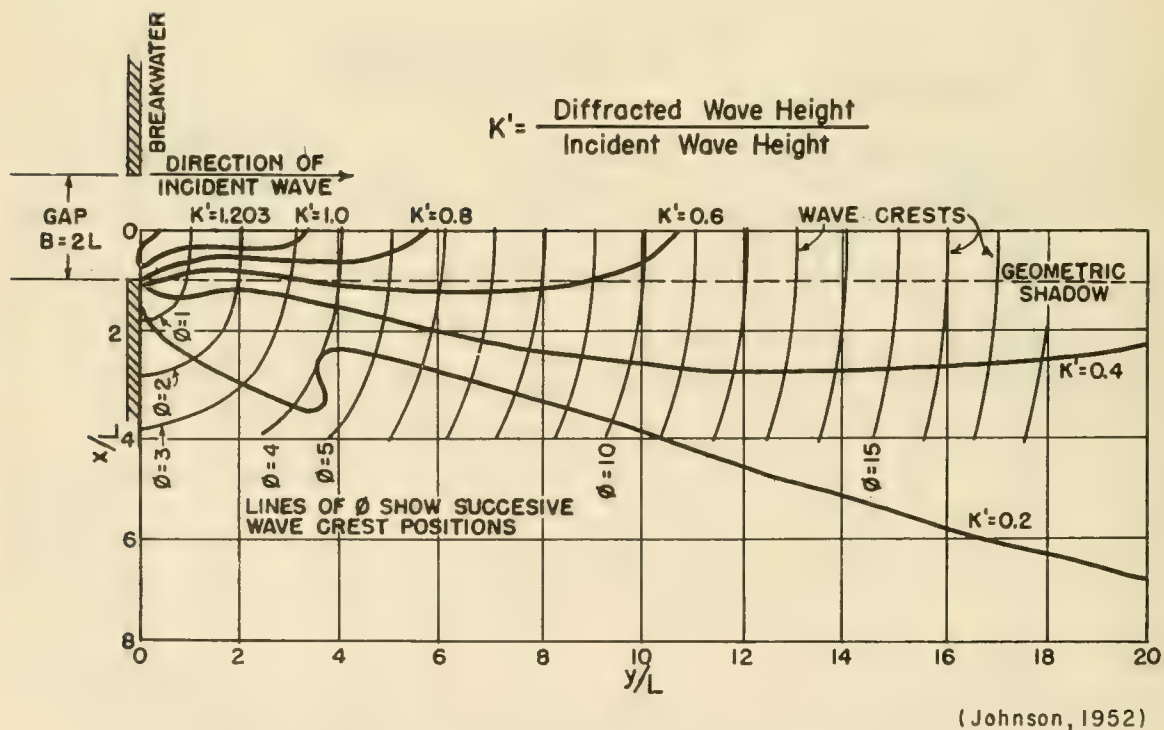
Figure 2-48.   Contours of Equal Diffraction Coefficient
              Gap Width = 2 Wave Lengths (B/L = 2)
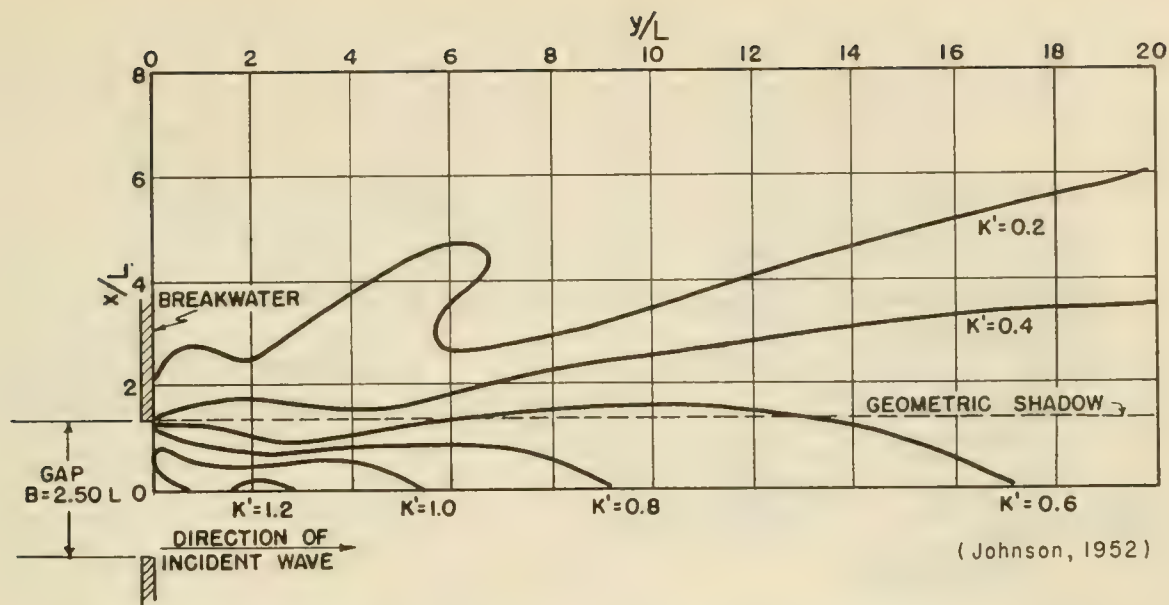
Figure 2-49. Contours of Equal Diffraction Coefficient
Gap Width = 2.50 Wave Lengths (B/L = 2.50)
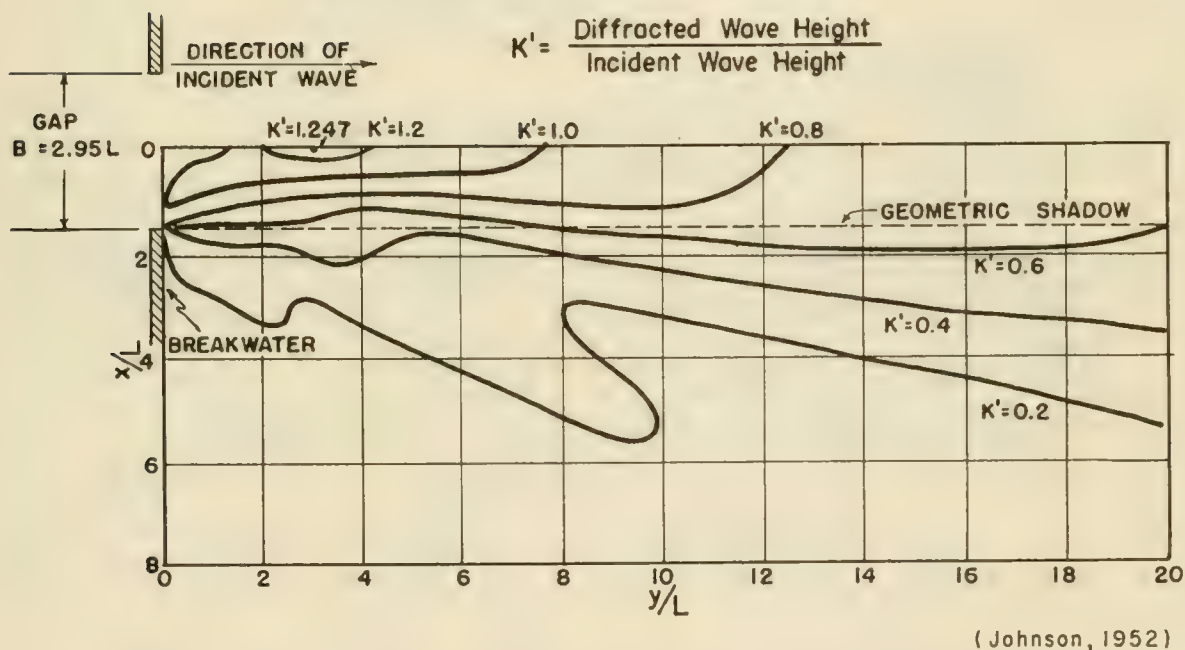
Figure 2-50. Contours of Equal Diffraction Coefficient
Gap Width = 2.95 Wave Lengths (B/L = 2.95)
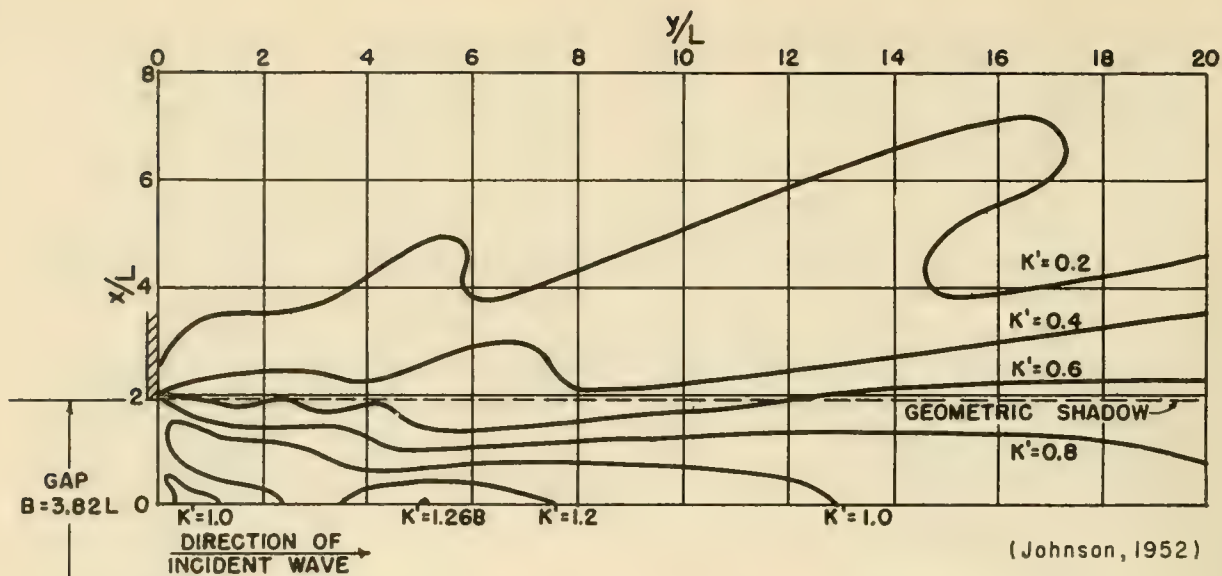
Figure 2-51. Contours of Equal Diffraction Coefficient
Gap Width = 3.82 Wave Lengths (B/L = 3.82)

$$K' = \frac{\text{Diffracted Wave Height}}{\text{Incident Wave Height}}$$
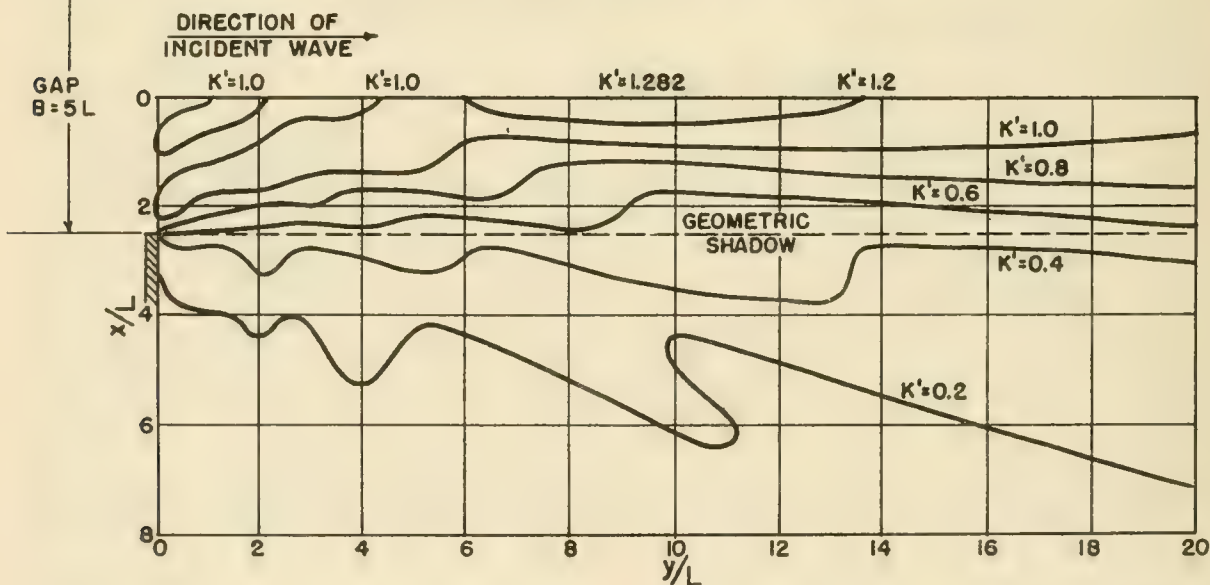
(Johnson, 1952)

Figure 2-52. Contours of Equal Diffraction Coefficient
Gap Width = 5 Wave Lengths (B/L = 5)

2-104
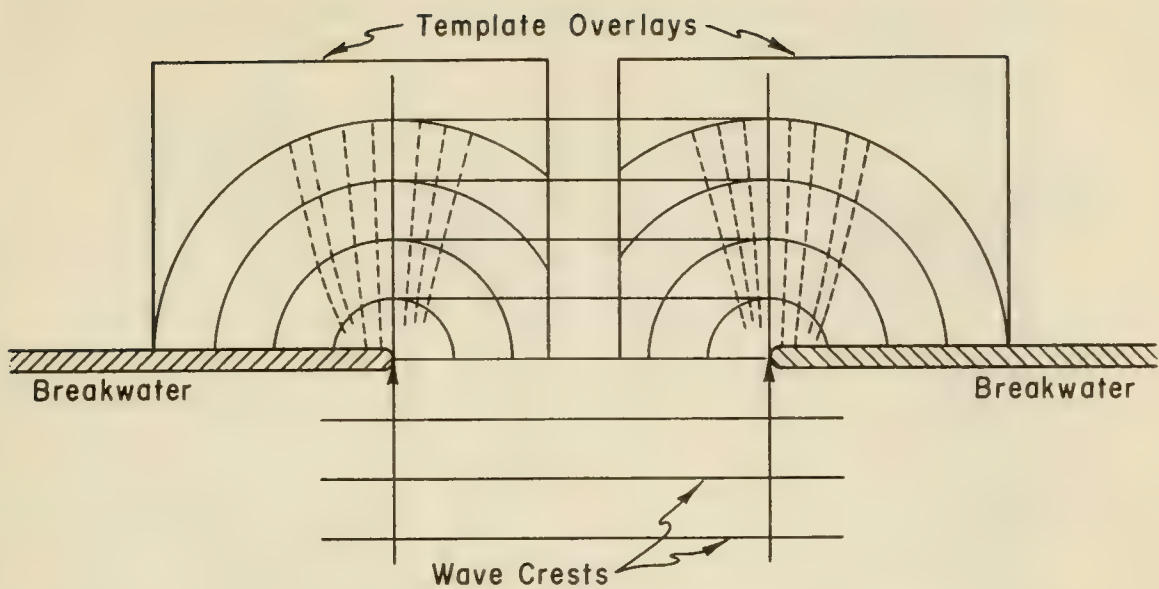
Figure 2-53.   Diffraction for a Breakwater Gap of Width > 5L (B/L > 5)
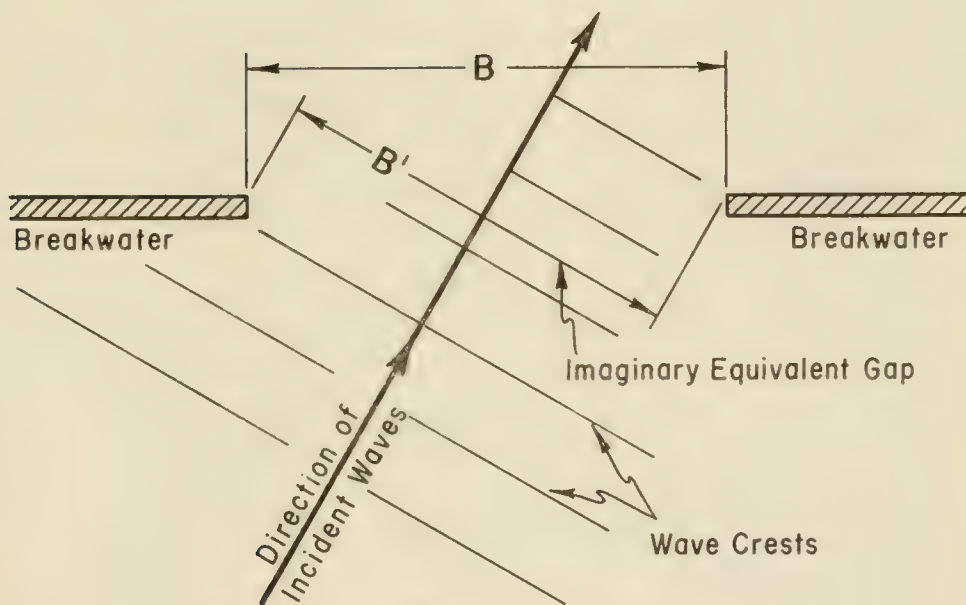
(Johnson, 1952)

Figure 2-54.   Wave Incidence Oblique to Breakwater Gap

2-105
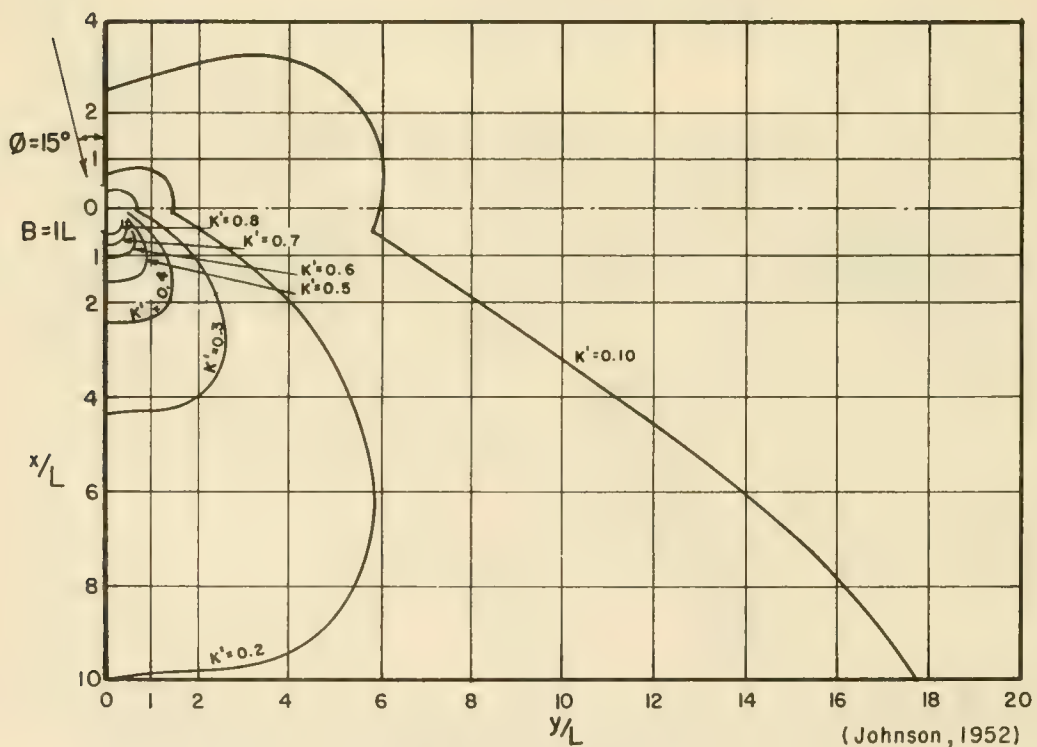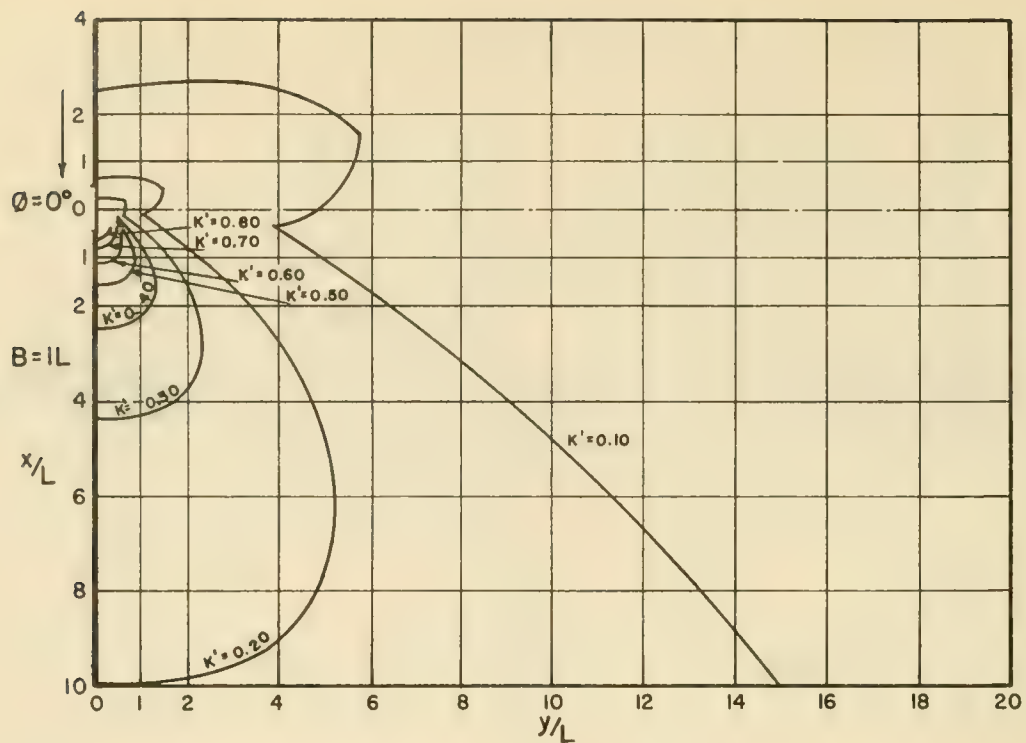
Figure 2-55. Diffraction for a Breakwater Gap of One Wave
Length Width (ϕ = 0 and 15°)
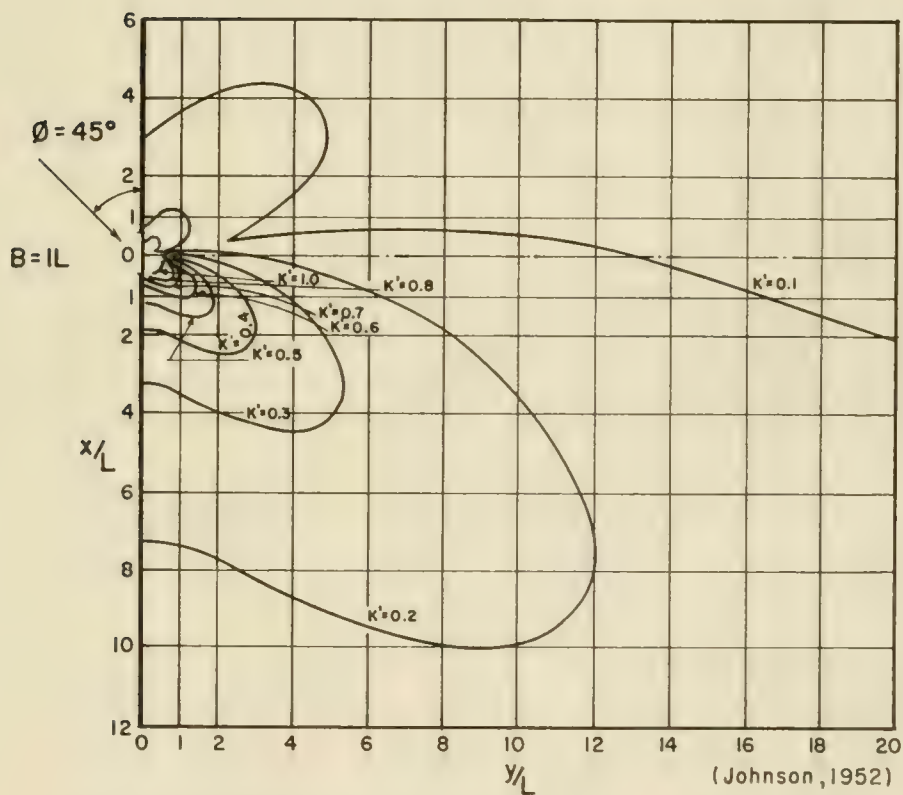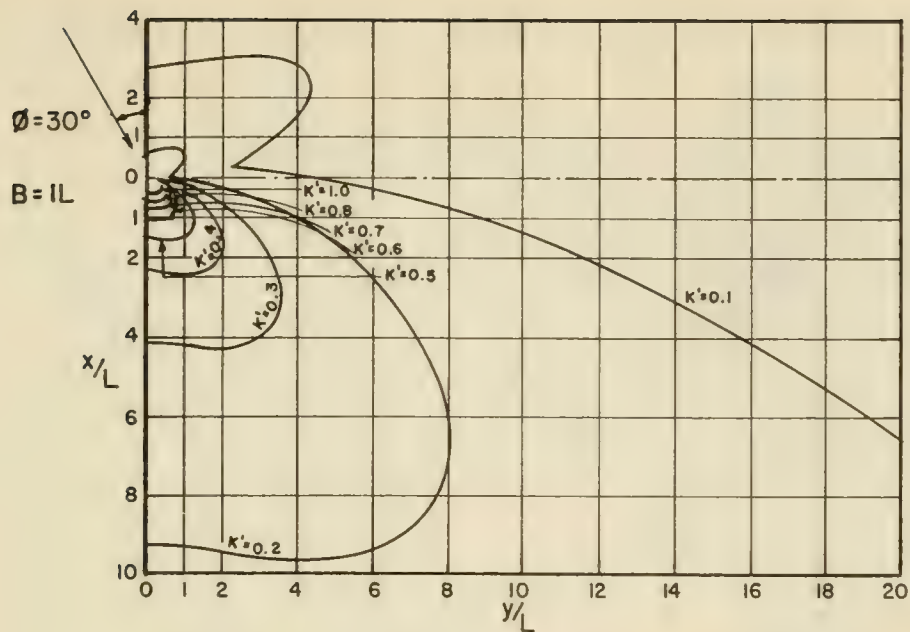
Figure 2-56. Diffraction for a Breakwater Gap of One
Wave Length Width (ϕ = 30 and 45°)

2-107
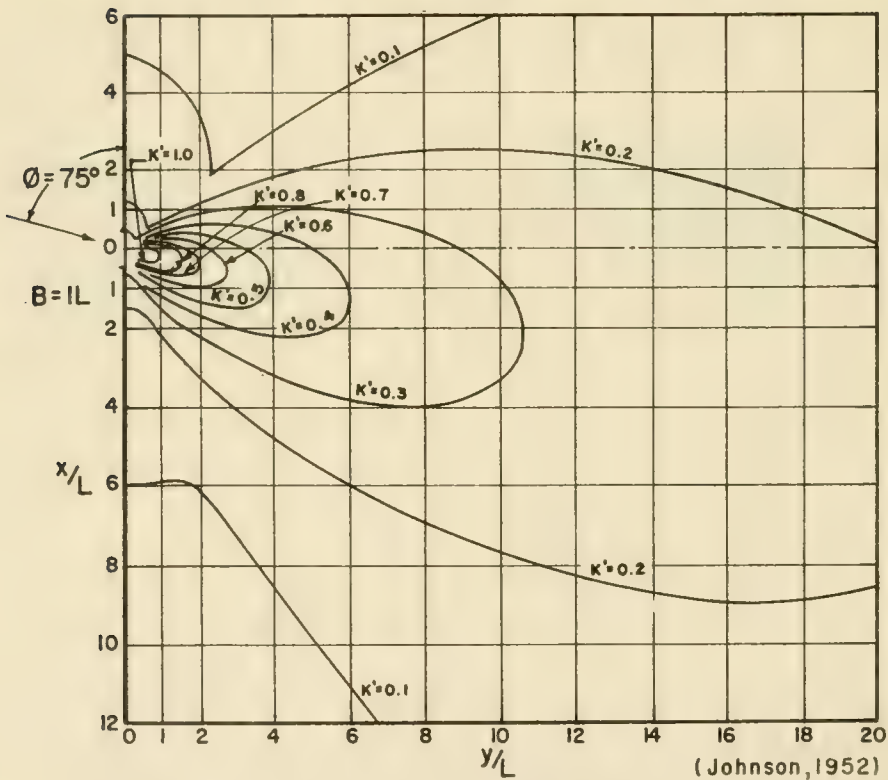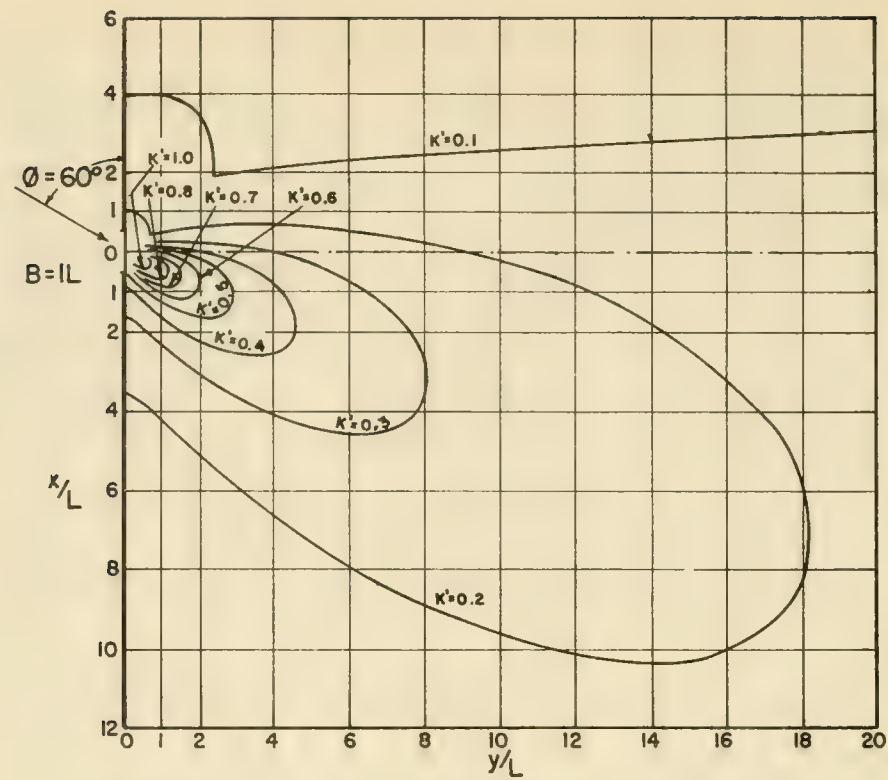
Figure 2-57.   Diffraction for a Breakwater Gap of One
Wavelength Width   (ϕ = 60 and 75°)

2-108
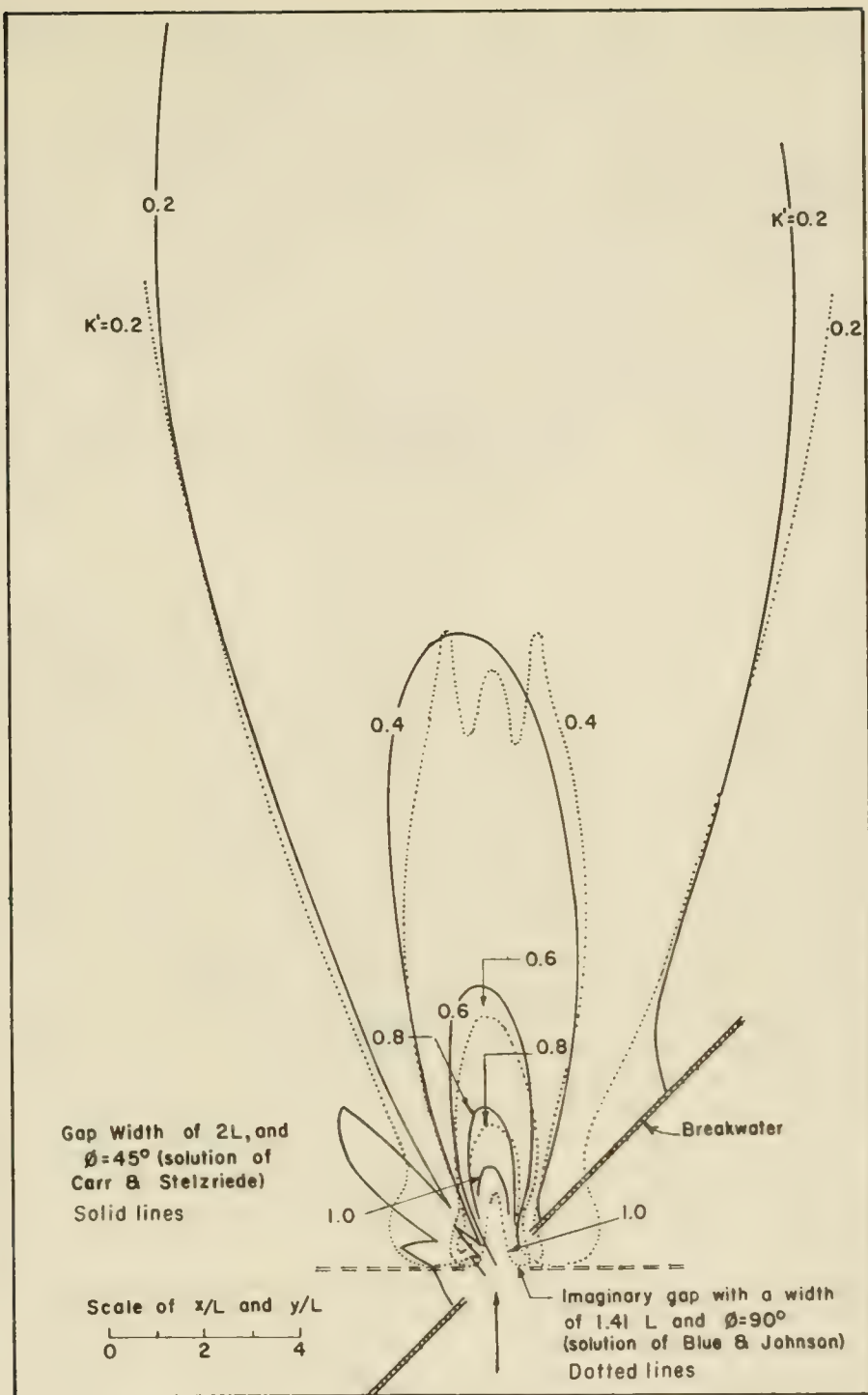
(Johnson, 1952)

Figure 2-58. Diffraction Diagram for a Gap of Two Wave
Lengths and a 45° Approach Compared with
That for a Gap Width $\sqrt{2}$ Wavelengths with
a 90° Approach

diagram shoreward to the breakwater; (b) at this point, constructing a diffraction diagram carrying successive crests three or four wavelengths shoreward, if possible; and (c) with the wave crest and wave direction indicated by the last shoreward wave crest determined from the diffraction diagram, constructing a new refraction diagram to the breaker line. The work of Mobarek (1962) on the effect of bottom slope on wave diffraction indicates that the method presented here is suitable for medium-period waves. For long-period waves the effect of shoaling (Section 2.32) should be considered. For the condition when the bottom contours are parallel to the wave crests, the sloping bottom probably has little effect on diffraction. A typical refraction-diffraction diagram and the method for determining combined refraction-diffraction coefficients are shown in Figure 2-59. When a wave crest is not of uniform height, as when a wave is undergoing refraction, a lateral flow of energy - wave diffraction - will occur along the wave crest. Therefore diffraction can occur without the wave moving past a structure although the diffraction effects are visually more dramatic at the structure.

2.5   WAVE REFLECTION

2.51   GENERAL

Water waves may be either partially or totally reflected from both natural and manmade barriers. (See Figure 2-60.) Wave reflection may often be as important a consideration as refraction and diffraction in the design of coastal structures, particularly for structures associated with development of harbors. Reflection of waves implies a reflection of wave energy as opposed to energy dissipation. Consequently, multiple reflections and absence of sufficient energy dissipation within a harbor complex can result in a buildup of energy which appears as wave agitation and surging in the harbor. These surface fluctuations may cause excessive motion of moored ships and other floating facilities, and result in the development of great strains on mooring lines. Therefore seawalls, bulkheads and revetments inside of harbors should dissipate rather than reflect incident wave energy whenever possible. Natural beaches in a harbor are excellent wave energy dissipaters and proposed harbor modifications which would decrease beach areas should be carefully evaluated prior to construction. Hydraulic model studies are often necessary to evaluate such proposed changes. The importance of wave reflection and its effect on harbor development are discussed by Bretschneider (1966), Lee (1964), and LeMehaute (1965); harbor resonance is discussed by Raichlen (1965).

A measure of how much a barrier reflects waves is given by the ratio of the reflected wave height H_r, to the incident wave height H_i, which is termed the reflection coefficient χ; hence $\chi = H_r/H_i$. The magnitude of χ varies from 1.0 for total reflection to 0 for no reflection; however, a small value of χ does not necessarily imply that wave energy is dissipated by a structure since energy may be transmitted through such structures as permeable, rubble-mound breakwaters. A transmission coefficient may be defined as the ratio of transmitted wave height H_t, to incident wave height H_i. In general, both the reflection coefficient
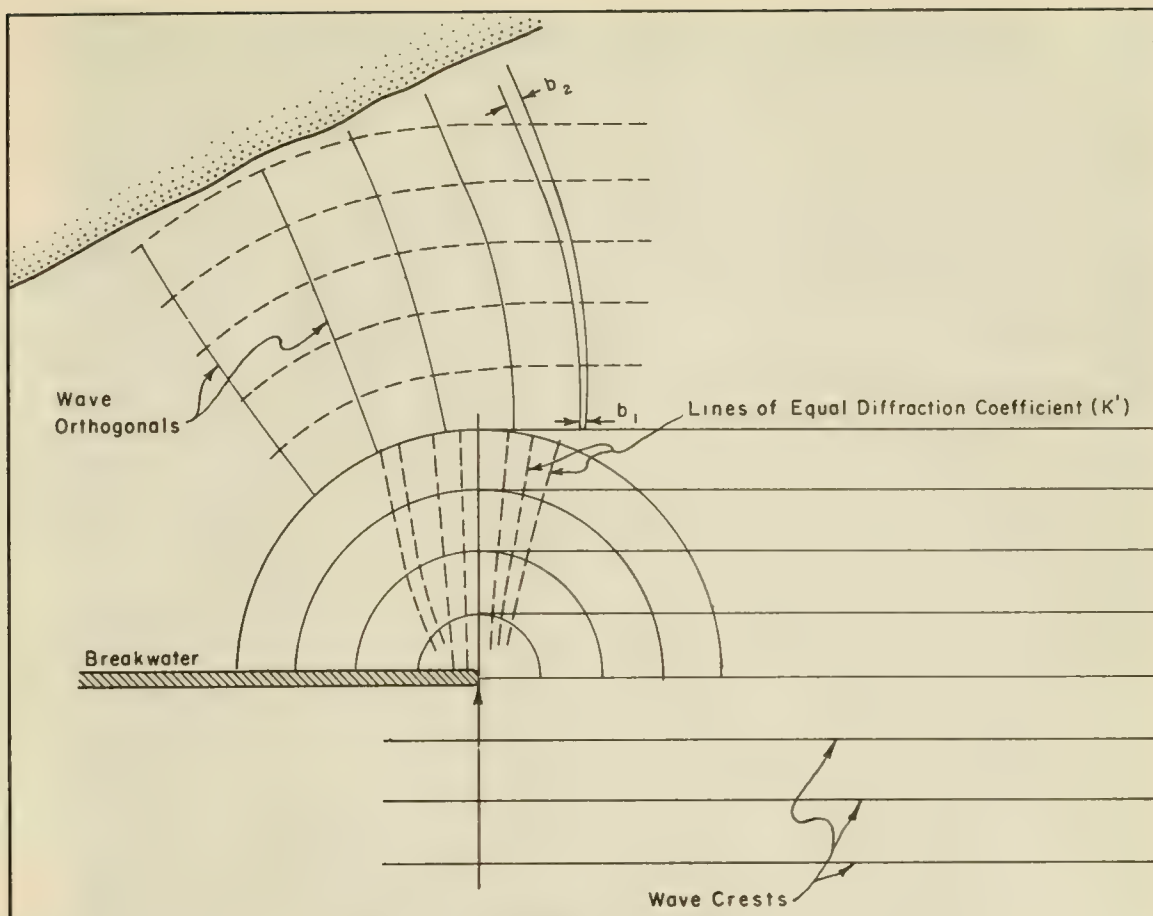
Over-all refraction–diffraction coefficient is given
   by $(K_R) (K^I) \sqrt{b_1 / b_2}$
Where K_R = Refraction coefficient to breakwater.
    K^I = Diffraction coefficient at point on
        diffracted wave crest from which
        orthogonal is drawn.
    b_1 = Orthogonal spacing at diffracted wave
        crest.
    b_2 = Orthogonal spacing nearer shore.

Figure 2-59. Single Breakwater - Refraction - Diffraction Combined
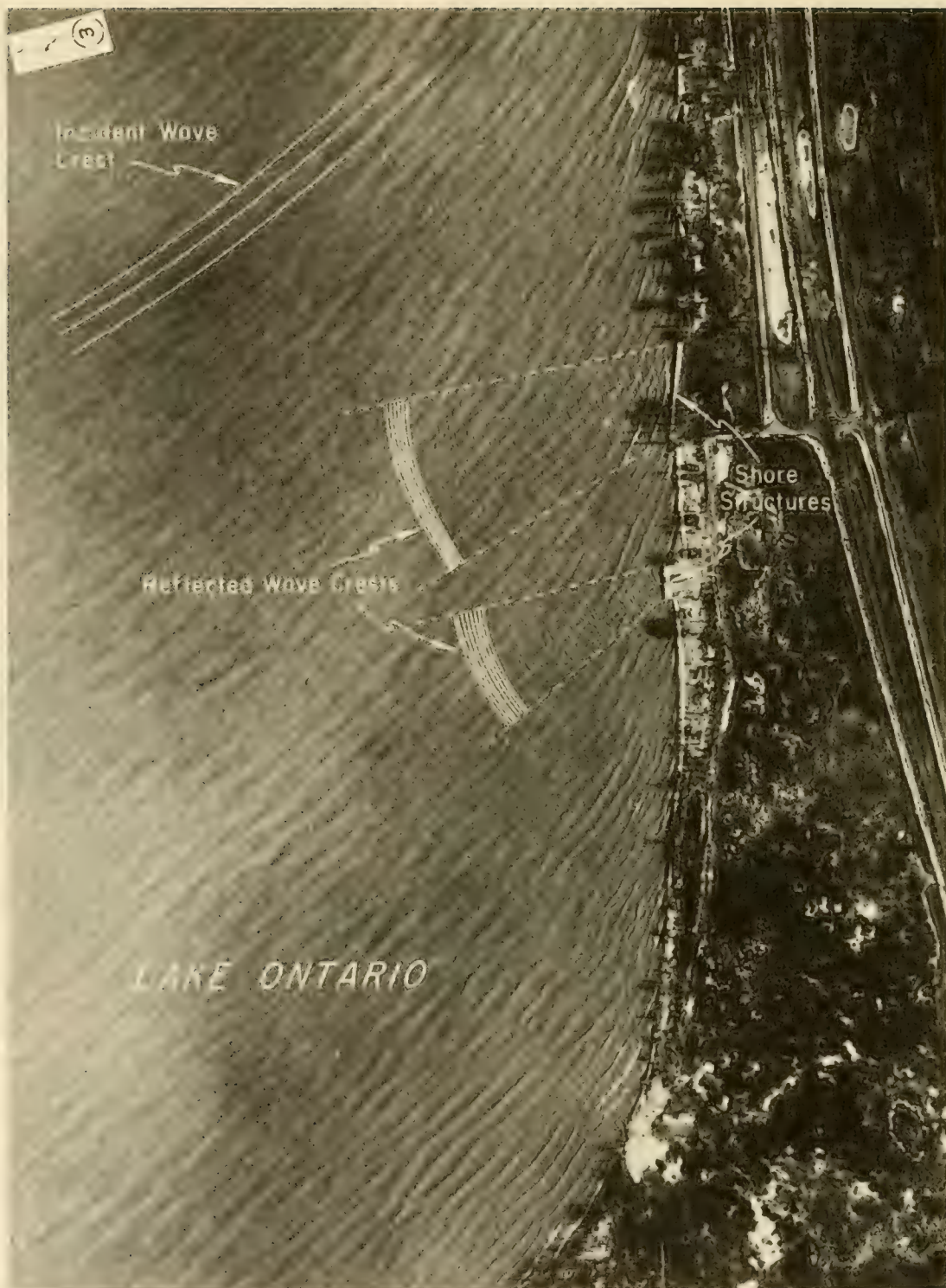
December 1952

Figure 2-60. Wave Reflection at Hamlin Beach, New York

2-112

and the transmission coefficient will depend upon the geometry and composition of a structure and the incident wave characteristics such as wave steepness and relative depth d/L, at the structure site.

2.52 REFLECTION FROM IMPERMEABLE, VERTICAL WALLS (LINEAR THEORY)

Impermeable vertical walls will reflect almost all incident wave energy unless they are fronted by rubble toe protection or are extremely rough. The reflection coefficient χ is therefore equal to approximately 1.0 and the height of a reflected wave will be equal to the height of the incident wave. Although some experiments with smooth, vertical, impermeable walls appear to show a significant decrease of χ with increasing wave steepness, Domzig (1955), Goda and Abe (1968) have shown that this paradox probably results from the experimental technique, based on linear wave theory, used to determine χ. The use of a higher order theory to describe the water motion in front of the wall gives a reflection coefficient of 1.0 and satisfies the conservation of energy principle.

Wave motion in front of a perfectly reflecting vertical wall subjected to monochromatic waves moving in a direction perpendicular to the barrier can be determined by superposing two waves with identical wave numbers, periods and amplitudes but traveling in opposite directions. The water surface of the incident wave is given to a first order (linear) approximation by Equation 2-10,

$$\eta_i = \frac{H_i}{2} \cos \left(\frac{2\pi x}{L} - \frac{2\pi t}{T} \right),$$

(2-10)

and the reflected wave by,

$$\eta_r = \frac{H_r}{2} \cos \left(\frac{2\pi x}{L} + \frac{2\pi t}{T} \right).$$

Consequently, the water surface is given by the sum of η_i and η_r or, since $H_i = H_r$,

$$\eta = \eta_i + \eta_r = \frac{H_i}{2} \left[\cos \left(\frac{2\pi x}{L} - \frac{2\pi t}{T} \right) + \cos \left(\frac{2\pi x}{L} + \frac{2\pi t}{T} \right) \right],$$

which reduces to

$$\eta = H_i \cos \frac{2\pi x}{L} \cos \frac{2\pi t}{T}.$$

(2-79)

Equation 2-79 represents the water surface for a standing wave or *clapotis* which is periodic in time and in x having a maximum height of $2H_i$ when both $\cos(2\pi x/L)$ and $\cos(2\pi t/T)$ equal 1. The water surface profile as a function of $2\pi x/L$ for several values of $2\pi t/T$ are shown in Figure 2-61. There are some points (nodes) on the profile where the water surface
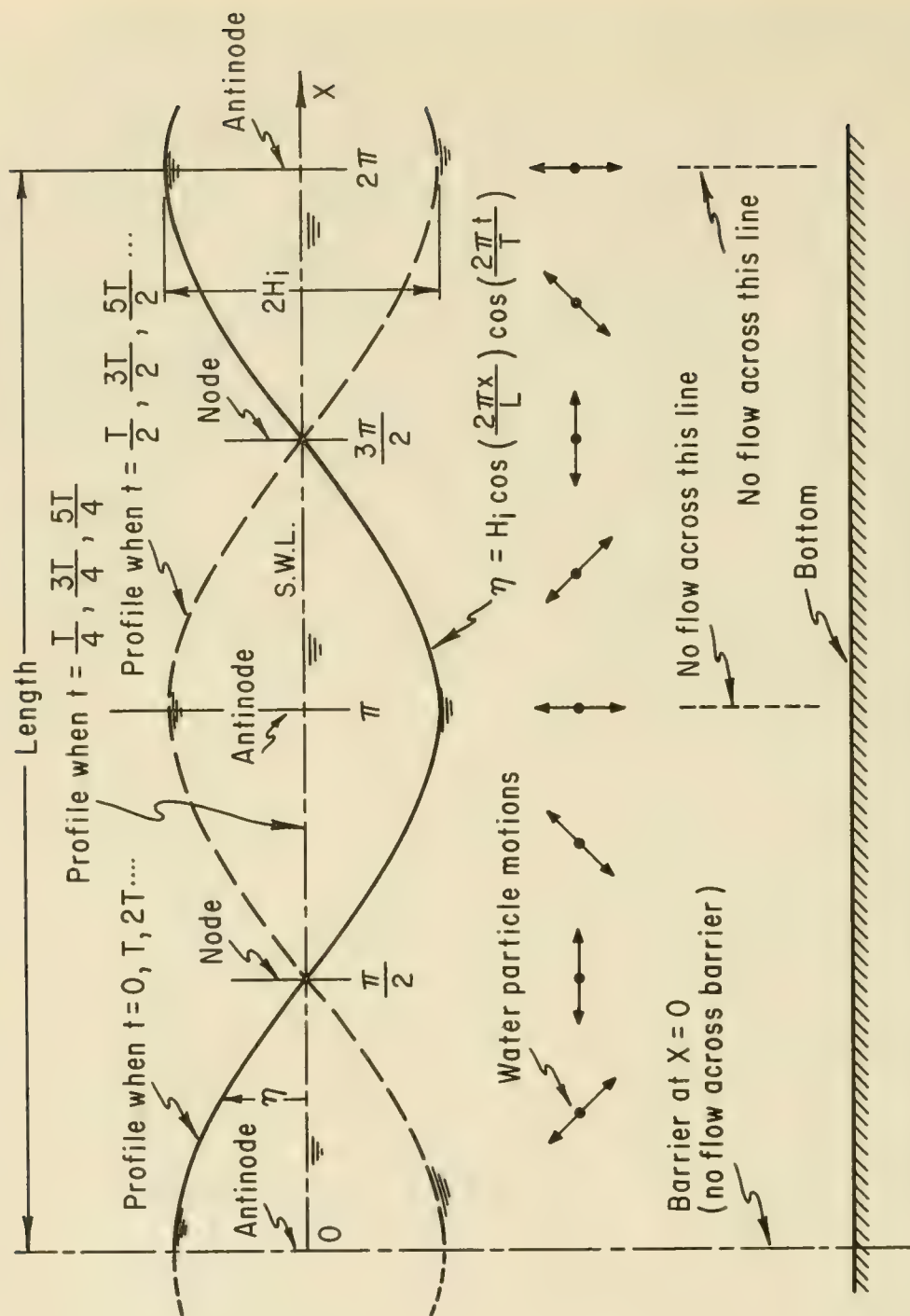
Figure 2-61. Standing Wave (Clapotis) System - Perfect Reflection from a Vertical Barrier - Linear Theory

2-114

remains at the SWL for all values of t and other points (antinodes) where
the water particle excursion at the surface is $2 H_i$ or twice the incident
wave height. The equations describing the water particle motion show that
the velocity is always horizontal under the nodes and always vertical under
the antinodes. At intermediate points, the water particles move along
diagonal lines as shown in Figure 2-61. Since water motion at the anti-
nodes is purely vertical, the presence of a vertical wall at any antinode
will not change the flow pattern described since there is no flow across
the vertical barrier and equivalently, there is no flow across a vertical
line passing through an antinode. (For the linear theory discussion here,
the water contained between any two antinodes will remain between those
two antinodes.) Consequently, the flow described here is valid for a
barrier at $2\pi x/L = 0$ (x = 0) since there is an antinode at that location.

2.53   REFLECTIONS IN AN ENCLOSED BASIN

Some insight can be obtained about the phenomenon of the resonant
behavior of harbors and other enclosed bodies of water by examining the
standing wave system previously described. The possible resonant oscillat-
tions between two vertical walls can be described by locating the two
barriers so that they are both at antinodes; for example, barriers at
x = 0 and π or x = 0 and 2π, etc. represent possible modes of oscillation.
If the barriers are taken at x = 0 and x = π,   there is one-half of a wave
in the basin or, if ℓ_B is the basin length, $\ell_B = L/2$. Since the wave-
length is given by Equation 2-4

$$ L = \frac{gT^2}{2\pi} \tanh \left(\frac{2\pi d}{L} \right) , $$

the period of this fundamental mode of oscillation is,

$$ T = \left[\frac{4\pi \ell_B}{g \tanh \left(\pi d/\ell_B \right)} \right]^{\frac{1}{2}} \tag{2-80} $$

The next possible resonant mode occurs when there is one complete wave in
the basin (barriers at x = 0 and x = 2π) and the next mode when there are
3/2 waves in the basin (barriers at x = 0 and x = $3\pi/2$, etc. In general,
$\ell_B = jL/2$, where j = 1, 2, ... In reality, the length of a natural or
manmade basin ℓ_B, is fixed and the wavelength of the resonant wave con-
tained in the basin will be the variable; hence,

$$ L = \frac{2\ell_B}{j} \quad j = 1, 2, \cdots , \tag{2-81} $$

may be thought of as defining the wavelengths capable of causing resonance
in a basin of length ℓ_B. The general form of Equation 2-80 is found by

substituting Equation 2-81 into the expression for the wavelength; there-
fore,

$$T_j = \left[\frac{4\pi \ell_B}{jg \, \tanh \, (\pi j d / \ell_B)}\right]^{1/2} , \; j = 1, 2, \cdots \cdot \qquad (2\text{-}82)$$

For an enclosed harbor, of approximately rectangular planform with length,
ℓ_B, waves entering through a breakwater gap having a predominant period
close to one of those given by Equation 2-82 for small values of j, may
cause significant agitation unless some effective energy dissipation
mechanism is present. The addition of energy to the basin at the resonant
(or excitation) frequency $(f_j = 1/T_j)$ is said to *excite* the basin.

Equation 2-82 was developed by assuming the end boundaries to be
vertical; however, it is still approximately valid so long as the end
boundaries remain highly reflective to wave motion. Sloping boundaries,
such as beaches, while usually effective energy dissipaters, may be signifi-
cantly reflective if the incident waves are extremely long. The effect of
sloping boundaries and their reflectivity to waves of differing character-
istics is given in Section 2.54, Wave Reflection from Beaches.

Long-period resonant oscillations in large lakes and other large
enclosed bodies of water are termed *seiches*. The periods of seiches may
range from a few minutes up to several hours, depending upon the geometry
of the particular basin. In general, these basins are shallow with respect
to their length; hence, tanh $(\pi j d / \ell_B)$ in Equation 2-82 becomes approximately
equal to $\pi j d / \ell_B$ and

$$T_j = \frac{2\ell_B}{j} \frac{1}{(gd)^{1/2}} \quad j = 1, 2, \cdots \cdot \text{ (small values)} . \qquad (2\text{-}83)$$

Equation 2-83 is termed Merian's equation. In natural basins, complex
geometry and variable depth will make the direct application of Equation
2-83 difficult; however, it may serve as a useful first approximation for
enclosed basins. For basins open at one end, different modes of oscilla-
tion exist since resonance will occur when a node is at the open end of
the basin and the fundamental oscillation occurs when there is one quarter
of a wave in the basin; hence, $\ell_{B'} = L/4$ for the fundamental mode and
$T = 4\ell_B / \sqrt{gd}$. In general $\ell_{B'} = (2j - 1)L/4$, and

$$T_j = \frac{4\ell_{B'}}{(2_j - 1)} \frac{1}{(gd)^{1/2}} \quad j = 1, 2, \cdots \cdot \text{ (small values)} . \qquad (2\text{-}84)$$

Note that higher modes occur when there are 3, 5, ..., $2_j - 1$, etc.,
quarters of a wave within the basin.

GIVEN: Lake Erie has a mean depth of d = 61 feet and its length ℓ_B is 220 miles or 116,160 feet.

FIND: The fundamental period of oscillation T_j, if j = 1.

SOLUTION: From Equation 2-83 for an enclosed basin,

$$T_1 = \frac{2\ell_B}{j} \frac{1}{(gd)^{1/2}}$$

$$T_1 = \frac{2(116,160)}{1} \frac{1}{[32.2(61)]^{1/2}}$$

$$T_1 = 52,420 \text{ sec. or } 14.56 \text{ hrs.}$$

Considering the variability of the actual lake cross-section, this result is surprisingly close to the actual observed period of 14.38 hours (Platzman and Rao, 1963). Such close agreement may not always result.

* *

Note: Additional discussion of seiching is presented in Section 3.84.

2.54 WAVE REFLECTION FROM BEACHES

The amount of wave energy reflected from a beach depends upon the roughness, permeability and slope of the beach in addition to the steepness and angle of approach of incident waves. Miche (1951) assumed that the reflection coefficient for a beach χ, could be described as the product of two factors by the expression,

$$\chi = \chi_1 \chi_2 , \qquad\qquad (2-85)$$

where χ_1 depends on the roughness and permeability of the beach and is independent of the slope, while χ_2 depends on the beach slope and the wave steepness.

Based on measurements made by Schoemaker and Thijsse (1949), Miche found that $\chi_1 \approx 0.8$ for smooth impervious beaches. A value of $\chi_1 \approx 0.3$

to 0.6 has been recommended for rough slopes and step-faced structures. The second factor χ_2 is given by

$$\chi_2 = \begin{cases} \dfrac{H_o/L_o \,_{max}}{H_o/L_o} \quad , \left(\dfrac{H_o}{L_o}\right) > \left(\dfrac{H_o}{L_o}\right)_{max} & (2\text{-}86a) \\[20pt] 1 \qquad , \left(\dfrac{H_o}{L_o}\right) \leq \left(\dfrac{H_o}{L_o}\right)_{max} & (2\text{-}86b) \end{cases}$$

where $(H_o/L_o)_{max}$ is constant for a particular beach slope and is given by

$$\left(\frac{H_o}{L_o}\right)_{max} = \left(\frac{2\beta}{\pi}\right)^{\frac{1}{2}} \frac{\sin^2\beta}{\pi} \quad , \tag{2-87}$$

in which β is the angle the beach makes with the horizontal (tan β = beach slope), and H_o/L_o is the incident wave steepness in deep water. $(H_o/L_o)_{max}$ can be considered a cut-off steepness; waves steeper than $(H_o/L_o)_{max}$ will be only partially reflected while waves with a steepness less than $(H_o/L_o)_{max}$ will be almost totally reflected. Equation 2-87 is given in graphical form in Figure 2-62, and Equation 2-86 is shown in Figure 2-63. These equations and figures are valid for impervious beaches with waves approaching at a right angle to the beach.

* * * * * * * * * * * * * *   EXAMPLE PROBLEM   * * * * * * * * * * * * * * *

GIVEN: A wave with a period of T = 10 second, and a deepwater height of H_O = 5 feet impinges on an impermeable revetment with a slope of tan β = 0.20.

FIND:

(a) Determine the reflection coefficient x.

(b) What will be the steepest incident wave almost totally reflected from the given revetment?

SOLUTION. Calculate:

$$\tan \beta = 0.20; \quad \frac{1}{\tan \beta} = 5.0 = \cot \beta$$

$$L_o = \frac{gT^2}{2\pi} = \frac{32.2(100)}{2\pi} = 512 \text{ feet.}$$

$$\frac{H_o}{L_o} = \frac{5}{512} = 0.00975 \approx 0.01 \ .$$

2-118

Figure 2-62. $(H_0/L_0)_{max}$ Versus Beach Slope

The figure contains the equation:

$$\left(\frac{H_0}{L_0}\right)_{max} = \sqrt{\frac{2\beta}{\pi}} \frac{\sin^2\beta}{\pi}$$

x-axis: $\text{cotangent } \beta = \frac{1}{\text{tangent } \beta}$

(after Miche, 1951)
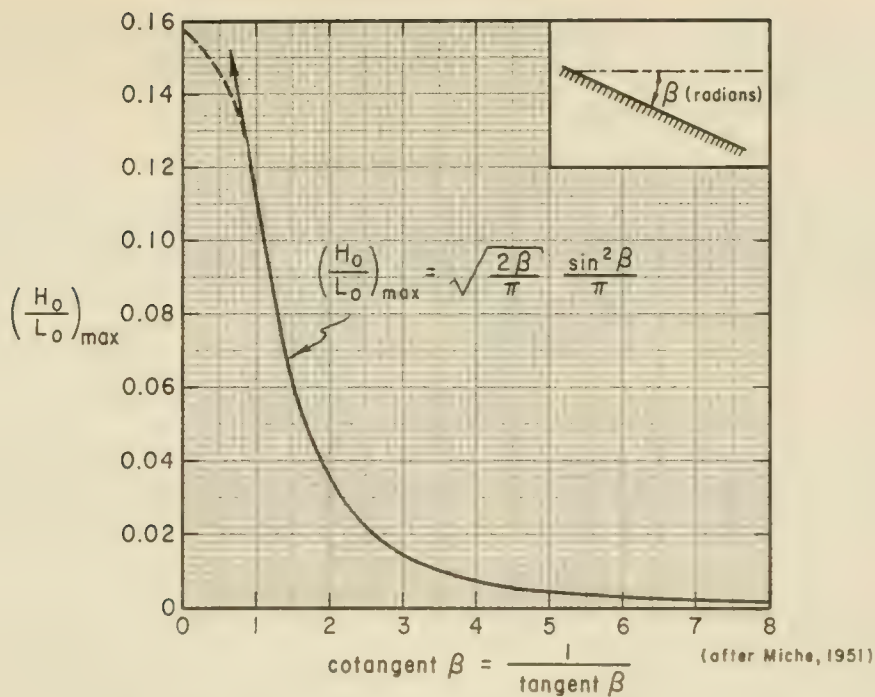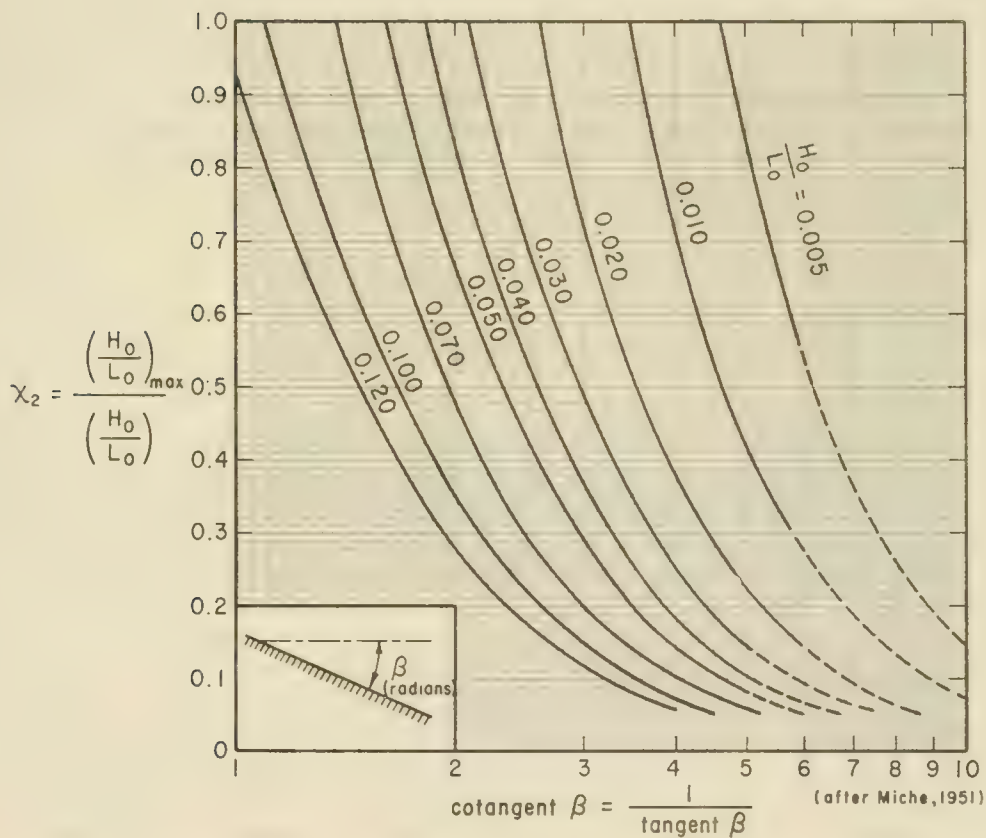
Figure 2-63. X_2 Versus Beach Slope for Various Values of H_0/L_0

y-axis: $X_2 = \dfrac{\left(\dfrac{H_0}{L_0}\right)_{max}}{\left(\dfrac{H_0}{L_0}\right)}$

x-axis: $\text{cotangent } \beta = \frac{1}{\text{tangent } \beta}$

(after Miche, 1951)

2-119

Entering Figure 2-63 with cot β = 5, and using the curve for H_O/L_O = 0.01, a value of χ_2 = 0.41 is found. Assuming that since the beach is impermeable, χ_1 = 0.8 and

$$\chi = \chi_1 \, \chi_2 = 0.8(0.41) = 0.33 \, .$$

The steepest incident wave which will be nearly perfectly reflected from the given revetment is, from Figure 2-62,

$$\left(\frac{H_o}{L_o}\right)_{max} = 0.005 \, .$$

It is interesting to note the effectiveness of flat beaches in dissipating wave energy by considering the above wave on a beach having a slope of 0.02 (1:50). From Equation 2-87 (noting that $\beta \approx \sin \beta \approx \tan \beta$ = 0.02),

$$\left(\frac{H_o}{L_o}\right)_{max} = 0.000014 \, .$$

Hence

$$\chi = \chi_1 \, \chi_2 = 0.8 \, (0.0014) = 0.0011 \, ,$$

or the height of the reflected wave is about 0.1 percent of the incident wave height.

As indicated by the dependence of reflection coefficient on incident wave steepness, a beach will selectively dissipate wave energy, dissipating the energy of relatively short steep waves and reflecting the energy of the longer, flatter waves.

* *

2.6   BREAKING WAVES

2.61   DEEP WATER

The maximum height of a wave travelling in deep water is limited by a maximum wave steepness for which the wave form can remain stable. Waves reaching the limiting steepness will begin to break and in so doing, will dissipate a part of their energy. Based on theoretical considerations, Michell (1893) found the limiting steepness to be given by,

$$\frac{H_o}{L_o} = 0.142 \approx \frac{1}{7} \, . \tag{2-88}$$

which occurs when the crest angle as shown in Figure 2-64 is 120°. This limiting steepness occurs when the water particle velocity at the wave crest just equals the wave celerity; a further increase in steepness would

result in particle velocities at the wave crest greater than the wave celerity and, consequently, instability.
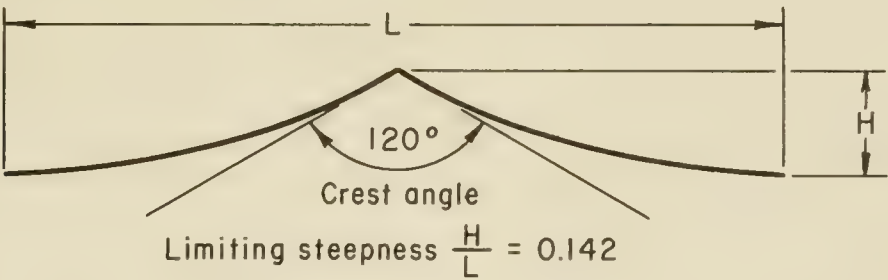
Figure 2-64. Wave of Limiting Steepness in Deep Water

2.62 SHOALING WATER

When a wave moves into shoaling water, the *limiting steepness* which it can attain decreases, being a function of both the relative depth d/L, and the beach slope m, perpendicular to the direction of wave advance. A wave of given deepwater characteristics will move toward a shore until the water becomes shallow enough to initiate breaking, this depth is usually denoted as d_b and termed the breaking depth. Munk (1949) derived several relationships from a modified solitary wave theory relating the breaker height H_b, the breaking depth d_b, the unrefracted deepwater wave height H_o', and the deepwater wavelength L_o. His expressions are given by

$$\frac{H_b}{H_o'} = \frac{1}{3.3 \, (H_o'/L_o)^{\frac{1}{3}}} \, , \tag{2-89}$$

and

$$\frac{d_b}{H_b} = 1.28 \, . \tag{2-90}$$

The ratio H_b/H_o' is frequently termed the breaker height index. Subsequent observations and investigations by Iversen (1952, 1953), Galvin (1969), and Goda (1970) among others, have established that H_b/H_o' and d_b/H_b depend on beach slope and on incident wave steepness. Figure 2-65 shows Goda's empirically derived relationships between H_b/H_o' and H_o'/L_o for several beach slopes. Curves shown on the figure are fitted to widely scattered data; however they illustrate a dependence of H_b/H_o' on the beach slope. Empirical relationships between d_b/H_b and H_b/gT^2 for various beach slopes are presented in Figure 2-66. It is recommended that Figures 2-65 and 2-66 be used, rather than Equations 2-89 and 2-90, for making estimates of the depth at breaking or the maximum breaker
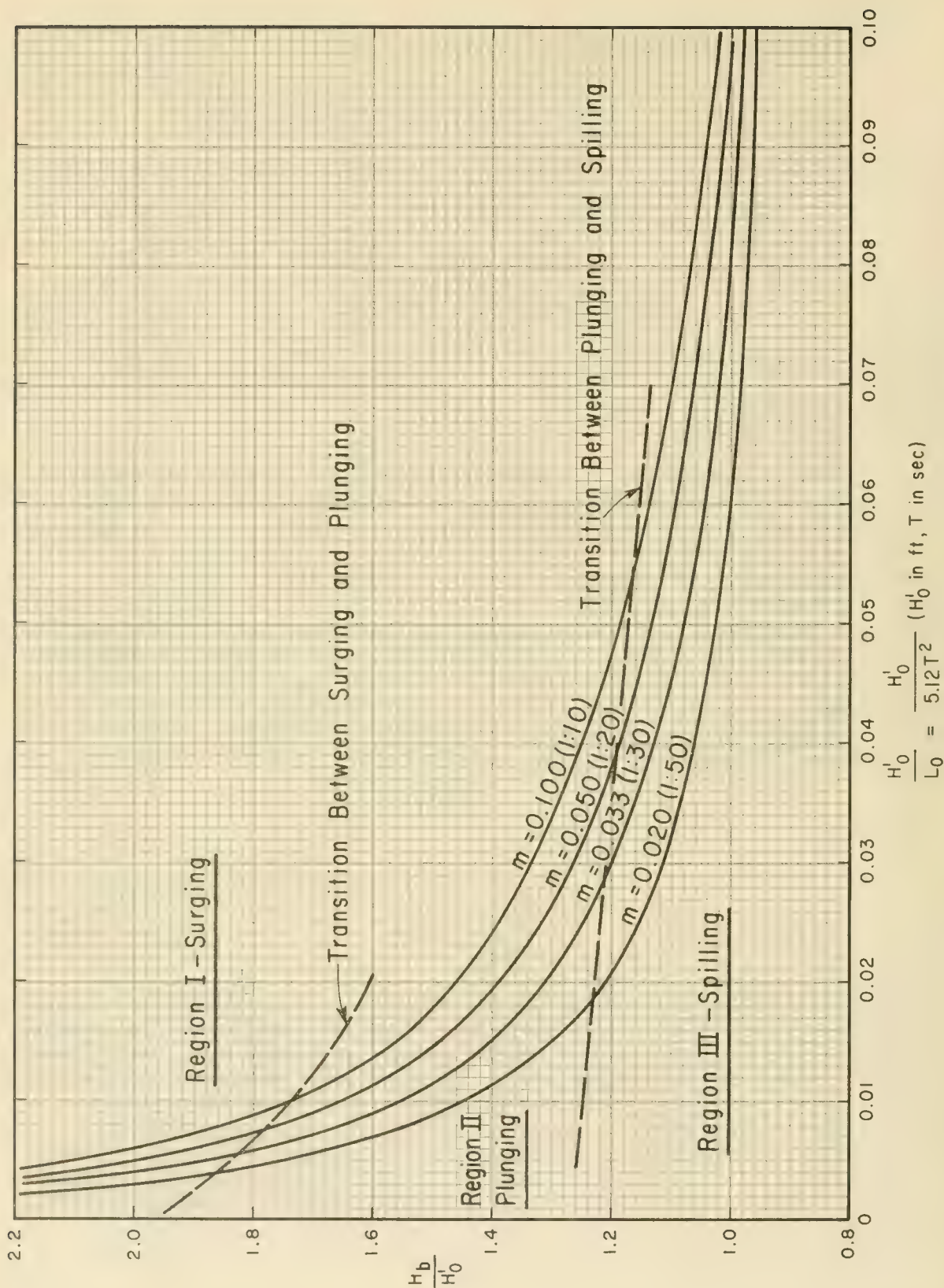
Figure 2-65. Breaker Height Index Versus Deep Water Wave Steepness
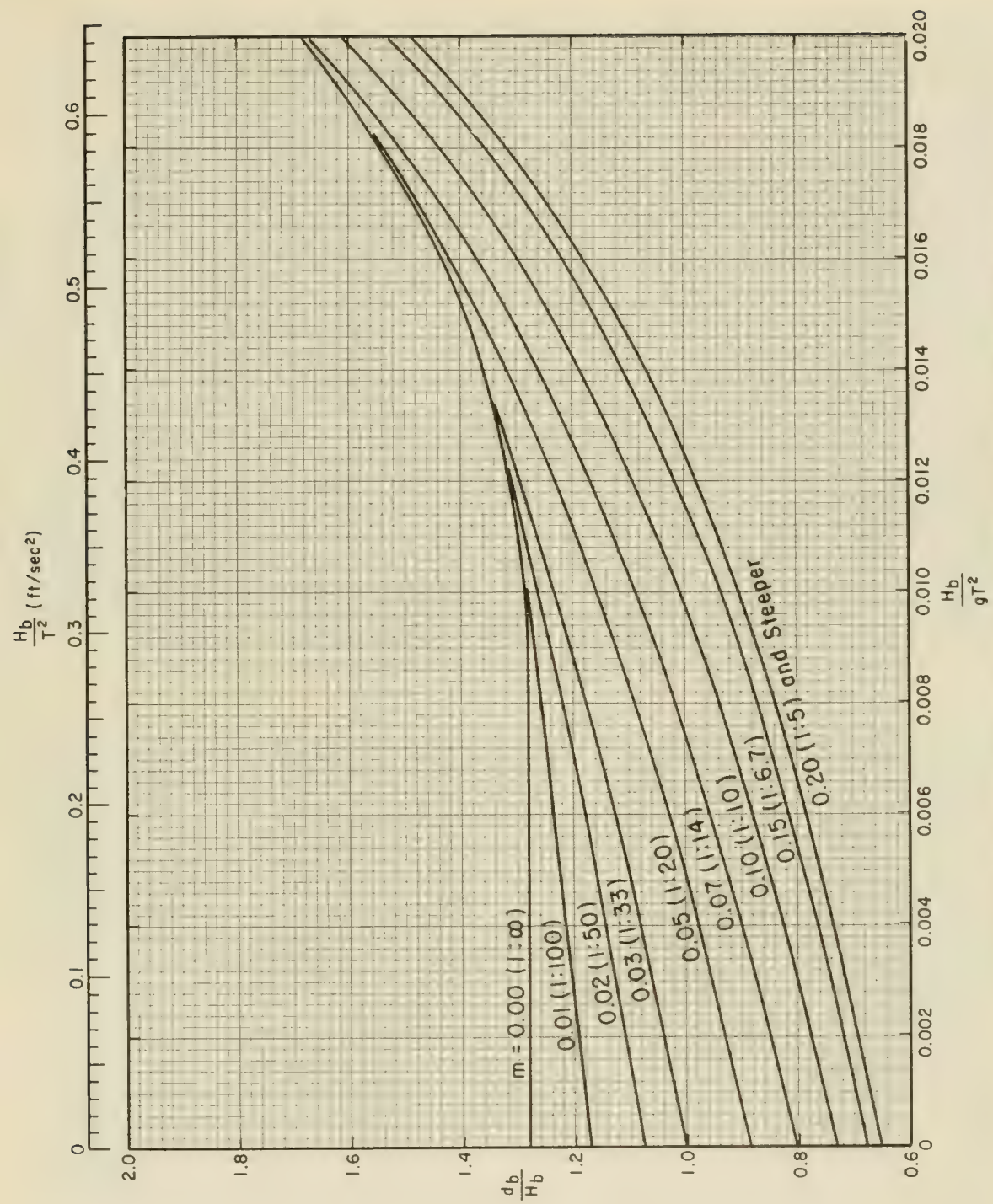
Figure 2-66. Dimensionless Depth at Breaking Versus Breaker Steepness

height in a given depth since the figures take into consideration the observed dependence of d_b/H_b and H_b/H_O' on beach slope. The curves in Figure 2-66 are given by

$$\frac{d_b}{H_b} = \frac{1}{b - (aH_b/gT^2)} \; , \tag{2-91}$$

where a and b are functions of the beach slope m, and may be approximated by

$$a = 1.36g\,(1 - e^{-19m}) \tag{2-92}$$

$$b = \frac{1.56}{(1 + e^{-19.5\,m})} \; . \tag{2-93}$$

Breaking waves have been classified as spilling, plunging or surging depending on the way in which they break (Patrick and Wiegel, 1955), and (Wiegel, 1964). Spilling breakers break gradually and are characterized by *white water* at the crest. (See Figure 2-67.) Plunging breakers curl over at the crest with a plunging forward of the mass of water at the crest. (See Figure 2-68.) Surging breakers build up as if to form a plunging breaker but the base of the wave surges up the beach before the crest can plunge forward. (See Figure 2-69.) Further subdivision of breaker types has also been proposed. The term collapsing breaker is sometimes used (Galvin, 1968) to describe breakers in the transition from plunging to surging. (See Figure 2-70.) In actuality, the transition from one breaker type to another is gradual without distinct dividing lines; however, Patrick and Wiegel (1955) presented ranges of H_O'/L_O for several beach slopes for which each type of breaker can be expected to occur. This information is also presented in Figure 2-65 in the form of three regions on the H_b/H_O' vs. H_O'/L_O plane. An example illustrating the estimation of breaker parameters follows.

* * * * * * * * * * * * * *   EXAMPLE PROBLEM   * * * * * * * * * * * * * *

GIVEN: A beach having a 1:20 slope; a wave with deepwater height of H_O = 5 feet and a period of T = 10 seconds. Assume that a refraction analysis gives a refraction coefficient, $K_R = (b_o/b)^{1/2}$ = 1.05 at the point where breaking is expected to occur.

FIND: The breaker height H_b and the depth d_b at which breaking occurs.

SOLUTION: The unrefracted deepwater height H_O' can be found from

$$\frac{H_O'}{H_o} = K_R = \left(\frac{b_o}{b}\right)^{\frac{1}{2}} \qquad \text{(See Section 2.32)},$$

2-124
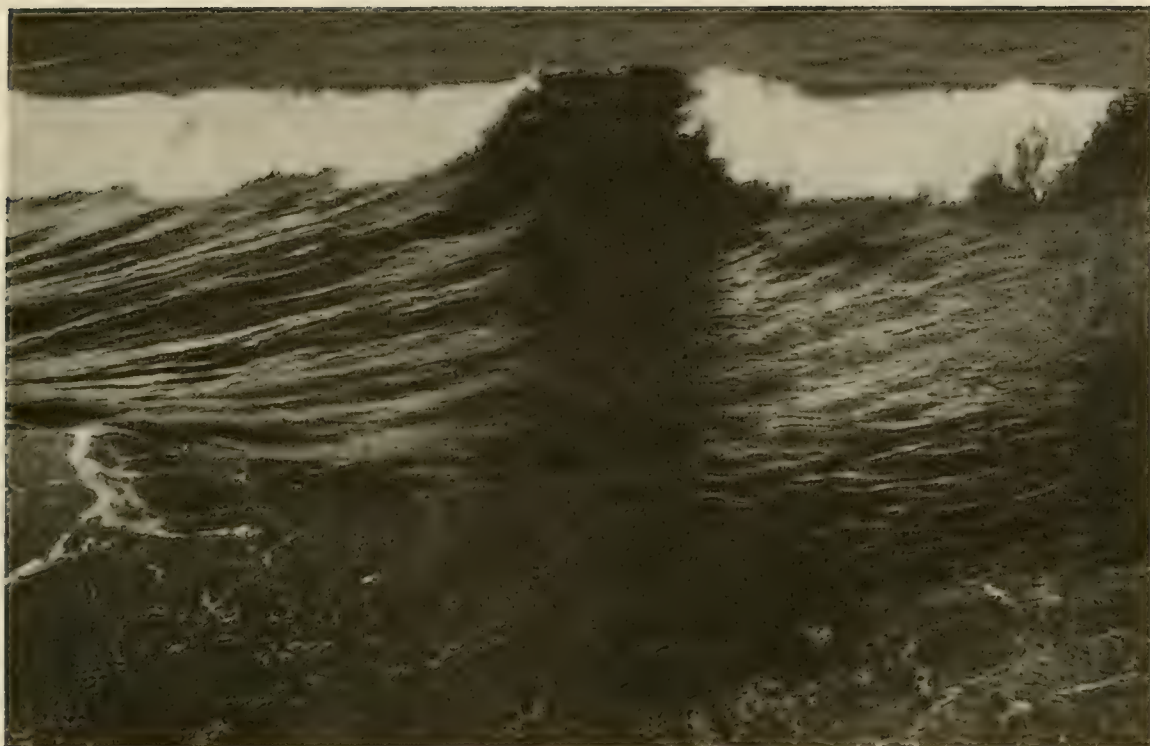
Figure 2-67. Spilling Breaking Wave

Figure 2-68. Plunging Breaking Wave

Figure 2-69. Surging Breaking Wave

Figure 2-70. Collapsing Breaking Wave

hence,

$$H_o' = 1.05(5) = 5.25 \text{ feet},$$

and since, $L_O = 5.12T^2$ (linear wave theory),

$$\frac{H_o'}{L_o} = \frac{5.25}{5.12\,(10)^2} = 0.010.$$

From Figure 2-65, entering with $H_o'/L_O = 0.010$ and intersecting the curve for a slope of 1:20 (m = 0.05) results in $H_b/H_o' = 1.65$. Therefore

$$H_b = \left(\frac{H_b}{H_o'}\right)H_o'$$

$$H_b = 1.65\,(5.25) = 8.66 \text{ feet}.$$

To determine the depth at breaking calculate:

$$\frac{H_b}{gT^2} = \frac{8.66}{32.2\,(10)^2} = 0.00269,$$

and enter Figure 2-66 for m = 0.050.

$$\frac{d_b}{H_b} = 0.90.$$

Thus $d_b = 0.90\,(8.66) = 7.80$ feet, and therefore the wave will break when it is approximately $7.80/(0.05) = 156$ feet from the shoreline, assuming a constant nearshore slope. The initial value selected for the refraction coefficient should now be checked to determine if it is correct for the actual breaker location as found in the solution. If necessary, a corrected value for the refraction coefficient should be used and the breaker height recomputed. The example wave will result in a plunging breaker. (See Figure 2-65.)

* *

AIRY, G.B., "On Tides and Waves," *Encyclopaedia Metropolitana,* 1845. (Date of original writing unknown.)

ARTHUR, R.S., MUNK, W.H., and ISSACS, J.D., "The direct Construction of Wave Rays," *Transactions of the American Geophysical Union,* Vol. 33, No. 6, 1952, pp. 855-865.

BATTJES, J.A., "Refraction of Water Waves," *Journal of the Waterways and Harbors Division,* ASCE, Vol. 94, WW4, No. 6206, Nov. 1968.

BEITINJANI, K.I., and BRATER, E.F., "Study on Refraction of Waves in Prismatic Channels," *Journal of the Waterways and Harbors Division,* ASCE, Vol. 91, WW3, No. 4434, 1965, pp. 37-64.

BLUE, F.L., JR. and JOHNSON, J.W., "Diffraction of Water Waves Passing through a Breakwater Gap," *Transactions of the American Geophysical Union,* Vol. 30, No. 5, Oct. 1949, pp. 705-18.

BORGMAN, L.E., "Directional Spectra Models for Design Use," HEL-1-12, University of California, Berkeley, 1969.

BOUSSINESQ, J., "Theory of Waves and Swells Propagated in a Long Horizontal Rectangular Canal, and Imparting to the Liquid Contained in this Canal Approximately Equal Velocities from the Surface to the Bottom," *Journal de Mathematiques Pures et Appliquees,* Vol. 17, Series 2, 1872.

BOUSSINESQ, J., "Essai sur la Theorie des Eaux Courantes," Mem. divers Savants a L'Academie des Science, 32:56, 1877.

BRETSCHNEIDER, C.L., "Wave Refraction, Diffraction and Reflection," *Estuary and Coastline Hydrodynamics,* A.T. Ippen, ed., McGraw-Hill, New York, 1966, pp. 257-280.

CALDWELL, J.M., "Reflection of Solitary Waves," TM-11, U.S. Army, Corps of Engineers, Beach Erosion Board, Washington, D.C., Nov. 1949.

CARR, J.H. and STELZRIEDE, M.E., "Diffraction of Water Waves by Breakwaters," *Gravity Waves,* Circ. No. 521, National Bureau of Standards, Washington, D.C., Nov. 1952, pp. 109-125.

CHAO, Y.Y., "The Theory of Wave Refraction in Shoaling Water," TR-70-7, Department of Meteorology and Oceanography, New York University, New York, 1970.

CHIEN, NING, "Ripple Tank Studies of Wave Refraction," *Transactions of the American Geophysical Union,* Vol. 35, No. 6, 1954, pp. 897-904.

COUDERT, J.F., and RAICHLEN, F., "Wave Refraction Near San Pedro Bay, California," *Journal of the Waterways, Harbors and Coastal Engineering Division,* ASCE, WW3, 1970, pp. 737-747.

DAILY, J.W. and STEPHAN, S.C.,JR., "Characteristics of a Solitary Wave," *Transactions of the American Society of Civil Engineers*, Vol. 118, 1953, pp. 575-587.

DANEL, P., "On the Limiting Clapotis," *Gravity Waves*, Circ. No. 521, National Bureau of Standards, Washington, D.C., 1952, pp. 35-38.

DEAN, R.G., "Stream Function Representation of Nonlinear Ocean Waves," *Journal of the Geophysical Research*, Vol. 70, No. 18, Sep. 1965a.

DEAN, R.G., "Stream Function Wave Theory; Validity and Application," *Coastal Engineering, Santa Barbara Specialty Conference*, Ch. 12, Oct. 1965b.

DEAN, R.G., "Relative Validities of Water Wave Theories," *Proceedings of the Conference on Civil Engineering in the Oceans I*, San Francisco, Sep. 1967.

DEAN, R.G., "Evaluation and Development of Water Wave Theories for Engineering Application," Engineering and Industrial Experiment Station Report, College of Engineering, University of Florida, Gainesville, 1970, (Draft copy.)

DEAN, R.G., "Evaluation and Development of Water Wave Theories for Engineering Application, U.S. Army, Corps of Engineers, Coastal Engineering Research Center. (To be published in 1973).

DEAN, R.G. and LE MÉHAUTÉ, B., "Experimental Validity of Water Wave Theories," *National Structural Engineering Meeting*, ASCE, Portland, Oregon, Apr. 1970.

---*Reprints on Stream Function Wave Theory and Application to Wave Force Calculations*, Engineering and Industrial Experiment Station, College of Engineering, University of Florida, Gainesville, 1970.

DOBSON, R.S., "Some Applications of Digital Computers to Hydraulic Engineering Problems," TR-80, Ch. 2, Department of Civil Engineering, Stanford University, Calif., Jun. 1967.

DOMZIG, H., "Wellendruck und druckerzeugender Seegang," *Mitteilungen der Hannoverschen Versuchsanstalt für Grundbau und Wasserbau*, Hannover, Germany, Heft 8, 1955.

DRAPER, L., "Attenuation of Sea Waves with Depth," *La Houille Blanche*, Vol. 12, No. 6, 1957, pp. 926-931.

EAGLESON, P.S. and DEAN, R.G., "Small Amplitude Wave Theory," *Estuary and Coastline Hydrodynamics*, A.T. Ippen, ed., McGraw-Hill, New York, 1966, pp. 1-92.

ESTEVA, D. and HARRIS, D.L., "Comparison of Pressure and Staff Wave Gages Records," *Proceedings of the 12th Conference on Coastal Engineering*, Washington, D.C., 1971.

FAN, S.S., "Diffraction of Wind Waves," HEL-1-10, Hydraulics Laboratory, University of California, Berkeley, Aug. 1968.

FAN, S.S. and BORGMAN, L.E., "Computer Modeling of Diffraction of Wind Waves," *Proceedings of the 12th Conference on Coastal Engineering,* Washington, D.C., Sep. 1970.

GALVIN, C.J., JR., "Breaker Type Classification on Three Laboratory Beaches," *Journal of Geophysical Research,* Vol. 73, No. 12, 1968.

GALVIN, C.J., JR., "Breaker Travel and Choice of Design Wave Height," *Journal of the Waterways and Harobrs Division,* ASCE, WW2, No. 6569, 1969, pp. 175-200.

GATEWOOD, R., in GAILLARD, D.D., "Wave Action in Relation to Engineering Structures," *Professional Paper No. 31,* U.S. Army, Corps of Engineers, 1904.

GERSTNER, F., "Theorie die Wellen," *Abhandlungen der Konigichen Bohmischen Gesellschaft der Wissenschaften,* Prague, 1802.

GODA, Y, "A Synthesis of Breaker Indices," *Transactions of the Japanese Society of Civil Engineers,* Vol. 2, Part 2, 1970.

GODA, Y. and ABE, Y., "Apparent Coefficient of Partial Reflection of Finite Amplitude Waves," Rpt. No. 3, Vol. 7, Port and Harbor Research Institute, Nagase, Yokosuka, Japan, Sep. 1968.

GRACE, R.A., "How to Measure Waves," *Ocean Industry,* Vol. 5, No. 2, 1970, pp. 65-69.

GRESLAU, L. and MAHÉ Y., "Study of the Reflection Coefficient of a Wave on an Inclined Plane," *Proceedings of the 5th Conference on Coastal Engineering,* Grenoble, France (French), Sep. 1954.

GRISWOLD, G.M., "Numerical Calculation of Wave Refraction," *Journal of Geophysical Research,* Vol. 68, No. 6, 1963.

HARDY, J.R., "Some Grid and Projection Problems in the Numerical Calculation of Wave Refraction," *Journal of Geophysical Research,* Vol. 73, No. 22, Nov. 1968.

HARRISON, W. and WILSON, W.S., "Development of a Method for Numerical Calculation of Wave Refraction," TM-6, U.S. Army, Corps of Engineers, Coastal Engineering Research Center, Washington, D.C., 1964.

HAVELOCK, T.H., "Periodic Irrotational Waves of Finite Height," *Proceedings of the Royal Society of London,* Vol. 95, Series A, No. A665, 1918, pp. 37-51.

HEALY, J.J., "Wave Damping Effect of Beaches," *Conference of International Hydraulics,* IAHR-ASCE, Minneapolis, Sep. 1953.

HOM-MA, M., HORIKAWA, K., and KOMORI, S., "Response Characteristics of Underwater Wave Gauge," *Proceedings of the 10th Conference on Coastal Engineering*, Vol. 1, Tokyo, 1966, pp. 99-114.

HUNT, I.A., "Winds, Wind Setup and Seiches on Lake Erie," U.S. Army Engineer District, Lake Survey, 1959.

IPPEN, A.T., "Waves and Tides in Coastal Processes," *Journal of the Boston Society of Civil Engineers*, Vol. 53, No. 2, 1966a., pp. 158-181.

IPPEN, A.T., ed., *Estuary and Coastline Hydrodynamics*, McGraw-Hill, New York, 1966b.

IPPEN, A. and KULIN, G., "The Shoaling and Breaking of the Solitary Wave," *Proceedings of the 5th Conference on Coastal Engineering*, Grenoble, France, 1954, pp. 27-49.

IVERSEN, H.W., "Laboratory Study of Breakers," *Gravity Waves*, Circ. No. 521, National Bureau of Standards, Washington, D.C., 1952.

IVERSEN, H.W., "Waves and Breakers in Shoaling Water," *Proceedings of the 3rd Conference on Coastal Engineering*, Cambridge, Mass., 1953.

IWASA, Y., "Analytical Consideration on Cnoidal and Solitary Waves," *Memoirs of the Faculty of Engineering*, Reprint, Kyoto University, Japan, 1955.

JOHNSON, J.W., "The Refraction of Surface Waves by Currents," *Transactions of the American Geophysical Union*, Vol. 28, No. 6, Dec. 1947, pp. 867-874.

JOHNSON, J.W., "Generalized Wave Diffraction Diagrams," *Proceedings of the 2nd Conference on Coastal Engineering*, Houston, Texas, 1952.

JOHNSON, J.W., "Engineering Aspects of Diffraction and Refraction," *Transactions of the American Society of Civil Engineers*, Vol. 118, No. 2556, 1953, pp. 617-652.

JOHNSON, J.W., O'BRIEN, M.P., and ISAACS, J.D., "Graphical Construction of Wave Refraction Diagrams," HO No. 605, TR-2, U.S. Naval Oceanographic Office, Washington, D.C., Jan. 1948.

KAPLAN, K., "Effective Height of Seawalls," Vol. 6, Bul. No. 2, U.S. Army, Corps of Engineers, Beach Erosion Board, Washington, D.C., 1952.

KELLER, J.B., "Surface Waves on Water of Non-uniform Depth," *Journal of Fluid Mechanics*, Vol. 4, 1958, pp. 607-614.

KEULEGAN, G.H., "Gradual Damping of Solitary Waves," *Journal of Research of the National Bureau of Standards*, Reprint, Vol. 40, 1948, pp. 487-498.

KEULEGAN, G.H. and HARRISON, J., "Tsunami Refraction Diagrams by Digital Computer," *Journal of the Waterways, Harbors and Coastal Engineering Division*, ASCE, Vol. 96, WW2, No. 7261, May 1970, pp. 219-233.

KEULEGAN, G.H. and PATTERSON, G.W., "Mathematical Theory of Irrotational Translation Waves," RP No. 1272, National Bureau of Standards, Washington, D.C., 1940, pp. 47-101.

KINSMAN, B., *Wind Waves, their Generation and Propagation on the Ocean Surface*, Prentice Hall, New Jersey, 1965.

KORTEWEG, D.J. and DE VRIES, G., "On the Change of Form of Long Waves Advancing in a Rectangular Canal, and on a New Type of Long Stationary Waves," *Philosophical Magazine*, 5th Series, 1895, pp. 422-443.

LACOMB, H., "The Diffraction of a Swell - A Practical Approximate Solution and Its Justification," *Gravity Waves*, Circ. No. 521, National Bureau of Standards, Washington, D.C., 1952, pp. 129-140.

LAITONE, E.V., "Higher Approximation to Non-linear Water Waves and the Limiting Heights of Cnoidal, Solitary and Stokes Waves," TM-133, U.S. Army, Corps of Engineers, Beach Erosion Board, Washington, D.C., 1963.

LAMB, H., *Hydrodynamics*, 6th ed. Cambridge University Press, London - New York, 1932.

LEE, C., "On the Design of Small Craft Harbors," *Proceedings of the 9th Conference on Coastal Engineering*, Lisbon, Portugal, Jun 1964.

LE MÉHAUTÉ, B., "Wave Absorbers in Harbors," Contract Report No. 2-122, National Engineering Science Company for the U.S. Army, Waterways Experiment Station, Vicksburg, Miss., Jun. 1965.

LE MÉHAUTÉ, B., "An Introduction to Hydrodynamics and Water Waves," *Water Wave Theories*, Vol. II, TR ERL 118-POL-3-2, U.S. Department of Commerce, ESSA, Washington, D.C., 1969.

LEWIS, R.M., BLEISTEIN, N., and LUDWIG, D., "Uniform Assymptolic Theory of Creeping Waves," *Communications on Pure and Applied Mathematics*, Vol. 20, No. 2, 1967.

LONGUET-HIGGINS, M.S., "Mass Transport in Water Waves," *Philosophical Transactions of the Royal Society of London*, Series A, Vol. 245, No. 903, 1953.

LONGUET-HIGGINS, M.S., "On the Transformation of a Continuous Spectrum by Refraction," *Proceedings of the Cambridge Philosophical Society*, Vol. 53, Part I, 1957, pp. 226-229.

LONGUET-HIGGINS, M.S., "Mass Transport in the Boundary Layer at a Free Oscillating Surface," Vol. 8, National Institute of Oceanography, Wormley, Surrey, England, 1960.

LOWELL, S.C., "The Propagation of Waves in Shallow Water," *Communications on Pure and Applied Mathematics*, Vol. 12, Nos. 2 and 3, 1949.

McCOWAN, J., "On the Solitary Wave," *Philosophical Magazine*, 5th Series, Vol. 32, No. 194, 1891, pp. 45-58.

MASCH, F.D., "Cnoidal Waves in Shallow Water," *Proceedings of the 9th Conference of Coastal Engineering*, Ch. 1, Lisbon, 1964.

MASCH, F.D. and WIEGEL, R.L., "Cnoidal Waves. Tables of Functions," *Council on Wave Research, The Engineering Foundation*, Richmond, Calif., 1961.

MATTSSON, A., "Reflection of Gravity Waves," *Congress on the International Association of Hydraulic Research*, London, 1963.

MEHR, E., "Surf Refraction - Computer Refraction Program," Statistical Laboratory, New York University, New York, Sep. 1962.

MICHE, M., "Mouvements Ondulatoires de la Mer en Profondeur Constante ou Décroissante," *Annales des Ponts et Chaussées*, 1944, pp. 25-78, 131-164, 270-292, and 369-406.

MICHE, M., "The Reflecting Power of Maritime Works Exposed to Action of the Waves," *Annals des Ponts et Chaussées*, Jun. 1951. (Partial translation by the Beach Erosion Board, Vol. 7, Bul. No. 2, Apr. 1953.)

MICHELL, J.H., "On the Highest Waves in Water," *Philosophical Magazine*, 5th Series, Vol. 36, 1893, pp. 430-437.

MITCHIM, C.F., "Oscillatory Waves in Deep Water," *The Military Engineer*, March-April 1940, pp. 107-109.

MOBAREK, ISMAIL, "Effect of Bottom Slope on Wave Diffraction," HEL-1-1, University of California, Berkeley, Nov. 1962.

MONKMEYER, P.L., "Higher Order Theory for Symmetrical Gravity Waves," Ch. 33, *Proceedings of the 12th Conference on Coastal Engineering*, Washington, D.C., 1970.

MORISON, J.R. and CROOKE, R.C., "The Mechanics of Deep Water, Shallow Water, and Breaking Waves," TM-40, U.S. Army, Corps of Engineers, Beach Erosion Board, Washington, D.C., 1953.

MORSE, P.M. and RUBINSTEIN, P.J., "The Diffraction of Waves by Ribbons and Slits," *Physical Reviews*, Vol. 54, Dec. 1938, pp. 895-898.

MUNK, W.H., "The Solitary Wave Theory and Its Application to Surf Problems," *Annals of the New York Academy of Sciences*, Vol. 51, 1949, pp. 376-462.

MUNK, W.H. and ARTHUR, R.S., "Wave Intensity Along a Refracted Ray," *Symposium on Gravity Waves*, Circ. 521, National Bureau of Standards, Washington, D.C., 1951.

MUNK, W.H. and TRAYLOR, M.A., "Refraction of Ocean Waves," *Journal of Geology*, Vol. LV, No. 1, 1947.

NIELSEN, A.H., "Diffraction of Periodic Waves Along a Vertical Breakwater of Small Angles of Incidence," HEL-1-2, Institute of Engineering Research, University of California, Berkeley, Dec. 1962.

O'BRIEN, M.P., "A Summary of the Theory of Oscillatory Waves," TR-2, U.S. Army, Corps of Engineers, Beach Erosion Board, Washington, D.C., 1942.

ORR, T.E. and HERBICH, J.B., "Numerical Calculation of Wave Refraction by Digital Computer," COE Rpt. No. 114, *Sea Grant Publication*, No. 209, Department of Coastal and Ocean Engineering, Texas A&M University, Dec. 1969.

PALMER, R.Q., "Wave Refraction Plotter," Vol. 11, Bul. No. 1, U.S. Army, Corps of Engineers, Beach Erosion Board, Washington, D.C., 1957.

PATRICK, D.A. and WIEGEL, R.L., "Amphibian Tractors in the Surf," *Proceedings of the First Conference on Ships and Waves, Council on Wave Research and Society of Naval Architects and Marine Engineers*, 1955.

PENNEY, W.G. and PRICE, A.T., "Diffraction of Sea Waves by a Breakwater," *Artificial Harbors*, Technical History No. 26, Sec. 3-D, Directorate of Miscellaneous Weapons Development, 1944.

PIERSON, W.J., JR., "The Interpretation of Crossed Orthogonals in Wave Refraction Phenomena," TM-21, U.S. Army, Corps of Engineers, Beach Erosion Board, Washington, D.C., 1950.

PIERSON, W.J., JR., "The Accuracy of Present Wave Forecasting Methods with Reference to Problems in Beach Erosion on the New Jersey and Long Island Coasts," TM-24, U.S. Army, Corps of Engineers, Beach Erosion Board, Washington, D.C., 1951.

PIERSON, W.J., JR., "Observing and Forecasting Ocean Waves," H.O. No. 603, U.S. Naval Oceanographic Office, Washington, D.C., 1965.

PLATZMAN, G.W., and RAO, D.B., "The Free Oscillations of Lake Erie," TR-8, Department of Geophysical Sciences, University of Chicago, for the U.S. Weather Bureau, Sep. 1963.

POCINKI, L.S., "The Application of Conformal Transformations to Ocean Wave Refraction Problems," Department of Meteorology and Oceanography, New York University, New York, 1950.

PUTNAM, J.A. and ARTHUR, R.S., "Diffraction of Water Waves by Breakwaters," *Transactions of the American Geophysical Union*, Vol. 29, No. 4, Aug. 1948, pp. 317-374.

RAICHLEN, F., "Long Period Oscillations in Basins of Arbitrary Shapes," *Coastal Engineering Santa Barbara Specialty Conference*, Ch. 7, Oct. 1965, pp. 115-148, American Society of Coastal Engineering, New York, 1966.

RALLS, G.C., "A Ripple Tank Study of Wave Refraction," *Journal of the Waterways and Harbors Division*, ASCE, Vol. 82, WW1, No. 911, Mar. 1956.

RAYLEIGH, LORD, "On Waves," *Philosophical Magazine and Journal of Science*, Vol. 1, No. 4, 1876, pp. 257-279.

RUSSELL, J.S., "Report of the Committee on Waves," *7th Meeting of the British Association for the Advancement of Science*, 1838, p. 417.

RUSSELL, J.S., "Report on Waves," *14th Meeting of the British Association for the Advancement of Science*, 1845, p. 311.

RUSSELL, R.C.H. and OSORIO, J.D.C., "An Experimental Investigation of Drift Profiles in a Closed Channel," *Proceedings of the 6th Conference on Coastal Engineering*, Miami, Council on Wave Research, University of California, Berkeley, 1958, pp. 171-183.

SAVILLE, T., JR., and KAPLAN, K., "A New Method for the Graphical Construction of Wave Refraction Diagrams," Vol. 6, Bul. No. 3, U.S. Army, Corps of Engineers, Beach Erosion Board, Washington, D.C., 1952, pp. 23-24.

SHOEMAKER, H.J. and THIJSSE, J.TH. "Investigations of the Reflection of Waves," *3rd. Meeting of the International Association for Hydraulic Structures Research*, Grenoble, France, Sep. 1949.

SILVESTER, R., "Design Wave for Littoral Drift Model," *Journal of the Waterways and Harbors Division*, ASCE, Vol. 89, WW3, No. 360, Aug. 1963.

SKJELBREIA, L., *Gravity Waves. Stokes' Third Order Approximation. Tables of Functions*, University of California, Council on Wave Research, The Engineering Foundation, Berkeley, 1959.

SKJELBREIA, L. and HENDRICKSON, J.A., *Fifth Order Gravity Wave Theory and Tables of Functions*, National Engineering Science Company, 1962.

SOMMERFELD, A., "Mathematische Theorie der Diffraction," *Mathematische Annals*, Vol. 47, 1896, pp. 317-374.

STOKES, G.C., "On the Theory of Oscillatory Waves," *Mathematical and Physical Papers*, Vol. 1, Cambridge University Press, Cambridge, 1880.

SVERDRUP, H.U. and MUNK, W.H., "Wind, Sea, and Swell: Theory of Relations for Forecasting," TR-1, H.O. No. 601, U.S. Naval Hydrographic Office, Washington, D.C., 1947, p. 7.

U.S. ARMY, CORPS OF ENGINEERS, "A Summary of the Theory of Oscillatory Waves," TR-2, Beach Erosion Board, Washington, D.C., 1942.

URSELL, F., "Mass Transport in Gravity Waves," *Proceedings of the Cambridge Philosophical Society*, Vol. 49, Pt. 1, Jan. 1953, pp. 145-150.

WEGGEL, J.R., "Maximum Breaker Height," *Journal of the Waterways, Harbors and Coastal Engineering Division*, ASCE, Vol. 98, WW4, Nov. 1972.

WHALIN, R.W., "The Limit of Applicability of Linear Wave Refraction Theory in a Convergence Zone," H-71-3, U.S. Army, Corps of Engineers, Waterways Experiment Station, Washington, D.C., 1971, pp. 156.

WIEGEL, R.L., *Gravity Waves. Tables of Functions*, University of California, Council on Wave Research, The Engineering Foundation, Berkeley, 1954.

WIEGEL, R.L., "A Presentation of Cnoidal Wave Theory for Practical Application," *Journal of Fluid Mechanics*, Vol. 7, Pt. 2, Cambridge University Press, 1960, pp. 273-286.

WIEGEL, R.L., "Diffraction of Waves by a Semi-infinite Breakwater," *Journal of the Hydraulics Division*, ASCE, Vol. 88, HY1, Jan. 1962, pp. 27-44.

WIEGEL, R.L., *Oceanographical Engineering*, Fluid Mechanics Series, Prentice Hall, New Jersey, 1964.

WIEGEL, R.L. and ARNOLD, A.L., "Model Studies of Wave Refraction," TM-103, U.S. Army, Corps of Engineers, Beach Erosion Board, Washington, D.C., Dec. 1957.

WILLIAMS, L.C., "CERC Wave Gages," TM-30, U.S. Army, Corps of Engineers, Coastal Engineering Research Center, Washington, D.C., 1969.

WILSON, W.S., "A Method for Calculating and Plotting Surface Wave Rays," TM-17, U.S. Army, Corps of Engineers, Coastal Engineering Research Center, Washington, D.C., Feb. 1966.

WILTON, J.R., "On Deep Water Waves," *Philosophical Magazine*, 6th Series, 1914, pp. 385-394.

WORTHINGTON, H.W. and HERBICH, J.B., "A Computer Program to Estimate the Combined Effects of Refraction and Diffraction of Water Waves," *Sea Grant Publication*, No. 219, Texas A&M University, Aug. 1970.

CHAPTER 3

WAVE AND
WATER LEVEL
PREDICTIONS

OCEAN CITY, NEW JERSEY — 9 March 1962

CHAPTER 3

WAVE AND WATER-LEVEL PREDICTIONS

3.1 INTRODUCTION

Chapter 2, treated phenomena associated with surface waves as though each phenomenon could be considered separately without regard to other phenomena. Surface waves were discussed from the standpoint of motions and transformations without regard to wave generation. Furthermore, the water level, *stillwater level (SWL)*, on which the waves propagated was assumed known.

In this chapter, wave observations are presented to show characteristics of surface waves in nature. The characteristics of real waves are much less regular than those implied by theory. Also presented are procedures for representing the complexity of the real sea by a small number of parameters. Deviations between the actual waves and the parameter values are discussed.

Theory for wave generation is reviewed to show progress in explaining and predicting the actual complexity of the sea. Wave prediction is called *hindcasting* when based on past meteorological conditions, and *forecasting* when based on predicted conditions. The same procedures are used for hindcasting and forecasting; the only difference is the source of meteorological data. The most advanced prediction techniques currently available can be used only in a few laboratories, because of the need for electronic computers, the sophistication of the models, and the need for correct weather data. However, simplified wave prediction techniques, suitable for use by field offices or a design group are presented.

While simplified prediction systems will not solve all problems, they can be used to indicate probable wave conditions for most design studies. Simplified wave prediction can also be used to obtain statistical wave data over several years.

Review of prediction theories is presented to give the reader more perspective for the simplified prediction methods that are presently available. This will justify confidence in some applications of the simplified procedures, will aid in recognizing unexpected difficulties when they occur, and will indicate some conditions in which they are not adequate.

The graphs in Sections 3.5, Simplified Wave Prediction Models, and 3.6, Wave Forecasting for Shallow Water Areas, may be read with the precision justified by the underlying theory. The equations were derived originally from graphs, and do not provide any physical understanding. Calculations with the graphs should be carried out to tenths or hundredths where this is feasible, and then rounded off in the final result.

Predictions are compared with available observations wherever possible to indicate their accuracy. Calibration of techniques applied to a specific geographic area by comparison with available observations is always desirable.

The problem of obtaining wind information for wave hindcasting is discussed, and specific instructions for estimating wind parameters are given.

Water levels continuously change. Changes due to astronomical tides are predictable, and are well documented for many areas. Fluctuations due to meteorological conditions are not as predictable, and are less well documented.

Many factors govern water levels at a shore during a storm. The principle factor is the effect of wind blowing over water. Some of the largest increases in water level are due to severe storms, such as hurricanes, which can cause storm surges higher than 25 feet at some locations on the open coast and even higher water levels in bays and estuaries. Estimating water levels caused by meteorological conditions is complex, even for the simplest cases; and unfortunately, the best approaches available for predicting these water levels are elaborate computational techniques which require the use of large digital computers.

3.2 CHARACTERISTICS OF OCEAN WAVES

The earlier discussion of waves was concerned with idealized, monochromatic waves. The pattern of waves on any body of water exposed to atmospheric winds generally contains waves of many periods. Typical records from a recording gage during periods of steep waves (Fig. 3-1) indicate that heights and periods of real waves are not as constant as is assumed in theory. Wavelengths and directions of propagation are also variable. (See Figure 3-2.) The prototype is so complex that some idealization is required.

3.21 SIGNIFICANT WAVE HEIGHT AND PERIOD

An early idealized description of ocean waves postulated a *significant height* and *significant period*, that would represent the characteristics of the real sea in the form of monochromatic waves.

The representation of a wave field by significant height and period has the advantage of retaining much of the insight gained from the theoretical studies. Its value has been demonstrated in the solution of engineering problems. For some problems this representation appears adequate; for others it is useful, but not entirely satisfactory.

To apply the significant wave concept it is necessary to define the height and period parameters from wave observations. Munk (1944) defined *significant wave height*, as the *average height of the one-third highest waves*, and stated that it was about equal to the average height of the waves as estimated by an experienced observer. This definition, while useful, has some drawbacks in wave-record analysis. It is not always clear which irregularities in the wave record should be counted to determine the total number of waves on which to compute the average height of the one-third highest. The significant wave height is written as $H_{1/3}$ or simply H_s.
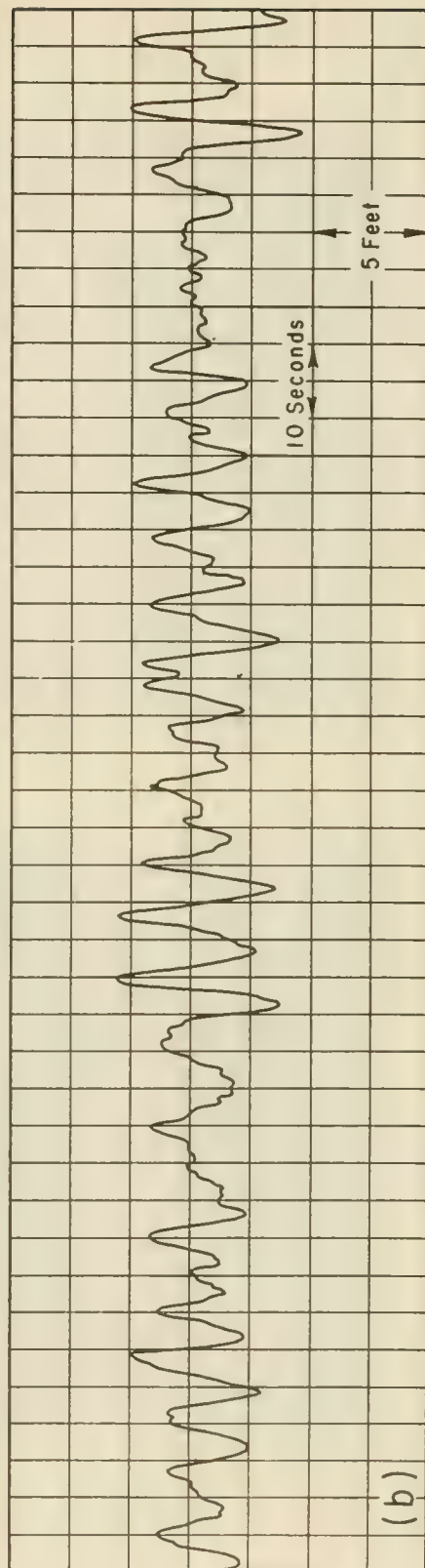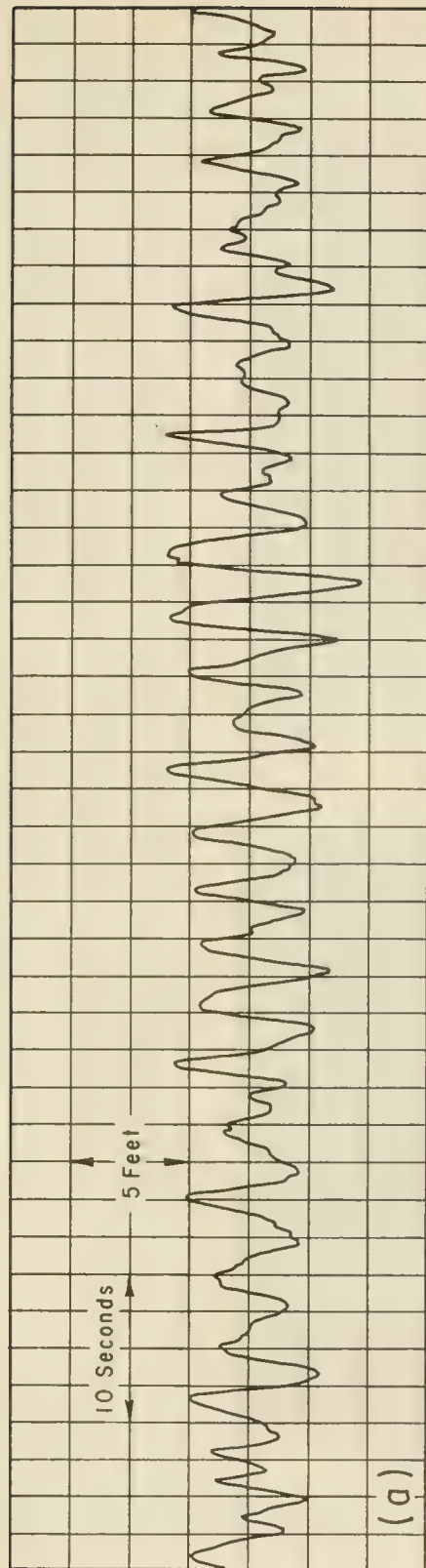
Figure 3-1. Sample Wave Records. (a) Chesapeake Bay Bridge Tunnel, Portal Island, significant height 5.5 feet, period 4 seconds (b) Huntington Beach, California, Significant height 5.5 feet, period 8 seconds.
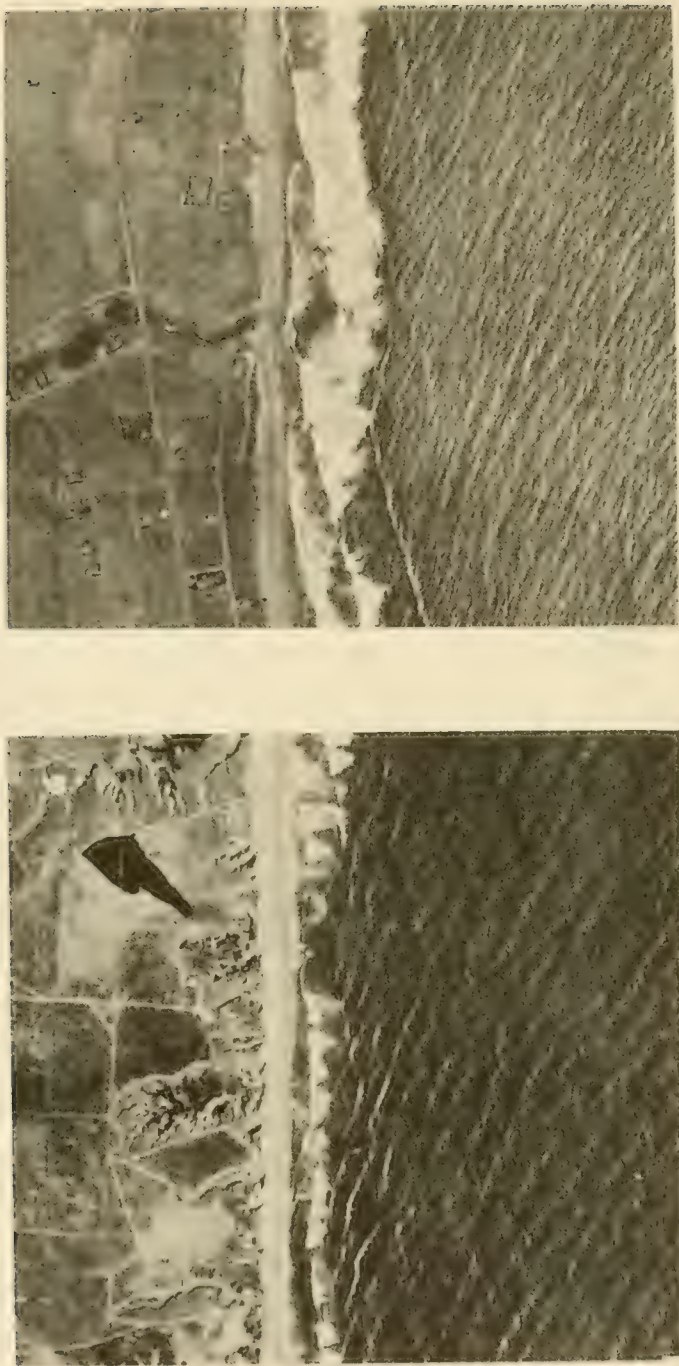
Figure 3-2. Waves in a Coastal Region. The left photo shows two wave trains approaching the shore simultaneously forming an irregular pattern of short-crested waves. The right photo shows long swell obscured by local wind waves almost until the breaking point

3-4

The significant wave period obtained by visual observations of waves is likely to be the average period of 10 to 15 successive prominent waves. When determined from gage records, the significant period is apt to be the average period of the subjectively estimated most prominent waves, or the average period of all waves whose troughs are below and whose crests are above the mean water level, (zero up crossing method).

3.22 WAVE HEIGHT VARIABILITY

When the heights of individual waves on a wave record are ranked from the highest to lowest, the frequency of occurrence of waves above any given value is given to a close approximation by the cumulative form of the Rayleigh distribution. This fact can be used to estimate the average height of the one-third highest waves from measurements of a few of the highest waves, or to estimate the height of a wave of any arbitrary frequency from a knowledge of the significant wave height. According to the Rayleigh distribution function, the probability that the wave height H is more than some arbitrary value of H referred to as $\widehat{H}$ is given by

$$P(H > \widehat{H}) = e^{-\left(\frac{\widehat{H}}{H_{rms}}\right)^2} \tag{3-1}$$

where H_{rms} is a parameter of the distribution, and $P(H > \widehat{H})$ is the number n of waves larger than $\widehat{H}$ divided by the total number N of waves in the record. Thus P has the form n/N. The value H_{rms} is called the *root-mean-square height* and is defined by

$$H_{rms} = \sqrt{\frac{1}{N} \sum_{j=1}^{N} H_j^2}. \tag{3-2}$$

It was shown in Section 2.238, Wave Energy and Power, that the total energy per unit surface area is given by

$$\bar{E} = \frac{\rho g H^2}{8}$$

The average energy per unit surface area for a number of waves is given by

$$(\bar{E})_A = \frac{\rho g}{8} \frac{1}{N} \sum_{j=1}^{N} H_j^2, \tag{3-3}$$

where H_j is the height of successive individual waves, and $(\bar{E})_A$ is the average energy per unit surface area of all waves considered. Thus H_{rms} is a measure of average wave energy. Calculation of H_{rms} by Equation 3-2 is somewhat less subjective than direct evaluation of the H_S because more emphasis is placed on the larger, better defined waves. The calculation can be made more objective by substitution of n/N for $P(H > \widehat{H})$ in Equation 3-1 and taking natural logarithms of both sides to obtain

$$Ln(n) = Ln(N) - (H_{rms}^{-2})\widehat{H}^2. \tag{3-4}$$

3-5

By making the substitutions

$$y(n) = Ln(n), \quad a = Ln(N), \quad b = -H_{rms}^{-2}, \quad x(n) = \widehat{H}^2(n) .$$

Equation 3-4 may be written as

$$y(n) = a + bx(n). \tag{3-5}$$

The constants a and b can be found graphically or by fitting a least-square regression line to the observations. The parameters N and H_{rms} may be computed from a and b. The value of N found in this way, is the value that provides the best fit between the observed distribution of identified waves and the Rayleigh distribution function. It is generally a little larger than the number of waves actually identified in the record. This seems reasonable because some very small waves are generally neglected in interpreting the record. When the observed wave heights are scaled by H_{rms}, that is, made dimensionless by dividing each observed height by H_{rms}, then data from all observations may be combined into a single plot. Points from scaled 15-minute samples are superimposed on Figure 3-3 to show the scatter to be expected from analyzing individual observations in this manner.

Data from 72 scaled 15-minute samples representing 11,678 observed waves have been combined in this manner to produce Figure 3-4. The theoretical height appears to be about 5 percent greater than the observed height for a probability of 0.01 and 15 percent at a probability of 0.0001. It is possible that the difference between the actual and theoretical heights of highest waves is due to breaking of the very highest waves before they reach the coastal wave gages.

Equation 3-1 can be established rigorously for restrictive conditions, and empirically for a much wider range of conditions. If Equation 3-1 is accepted as an exact law, the probability density function can be obtained in the form

$$f[(\widehat{H} - \Delta H) \leq H \leq (\widehat{H} + \Delta H)] = \left(\frac{2}{H_{rms}^2}\right) H e^{-\left(\frac{\widehat{H}}{H_{rms}}\right)^2} . \tag{3-6}$$

The height of the wave with any given probability n/N of being exceeded may be determined approximately from curve a in Figure 3-5 or from the equation,

$$\left(\frac{\widehat{H}}{H_{rms}}\right) = \left[-Ln\left(\frac{n}{N}\right)\right]^{1/2} \tag{3-7}$$
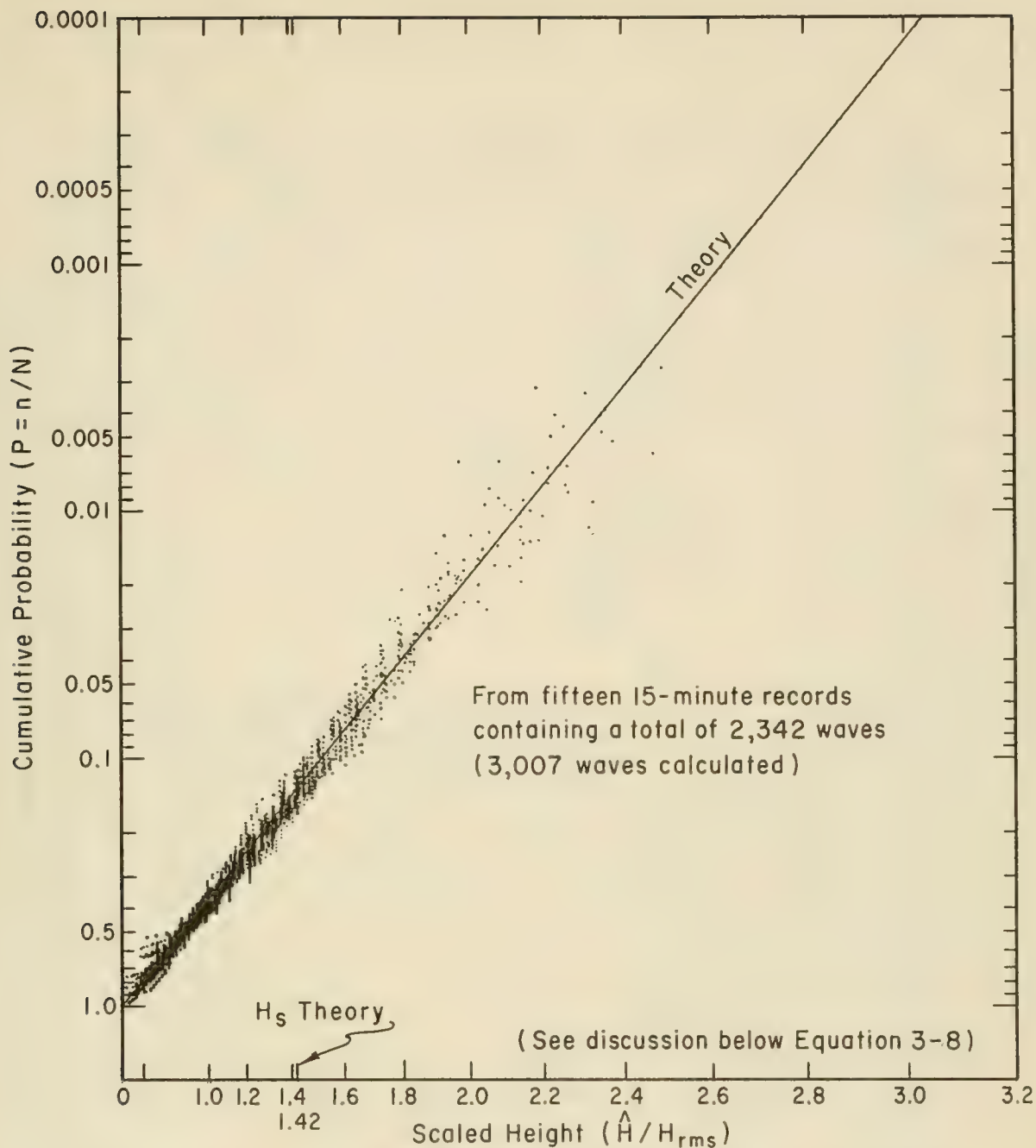
Figure 3-3. Theoretical and Observed Wave-Height Distributions. Observed distributions for 15 individual 15-minute observations from several Atlantic coast wave gages are superimposed on the Rayleigh distribution curve
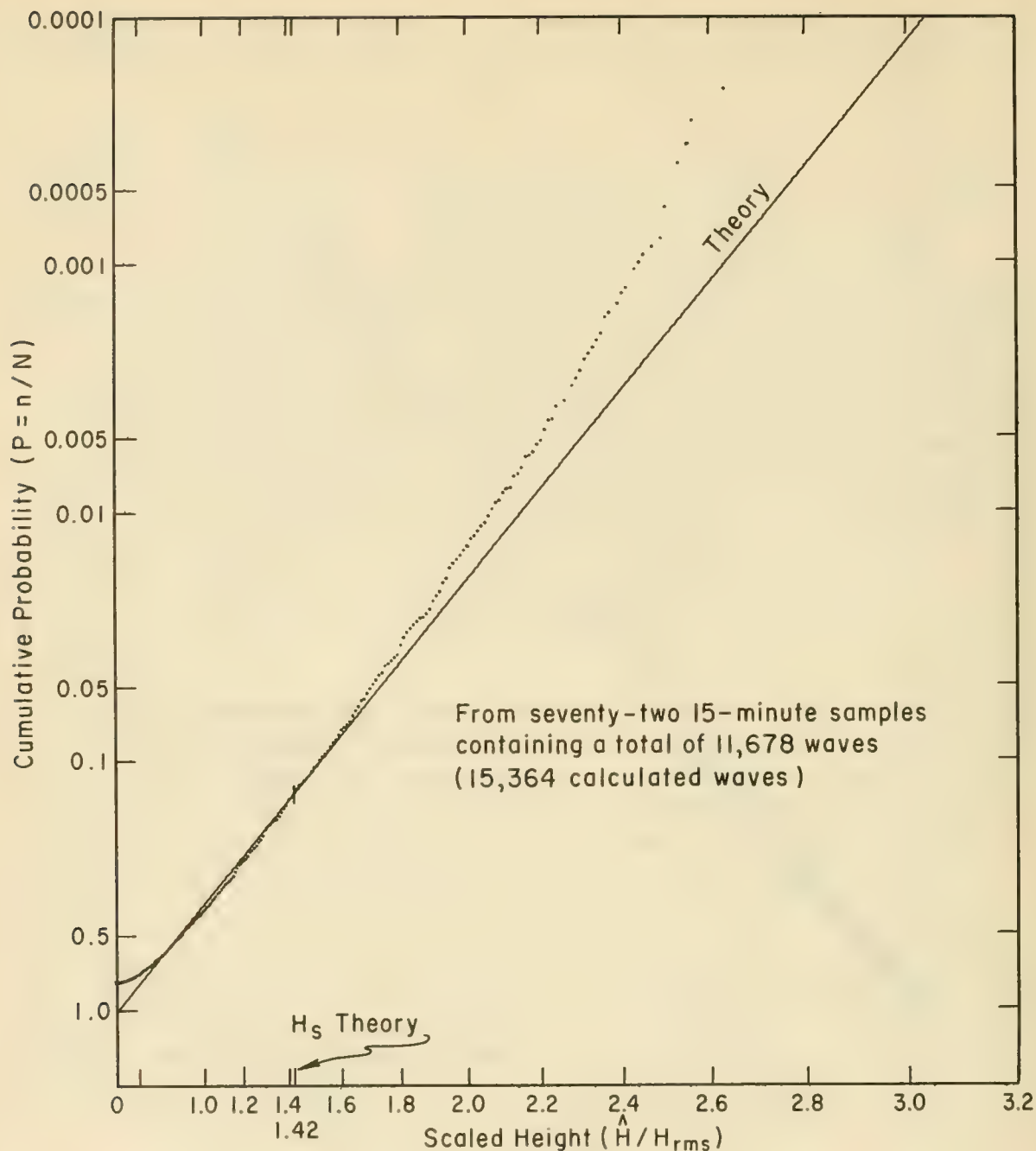
Figure 3-4. Theoretical and Observed Wave-Height Distributions. Observed waves from 72 individual 15-minute observations from several Atlantic coast wave gages are superimposed on the Rayleigh distribution curve

3-8
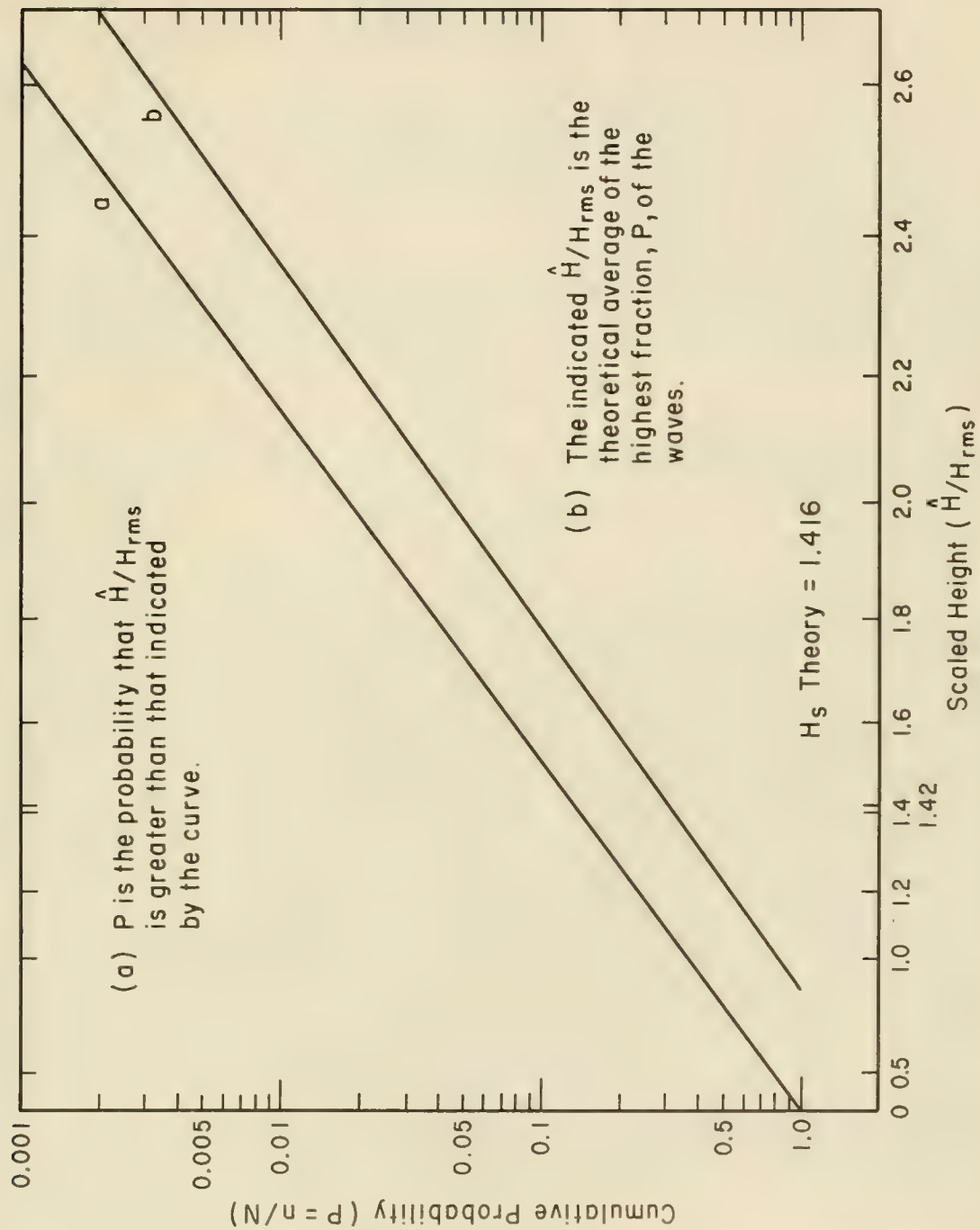
Figure 3-5. Theoretical Wave-Height Distributions

The average height of all waves with heights greater than $\overline{H}$ (H) can be obtained from the equation.

$$\overline{H}(\widehat{H}) = \frac{\displaystyle\int_{\widehat{H}}^{\infty} H^2 \, e^{-\left(\frac{H}{H_{rms}}\right)^2} \, dH}{\displaystyle\int_{\widehat{H}}^{\infty} H \, e^{-\left(\frac{H}{H_{rms}}\right)^2} \, dH} \; , \qquad (3\text{-}8)$$

or from curve b in Figure 3-5. By setting $\widehat{H} = 0$, all waves are considered, and it is found that the average wave height is given by

$$\overline{H} = 0.886 \, H_{rms} \, , \qquad (3\text{-}9)$$

and the significant wave height is given by

$$H_s = 1.416 H_{rms} \approx \sqrt{2} \, H_{rms} \, . \qquad (3\text{-}10)$$

In the analysis system used by CERC from 1960 to 1970, and whenever digital recordings cannot be used, the average period of a few of the best formed waves is selected as the significant wave period. An estimated number of equivalent waves in the record is obtained by dividing the duration of the record by this significant period. The highest waves are then ranked in order with the highest wave ranked 1. The height of the wave ranked nearest 0.135 times the total number of waves is taken as the significant wave height. The derivation of this technique is based on the assumption that the Rayleigh distribution law is exact. Harris (1970) showed that this procedure agrees closely with values obtained by more rigorous procedures which require the use of a computer. These procedures are described in Section 3.23, Energy Spectra of Waves.

The following problem illustrates the use of the theoretical wave height distribution curves given in Figure 3-5.

* * * * * * * * * * * * * *   EXAMPLE PROBLEM   * * * * * * * * * * * * * * *

GIVEN: Based on an analysis of wave records at a coastal location, the significant wave height H_s was estimated to be 10 feet.

FIND:

(a) H_{10} (Average of the highest 10 percent of all waves)

(b) H_1 (Average of the highest 1 percent of all waves)

SOLUTION: $\hat{H} = H_s = 10$ feet

Using Equation 3-10

$$H_s = 1.416\,H_{rms}$$

or

$$H_{rms} = \frac{H_s}{1.416} = \frac{10}{1.416} = 7.06 \text{ ft} .$$

(a)   From Figure 3-5, curve b, it is seen that for P = 0.1 (10 percent)

$$\frac{H_{10}}{H_{rms}} \approx 1.80; \ H_{10} = 1.80\,H_{rms} = 1.80\,(7.06) = 12.7 \text{ feet, say 13 feet.}$$

(b)   Similarly, for P = 0.01 (1 percent)

$$\frac{H_1}{H_{rms}} \approx 2.36; \ H_1 = 2.36\,H_{rms} = 2.36\,(7.06) = 16.7 \text{ ft., say 17 ft.}$$

Note that:

$$\frac{H_{10}}{H_s} = \frac{12.7}{10} \text{ or } H_{10} = 1.27\,H_s ,$$

and

$$\frac{H_1}{H_s} = \frac{16.7}{10} \text{ or } H_1 = 1.67\,H_s .$$

* *

Goodknight and Russell (1963) analyzed wave-gage observations taken on an oil platform in the Gulf of Mexico during four hurricanes. They found agreement adequate for engineering application between such important parameters as H_s, H_{10}, H_{max}, H_{rms}, and $\bar{H}$, although they did not find consistently good agreement between measured wave-height distributions and the entire Rayleigh distribution. Borgman (1972) substantiates this conclusion from wave observations from other hurricanes. These findings are consistent with Figures 3-3, and 3-4, based on wave records recently obtained by CERC from shore-based gages. The CERC data include waves from both extratropical storms and hurricanes.

3.23 ENERGY SPECTRA OF WAVES

The significant wave analysis, although simple in concept, is diffi-cult to do objectively, and does not provide all of the information needed in engineering design.

It appears from Figure 3-1 that the wave field might be better described by a sum of sinusoidal terms. That is, the curves in Figure 3-1 might be better represented by expressions of the type

$$\eta(t) = \sum_{j=1}^{N} a_j \cos(\omega_j - \phi_j),$$ (3-11)

where $\eta(t)$ is the departure of the water surface from its average position as a function of time, a_j is the amplitude, ω_j is the frequency, and ϕ_j is the phase of the jth wave at the time $t = 0$. The values of ω are arbitrary, and ω may be assigned any value within suitable limits. In analyzing records, however, it is convenient to set $\omega_j = 2\pi j/D$, where j is an integer and D is the duration of the observation. The a_j will be large only for those ω_j that are prominent in the record. When analyzed in this manner, the significant period may be defined as D/j, where j is the value of j corresponding to the largest a_j.

It was shown by Kinsman (1965), that the average energy of the wave train is proportional to the average value of $[\eta(t)]^2$. This is identical to σ^2 where σ is the standard deviation of the wave record. It can also be shown that

$$\sigma^2 = \frac{1}{2} \sum_{j=1}^{N} a_j^2.$$ (3-12)

Experimental results and calculations based on the Rayleigh distribution function show that the significant wave height is approximately equal to 4σ. Thus, recalling that

$$H_s \approx \sqrt{2} \; H_{rms},$$

and

$$H_s \approx 4\sigma,$$

then

$$\sigma \approx 0.25 \sqrt{2} \; H_{rms},$$ (3-13)

or

$$H_{rms} \approx 2 \sqrt{2} \; \sigma.$$ (3-14)

The a_j^2 may be regarded as approximations to the energy spectrum function $E(\omega)$ where

$$E(\omega) \, \Delta\omega = \frac{a_j^2}{2}.$$ (3-15)

Thus

$$\sigma^2 = \int\limits_{0}^{\infty} E(\omega)\, d\omega \,. \qquad (3\text{-}16)$$

The spectrum $E(\omega)$ permits one to assign specific portions of the total wave energy to specific frequency intervals, to recognize that two or more periods may be important in describing the wave field, and to give an indication of their relative importance. This also permits a first approximation to the calculation of velocities and accelerations from a record of the wave height in a complex wave field. Several energy spectra, computed from coastal zone wave records obtained by CERC, are shown in Figure 3-6.

The international standard unit for frequency measure is the *hertz*, defined as one cycle per second. The units *cycles per second* and *radians per second* are also widely used. One hertz = 2π radians per second.

3.24 DIRECTIONAL SPECTRA OF WAVES

A more complete description of the wave field is required to recognize that not all waves are traveling in the same direction. This may be written as,

$$\eta(x, y, t) = \Sigma\, a_j \, \cos\left[\omega_j t - \phi_j - k\,(x\cos\theta_j + y\sin\theta_j)\right], \qquad (3\text{-}17)$$

where $k = 2\pi/L$, and θ_j is the angle between the x axis and the direction of wave propagation, and ϕ_j is the phase of the jth wave at $t = 0$. The energy density $E(\theta,\omega)$ represents the concentration of energy at a particular wave direction θ, and frequency ω, therefore the total energy is obtained by integrating $E(\theta,\omega)$ over all directions and frequencies, thus

$$E = \int\limits_{0}^{2\pi} \int\limits_{0}^{\infty} E(\theta, \omega)\, d\omega\, d\theta \,. \qquad (3\text{-}18)$$

The concept of directional wave spectra is essential for advanced wave-prediction models, but technology has not yet reached the point where directional spectra can be routinely recorded or used in engineering design studies. Therefore, directional wave spectra are not discussed extensively here.

Savannah Coast Guard Light Tower

Nags Head, N.C.
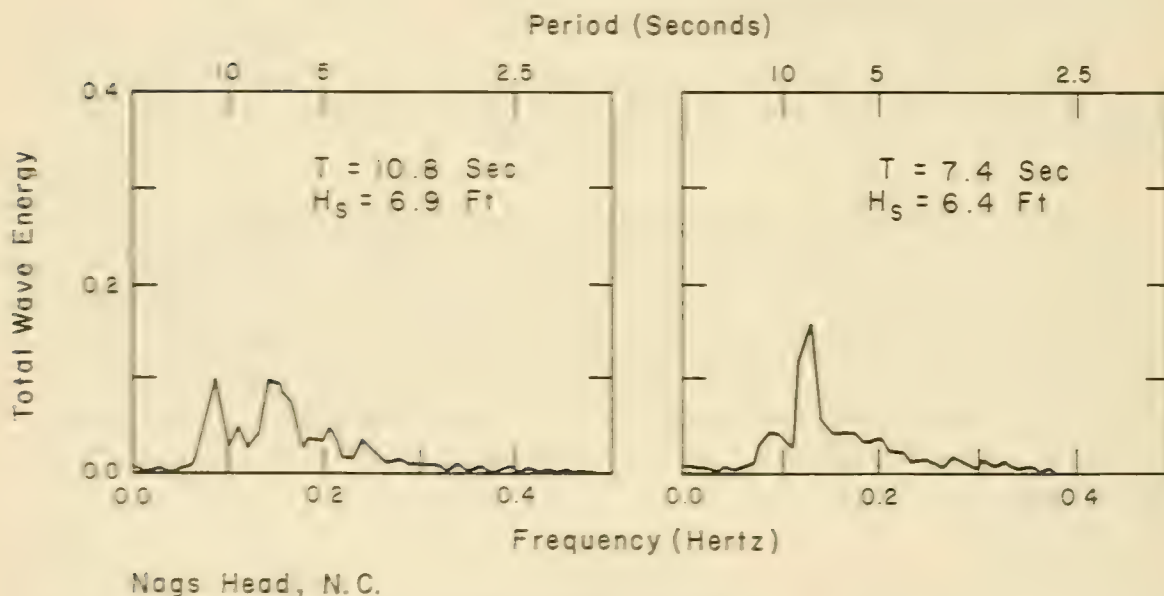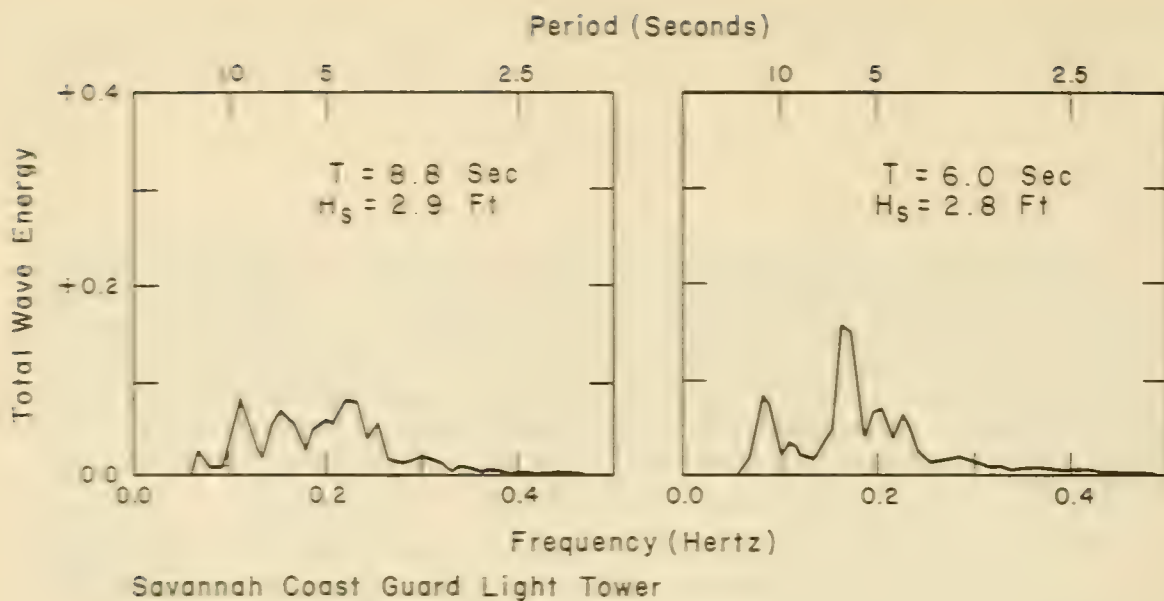
Figure 3-6. Typical Wave Spectra from the Atlantic Coast.
The ordinate scale is the fraction of total
wave energy in each frequency band of 0.011
Hertz, (one Hertz is one cycle/second). A
linear frequency scale is shown at the bottom
of each graph and a nonlinear period scale
at the top of each graph.

3.3 WAVE FIELD

3.31 DEVELOPMENT OF A WAVE FIELD

Various descriptions of the mechanism of wave generation by wind have been given, and significant progress in explaining the mechanism was reported by Miles (1957) and Phillips (1957). Integraged discussions of the results of many of the more prominent descriptions of wave generation by wind are given by Kinsman (1965), Phillips (1966), and Ewing (1971).

Laboratory studies, (Hidy and Plate, 1966) and (Shemdin and Hsu, 1966), carefully designed to match the assumptions made by Miles and by Phillips show reasonably good agreement with the theoretical predictions. Summaries of various filed studies, (Inoue, 1966, 1967) demonstrate that theory provides a reasonable framework for the analysis of observations.

The Miles-Phillips theory as extended and corrected by experimental data permits the formulation of a differential equation governing the growth of wave energy. This equation can be written in a variety of ways. (Inoue, 1966, 1967) and Barnett, 1968). This approach will not be discussed in detail because it requires a large capacity computer and more meteorological data than is likely to be found except in a major forecast center.

A brief discussion of the physical concepts employed in the computer wave forecast, however, is presented to show the shortcomings and merits of simpler procedures that can be used in wave forecasting.

Growth and dissipation of wave energy are very sensitive to wave frequency and wave direction relative to the wind direction. Thus it is desirable to consider each narrow band of directions and frequencies separately. A change in wave energy depends on the advection of energy into and out of a region; transformation of the wind's kinetic energy into the energy of water waves; dissipation of wave energy into turbulence and by friction, viscosity and breaking; and transformation of wave energy at one frequency into wave energy at other frequencies.

Wave energy is discussed in Section 2.238. Wave Energy and Power. Although it is known that energy transfers from one band of wave frequencies to another do take place, this process is secondary to the transfer of energy from the atmosphere to the sea, and is not yet well enough understood to justify its consideration in a practical wave prediction scheme.

Phillips (1957) showed that the turbulence associated with the flow of wind near the water would create traveling pressure pulses. These pulses generate waves traveling at a speed appropriate to the dimensions of the pressure pulse. Wave growth by this process is most rapid when the waves are short and when their speed is identical with the component of the wind velocity in the direction of wave travel. The empirical data analyzed by Inoue (1966, 1967) indicates that the effect of turbulent pressure pulses is real, but is only about one-twentieth as large as the original theory indicated.

Miles (1957) showed that the waves on the sea surface must be matched by waves on the bottom surface of the atmosphere. The speed of air and water must be equal at the water surface. Under most meteorological conditions, the air speed increases from near 0 to 60 - 90 percent of the free air value within 66 feet (20 meters) of the water surface. Within a shear zone of this type, energy is extracted from the mean flow of the wind and transferred to the waves. The magnitude of this transfer at any frequency is proportional to the wave energy already present at that frequency. Growth is normally most rapid at high frequencies. The energy transfer is also a complex function of the wind profile, the turbulence of the air stream, and the vector difference between wind and wave velocities.

The theories of Miles and Phillips predict that waves grow most rapidly when the component of the wind speed in the direction of wave propagation is equal to the speed of wave propagation.

The wave generation process discussed by Phillips is very sensitive to the structure of the turbulence. This is affected significantly by any existing waves, and the temperature gradient in the air near the water surface. The turbulence structure in an offshore wind is also affected by land surface roughness near the shore.

The wave generation process discussed by Miles is very sensitive to the vertical profile of the wind. This is determined largely by turbulence in the wind stream, the temperature profile in the air, and by the roughness of the sea surface.

Shorter waves grow most rapidly. Those waves which propagate obliquely to the wind are favored, for they are better matched to the component of the wind velocity in the direction of wave propagation than those moving parallel to the wind. Thus, the first wave pattern to appear for short fetches and durations consists of two wave trains forming a rhombic pattern with one diagonal along the direction of the mean wind.

There is a limit to the steepness to which a wave can grow without breaking. Shorter waves reach their limiting growth rather quickly; longer waves, which grow more slowly but can obtain greater heights, then become more prominent. Thus, the apparent direction of propagation of the two wave trains tends to coalesce with increasing fetch and duration. The length of the region in which a rhombic pattern is apparent may extend from a few meters to a few kilometers depending on the width of the basin, the wind speed, and previously existing waves.

Wave growth is significantly affected by any preexisting waves. The empirical data analyzed by Inoue (1966, 1967) indicated that the magnitude of the effect of seas already present is about eight times the value given in the original Miles (1957) theory. Neglecting this effect in early wave prediction theories has led to large errors in computing the duration required for a fully arisen sea. There are many situations in which the largest waves and the waves growing most rapidly are not being propagated in the wind direction.

3.32 VERIFICATION OF WAVE HINDCASTING

Inoue (1967) prepared hindcasts for Weather Station J (located near 53°N, 18°W), for the period 15-28 December, 1959, using a differential equation embodying the Miles-Phillips theory to predict wave growth. A comparison of significant wave heights from shipboard observations and by hindcasting at two separate locations near the weather ships is shown in Figure 3-7. The location of Ocean Weather Ship J, the mesh points used in the numerical calculations, and four other locations discussed below are are shown in Figure 3-8. The calculations required meteorological data from 519 grid points over the Atlantic Ocean as shown in Figure 3-8. The agreement between observed and computed values seems to justify a high level of confidence in the basic prediction model. Observed meteorological data were interpolated in time and space to provide the required data, thus these predictions were hindcasts.

Bunting and Moskowitz (1970) and Bunting (1970) have compared fore-cast wave heights with observations, using the same model with comparable results.

By 1970, it was generally believed that the major remaining difficulty in wind wave prediction was the determination of the surface wind field over the ocean. (Pore and Richardson, 1967), and (Bunting, 1970). It is partly because of the difficulty in obtaining a satisfactory specification of the wind field over the sea that simpler wave prediction systems are still being used operationally. (Pore and Richardson, 1969), (Shields and Burdwell, 1970), and (Francis, 1971.)

3.33 DECAY OF A WAVE FIELD

Wind-energy can be transferred directly to the waves only when the component of the surface wind in the direction of wave travel exceeds the speed of wave propagation. Winds may decrease in intensity, pass over land, or change in direction to such an extent that wave generation ceases, or the waves may propagate out of the generation area. When any of these events occurs, the wave field begins to decay. Wave energy travels at a speed which increases with the wave period. Thus the energy packet leaving the generating area spreads out over a larger area with increasing time. The apparent period at the energy front increases and the wave height decreases. If the winds subside before the sea is fully arisen, the longer waves may begin to decay while the shorter waves are still growing. This possibility is recognized in advanced wave prediction techniques. The hindcast spectra, computed by the Inoue (1967) model and published by Guthrie (1971) show many examples of this for low swell, as do the aerial photographs and spectra given by Harris (1971). (See Figures 3-2 and 3-6.) This swell is frequently overlooked in visual observations and even in the subjective analysis of pen and ink records from coastal wave gages.

Most coastal areas of the United States are so situated that most of the waves reaching them are generated in water so deep that depth has no effect on wave generation. In many of these areas, wave characteristics
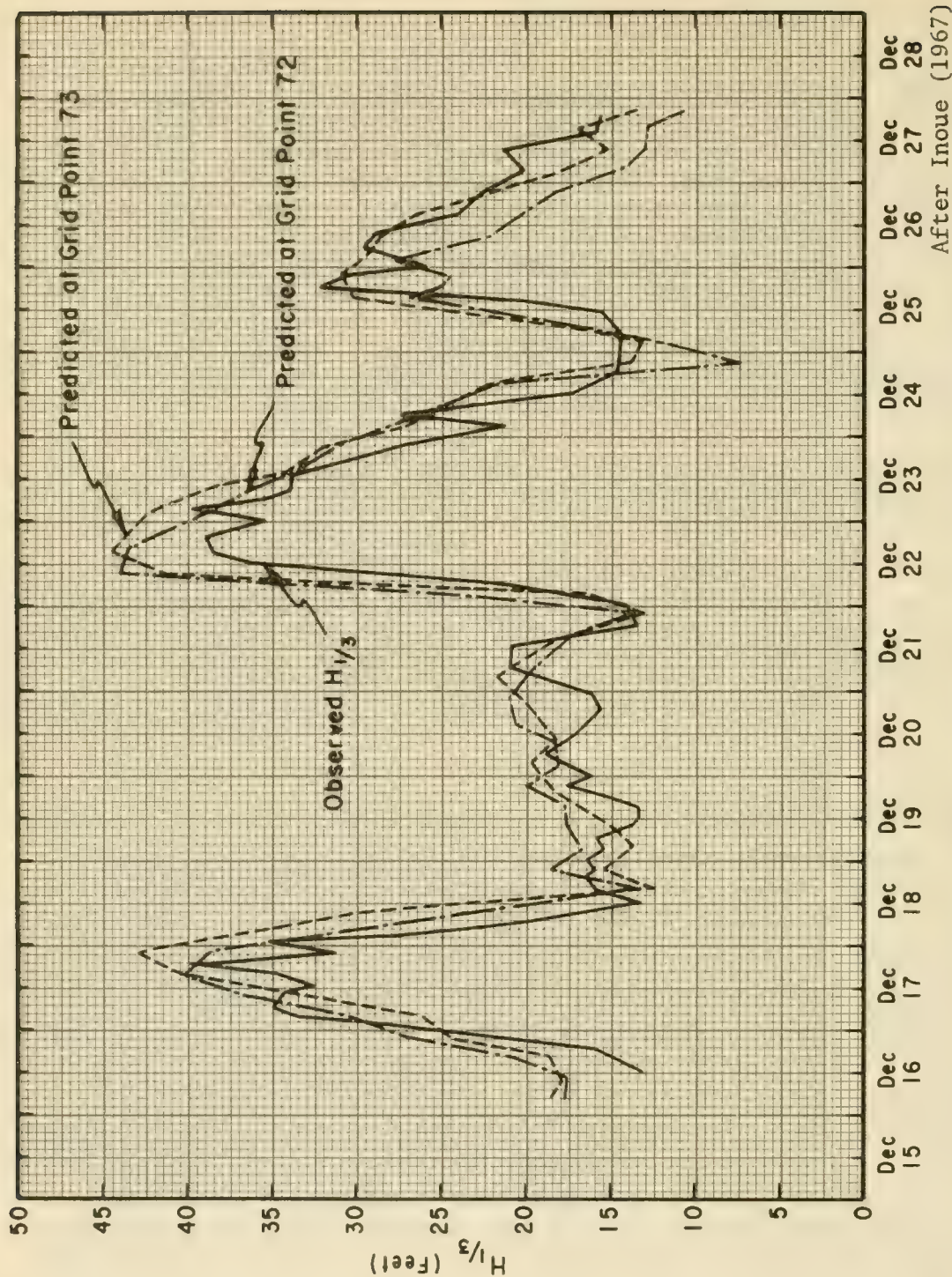
Figure 3-7. Observed and Hindcasted Significant Wave Heights versus Time (GMT), December, 1959, at and near the Weather Station J in the North Atlantic. Location of mesh points 72 and 73 and Ocean Weather Ship J are shown in Figure 3-8.

After Inoue (1967)

3-18
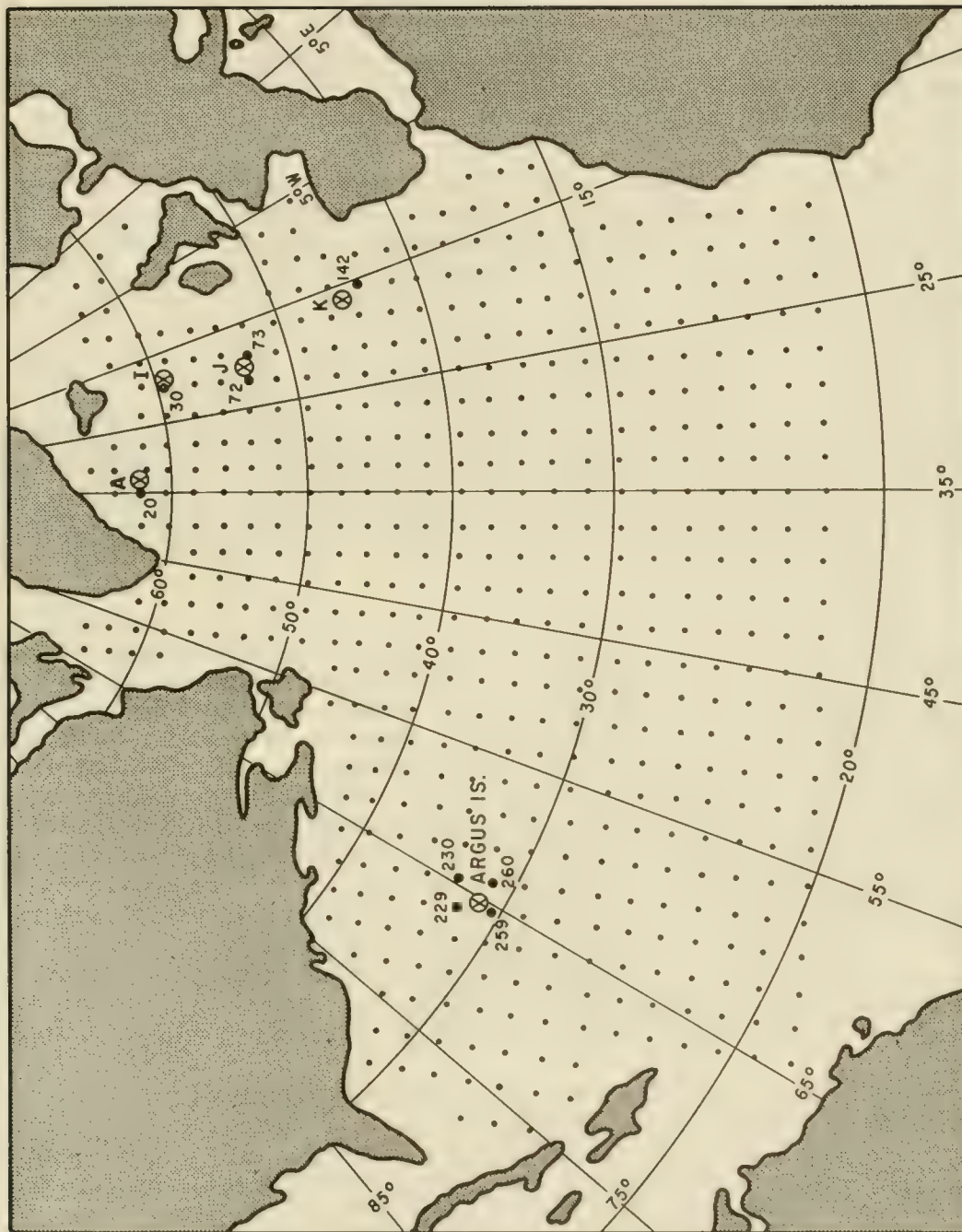
Figure 3-8. Map of North Atlantic Grid Points, Ocean Weather Ship (OWS) Stations and Argus Island

(from Bunting and Moskowitz (1970))

may be determined by first analyzing meteorological data to find deep-water conditions. Then, by analyzing refraction (Section 2.32, General - Refraction by Bathymetry.), the changes in wave characteristics as the wave moves through shallow water to the shore may be found. In other areas, in particular along the North Atlantic coast, where the bathymetry is complex, refraction procedure results are frequently difficult to interpret, and the conversion of deepwater wave data to shallow-water and nearshore data becomes laborious and sometimes inaccurate.

Along the Gulf coast and in many inland lakes, generation of waves by wind is appreciably affected by water depth. In addition, the nature and extent of transitional and shallow-water regions complicate ordinary refraction analysis by introducing a bottom-friction factor and associated wave energy dissipation.

3.4 WIND INFORMATION NEEDED FOR WAVE PREDICTION

Wave prediction from first principles, as described above, requires very detailed specification of the wind field near the water surface. This is generally developed in two steps: (1) Estimation of the mean *free* air wind speed and direction, (This step may be omitted for reservoirs and small lakes if surface wind observations are available.), and (2) Estimation of the mean *surface* wind speed and direction.

When the full wave generation process is considered, a large capacity computer must be used for the calculations, and fairly complex procedures may be used for determining the wind field. Engineers who require wave hindcasts for only a few locations, and perhaps for only a few dates must employ simpler techniques. A brief discussion of the processes involved in determining the surface wind and techniques suitable for use in determining the characteristics of the wind field needed for the simplified wave prediction model described in Section 3.5, Simplified Wave Prediction Models, are given in this section. These procedures will be accurate (within 20 percent) about two-thirds of the time. The following discussion provides guidance for recognizing cases in which the simplified procedures are not appropriate. Errors resulting from disregarding the exceptional situations tend to be random. Thus climatological summaries, based on hindcast data, may be much more accurate than the individual values that go into them.

Wind reports from ships at sea are generally estimates based on the appearance of the waves, the drifting of smoke, or the flapping of flags - although some are anemometer measurements. Actually, even if all ships were equipped with several aneometers, the wind field over the sea would still not be known in sufficient detail or precision to permit full exploitation of modern theories for wave generation.

Fortunately, estimates of the surface wind field that are usefully accurate most of the time can be based on the isobaric pattern of synoptic weather charts.

Horizontal pressure gradients arise in the atmosphere primarily because of density differences, which in turn are generated primarily by temperature differences. Wind results from nature's efforts to eliminate the pressure gradients, but is modified by many other factors.

The pressure gradient is nearly always in approximate equilibrium with the acceleration produced by the rotation of the earth. The *geostrophic wind* is defined by assuming that exact equilibrium exists, and is given by

$$U_g = \frac{1}{\rho_a f} \frac{dp}{dn} \; , \qquad (3\text{-}19)$$

where U_g is the wind speed, ρ_a the density of the air, f the coriolis parameter, $f = 2\omega \sin\phi$, where $\omega = 7.292 \times 10^{-5}$ radians/second and ϕ is the latitude, and dp/dn is the horizontal gradient of atmospheric pressure. A graphic solution of this equation is given in Figure 3-11, Section 3.41, Estimating the Wind Characteristics. The geostrophic wind blows parallel to the isobars with low pressure to the left, when looking in the direction toward which the wind is blowing, in the Northern Hemisphere, and low pressure to the right in the Southern Hemisphere. Geostrophic wind is usually the best simple estimate of the true wind in the free atmosphere.

When the trajectories of air particles are curved, equilibrium wind speed is called *gradient wind*. Gradient wind is stronger than geostrophic wind for flow around a high pressure area, and weaker than geostrophic wind for flow around low pressure. The magnitude of the difference between geostrophic and gradient winds is determined by the curvature of the trajectories. If the pressure pattern does not change with time and friction is neglected, trajectories are parallel with the isobars. The isobar curvature can be measured from a single weather map, but at least two maps must be used to estimate trajectory curvature. There is a tendency by some analysts to equate the isobars and trajectories at all times, and to compute the gradient wind correction from the isobar curvature. When the curvature is small, but the pressure is changing, this tendency may lead to incorrect adjustments. Corrections to the geostrophic wind that cannot be determined from a single weather map are usually neglected, even though they may be more important than the isobaric curvature effect.

The equilibrium state is further disturbed near the surface of the earth by friction. Friction causes the wind to cross the isobars toward low pressure at a speed lower than the wind speed in the free air. Over water, the average surface wind speed is generally about 60 to 75 percent of the free air value, and wind crosses the isobars at an angle of 10 to 20 degrees. In individual situations, the magnitude of the ratio between the surface wind speed and the computed free air speed may vary from 20 to more than 100 percent, and the crossing angle may vary from $0°$ to more than $90°$. The magnitude of these changes is determined by the vertical temperature profile and the turbulent viscosity in the atmosphere.

3.41 ESTIMATING THE WIND CHARACTERISTICS

To predict wave properties from meteorological data by any of the simplified techniques, it is necessary to:

(a) Estimate the mean surface wind speed and direction, as discussed in Section 3.4, Wind Information Needed for Wave Prediction;

(b) delineate a fetch over which the wind is reasonably constant in speed and direction, and measure the fetch length, and

(c) estimate wind duration over the fetch.

These determinations may be made in many ways depending on the location and the type of meterological data available. For restricted bodies of water, such as lakes, the fetch length is often the distance from the forecasting point to the opposite shore measured along the wind direction. There is no decay distance, and it is often possible to use observational data to determine wind speeds and durations.

When forecasting for oceans or other large bodies of water, the most common form of meteorological data used is the synoptic surface weather chart. (*Synoptic* means that the charts are drawn by analysis of many individual items of meteorological data obtained simultaneously over a wide area.) These charts depict lines of equal atmospheric pressure, called isobars. Wind estimates at sea, based on an analysis of the sea-level atmoshperic pressure are generally more reliable than wind observations because pressure, unlike wind, can be measured accurately on a moving ship. Pressures are recorded in millibars, 1,000 dynes per square centimeter. One thousand millibars (a bar) equals 29.53 inches of mercury and is 98.7 percent of normal atmoshperic pressure.

A simplified surface chart for the Pacific Ocean is shown in Figure 3-9, which is drawn for 27 October 1950 at 0030Z (0030 Greenwich mean time). Note the area labelled L in the right center of the chart, and the area labelled H in the lower left corner of the chart. These are low- and high-pressure areas; the pressures increase moving out from L (isobars 972, 975, etc.) and decrease moving out from H (isobars 1026, 1023, etc.).

Scattered about the chart are small arrow shafts with a varying number of feathers or barbs. The direction of a shaft shows the direction of the wind; each one-half feather represents a unit of 5 knots (2.5 meters/second) in wind speed. Thus, in Figure 3-9 near the point 35°N. latitude, 135°W. longitude, there are three such arrows, two with $3\frac{1}{2}$ feathers which indicate a wind force of 31 to 35 knots (15 to 17.5 meters/second), and one with 3 feathers indicating a force of 26 to 30 knots (13 to 15 meters/second).

On an actual chart, much more meteorological data than wind speed and direction are shown for each station. This is accomplished by the use of
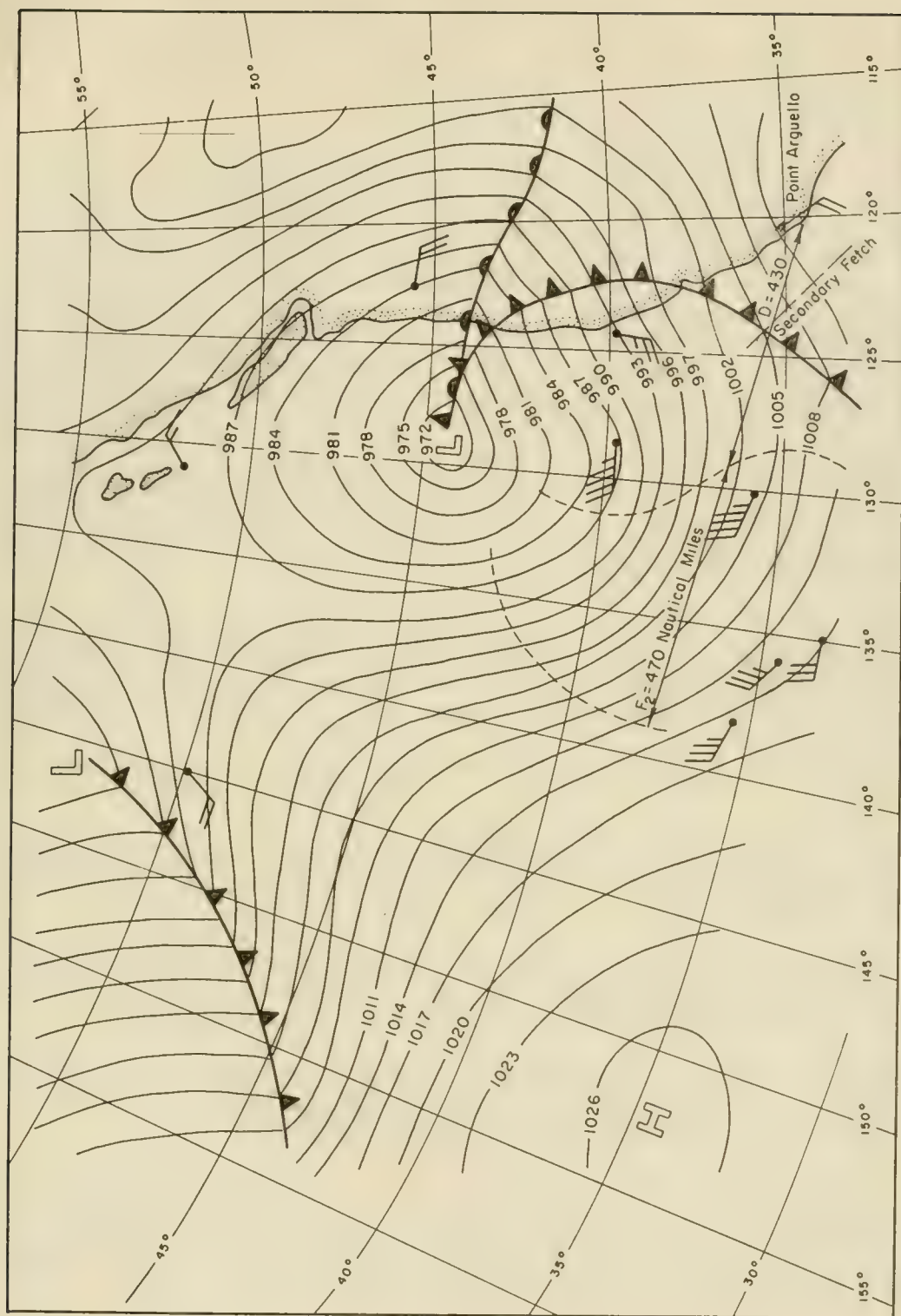
Figure 3-9. Surface Synoptic Chart for 0030Z, 27 October 1950

3-23

coded symbols, letters, and numbers placed at definite points in relation to the station dot. A sample model report, showing the amount of information possible to report on a chart, is shown in Figure 3-10. Not all of the data shown on this plot are included in each report, and not all of the data in the report are plotted on each map.

Figure 3-11 may be used to facilitate computation of the geostrophic wind speed. A measure of the average pressure gradient over the area is required. Most synoptic charts are drawn with either a 3- or 4-millibar spacing. Sometimes when isobars are crowded, intermediate isobars are omitted. Either of these standard spacings is adequate as a measure of the geographical distance between isobars. Using Figure 3-11, the distance between isobars on a chart is measured in degrees of latitude (an average spacing over a fetch is ordinarily used), and the latitude position of the fetch is determined. Using the spacing as ordinate and location as abscissa, the plotted or interpolated slant line at the intersection of these two values gives the geostrophic wind speed. For example, in Figure 3-9, a chart with 3-millibar isobar spacing, the average isobar spacing (measured normal to the isobars) over F_2, located at 37°N. latitude, is 0.70° of latitude. Using the scales on the bottom and right side of Figure 3-11, a geostrophic wind of 67 knots is found.

Geostrophic wind speeds are generally higher than surface wind speeds. The following instructions, U.S. Fleet Weather Facility Manual (1966), are recommended for obtaining estimates of the surface wind speeds over the open sea from the geostrophic wind speeds:

(a) For moderately curved to straight isobars - no correction is applied.

(b) For great anticyclonic (clockwise movement about a high pressure center in Northern Hemisphere and counter-clockwise in Southern Hemisphere) curvature - add 10 percent to the geostrophic wind speed.

(c) For great cyclonic (counter-clockwise movement about a low pressure center in Northern Hemisphere and clockwise in Southern Hemisphere) curvature - subtract 10 percent from the geostrophic wind speed.

Frequently the curvature correction can be neglected since isobars over a fetch are often relatively straight. The gradient wind can always be computed if more refined computations are desired.

To correct for air mass stability, the sea-air temperature difference must be computed. This can be done from ship reports in or near the fetch area, aided by climatic charts of average monthly sea surface temperatures when data are too scarce. The correction to be applied is given in Table 3-1. (U.S. Fleet Weather Facility Manual, 1966.)

Over oceans, the surface winds generally cross the isobars toward low pressure at an angle of 10° to 20°.
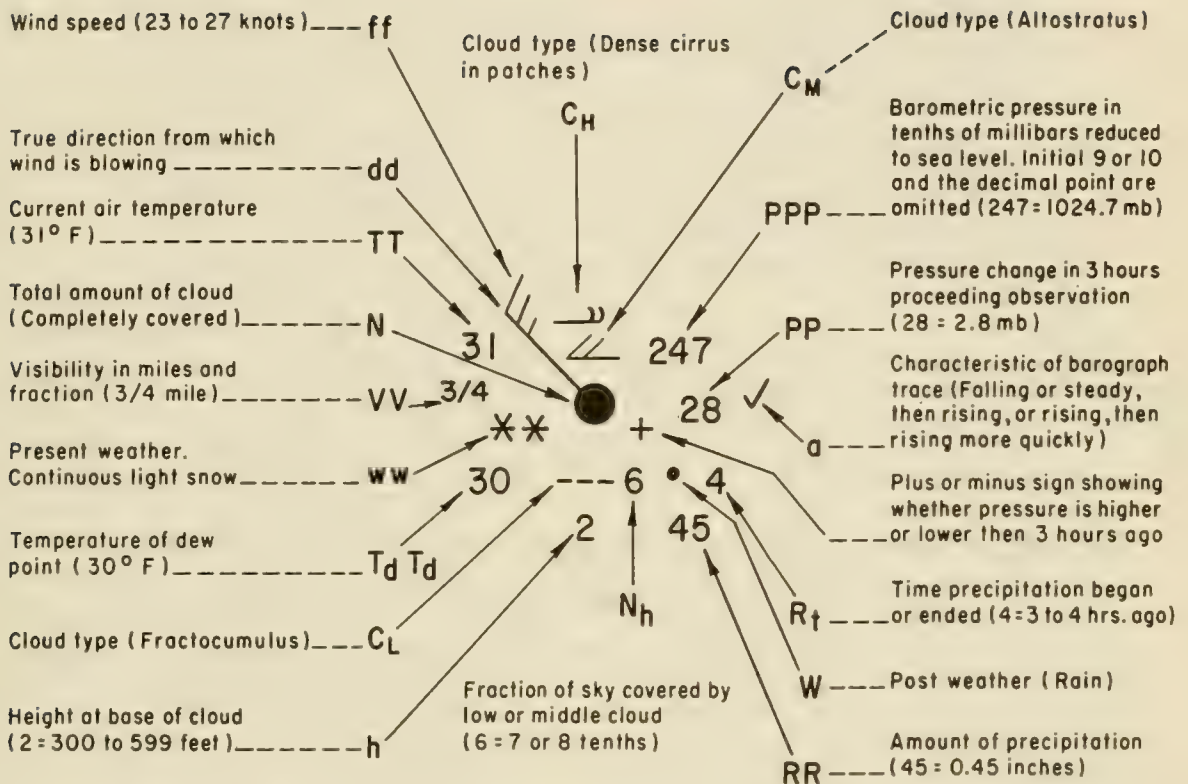
Figure 3-10.   Sample Plotted Report

$$U_g = \frac{1}{\rho_a f} \frac{\Delta p}{\Delta n}$$

For T = 10° C

   Δp = 3 mb and 4 mb

   Δn = isobar spacing measured in degrees latitude

   p = 1013.3 mb

   ρ_a = 1.247 × 10⁻³ gm/cm³

   f = Coriolis parameter = $2\omega \sin \emptyset$

where

   ω = angular velocity of earth, 0.2625 radians/hour

   $\emptyset$ = latitude in degrees

GEOSTROPHIC WIND VELOCITY, U_g
IN KNOTS
Left Scale — 3mb Isobar Spacing
Right Scale — 4mb Isobar Spacing

(after Bretschneider, 1952a)
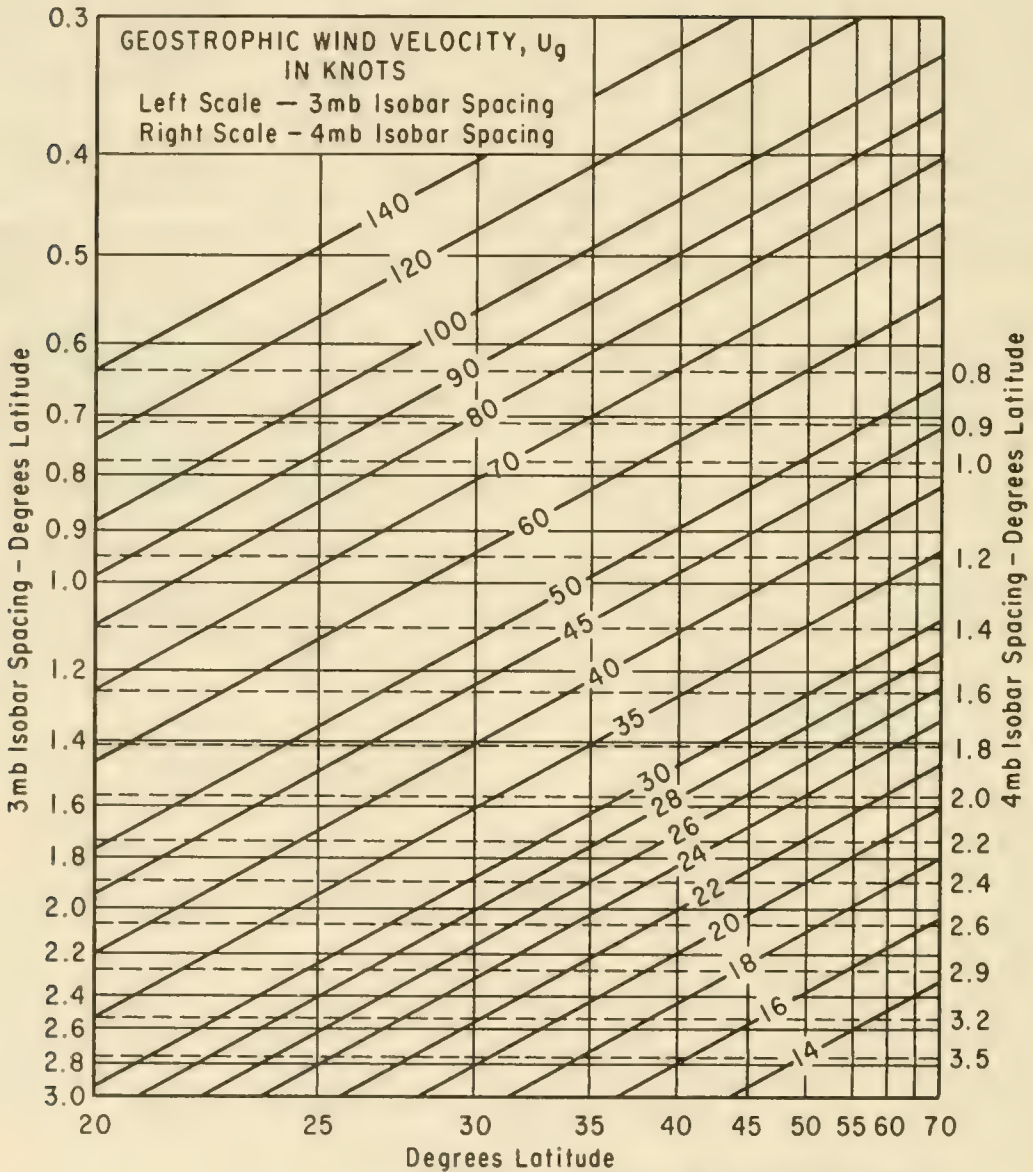
Figure 3-11.   Geostrophic Wind Scale

Table 3-1. Correction for Sea-Air Temperature*

Sea Temperature minus Air Temperature	Ratio of Surface Wind Speed to Geostrophic Wind Speed, U/Ug
0 or negative	0.60
0 to 10	0.65
10 to 20	0.75
20 or above	0.90

*Pore and Richardson (1969) and Hasse and Wagner (1971)
report recent studies designed to refine the above table.
Neither were able to find enough high quality observa-
tions of large differences between air and sea tempera-
tures to rigorously establish any effect of the sea-air
temperature difference on the ratio of the surface wind
speed to the gradient wind speed over the ocean. Both
recommended the use of a constant value near 0.6 for
most routine work.

   If there are several observed wind reports within the fetch region,
and these consistently deviate in the same manner from wind speeds arrived
at by the instructions given above, an average between the reported values
and those computed by the above instructions will usually be the best
estimate.

   Over the Great Lakes and some coastal regions, large temperature
inversions (temperature increasing with elevation) may be observed.
Bellaire (1965) reports air temperatures more than $15^{\circ}C$ ($27^{\circ}F$) greater
than the water temperature in May 1964. When air temperature is much
greater than that of the sea, all turbulent motion in the lower atmosphere
is suppressed, and the wind near the surface has little relation to the
wind estimate determined from a synoptic weather chart. Near mountainous
coasts and particularly in fjords, the wind near the sea is often channeled
to flow parallel to the mountains. The local temperature contrast between
snow-covered mountains and relatively warm open water may have more control
over the wind near the water than the isobaric pressure pattern from
weather maps. In these cases, the wind determined from the pressure
analysis on a weather map has little if any value for wave prediction.
For these exceptional cases, there is no valid substitute for wind
observations.

3.42 DELINEATING A FETCH

   The fetch has been defined subjectively as a region in which the wind
speed and direction are reasonably constant. Confidence in the computed
results begins to deteriorate slightly when wind direction variations
exceed 15°, and deteriorates significantly when direction deviations
exceeding 45° are accepted in the fetch area. The computed results are
sensitive to changes in wind speed as small as 1 knot (0.5 meter/second),
but it is not possible to estimate the wind speed over any sizable region

with this precision. For practical wave predictions it is usually satis-
factory to regard the wind speed as reasonably constant if variations do
not exceed 5 knots (2.5 meters/second) from the mean. A coastline upwind
from the point of interest always limits a fetch. An upwind limit to the
fetch may also be provided by curvature or spreading of the isobars as
indicated in Figure 3-12 (Shields and Burdwell, 1970), or by a definite
shift in wind direction. Frequently the discontinuity at a weather front
will limit a fetch, although this is not always so.
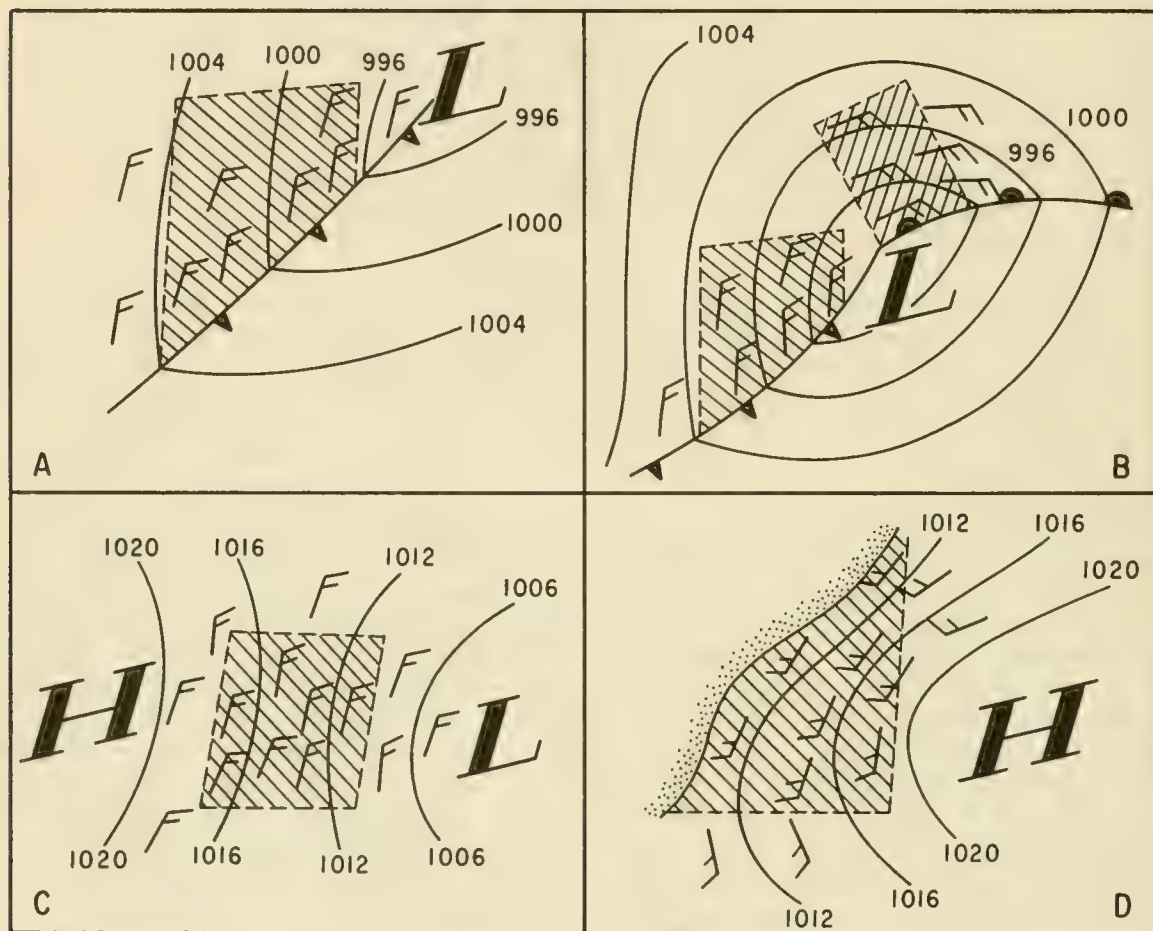
Figure 3-12. Possible Fetch Limitations

    Estimates of the duration of the wind are also needed for wave predic-
tion. Computed results, especially for short durations and high wind speeds
may be sensitive to differences of only a few minutes in the duration. Com-
plete synoptic weather charts are prepared only at 6-hour intervals. Thus
interpolation between charts to determine the duration may be necessary.
Linear interpolation is adequate for most uses, and, when not obviously
incorrect, is usually the best procedure.

3.43 FORECASTS FOR LAKES, BAYS, AND ESTUARIES

3.431 Wind Data. The techniques referred to for determination of wind speeds and directions from isobaric patterns apply generally to ocean areas. The friction that causes winds to spiral when crossing isobars and to have a velocity lower than geostrophic or gradient winds is more variable over land areas. When a fetch is close to land, this variability will alter anticipated wind directions and velocities. In enclosed or semienclosed bodies of water, such as lakes and bays, wind speeds and directions should be taken from actual weather station reports whenever possible.

In enclosed bodies of water, or in other areas where the wind blows off the land, differing frictional effects of land and water should be considered, and indicated wind speeds should be adjusted for these effects. Studies by Myers (1954) and Graham and Nunn (1959) indicate recommended adjustments in wind speeds. (See Table 3-2.) The adjustment factor may vary considerably depending on the shoreline frictional characteristics. This adjustment is used only for short fetches such as those in reservoirs and small lakes.

Often, over small or well-defined fetch areas, it is not convenient or even possible to utilize surface charts to determine wind characteristics. Where wind records exist for locations in or near a fetch area, these may be utilized. The accuracy of the forecast will depend on the completeness of the records, the extent of fetch, and the wave prediction technique employed. Where wind duration records are not available, local wind speed reports may still be utilized to forecast waves assuming unlimited durations, that is, wave growth is limited by the available fetch. Wave characteristics deduced in this way are only qualitative.

Table 3-2. Wind-Speed Adjustment, Nearshore

Wind Direction	Location of Wind Station	Ratio*
Onshore	2 to 3 miles offshore	1.0
Onshore	At coast	0.9
Onshore	5 to 10 miles inland	0.7
Offshore	At coast	0.7
Offshore	10 miles offshore	1.0

(Graham and Nunn, 1959)

*Ratio of wind speed at location to overwater wind speed (both at 30-ft. level).

3.432 Effective Fetch. The effect of fetch width or limiting ocean wave growth in a generating area may usually be neglected since nearly all ocean fetches have widths about as large as their lengths. In inland waters (bays, rivers, lakes, and reservoirs), fetches are limited by land forms surrounding the body of water. Fetches that are long in comparison to width are frequently found, and the fetch width may become quite important, resulting in wave generation significantly lower than that expected from the same generating conditions over more open waters.

Saville (1954) proposed a method to determine the effect of fetch width on wave generation. Figure 3-13, based on this method, indicates the effective fetch for a relatively uniform fetch width. The following problem demonstrates the use of Figure 3-13.

* * * * * * * * * * * * * *   EXAMPLE PROBLEM   * * * * * * * * * * * * * * * *

GIVEN: Consider a channel with a fetch length F = 20 miles, a width W = 5 miles, an average depth d = 35 feet, and a windspeed U = 50 mph along the long axis.

FIND: Estimate the significant wave height H_s, and the significant wave period T_s.

SOLUTION: Compute W/F = 5/20 = 0.25

From Figure 3-13 for W/F = 0.25, F_E/F = 0.45

Compute F_E = 0.45 x 20 = 9 miles or 47,500 feet.

Using the forecasting relations given in Section 3.6, Wave Forecasting for Shallow Water, for a fetch of 47,500 feet and a wind speed of 50 mph and an average uniform depth of 35 feet, the significant wave height may be determined from Figure 3-27 to be H_s = 5.2 feet, say 5 feet and the significant wave period will be T_s = 4.6 seconds, say 5 seconds.

* *

The preceding example presents a simplified method of determining the effective fetch. Shorelines are usually irregular, and the uniform-width method indicated in Figure 3-13 is not applicable. A more general method must be applied. This method is based on the concept that the width of a fetch in reservoirs normally places a very definite restriction on the length of the effective fetch; the less the width-length ratio, the shorter the effective fetch. A procedure for determining the effective fetch distance is illustrated in Figure 3-14. It consists of constructing 15 radials from the wave station at intervals of 6° (limited by an angle of 45° on either side of the wind direction) and extending these radials until they first intersect the shoreline. The component of length of each radial in a direction parallel to the wind direction is measured and multiplied by the cosine of the angle between the radial and the wind direction. The resulting values for each radial are summed and divided by the sum of the cosines of all the individual angles. This method is based on the following assumptions:

(a) Wind moving over a water surface transfers energy to the water surface in the direction of the wind and in all directions within 45° on either side of the wind direction.

(b) The wind transfers a unit amount of energy to the water along the central radial in the direction of the wind and along any other radial an amount modified by the cosine of the angle between the radial and the wind direction.
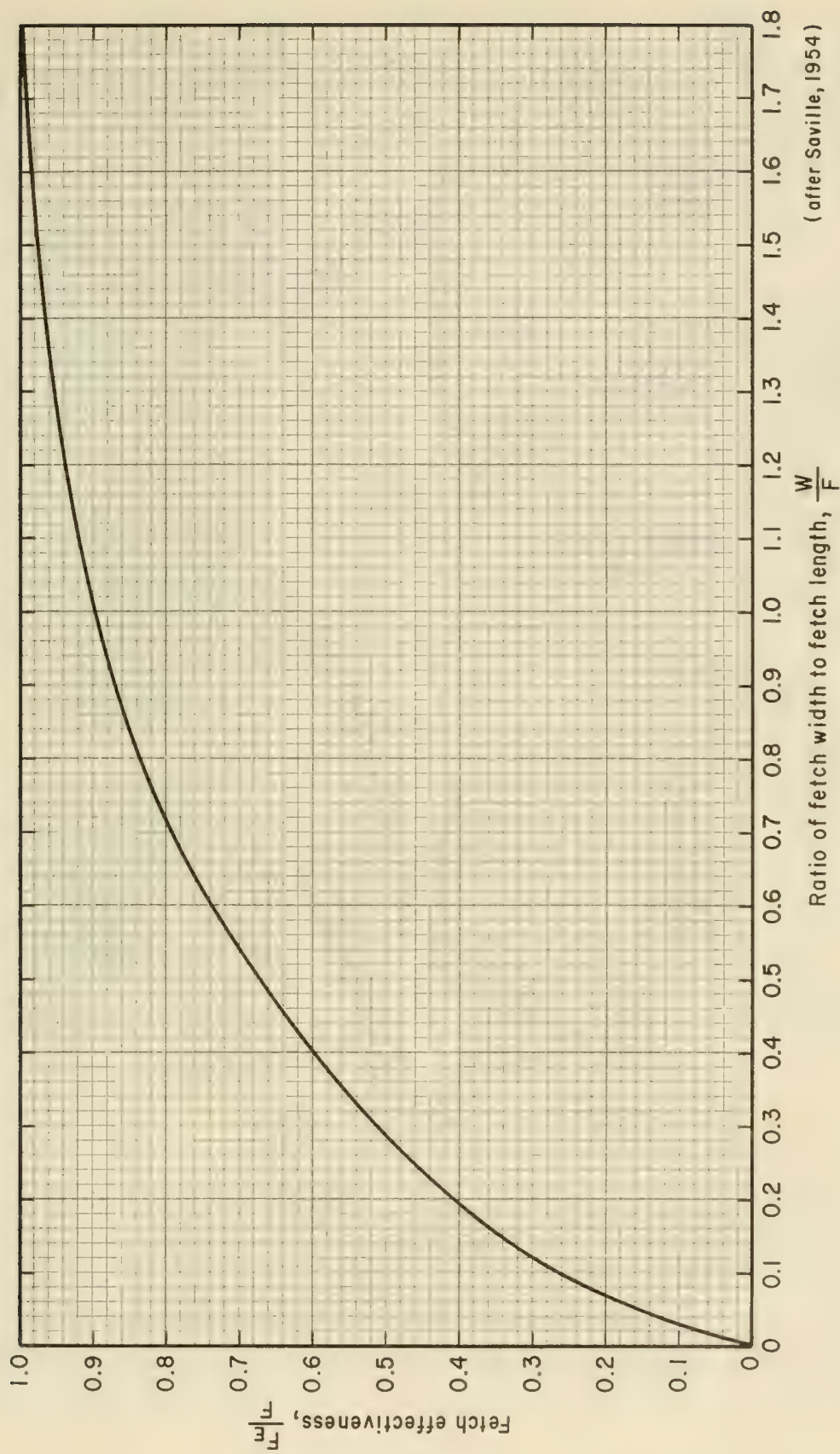
Figure 3-13. Relation of Effective Fetch to Width-Length Ratio for Rectangular Fetches

α	Cos α	X_i	X_iCosα
42	.743	5.1	3.79
36	.809	5.5	4.45
30	.866	7.8	6.75
24	.914	9.0	8.23
18	.951	14.2	13.50
12	.978	13.8	13.50
6	.995	16.7	16.62
0	1.000	24.7	24.70
6	.995	24.1	23.98
12	.978	22.7	22.20
18	.951	6.2	5.90
24	.914	4.8	4.39
30	.866	3.3	2.86
36	.809	3.1	2.51
42	.743	2.8	2.08
Total	13.512		155.46

Wind Direction

Central Radial

25 · 20 · 15 · 10 · 5

Shoreline

N

617

45°

6°

X_i

Station A

Denison Dam

$$F_{eff} = \frac{\sum X_i \cdot \text{Cos } \alpha}{\sum \text{Cos } \alpha}$$

$$F_{eff.} = \frac{155.46}{13.512} = 11.51 \text{ Units}$$

Where based on map scale
One Unit = 1714 feet

$$F_{eff} = 11.51 \times \frac{1714}{5280} = 3.7 \text{ Miles}$$

0   6000   12000
Scale in feet

Figure 3-14. Computation of Effective Fetch for Irregular Shoreline

(c) Waves are completely absorbed at shorelines.

Fetch distances determined in this manner usually are less than those based on maximum straight-line distances over open water. This is true because the width of the fetch places restrictions on the total amount of energy transferred from wind to water until the fetch width exceeds twice the fetch length.

While 6° spacing of the radials is used in this example, any other angular spacing could be used in the same procedure.

3.5 SIMPLIFIED WAVE-PREDICTION MODELS

Use of the wave-prediction models discussed in Section 3.3, Wave Field, requires an enormous computational effort and more meteorological data than one is likely to find outside of a major forecasting center. The Fleet Numerical Weather Center, Monterey, California began using this model on an experimental basis for a small part of the globe early in 1972. Expansion to larger regions is planned. Wave prediction begins with a computation of the existing wave field (often called a zero-time prediction), and continues with a calculation of the effects of predicted winds on the waves. A few years after this system is operational, it should be possible to supply the needs for wave-hindcast statistics by compilations of zero-time predictions. In the meantime, engineers who require wave statistics derived by hindcasting techniques for design consideration must accept simpler techniques.

Computational effort required for the model discussed in Section 3.31, Development of a Wave Field, can be greatly reduced by the use of simplified assumptions with only a slight loss in accuracy for wave height calculations, but sometimes with significant loss of detail on the distribution of wave energy with frequency. One commonly used approach is to assume that both duration and fetch are large enough to permit an equilibrium state between the mean wind, turbulence, and waves. If this condition exists, all other variables are determined by the wind speed.

Pierson and Moskowitz (1964) consider three analytic expressions which satisfy all of the theoretical constraints for an equilibrium spectrum. Empirical data, described by Moskowitz (1964) were used to show that the most satisfactory of these is

$$E(\omega)\,d\omega = (\alpha g^3/\omega^5)\,e^{-\beta\,(\omega_o^4/\omega^4)}\,d\omega, \qquad (3\text{-}20)$$

where α and β are dimensionless constants, $\alpha = 8.1 \times 10^{-3}$, $\beta = 0.74$ and $\omega_O = g/U$, where g is the acceleration of gravity and U is the wind speed reported by weather ships, and ω is the wave frequency considered.

Equation 3-20 may be expressed in many other forms. Bretschneider (1959, 1963) gave an equivalent form, but with different values for α and β. A similar expression was also given by Roll and Fischer (1956). The condition in which waves are in equilibrium with the wind is called a

fully arisen sea. The assumption of a universal form for the fully arisen sea permits the computation of other wave characteristics such as total wave energy, significant wave height, and period of maximum energy. The equilibrium state between wind and waves rarely occurs in the ocean, and may never occur for higher wind speeds.

A more general model may be constructed by assuming that the sea is calm when the wind begins to blow. Integration of the equations governing wave growth then permits the consideration of changes in the shape of the spectrum with increasing fetch and duration. If enough wave and wind records are available, empirical data may be analyzed to provide similar information. Pierson, Neumann, and James (1955) introduced this type of wave prediction scheme based almost entirely on empirical data. Inoue (1966, 1967) repeated this exercise in a manner more consistent with the Miles-Phillips theory using a differential equation for wave growth. Inoue was a member of Pierson's group when this work was carried out, and his prediction scheme may be regarded as a replacement for the earlier Pierson-Neuman-James (PNJ) wave prediction model. The topic has been extended by Silvester and Vongvisessomjai (1971) and others.

These simplified wave prediction schemes are based on the implicit assumption that the waves being considered are due entirely to a wind blowing at constant speed and direction for an overwater distance called the *fetch* and for a time period called the *duration*.

In principle it would be possible to consider some effects of variable wind velocity by tracing each wave train. Once waves leave a generating area and become swell, the wave energy is then propagated according to the group velocity. The total energy at a point, and the square of the significant wave height could be obtained by adding contributions from individual wave trains. Without a computer, this procedure is too laborious, and theoretically inaccurate.

A more practical procedure is to relax the restrictions implied by derivation of these schemes. Thus wind direction may be considered constant if it varies from the mean by less than some finite value, say 30°. Wind speed may be considered constant if it varies from the mean by less than ± 5 knots (2.5 meters/second) or ½ barb on the weather map. This assumption is not much greater than the uncertainty inherent in wind reports from ships. In this procedure, average values are used and are assumed constant over the fetch area, and for a particular duration.

The theoretical spectra for the partially arisen sea can be used to develop formulas for such wave parameters as total energy, significant wave height and period of maximum energy density.

Similar formulas can also be developed empirically from wind and wave observations. A quasi-empirical - quasi-theoretical procedure was used by Sverdrup and Munk (1947) to construct the first widely used wave prediction system. The Sverdrup-Munk prediction curves were revised by Bretschneider (1952a, 1958) with additional empirical data. Thus, this prediction system is often called the Sverdrup-Munk-Bretschneider (SMB) method. It is the most convenient wave prediction system to use when a limited amount of data and time are available.

Revisions of earlier SMB forecasting curves are seen in Figures 3-15 and 3-16. The curves represent dimensional plots from the empirical equations,

$$\frac{gH}{U^2} = 0.283 \tanh \left[0.0125 \left(\frac{gF}{U^2} \right)^{0.42} \right], \tag{3-21}$$

$$\frac{gT}{2\pi U} = 1.20 \tanh \left[0.077 \left(\frac{gF}{U^2} \right)^{0.25} \right], \tag{3-22}$$

and,

$$\frac{gt}{U} = K \exp \left\{ \left[A \left(\ln \left(\frac{gF}{U^2} \right) \right)^2 - B \ln \left(\frac{gF}{U^2} \right) + C \right]^{\frac{1}{2}} + D \ln \left(\frac{gF}{U^2} \right) \right\}, \tag{3-23}$$

where

$$\exp \{x\} = e^{\{x\}}$$
$$\ln = \log_e$$
$$K = 6.5882$$
$$A = 0.0161$$
$$B = 0.3692$$
$$C = 2.2024$$

and

$$D = 0.8798 .$$

With these relationships, the significant wave height H_F, and significant wave period T_F, at the end of a fetch may be estimated when wind speed, fetch length, and duration of wind over the fetch are given. Estimation of wind parameters is discussed in Section 3.4, Wind Information Needed for Wave Prediction, following the evaluation of simplified prediction techniques. In using Figures 3-15 or 3-16 the estimated wind velocity U, the fetch length F, and the estimated wind duration t, when a fetch first appears on a weather chart, are tabulated. Figure 3-15 or 3-16 is then entered with the value of U, using the scale on the left if U is in knots, or the scale on the right if U is in statute miles per hour. This U line is then followed from the left side of the graph across to its intersection with the fetch length or F line, or the duration t line, whichever comes first.
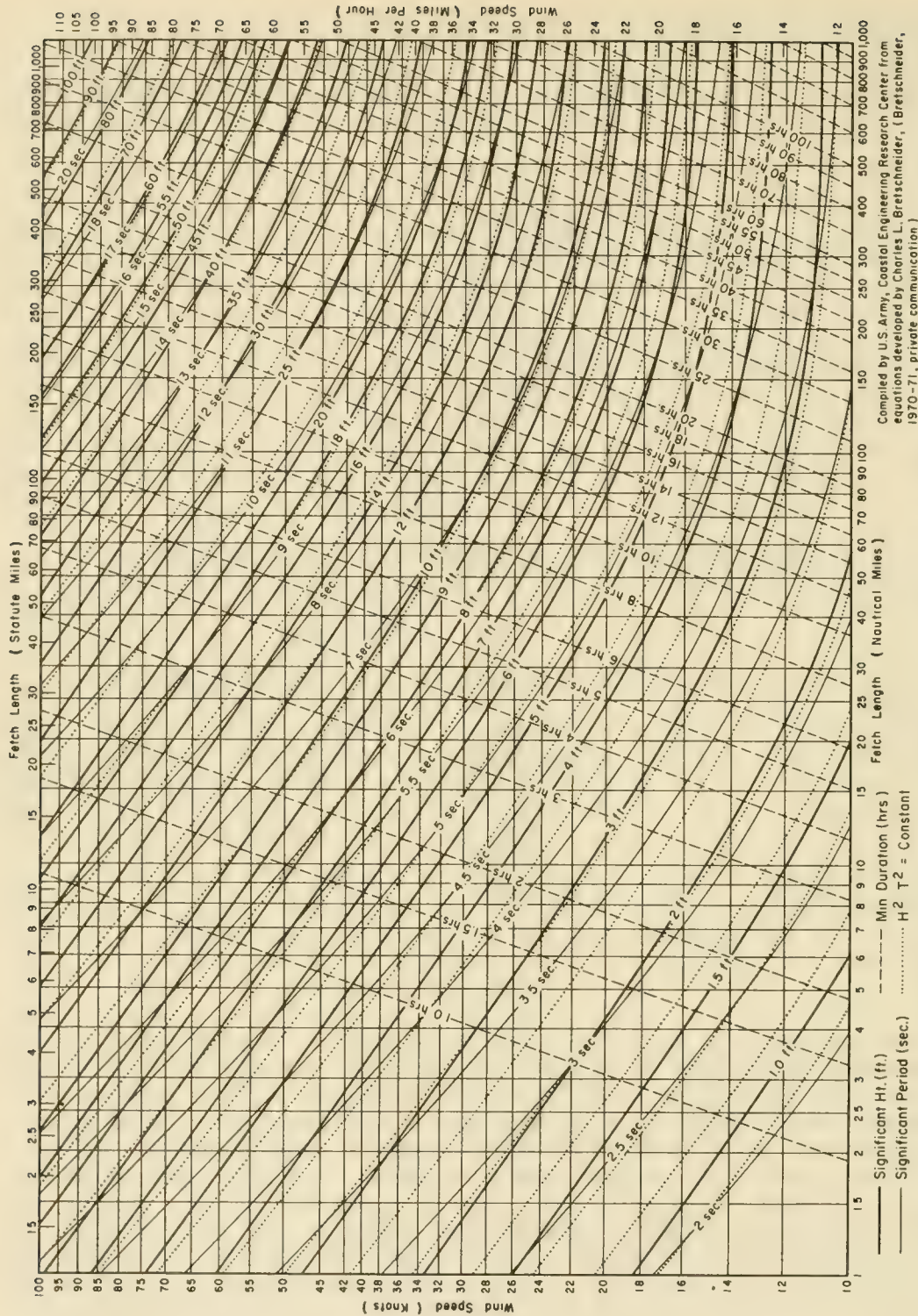
Figure 3-15. Deepwater Wave Forecasting Curves as a Function of Wind Speed, Fetch Length, and Wind Duration (for Fetches 1 to 1,000 miles)

3-36
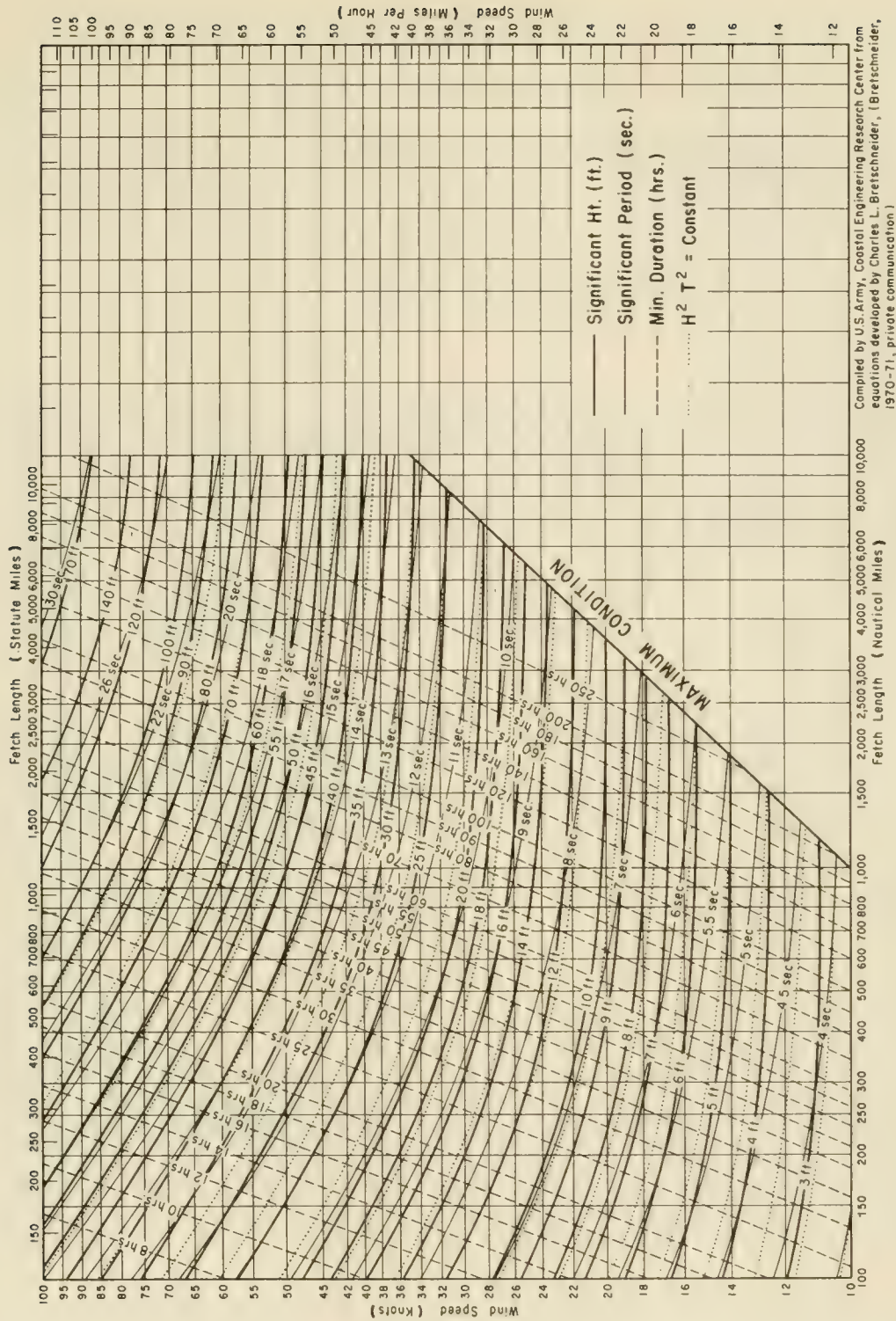
Figure 3-16. Deepwater Wave Forecasting Curves as a Function of Wind Speed, Fetch Length, and Wind Duration (for Fetches of 100 to more than 1,000 miles)

3-37

* * * * * * * * * * * * *   EXAMPLE PROBLEM   * * * * * * * * * * * * * * *

GIVEN: A wind speed U = 35 knots (40 mph) and a duration t = 10 hours.

FIND: The significant wave height H_F, and the significant period T_F, at the fetch front for:

  (a) A fetch length, F = 200 nautical miles and

  (b) a fetch length, F = 80 nautical miles.

SOLUTION:

  (a) Enter Figure 3-15 from the left side at U = 35 knots and move horizontally across the figure from the left toward the right, until intersecting the dashed line for a duration of 10 hours that comes before the line indicating a fetch length of 200 nautical miles. At the 10-hour duration line F = 92 nautical miles; this is the minimum fetch F_m for this case.

  With U = 35 knots, t = 10 hours, and F = 200 nautical miles then H_F = 13.1 feet, T_F = 8.0 seconds, t_m equals 10 hours, and F_m = 92 nautical miles.

  (b) Entering Figure 3-15 as above, when F = 80 nautical miles and t = 10 hours, then the heights, periods, minimum duration and fetch would be H_F = 12.6 feet, T_F = 7.8 seconds, and t_m = 9.0 hours. The minimum duration t_m is 9 hours, corresponding to the miles which limit generation, and comes before a duration of 10 hours.

  In this example problem, the wave pattern in (a) is limited by the duration; the wave pattern in (b) is limited by the fetch.

* *

  When a series of surface synoptic weather charts (Fig. 3-9) are used to determine wave patterns, the values of U, F and t can be tabulated for the first chart. For the same fetch on a later chart drawn for a time Z, after the first chart, U, F, and t are again tabulated. Using the subscript 2 to refer to those of the second chart and subscript 1 to refer to those of the first chart, if U_2 = U_1, the above procedures should be followed using either t_2 = t_{m1} + Z or F_2. If, however, $U_2 \neq U_1$, certain additional assumptions must be made before using the forecasting curves.

  A change in wind speed from U_1 to U_2 in a time Z between charts may be assumed to take place instantaneously at a time Z/2. Waves due to U_1 may then be calculated by assuming that the first chart minimum duration time has been lengthened by an amount Z/2 or that its minimum fetch has been changed by $\Delta F/2$, where ΔF represents the change in fetch length between weather charts. Since at the assumed abrupt change in wind speed,

the energy imparted to the waves by U_1, with a minimum duration $t_{m1} + Z/2$ for a minimum fetch $F_{m1} + F/2$, does not change, U_2 will be assumed to impart energy to waves which already contain energy due to U_1.

Plotted on Figures 3-15 and 3-16 are dotted lines of constant H^2T^2 which are considered lines of constant wave energy. To a first approximation, deepwater wave energy is given by

$$E_o = \frac{\rho g H^2 L_o}{8} = \frac{5.12 \, \rho g \, (HT)^2}{8} \, . \tag{3-24}$$

If energy had been imparted to the waves by U_2 acting alone, these waves would be of length and height given in Figures 3-15 or 3-16 by the inter-section of the U_2 ordinate with the constant energy line (plotted or interpolated) corresponding to energy imparted by U_1 with a minimum duration of $t_{m1} + Z/2$ or a minimum fetch $F_{m1} + F/2$. By increasing the minimum duration at this point by an amount $Z/2$ or by changing the minimum fetch by an amount $\Delta F/2$, wave conditions under U_2 at the time of the second chart may be approximated.

For example, if the wind speed increases so that U_2 = 40 knots, and with U_1 = 35 knots, t_{m1} = 10 hours, F_{m1} = 92 nautical miles, $t_{m1} + Z/2$ = 13 hours; an interpolated (by eye) dotted line of constant H^2T^2 would be followed up to the U_2 = 40-knot line where the duration = 6.5 hours. To this value $Z/2$ or 3 hours is added and then moving horizontally along the line U_2 = 40 knots to t = 6.5 + 3.0 = 9.5 hours, it is found that H_{F2} = 15.6 feet, T_{F2} = 8.7 seconds, t_{m2} = 9.5 hours, and F_{m2} = 95 nautical miles. If the measured fetch F_2 had been less than 95 nautical miles, this length of fetch would limit the growth of waves. Although the pre-ceding discussion would indicate that ΔF should be calculated, in practice this need not be done; the results obtained through calculation of ΔF would be found by reading off wave heights at the intersection of U_2 and F_2 if F_2 is limiting. Therefore, if F_2 had equalled 85 nautical miles, in this case less than 95 miles and therefore limiting, at the intersection of U_2 = 40 knots, then H_{F2} = 15.0 feet, T_{F2} = 8.5 seconds, T_{m2} = 8.8 hours, and F_{m2} = 85 nautical miles. Note this important distinction: t_1, F_1 and F_2 are calculated by use of Figure 3-15. Some of the measured and calculated values will be the same, but not all of them.

If the wind velocity U_2 is less than U_1, the procedures followed are nearly the same. From the intersection of U_1 and $t_{m1} + Z/2$ a constant energy line is followed to its intersection, if there is one,

with either U_2 or F_2 whichever comes first from the left side of the figure. If U comes first, Z/2 is added to the duration at this point, and the U_2 ordinate is followed to either this new duration or to the F_2 whichever is first from the left side of the chart. (Compare with the preceding paragraph.) At this point, H_{F2}, T_{F2}, t_{m2}, and F_{m2} inclusive, are read off. If the constant energy line had intersected F_2 before U_2, it is only necessary to drop down along the F_2 abscissa to its intersection with U_2, and at this point read H_{F2}, T_{F2}, t_{m2} and F_{m2}. (This procedure could be used for many cases in which U_2 is greater than U_1.)

The major differences in technique are used when U_2 is less than U_1 and the H^2T^2 = constant line from the intersection of U_1 and $t_{m1} + Z/2$ does not intersect either U_2 or F_2. Forecasting theory used here predicts that waves due to a constant wind blowing over an unlimited fetch for an unlimited duration will eventually reach limiting height and period distributions beyond which growth will not continue. In Figure 3-16 the limit of this state is delineated by the line labelled *maximum condition*. To the right of this line, it is assumed that any energy transport to the waves by the wind is compensated by wave breaking, hence no wave growth occurs.

3.52 EFFECTS OF MOVING STORMS AND A VARIABLE WIND SPEED AND DIRECTION

In principle, it should be possible to extend the Inoue differential equation for wave growth to highly irregular conditions, but no experimental verification of this concept has been published. Kaplan (1953) and Wilson (1955) have proposed techniques for applying the simplified prediction techniques to variable wind fields and changing fetches. The procedures appear reasonable and these techniques are used, although no statistics are available for verification.

3.53 VERIFICATION OF SIMPLIFIED WAVE HINDCAST PROCEDURES

Comparisons of hindcast wave heights and observed wave heights, similar to Figure 3-7, have been given by Jacobs (1965) for the PNJ wave-prediction system, by Bates (1949) and Isaacs and Saville (1949) for the early Sverdrup-Munk method, by Kaplan and Saville (1954), for the early SMB method, and by Bretschneider (1965) for a later revision. The basic data from which the prediction curves were derived, summarized by Bretschneider (1951), also indicate the range of variation that may be expected.

It is generally believed that much of the discrepancy between observed and predicted waves is random, and that statistical summaries of observations and predicted values will agree much better than the individual observations. Saville (1954) and Pierson, Neumann and James (1955) give summaries of results from a systematic program for deepwater hindcasting waves at the four locations shown in Figure 3-17. The U.S. Naval Weather
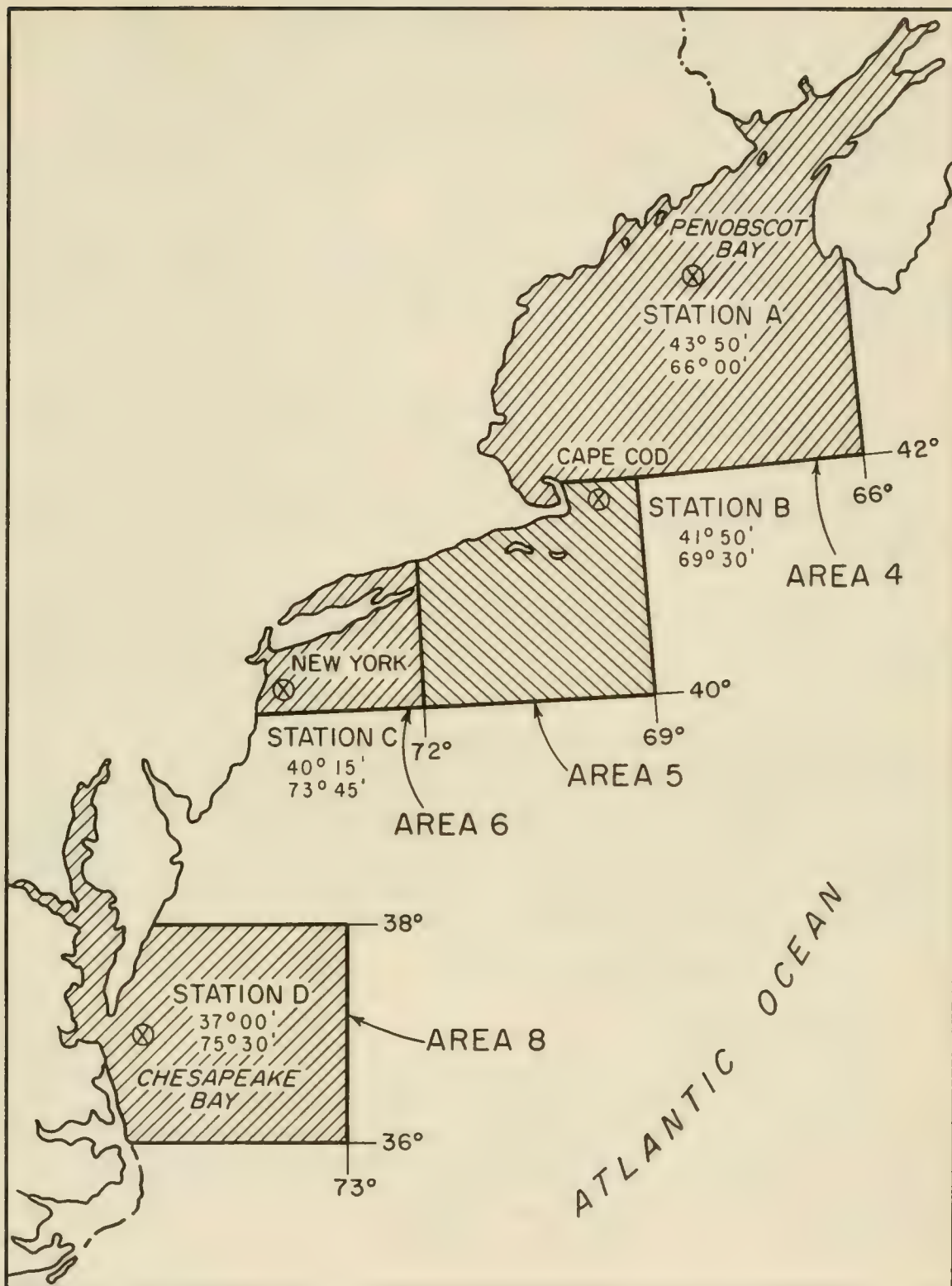
Figure 3-17. Location of Wave Hindcasting Stations and Summary of Synoptic Meterological Observations (SSMO) Areas

3-41

Service Command (1970) provides summaries of shipboard wave observations, Summary of Synoptic Meteorological Observations (SSMO) for the hatched areas indicated in Figure 3-17. Cumulative distribution functions for wave heights as determined by both hindcasting techniques and the shipboard observations are given in Figure 3-18. The average of the two forecasting methods agrees reasonably well with the shipboard observations.

3.54 ESTIMATING WAVE DECAY IN DEEP WATER

Figures 3-19 and 3-20 are used to estimate wave characteristics after the waves have left the fetch area but are still travelling in deep water. With Figure 3-19, and given H_F, T_F, F_m and D (the decay distance), it is possible to compute the ratios

$$\frac{\text{decayed wave height}}{\text{fetch wave height}} = \frac{H_D}{H_F}, \text{ and } \frac{\text{decayed wave period}}{\text{fetch wave period}} = \frac{T_D}{T_F}$$

With Figure 3-20, it is possible to compute wave travel time between a fetch and a coast, knowing the decayed wave period T_D and the decay distance D.

This *travel time* t_D is determined by dividing the decay distance by the deepwater group velocity for waves having a period equal to the decayed period T_D. These values enable the estimation of arrival times for waves at the end of the decay distance.

Waves, after leaving a generating area, will generally follow a great-circle path toward a coast. However, sufficient accuracy is usually obtained by assuming wave travel in a straight line on the synoptic chart. Decay distance is found by measuring the straight line distance between the front of a fetch and the point for which the forecast is being made. If a forecast is being made for a coastal area, the effects of shoaling, refraction, bottom friction and percolation will have to be considered in translating the deepwater forecast to the shore.

3.6 WAVE FORECASTING FOR SHALLOW WATER

3.61 FORECASTING CURVES

Water depth affects wave generation. For a given set of wind and fetch conditions, wave heights will be smaller and wave periods shorter if generation takes place in transitional or shallow water rather than in deep water. Several forecasting approaches have been made; the method given by Bretschneider as modified using the results of Ijima and Tang (1966) is presented here. Bretschneider and Reid (1953) consider bottom friction and percolation in the permeable sea bottom.

There is no single theoretical development for determining the actual growth of waves generated by winds blowing over relatively shallow water. The numerical method presented here is based on successive approximations
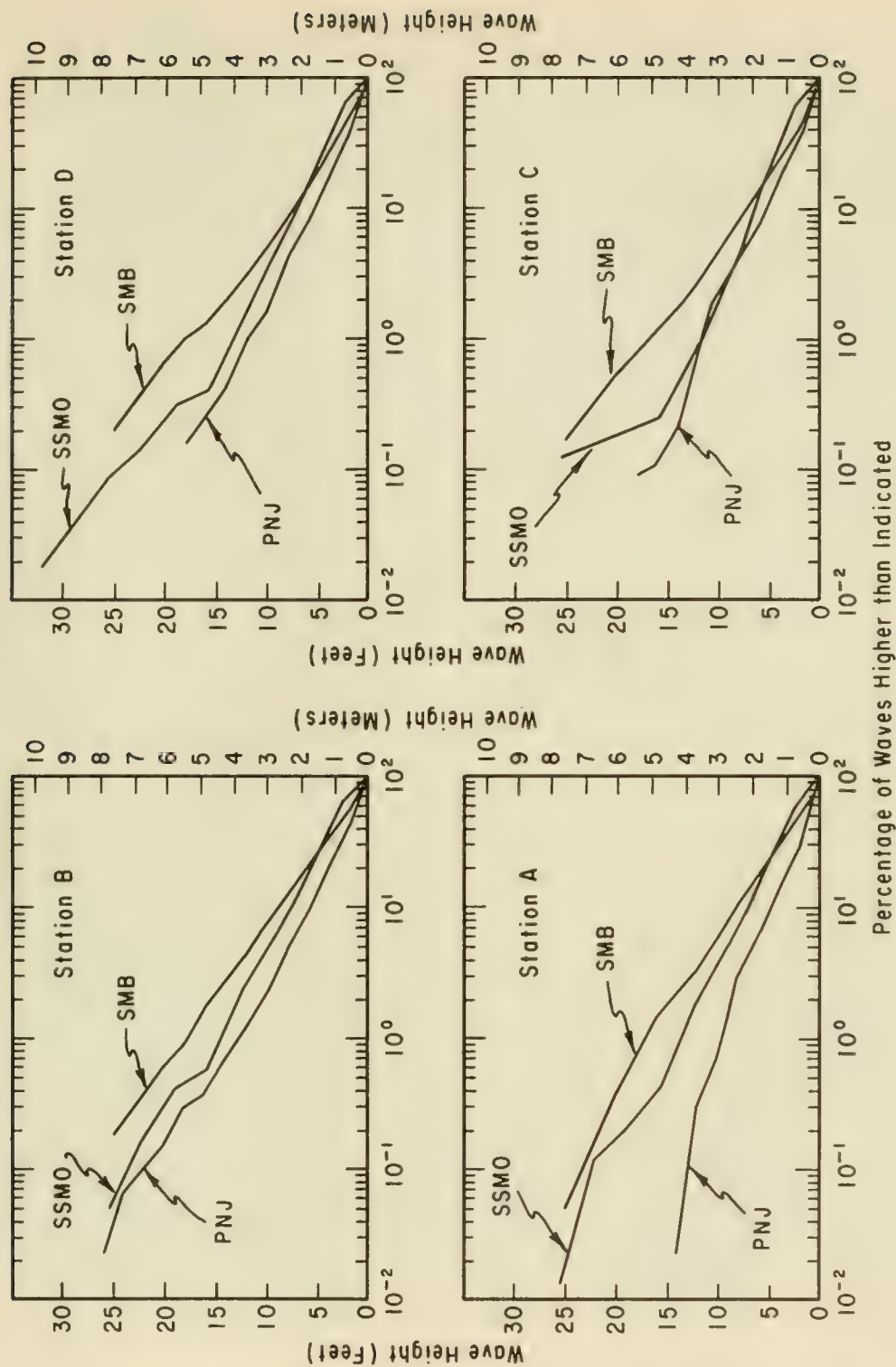
Figure 3-18. A Comparison of Shipboard Observations and Hindcasts. Based on shipboard observations for the years 1963-1968 and on hindcasts by SMB (1951) procedures for the years 1948-1950 and PNJ (1955) procedures for the years 1947-1949.

3-43

Figure 3-19. Decay Curves   (Bretschneider, 1952 a)

3-44
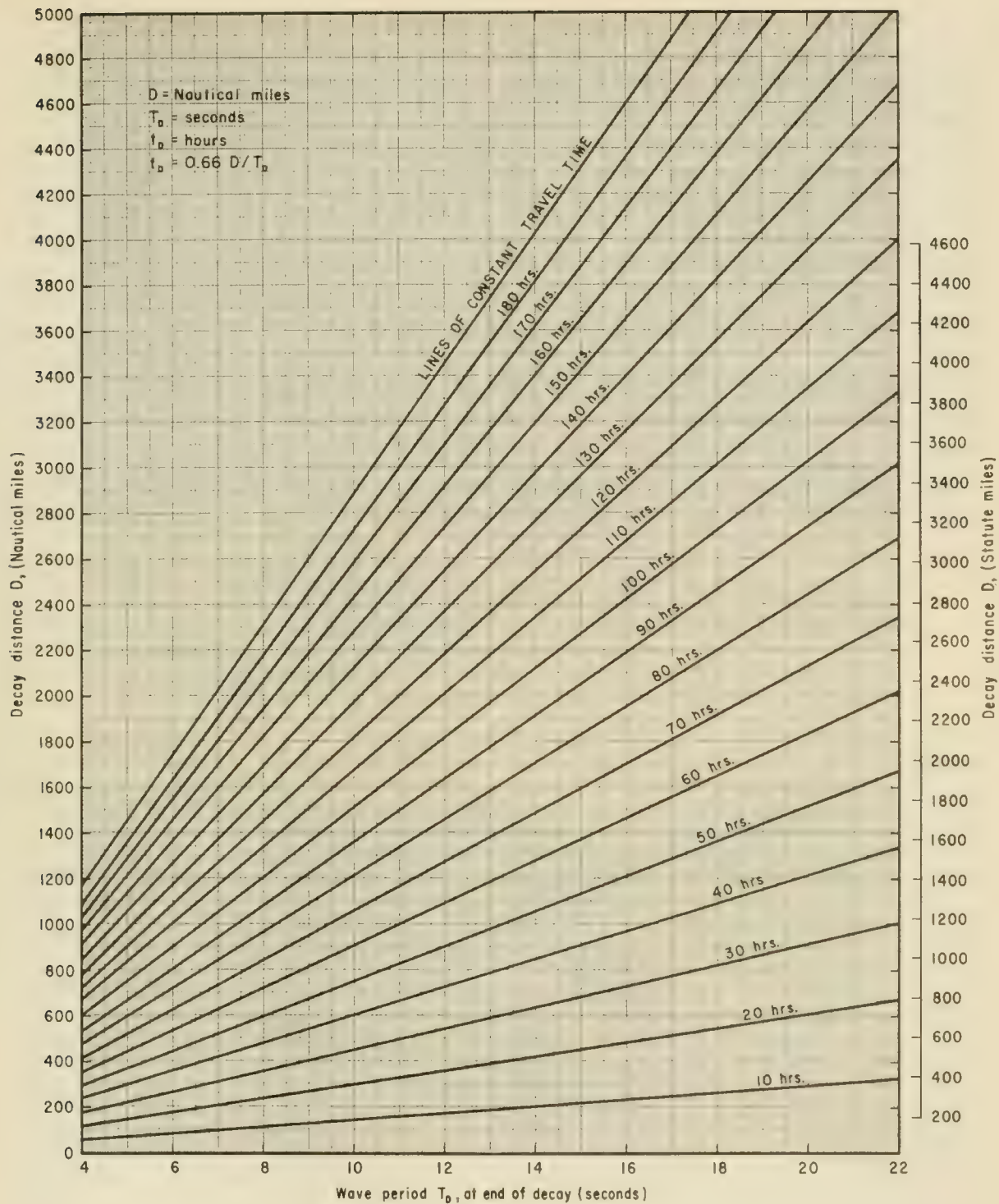
Figure 3-20. Travel Time of Swell Based on $t_D = D/C_g$

in which wave energy is added due to wind stress and subtracted due to bottom friction and percolation. This method uses deepwater forecasting relationships originally developed by Sverdrup and Munk (1947) and revised by Bretschneider (1951) to determine the energy added due to wind stress. Wave energy lost due to bottom friction and percolation is determined from the relationships developed by Bretschneider and Reid (1953). Resultant wave heights and periods are obtained by combining the above relationships by numerical methods. The basic assumptions applicable to development of deepwater wave-generation relationships (Bretschneider, 1952b) as well as development of relationships for bottom friction loss (Putnam and Johnson, 1949) and percolation loss (Putnam, 1949) apply.

The choice of an appropriate bottom friction factor f_f for use in the forecasting technique is a matter of judgement; a value of $f_f = 0.01$ has been used for the preparation of Figures 3-21 through 3-30 which are forecasting curves for shallow-water areas of constant depth. These curves, which may be used like Figures 3-15 and 3-16, are given by the equations:

$$\frac{gH}{U^2} = 0.283 \, \tanh\left[0.530\left(\frac{gd}{U^2}\right)^{0.75}\right] \tanh\left\{\frac{0.0125\left(\frac{gF}{U^2}\right)^{0.42}}{\tanh\left[0.530\left(\frac{gd}{U^2}\right)^{0.75}\right]}\right\}, \quad (3\text{-}25)$$

and

$$\frac{gT}{2\pi U} = 1.20 \, \tanh\left[0.833\left(\frac{gd}{U^2}\right)^{0.375}\right] \tanh\left\{-\frac{0.077\left(\frac{gF}{U^2}\right)^{0.25}}{\tanh\left[0.833\left(\frac{gd}{U^2}\right)^{0.375}\right]}\right\}, (3\text{-}26)$$

which in deep water reduce to Equations 3-21 and 3-22 respectively.

* * * * * * * * * * * * *   EXAMPLE PROBLEM   * * * * * * * * * * * * * *

GIVEN: Fetch, F = 80,000 feet, wind speed, U = 50 mph., water depth, d = 35 feet (average constant depth), bottom friction factor $f_f = 0.01$ (assumed).

FIND: Wave height H and wave period T.
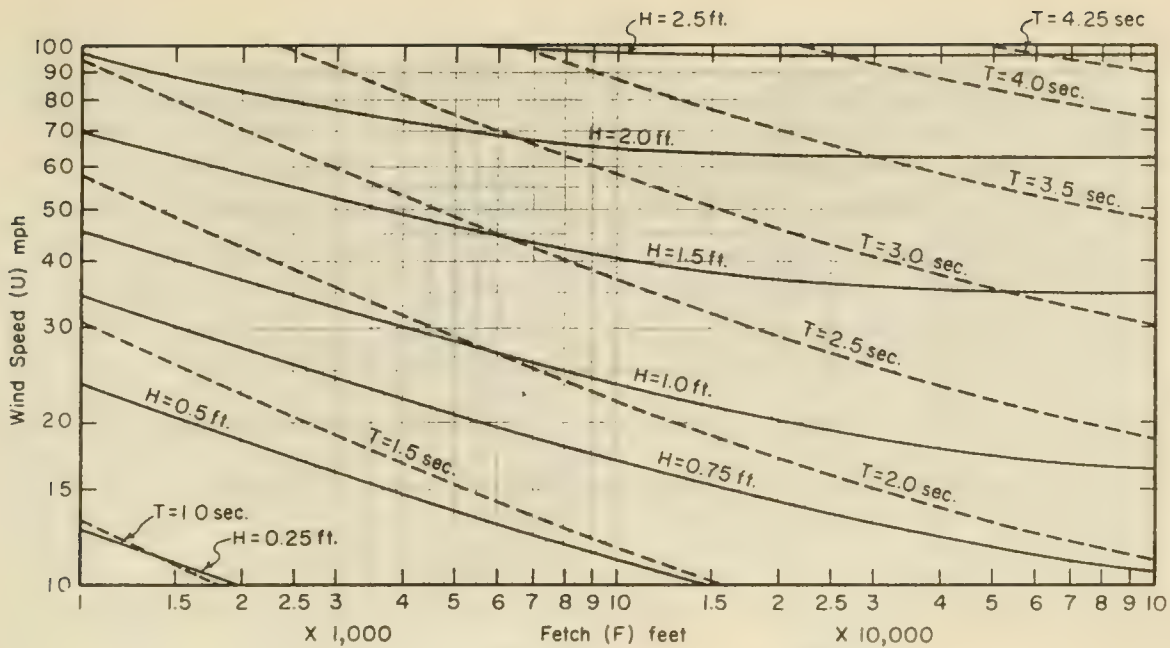
Figure 3-21. Forecasting Curves for Shallow-Water Waves
Constant Depth = 5 feet.
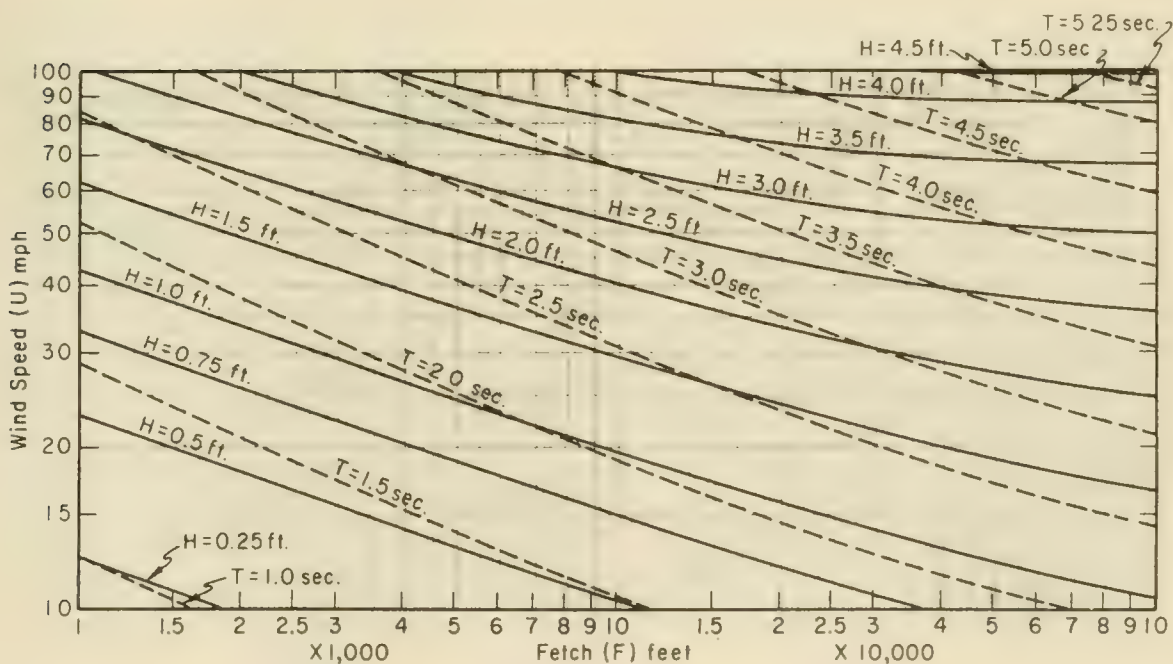
Figure 3-22. Forecasting Curves for Shallow-Water Waves
Constant Depth = 10 feet.

3-47

Figure 3-23. Forecasting Curves for Shallow-Water Waves
Constant Depth = 15 feet.

Figure 3-24. Forecasting Curves for Shallow-Water Waves
Constant Depth = 20 feet.

3-48
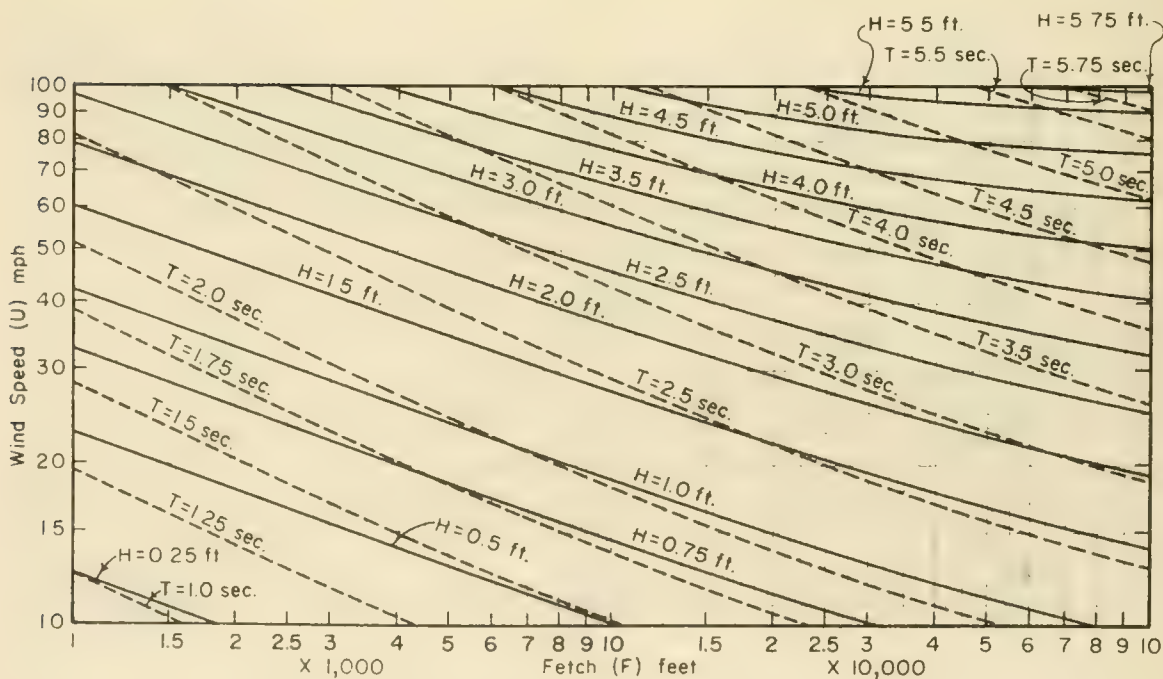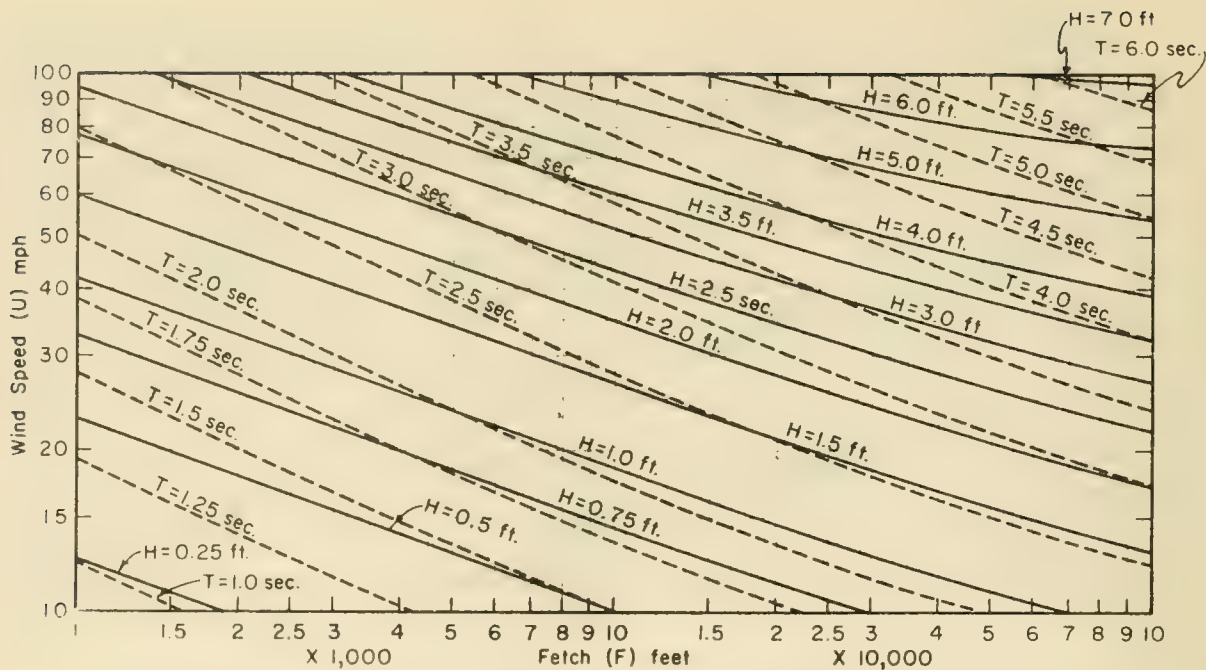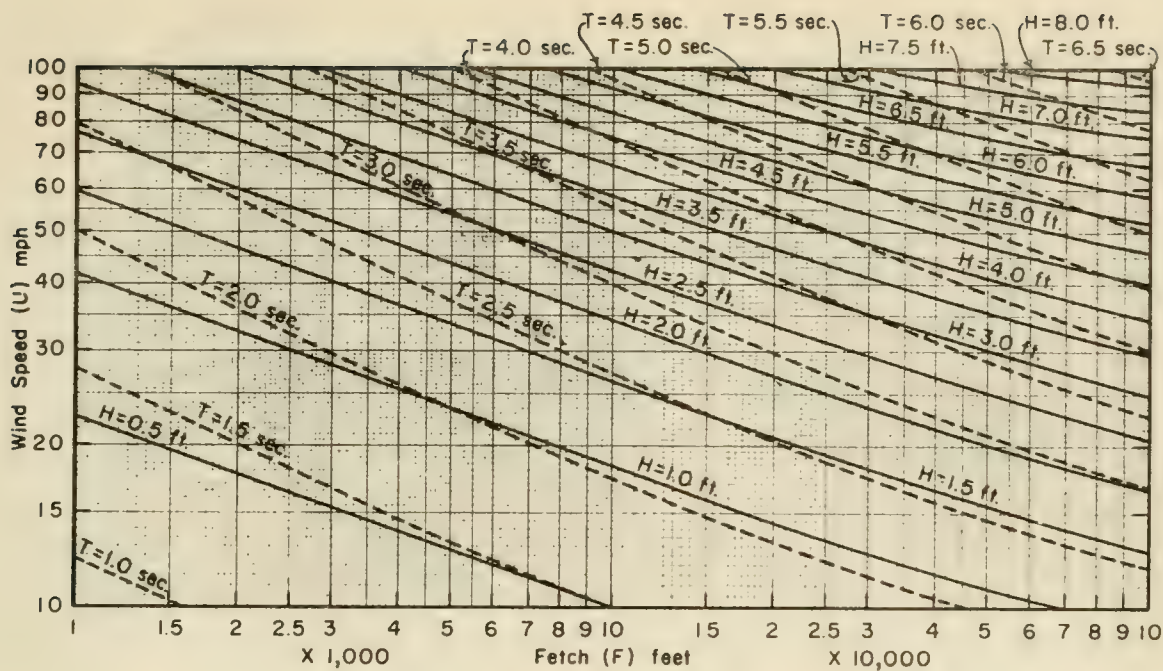
Figure 3-25.   Forecasting Curves for Shallow-Water Waves
Constant Depth = 25 feet.
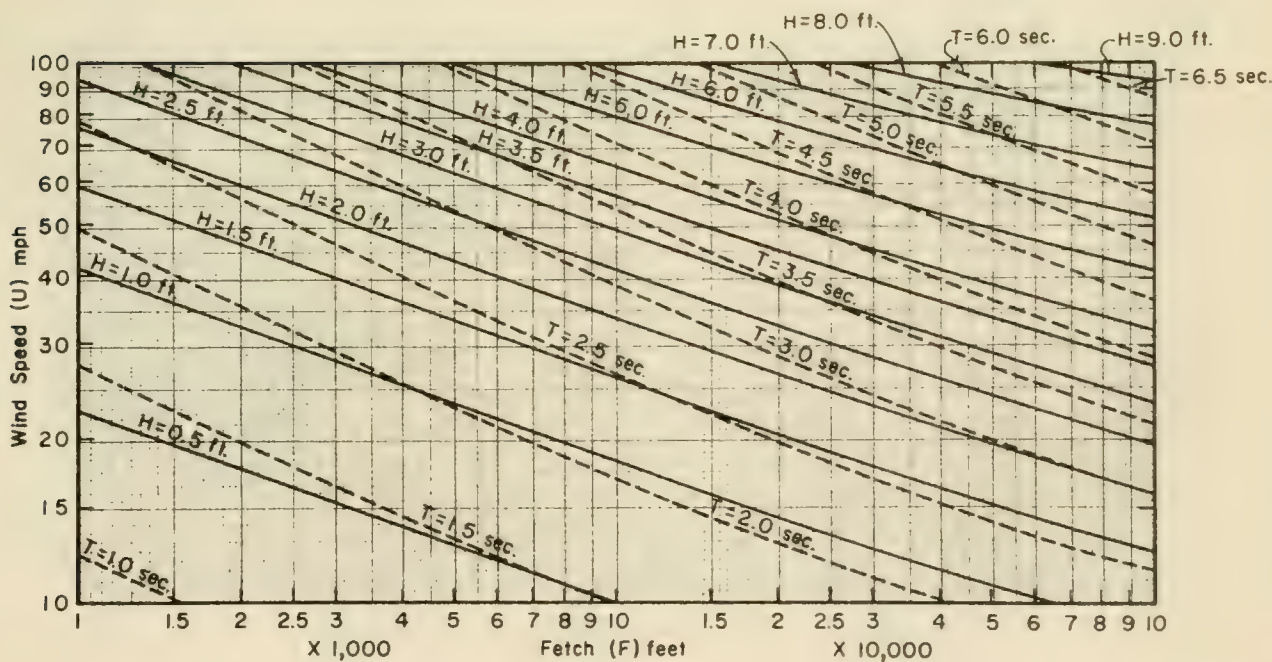
Figure 3-26.   Forecasting Curves for Shallow-Water Waves
Constant Depth = 30 feet.
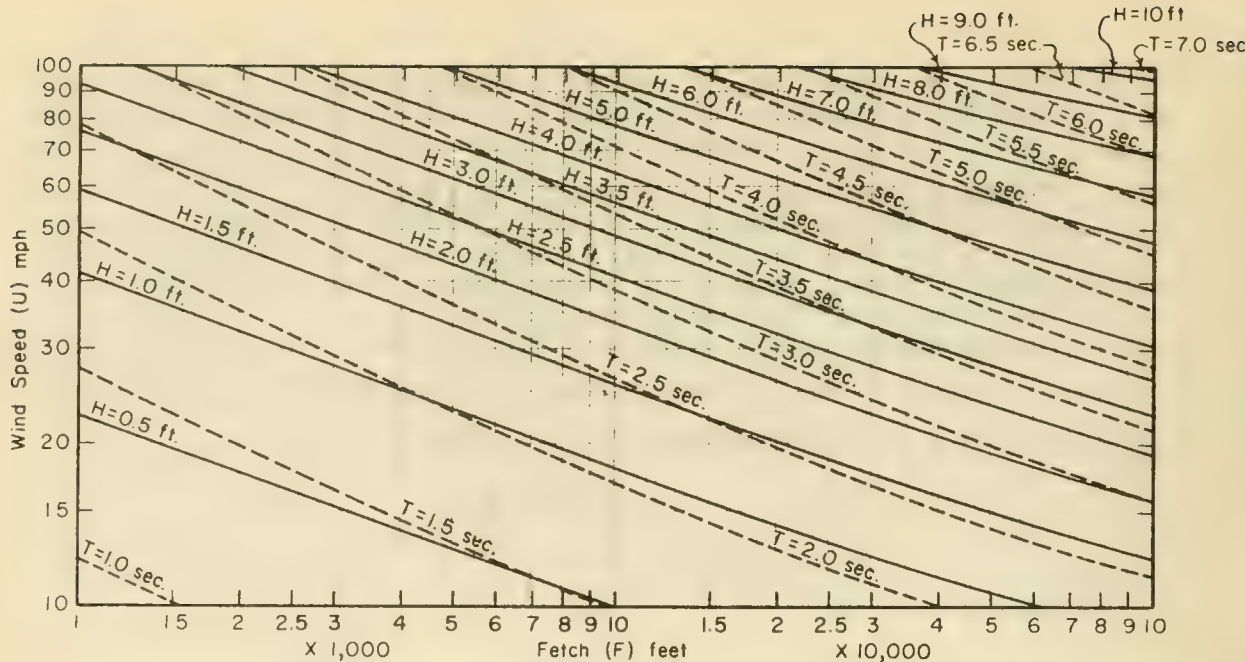
Figure 3-27.   Forecasting Curves for Shallow-Water Waves
Constant Depth = 35 feet.
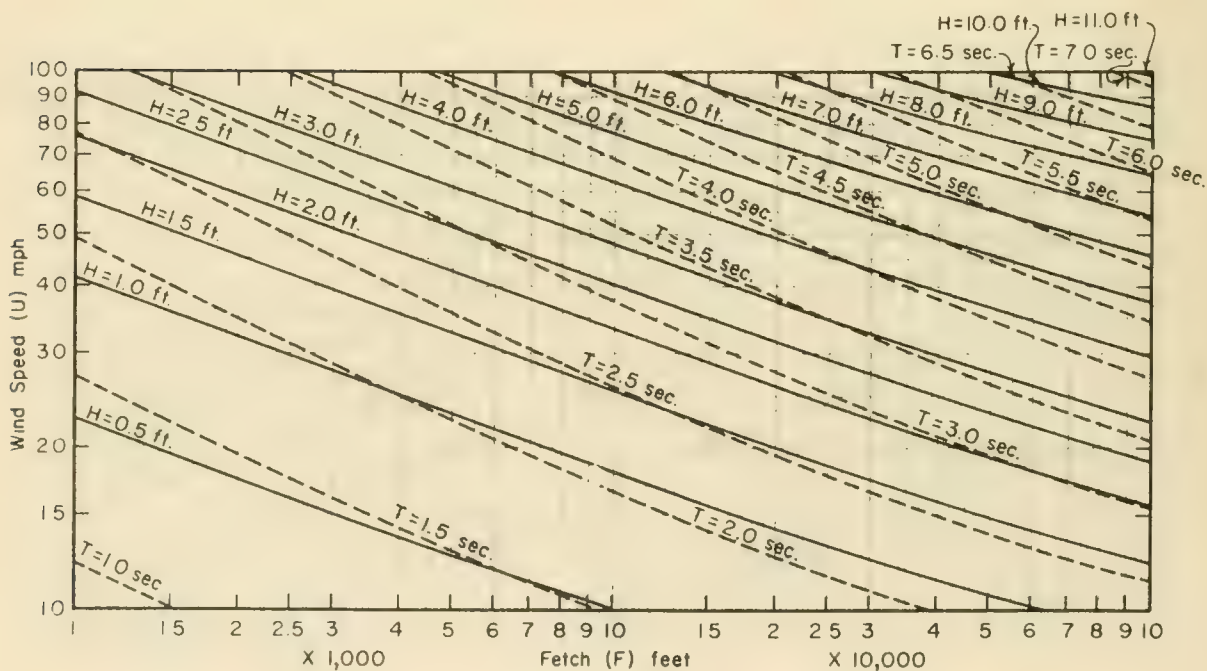
Figure 3-28.   Forecasting Curves for Shallow-Water Waves
Constant Depth = 40 feet.
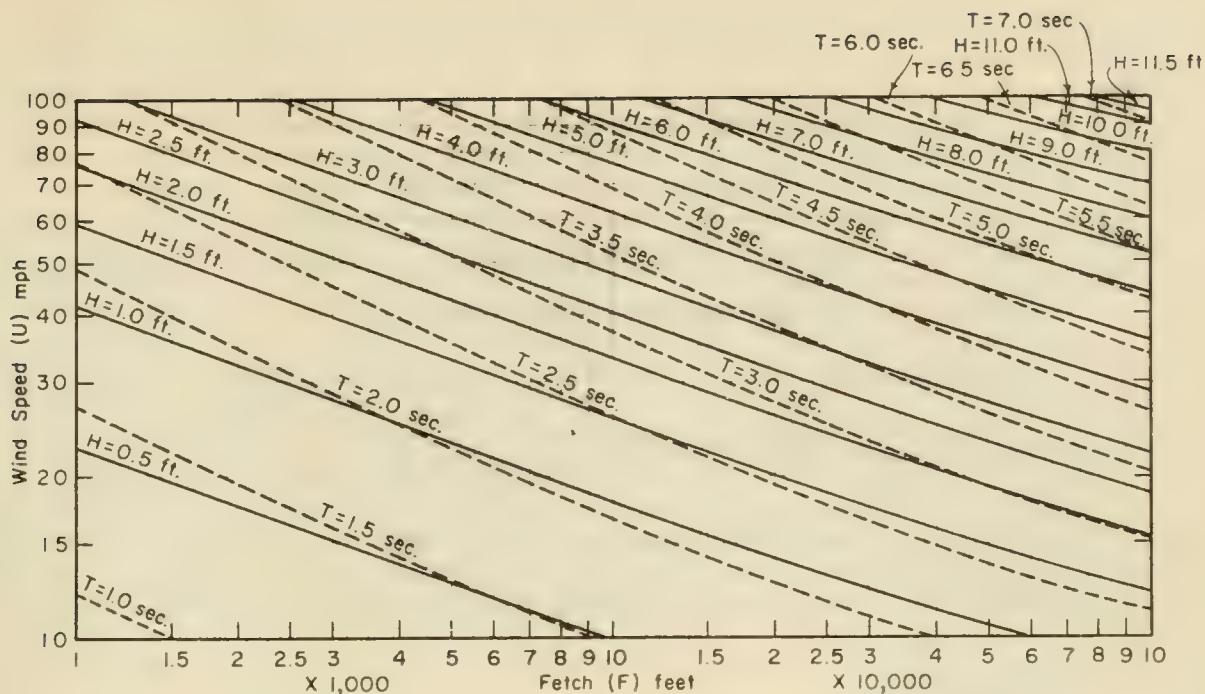
Figure 3-29.   Forecasting Curves for Shallow-Water Waves
Constant Depth = 45 feet.
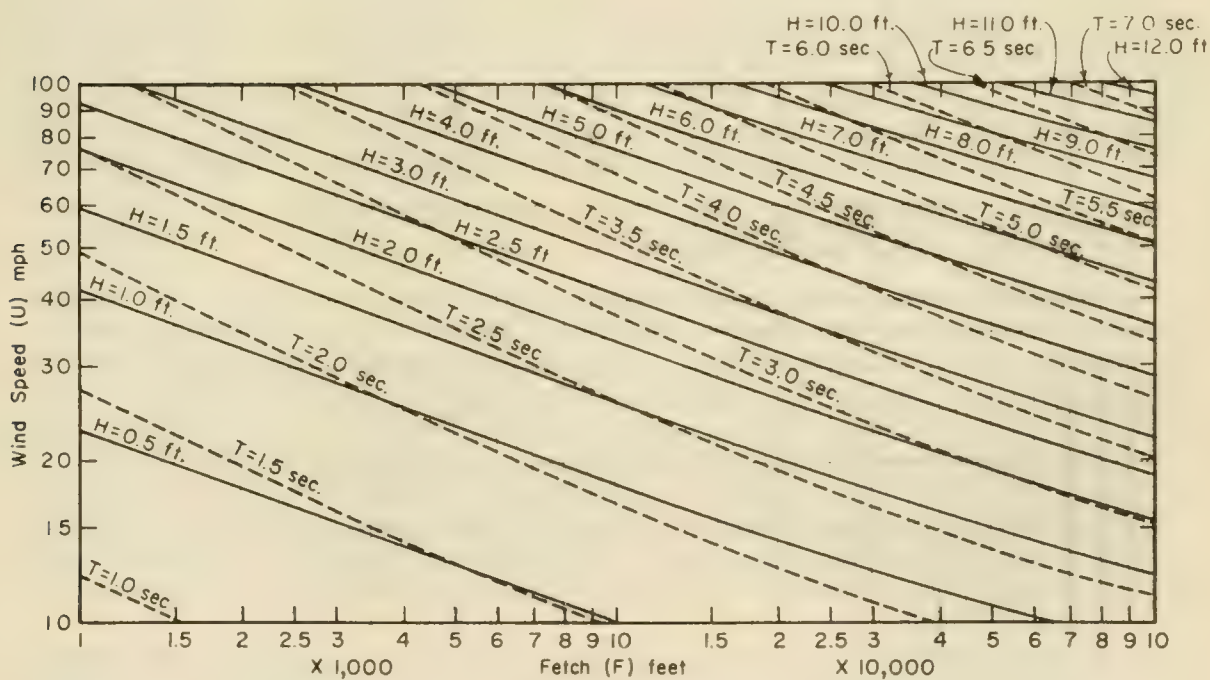
Figure 3-30.   Forecasting Curves for Shallow-Water Waves
Constant Depth = 50 feet.

SOLUTION: From Figure 3-27 for constant depth, d = 35 feet,

for

$$F = 80,000 \text{ feet,}$$

and

$$U = 50 \text{ mph.}$$

Then

$$H = 5.9 \text{ feet, say 6 feet,}$$

and

$$T = 5.1 \text{ seconds, say 5 seconds.}$$

* *

3.62   DECAY IN LAKES, BAYS, AND ESTUARIES

Section 3.33. Decay of A Wave Field applies to water areas contiguous with land as well as those in the open ocean. Most fetches in inland waters will be limited at the front and at the rear by a land mass and decay distances will usually be relatively small or nonexistent.

3.7   HURRICANE WAVES

When predicting wave generation by hurricanes, the determination of fetch and duration from a wind field is more difficult than for more normal weather conditions discussed earlier. The large changes in wind speed and direction with both location and time cause the difficulty. Estimation of the free air wind field must be approached through mathematical models, because of the scarcity of observations in severe storms. However, the vertical temperature profile and atmospheric turbulence characteristics associated with hurricanes differ less from one storm to another than for other types of storms. Thus the relation between the free air winds and the surface winds is less variable for hurricanes than for other storms.

3.71 DESCRIPTION OF HURRICANE WAVES

In hurricanes, fetch areas in which wind speed and direction remain reasonably constant are always small; a fully arisen sea state never develops. In the high-wind zones of a storm, however, long-period waves which can outrun the storm may be developed within fetches of 10 to 20 miles and over durations of 1 to 2 hours. The wave field in front, or to either side, of the storm center will consist of a locally generated sea, and a swell from other regions of the storm. Samples of wave spectra, obtained during hurricane Agnes, 1972, are shown in Figure 3-31. Most of the spectra display evidence of two or three distinct wave trains; thus, the physical implications of a *significant wave period* is not clear.

Other hurricane wave spectra computed with an analog spectrum analyzer from wave records obtained during Hurricane Donna, 1959, have been published by Bretschneider (1963). Most of these spectra also contained two distinct peaks.
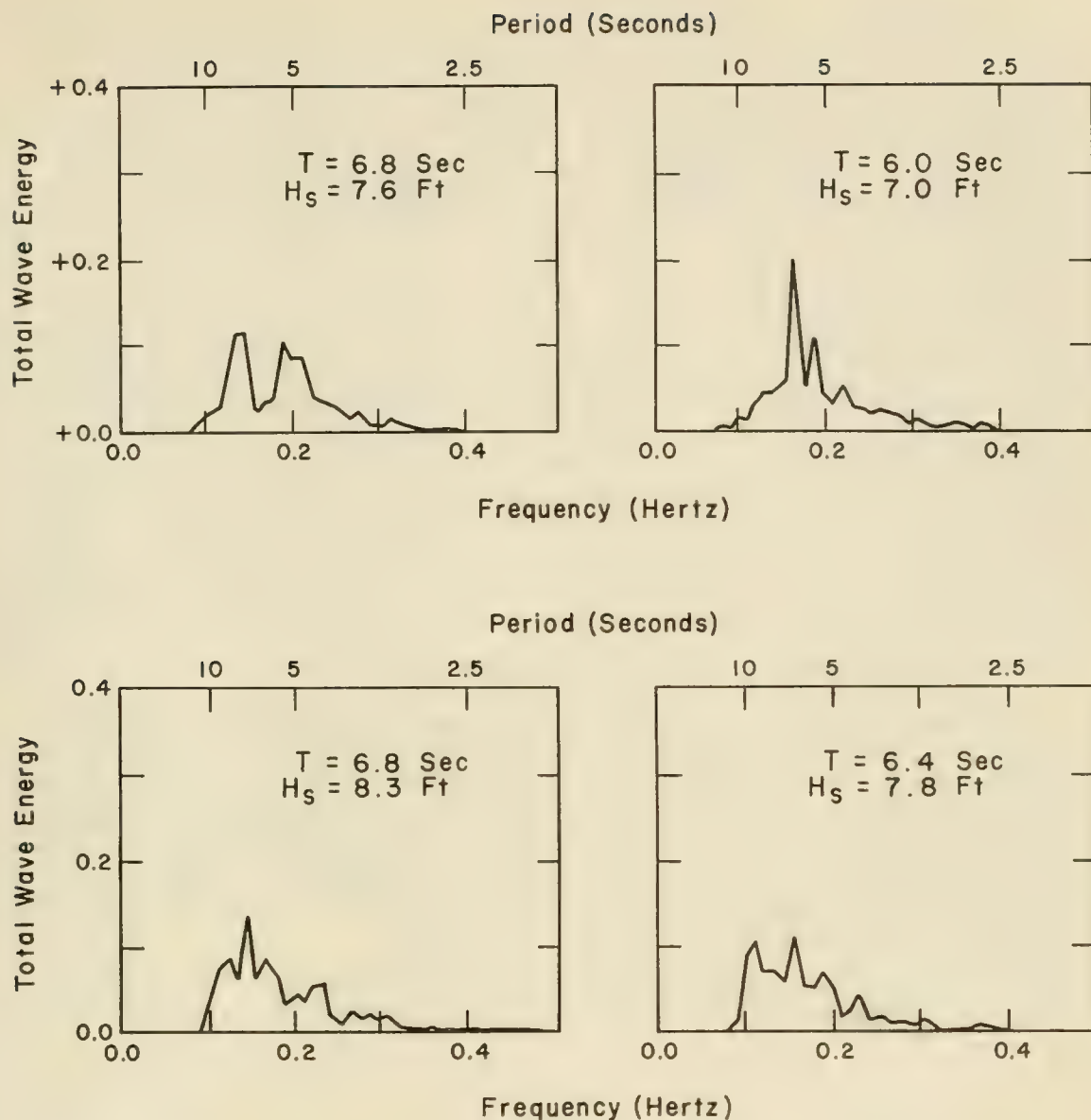
Figure 3-31.   Typical Hurricane Wave Spectra.   Typical Hurricane
Wave Spectra from the Atlantic Coast of the United
States.   The ordinate scale is the fraction of
total wave energy in each frequency band of 0.0011
Hertz (one Hertz is one cycle/second).   A linear
frequency scale is shown at bottom of each graph
and a non-linear period scale at top of each graph.

An indication of the distribution of waves throughout a hurricane can be obtained by plotting composite charts of shipboard wave observations. The position of a report is determined by its distance from the storm center and its direction from the storm track. Changes in storm intensity and shape are often small enough to permit all observations obtained during a period of 24 to 36 hours to be plotted on a single chart. Several plots of this type from Pore (1957) are given in Figure 3-32. Additional data of the same type have been presented by Arakawa and Suda (1953), Pore (1957) and Harris (1962).

Goodknight and Russell (1963) give a tabulation of the significant height and period for waves recorded on an oil drilling platform in approximately 33 feet of water, 1.5 miles from shore near Burrwood, Louisiana during hurricanes Audrey, 1957, and Ella, 1950, and tropical storms Bertha, 1957, and Esther, 1957. These wave records were used to evaluate the applicability of the Rayleigh distribution function (Section 3.22. Wave Height Variability) to hurricane statistics for wave heights and periods. They concluded that the Rayleigh distribution function is adequate for deriving the ratios between H_s, H_{10}, $\overline{H}$, etc., with sufficient accuracy for engineering design, but that its acceptance as a basic law for wave height distributions is questionable.

3.72 MODEL WIND AND PRESSURE FIELDS FOR HURRICANES

Many mathematical models have been proposed, for use in studying hurricanes. Each is designed to simulate some aspect of the storm as accurately as possible without making excessively large errors in describing other aspects of the storm. Each model leads to a slightly different specification of the surface wind field. Available wind data are sufficient to show that some models duplicate certain aspects of the wind field better than certain other models; but there are not enough data for a determination of a *best model* for all purposes.

One of the simplest and earliest models for the hurricane wind field is the Rankin vortex. For this model, it is assumed that

$$U = Kr \quad \text{for } r \leq R ,$$

$$U = \frac{KR^2}{r} \quad \text{for } r \geq R , \qquad (3\text{-}27)$$

where K is a constant, R is the radial distance from the storm center to the region of maximum wind speed, and r is the radial distance from the storm center to any specified point in the storm system.

This model can be improved by adding a translational component to account for storm movement and a term producing cross-isobar flow toward the storm center.

Extensions of this model are still being used in some engineering studies (Collins and Viehman, 1971). This model gives an artificial discontinuity in the horizontal gradient of the wind speed at the radius of maximum winds, and does not reproduce the well-known area of calm winds near the storm center.
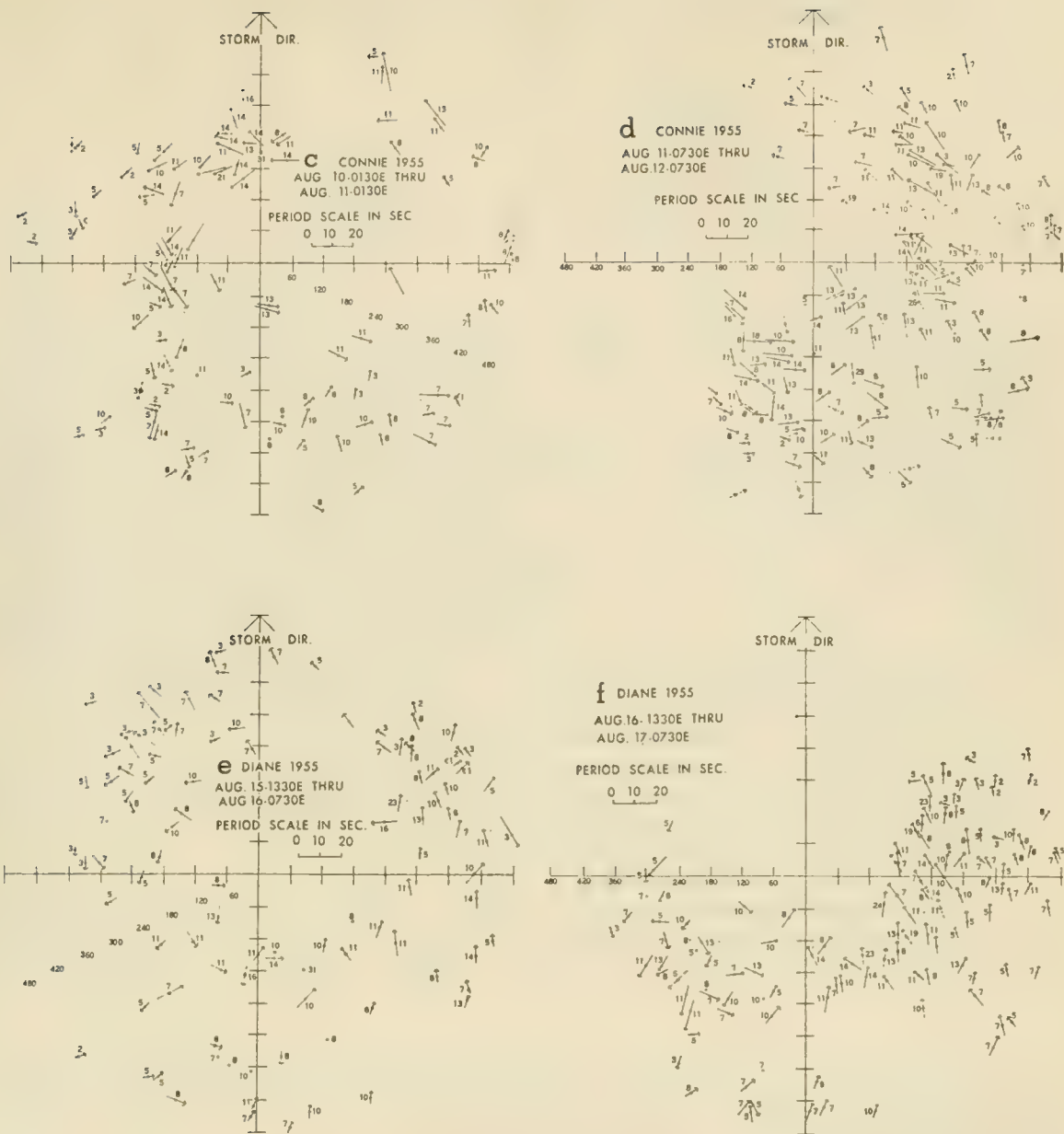
(after Pore, 1957)

Figure 3-32.   Compositive Wave Charts. The wave height in feet is plotted
beside the arrow indicating direction from which the waves
came.   The length of the arrow is proportional to the wave
period.   Dashed arrow indicates unknown period.   Distances
are marked along the radii at intervals of 60 nautical miles.

3-55

A more widely used model was given by Myers (1954). A concise mathematical description of this model is given by Harris (1958) as follows:

$$\frac{p - p_o}{p_n - p_o} = e^{-\frac{R}{r}} , \qquad (3-28)$$

$$\frac{U_{gr}^2}{r} + fU_{gr} = \frac{1}{\rho_a} \left(p_n - p_o\right) \frac{R}{r^2} e^{-\frac{R}{r}} , \qquad (3-29)$$

where p is the pressure at a point located at a distance r from the storm center, p_o is the central pressure, p_n is the pressure at the outskirts of the storm, ρ_a is the density of air, and U_{gr} is the gradient wind speed. Agreement between this model and the characteristics of a well-observed hurricane is shown in Figure 3-33. The insert map gives the storm track; dots indicate the observed pressure at several stations in the vicinity of Lake Okeechobee, Florida; the solid line (Fig. 3-33a) gives the theoretical pressure profile fitted to three points within 50 miles of the storm center. The corresponding theoretical wind profile is given by the upper curve of Figure 3-33b. Observed winds at one station are indicated by dots below this curve. A solid line has been drawn through these dots by eye to obtain a smooth profile. The observed wind speed varies in a systematic way from about 65 percent of the computed wind speed at the outer edge to almost 90 percent of the predicted value near the zone of maximum wind speed. Reasonably good agreement between the theoretical and observed wind speeds has been obtained in only a few storms. This lack of agreement between the theoretical and observed winds is due in part to the elementary nature of the model, but perhaps equally to the lack of accurate wind records near the center of hurricanes.

Parameters obtained from fitting this model to a large number of storms were given by Myers (1954). Parameters for these other storms (and for additional storms) are given by Harris (1958). Equation 3-29 will require some form of correction for a moving storm.

This model is purely empirical, but it has been used extensively and it provides reasonable agreement with observations in many storms. Other equally valid models could be derived; however, alternative models should not be adopted without extensive testing.

In the northern hemisphere, wind speeds to the right of the storm track are always higher than those on the left, and a correction is needed when any stationary storm model is being used for a moving storm. The effect of storm motion on the wind field decreases with distance from the zone of highest wind speeds. Thus the vectorial addition of storm motion to the wind field of the stationary storm is not satisfactory. Jelesnianski (1966) suggests the following simple form for this correction,

$$U_{SM}(r) = \frac{Rr}{R^2 + r^2} V_F , \qquad (3-30)$$
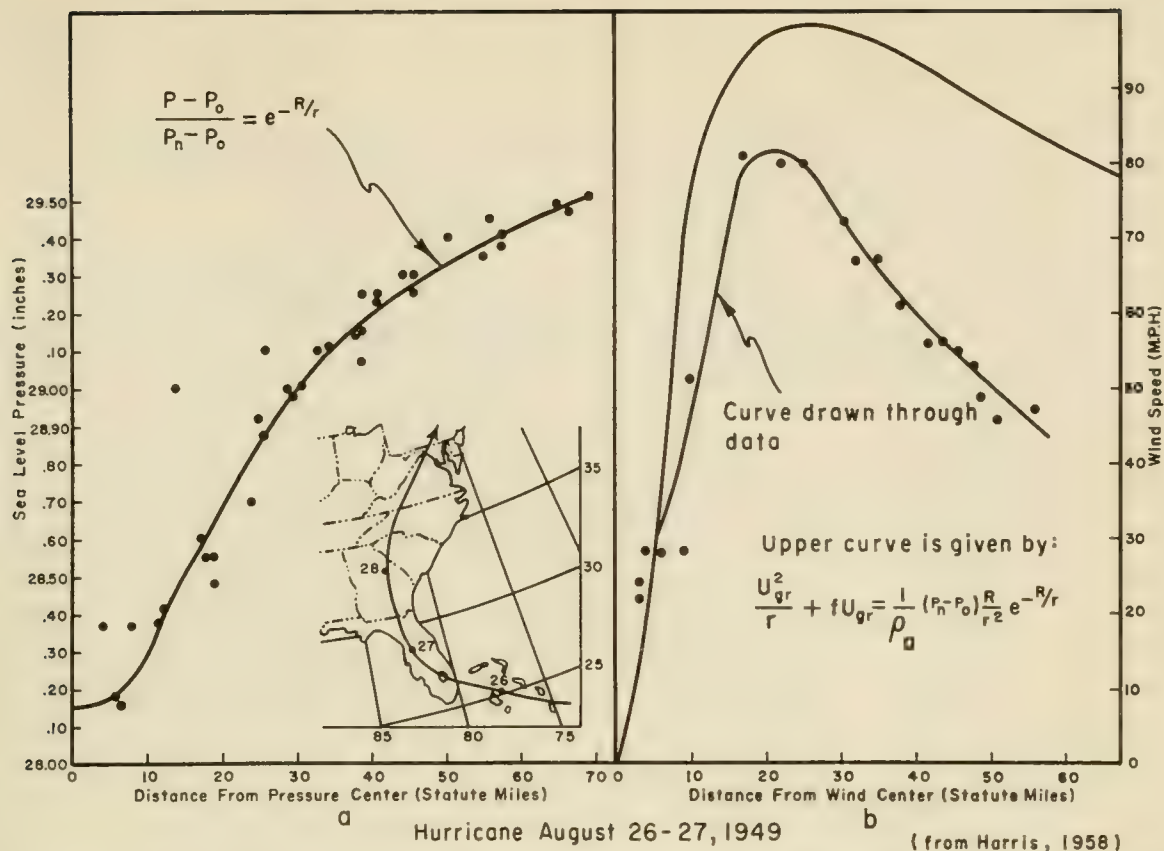
Figure 3-33.   Pressure and Wind Distribution in Model Hurricane.   Plotted dots represents observations

where V_F is the velocity of the storm center, and $U_{SM}(r)$ is the convective term which is to be added vectorially to the wind velocity at each value of r.   Wilson (1955, 1961) and Bretschneider (1959, 1972) have suggested other correction terms.

3.73 PREDICTION TECHNIQUE

For a slowly moving hurricane, the following formulas can be used to obtain an estimate of the deepwater significant wave height and period at the point of maximum wind:

$$H_o = 16.5 \, e^{\frac{R\Delta p}{100}} \left[1 + \frac{0.208 \, \alpha \, V_F}{\sqrt{U_R}} \right], \qquad (3\text{-}31)$$

and

$$T_s = 8.6 \, e^{\frac{R\Delta p}{200}} \left[1 + \frac{0.104 \, \alpha \, V_F}{\sqrt{U_R}} \right], \qquad (3\text{-}32)$$

where

H_O = deepwater significant wave height in feet

T_s = the corresponding significant wave period in seconds

R = radius of maximum wind in nautical miles

Δp = $p_n - p_o$, where p_n is the normal pressure of 29.92 inches of mercury, and p_o is the central pressure of the hurricane

V_F = The forward speed of the hurricane in knots

U_R = The maximum sustained wind speed in knots, calculated for 30 feet above the mean sea surface at radius R where

$$U_R = 0.865 \, U_{max} \quad \text{(For stationary hurricane)} \qquad (3-33)$$

$$U_R = 0.865 \, U_{max} + 0.5 \, V_F \quad \text{(For moving hurricane)} \qquad (3-34)$$

U_{max} = Maximum gradient wind speed in knots 30 feet above the water surface

$$U_{max} = 0.868 \, [73 \, (p_n - p_o)^{1/2} - R(0.575f)] \qquad (3-35)$$

f = Coriolis parameter = $2\omega \sin\phi$, where ω = angular velocity of earth = $2\pi/24$ radians per hour

Latitude (ϕ)	25°	30°	35°	40°
f (rad/hr)	0.221	0.262	0.300	0.337

α = a coefficient depending on the forward speed of the hurricane and the increase in effective fetch length, because the hurricane is moving. It is suggested that for slowly moving hurricane α = 1.0.

Once H_O is determined for the point of maximum wind from Equation 3-31 it is possible to obtain the approximate deepwater significant wave height H_O for other areas of the hurricane by use of Figure 3-34.

The corresponding approximate wave period may be obtained from

$$T = 2.13 \sqrt{H_O} \quad \text{(in seconds)}, \qquad (3-36)$$

where H_O is in feet (derived from empirical data showing that the wave steepness H/T^2 will be about 0.22).
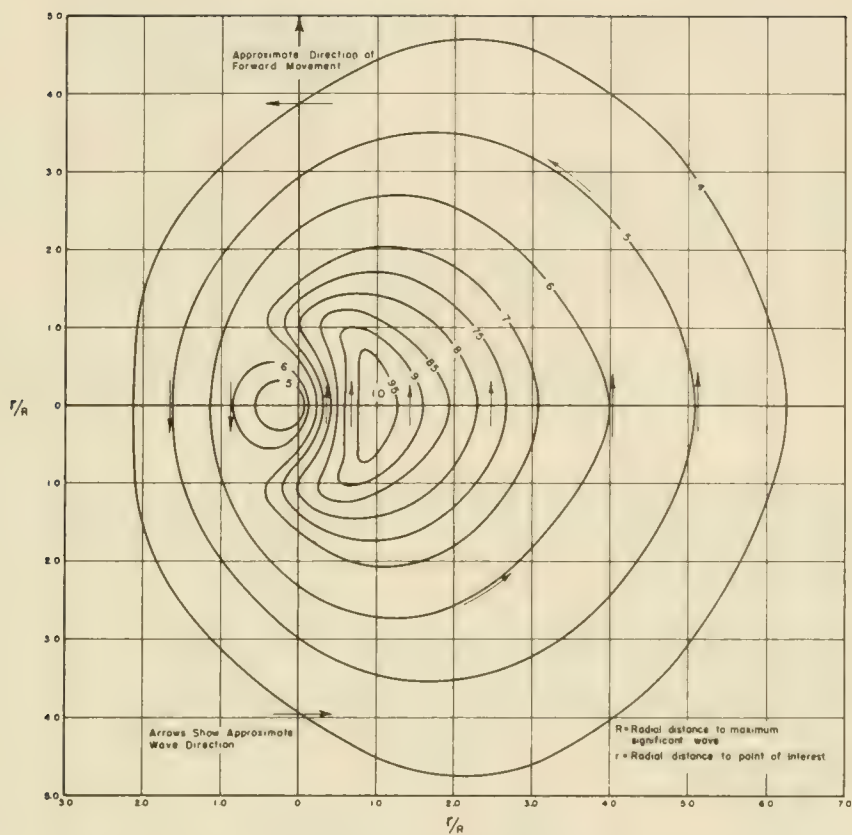
Figure 3-34.   Isolines of Relative Significant Wave
Height for Slow Moving Hurricane

GIVEN: Consider a hurricane at latitude 35°N. with R = 36 nautical miles, Δp = 29.92 - 27.61 = 2.31 inches of mercury, and V_F, forward speed, = 26 knots.   Assume for simplicity that α = 1.0.

FIND: The deepwater significant wave height and period.

SOLUTION:

  Using Equation 3-35

$$U_{max} = 0.868 \left[73 \left(P_n - P_o \right)^{\frac{1}{2}} - R\,(0.575f) \right]$$

$$U_{max} = 0.868 \left[73\,(2.31)^{\frac{1}{2}} - 36\,(0.575 \times 0.300) \right]$$

$$U_{max} = 0.868\,(110.95 - 6.23) = 90.9 \text{ knots.}$$

  Using Equation 3-34

$$U_R = 0.865\,U_{max} + 0.5\,V_F$$

$$U_R = 0.865\,(90.9) + 0.5\,(26) = 91.6 \text{ knots.}$$

  Using Equation 3-31

$$H_o = 16.5\ e^{\frac{R\Delta p}{100}} \left[1 + \frac{0.208\,\alpha V_F}{\sqrt{U_R}} \right],$$

  where the exponent

$$\frac{R\Delta p}{100} = \frac{36\,(2.31)}{100} = 0.832,$$

  and

$$e^{0.832} = 2.30$$

  then

$$H_o = 16.5\ e^{0.832} \left[1 + \frac{0.208 \times 1 \times 26}{\sqrt{91.6}} \right]$$

$$H_o = 16.5\,(2.30)\,(1.564) = 59.4 \text{ feet.}$$

3-60

Using Equation 3-32

$$T_s = 8.6 \ e^{\frac{R\Delta p}{200}} \left[1 + \frac{0.104 \ \alpha \ V_F}{\sqrt{U_R}} \right],$$

where the exponent

$$\frac{R\Delta P}{200} = \frac{36 \ (2.31)}{200} = 0.416$$

$$T_s = 8.6 \ e^{0.416} \left[1 + \frac{0.104 \times 1 \times 26}{\sqrt{91.6}} \right]$$

$$T_s = 8.6 \ (1.52) \ (1.282) = 16.8 \ \text{seconds}.$$

Alternately, by Equation 3-36, it is seen that

$$T_s = 2.13 \sqrt{59.4} = 16.4 \ \text{seconds}.$$

It should be noted that computing the values of wave height and period to three significant figures does not imply the degree of accuracy of the method; it is done to reduce the computational error.

Referring to Figure 3-34, H_o = 59.4 feet corresponds to the relative significant wave height of 1.0 at r/R = 1.0, the point of maximum winds located, for this example, 36 nautical miles to the right of the hurricane center. At that point the wave height is about 60 feet, and the wave period T is about 16 seconds. At r/R = 1.0 to the left of the hurricane center, from Figure 3-34 the ratio of relative significant height is about 0.62, whence H_o = 0.62 (59.4) = 36.8 feet. This wave is moving in a direction opposite to that of the 59.4-foot wave. The significant wave period for the 36.8-foot wave is: $T_s = 2.13 \sqrt{36.8} = 12.9$ seconds, say 13 seconds.

The most probable maximum wave is assumed to depend on the number of waves considered applicable to the significant wave, H_o = 59.4 feet. This number N depends on the length of the section of the hurricane for which near steady state exists and the forward speed of the hurricane. It has been found that maximum wave conditions occur over a distance equal to the radius of maximum wind. The time it takes the radius of maximum wind to pass a particular point is

$$t = \frac{R}{V_F} = \frac{36}{26} = 1.38 \ \text{hours} = 4,970 \ \text{seconds}; \tag{3-37}$$

the number of waves will be

$$N = \frac{t}{T_s} = \frac{4970}{16.4} \approx 303. \tag{3-38}$$

3-61

The most probable maximum waves can be obtained by using

$$H_n = 0.707 \ H_o \ \sqrt{\log_e \frac{N}{n}} . \qquad (3\text{-}39)$$

The most probable maximum wave is obtained by setting n = 1, and using Equation 3-39

$$H_1 = 0.707 \ (59.4) \ \sqrt{\log_e \frac{303}{1}} = 100.4 \ \text{feet, say } 100 \ \text{feet.}$$

Assuming that the 100-foot wave occurred, then the most probable second highest wave is obtained by setting n = 2, the third from n = 3, etc.

$$H_2 = 0.707 \ (59.4) \ \sqrt{\log_e \frac{303}{2}} = 94.1 \ \text{feet, say } 94 \ \text{feet;}$$

$$H_3 = 0.707 \ (59.4) \ \sqrt{\log_e \frac{303}{3}} = 90.2 \ \text{feet, say } 90 \ \text{feet.}$$

The problem now is to determine the changes in the deepwater waves as they cross the Continental Shelf, taking into account the combined effects of bottom friction, refraction, the continued action of the wind, and the forward speed of the hurricane. This requires numerical integration, using Table 3-3, Figure 3-35, and refraction diagrams. It is also necessary to obtain an effective fetch length, by use of

$$F_e = \left[\frac{H_o}{0.0555 \ U_R} \right]^2 , \qquad (3\text{-}40)$$

where

F_e is the effective fetch in nautical miles,

H_o is the deepwater significant wave height in feet,

and

U_R is the maximum sustained wind speed in knots.

For this example, using Equation 3-40

$$F_e = \left[\frac{59.4}{0.0555 \ (91.6)} \right]^2 = (11.69)^2 = 137 \ \text{nautical miles.}$$

3-62

Table 3-3. Values of K_s or (H/H'_o)

T^2/d *	0.00	0.01	0.02	0.03	0.04	0.05	0.06	0.07	0.08	0.09
0.1	1.000	1.000	1.000	1.000	1.000	1.000	1.000	1.000	1.000	1.000
0.2	1.000	1.000	1.000	1.000	1.000	1.000	1.000	0.999	0.999	0.999
0.3	0.998	0.998	0.997	0.997	0.996	0.995	0.994	0.993	0.992	0.991
0.4	0.990	0.989	0.987	0.986	0.984	0.982	0.981	0.980	0.978	0.976
0.5	0.974	0.973	0.971	0.969	0.967	0.965	0.963	0.961	0.960	0.959
0.6	0.957	0.955	0.954	0.952	0.951	0.949	0.948	0.946	0.945	0.943
0.7	0.942	0.941	0.939	0.938	0.937	0.936	0.935	0.934	0.932	0.931
0.8	0.930	0.929	0.929	0.928	0.927	0.926	0.925	0.924	0.924	0.923
0.9	0.922	0.922	0.921	0.921	0.920	0.919	0.919	0.918	0.918	0.917
1.0	0.917	0.917	0.916	0.916	0.916	0.915	0.915	0.915	0.915	0.914
1.1	0.914	0.914	0.914	0.914	0.914	0.913	0.913	0.913	0.913	0.913
1.2	0.913	0.913	0.913	0.913	0.913	0.913	0.913	0.913	0.913	0.913
1.3	0.913	0.913	0.914	0.914	0.914	0.914	0.914	0.914	0.914	0.915
1.4	0.915	0.915	0.915	0.915	0.915	0.916	0.916	0.916	0.916	0.917
1.5	0.917	0.917	0.917	0.918	0.918	0.918	0.919	0.919	0.919	0.919
1.6	0.920	0.920	0.920	0.920	0.921	0.921	0.921	0.922	0.922	0.922
1.7	0.923	0.923	0.924	0.924	0.924	0.925	0.925	0.925	0.926	0.926
1.8	0.927	0.927	0.927	0.928	0.928	0.928	0.929	0.929	0.930	0.930
1.9	0.931	0.931	0.931	0.932	0.932	0.933	0.933	0.933	0.934	0.934
2.0	0.935	0.935	0.936	0.936	0.936	0.937	0.937	0.938	0.938	0.939
2.1	0.939	0.940	0.940	0.941	0.941	0.942	0.942	0.942	0.943	0.943
2.2	0.943	0.944	0.945	0.945	0.946	0.946	0.947	0.947	0.947	0.948
2.3	0.948	0.949	0.949	0.950	0.950	0.951	0.951	0.951	0.952	0.952
2.4	0.953	0.953	0.954	0.954	0.955	0.955	0.956	0.956	0.956	0.957
2.5	0.957	0.958	0.958	0.959	0.959	0.960	0.960	0.961	0.961	0.962
2.6	0.962	0.963	0.963	0.964	0.964	0.965	0.965	0.966	0.966	0.967
2.7	0.967	0.968	0.968	0.969	0.969	0.969	0.970	0.970	0.971	0.971
2.8	0.972	0.972	0.973	0.973	0.974	0.974	0.975	0.975	0.976	0.976
2.9	0.977	0.977	0.977	0.978	0.979	0.979	0.979	0.980	0.980	0.981
3.0	0.981	0.981	0.982	0.983	0.983	0.984	0.984	0.985	0.985	0.986
3.1	0.986	0.987	0.987	0.987	0.988	0.988	0.989	0.990	0.990	0.990
3.2	0.991	0.991	0.992	0.992	0.992	0.992	0.994	0.994	0.994	0.995
3.3	0.995	0.996	0.996	0.997	0.997	0.998	0.998	0.999	0.999	0.999
3.4	1.000	1.000	1.000	1.001	1.002	1.003	1.003	1.003	1.004	1.004
3.5	1.005	1.005	1.006	1.006	1.006	1.007	1.007	1.008	1.008	1.009
3.6	1.009	1.010	1.010	1.011	1.011	1.012	1.012	1.012	1.013	1.013
3.7	1.014	1.014	1.015	1.015	1.015	1.016	1.016	1.017	1.017	1.017
3.8	1.018	1.018	1.019	1.019	1.019	1.020	1.021	1.021	1.022	1.022
3.9	1.023	1.023	1.024	1.024	1.024	1.025	1.025	1.025	1.026	1.026
4.0	1.027	1.027	1.028	1.028	1.029	1.029	1.030	1.030	1.030	1.031

T^2/d	0.0	0.1	0.2	0.3	0.4	0.5	0.6	0.7	0.8	0.9
4	1.027	1.032	1.036	1.040	1.044	1.048	1.053	1.056	1.060	1.064
5	1.068	1.073	1.077	1.080	1.085	1.089	1.092	1.097	1.100	1.103
6	1.107	1.111	1.115	1.118	1.121	1.125	1.128	1.131	1.135	1.139
7	1.142	1.146	1.149	1.152	1.155	1.159	1.162	1.164	1.168	1.171
8	1.174	1.177	1.180	1.185	1.187	1.189	1.193	1.196	1.199	1.201
9	1.205	1.207	1.211	1.213	1.216	1.218	1.221	1.225	1.227	1.230
10	1.233	1.236	1.239	1.240	1.243	1.246	1.249	1.251	1.253	1.257

*Units of sec^2/ft.
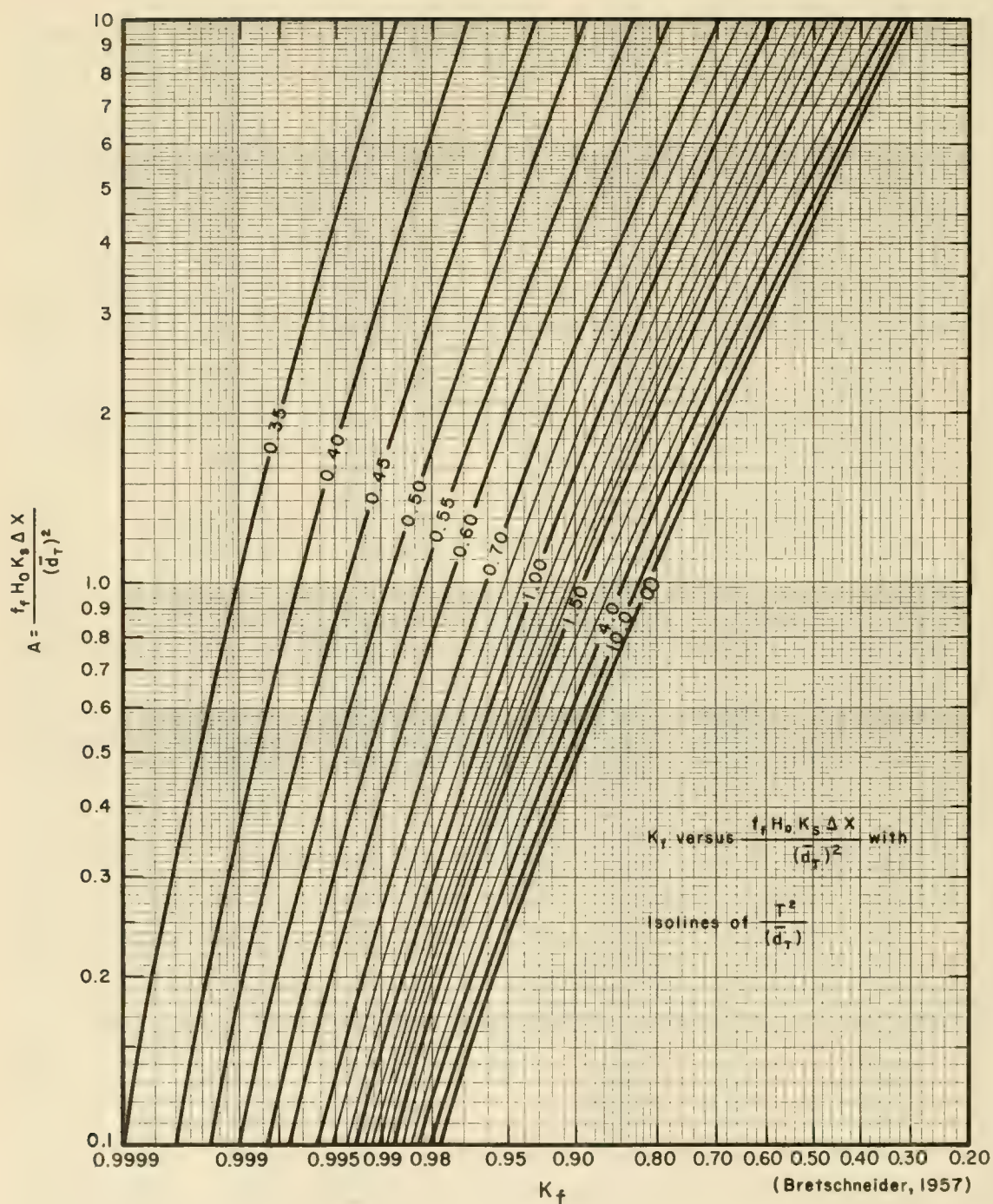
Figure 3-35. Relationship for Friction Loss Over a Bottom of Constant Depth

3-64

For the remaining part of this problem, either the value of F_{min} equal to 220 nautical miles as determined from Figure 3-15 for $U_R = 91.6$, $H_O = 59.4$ can be used with the deepwater forecasting curves, or else Equation 3-40 can be used, as modified,

$$H_o = 0.0555 \ U_R \ \sqrt{F'_e + \Delta F}$$

along with Equation 3-36

$$T_o = 2.13 \ \sqrt{H_o} \ .$$

F'_e is defined below.

The latter being a numerical method is easier to use and more accurate than the graphical method of using forecasting curves.

The procedure for computing wind waves over the Continental Shelf will be illustrated by using the bottom profile off the mouth of the Chesapeake Bay and the standard project hurricane developed for the Norfolk area. The storm surge computed for the standard project hurricane and 2.5 feet of astronomical tide are added to the mean low water depths to obtain the total water depth for wave generation. Refraction is neglected in this example, i.e., $K_R = 1.0$. The results of these computations are given in Table 3-4 followed by examples and explanations.

Column 1 of Table 3-4 is the distance in nautical miles measured seaward of the entrance to Chesapeake Bay, using increments of 5 nautical miles for each section.

Column 2, d_x, is the depth in feet referred to mean low water at the shoreward end of each section, denoted by X of Column 1.

Column 3 is the depth d_1 at the beginning of each section.

Column 4 is the depth d_2 at the shoreward end of each section. These depths are the water depths below MLW plus the 2.5-foot astronomical tide plus the hurricane surge and are then rounded off to the nearest foot.

Column 5, $\overline{d_T}$, is the average of Columns 3 and 4 to the nearest foot.

Column 6 is the effective fetch F_e (nautical miles), and is obtained for the first step directly from Equation 3-40. For successive steps, $F_e = F'_e + \Delta F \leq 137$ n.mi. where F'_e is given in Column 14 one line above in each case (e.g., line X = 40, $F_e = 80.6 + 5.0 = 85.6$) and ΔF is 5 n.mi. F'_e is defined for Column 14.

Table 3-4. Computations for Wind Waves Over the Continental Shelf.

1	2	3	4	5	6	7	8	9	10	11	12	13	14	15	16	17	18	19	20
X	d_x MLW	d_1	d_2	$\bar{d}_T$	F_e	H_o	T_o	$\dfrac{T_o^2}{d_T}$	K_s	A	K_f	H_o'	F_e'	T_o'	$\dfrac{(T_o')^2}{d_2}$	K_{s2}	H	N	H_{max}
65	500	1004	504	754	137	59.4	16.4	0.36	0.994	0.0316	1.00	59.4	136.7	16.4	0.53	0.969	57.6	303	97.3
60	190	504	194	349	137	59.4	16.4	0.77	0.934	0.138	0.995	59.1	135.3	16.4	1.39	0.915	54.1	303	91.4
55	154	194	158	176	137	59.4	16.4	1.53	0.918	0.536	0.94	55.8	120.6	15.9	1.60	0.920	51.3	313	87.1
50	116	158	122	140	125.6	56.9	16.1	1.85	0.928	0.819	0.90	51.2	101.6	15.2	1.89	0.930	47.6	327	81.0
45	112	122	116	119	106.6	52.4	15.4	1.99	0.934	1.050	0.87	45.6	80.6	14.4	1.77	0.925	42.2	345	72.1
40	110	116	116	116	85.6	47.0	14.6	1.84	0.928	0.990	0.88	41.4	66.4	13.7	1.62	0.920	38.1	363	65.4
35	104	116	110	113	71.4	42.9	14.0	1.73	0.924	0.943	0.89	38.2	56.6	13.2	1.58	0.919	35.1	377	60.4
30	82	110	88	99	61.6	39.9	13.5	1.84	0.928	1.15	0.80	34.3	45.6	12.5	1.78	0.926	31.8	398	55.0
25	70	88	78	83	50.6	36.1	12.8	1.97	0.933	1.49	0.825	29.8	34.4	11.6	1.73	0.924	27.5	428	47.9
20	60	78	68	73	39.4	30.0	11.7	1.88	0.930	1.59	0.83	24.9	24.0	10.5	1.62	0.920	22.9	473	40.2
15	52	68	62	65	29.0	27.4	11.1	1.90	0.931	1.84	0.78	21.4	17.7	9.9	1.58	0.919	19.7	502	34.7
10	42	62	52	57	22.7	24.2	10.5	1.93	0.932	2.11	0.76	18.4	13.1	9.1	1.59	0.919	16.9	546	30.0
5	32	52	44	48	18.1	21.6	9.9	2.04	0.936	2.67	0.73	15.8	9.7	8.5	1.64	0.921	14.6	585	26.0
0	24	44	36	40	14.7	19.5	9.4	2.21	0.944	3.50	0.66	12.9	6.5	7.6	1.60	0.920	11.9	654	21.4

3-66

Column 7 is the deepwater significant wave height H_o and is obtained from Equation 3-40:

$$H_o = 0.0555 \ U_R \ \sqrt{F_e} = 5.08 \ \sqrt{F_e}, \text{ where } U_R = 91.6 \text{ knots}$$

and F_e is obtained from Column 6.

Column 8 is the deepwater significant wave period T_o and is obtained from Equation 3-36:

$$T_o = 2.13 \ \sqrt{H_o} \text{ where } H_o \text{ is obtained from Column 7.}$$

Column 9 is $T_o^2/\bar{d}_T$, or Column 8 squared over Column 5.

Column 10 is the shoaling coefficient (H/H_o') or K_s corresponding to the value of $T_o^2/\bar{d}_T$, Column 9, and is obtained from Table 3-3 K_s versus T^2/d.

Column 11 is the friction loss parameter and is equal to

$$A = \frac{f_f H_o \ K_s \Delta X}{\left(\bar{d}_T\right)^2} = \frac{0.01 \ H_o \ K_s \ (5) \ (6,080)}{\left(\bar{d}_T\right)^2} = \frac{304 \ H_o \ K_s}{\left(\bar{d}_T\right)^2} \tag{3-41}$$

where f_f is assumed as 0.01, $\Delta X = 5(6,080) = 30,400$ ft., $\bar{d}_T$ is the average water depth of the increment ΔX.

Column 12 is the friction factor K_f and is obtained from Figure 3-35 where K_f is a function of $T^2/\bar{d}_T$ (Column 9) and

$$\frac{f_f H_o \ K_s \ \Delta X}{\left(\bar{d}_T\right)^2} = A \text{ (Column 11).}$$

Column 13 is the equivalent deepwater wave height H_o' and is obtained from $H_o' = H_o K_f$ (the product of Columns 7 and 12).

Column 14 is the equivalent effective fetch length for H_o' and is obtained from Equation 3-40

$$F_e' = \left[\frac{H_o'}{\left(0.0555 \ U_R\right)}\right]^2 = \left[\frac{H_o'}{5.08}\right]^2 \text{ where } U_R = 91.6 \text{ knots (moving hurricane).}$$

Column 15 is obtained by using Equation 3-36 $T_o' = 2.13 \ \sqrt{H_o'}$.

Column 16 is $(T_o')^2/d_2$, where d_2 is the water depth at shoreward end of section ΔX.

Column 17 is the shoaling coefficient K_{s2} related to the values of $(T'_o)^2/d_2$ (Column 16).

Column 18 is $H = H'_o \times K_{s2}$ (product of Columns 13 and 17).

Column 19 is obtained by using Equation 3-38

$$N = \frac{t}{T'_o} = \frac{4,970}{T'_o} \quad \text{where } t = R/V_F = \frac{36}{26} = 1.38 \text{ hours or } 4,970 \text{ seconds.}$$

Column 20 is $H_{max} = 0.707 \, H \sqrt{\log_e N}$, H is from Column 18.

After one line of computations across is completed, the next line is begun, using $F_e = F'_e + \Delta F \le 137$ where F'_e is from Column 14 of the preceding completed line. For example, consider the line corresponding to X = 40 being completed. Then the computation for the next line X = 35 is as follows:

$$F'_e = 66.4 \text{ from line X} = 40, \text{ Column 14.}$$

Column 6, F_e = 66.4 + 5 = 71.4 nautical miles for line X = 35 .

Compute

Column 7, H_o = 5.08 $\sqrt{71.4}$ = 42.9 feet .

Column 8, T_o = 2.13 $\sqrt{42.9}$ = 14.0 seconds .

Column 9, $\dfrac{T_o^2}{d_T} = \dfrac{(14)^2}{113} = 1.73$.

Column 10, K_s = 0.924 (Table 3-3) for values of $\dfrac{T_o^2}{d_T} = 1.73.$

Column 11, $A = \dfrac{304 \, H_o \, K_s}{(\bar{d}_T)^2} = \dfrac{(304 \, (42.9) \, (0.924)}{(113)^2} = 0.943$.

Column 12, K_f = 0.89 (from Figure 3-35) for values of $\dfrac{T_o^2}{d_T} = 1.73$ and A = 0.943 .

Column 13, $H'_o = H_o \, K_f$ = 42.9 (0.89) = 38.2 feet .

Column 14, $F'_e = \left[\dfrac{H'_o}{5.08}\right]^2 = \left[\dfrac{38.2}{5.08}\right]^2 = 56.6$ nautical miles .

3-68

Column 15, $T_o' = 2.13 \sqrt{38.2} = 13.2$ seconds .

Column 16, $\dfrac{(T_o')^2}{d_2} = 1.58$.

Column 17, $K_{s2} = 0.919$.

Column 18, $H = 0.919 (38.2) = 35.1$ feet, which is the shallow-water height for depth $d_2 = 110$ feet, corresponding to MLW of 104 feet.

Column 19, $N = \dfrac{4{,}970}{T_o'} = 377$ or the total number of waves applicable to

steady-state significant wave of $H = 35.1$ feet, say 35 feet .

Column 20, $H_{max} = 35.1 (0.707) \sqrt{\log_e 377} = 60.4$ feet, say 60 feet .

* *

The moving fetch model of Wilson (1955) has been adapted for computer usage by Wilson (1961). The basic equations were modified by Wilson (1966). The Bretschneider (1959) model for hurricane wave prediction was modified by Bretschneider (1972). Borgman (1972) used the results of Wilson (1957) to develop an approach for estimating the maximum wave in a storm which may be considered as an alternate to that presented here.

3.8   WATER LEVEL FLUCTUATIONS

The focus now changes from wave prediction to water level fluctuations in oceans and other bodies of water which have periods substantially longer than those associated with surface waves. Several known physical processes combine to cause these longer-term variations of the water level.

The expression *water level* is used to indicate the mean elevation of the water when averaged over a period of time long enough (about 1 minute) to eliminate high frequency oscillations caused by surface gravity waves. In the discussion of gravity waves the water level was also referred to as the *stillwater level* (SWL) to indicate the elevation of the water if all gravity waves were at rest. In the field, water levels are determined by measuring water surface elevations in a stilling well. Inflow and outflow of the well is restricted so that the rapid responses produced by gravity waves are filtered out, thus reflecting only the mean water elevation.

Water level fluctuations -- classified by the characteristics and type of motion which take place -- may be identified as:

     (a)   astronomical tides
     (b)   tsunamis
     (c)   seiches
     (d)   wave setup
     (e)   storm surges
     (f)   climatological variations
     (g)   secular variations

The first five have periods that range from a few minutes to a few days; the last two have periods that range from semi-annually to many years. Although important in long-term changes in water elevations, climatological and secular variations are not discussed here.

Forces caused by the graviational attraction between the moon, the sun, and the rotating earth result in periodic level changes in large bodies of water. The vertical rise and fall resulting from these forces is called the *tide* or *astronomical tide;* the horizontal movements of water are called *tidal currents*. The responses of water level changes to the tidal forces are modified in coastal regions because of variations in depths and lateral boundaries; tides vary substantially from place to place. Astronomical tide generating forces are well understood, and can be predicted many years in advance. The response to these forces can be determined from an analysis of tide gage records. Tide predictions are routinely made for many locations for which analyzed tide observations are available. In the United States, tide predictions are made by the National Ocean Survey, National Oceanographic and Atmospheric Administration

Tsunamis are generated by several mechanisms: submarine earthquakes, submarine landslides, and underwater volcanos. These waves may travel distances of more than 5,000 miles across an ocean with speeds at times exceeding 500 miles per hour. In open oceans, the heights of these waves are generally unknown but small; heights in coastal regions have been greater than 100 feet.

Seiches are long-period standing waves that continue after the forces that start them have ceased to act. They occur commonly in enclosed or partially enclosed basins.

Wave setup is defined as the superelevation of the water surface due to the onshore mass transport of the water by wave action alone. Isolated observations have shown that wave setup does occur in the surf zone.

Surges are caused by moving atmospheric pressure jumps and by the wind stress accompanying moving storm systems. Storm systems are significant because of their frequency and potential for causing abnormal water levels at coastlines. In many coastal regions, maximum storm surges are produced by severe tropical cyclones called hurricanes.

Prediction of water level changes is complex because many types of water level fluctuations can occur simultaneously. It is not unusual for surface wave setup, high astronomical tides, and storm surge to occur coincidently at the shore on the open coast. It is difficult to determine how much rise can be attributed to each of these causes. Although astronomical tides can be predicted rather well where levels have been recorded for a year or more, there are many locations where this information is not available. Furthermore, the interaction between tides and storm surge in shallow water is not well defined.

3.81 ASTRONOMICAL TIDES

Tide is a periodic rising and falling of sea level caused by the gravitational attraction of the moon, sun, and other astronomical bodies acting on the rotating earth. Tides follow the moon more closely than they do the sun. There are usually two high and and two low waters in a tidal or lunar day. As the lunar day is about 50 minutes longer than the solar day, tides occur about 50 minutes later each day. Typical tide curves for various locations along the Atlantic, Gulf, and Pacific coasts of the United States are shown in Figures 3-36 and 3-37. Along the Atlantic coast, the two tides each day are of nearly the same height. On the Gulf coast, the tides are low but in some instances have a pronounced diurnal inequality. Pacific coast tides compare in height with those on the Atlantic coast but in most cases have a decided diurnal inequality. (See Appendix A, Figure A-10.)

The dynamic theory of tides was formulated by Laplace (1775) and special solutions have been obtained by Doodson and Warburg (1941) among others. The use of simplified theories for the analysis and prediction of tides has been described by Schureman (1941), Defant (1961) and Ippen (1966). The computer program for tide prediction, currently being used for official tide prediction in the United States is described by Pore and Cummings (1967).

Data concerning tidal ranges along the seacoasts of the United States are given to the nearest foot in Table 3-5. Spring ranges are shown for areas having approximately equal daily tides; diurnal ranges are shown for areas having either a diurnal tide or a pronounced diurnal inequality. Detailed data concerning tidal ranges are published annually in Tide Tables, U.S. Department of Commerce, National Ocean Survey.

3.82 TSUNAMIS

Long period gravity waves generated by such disturbances as earthquakes, landslides, volcano eruptions and explosions near the sea surface are called tsunamis. The Japanese word *tsunami* has been adopted to replace the expression *tidal wave* to avoid confusion with the astronomical tides.

Most tsunamis are caused by earthquakes that extend at least partly under the sea, although not all submarine earthquakes produce tsunamis. Severe tsunamis are rare events.

Tsunamis may be compared to the wave generated by dropping a rock in a pond. Waves (ripples) move outward from the source region in every direction. In general, the tsunami wave amplitudes decrease but the number of individual waves increases with distance from the source region. Tsunami waves may be reflected, refracted, or diffracted by islands, seamounts, submarine ridges or shores. The longest waves travel across the deepest part of the sea as shallow-water waves, and may obtain speeds of several hundred knots. The travel time required for the first tsunami disturbance to arrive at any location can be determined within a few percent of the actual travel time by the use of suitable tsunami travel-time charts.
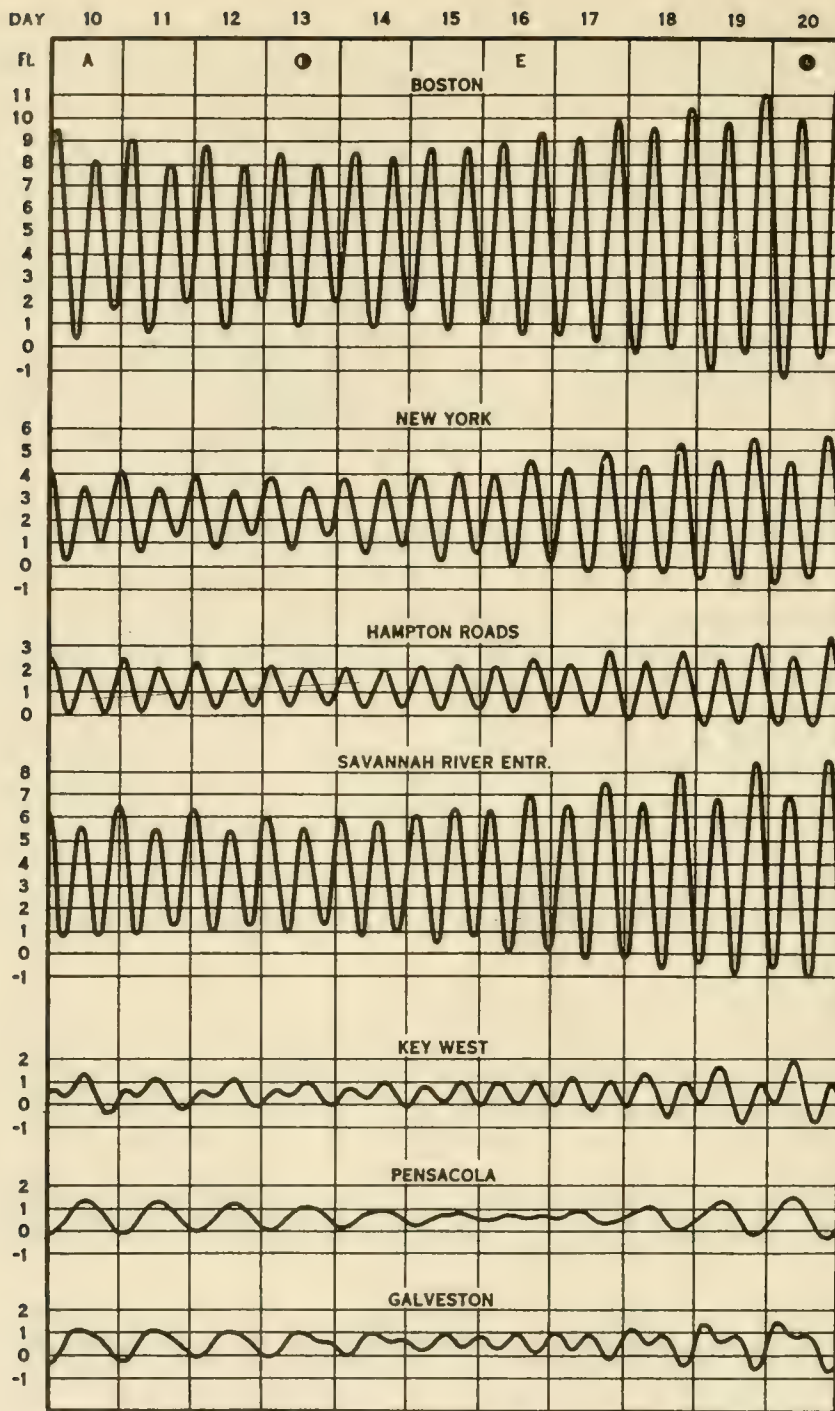
Lunar data: max. S. declination, 9th; apogee, 10th; last quarter, 13th; on equator, 16th; new moon, 20th; perigee, 22d; max. N. declination, 23d.

(from National Ocean Survey, NOAA, Tide Tables)

Figure 3-36. Typical Tide Curves Along Atlantic and Gulf Coasts

3- 72

Lunar data: max. S. declination, 9th; apogee, 10th; last quarter, 13th; on equator, 16th; new moon, 20th; perigee, 22d; max. N. declination, 23d.

(from National Ocean Survey, NOAA, Tide Tables)
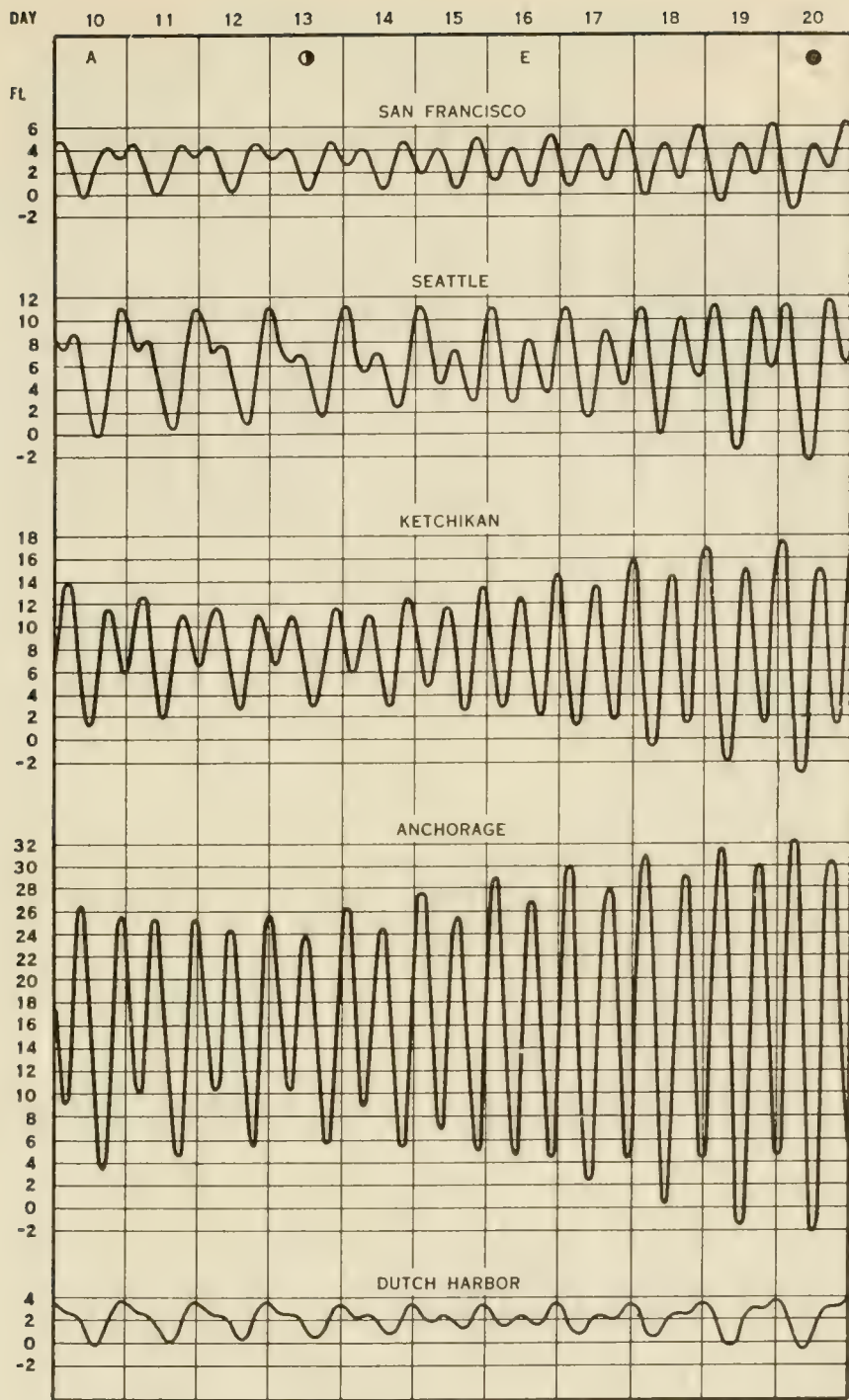
Figure 3-37.   Typical Tide Curves Along Pacific Coasts of the
United States

3-73

Table 3-5. Tidal Ranges

Station	Approximate Ranges (feet)		
	Mean	Diurnal	Spring
Atlantic Coast			
Calais, Maine	20		23
W. Quoddy Head, Maine	16		18
Englishman Bay, Maine	12		14
Belfast, Maine	10		11
Provincetown, Mass.	9		11
Chatham, Mass.	7		8
Cuttyhunk, Mass.	3		4
Saybrook, Conn.	4		4
Montauk Point, N.Y.	2		2
Sandy Hook, N.J.	5		6
Cape May, N.J.	4		5
Cape Henry, Va.	3		3
Charleston, S.C.	5		6
Savannah, Ga.	7		8
Mayport, Fla.	5		5
Gulf Coast			
Key West, Fla	1		2
Apalachicola, Fla.		1	
Atchafalaya Bay, La.	1	2	
Port Isabel, Tex.	1	1	
Pacific Coast			
Point Loma, Calif.	4	5	
Cape Mendocino, Calif.	4	6	
Siuslaw River, Ore.	5	7	
Columbia River, Wash.	6	8	
Port Townsend, Wash.	7	10	
Puget Sound, Wash.	11	15	

Tsunamis cross the sea as very long waves of low amplitude. A wavelength of 100 miles and an amplitude of 2 feet is not unreasonable. The wave may be greatly amplified by shoaling, diffraction, convergence, and resonance when it reaches land. Sea water has been carried higher than 35 feet above sea level in Hilo, Hawaii by tsunamis. Tide gage records of the tsunami of 23-26 May 1960 at these locations are shown in Figure 3-38. The tsunami appears as a quasi-periodic oscillation, superimposed on the normal tide. The characteristic period of the disturbance, as well as the amplitude, is different at each of the three locations. It is generally assumed that the recorded disturbance results from forced oscillations of hydraulic basin systems, and that the periods of greatest response are determined by basin geometry.
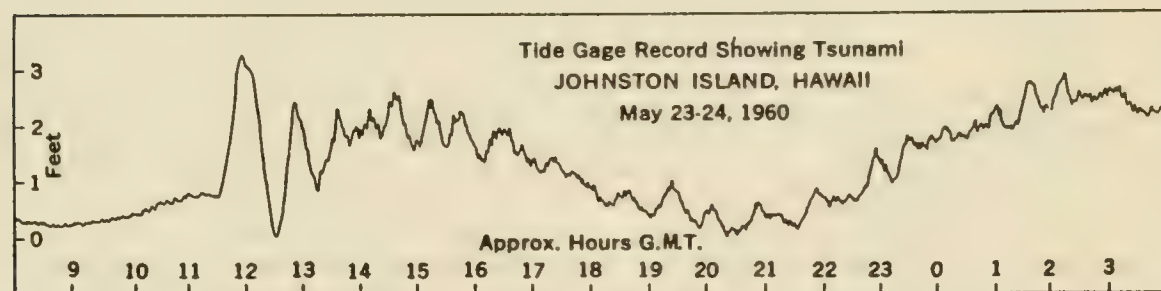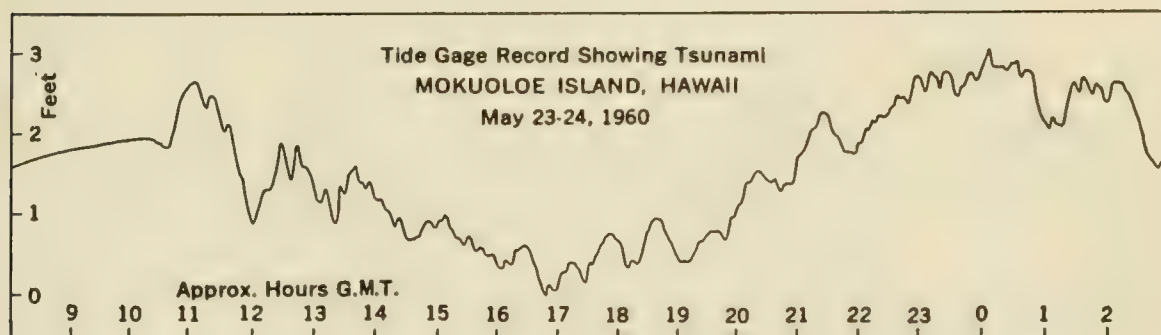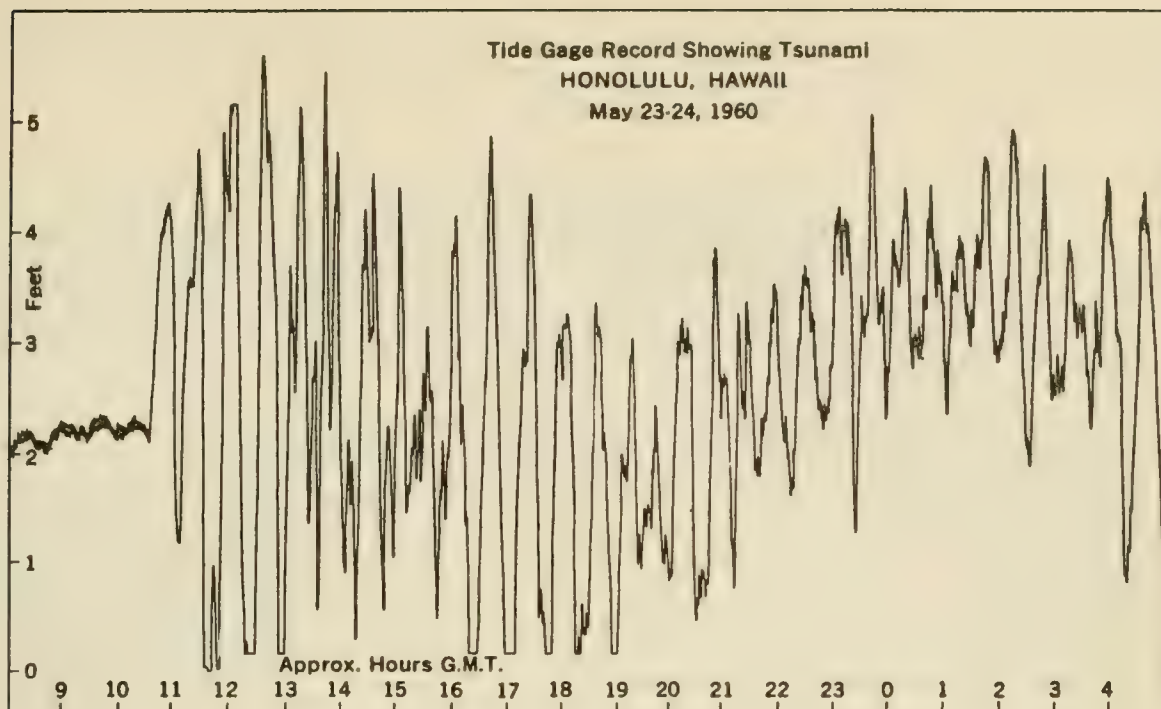
Figure 3-38. Sample Tsunami Records from Tide Gages

Theoretical and applied research dealing with tsunami problems has been greatly intensified since 1960. Preisendorfer (1971) lists more than 60 significant theoretical papers published since 1960. The list does not include observational papers concerned with the warning system.

3.83 LAKE LEVELS

Lakes have insignificant tidal variations, but are subject to seasonal and annual hydrologic changes in water level and to water level changes caused by wind setup, barometric pressure variations, and seiches. Additionally some lakes are subject to occasional water level changes by regulatory control works.

Water surface elevations of the Great Lakes vary irregularly from year to year. During each year, the water surfaces consistently fall to their lowest stages during the winter and rise to their highest stages during the summer. Nearly all precipitation in the watershed areas during the winter is snow or rainfall transformed to ice. When the temperature begins to rise there is substantial runoff - thus the higher stages in the summer. Typical seasonal and yearly changes in water levels for Lake Erie are shown in Figure 3-39. The maximum and minimum monthly mean stages for the lakes are summarized in Table 3-6.

Table 3-6. Fluctuations in Water Levels — Great Lakes System (1860 through 1973).

Lake	Datum* Factor	Low† Water Chart Datum	Surface Elevation	Alltime Monthly Means				
				High (feet)	Date	Low (feet)	Date	Difference
Superior	1.71	600.0	600.37	602.06	8/1876	598.23	4/1926	3.83
Michigan-Huron	1.74	576.8	578.68	581.94	6/1886	575.35	3/1964	6.59
St. Clair‡	1.82	571.7	573.01	576.22	6/1973	569.86	1/1936	6.36
Erie	1.94	568.6	570.38	573.52	6/1973	567.49	2/1936	6.03
Ontario	1.23	242.8	244.77	248.06	6/1952	241.45	11/1934	6.61

Elevations are in feet above mean water level at Father Point, Quebec.
International Great Lakes Datum (IGLD) (1955).

* To convert to U.S. Lake Survey 1935 Datum, add datum factor to IGLD (USLS 1935 = IGLD + datum factor).

† Low water datum is the zero plane on Lake Survey Charts to which charts are referred. Thus the zero (low water) datum on a USLS Lake Superior chart is 600 feet above mean waterlevel at Father Point, Quebec.

‡ Lake St. Clair elevations are available only for 1898 to date.

In addition to seasonal and annual fluctuations, the Great Lakes are subject to occasional seiches of irregular amount and duration. These sometimes result from a resonant coupling which arises when the propagation speed of an atmospheric disturbance is nearly equal to the speed of free waves on a lake. (Ewing, Press and Donn, 1954), (Harris, 1957), Platzman, 1958, 1965.) The lakes, also and sometimes simultaneously, are affected by wind stresses which raise the water level at one end and lower it at the other. These mechanisms may produce changes in water elevation ranging from a few inches to more than 6 feet. Lake Erie, shallowest of

Figure 3-39. Typical Water Level Variations in Lake Erie

the Great Lakes, is subject to greater wind-induced surface fluctuations, that is, wind setup, than any other Lake. Wind setup is discussed in Section 3.86, Storm Surge and Wind Setup.

In general, the maximum amount of these irregular changes in lake level must be determined for each location under consideration. Table 3-7 shows short-period observed maximum and minimum water level elevations at selected gage sites. More detailed data on seasonal lake levels and wind setup may be obtained for specific locations from the Lake Survey Center, National Oceanic and Atmospheric Administration, U.S. Department of Commerce.

Table 3-7. Short-Period Fluctuations in Lake Levels at Selected Gage Sites

Lake and Gage Location	Period of Gage Record	Maximum Recorded	
		Rise in Feet (MSE)*	Fall in Feet (MSE)*
SUPERIOR at Marquette	1903-1971	3.7	2.9
MICHIGAN at Calument Harbor (Chicago)	1903-1971	4.5	5.2
HURON at Harbor Beach	1902-1971	3.3	4.5
ERIE at Buffalo	1900-1971	8.7	6.2
ERIE at Toledo	1940-1971	5.3	8.9
ONTARIO at Oswego	1933-1971	4.2	3.8

*The mean surface elevation (MSE) refers to the water level that represents the average water elevation for the period of record. It corresponds to the mean surface elevation given in Table 3-6.

3.84 SEICHES

Seiches are standing waves (Fig. 3-40) of relatively long periods that occur in lakes, canals, bays and along open seacoasts. Lake seiches are usually the result of a sudden change, or a series of intermittent-periodic changes, in atmospheric pressure or wind velocity. Standing waves in canals can be initiated by suddenly adding or subtracting large quantities of water. Seiches in bays can be generated by local changes in atmospheric pressure and wind and by oscillations transmitted through the mouth of the bay from the open sea. Open-sea seiches can be caused by changes in atmospheric pressure and wind, or tsunamis. Standing waves of large amplitude are likely to be generated if the causative force which sets the water basin in motion is periodic in character, especially if the period of this force is the same as, or is in resonance with, the natural or free oscillating period of the basin. (See Section 2.5, Wave Reflection.)

3-78

Free oscillations have periods that are dependent upon the horizontal and vertical dimensions of the basin, the number of nodes of the standing wave, that is, lines where deviation of the free surface from its undisturbed value is zero, and friction. The period of a true forced-wave oscillation is the same as the period of the causative force. Forced oscillations, however, are usually generated by intermittent external forces, and the period of the oscillation is determined partly by the period of the external force and partly by the dimensions of the water basin and the mode of oscillation. Oscillations of this type have been called forced seiches (Chrystal, 1905) to distinguish them from free seiches in which the oscillations are free.
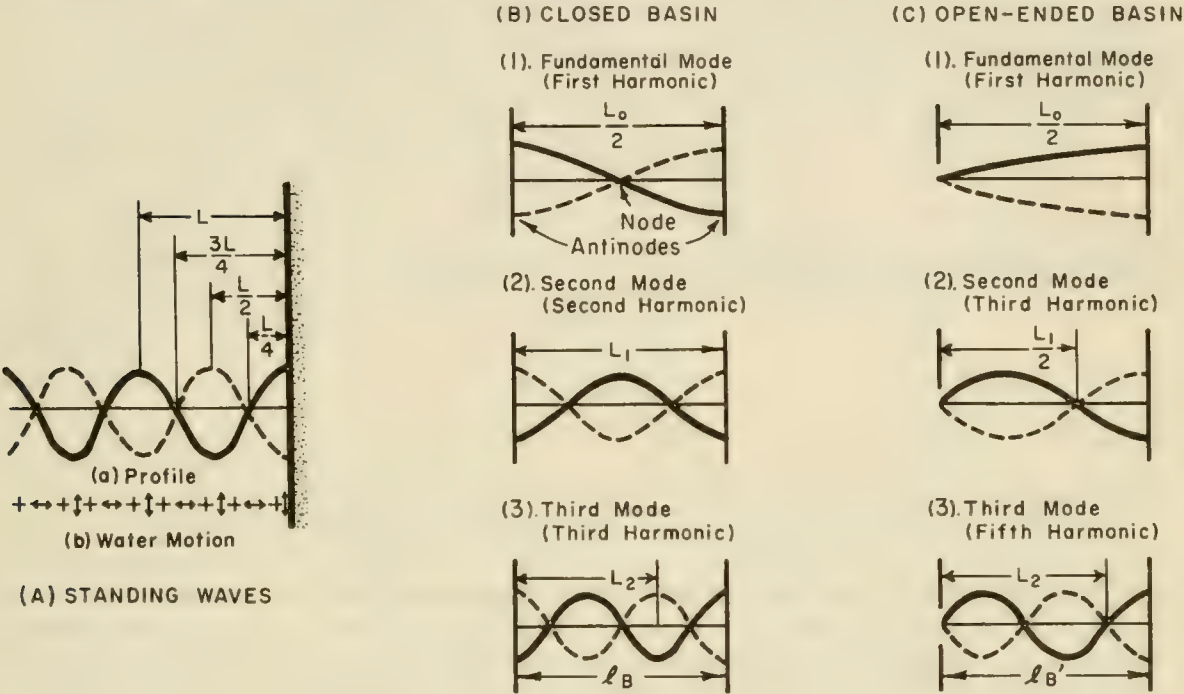
Surface profiles for oscillating waves

(after Carr, 1953)

Figure 3-40. Long-Wave Surface Profiles

For the simplest form of a standing one-dimensional wave in a closed rectangular basin with vertical sides and uniform depth (Fig. 3-40(B)), wave antinodes, that is, lines where deviation of the free surface from its undisturbed value is a relative maxima or minima, are situated at the ends (longitudinal seiche) or sides (transverse seiche). The number of nodes and antinodes in a basin depends on which mode or modes of oscillation are present. If n = number of nodes along a given basin axis, d = basin depth, and ℓ_B = basin length along that axis, then T_n, the natural free oscillating period is given by

$$T_n = \frac{2\ell_B}{n\sqrt{gd}} \, .$$

(3-42)

3-79

The fundamental and maximum period (T_n for n = 1) becomes

$$T_1 = \frac{2\ell_B}{\sqrt{gd}} .$$ (3-43)

Equation 3-43 is called Merian's formula. (Sverdrup, Johnson and Fleming, 1942.)

In an open rectangular basin of length $\ell_{B'}$ and constant depth d, the simplest form of a one-dimensional, non-resonant, standing longitudinal wave is one with a node at the opening, antinode at the opposite end, and n' nodes in between. (See Figure 3-40(C).) The free oscillation period $T'_{n'}$ in this case is

$$T'_{n'} = \frac{4\ell_{B'}}{(1 + 2n')\sqrt{gd}} .$$ (3-44)

For the fundamental mode (n' = 0), T'_n becomes

$$T'_0 = \frac{4\ell_{B'}}{\sqrt{gd}} .$$ (3-45)

The basin's total length is occupied by one-fourth of a wave length.

This simplified theory must be modified for most actual basins, because of the variation in width and depth along the basin axes.

Defant (1961) outlines a method to determine the possible periods for one-dimensional free oscillations in long narrow lakes of variable width and depth. Defant's method is useful in engineering work because it permits computation of periods of oscillation, relative magnitudes of the vertical displacements along chosen axes, and the positions of nodal and antinodal lines. This method, applicable only to free oscillations, can be used to determine the nodes of oscillation of multinodal and uninodal seiches. The theory for a particular forced oscillation was also derived by Defant and is discussed by Sverdrup et al (1942). Hunt (1959) discusses some complexities involved in the hydraulic problems of Lake Erie, and offers an interim solution to the problem of vertical displacement of water at the eastern end of the lake. More recently, work has been done by Simpson and Anderson (1964), Platzman and Rao (1963), and Mortimer (1965). Rockwell (1966) computed the first five modes of oscillation for each of the Great Lakes by a procedure based on the work of Platzman and Rao (1965). Platzman (1972) has developed a method for evaluating natural periods for basins of general two-dimensional configuration.

3.85 WAVE SETUP

Field observations indicate that part of the variation in mean water level near shore is a function of the incoming wave field. However these

observations are insufficient to provide quantitative trends. (Savage, 1957; Fairchild, 1958; Dorrestein, 1962; Galvin and Eagleson, 1965.) A laboratory study by Saville (1961) indicated that for waves breaking on a slope there would be a decrease in the mean water level relative to the stillwater level just prior to breaking, with a maximum depression or set-down at about the breaking point. This study also indicated that from the breaking point the mean water surface slopes upward to the point of inter-section with the shore and has been termed wave setup. *Wave setup is defined as that super-elevation of the mean water level caused by wave action alone.* This phenomenon is related to a conversion of kinetic energy of wave motion to a quasi-steady potential energy.

Theoretical studies of wave setup have been made by Dorrestein (1962), Fortak (1962), Longuet-Higgins and Stewart (1960, 1962, 1963, 1964), Bowen, Inman, and Simmons (1968), and Hwang and Divoky (1970). Theoretical devel-opments can account for many of the principal processes, but contain factors that are often difficult to specify in practical problems.

R.O. Reid (personal communication) has suggested the following approach for estimating the wave setup at shore, using Longuet-Higgins and Stewart (1963) theory for the setdown at the breaking zone and solitary wave theory. The theory for setdown at the breaking zone indicates that

$$S_b = -\frac{g^{1/2} H_o^2 T}{64 \pi d_b^{3/2}} \qquad (3\text{-}46)$$

in which S_b is the setdown at the breaking zone, T is the wave period, H_o is the deepwater significant wave height, d_b is the depth of water at the breaker point and g is gravity. The laboratory data of Saville (1961) gives somewhat larger values than those obtained by use of Equation 3-46.

By using relations derived from solitary wave theory relating d_b to the breaker height of the significant wave, H_b, and d_b/H_o to H_o/L_o, the above relation can be converted to

$$S_b = -\frac{0.536 H_b^{3/2}}{g^{1/2} T} . \qquad (3\text{-}47)$$

Longuet-Higgins and Stewart (1963) show from an analysis of Saville's data that the wave setup ΔS between the breaker zone and shore is given approximately by $\Delta S = 0.15 d_b$. Assuming that $d_b = 1.28 H_b$, this becomes $\Delta S = 0.19 H_b$.

The net wave setup at the shore is

$$S_W = \Delta S + S_b , \qquad (3\text{-}48)$$

or

$$S_W = 0.19 \left[1 - 2.82 \left(\frac{H_b}{gT^2} \right)^{\frac{1}{2}} \right] H_b . \qquad (3\text{-}49)$$

3-81

Equation 3-49 provides a conservative estimate for wave setup at the shore. The difference between laboratory data and theory, however, is not likely to exceed the uncertainties of field data.

* * * * * * * * * * * * * *   EXAMPLE PROBLEM   * * * * * * * * * * * * * *

GIVEN: H_b = 20 feet, T = 12 seconds.

FIND: Wave setup, S_W.

SOLUTION: Using Equation 3-49,

$$S_W = 0.19 \left[1 - 2.82 \left(\frac{H_b}{gT^2} \right)^{\frac{1}{2}} \right] H_b ,$$

$$S_W = 0.19 \left[1 - 2.82 \left(\frac{20}{32.2 \, (12)^2} \right)^{\frac{1}{2}} \right] 20 ,$$

$$S_W = 3.1 \text{ feet . Say 3 feet .}$$

Equation 3-49 is only applicable to normal beach slopes.

* *

3.86 STORM SURGE AND WIND SETUP

3.861 General. Reliable estimates of water-level changes under storm conditions are essential for the planning and design of coastal engineering works. Determination of design water elevations during storms is a complex problem involving interaction between wind and water, differences in atmospheric pressure, and effects caused by other mechanisms unrelated to the storm. Winds are responsible for the largest changes in water level when considering only the storm-surge generating processes. A wind blowing over a body of water exerts a horizontal force on the water surface and induces a surface current in the general direction of the wind. The force of wind on the water is partly due to inequalities of air pressures on the windward side of gravity waves, and partly due to shearing stresses at the water surface. Horizontal currents induced by the wind are impeded in shallow water areas, thus causing the water level to rise downwind while at the windward side the water level falls. The term *storm surge* is used to indicate departure from normal water level due to the action of storms. The term *wind setup* is often used to indicate rises in lakes, reservoirs and smaller bodies of water. A fall of water level below the normal level at the upwind side of a basin is generally referred to as *setdown*.

Severe storms may produce surges in excess of 25 feet on the open coast and even higher in bays and estuaries. Generally, setups in lakes and reservoirs are less, and setdown in these enclosed basins is about equivalent to the setup. Setdown in open oceans is insignificant because the volume of water required to produce the setup along the shallow regions of the coast is small compared to the volume of water in the ocean. However, setdown may be appreciable when a storm traverses a relatively narrow

3-82

landmass such as southern Florida and moves offshore. High offshore winds in this case can cause the water level to drop several feet.

Setdown in semienclosed basins (bays and estuaries) also may be substantial, but the fall in water level is influenced by the coupling to the sea. There are some detrimental effects as a result of setdown, such as making water-pumping facilities inoperable due to exposure of the intake, increasing the pumping heads of such facilities, and causing navigational hazards because of decreased depths.

However, rises in water levels (setup rather than setdown) are of most concern. Abnormal rises in water level in nearshore regions will not only flood low-lying terrain, but provide a base on which high waves can attack the upper part of a beach and penetrate farther inland. Flooding of this type combined with the action of surface waves can cause severe damage to low-lying land and backshore improvements.

Wind-induced surge, accompanied by wave action, accounts for most of the damage to coastal engineering works and beach areas. Displacement of stone armor units of jetties, groins and breakwaters, scouring around structures, accretion and erosion of beach materials, cutting of new inlets through barrier beaches, and shoaling of navigational channels can often be attributed to storm surge and surface waves. Moreover, surge can increase hazards to navigation, impede vessel traffic, and hamper harbor operations. A knowledge of the increase and decrease in water levels that can be expected during the life of a coastal structure or project is necessary to design structures that will remain functional.

3.862 _Storms_. A storm is an atmospheric disturbance characterized by high winds which may or may not be accompanied by precipitation. Two distinctions are made in classifying storms: a storm originating in the tropics is called a _tropical storm_; a storm resulting from a cold and warm front is called an _extratropical storm_. Both of these storms can produce abnormal rises in water level in shallow water near the edge of water bodies. The highest water levels produced along the entire gulf coast and from Cape Cod to the south tip of Florida on the east coast generally result from tropical storms. High water levels are rarely caused by tropical storms on the lower coast of California. Extreme water levels in some enclosed bodies, such as Lake Okeechobee, Florida can also be caused by a tropical storm. Highest water levels at other coastal locations and most enclosed bodies of water result from extratropical storms.

A severe tropical storm is called a _hurricane_ when the maximum sustained wind speeds reach 75 miles per hour (65 knots). Hurricane winds may reach sustained speeds of more than 150 miles per hour (130 knots). Hurricanes, unlike less severe tropical storms, generally are well organized and have a circular wind pattern with winds revolving around a center or _eye_ (not necessarily the geometric center). The eye is an area of low atmospheric pressure and light winds. Atmospheric pressure and wind speed increase rapidly with distance outward from the eye to a zone of maximum wind speed which may be anywhere from 4 to 60

nautical miles from the center. From the zone of maximum wind to the periphery of the hurricane, the pressure continues to increase; however, the wind speed decreases. The atmospheric pressure within the eye is the best single index for estimating the surge potential of a hurricane. This pressure is referred to as the *central pressure index* (CPI). Generally for hurricanes of fixed size, the lower the CPI, the higher the wind speeds. Hurricanes may also be characterized by other important elements, such as the radius of maximum winds (R) which is an index of the size of the storm, and the speed of forward motion of the storm system (V_F). A discussion of the formation, development and general characteristics of hurricanes is given by Dunn and Miller (1964).

Extratropical storms that occur along the northern part of the east coast of the United States accompanied by strong winds blowing from the northeast quadrant are called *northeasters*. Nearly all destructive northeasters have occurred in the period from November to April; the hurricane season is from about June to November. A typical northeaster consists of a single center of low pressure and the winds revolve about this center, but wind patterns are less symmetrical than those associated with hurricanes.

3.863 <u>Factors of Storm Surge Generation</u>. The extent to which water levels will depart from normal during a storm depends on several factors. The factors are related to the:

    (a)   characteristics and behavior of the storm;
    (b)   hydrography of the basin;
    (c)   initial state of the system; and
    (d)   other effects that can be considered external to the system.

Several distinct factors that may be responsible for changing water levels during the passage of a storm may be identified as:

    (a)   astronomical tides
    (b)   direct winds
    (c)   atmospheric pressure differences
    (d)   earth's rotation
    (e)   rainfall
    (f)   surface waves and associated wave setup
    (g)   storm motion effects.

The elevation of setup or setdown in a basin depends on storm intensity, path or track, overwater duration, atmospheric pressure variation, speed of translation, storm size, and associated rainfall. Basin characteristics that influence water-level changes are basin size and shape, and bottom configuration and roughness. The size of the storm relative to the size of the basin is also important. The magnitude of storm surges is shown in Figures 3-41 and 3-42. Figure 3-41 shows the difference between observed water levels and predicted astronomical tide levels during Hurricane Carla (1961) at several Texas and Louisiana coast tide stations. Figure 3-42 shows high water marks obtained from a storm survey made after Hurricane Carla. Harris (1963b) gives similar data from other hurricanes.

<div align="center">3-84</div>

3.864 Initial Water Level. Water surfaces on the open coast or in en-
closed or semienclosed basins are not always at their normal level prior
to the arrival of a storm. This departure of the water surface from its
normal position in the absence of astronomical tides, referred to as an
initial water level, is a contributing factor to the water level reached
during the passage of a storm system. This level may be 2 feet above
normal for some locations along the U.S. Gulf coast. Some writers refer
to this difference in water level as a *forerunner* in advance of the storm
due to initial circulation and water transport by waves particularly when
the water level is above normal. Harris (1963b) on the other hand, indi-
cates that this general rise may be due to short-period anomalies in the
mean sea level not related to hurricanes. Whatever the cause, the initial
water level should be considered when evaluating the components of open-
coast storm surge. The existence of an initial water level preceeding the
approach of Hurricane Carla is shown in Figure 3-41 and in a study of the
synoptic weather charts for this storm. (Harris, 1963b.) At 0700 hours
(Eastern Standard Time) 9 September 1961, the winds at Galveston, Texas
were about 10 mph, but the open coast tide station (Pleasure Pier) shows
the difference between the observed water level and astronomical tide to
be above 2 feet. Rises of this nature on the open coast can also affect
levels in bays and estuaries.

     There are other causes for departures of the water levels from normal
in semienclosed and enclosed basins, such as the effects of evaporation
and rainfall. Generally, rainfall plays a more dominant role since these
basins are affected by direct rainfall and can be greatly affected by
rainfall runoff from rivers. The initial rise caused by rainfall is due
to rains preceding the storm; rains during the passage of a storm have a
time-dependent effect on the change in water level.

3.865 Storm Surge Prediction. The design of coastal engineering works is
usually based on a life expectancy for the project and on the degree of
protection the project is expected to provide. This design requires that
the *design storm* have a specified frequency of occurrence for the partic-
ular area. An estimate of the frequency of occurrence of a particular
storm surge is required. One method of making this estimate is to use
frequency curves developed from statistical analyses of historical water
level data. Table 3-8, based on National Ocean Survey tide gage records,
indicates observed extreme storm surge water levels including wave setup
The water levels are those actually recorded at the various tide stations,
and do not necessarily reflect the extreme water levels that may have
occurred near the gages. Values in this table may differ from gage-station
values because of corrections for seasonal and secular anaomalies. The
frequency of occurrence for the highest and lowest water levels may be
estimated by noting the length of time over which observations were made.
The average yearly highest water level is an average of the highest water
level from each year during the period of observation. Extreme water
levels are rarely recorded by water level gages, partly because the gages
tend to become inoperative with extremely high waves, and partly because
the peak storm surge often occurs between tide gage stations. Post-storm
surveys showed water levels, as the result of Hurricane Camille, August
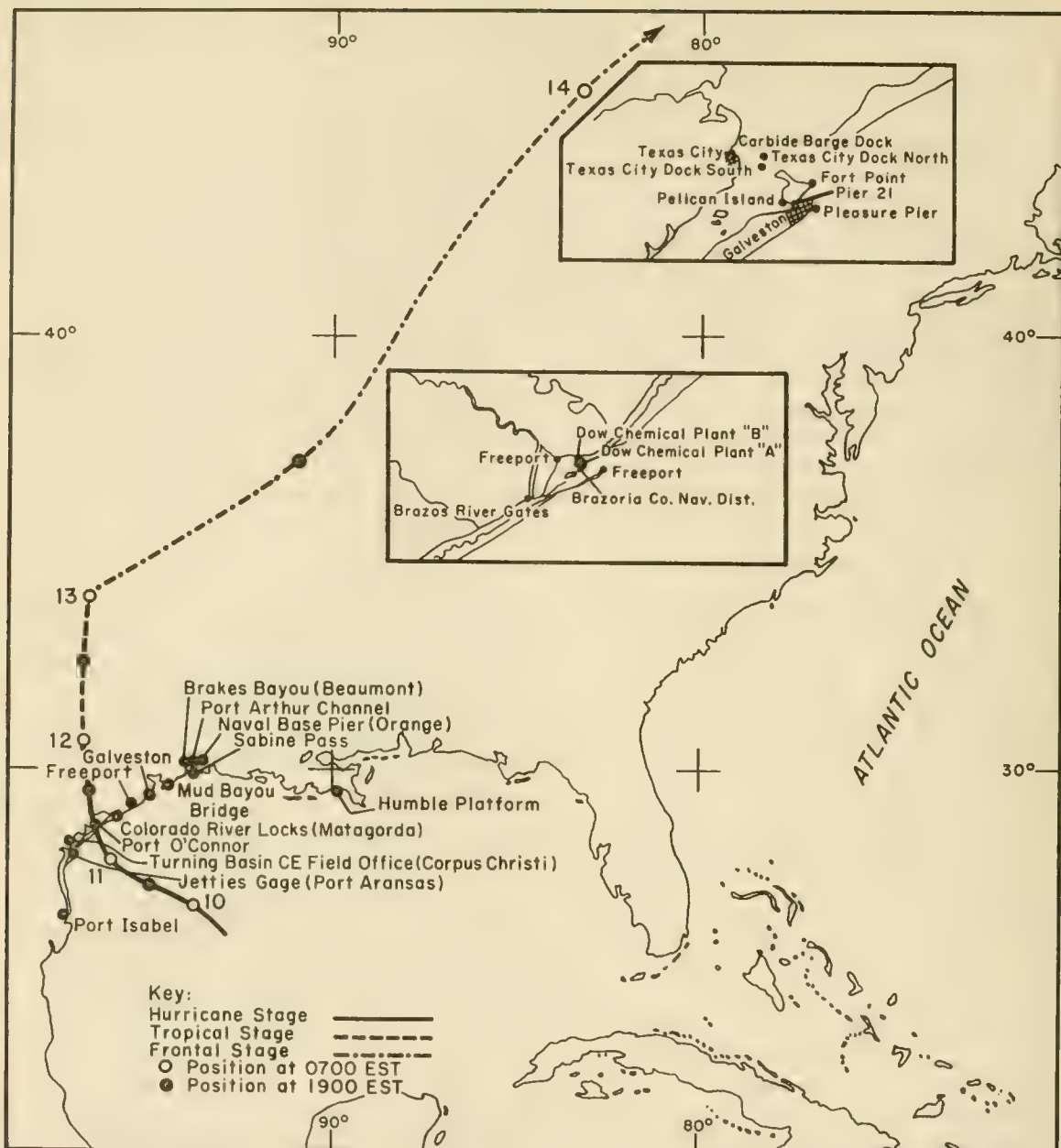
(from Harris, 1963 b)

Figure 3-41.   Storm Surge and Observed Tide Chart.   Hurricane Carla,
7-12 September 1961.   Insert Maps for Freeport and
Galveston, Texas, Areas
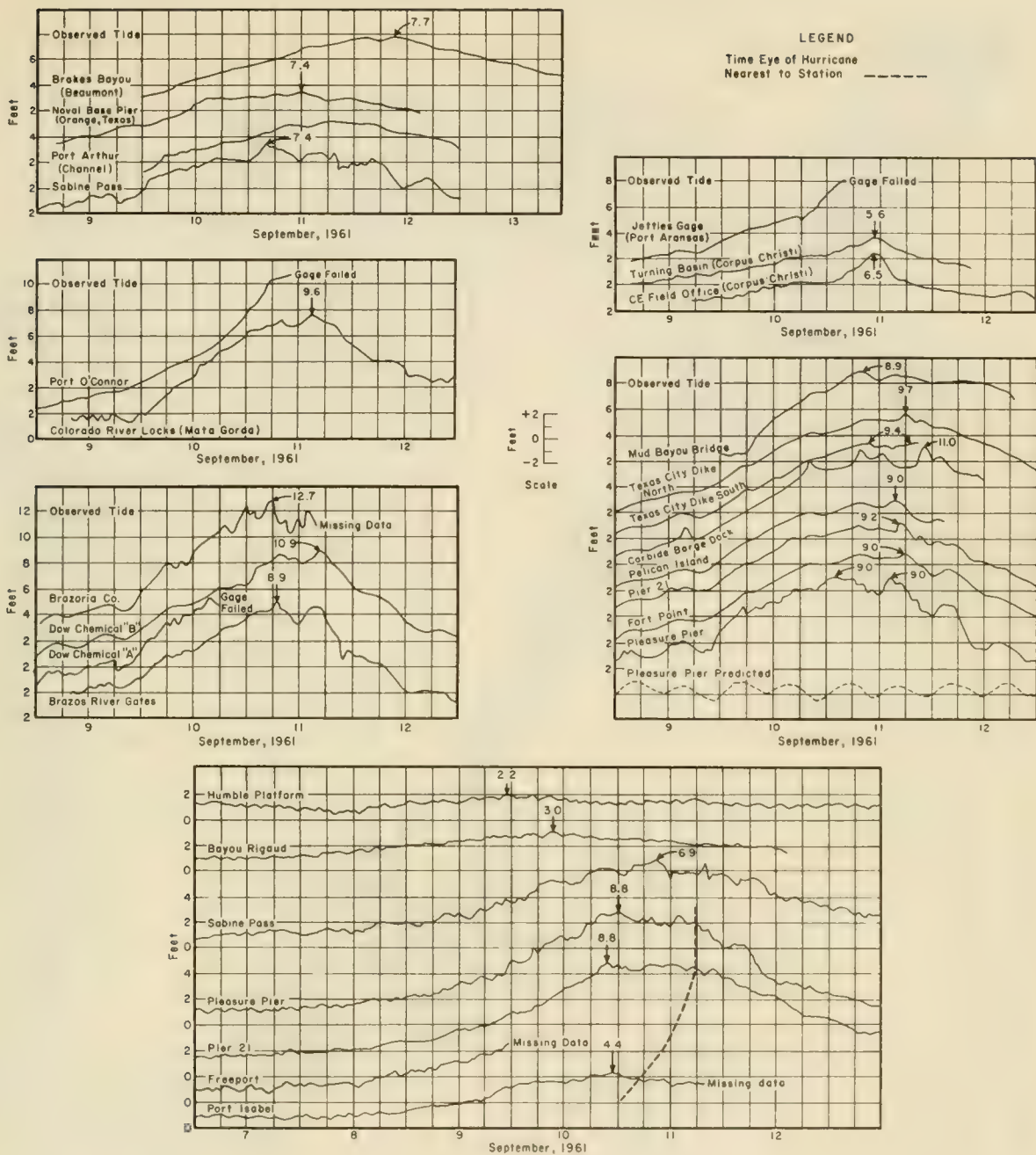
Figure 3-41. Storm Surge and Observed Tide Chart. Hurricane Carla,
7-12 September 1961. Insert Maps for Freeport and
Galveston, Texas, Areas -- Continued

(from Harris,1963b)
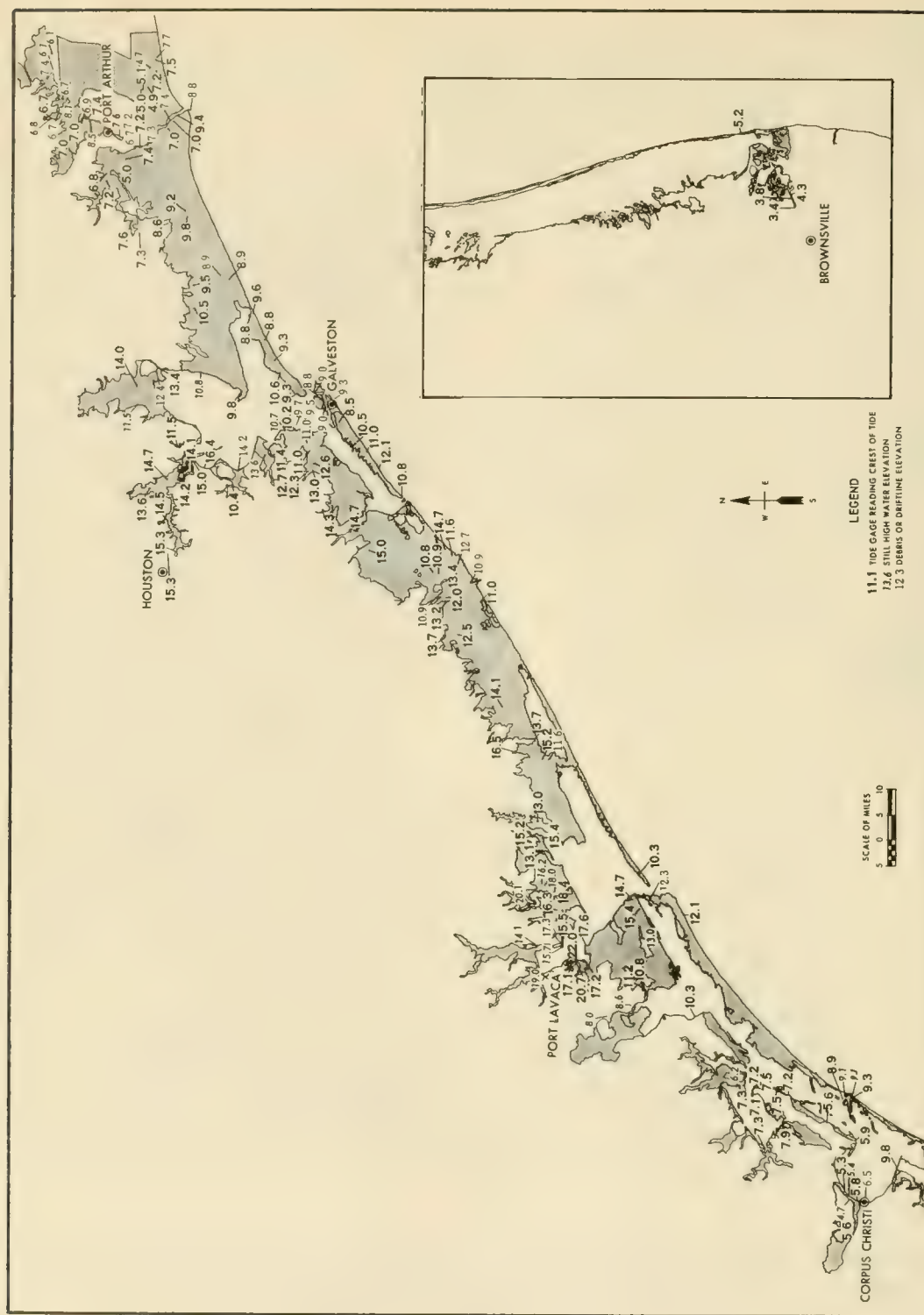
Figure 3-42. High Water Mark Chart for Texas, Hurricane Carla, 7-12 September 1961. Shaded area indicates the extent of flooding.

Table 3-8. Highest and Lowest Water Levels

Location	Observation Period	Mean Range (feet)	Highest Water Levels Above Mean High Water (feet)			Lowest Water Levels Below Low Water (feet)		
			Average Yearly Highest	Extreme High	Date of Record	Average Yearly Lowest	Extreme Low	Date of Record
ATLANTIC COAST								
Eastport, Maine	1930-69	18.2	3.9	4.9	21 Dec 68	3.9	4.4	7 Jan 43 23 May 59 30 Dec 63
Portland, Maine	1912-69	9.0	2.8	4.0	30 Nov 44 20 Nov 45	2.8	3.7	30 Nov 55
Bar Harbor, Maine	1947-70	10.5	3.1	4.3	29 Dec 59	2.8	3.6	30 Dec 53
Portsmouth, N.H.	1927-70	8.1	2.8	3.7	30 Nov 44 29 Dec 59	2.7	3.4	30 Nov 55
Boston, Mass.	1922-70	9.5	3.0	4.4	29 Dec 59	3.1	3.8	25 Jan 28 24 Mar 40
Woods Hole, Mass.	1933-70	1.8	2.9	9.2	21 Sep 38	2.0	2.7	8 Jan 68
Providence, R.I.	1938-47 1957-70	4.6	3.7	13.1	21 Sep 38	2.5	3.4	5 Jan 59
Newport, R.I.	1931-70	3.5	2.7	10.0	21 Sep 38	2.1	2.9	25 Jan 36
New London, Conn.	1938-70	2.6	3.2	8.1	21 Sep 38	2.3	3.4	11 Dec 43
Willets Point, N.Y.	1932-70	7.1	3.8	9.6	21 Sep 38	3.2	4.1	24 Mar 40
Battery, N.Y.	1920-70	4.5	2.9	5.7	12 Sep 60	3.0	4.0	8 Mar 32 5 Jan 59
Montauk, N.Y.	1948-70	2.1	3.2	6.6	31 Aug 54	1.9	2.6	8 Feb 51
Sandy Hook, N.J.	1933-70	4.6	3.1	5.7	12 Sep 60	2.9	4.1	31 Dec 62
Atlantic City, N.J.	1912-20 1923-70	4.1	2.8	5.2	14 Sep 44	2.7	3.7	8 Mar 32
Philadelphia, Pa.	1900-20 1922-70	5.9	2.2	4.7	25 Nov 50	3.1	6.7	31 Dec 62
Lewes, Del. Breakwater Harbor	1936-70	4.1	3.0	5.4	6 Mar 62	2.5	3.0	28 Mar 55
Baltimore, Md.	1902-70	1.1	2.3	6.7	23 Aug 33	3.4	5.0	24 Jan 08
Annapolis, Md.	1929-70	0.9	2.2	5.4	23 Aug 33	2.8	3.8	31 Dec 62
Solomons Island, Md.	1938-70	1.2	2.0	3.4	13 Aug 55	2.1	3.4	31 Dec 62
Washington, D.C.	1931-70	2.9	2.8	8.4	17 Oct 42	2.9	3.9	31 Dec 62
Portsmouth, Va.	1935-70	2.8	3.0	5.7	18 Sep 36	2.0	2.4	25 Jan 36 4 Dec 42 8 Feb 59

Table 3-8. Highest and Lowest Water Levels — Continued

Location	Observation Period	Mean Range (feet)	Highest Water Levels Above Mean High Water (feet)			Lowest Water Levels Below Low Water (feet)		
			Average Yearly Highest	Extreme High	Date of Record	Average Yearly Lowest	Extreme Low	Date of Record
ATLANTIC COAST								
Norfolk, Va.								
Sewells Point	1928-70	2.5	2.8	6.0	23 Aug 33	2.1	3.0	23 Jan 28 26 Jan 28
Morehead City, N.C.	1953-57	2.8	——	4.2	15 Oct 54 19 Sep 55	——	1.7	11 Dec 54
Wilmington, N.C.	1935-70	3.6	1.7	4.3	15 Oct 54	1.4	2.0	3 Feb 40
Southport, N.C.	1933-53	4.1	2.4	3.4	2 Nov 47	1.2	1.9	28 Jan 34
Charleston, S.C.	1922-70	5.2	2.2	5.2	11 Aug 40	2.4	3.6	30 Nov 63
Fort Pulaski, Ga.	1936-70	6.9	2.5	4.2	15 Oct 47	2.9	4.4	20 Mar 36
Fernandina, Fla.	1897-1924 1939-1970	6.0	2.5	7.7	2 Oct 1898	2.5	3.9	24 Jan 1940
Mayport, Fla.	1928-70	4.5	1.9	3.0	9 Sep 64	2.0	3.2	24 Jan 40
Miami Beach, Fla.	1931-51 1955-70	2.5	1.6	3.9	8 Sep 65	1.3	1.6	24 Mar 36
GULF COAST								
Key West, Fla.	1926-70	1.3	1.3	2.5	8 Sep 65	1.2	1.6	19 Feb 28
St. Petersburg, Fla.	1947-70	2.3*	1.6	3.0	5 Sep 50	1.7	2.1	3 Jan 58
Cedar Key, Fla.	1914-25 1939-70	2.6	2.2	3.2	15 Feb 53 11 Sep 64	2.8	3.5	27 Aug 49 21 Oct 52 4 Feb 63
Pensacola, Fla.	1923-70	1.3*	1.6	7.6	20 Sep 26	1.4	2.2	6 Jan 24
Grand Isle, La.								
Humble Platform	1949-70	1.4*	1.5	2.2	25 Sep 53 22 Sep 56	1.4	1.7	22 Nov 49 3 Feb 51
Bayou Rigaud	1947-70	1.0*	1.9	3.9	24 Sep 56	1.1	1.5	3 Feb 51 13 Jan 64
Eugene Island, La.	1939-70	1.9*	2.5	6.0	27 Jun 57	1.6	2.4	25 Jan 40
Galveston, Tex.	1908-70	1.4*	2.2	10.1	16,17 Aug 15	2.6	5.3	11 Jan 08
Port Isabel, Tex.	1944-70	1.3*	1.5	3.8	11 Sep 61	1.4	1.7	31 Dec 56 7 Jan 62

* Diurnal Range

Table 3-8. Highest and Lowest Water Levels — Continued

Location	Observation Period	Diurnal Range (feet)	Highest Water Levels Above Mean High Water (feet)			Lowest Water Levels Below Low Water (feet)		
			Average Yearly Highest	Extreme High	Date of Record	Average Yearly Lowest	Extreme Low	Date of Record
PACIFIC COAST†								
San Diego, Calif.	1906-70	5.7	1.8	2.6	20 Dec 68 29 Dec 59	2.0	2.8	17 Dec 33 17 Dec 37
La Jolla, Calif.	1925-53 1956-70	5.2	1.8	2.4	20 Dec 68	1.9	2.6	17 Dec 33
Los Angeles, Calif.	1924-70	5.4	1.8	2.3	19,20 Dec 68	1.8	2.6	26 Dec 32 17 Dec 33
Santa Monica, Calif.	1933-70	5.4	1.8	2.1	27 Dec 36 17,18 Jul 51	1.8	2.7	17 Dec 33
San Francisco, Calif.	1898-1970	5.7	1.5	2.3	24 Dec 40 19 Jan 69 9 Jan 70	2.1	2.7	26 Dec 32 17 Dec 33
Crescent City, Calif.	1933-46 1950-70	6.9	2.4	3.1	4 Feb 58	2.4	2.9	22 May 55
Astoria, Oreg.	1925-70	8.3	2.6	3.8	17 Dec 33	1.9	2.8	16 Jan 30
Neah Bay, Wash.	1935-70	8.2	2.9	4.1	30 Nov 51	3.1	3.8	29 Nov 36
Seattle, Wash.	1899-1970	11.3	2.2	3.3	6 Feb 04 5 Dec 67	3.9	4.7	4 Jan 16 20 Jun 51
Friday Harbor, Wash.	1934-70	7.7	2.3	3.2	30 Dec 52	3.2	4.0	7 Jan 47
Ketchikan, Alaska	1919-70	15.3	4.4	5.9	2 Dec 67	4.5	5.2	8 Dec 19 16 Jan 57 30 Dec 59
Juneau, Alaska	1936-41 1944-70	16.4	5.0	6.3	2 Nov 48	4.5	5.7	16 Jan 57
Skagway, Alaska	1945-62	16.7	4.9	6.7	22 Oct 45	5.0	6.0	16 Jan 57
Sitka, Alaska	1938-70	9.9	3.4	4.7	2 Nov 48	3.2	3.8	19 Jun 51 16 Jan 57
Yakutat, Alaska	1940-70	10.1	3.7	4.8	2 Nov 48	3.1	3.9	29 Dec 51 16 Jan 57
Seward, Alaska	1925-38	10.6	3.4	4.1	13 Oct 27	3.5	4.2	14 Jan 30
Kodiak Island, Alaska Womens Bay	1949-63	8.8	2.8	3.7	21 Nov 49	2.9	3.6	15,16 Jan 57
Unalaska Island, Alaska Dutch Harbor	1934-39 1946-70	3.7	2.0	2.9	14,15 Jan 38	2.0	2.7	13 Nov 50
Adak Island, Alaska Sweeper Cove	1943-70	3.7	1.8	2.7	28 Dec 66	2.3	3.3	11 Nov 50
Attu Island, Alaska Massacre Bay	1943-69	3.3	1.6	2.4	6 Jan 66	1.7	2.4	12,13 Nov 50

† Tsunami levels not included.

1969, in excess of 20 feet MSL over many miles of the open Gulf Coast, with a peak value of 24 feet MSL near Pass Christian, Mississippi. High water levels in excess of 12 feet MSL on the open coast and 20 feet within bays were recorded along the Texas coast as the result of Hurricane Carla, September, 1961. Water levels above 13 feet MSL were recorded in the Florida Keys during Hurricane Donna, 1960.

Accumulation of data over many years in some areas, such as regions near the North Sea, has led to relatively accurate empirical techniques of storm surge prediction for some locations. However, these empirical methods are not applicable to other locations. In general, not enough storm surge observations are available in the United States to make accurate predictions of storm surge. Therefore, it has been general practice to use hypothetical design storms, and to estimate the storm-induced surge by physical or mathematical models. Mathematical models are usually used for predicting storm surge, since it is difficult to represent some of the storm surge generating processes (such as the direct wind effects and Coriolis effects) in physical laboratory models.

a. Hydrodynamic Equations. Equations that describe the storm surge generation processes are the continuity equation expressing conservation of mass and the equations of motion expressing Newton's second law. The derivations are not presented here; references are cited below. The equations of motion and continuity given here represent a simplification of the more complete equations. A more simplified form is obtained by vertically integrating all governing equations and then expressing everything in terms of either the mean horizontal current velocity or volume transport. Vertically integrated equations are generally preferred in storm-surge calculations since interest is centered in the free surface motion and mean horizontal flow. Integration of the equations for the storm surge problem are given by Haurwitz (1951), Welander (1961), Fortak (1962), Platzman (1963), Reid (1964), and Harris (1967).

The equations given here are obtained by assuming:

(1) vertical accelerations are negligible,
(2) curvature of the earth and effects of surface
     waves can be ignored,
(3) the fluid is inviscid, and
(4) the bottom is fixed and impermeable.

The notation and the coordinate scheme employed are shown schematically in Figure 3-43. D is the total water depth at time t, and is given by D = d + S, where d is the undisturbed water depth and S is the height of the free surface above or below the undisturbed depth resulting from the surge. The Cartesian coordinate axes, x and y, are in the horizontal plane at the undisturbed water level and the z axis is directed positively upward. The x axis is taken normal to the shoreline (positive in the shoreward direction), and the y axis is taken alongshore (positive to the left when facing the shoreline from the sea).

3-92

PROFILE

PLAN VIEW
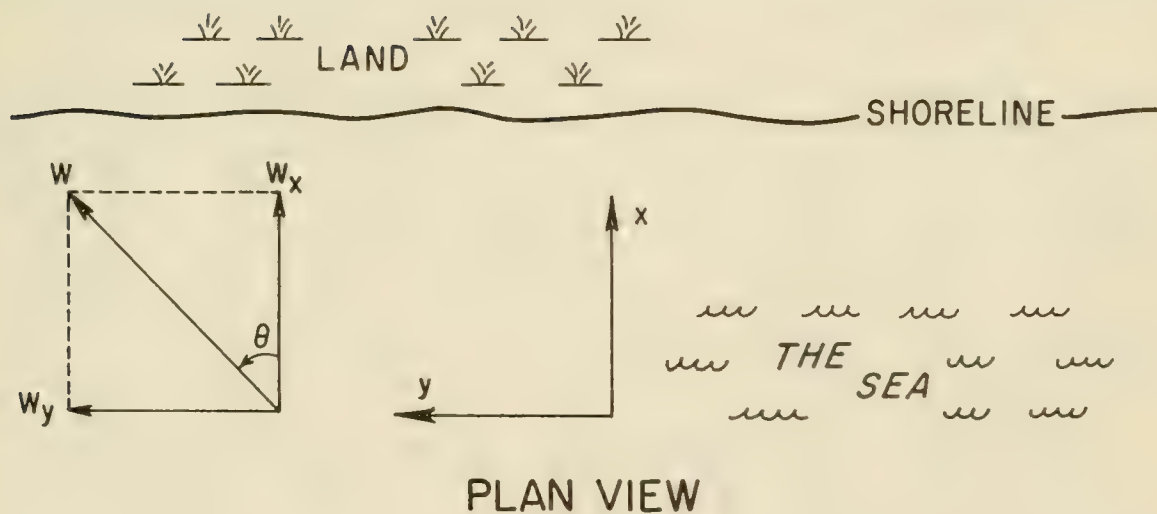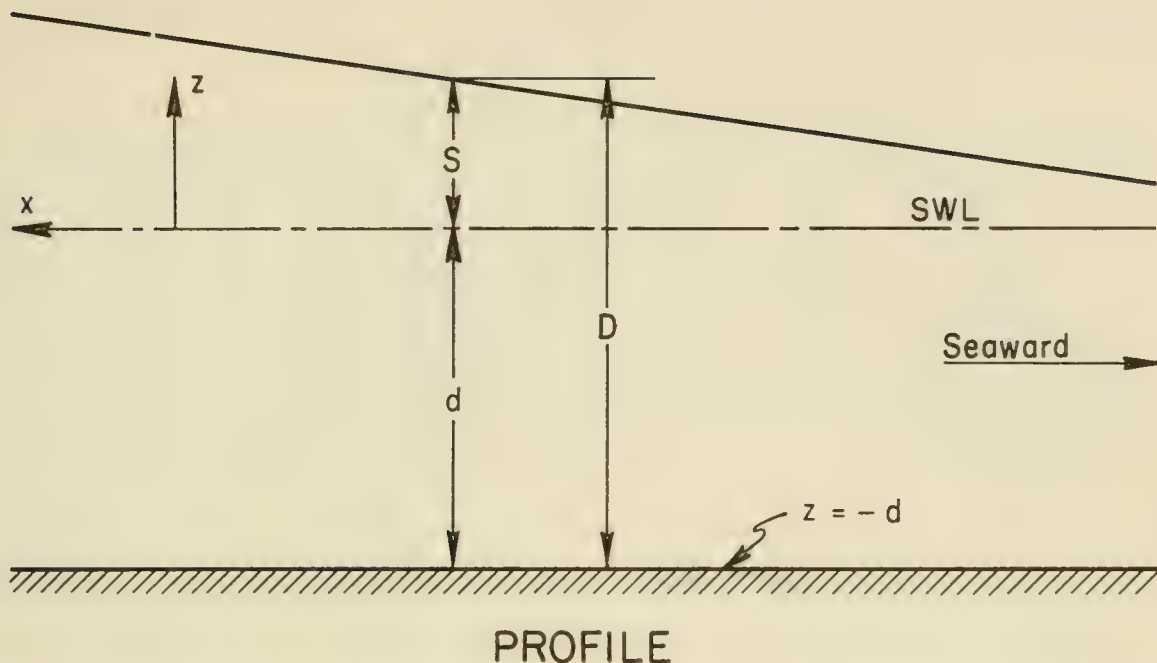
Figure 3-43. Notation and Reference Frame

The differential equations appropriate for tropical or extratropical storm surge problems on the open coast and in enclosed and semienclosed basins are as follows:

$$\frac{\partial U}{\partial t} + \underbrace{\frac{\partial M_{xx}}{\partial x} + \frac{\partial M_{xy}}{\partial y}}_{\substack{\text{Advection of}\\ \text{Momentum}}} = \underbrace{fV}_{\text{Coriolis}} - \underbrace{gD\,\frac{\partial S}{\partial x}}_{\text{Surface Slope}} + \underbrace{gD\,\frac{\partial \xi}{\partial x}}_{\substack{\text{Inverse}\\ \text{Barometer}}} + \underbrace{gD\,\frac{\partial \zeta}{\partial x}}_{\substack{\text{Astro. Tide}\\ \text{Potential}}} + \underbrace{\frac{\tau_{sx}}{\rho}}_{\text{Wind Stress}} - \underbrace{\frac{\tau_{bx}}{\rho}}_{\text{Bottom Stress}} + \underbrace{W_x P}_{\text{Rainfall Rate}} \quad (3\text{-}50)$$

$$\frac{\partial V}{\partial t} + \frac{\partial M_{yy}}{\partial y} + \frac{\partial M_{xy}}{\partial x} = - fU - gD\,\frac{\partial S}{\partial y} + gD\,\frac{\partial \xi}{\partial y} + gD\,\frac{\partial \zeta}{\partial y} + \frac{\tau_{sy}}{\rho} - \frac{\tau_{by}}{\rho} + W_y P \quad (3\text{-}51)$$

$$\frac{\partial S}{\partial t} + \frac{\partial U}{\partial x} + \frac{\partial V}{\partial y} = P \ . \tag{3-52}$$

where

$$M_{xx} = \int_{-d}^{S} u^2\, dz; \quad M_{yy} = \int_{-d}^{S} v^2\, dz; \quad M_{xy} = \int_{-d}^{S} uv\, dz;$$

$$U = \int_{-d}^{S} u\, dz; \qquad V = \int_{-d}^{S} v\, dz \ .$$

The symbols are defined as:

U, V = x and y components, respectively, of the volume transport per unit width;

t = time;

M_{xx}, M_{yy}, M_{xy} = momentum transport quantities;

f = $2\omega \sin \phi$ = Coriolis parameter;

3-94

ω = angular velocity of earth
(7.29 x 10^{-5} radians/second);

ϕ = geographical latitude;

τ_{sx}, τ_{sy} = x and y components of surface wind stress;

τ_{bx}, τ_{by} = x and y components of bottom stress;

ρ = mass density of water;

W_x, W_y = x and y components of wind speed;

ξ = atmospheric pressure deficit in head of water;

ζ = astronomical tide potential in head of water;

u, v = x and y components, respectively, of current velocity;

P = precipitation rate (depth/time);

g = gravitational acceleration; and

θ = angle of wind measured counterclockwise from the x axis.

Equations 3-50 and 3-51 are approximate expressions for the equations of motion and Equation 3-52 is the continuity relation for a fluid of constant density. These basic equations provide, for all practical pur- poses, a complete description of the water motions associated with nearly horizontal flows such as the storm surge problem. Since these equations satisfactorily describe the phenomenon involved, a nearly exact solution can only be obtained by using these relations in complete form.

It is possible to obtain useful approximations by ignoring some terms in the basic equations when they are either equivalent to zero or are negligible, but accurate solutions can be achieved only by retaining the full two-dimensional characteristics of the surge problem. Various sim- plifications (discussed later) can be made by ignoring some of the physi- cal processes. These simplifications may provide a satisfactory estimate, but they must always be considered as only an approximation.

In the past, simplified methods were used extensively to evaluate storm surge because it was necessary to make all computations manually. Manual solutions of the complete basic equations in two dimensions were prohibitively expensive because of the enormous computational effort. With high speed computers, it is possible to resolve the basic hydro- dynamic relations efficiently and economically. As a result of computers, several workers have recently developed useful mathematical models for computing storm surge. These models have substantially improved accuracy, and provide a means for evaluating the surge in the two horizontal dimen- sions. These more accurate methods are not covered here, but are highly recommended for resolving storm-surge problems where more exactness is

warranted by the size or importance of the problem. These methods are recommended only if a computer is available. A brief description of these methods and references to them follows.

Solutions to the basic equations given can be obtained by the techniques of numerical integration. The differential equations are approximated by finite differences resulting in a set of equations referred to as the numerical analogs. The finite-difference analogs, together with known input data and properly specified boundary conditions, allow evaluation at discrete points in space of both the fields of transport and water level elevations. Because the equations involve a transient problem, steps in time are necessary; the time interval required for these steps is restricted to a value between a few seconds and a few minutes depending on the resolution desired and the maximum total water depth. Thus solutions are obtained by a repetitive process where transport values and water-level elevations are evaluated at all prescribed spatial positions for each time level throughout the temporal range.

These techniques have been applied to the study of long-wave propagation in various water bodies by numerous investigators. Some investigations of this type are listed below. Mungall and Matthews (1970) developed a variable-boundary, numerical tidal model for a fjord inlet. The problem of surge on the open coast has been treated by Miyazaki (1963), Leendertse (1967), and Jelesnianski (1966, 1967, and 1970). Platzman (1958) developed a model for computing the surge on Lake Michigan resulting from a moving pressure front, and also developed a dynamical wind tide model for Lake Erie. (Platzman, 1963.) Reid and Bodine (1968) developed a numerical model for computing surges in a bay system taking into account flooding of adjacent low lying terrain and overtopping of low barrier islands.

b. Simplified Techniques for Determining Storm Surge. The techniques described here for the determination of storm surge are simple, and it is possible to carry out all storm surge calculations manually, using a desk calculator or slide rule. In most cases, however, it is desirable to employ a digital computer for the computations to reduce the effort and to improve accuracy. It is sometimes possible to estimate surge with satisfactory accuracy using a set of simplified equations, if the particular problem is not too complex, and if the simplified technique can be verified from actual prototype field data. Simpler schemes for computing storm surge are obtained by including only those phenomena that appear significant to the investigation; thus some of the less important terms are omitted from Equations 3-50, 3-51 and 3-52.

(1) Storm Surge on the Open Coast. Ocean basins are large and deep beyond the shallow waters of the Continental Shelf. The expanse of ocean basins permits large tropical or extratropical storms to be situated entirely over water areas allowing tremendous energy to be transferred from the atmosphere to the water. Wind-induced surface currents, when moving from the deep ocean to the coast, are impeded by the shoaling bottom, causing an increase in water level over the Continental Shelf.

Onshore winds cause the water level to begin to rise at the edge of the Continental Shelf. The amount of rise increases shoreward to a maximum level at the shoreline. Storm surge at the shoreline can occur over long distances along the coast. The breadth and width of the surge will depend on the storm's size, intensity, track and speed of forward motion as well ' as the shape of the coastline, and the offshore bathymetry. The highest water level reached at a location along the coast during the passage of a storm is called the *maximum surge* for that location; the highest maximum surge is called the *peak surge*. Maximum water levels along a coast do not necessarily occur at the same time. The time of the maximum surge at one location may differ by several hours from the maximum surge at another location. The variation of maximum surge values and their time for many locations along the east coast during Hurricane Carol, 1954, are shown in Figure 3-44. This hurricane moved a long distance along the coast before making landfall, and altered the water levels along the entire east coast. The location of the peak surge relative to the location of the landfall where the eye crosses the shoreline depends on the seabed bathymetry, wind-field, configuration of the coastline, and the path the storm takes over the shelf. For hurricanes moving more or less perpendicular to a coast with relatively straight bottom contours, the peak surge will occur close to the point where the region of maximum winds intersects the shoreline, approximately at a distance R, to the right of the storm center. Peak surge is generally used by coastal engineers to establish design water levels at a site.

Attempts to evaluate storm surge on the open coast, and also in bays and estuaries, when obtained entirely from theoretical considerations, require verification particularly when simplified models are used. The surge is verified by comparing the theoretical system response and computed water levels with those observed during an actual storm. The comparison is not always simple, because of the lack of field data. Most water-level data obtained from past hurricanes were taken from high water marks in low-lying areas some distance inland from the open coast. The few water-level recording stations along the open coast are too widely separated for satis-factory verification. Estimates of the water level on the open coast from levels observed at inland locations are unreliable, since corrective adjust-ments must be made to the data, and the transformation is difficult.

Systematic acquisition of hurricane data by a number of organizations and individuals began during the first quarter of this century. Harris (1963b) presented water-level data and synoptic weather charts for 28 hurricanes occurring from 1926 to 1961. Such data are useful for verifying surge prediction techniques.

Because of the limited availability of observed hurricane surge data for the open coast, design analysis for coastal structures is not always based on observed water levels. Consequently a statistical approach has evolved that takes into account the expected probability of the occurrence of a hurricane with a specific CPI at any particular coastal location. Statistical evaluation of hurricane parameters based on detailed analysis of many hurricanes, have been compiled for coastal zones along the Atlantic and Gulf coasts of the U.S. The parameters evaluated were the radius of
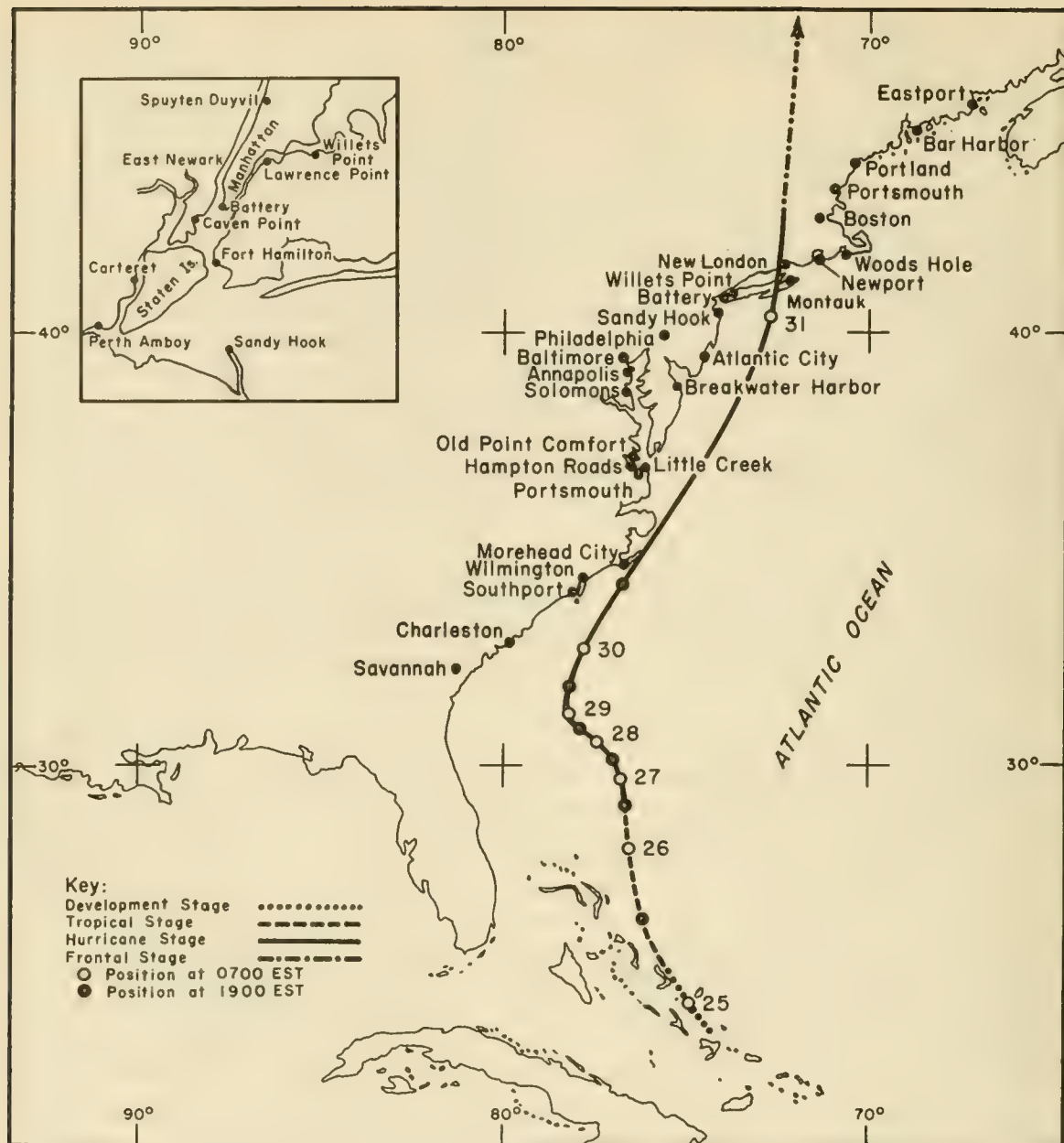
(from Harris, 1963 b)

Figure 3-44.   Storm Surge Chart.   Hurricane Carol, 30, 31 August 1951.
Insert Map for New York Harbor
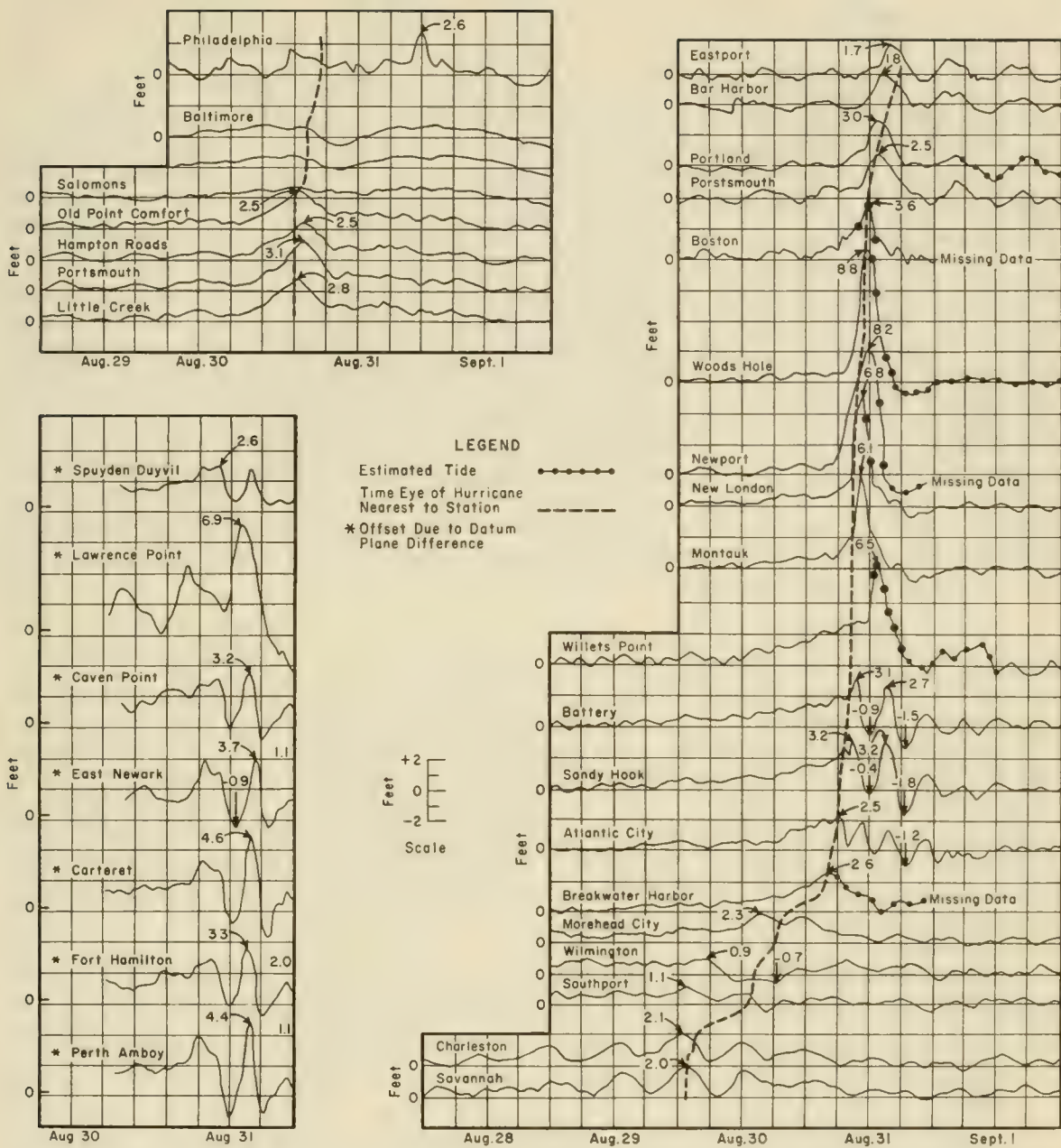
Figure 3-44. Storm Surge Chart. Hurricane Carol, 30, 31 August 1951.
Insert Map for New York Harbor -- Continued

maximum wind R; the minimum central pressure of the hurricanes p_0; the forward speed of the hurricane V_F, while approaching or crossing the coast; and the maximum sustained wind speed W, 30 feet above the mean water level.

Based on this analysis, the U.S. Weather Bureau (now the National Weather Service) and U.S. Army Corps of Engineers jointly established specific storm characteristics for use in the design of coastal structures. Because the parameters characterizing these storms are specified from statistical considerations and not from observations, the storms are termed *hypothetical hurricanes* or *hypo-hurricanes*. The parameters for such storms are assumed constant during the entire surge generation period. Graham and Nunn (1959) have developed criteria for a design storm where the central pressure has an occurrence probability of once in 100 years. This storm is referred to as the *standard project hurricane* (SPH). The mathematical model used for predicting the wind and pressure fields in the SPH is discussed in Section 3.72, Model Wind and Pressure Fields for Hurricanes. The SPH is defined as a "hypo-hurricane that is intended to represent the most severe combination of hurricane parameters that is *reasonably characteristic* of a region excluding extremely rare combinations." Most coastal structures built by the U.S. Army Corps of Engineers that are designed to withstand or protect against hurricanes are based on design water associated with the SPH.

The construction of nuclear-powered electric generating stations in the coastal zone made necessary the definition of an extreme hurricane called the *probable maximum hurricane* (PMH). The PMH has been adopted by the Atomic Energy Commission for design purposes to ensure public safety and the safety of nuclear-power facilities. Procedures for developing a PMH for a specific geographical location are given in U.S. Weather Bureau Interim Report HUR 7-97 (1968). The PMH was defined as "A hypothetical hurricane having that combination of characteristics which will make the most severe storm that is reasonably possible in the region involved, if the hurricane should approach the point under study along a critical path and at an optimum rate of movement."

Selection of hurricane parameters and the methods used for developing overwater wind speeds and directions for various coastal zones of the United States are discussed in detail by Graham and Nunn (1959) and in HUR 7-97 (1968) for the SPH and PMH. The basic design storm data should be carefully determined, since errors may significantly affect the final results.

Two simple methods are presented here for estimating storm surge on the *open coast:* one a quasi-static numerical scheme and the other a nomograph method. These methods should *never* be used for estimating the surge in bays, estuaries, rivers or in low-lying regions landward of the normal open-coast shoreline. Neither method is entirely satisfactory for all cases, but for many problems both appear to give reasonable solutions. The use of each method is illustrated by estimating the peak open-coast storm surge for an actual hurricane. The peak surges thus calculated are compared to the surge computed by a complete two-dimensional numerical model for the same storm.

(a) Quasi-Static Method for Prediction of Hurricane Surge.
This method for determining open-coast storm surge is based on theoretical approximations of the governing hydrodynamic equations originally proposed by Freeman, Baer, and Jung (1957). The term *quasi-static method* is used here to emphasize that this method should be restricted to slow-moving, large-scale storm systems. This method is called the *Bathystrophic Storm Tide Theory* and, unlike earlier one-dimensional theories, some of the effects of longshore flow and the apparent Coriolis force are considered. Such an approximation of the theory can be described as a quasi-static method in which a numerical solution is obtained by successively integrating wind stresses over the Continental Shelf from its seaward edge to the shore for a predetermined interval of time.

This simplified method assumes that storm surge responds instantaneously to the onshore wind stresses, advection of momentum can be ignored, longshore sea surface is uniform, and no flow is assumed normal to the shore which is treated as a seawall. Barometric effects and precipitation also can be neglected. Setup due to atmospheric pressure difference can be estimated from another source, and added to the final design water level. Based on the preceding assumptions, Equations 3-50 and 3-51 reduce to

$$gD \frac{\partial S}{\partial x} = fV + \frac{\tau_{sx}}{\rho} \qquad (3\text{-}53)$$

$$\frac{\partial V}{\partial t} = \frac{\tau_{sy} - \tau_{by}}{\rho} \qquad (3\text{-}54)$$

Conservation of mass is not considered because, (1) there is no flow perpendicular to shore, (2) the longshore flow is assumed independent of y and, (3) the water level is assumed slowly changing. The forces (expressed in mass times acceleration per unit area) involved and the corresponding response of the sea for the bathystrophic approximation are shown in Figure 3-45. As indicated in the figure, the surface shear force acting in the x-direction τ_{sx} and the apparent Coriolis force is balanced by the hydrostatic pressure force $\rho g \Delta (\partial S/\partial x)$. Moreover, the surface shear force acting in the y-direction τ_{sy} is balanced by the bottom shear force τ_{by} and the inertial force $\rho(\partial V/\partial t)$.

Bretschneider and Collins (1963) developed a computational model based on this Bathystrophic Theory and applied it to open-coast surge problems for the region around Corpus Christi, Texas. Marinos and Woodward (1968) modified the Bretschneider and Collins model and calibrated it for various reaches along the Texas coast by using three hurricanes of record, and also made parametric studies of hypo-hurricane surges for the entire coast of Texas.

In some cases the underlying assumptions made in the development of this theory are not satisfied. Thus, as a consequence of assuming that the onshore wind stresses cause an instantaneous change of the water level, i.e., U = 0, the traverse line (the line over the Continental Shelf along which computations are carried out) *must always* be taken perpendicular to

NOTE: Various scales have been distorted to give a clearer pictorial representation.
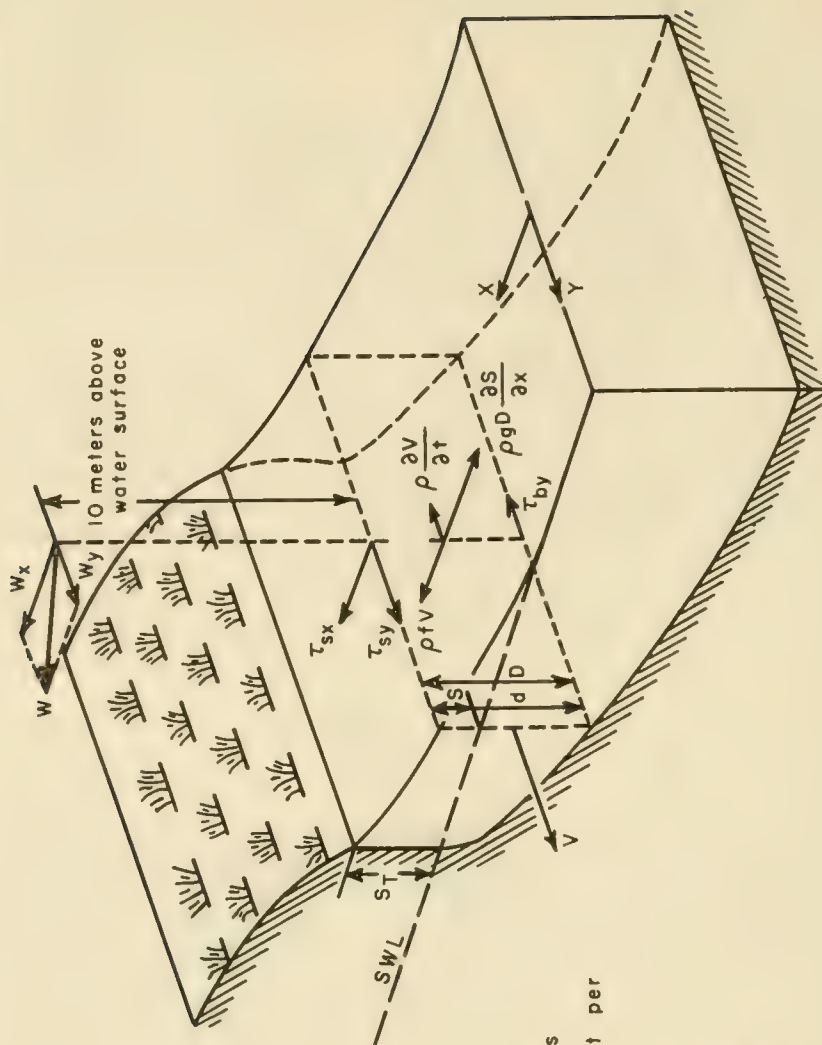
LEGEND:

SWL = Stillwater Level

S_T = Total Setup at Shore

S = Setup

d = depth below SWL

D = Total depth

τ_{sx}, τ_{sy} = x,y components of wind stress

V = y-component of water transport per unit width (of x)

W = Wind Speed

W_x, W_y = x,y components of wind speed

τ_{by} = y-component of bottom stress

f = coriolis parameter

ρ = density of water

g = gravity

t = time

3-102

Figure 3-45. Schematic of Forces and Responses for Bathystrophic Approximation

the bottom contours for valid computations. The above assumption also implies that there is no flooding landward of the shore; thus, there is a deficiency in the method when substantial flooding occurs.

The bottom contours of the actual seabed are rarely straight and parallel; however, the traverse line can often be oriented so that it is nearly perpendicular to the contours in an average way. For complex offshore bathymetry, such an approximation would be invalid. For storms moving more or less perpendicular to a coastline, the traverse line can be taken through, or anywhere to the right of, the region of maximum winds, but *never* to the left of this region. Many other factors such as the angle of approach of a storm, the coastline configuration, and inertial effects, limit the use of such a simple approach.

The computation model given here is based on Bathystrophic Storm Tide Theory as described by Bodine (1971). Although Bodine applied both manual and digital computer calculation methods to the open coast storm surge problem, only the manual method is presented.

The bottom and surface shear stresses are assumed to vary according to:

$$\frac{\tau_{by}}{\rho} = \frac{KV|V|}{D^2} \quad \text{(bottom shear stress)} \tag{3-55}$$

$$\frac{\tau_{sx}}{\rho} = kW^2 \cos\theta$$

$$\text{(wind shear stress)} \tag{3-56}$$

$$\frac{\tau_{sy}}{\rho} = kW^2 \sin\theta$$

in which K is a dimensionless bottom friction coefficient, k is a dimensionless surface friction coefficient, W is the wind speed, and θ is the angle between the x-axis and the local wind vector. The bottom friction coefficient K is related to the coefficient of Chezy C and the Darcy-Weisbach friction factor f_f as follows:

$$K = \frac{g}{C^2} = \frac{f_f}{2} \tag{3-57}$$

Typical bottom conditions result in a value of K that lies in the range between 2×10^{-3} and 5×10^{-3}. For a first estimate, a value of $K = 2.5 \times 10^{-3}$ may be assumed. This coefficient is used in calibrating the model. It not only accounts for energy dissipation at the bed, but may be used to adjust for inexact modeling and deficiencies caused by ignoring some of the hydrodynamic processes involved.

3-103

The wind stress coefficient is based on one given by Van Dorn (1953) and others which is assumed to be a function of wind speed; thus,

$$k = \bar{K}_1 , \qquad\qquad \text{for } W \le W_c \qquad\qquad (3\text{-}58)$$

$$k = K_1 + K_2 \left(1 - \frac{W_c}{W}\right)^2 \quad \text{for } W \ge W_c \qquad\qquad (3\text{-}59)$$

where the constants K_1 and K_2 are usually taken to be 1.1×10^{-6} and 2.5×10^{-6}, respectively. W_c is a critical wind speed taken as 14 knots (16 miles per hour).

Introducing the bottom and free-surface stress relations into Equations 3-53 and 3-54 gives

$$\frac{\partial S}{\partial x} = \frac{1}{gD} [fV + kW^2 \cos \theta] \qquad\qquad (3\text{-}60)$$

$$\frac{\partial V}{\partial t} = kW^2 \sin \theta - \frac{KV^2}{D} \qquad\qquad (3\text{-}61)$$

an estimate of the amount of setup that can be attributed to the onshore effects. The setup attributed to longshore effects can be obtained by rewriting Equation 3-60 in the following two-component form:

$$\frac{\partial S_x}{\partial x} = \frac{kW^2 \cos \theta}{gD} \qquad\qquad (3\text{-}62)$$

$$\frac{\partial S_y}{\partial x} = \frac{fV}{gD} \qquad\qquad (3\text{-}63)$$

The total setup along the x-axis is the sum of the two components or,

$$\frac{\partial S}{\partial x} = \frac{\partial S_x}{\partial x} + \frac{\partial S_y}{\partial x} \qquad\qquad (3\text{-}64)$$

In the finite-difference numerical solution of the reduced equations, values of S_x and S_y are evaluated at points spaced Δx apart along a single Cartesian axis (the traverse line). The values of S, the total setup for the increment, can be regarded as being the water level midway between two points along the traverse line, midway between x and $x + \Delta x$ at a time t. The longshore volume transport of water V is also evaluated between points. Wind stress data and the Coriolis parameter are supplied at the points x and $x + \Delta x$. The subscripts and superscripts i and n

are used to denote discrete points in space and time, respectively. The quantities Δx and Δt are allowed to be nonuniform spacings along the traverse line and time increments, respectively. The finite difference forms of Equations 3-61, 3-62, and 3-63 are then given as follows:

$$\left(\Delta S_x\right)_{i+\frac{1}{2}}^{n+1} = \frac{\Delta x}{2gD_{i+\frac{1}{2}}^{n+1}} \left(A_i + A_{i+1}\right)^{n+1} \tag{3-65}$$

$$\left(\Delta S_y\right)_{i+\frac{1}{2}}^{n+1} = \frac{\Delta x}{2gD_{i+\frac{1}{2}}^{n+1}} \left(f_i + f_{i+1}\right) V_{i+\frac{1}{2}}^{n+1} \tag{3-66}$$

$$V_{i+\frac{1}{2}}^{n+1} = \frac{\left(\frac{1}{4}\right)\left[\left(B_i + B_{i+1}\right)^n + \left(B_i + B_{i+1}\right)^{n+1}\right] \Delta t + V_{i+\frac{1}{2}}^n}{1 + K \left|V_{i+\frac{1}{2}}^n\right|\Delta t \left(D^{-2}\right)_{i+\frac{1}{2}}^{n+\frac{1}{2}}} \tag{3-67}$$

where A and B are the kinematic forms of the wind stress given by:

$$A = k W^2 \cos \theta \tag{3-68}$$

$$B = k W^2 \sin \theta \tag{3-69}$$

The time step specified by the ordinal number n represents a time level at which ΔS_x, ΔS_y and V are known, while $n + 1$ represents the new time level for which the quantities ΔS_x, ΔS_y and V are to be determined.

The total water depth at the mid-interval between two time steps is given by:

$$D_{i+\frac{1}{2}}^{n+\frac{1}{2}} = \frac{d_i + d_{i+1}}{2} + S_e + \frac{S_A^n + S_A^{n+1}}{2} + \left(S_x + S_y\right)_{i+\frac{1}{2}}^n \tag{3-70}$$

$$+ \left(\frac{1}{4}\right)\left(\left[\left(S_{\Delta p}\right)_i + \left(S_{\Delta p}\right)_{i+1}\right]^n + \left[\left(S_{\Delta p}\right)_i + \left(S_{\Delta p}\right)_{i+1}\right]^{n+1}\right)$$

where

$$S_e = \text{initial setup}$$

$$S_A = \text{astronomical tide}$$

$$S_{\Delta p} = \text{atmospheric pressure setup.}$$

3-105

The initial setup refers to the water level at the time the storm surge computations are started. An approximate relationship giving the atmospheric pressure setup in feet when pressure is expressed in inches of mercury is

$$S_{\Delta p} = 1.14 \left(p_n - p_o \right) \left(1 - e^{-R/r} \right) \tag{3-71}$$

where p_n is the pressure at the periphery of the storm, and r is the radial distance from the storm center to the computation point on the traverse line.

The total depth at the new time level is evaluated by the relation:

$$D_{i+\frac{1}{2}}^{n+1} = \frac{d_i + d_{i+1}}{2} + S_e + S_A^{n+1} + \left(S_x + S_y \right)_{i+\frac{1}{2}}^n \tag{3-72}$$

$$+ \frac{1}{2} \left[\left(S_{\Delta p} \right)_i + \left(S_{\Delta p} \right)_{i+1} \right]^{n+1}$$

The total water level rise at the coast is the sum of all component water level changes resulting from the meteorological storm plus those components which are not related to the storm. Hence the total setup is given by

$$S_T = S_x + S_y + S_{\Delta p} + S_e + S_A + S_W + S_L \tag{3-73}$$

where S_W is a component due to the wave setup in the region shoreward of the breaker line and is related to the breaker height by Equation 3-49. (See Section 3.85, Wave Setup.) The setup component S_L accounts for the setup resulting from local conditions such as bottom configuration, coastline shape, or other flows influencing the system, such as flows from bay inlets or rivers. This component can only be estimated from a full understanding of the influence of topographic and hydrographic features not considered in the numerical calculations. Contributions made by the various setup components to the total surge are shown in Figure 3-46.

Equations 3-65, 3-66, and 3-67 can be rewritten in a more useful form by introducing dimensional constants for terms frequently appearing in the equations. Hence,

$$\left(\Delta S_x \right)_{i+\frac{1}{2}}^{n+1} = \frac{C_1 \, \Delta x}{D_{i+\frac{1}{2}}^{n+1}} \left(A_i + A_{i+1} \right)^{n+1} \tag{3-74}$$

$$\left(\Delta S_y \right)_{i+\frac{1}{2}}^{n+1} = \frac{C_2 \, \Delta x}{D_{i+\frac{1}{2}}^{n+1}} \left[\left(\sin \phi \right)_i + \left(\sin \phi \right)_{i+1} \right] V_{i+\frac{1}{2}}^{n+1} \tag{3-75}$$

$$V_{i+\frac{1}{2}}^{n+1} = \frac{\left(\frac{1}{4} \right) \left[\left(B_i + B_{i+1} \right)^n + \left(B_i + B_{i+1} \right)^{n+1} \right] \left(\Delta t \right) + V_{i+\frac{1}{2}}^n}{1 + C_3 \mid V_{i+\frac{1}{2}}^n \mid \Delta t \, K \left(D^{-2} \right)_{i+\frac{1}{2}}^{n+\frac{1}{2}}} \tag{3-76}$$

3-106
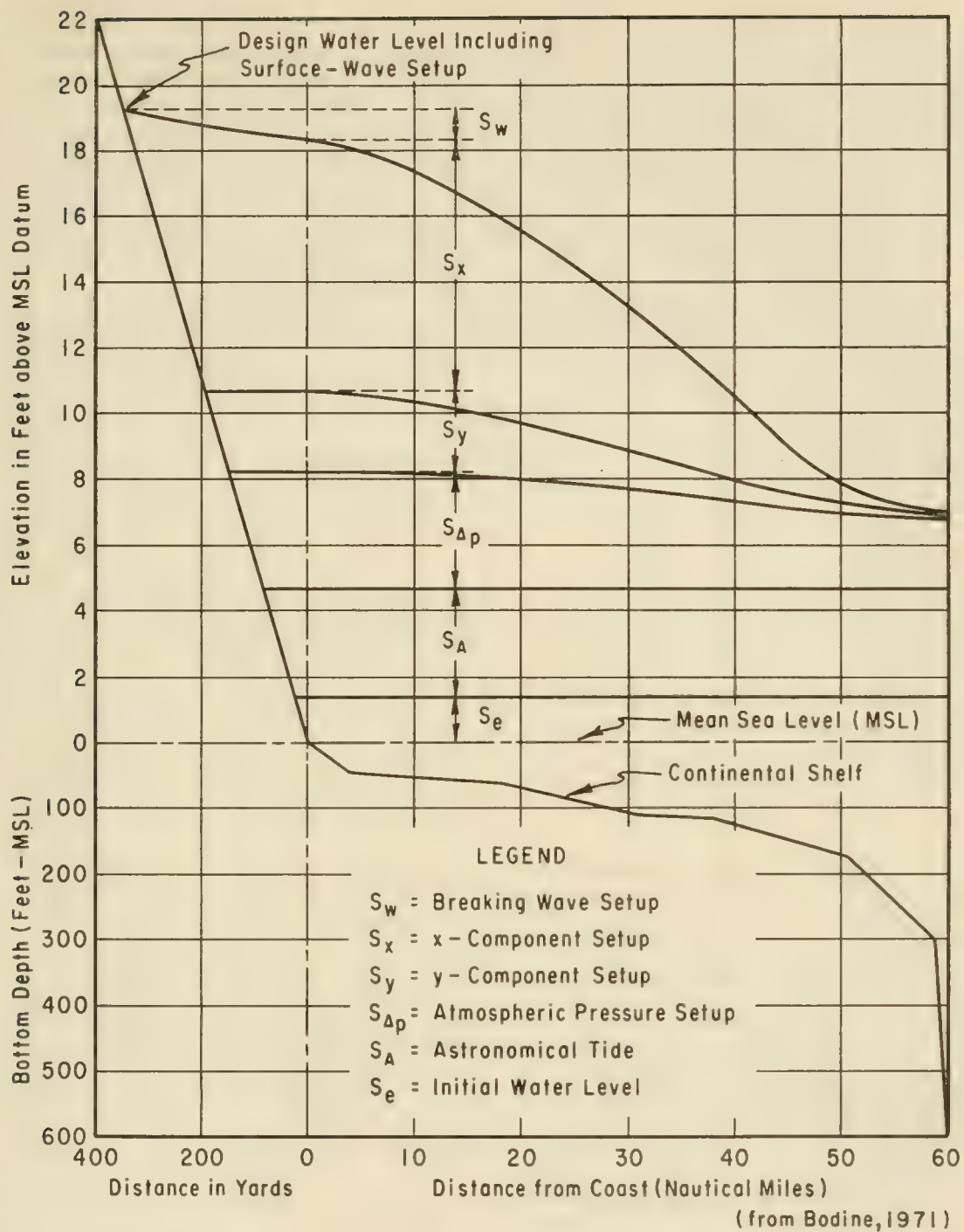
Figure 3-46. Various Setup Components Over the Continental Shelf

The values of the dimensional constants C_1, C_2, and C_3 in Equations 3-74, 3-75 and 3-76 depend on the units used in performing the calculations. Table 3-9 gives the dimensions of the variables used in the numerical scheme in three systems of units and the corresponding value of the constants for each system. The first column of units is given in the metric system while the other two are given in mixed units in the English system.

Table 3-9. Systems of Units for Storm Surge Computations

Parameters	Units and Constant Values		
	Metric	Mixed English	
Δx	km	nm	mi
ΔS_x, ΔS_y	m	ft	ft
g	m/sec^2	ft/sec^2	ft/sec^2
D	m	ft	ft
A, B	$(km/hr)^2$	$(nm/hr)^2$	$(mi/hr)^2$
V	km^2/hr	nm^2/hr	mi^2/hr
f	hr^{-1}	hr^{-1}	hr^{-1}
Δt	hr	hr	hr
C_1	3.94	269	176
C_2	2.06	141	92
C_3	$(1000)^2$	$(6080)^2$	$(5280)^2$

The assumptions for this model are reasonably good only when the momentum of the water is increasing under the influence of the wind, i.e., when the right side of Equation 3-76 is positive. This condition can be considered in the calculations by using the relation

$$V_{i+\frac{1}{2}}^{n+1} \leq \sqrt{\frac{\left| \left(B_i + B_{i+1} \right)^{n+1} \right| \left(D^2 \right)_{i+\frac{1}{2}}^{n+1}}{2 \, C_3 \, K}} \tag{3-77}$$

For a derivation of this equation see Bodine (1971). Should V at a particular time level, as evaluated from Equation 3-76, be less than the value obtained from Equation 3-77, then the result from Equation 3-77 is ignored. However, if the opposite is true, then as an estimate, V is taken equal to the maximum possible value as given by Equation 3-77.

It is customary to assume that the system is initially in a state of equilibrium and $V = 0$, and S is uniform along the traverse line at the start of the computational scheme. Thus, computations should be initiated for conditions prior to the arrival of strong winds over the Continental Shelf. Although the real system would seldom, if ever, be in a complete initial state of equilibrium, errors in assuming it to be are of little consequence in the computational scheme after several time steps in the calculations, because the effects of the forcing functions will eventually predominate.

To demonstrate the computational procedures, the storm surge in the Gulf of Mexico resulting from Hurricane Camille (1969) is calculated. Hurricane Camille was an extremely severe storm that crossed the eastern part of the Gulf of Mexico with the eye of the storm making landfall at Bay St. Louis, Mississippi, at about 0500 Greenwich Mean Time (GMT) on 18 August 1969. Unusually high water levels were experienced along the gulf coast during the passage of Camille because of the intense winds and relatively shallow water depths which extend far offshore. The storm surge is calculated and compared with the peak surge generated by Camille.

Information published by the U.S. Weather Bureau for Hurricane Camille in HUR 7-113 (1969) indicates that $R = 14$ nautical miles and $V_F = 13$ knots would be representative of these values which are assumed to be invariant while the storm moved over the Continental Shelf. The wind data and track for Hurricane Camille have been published by the Weather Bureau in HUR 7-113A (1970). The track, together with the traverse line used in the present calculations, is shown in Figure 3-47. Overwater wind speeds and directions are shown in Figure 3-48. A profile of the seabed along the traverse line is shown in Figure 3-49.

Tide records from the region affected by the storm show the mean water level to be about 1.2 feet above normal before being affected by the storm. This value is taken to represent the initial water level. The range of astronomical tides in this location is about 1.6 feet. A constant value of 0.8-foot above MSL is used in the computations; the final surge hydrograph at the coast can be subsequently corrected to account for the predicted variations of the tide. Variations in the initial water level and astronomical tides may be added algebraically to the storm surge calculations without seriously affecting the final results. The atmospheric pressure difference, $p_n - p_o$, is needed for evaluating the pressure setup component, $S_{\Delta p}$. Data given in HUR 7-113 (1969) suggest that $p_o = 26.73$ inches of mercury and $p_n = 29.92$ inches of mercury are representative for the hurricane. All of these values are assumed to remain constant for the calculations.

The wind data, basin profile, and hurricane characteristics provide the basic information needed in making an estimate of the peak storm surge associated with Hurricane Camille. The time intervals, distance increments along the traverse line, etc., are given in the computational steps to follow.
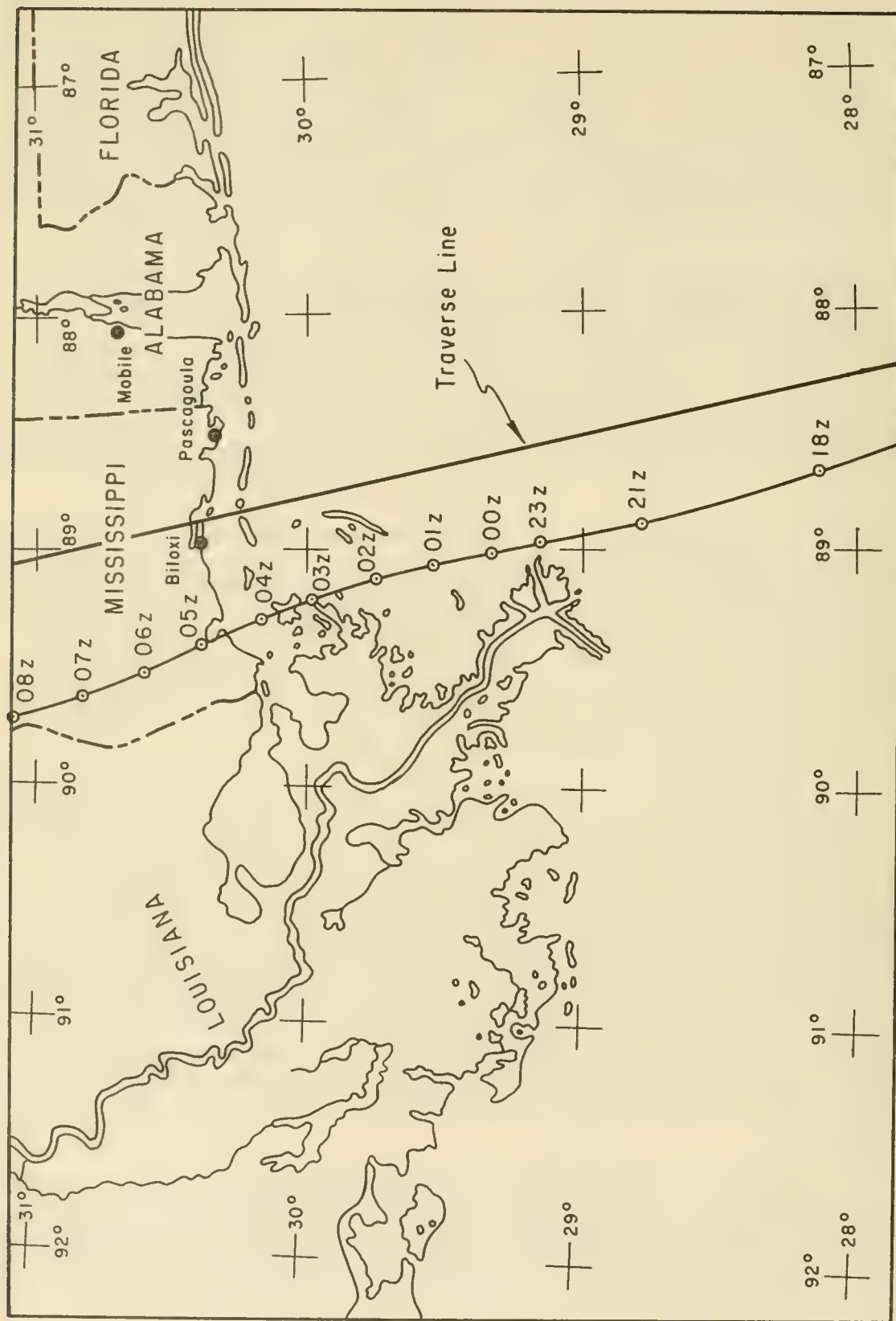
Figure 3-47. Track for Hurricane Camille, August 1969

(from Hur. 7-113A, 1970)
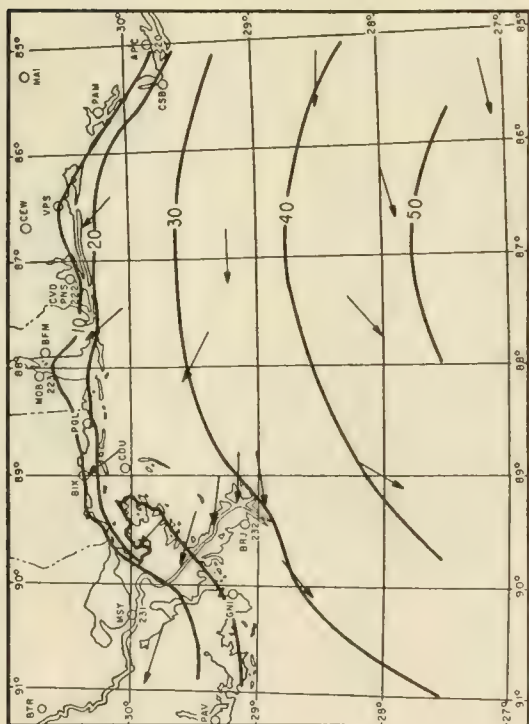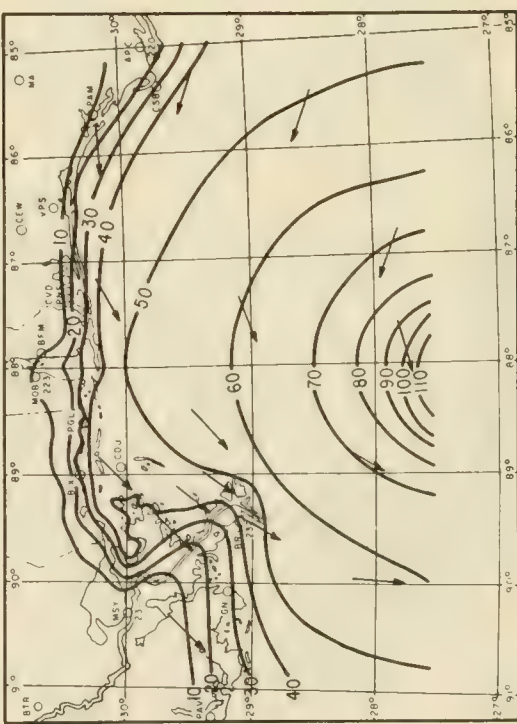
B 0600 GMT – 17 Aug 69

A 0000 GMT – 17 Aug 69
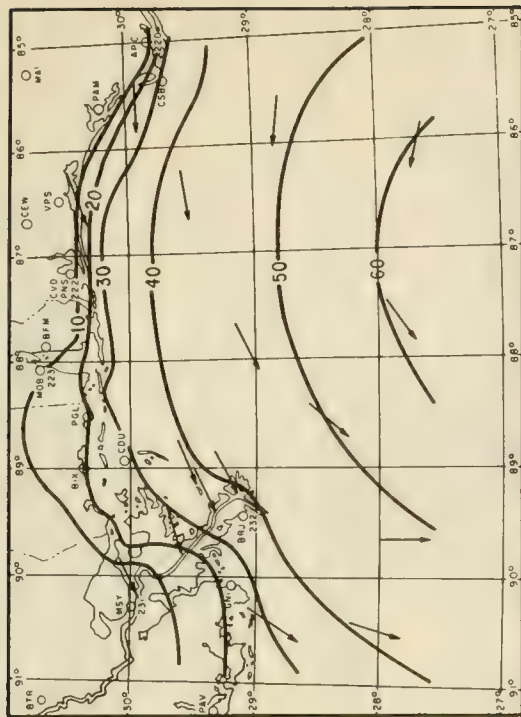
C 1200 GMT – 17 Aug 69

(from U.S. Weather Bureau Publication, HUR. 7-113A, 1970)

Figure 3-48. 30-Foot Surface Isovels (knots), Hurricane Camille
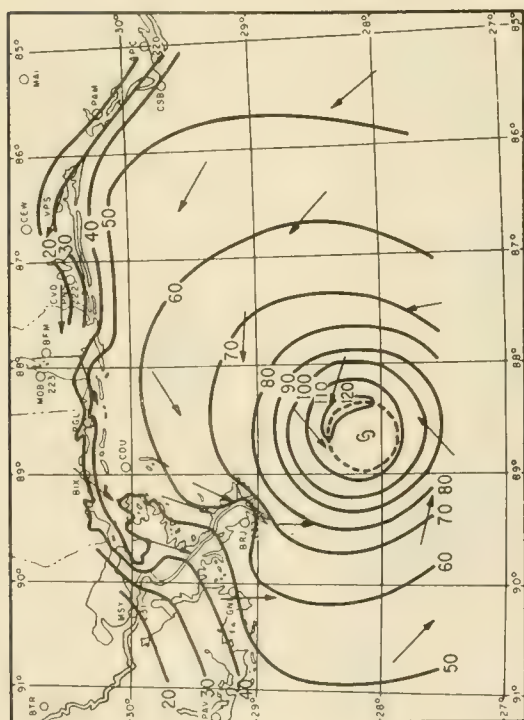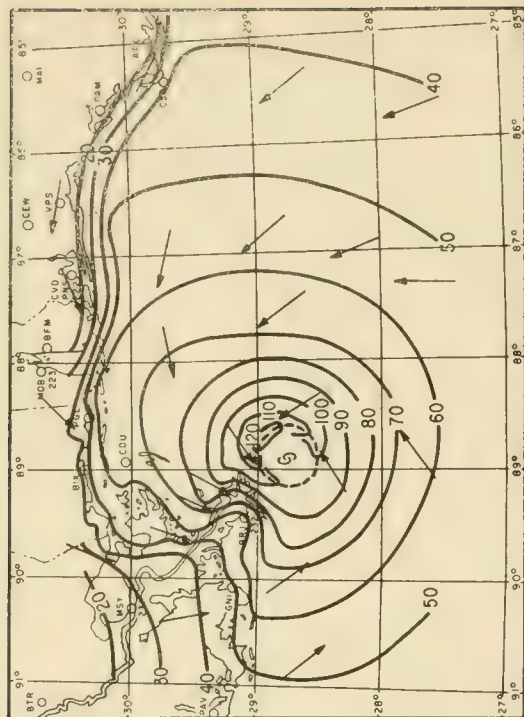
3-111

Figure 3-48. 30-Foot Surface Isovels (knots), Hurricane Camille -- Continued

3-112
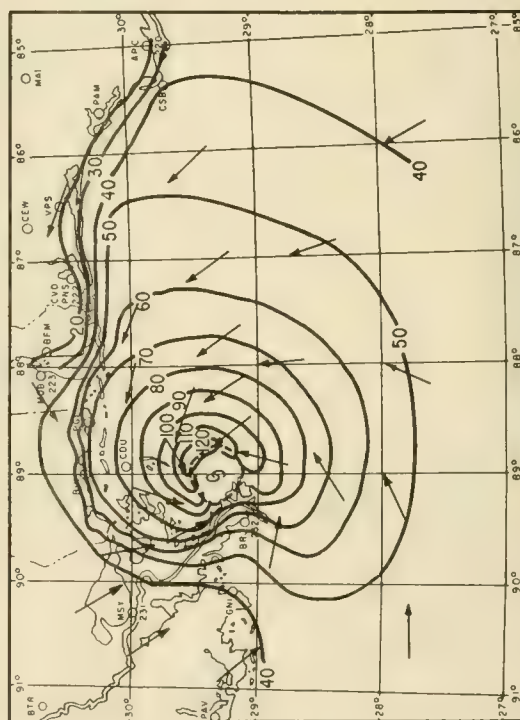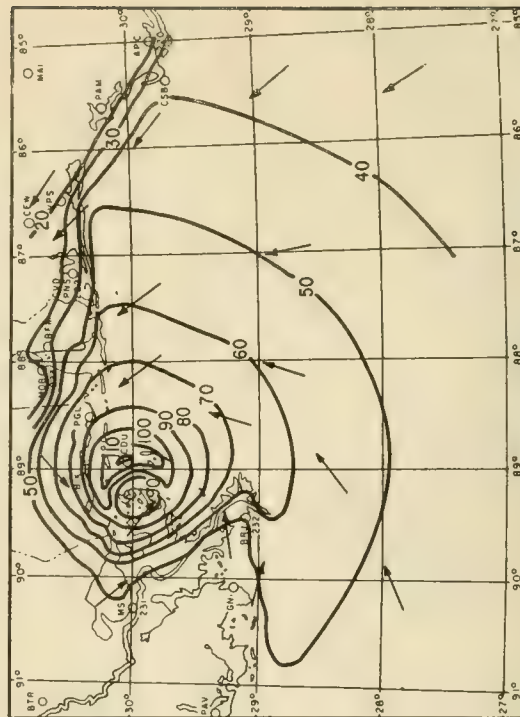
Figure 3-48.   30-Foot Surface Isovels (knots), Hurricane Camille -- Continued
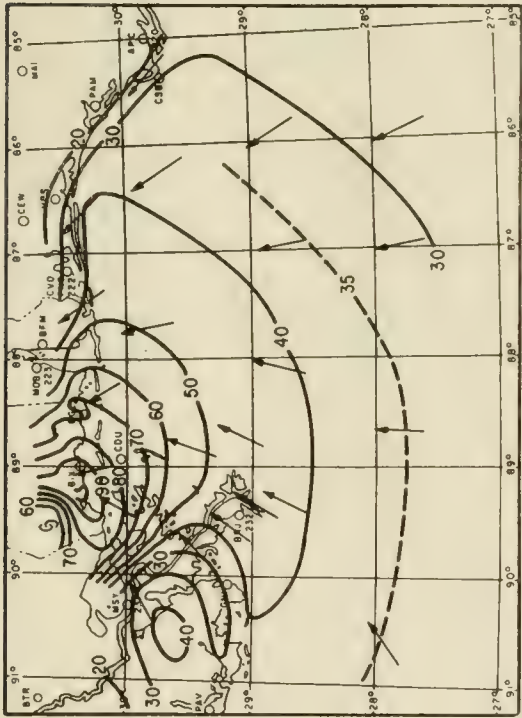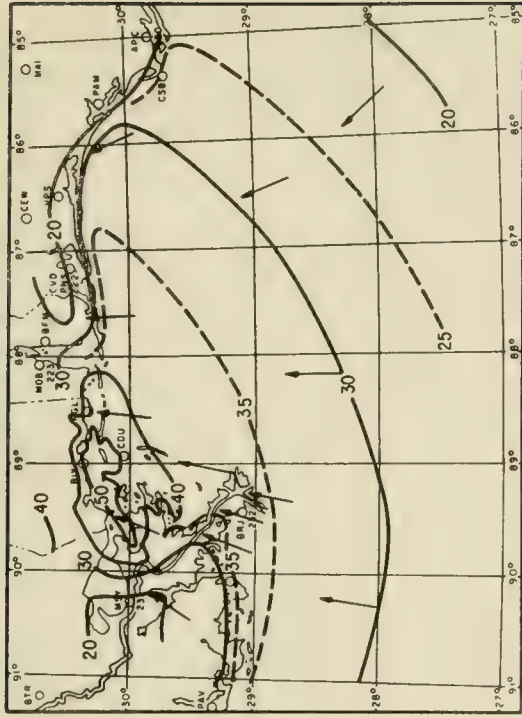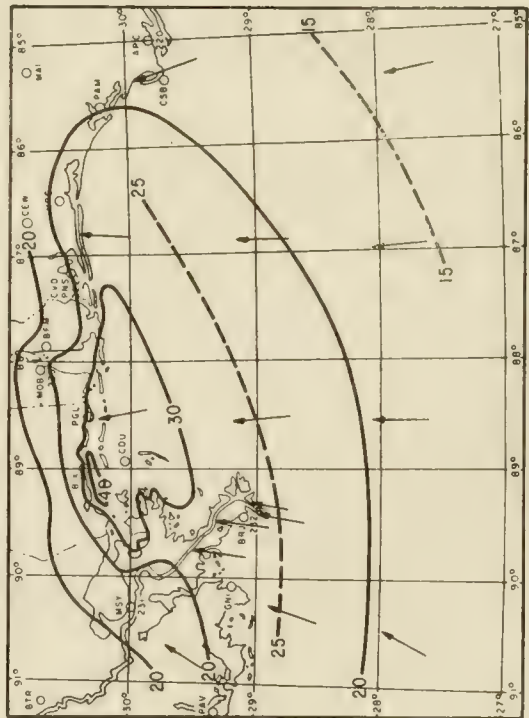
I   1200 GMT — 18 Aug 69

H   0600 GMT — 18 Aug 69

K   0000 GMT — 19 Aug 69

J   1800 GMT — 18 Aug 69
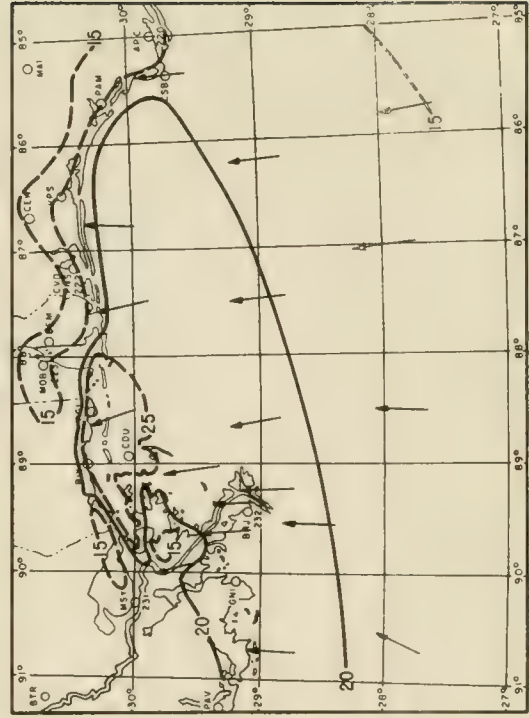
3-113
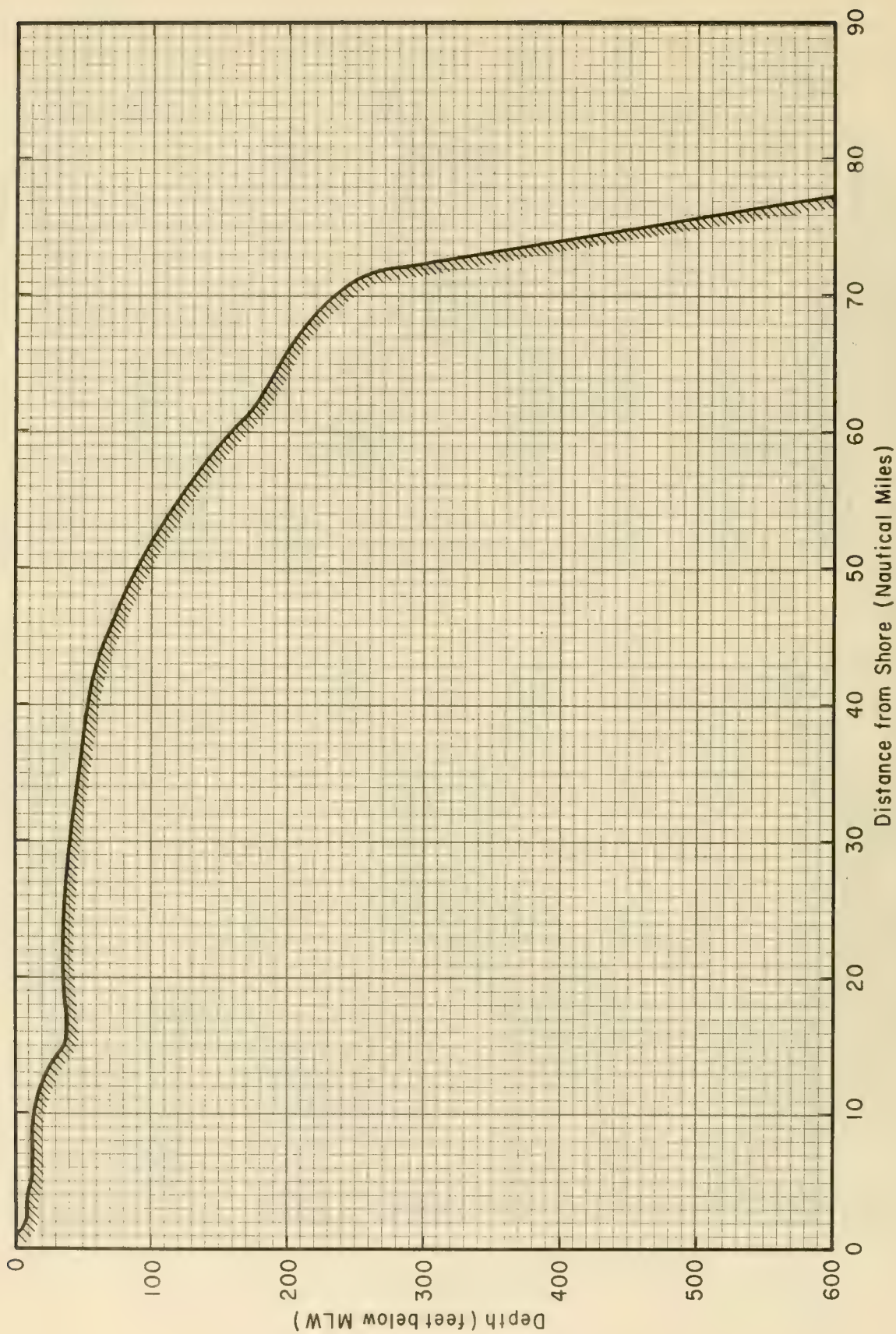
Figure 3-49. Seabed Profile Used for Hurricane Camille (August 1969)

This quasi-linear computational scheme can be used for manual computations; however, since the calculations are repetitive, they can be performed more efficiently by using a digital computer. When carried out manually, the technique is laborious, tedious and subject to error. Bodine (1971) gives a computer program based on the numerical scheme presented here. Other programs based on similar numerical schemes using the quasi-static methods have been developed.

When manual computation of storm surge is necessary, a systematic, tabular procedure must be adopted to permit stepping through all of the discrete computational points in space for each time increment. Table 3-10 represents a recommended procedure. One table is required for each time increment. Table 3-10 corresponds to the time of peak surge for Hurricane Camille; preceding tables required to bring the calculations to this point are not included since those calculations are similar. The first table in the series must reflect the initial conditions; thus V is taken to be zero and S is assumed uniform over the system.

Manual surge calculations for Hurricane Camille give a peak surge of 25.03 feet, say 25 feet (MLW) or 24.2 feet (MSL). The bottom friction coefficient selected for this particular example was K = 0.003 and the surge was found to be insensitive to small changes in the friction coefficient. Computer calculations using a friction coefficient of 0.003 resulted in a peak surge of 25.19 feet and a bottom friction coefficient of 0.0025 resulted in a peak surge of 25.40 feet. For some basins and storm systems, the bottom shear stresses are more significant in determining water levels. Therefore, it is important to select a bottom friction coefficient by verification (i.e., by comparing calculated results with observed water levels). After such verification, the model may be used to estimate the storm surge from hypothetical hurricanes for the same geographical region.

The surge hydrograph (water level as a function of time) for Hurricane Camille is shown in Figure 3-50 for the most landward computational point on the traverse line. This figure shows that the water level rose for about the first 8 hours, but then began to fall gradually until about 27 hours of computational period had elapsed, then began to rise rapidly. A study of the local wind fields during this period shows that the winds had an onshore component in the early stages of the storm, then the winds began blowing offshore for several hours before the principal rise at the coast.

(b) Nomograph Method. A simplified method for obtaining a first approximation to the peak storm surge of a hurricane can be based on an empirical analysis of past records, an empirical analysis of a systematic set of calculations with numerical models, or a combination of the two. Jelesnianski (1972) combined empirical data from Harris (1959) with his theoretical calculations to produce a set of nomograms that permit the rapid estimation of peak surge for any geographical location when a few parameters characterizing a storm are known.

The first nomogram (Fig. 3-51) permits an estimate of the peak surge S_I, generated by an idealized hurricane with specified CPI and radius of

Table 3-10. Manual Surge Computations at a Time Level Centered between t = 31.5 Hours and $t + \Delta t$ = 33.0 Hours

Line	(1) Distance Offshore and Δx (N.M.)	(2) Water Depth $d, \bar{d}$ (ft. MLW)	(3) $\sin \phi$	(4) Initial Water Level S_e (ft.)	(5) Astro. Tide S_A (ft.)	(6) Previous Wind Setup $S_x + S_y$ (ft.)	(7) Previous Pressure Setup $S^n_{\Delta p}$ (ft.)	(8) Previous Flux V^n (mi²/hr)	(9) Previous Wind Stress B^n (mi/hr)²	(10) Radial Distance $r, \bar{r}$ (N.M.)	(11) Wind Angle $\theta, \bar{\theta}$ (degrees)	(12) Wind Speed $W, \bar{W}$ (mi/hr)	(13) $R/\bar{r}$	(14) $e^{-R/\bar{r}}$	(15) $S^{n+1}_{\Delta p}$ (ft.) Eq. 3-71	(16) $\bar{W}^2 \cos\theta$ (mi/hr)²	(17) $\bar{W}^2 \sin\theta$ (mi/hr)²	(18) Wind Stress Coef. k Eq. 3-59	(19) $A^{n+1}=1.10\cdot k \cdot$Col 16 (mi/hr)²	(20) $B^{n+1}=1.10\cdot k \cdot$Col 17 (mi/hr)²
A	77.0 / Δx= 7.0	600.0 / $\bar{d}$=417.5	0.500	1.2	0.8	0.343	1.19	0.0870	0.0032	63.4 / 58.0	326.0 / 326.0	77.0 / 78.5	0.241	0.786	0.78	5110	−3447	2.70 × 10⁻⁶	0.0152	−0.0102
B	70.0 / 10.0	235.0 / 197.5	0.500	1.2	0.8	1.374	1.27	0.0801	0.0118	52.6 / 48.1	326.0 / 326.0	80.0 / 83.3	0.291	0.747	0.92	5761	−3886	2.76 × 10⁻⁶	0.0175	−0.0118
C	60.0 / 10.0	160.0 / 125.0	0.500	1.2	0.8	2.571	1.29	0.0519	0.0117	43.5 / 39.6	326.0 / 326.0	86.6 / 91.8	0.353	0.702	1.09	7008	−4727	2.84 × 10⁻⁶	0.0219	−0.0148
D	50.0 / 10.0	90.0 / 71.0	0.500	1.2	0.8	3.812	1.27	0.0327	0.0130	35.7 / 32.5	326.0 / 326.0	97.0 / 103.0	0.430	0.650	1.28	8899	−5840	2.92 × 10⁻⁶	0.0286	−0.0187
E	40.0 / 10.0	52.0 / 46.0	0.500	1.2	0.8	5.256	1.27	0.0188	0.0093	29.3 / 27.2	326.0 / 331.0	109.0 / 113.9	0.611	0.543	1.47	11368	−6247	2.97 × 10⁻⁶	0.0371	−0.0204
F	30.0 / 10.0	40.0 / 38.0	0.500	1.2	0.8	7.642	1.24	0.0178	0.0112	25.0 / 25.0	327.3 / 348.2	118.8 / 122.1	0.848	0.428	1.56	14240	−3313	3.00 × 10⁻⁶	0.0470	−0.0109
G	20.0 / 5.0	36.0 / 35.5	0.500	1.2	0.8	9.140	1.16	0.0185	0.0133	25.0 / 26.0	334.5 / 1.0	125.5 / 126.2	0.642	0.526	1.51	15935	+275	3.01 × 10⁻⁶	0.0528	+0.0009
H	15.0 / 5.0	35.0 / 24.0	0.500	1.2	0.8	10.926	1.09	0.0140	0.0137	27.0 / 27.6	2.0 / 5.0	127.0 / 126.5	0.507	0.602	1.44	15882	1378	3.00 × 10⁻⁶	0.0524	+0.0045
I	10.0 / 5.0	13.0 / 12.5	0.500	1.2	0.8	13.146	1.01	0.0096	0.0160	28.3 / 29.2	10.0 / 15.0	126.0 / 124.0	0.479	0.619	1.38	14810	3924	2.99 × 10⁻⁶	0.0487	0.0129
J	5.0 / 2.0	12.0 / 10.5	0.500	1.2	0.8	13.978	0.99	0.0089	0.0180	30.2 / 31.2	20.0 / 25.0	122.0 / 120.5	0.449	0.638	1.31	13125	6086	2.97 × 10⁻⁶	0.0470	0.0199
K	3.0 / 1.0	9.0 / 9.0	0.500	1.2	0.8	14.337	0.96	0.0087	0.0210	32.3 / 32.9	30.0 / 40.0	119.0 / 118.0	0.425	0.654	1.26	10620	8783	2.96 × 10⁻⁶	0.0346	0.0286
L	2.0 / 1.0	9.0 / 6.0	0.500	1.2	0.8	14.601	0.94	0.0073	0.0239	33.6 / 34.1	50.0 / 60.0	117.0 / 115.7	0.410	0.664	1.22	6641	11403	2.95 × 10⁻⁶	0.0215	0.0370
M	1.0 / 1.0	3.0 / 1.5	0.500	1.2	0.8	14.672	0.92	0.0061	0.0237	34.6 / 35.1	70.0 / 80.0	114.5* / 113.0	0.399	0.671	1.19	2242	12376	2.93 × 10⁻⁶	0.0072	0.0399
	0.0	0.0								35.7	90.0	111.5†								

NOTE: Columns 6 through 9 are values evaluated at previous time level.
Columns 10, 11 and 12 are values taken from curves given in Figure 3-48.
* Wind reduced by a factor of 0.945 due to interference with land mass.
† Wind reduced by a factor of 0.890 due to interference with land mass.

STORM CHARACTERISTICS AND OTHER BASIC INFORMATION

P_o = 26.73 inches of mercury

P_n = 29.92 inches of mercury

$\Delta p = (P_n - P_o)$ = 3.19 inches of mercury

V_F = 13.0 knots

R = 14.0 nautical miles

ϕ = 30° → sin φ = 0.500 (assumed constant in this case)

K = 0.003

Wind stress correction factor = 1.10

Table 3-10. Manual Surge Computations at a Time Level Centered between $t = 31.5$ Hours and $t + \Delta t = 33.0$ Hours—Continued

Line	21 $\frac{S_{\Delta p}^n + S_{\Delta p}^{n+1}}{2}$ (ft.)	22 $D^{n+\frac{1}{2}}$ Σ Cols 2, 4, 5, 6, 21 Eq. 3-70 (ft.)	23 D^{n+1} Σ Cols 2, 4, 5, 6, 15 Eq. 3-72 (ft.)	24 $\left(\frac{B^n + B^{n+1}}{2}\right)\Delta t$ (mi²/hr.)	25 $\left(\frac{5280}{D^{n+\frac{1}{2}}}\right)^2$	26 $1 + (Col\ 25 \cdot K \cdot \Delta t \cdot |V^n|)$	27 $V^{n+1} = \frac{Col\ 24 + V^n}{Col\ 26}$ Eq. 3-76 (mi²/hr.)	28 $K \cdot (5280)^2$	29 $|B^{n+1}| \cdot (D^{n+1})^2$	30 $V^{n+1} = \sqrt{\frac{Col\ 29}{Col\ 28}}$ Eq. 3-77 (mi²/hr.)‡	31 Value Used V^{n+1} (mi²/hr.)	32 $\frac{106 \cdot \Delta x}{D^{n+1}}$	33 $\Delta S_y = 2 \cdot \sin\phi \cdot Col\ 32 \cdot V^{n+1}$ Eq. 3-75 (ft.)	34 $S_y = \Sigma \Delta S_y$ (ft.)	35 $\Delta S_x = 106 \cdot \Delta x \cdot \frac{A^{n+1}}{D^{n+1}}$ Eq. 3-74 (ft.)	36 $S_x = \Sigma \Delta S_x$ (ft.)	37 Total Setup S_T Eq. 3-73 (ft.)
A	0.98	421.82	420.62	-0.0052	156.68	1.0613	0.0771	83,635	1804.59	0.1469	0.0771	1.764	0.136	0.136	0.103	0.103	3.02
B	1.09	201.96	201.79	0.0000	683.49	1.2464	0.0643	83,635	480.49	0.0758	0.0643	5.253	0.338	0.474	0.352	0.455	3.85
C	1.19	130.76	130.66	-0.0023	1630.49	1.3808	0.0359	83,635	253.67	0.0550	0.0359	8.113	0.291	0.765	0.680	1.135	4.99
D	1.27	78.08	78.09	-0.0043	4572.86	1.6729	0.0170	83,635	114.03	0.0369	0.0170	13.574	0.231	0.996	1.487	2.632	6.90
E	1.37	54.63	54.73	-0.0083	9341.26	1.7903	0.0059	83,635	61.11	0.0270	0.0059	19.368	0.114	1.110	2.752	5.374	9.95
F	1.40	49.04	49.20	0.0002	11592.22	1.9285	0.0093	83,635	26.38	0.0178	0.0093	21.545	0.200	1.310	3.878	9.252	14.12
G	1.33	47.97	48.15	0.0107	12115.14	2.0086	0.0145	83,635	2.09	0.0050	0.0050	11.007	0.055	1.365	2.226	11.478	16.35
H	1.26	38.19	38.37	0.0136	19114.74	2.2042	0.0125	83,635	6.63	0.0089	0.0089	13.813	0.123	1.488	2.772	14.250	19.18
I	1.19	28.84	29.03	0.0217	33517.94	2.4480	0.0128	83,635	10.87	0.0114	0.0114	18.257	0.208	1.696	3.287	17.537	22.61
J	1.15	27.63	27.79	0.0284	36517.92	2.4625	0.0151	83,635	15.37	0.0136	0.0136	7.629	0.104	1.800	1.254	18.791	23.90
K	1.11	26.45	26.60	0.0372	39848.91	2.5601	0.0179	83,635	20.24	0.0156	0.0156	3.985	0.062	1.862	0.528	19.319	24.44
L	1.08	23.99	23.82	0.0456	48440.36	2.5913	0.0204	83,635	20.99	0.0158	0.0158	4.450	0.070	1.932	0.366	19.685	24.84
M	1.06	19.52	19.36	0.0477	73165.82	3.0084	0.0179	83,635	14.95	0.0134	0.0134	5.475	0.073	2.005	0.151	19.836	25.03

‡ This is a test.
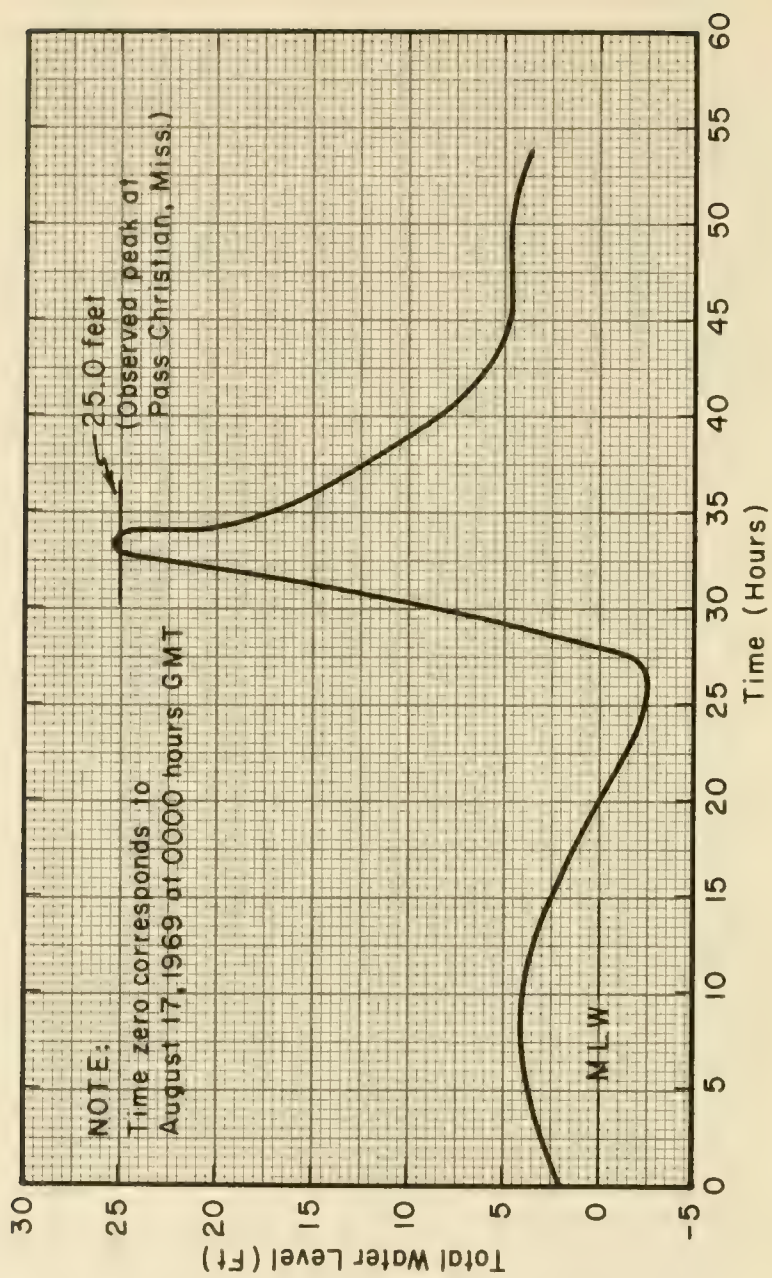
Figure 3-50. Open Coast Surge Hydrograph. Hurricane Camille, August 1969.
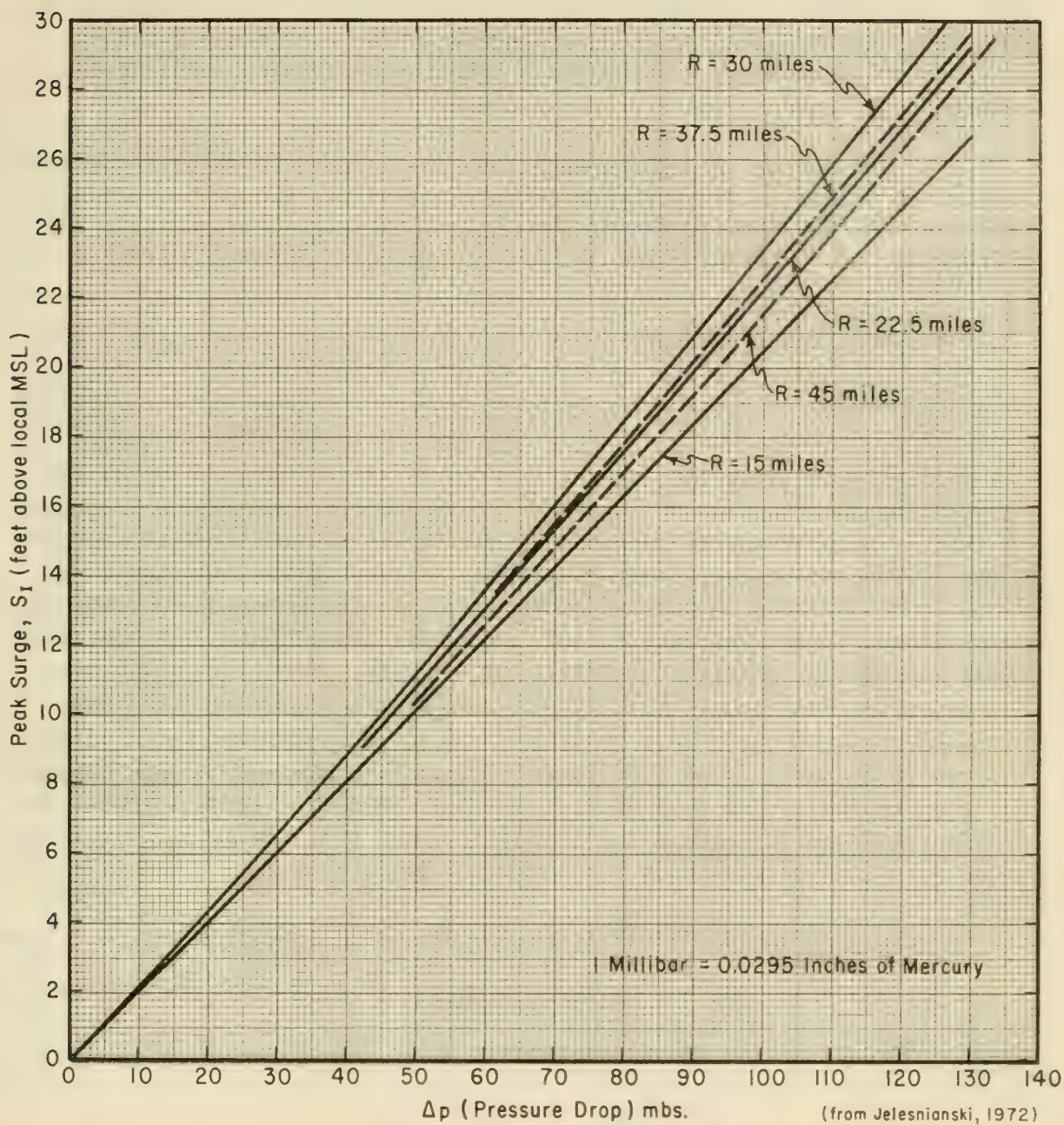
Figure 3-51. Preliminary Estimate of Peak Surge

maximum wind that is moving perpendicular to a shoreline with a speed of
15 MPH. This nomogram indicates there is a critical storm size as reflec-
ted by the radius of maximum winds, R. For a given pressure drop greater
than zero, the highest peak surge is produced for a critical value of R
equal to 30 miles and any value of R greater or less than this value
results in a lesser value of the peak surge.

A second factor F_S given in Figures 3-52 and 3-53 adjusts for the
effects of variations in bathymetric characteristics along the gulf and
Atlantic coasts. A third factor F_M given in Figure 3-54, adjusts for
the effects of storm speed and the angle with which the storm track
intercepts the coast.

The predicted peak storm surge S_p is then given by

$$S_p = S_I F_S F_M \tag{3-78}$$

Jelesnianski (1972) applied the scheme to the 43 storms given by Harris
(1959) that entered land south of New England during the period from 1893
to 1957. The peak surges reported by Harris are plotted against the peak
surges predicted by the nomograph method in Figure 3-55. The two-
dimensional hurricane model and storm surge prediction model described by
Jelesnianski (1967) was used for all calcualtions without adjustment for
local variations in friction coefficient or other efforts to calibrate
the model for individual storms. For many of the hurricanes, the post-
storm surveys conducted were of limited scope and probably did not disclose
the true peak surge. Thus, at least a part of the spread between observed
and computed values must be due to the observed data. In addition to the
peak surge, other nomograms for computing other storm surge parameters are
given by Jelesnianski (1967).

An example problem illustrating the use of the nomogram method follows:

* * * * * * * * * * * * * *   EXAMPLE PROBLEM   * * * * * * * * * * * * * * *

GIVEN: Parameters for Hurricane Camille are:

$$\Delta p = 3.19 \text{ inches of mercury (in. Hg.)}$$

$$V_F = 13 \text{ knots}$$

$$R = 14 \text{ nautical miles (n.m.)}$$

FIND: Estimate peak open-coast surge produced by Hurricane Camille.

Figure 3-52. Shoaling Factors on Gulf Coast
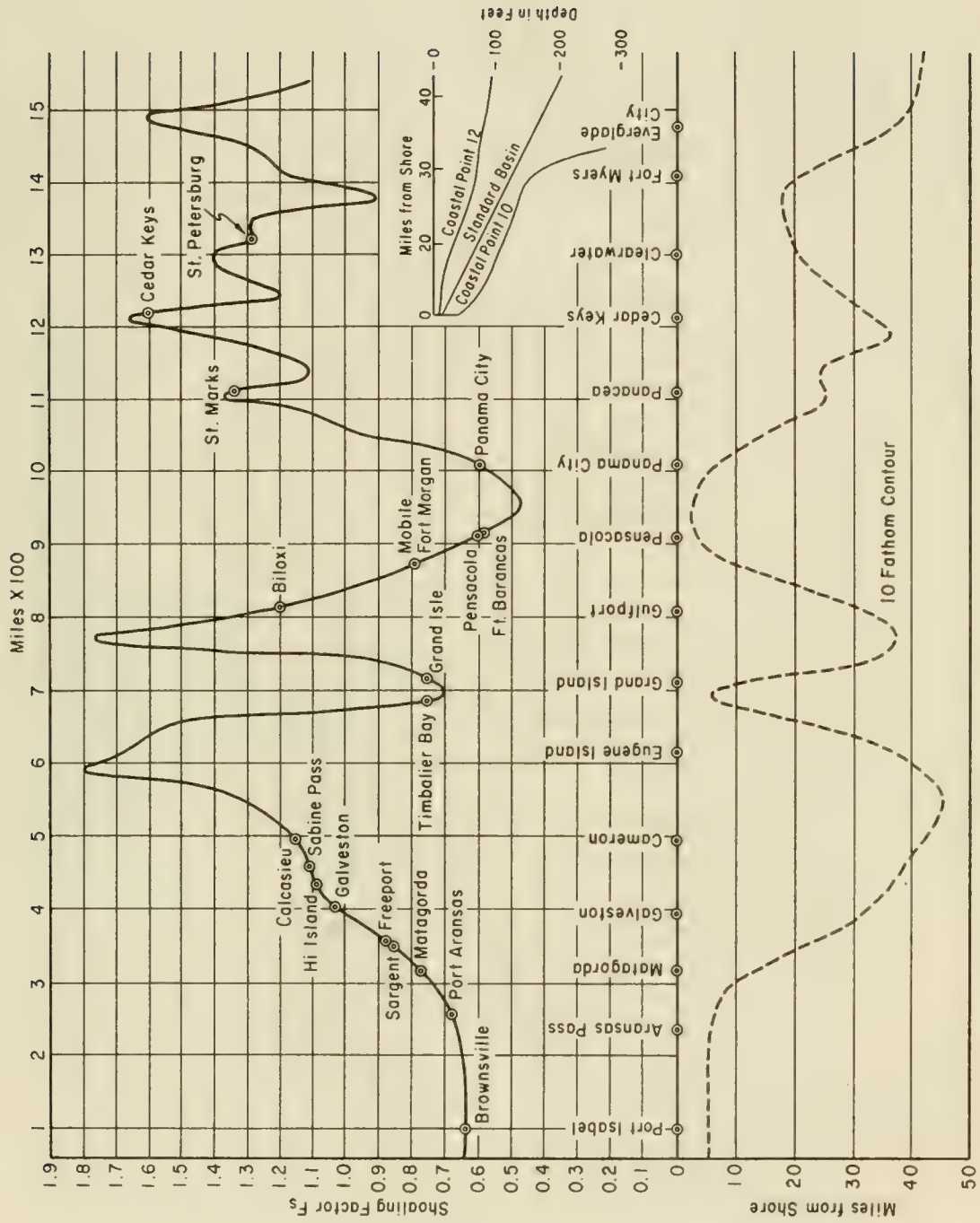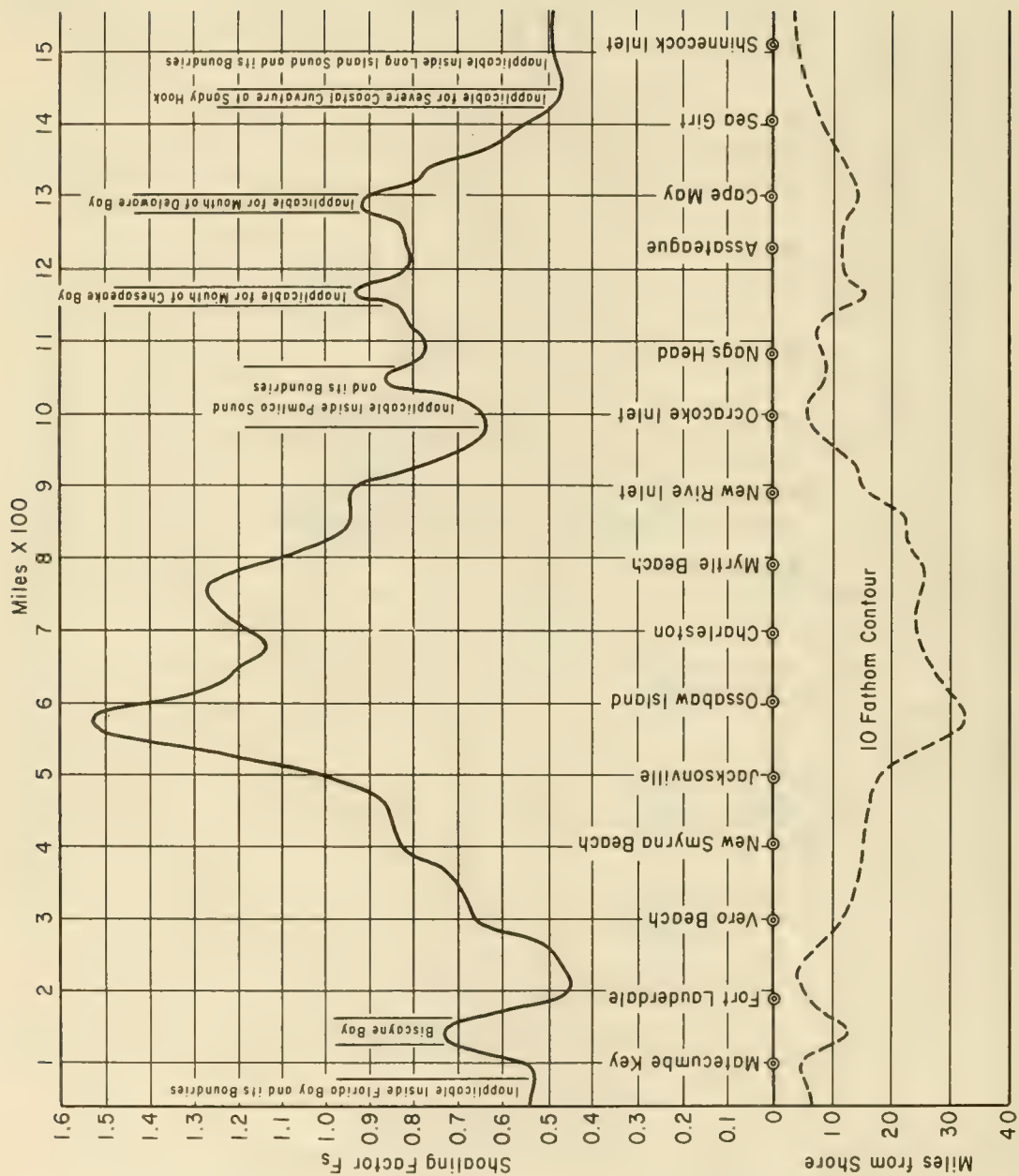
(Jelesnianski, 1972)

Figure 3-53. Shoaling Factors on East Coast

(Jelesnianski, 1972)

3-122

Figure 3-54. Correction Factor for Storm Motion

(from Jelesnianski, 1972)

3-123
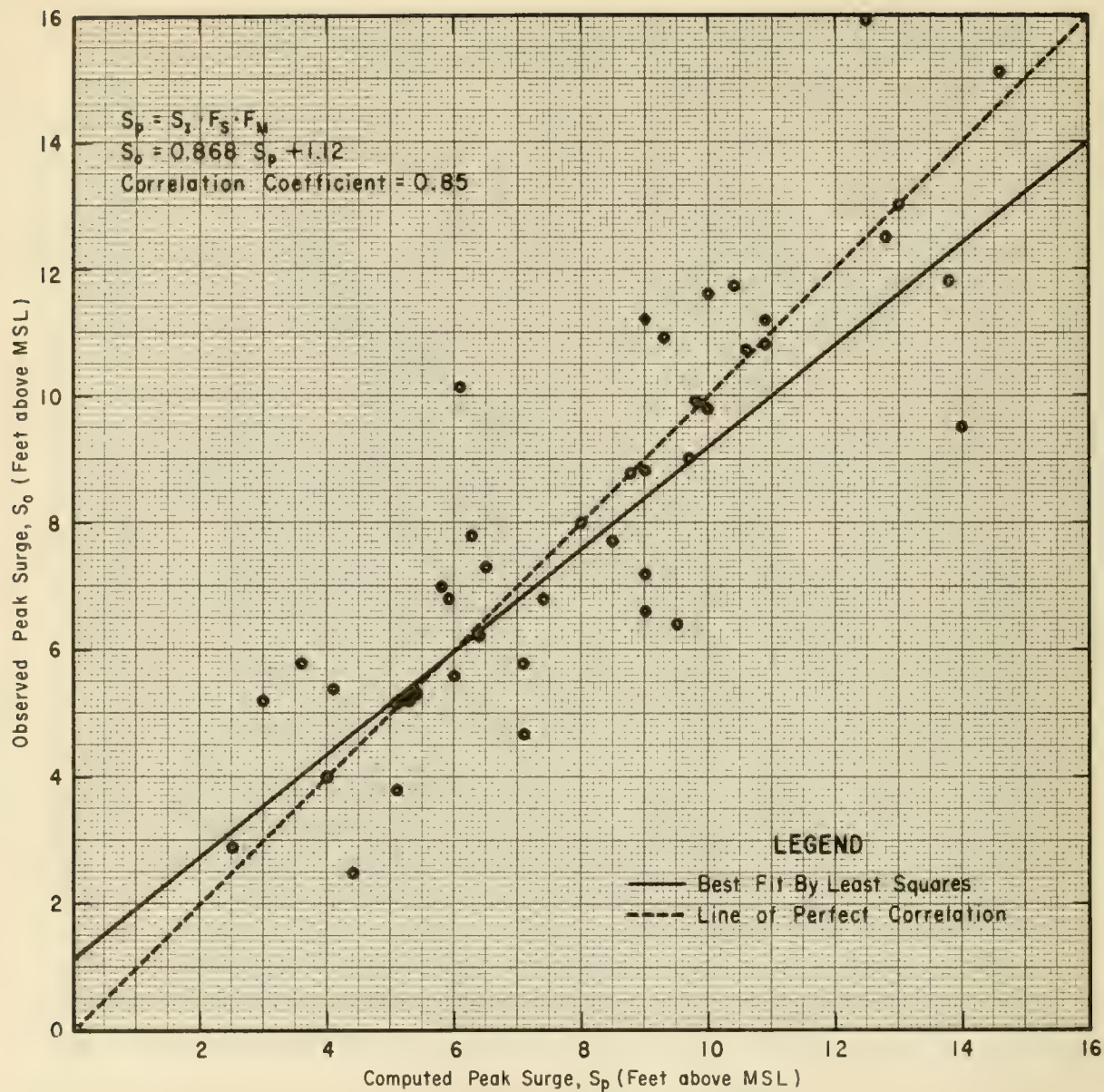
Figure 3-55. Comparison of Observed and Computed Peak Surges
(for 43 storms with a landfall south of New England
from 1893-1957)

3-124

SOLUTION: Because of the units used in the various nomograms, the units of the parameters are converted to

$$\Delta p = 3.19 \text{ in. Hg.} = \frac{3.19\,(1000)}{29.53} = 108 \text{ millibars .}$$

Note: 29.53 inches of Hg. $\approx$ 1000 millibars

$$V_F = 13 \text{ knots} \approx 14.5 \text{ mph}$$

$$R = 14 \text{ n.m.} \approx 15.6 \text{ miles.}$$

Using Figure 3-51 with values of Δp and R,

$$S_I \approx 22 \text{ feet (MSL)}$$

Based on the approximate landfall location (west of Biloxi) of Hurricane Camille (Fig. 3-47), the shoaling factor F_s is determined from Figure 3-52.

$$F_s \approx 1.23 \text{ .}$$

To evaluate the correction for storm motion F_M the angle of storm approach to the coast ψ must be first determined. The definition of the angle ψ is shown schematically in the insert in Figure 3-54. From Figure 3-47 ψ is estimated to be 102°. From Figure 3-54 for $\psi = 102°$ and $V_F = 14.5$ mph,

$$F_M \approx 0.97 \text{ .}$$

The peak surge given by Equation 3-78

$$S_p = S_I \, F_S \, F_M$$

$$S_p = (22)\,(1.23)\,(0.97)$$

$$S_p = 26.2 \text{ feet, say } 26 \text{ feet (MSL)}$$

3-125

Jelesnianski (1972) has calculated the open coast surge for Hurricane Camille with a full two-dimensional mathematical model. The maximum surge envelope along the coast, based on computations from this model, is shown in Figure 3-56 where the zero distance corresponds to the point of landfall of the hurricane eye. This figure shows that the peak surge estimated by this method is about 25+ feet MSL.

Thus, by three independent estimates, it has been found that the peak surge is about 25 feet MSL which corresponds approximately to that observed (U.S. Geological Survey) at Pass Christian, Mississippi of 24.2 feet MSL. It would be expected that a slightly higher peak water elevation occurred because Pass Christian is located a few miles left of the position where the maximum winds made landfall.

It is rare that such a close agreement is found when estimating the peak surge with these dissimilar models. Normally, because of the difference in these predictive schemes, it can be expected that peak surge estimates may deviate by as much as 25 percent. For well-formulated schemes properly applied, there is usually a trade-off between reliability of the estimate and the computational effort.

* *

(c) <u>Predicting Surge for Storms other than Hurricanes.</u> Although the basic equations for water motion in response to atmospheric stresses are equally valid for nonhurricane tropical and extratropical storms, the structures of these storms are not nearly so simple as that of a hurricane. Because the storms display much greater variability in structure, it is difficult to derive a proper wind field. Moreover, no system of classifying these storms by parameters has been developed similar to hurricane classification by such parameters as radius to maximum winds, forward motion of the storm center, and central pressure.

Criteria however have been established for a Standard Project Northeaster for the New England coast north of Cape Cod as given by Peterson and Goodyear (1964). Specific standard-project storms other than hurricanes are not presently available for other coastal locations. Estimates of design-storm wind fields can be made by meteorologists working directly with climatological weather maps, and by use of statistical wind records on land and assuming that they blow toward shore for a significant duration over a long, straight line fetch.

Once the wind field is determined, estimation of the storm surge may be determined by methods based on the complete basic formulas or the quasi-static method given. The nomogram method cannot be used, since this scheme is based on the hurricane parameters.

(2) <u>Storm Surge in Enclosed Basins.</u> An example of an inclined water surface caused by wind shearing stresses over an enclosed body of water occurred during passage of the hurricane of 26-27 August 1949 over the northern part of Lake Okeechobee, Florida. After the lake level was inclined by the wind, the wind direction shifted 180° in 3 hours, resulting

3-126
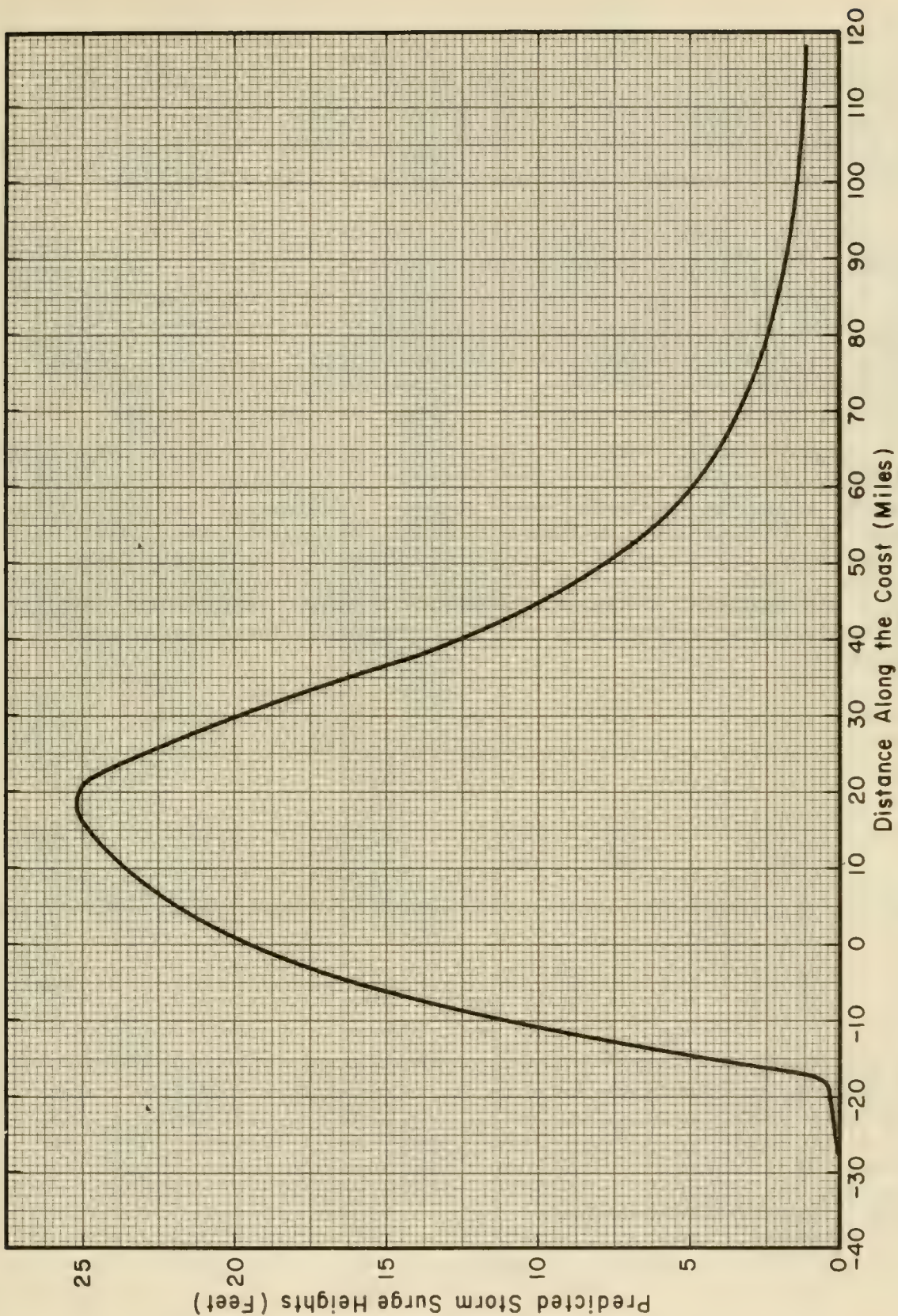
Figure 3-56. Surge Profile Along Coast. Hurricane Camille, August 1969. Zero distance represents point of landfall.

3-127

in a turning of the height contours of the lake surface. However, the turning of the contours lagged behind the wind so that for a time the wind blew parallel to the water level contours instead of perpendicular to them. Contour lines of the lake surface from 1800 hours on 26 August to 0600 hours on 27 August 1949 are shown in Figure 3-57. The map contours for 2300 hours on 26 August show the wind blowing parallel to the highest contours at two locations. (Haurwitz, 1951), (Saville, 1952), (Sibul, 1955), (Tickner, 1957), and (U.S. Army, Corps of Engineers, 1955).)

Recorded examples of wind setup on the Great Lakes are available from the U.S. Lake Survey, National Ocean Survey, and NOAA. These observations have been used for the development of theoretical methods for forecasting water levels during approaching storms and for the planning and design of engineering works. As a result of the need to predict unusually high stages on the Great Lakes, numerous theoretical investigations have been made of wind setup for that area. (Harris, 1953), (Harris and Angelo, 1962), (Platzman and Rao, 1963), (Jelesnianski, 1958), (Irish and Platzman, 1962), and (Platzman, 1958, 1963, 1965, and 1967).)

Water level variations in an enclosed basin cannot be estimated satisfactorily if a basin is irregularly shaped, or if natural barriers such as islands affect the horizontal water motions. However, if the basin is simple in shape and long compared to width, then water level elevations may be reasonably calculated using the hydrodynamic equations in one dimension. Thus if the motion is considered only along the x-axis (major axis), and advection of momentum, pressure deficit, astronomical effects and precipitation effects are neglected, then Equations 3-50 and 3-52 reduce to

$$\frac{\partial U}{\partial t} = -gD\frac{\partial S}{\partial x} + \frac{1}{\rho}\left(\tau_s - \tau_b\right) \qquad (3\text{-}79)$$

$$\frac{\partial S}{\partial t} = -\frac{\partial U}{\partial x} \qquad (3\text{-}80)$$

If it is further assumed that steady state exists, then Equation 3-79 becomes

$$\frac{dS}{dx} = \frac{1}{\rho gD}\left(\tau_s + \tau_b\right) \qquad (3\text{-}81)$$

The bottom stress is taken in the same direction as the wind stress, since for equilibrium conditions the flow near the bottom is opposite to flow induced by winds in the upper layers. Theoretical development of this wind setup equation was given by Hellstrom (1941), Keulegan (1951), and others. The mechanics of the various determinations have differed somewhat, but the resultant equation has been about the same. This wind setup equation is expressed as:

$$\Delta S = \frac{k'n\rho_a W^2 F}{\rho gD}\cos\theta \qquad (3\text{-}82)$$

3-128
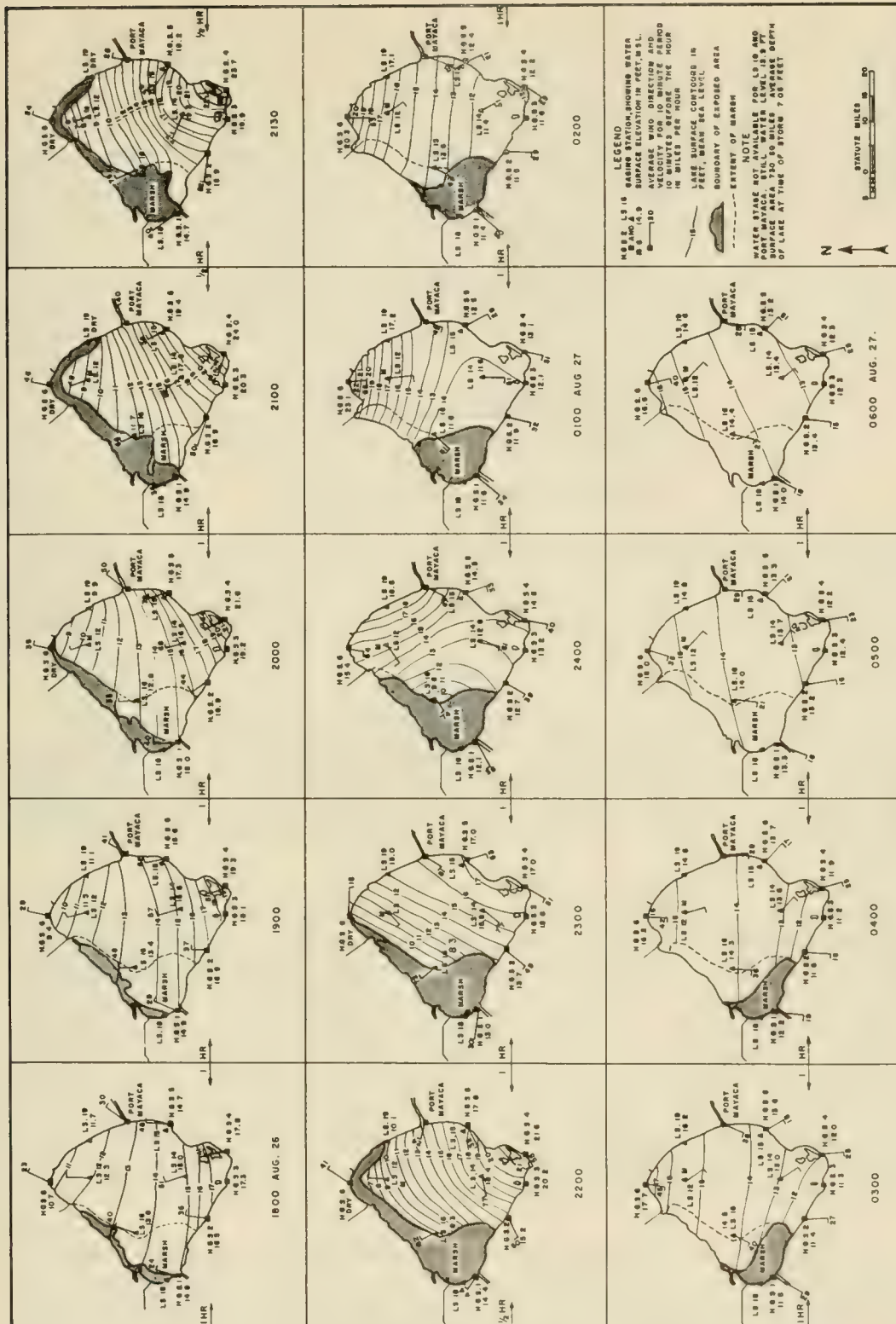
Figure 3-57. Lake Surface Contours on Lake Okeechobee, Florida. Hurricane, 26-27 August 1949.

(U.S. Army C of E, 1955)

where

$$k' = \text{a numerical constant} \approx 0.003$$

ρ_α = air density

W = Wind velocity

F = Fetch length

θ = angle between wind and the fetch

$n = 1 + \tau s/\tau b; \quad 1.15 \leq n \leq 1.30$

ΔS = Wind setup. This value represents
the difference in water level
between the two ends of the fetch

D = average depth of the fetch.

An approximate expression of Equation 3-82 is given by

$$\Delta S = \frac{CW^2 F}{D} \cos \theta \qquad (3-83)$$

where C is a coefficient having dimensions of time squared per unit
length. Saville (1952) in a comprehensive investigation of setup data
obtained from Lake Okeechobee found that C is approximately 1.165×10^{-3}
when W is given miles per hour, F in miles and D and ΔS in feet.
This coefficient is almost identical with that of the Netherlands Zuider
Zee formula (1.25×10^{-3}).

Equation 3-83 is often useful in making the first approximation of
the setup in an enclosed basin. Its advantage is that the setup can be
evaluated with fewer computations. The surge can be estimated more satis-
factorily by segmenting an enclosed basin into reaches and using a numeri-
cal integration procedure to solve Equation 3-81 for the various reaches
in the basin. Bretschneider (Ippen, 1966) presented solutions in parameter
form for Equation 3-81, and compiled these solutions in tables for different
conditions. These tables can be used to estimate the storm surge for a
rectangular channel of constant depth with either an exposed bottom or a
nonexposed bottom and a basin of regular shape. Such solutions may provide
an estimate of the water level variation in some basins.

A more complete scheme than those described above follows. This
method accounts for the time dependence of the problem; more specifically
Equations 3-79 and 3-80 are used. Although this more complete method
provides a better approximation of the surge problem, it is done at the
expense of increasing the computations.

When a basin enclosed with vertical sides has a well-defined major axis and a gradually varying cross section, it is possible to use a dynamic one-dimensional, computational model for evaluating fluctuations in water level resulting from a forcing mechanism such as wind stress, and also to account for some of the effects of a varying cross section. The validity of such a model depends on the behavior of the storm system and the geometric configuration of the basin.

Equations 3-79 and 3-80, when the varying width b of the basin is introduced, can be written in terms of the volume flow rate $Q(x,t)$ as

$$\frac{\partial Q}{\partial t} = - gA \frac{\partial S}{\partial x} + \frac{b}{\rho} \left(\tau_s - \tau_b\right) \qquad (3\text{-}84)$$

$$\frac{\partial S}{\partial t} = - \frac{1}{b} \frac{\partial Q}{\partial x} \qquad (3\text{-}85)$$

where x is taken along the major axis of the basin, and for any time t, A is the cross-section area, and D is the average depth A/b or D = d + S.

Various schemes have been proposed for evaluating the water level changes in an enclosed body of water by using the differential equations. (Equations 3-84 and 3-85.) The formulation of the problem and the numerical scheme given here is from Bodine, Herchenroder and Harris (1972).

The surface stress and bottom stress terms are taken identical to the terms given for the quasi-static method for open-coast surge. (See Equations 3-55 and 3-56, Section 3-865b(1)(a).) The stress terms, in terms of the volume flow rate, become

$$\frac{\tau_b}{\rho} = \frac{KQ|Q|}{(Db)^2} \qquad (3\text{-}86)$$

$$\frac{\tau_s}{\rho} = kWW_x = kW^2 \cos \theta \qquad (3\text{-}87)$$

Substituting Equations 3-86 and 3-87 into Equation 3-84 gives

$$\frac{\partial Q}{\partial t} = bkWW_x - gA \frac{\partial S}{\partial x} - \frac{KQ|Q|}{D^2 b} \qquad (3\text{-}88)$$

A finite difference representation of Equations 3-88 and 3-85 may be expressed in the form

$$Q_{i+1}^{n+1} = \frac{1}{G} \left[Q_{i+1}^{n} + \frac{\Delta t}{2} \left(b_{i+\frac{1}{2}} + b_{i+\frac{3}{2}} \right) \left(kW^2 \cos \theta \right)_{i+1}^{n+1} \right.$$

$$\left. + \frac{g\Delta t}{2\Delta x} \left(A_{i+\frac{1}{2}} + A_{i+\frac{3}{2}} \right)^{n} \left(S_{i+\frac{1}{2}} - S_{i+\frac{3}{2}} \right)^{n} \right]$$

(3-89)

$$S_{i+\frac{1}{2}}^{n+1} = S_{i+\frac{1}{2}}^{n} + \frac{\Delta t}{\Delta x\, b_{i+\frac{1}{2}}} \left(Q_i - Q_{i+1} \right)^{n+1}$$

(3-90)

where,

$$G = 1 + \frac{4K\Delta t\, |Q_{i+1}^{n}|}{\left(D_{i+\frac{1}{2}}^{2} + D_{i+\frac{3}{2}}^{2} \right)^{n} \left(b_{i+\frac{1}{2}} + b_{i+\frac{3}{2}} \right)}$$

(3-91)

The value of G is greater than unity for most flow conditions except for the case when the flow vanishes ($Q = 0$). The subscripts and superscripts i and n are used to denote discrete points in space and time, respectively. A schematic of the grid system used is shown in Figure 3-58. It is seen that S at the new time level $(t + \Delta t)$ is first evaluated based on the known values of Q, D, S, A and $b(x)$ lying on triangle (1) and subsequently followed by an evaluation of S at the new time level based on known values lying on triangle (2). The solutions at successive time levels are obtained by a marching process with Q evaluated at the new time level for all integer steps along x; S is evaluated for all mid-integer steps along x. Width as a function of x, $b(x)$, is taken constant for all t and the total depth D is permitted to vary with time. Thus the cross-section area of the basin A is a function of distance along the major axis of the basin and a function of time.

The computational scheme is a combined boundary and initial value problem. At each end of the basin, it is assumed that there is no flow across the boundary, thus $Q = 0$ at the boundary. The initial conditions assumed are that $Q = 0$ and S is uniform throughout the basin.

The scheme requires that for numerical stability, the time increment specified for successive calculations Δt be taken less than $\Delta x/\sqrt{gD_{max}}$, where D_{max} is the maximum depth $(d + S)$ anticipated in the basin during passage of a storm system. (Abbott, 1966.)

The restriction imposed by the criterion for numerical stability results in a trade-off between the resolution obtained in the solution and the number of calculations involved. Decreasing Δx gives better resolution of the surge, but requires a smaller Δt and increases the number of computational steps. It is important to choose Δx small enough so that reasonable resolution of the surge is obtained, but large enough to reduce the computations. The choice of a Δx depends on the problem involved.

Figure 3-58. Grid System

(from Bodine, Herchenroder and Harris, 1972)

3-133
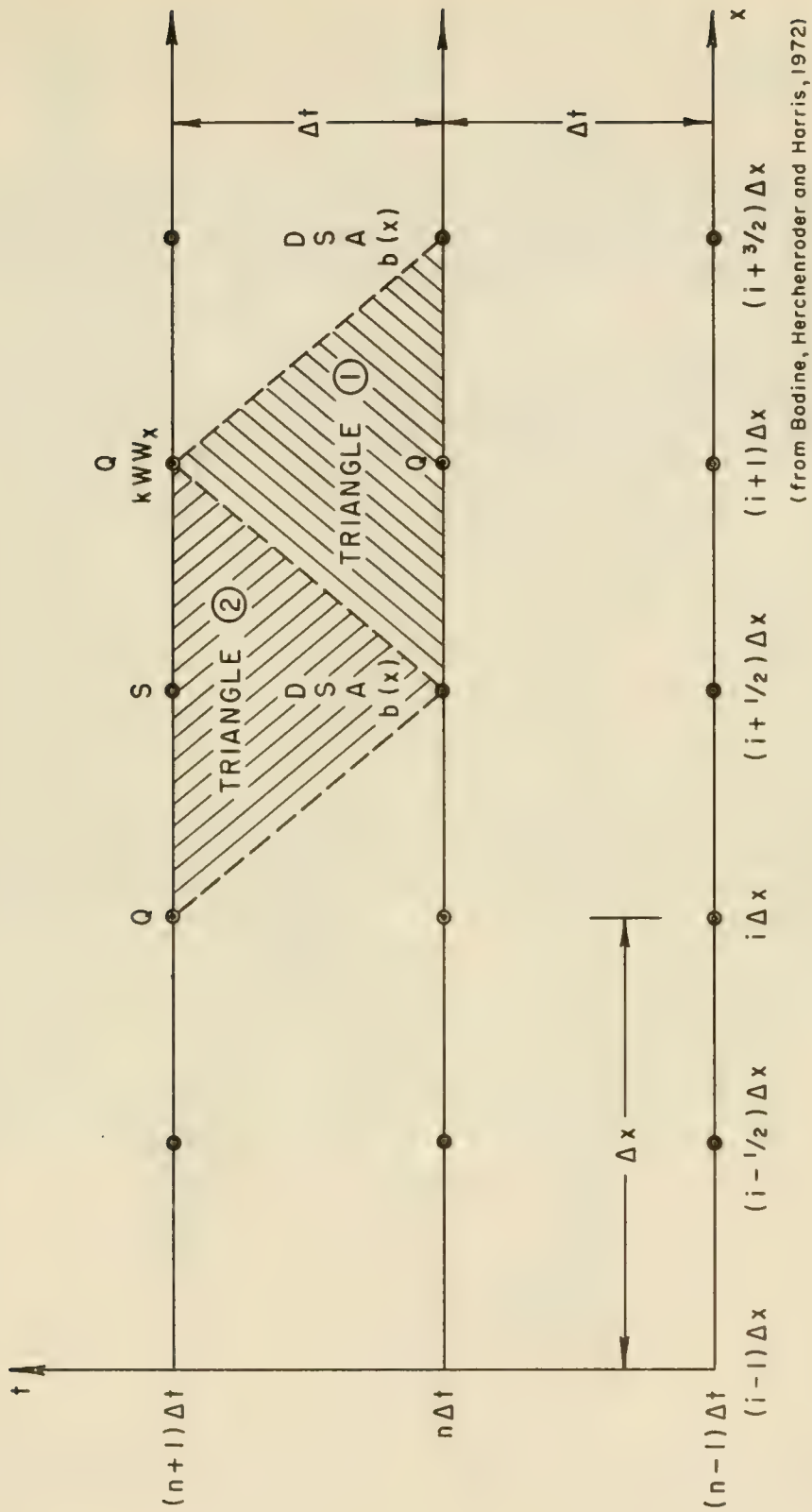
For such a recursive type calculation, computer computations reduce the effort required. However, since this is a one-dimensional formulation of the problem, it is possible to carry out the necessary computations manually.

The March 1955 storm on Lake Erie is used to demonstrate the scheme. A plan view of Lake Erie is shown in Figure 3-59. The width and cross-section area of the Lake are shown in Figure 3-60, mean bottom profile in Figure 3-61, and wind and wind direction data for the March 1955 storm in Figure 3-62.

In the following example problem computations are made at a single spatial point where Q is evaluated at a distance of $3\Delta x$ from Buffalo (Fig. 3-59) at a time when the wind speeds are approximately maximum. Tables similar to Table 3-10 should be used in manual calculations.

* * * * * * * * * * * * * * EXAMPLE PROBLEM * * * * * * * * * * * * * * *

GIVEN:

$$\Delta x = 10 \text{ miles}$$

$$\Delta t = 0.2 \text{ hrs.}$$

$$g = 79000 \text{ mi/hr}^2$$

$$K = 0.003$$

The wind at the new time level is 50.5 miles per hour and $\theta = 4.0°$. The corresponding water surface widths for this section are $b_{i+1/2} = 26.3$ miles and $b_{i+3/2} = 21.0$ miles. The values from preceding calculations at the previous time level are

$$Q_{i+1}^n = 0.0707 \text{ mi}^3/\text{hr.}$$

$$S_{i+1/'2}^n = 3.32 \text{ ft.}$$

$$S_{i+3/2}^n = 3.76 \text{ ft.}$$

$$A_{i+1/2}^n = 0.426 \text{ mi}^2$$

$$A_{i+3/2}^n = 0.278 \text{ mi}^2$$

$$D_{i+1/2}^n = 0.0162 \text{ mi.}$$

$$D_{i+3/2}^n = 0.0132 \text{ mi.}$$

Also required is the value of Q_i^{n+1} from the previous spatial step which is given as +0.0915 mi^3/hr.

Depth in Fathoms

Figure 3-59. Lake Erie

(after Platzman and Rao, 1963)
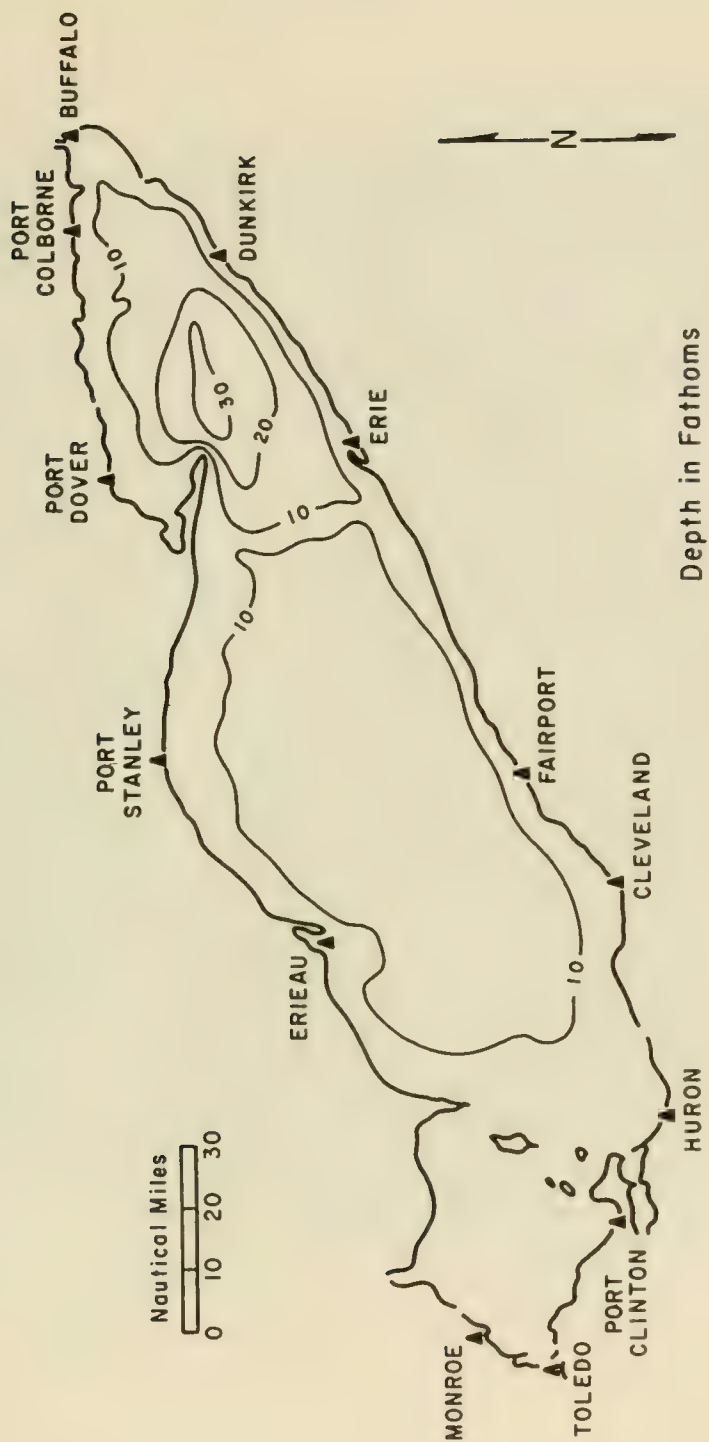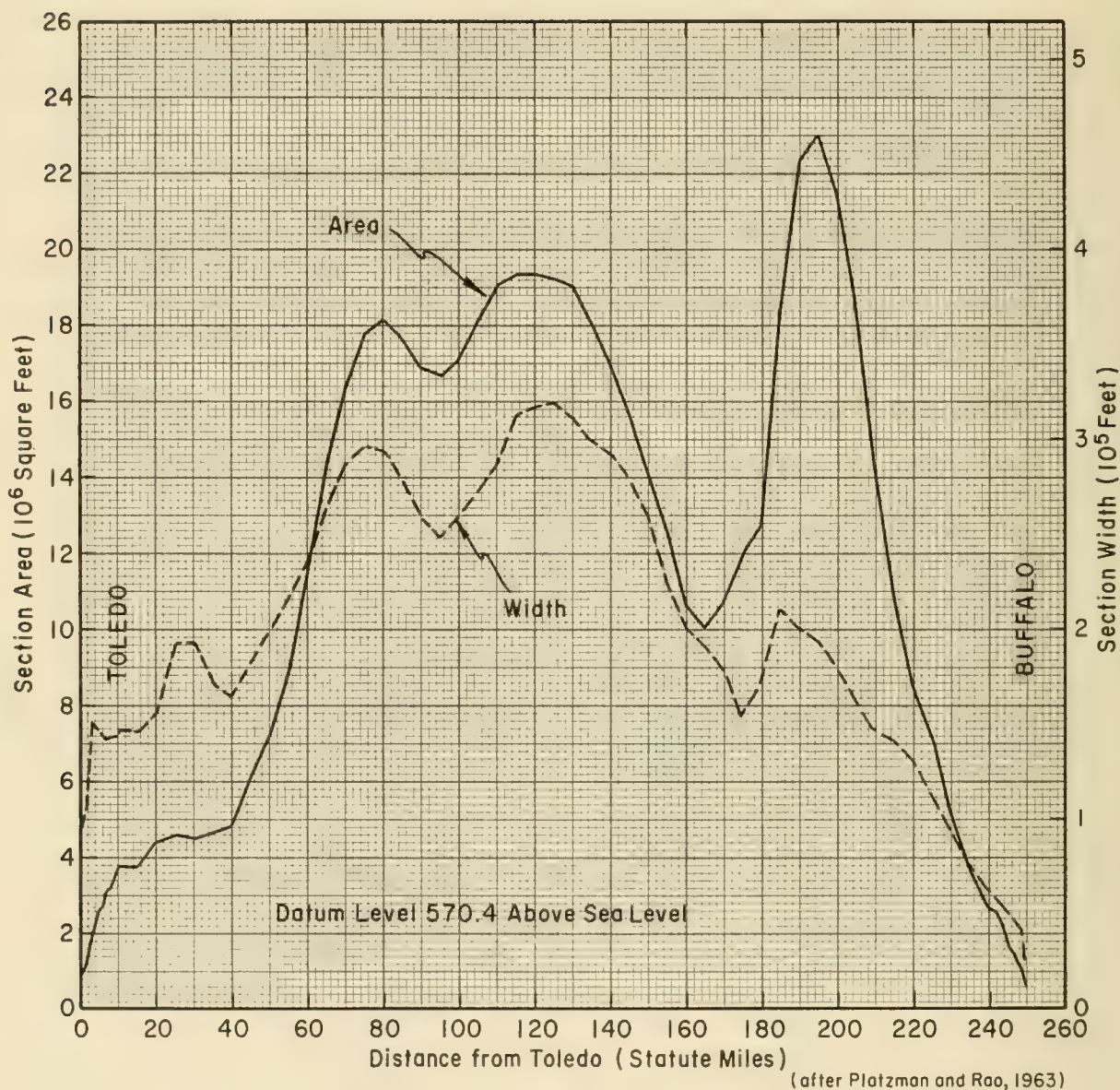
Figure 3-60. Cross-Section Area and Surface Width — Lake Erie

3-136
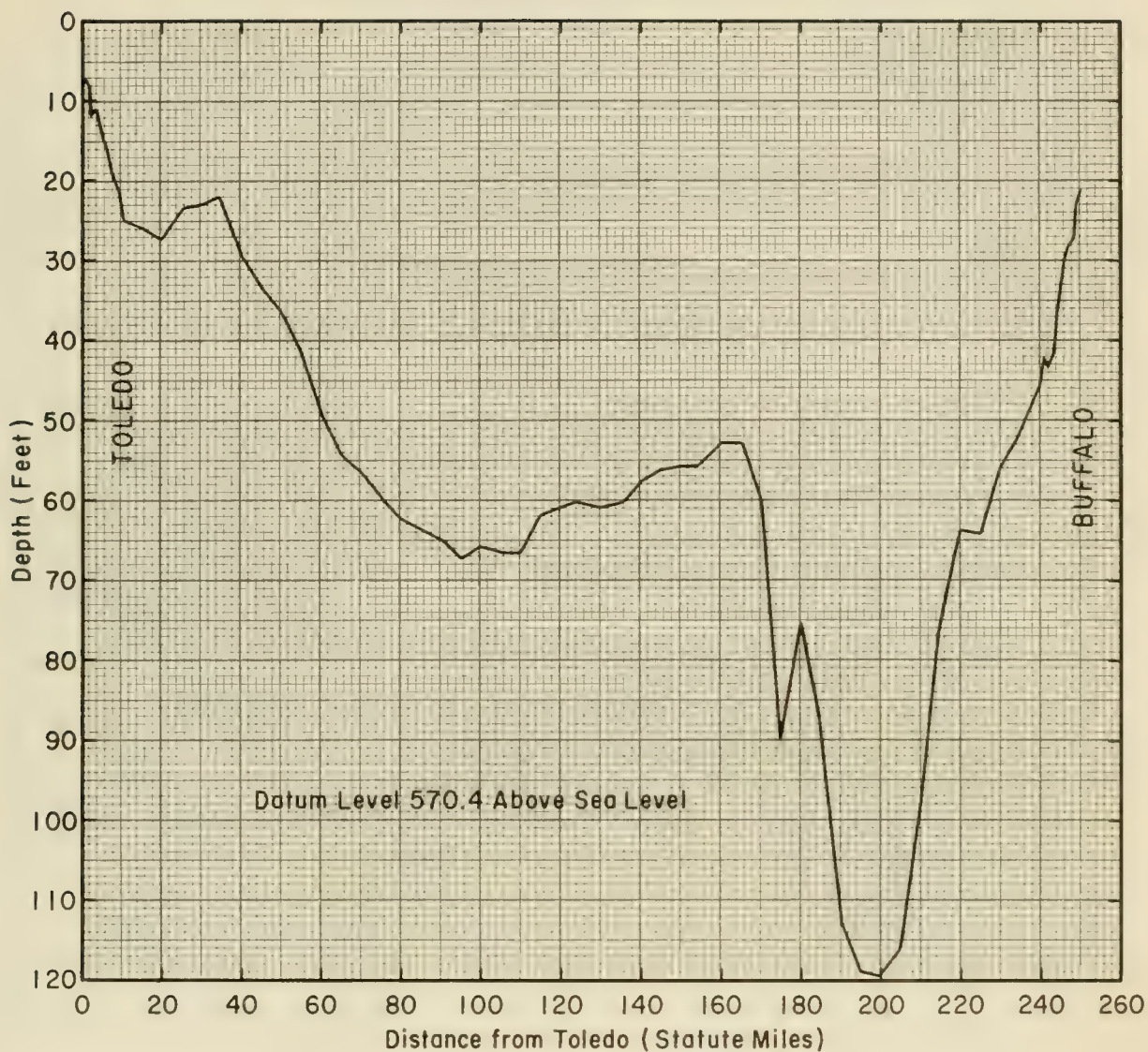
Figure 3-61. Mean Bottom Profile of Lake Erie

3-137
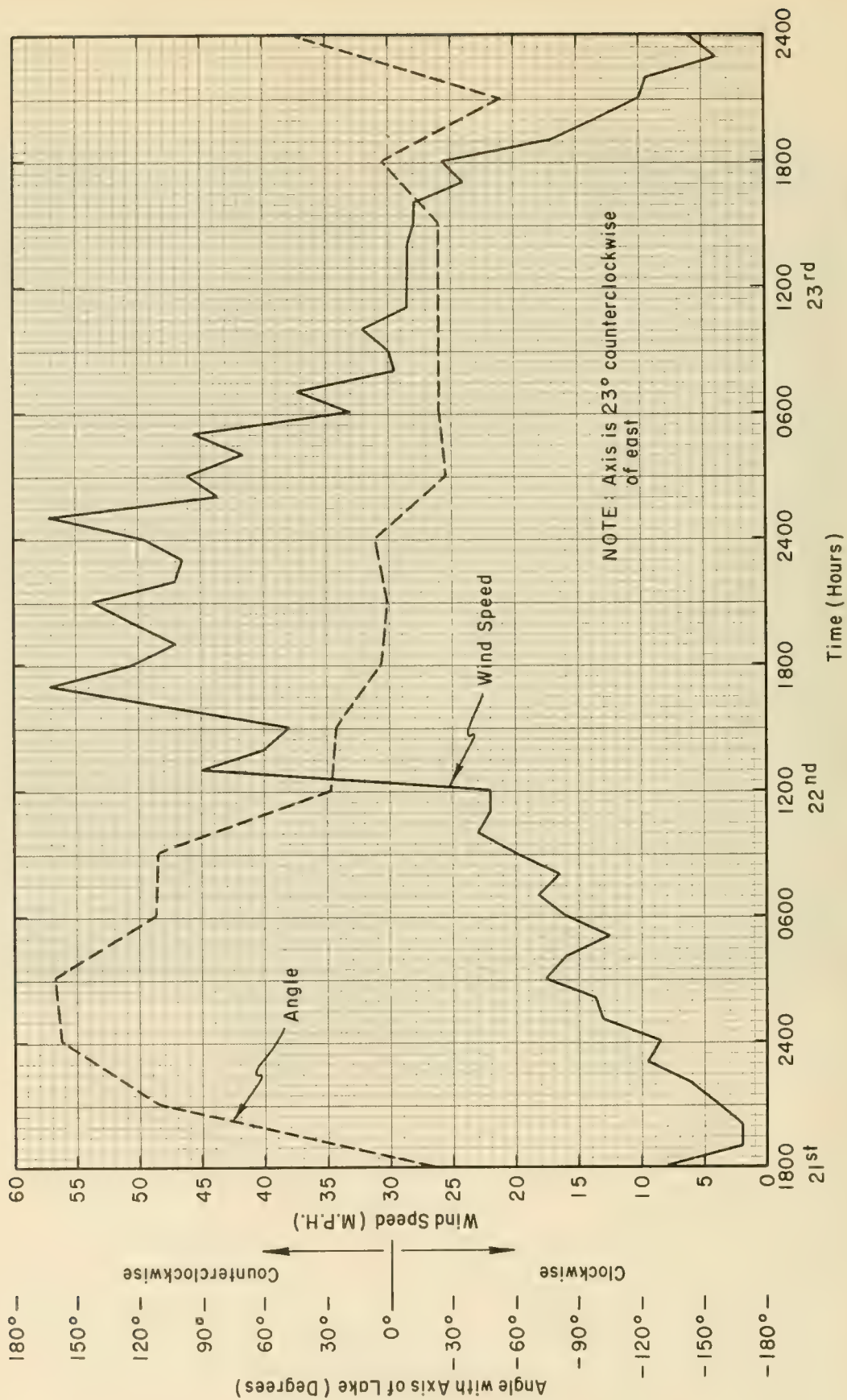
Figure 3-62. Wind Speed and Direction for Lake Erie – Storm, March 1955

3-138

FIND: Wind setup at the new time level.

SOLUTION: The wind stress coefficient given by Equation 3-59 is

$$k = K_1 + K_2 \left(1 - \frac{W_c}{W}\right)^2 = 1.1 \times 10^{-6} + 2.5 \times 10^{-6} \left(1 - \frac{16}{50.5}\right)^2$$

$$= 2.27 \times 10^{-6}$$

From Equation 3-91

$$G = 1 + \frac{4K\Delta t \, |Q_{i+1}^n|}{\left(D_{i+\frac{1}{2}}^2 + D_{i+3/2}^2\right)^n \left(b_{i+\frac{1}{2}} + b_{i+3/2}\right)}$$

$$G = 1 + \frac{4 \, (0.003) \, (0.2) \, | \, 0.0707 \, |}{[(0.0162)^2 + (0.0132)^2] \, (26.3 + 21.0)} = 1.01$$

The two terms needed in the evaluation of Q_{i+1}^{n+1} (Equation 3-89) are given by

$$\frac{\Delta t}{2} \left(b_{i+\frac{1}{2}} + b_{i+3/2}\right) \left(kW^2 \cos \theta\right)_{i+1}^{n+1}$$

$$= \frac{0.2}{2} \, (26.3 + 21.0) \, (2.27 \times 10^{-6}) \, (50.5)^2 \, (1) = 0.0274$$

and

$$\frac{g\Delta t}{2\Delta x} \left(A_{i+\frac{1}{2}} + A_{i+3/2}\right)^n \left(S_{i+\frac{1}{2}} - S_{i+3/2}\right)^n$$

$$= \frac{79,000 \, (0.2) \, (0.426 + 0.278) \, (3.32 - 3.76)}{(2) \, (10) \, (5,280)} = - \, 0.0463$$

The volume flow rate from Equation 3-89 is

$$Q_{i+1}^{n+1} = \frac{1}{1.0129} \, [0.070 + 0.0274 - 0.0463] = 0.0513 \text{ mi}^3 / \text{hr.}$$

3-139

and finally, the water level at this discrete point in space and time is given by Equation 3-90 as

$$S_{i+\frac{1}{2}}^{n+1} = S_{i+\frac{1}{2}}^{n} + \frac{\Delta t}{\Delta x \; b_{i+\frac{1}{2}}} \left(Q_i - Q_{i+1} \right)^{n+1}$$

$$= 3.32 + \frac{(0.2)(0.0915 - 0.0513)(5280)}{(10)(26.3)}$$

$$= 3.48 \text{ feet, say } 3.5 \text{ feet .}$$

The significant digits indicated in the above computations do not reflect the accuracy of the numerical procedure, but are retained to reduce the accumulation of round-off errors.

The wind setup hydrograph for the ends of the lake as determined by computer is shown in Figure 3-63. The storm winds blew in the general direction toward Buffalo at the northeastern end of the lake as indicated by the setdown at Toledo and the setup at Buffalo. The spatial steps Δx taken are quite large; smaller increments in Δx would give a more accurate estimate. Calculations with the mathematical model were initiated with the system in a calm state, i.e., $Q = S = 0$.

The wind setup profile along the major axis of the lake determined by the numerical scheme is shown in Figure 3-64 for three time periods during the storm. The nodal point where the computed water surface crosses the stillwater level occurs near the center of the lake, but this nodal point can vary with time.

Although the comparison of the computed and observed wind setup is not in complete agreement, particularly at the beginning and late stages of the storm, the method gives reasonable results for the wind setup amplitudes. To engineers, it is frequently the maximum departure of the water level from its normal position that is of greatest concern. Results of the simplified model should be interpreted with care, since many of the physical processes which may be significant have been neglected. Wind and bottom stress laws, in particular, are oversimplified for the Lake Erie problem. Better agreement can be expected with two-dimensional schemes such as the one developed by Platzman (1963), since they more accurately model for the physical processes involved.

* *

(3) Storm Surge in Semienclosed Basins. It is generally impossible to make reliable estimates of storm surge in semienclosed basins (bays, and estuaries) with less exact procedures such as those described for specific problems within enclosed basins or on the open coast. This is because bays and estuaries are nearly always irregular in shape, and basin geometry is often further complicated by the presence of islands, navigational channels, and harbors. Moreover, many of these basins have

3-140

NOTE: Calculations were started at 0100 20 March with the lake surface horizontal and no currents. 1800 21 March was used to eliminate start-up transients.
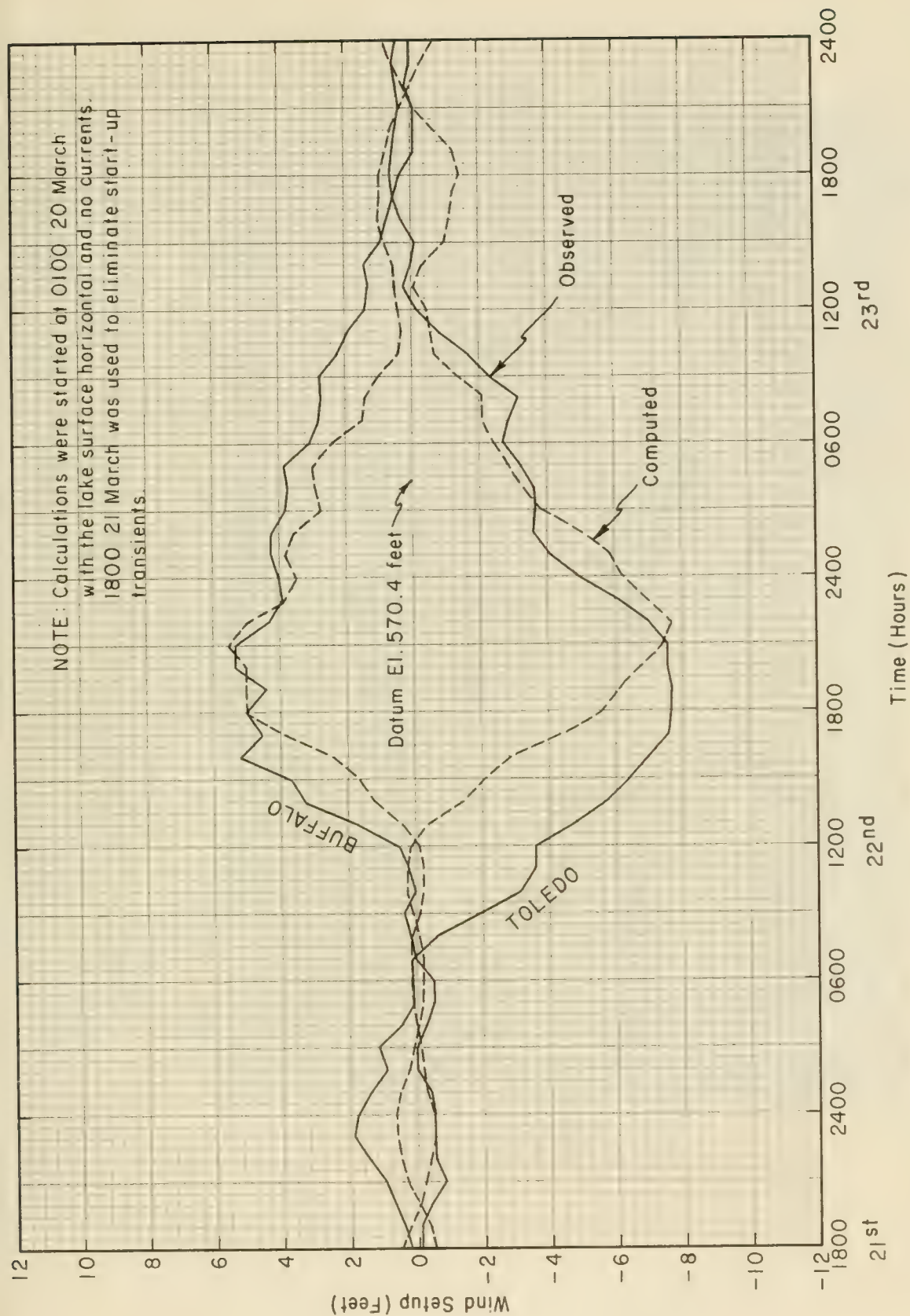
Figure 3-63. Wind Setup Hydrograph for Buffalo and Toledo – Storm, March 1955

3-141
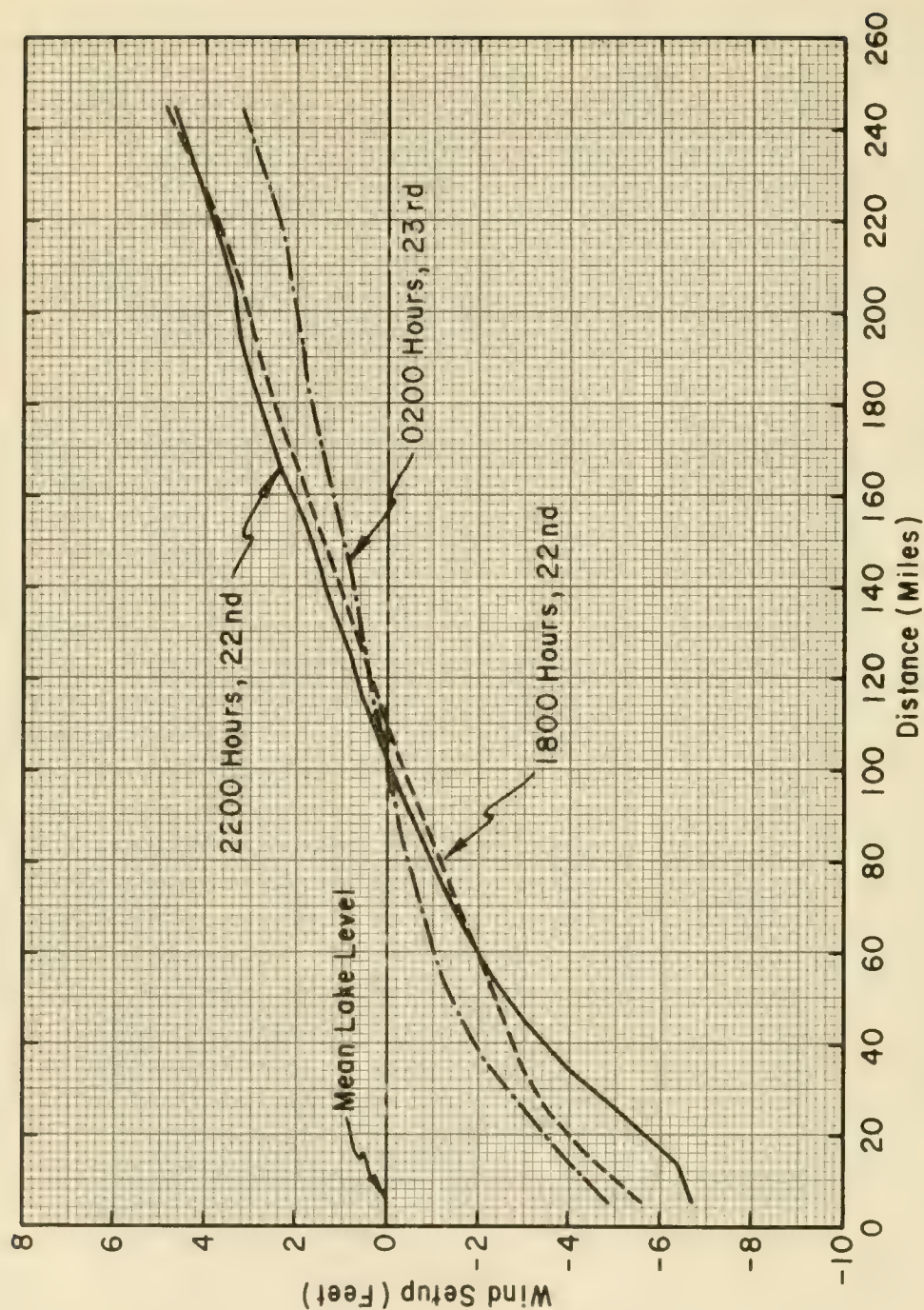
Figure 3-64. Wind Setup Profile for Lake Erie. Storm, March 1955.

extensive low-lying areas surrounding them which may be subject to extensive flooding during severe storm conditions. Also, these basins are usually shallow, and on the windward side of the basin substantial bottom areas can become exposed. Thus, during the passage of a storm system, many semienclosed basins have time-dependent moving boundaries. The water present at any time in a bay or estuary is also dependent upon the sea state because of the interrelation between these two bodies of water. Because of the above characteristics of semienclosed basins, a simplified approach does not usually provide a satisfactory estimate of water motions, and methods based on full two-dimensional dynamic approaches should be employed.

REFERENCES AND SELECTED BIBLIOGRAPHY

ABBOTT, M.B., *An Introduction to the Method of Characteristics*, American Elsevier, New York, 1966, 243 pp.

ARAKAWA, H., and SUDA, K., "Analysis of Winds, Wind Waves, and Swell Over the Sea to the East of Japan During the Typhoon of September 26, 1935," *Monthly Weather Review*, Vol. 81, No. 2, Feb. 1953, pp. 31-37.

BAER, J., "An Experiment in Numerical Forecasting of Deep Water Ocean Waves," Lockheed Missile and Space Co., Sunnyvale, Calif., 1962.

BARNETT, T.P., "On the Generation, Dissipation, and Prediction of Ocean Wind Waves," *Journal of Geophysical Research*, Vol. 73, No. 2, 1968, pp. 531-534.

BATES, C.C., "Utilizations of Wave Forecasting in the Invasions of Normandy, Burma, and Japan," *Annals of the New York Academy of Sciences*, Vol. 51, Art. 3, "Ocean Surface Waves," 1949, pp. 545-572.

BELLAIRE, F.R., "The Modification of Warm Air Moving Over Cold Water," *Proceedings, Eight Conference on Great Lakes Research*, 1965.

BODINE, B.R., "Storm Surge on the Open Coast: Fundamentals and Simplified Prediction," TM-35, U.S. Army, Corps of Engineers, Coastal Engineering Research Center, Washington, D.C., May 1971.

BODINE, B.R., HERCHENRODER, B.E., and HARRIS, D.L., "A Numerical Model for Calculating Storm Surge in a Long Narrow Basin with a Variable Cross Section," Report in preparation, U.S. Army, Corps of Engineers, Coastal Engineering Research Center, Washington, D.C., 1972.

BORGMAN, L.E., "The Extremal Rayleigh Distribution: A Simple Approximation for Maximum Ocean Wave Probabilities in a Hurricane with Varying Intensity," Stat. Lab Report No. 2004, University of Wyoming, Laramie, Wyo., Jan. 1972.

BOWEN, A.J., INMAN, D.L., and SIMMONS, V.P., "Wave 'Setdown' and Set-up," *Journal of Geophysical Research*, Vol. 73, No. 8, 1968.

BRETSCHNEIDER, C.L., "Revised Wave Forecasting Curves and Procedures," Unpublished Manuscript, Institute of Engineering Research, University of California, Berkeley, Calif., 1951.

BRETSCHNEIDER, C.L. "Revised Wave Forecasting Relationships," *Proceedings of the Second Conference on Coastal Engineering*, ASCE, Council on Wave Research, 1952a.

BRETSCHNEIDER, C.L., "The Generation and Decay of Wind Waves in Deep Water," *Transactions of the American Geophysical Union*, Vol. 33, 1952b, pp. 381-389.

BRETSCHNEIDER, C.L., "Hurricane Design-Wave Practice," *Journal of the Waterways and Harbors Division*, ASCE, Vol. 83, WW2, No. 1238, 1957.

BRETSCHNEIDER, C.L., "Revisions in Wave Forecasting; Deep and Shallow Water," *Proceedings of the Sixth Conference on Coastal Engineering*, ASCE, Council on Wave Research, 1958.

BRETSCHNEIDER, C.L., "Wave Variability and Wave Spectra for Wind-Generated Gravity Waves," TM-118, U.S. Army, Corps of Engineers, Beach Erosion Board, Washington, D.C., Aug. 1959.

BRETSCHNEIDER, C.L., "A One Dimensional Gravity Wave Spectrum," *Ocean Wave Spectra*, Prentice-Hall, New York, 1963.

BRETSCHNEIDER, C.L., "Investigation of the Statistics of Wave Heights," *Journal of the Waterways and Harbors Division*, ASCE, Vol. 90, No. WW1, 1964, pp. 153-166.

BRETSCHNEIDER, C.L., "Generation of Waves by Wind; State of the Art," Report SN-134-6, National Engineering Science Co., Washington, D.C., 1965.

BRETSCHNEIDER, C.L., Department of Ocean Engineering, University of Hawaii, Honolulu, Hawaii, Consultations, 1970-71.

BRETSCHNEIDER, C.L., "A Non-Dimensional Stationary Hurricane Wave Model," *Offshore Technology Conference*, Preprint No. OTC 1517, Houston, Tex., May, 1972.

BRETSCHNEIDER, C.L., and COLLINS, J.I., "Prediction of Hurricane Surge; An Investigation for Corpus Christi, Texas and Vicinity," Technical Report No. SN-120, National Engineering Science Co., Washington, D.C., 1963. (for U.S. Army Engineering District, Galveston, Tex.)

BRETSCHNEIDER, C.L., and REID, R.O., "Change in Wave Height Due to Bottom Friction, Percolation and Refraction," *34th Annual Meeting of American Geophysical Union*, 1953.

BUNTING, D.C., "Evaluating Forecasts of Ocean-Wave Spectra," *Journal of Geophysical Research*, Vol. 75, No. 21, 1970, pp. 4131-4143.

BUNTING, D.C., and MOSKOWITZ, L.I., "An Evaluation of a Computerized Numerical Wave Prediction Model for the North Atlantic Ocean," Technical Report No. TR 209, U.S. Naval Oceanographic Office, Washington, D.C., 1970.

CHRYSTAL, G., "Some Results in the Mathematical Theory of Seiches," *Proceedings of the Royal Society of Edinburgh*, Session 1903-04, Robert Grant and Son, London, Vol. XXV, Part 4, 1904, pp. 328-337.

CHRYSTAL, G., "On the Hydrodynamical Theory of Seiches, with a Bibliographical Sketch," *Transactions of the Royal Society of Edinburgh*, Robert Grant and Son, London, Vol. XLI, Part 3, No. 25, 1905.

COLE, A.L., "Wave Hindcasts vs Recorded Waves," Supplement No. 1 to Final Report 06768, Department of Meteorology and Oceanography, University of Michigan, Ann Arbor, Mich., 1967.

COLLINS, J.I., and VIEHMAN, M.J., "A Simplified Empirical Model for Hurricane Wind Fields," *Offshore Technology Conference*, Vol. 1, Preprints, Houston, Tex., Apr. 1971.

CONNER, W.C., KRAFT, R.H., and HARRIS, D.L., "Empirical Methods of Forecasting the Maximum Storm Tide Due to Hurricanes and Other Tropical Storms," *Monthly Weather Review*, Vol. 85, No. 4, Apr. 1957, pp. 113-116.

COX, D.C., ed., *Proceedings of the Tsunami Meetings Associated with the 10th Pacific Science Congress*, Honolulu, Hawaii, 1961.

DARWIN, G.H., *The Tides and Kindred Phenomena in the Solar System*, W.H. Freeman, San Francisco, 1962, 378 pp.

DAWSON, W. BELL, "The Tides and Tidal Streams," Department of Naval Services, Ottawa, 1920.

DEFANT. A., "Gezeitlichen Probleme des Meeres in Landnähe," *Probleme der Kosmischen Physik*, VI, Hamburg, 1925.

DEFANT, A., *Ebbe und Flut des Meeres, der Atmosphare, und der Erdfeste*, Springer, Berlin-Gottingen-Heidelberg, 1953.

DEFANT, A., *Physical Oceanography*, Vol. 2, Pergamon Press, New York, 1961, 598 pp.

DOODSON, A.T., and WARBURG, H.D., *Admiralty Manual of Tides*, Her Majesty's Stationery Office, London, 1941, 270 pp.

DORRESTEIN, R., "Wave Setup on a Beach," *Proceedings, Second Technical Conference on Hurricanes*, National Hurricane Research Report No. 50, 1962, pp. 230-241.

DRAPER, L., "The Analysis and Presentation of Wave Data - A Plea for Uniformity," *Proceedings of the 10th Conference on Coastal Engineering*, ASCE, New York, 1967.

DUNN, G.E., and MILLER, B.I., *Atlantic Hurricanes*, Rev. ed., Louisiana State University Press, New Orleans, 1964.

EWING, J.A., "The Generation and Propagation of Sea Waves," *Dynamic Waves in Civil Engineering*, Wiley, New York, 1971, pp. 43-56.

EWING, M., PRESS, F., and DONN, W.L., "An Explanation of the Lake Michigan Wave of 26 June, 1954," *Science*, Vol. 120, 1954, pp. 684-686.

FAIRCHILD, J.C., "Model Study of Wave Setup Induced by Hurricane Waves at Narragansett Pier, Rhode Island," *The Bulletin of the Beach Erosion Board*, Vol. 12, July 1958, pp. 9-20.

FORTAK, H., "Concerning the General Vertically Averaged Hydrodynamic Equations with Respect to Basic Storm Surge Equations," National Hurricane Research Project, Report No. 51, U.S. Weather Bureau, Washington, D.C. 1962.

FRANCIS, G.W., "Weather Routing Procedures in the United States," *The Marine Observer*, Vol. XLI, No. 232, Apr. 1971.

FREEMAN, J.C., JR., BAER, L., and JUNG, C.H., "The Bathystrophic Storm Tide," *Journal of Marine Research*, Vol. 16, No. 1, 1957.

GALVIN, C.J., JR., and EAGLESON, P.S., "Experimental Study of Longshore Currents on a Plane Beach," TM-10, U.S. Army, Corps of Engineers, Coastal Engineering Research Center, Washington, D.C., Jan. 1965.

GOODKNIGHT, R.C., and RUSSELL, T.L., "Investigation of the Statistics of Wave Heights," *Journal of the Waterways and Harbors Division*, ASCE, Vol. 89, No. WW2, Proc. Paper 3524, May 1963, pp. 29-54.

GRAHAM, H.E., and NUNN, D.E., "Meteorological Considerations Pertinent to Standard Project Hurricane, Atlantic and Gulf Coasts of the United States," National Hurricane Research Project, Report No. 33, U.S. Weather Bureau, Washington, D.C., 1959.

GROVES, G.W., *McGraw-Hill Encyclopedia of Science and Technology*, McGraw-Hill, New York, 1960, pp. 632-640.

GUTHRIE, R.C., "A Study of Ocean Wave Spectra for Relation to Ships Bending Stresses," Informal Report No. IR 71-12, U.S. Naval Oceanographic Office, Washington, D.C., 1971.

HARRIS, R.A., "Currents, Shallow-Water Tides, Meteorological Tides, and Miscellaneous Matters", *Manual of Tides*, Part V, App. 6, Superintendent of the Coast and Geodetic Survey, Washington, D.C., 1907.

HARRIS, D.L. "Wind Tide and Seiches in the Great Lakes," *Proceedings of the Fourth Conference on Coastal Engineering*, ASCE, 1953, pp. 25-51.

HARRIS, D.L., "The Effect of a Moving Pressure Disturbance on the Water Level in a Lake," *Meteorological Monographs*, Vol. 2, No. 10, "Interaction of Sea & Atmosphere: a Group of Contributions," 1957, pp. 46-57.

HARRIS, D.L., "Meteorological Aspects of Storm Surge Generation," *Journal of the Hydraulics Division*, ASCE, No. HY7, Paper 1859, 1958, 25 pp.

HARRIS, D.L., "An Interim Hurricane Storm Surge Forecasting Guide," National Hurricane Research Project, Report No. 32, U.S. Weather Bureau, Washington, D.C., 1959.

HARRIS, D.L., "Wave Patterns in Tropical Cyclones," *Mariners Weather Log*, Vol. 6, No. 5, Sept., 1962, pp. 156-160.

HARRIS, D.L., "Coastal Flooding by the Storm of March 5-7, 1962," *Presented at the American Meteorological Society Annual Meeting*, Unpublished Manuscript, U.S. Weather Bureau, 1963a.

HARRIS, D.L., "Characteristics of the Hurricane Storm Surge," Technical Paper No. 48, U.S. Dept. of Commerce, Washington, D.C., 1963b.

HARRIS, D.L., "A Critical Survey of the Storm Surge Protection Problem," *The 11th Symposium of Tsunami and Storm Surges*, 1967, pp. 47-65.

HARRIS, D.L., "The Analysis of Wave Records," *Proceedings of the 12th Coastal Engineering Conference*, ASCE, Washington, D.C., 1970.

HARRIS, D.L., "Characteristics of Wave Records in the Coastal Zone," Unpublished Manuscript, U.S. Army, Corps of Engineers, Coastal Engineering Research Center, Washington,D.C., 1971.

HARRIS, D.L., and ANGELO, A.T., "A Regression Model for the Prediction of Storm Surges on Lake Erie," *Proceedings, Fifth Conference on Great Lakes Research*, Toronto, 1962.

HASSE L., and WAGNER, V., "On the Relationship Between Geostrophic and Surface Wind at Sea," *Monthly Weather Review*, Vol. 99, No. 4, Apr. 1971, pp. 255-260.

HAURWITZ, B., "The Slope of Lake Surfaces under Variable Wind Stresses," TM-25, U.S. Army, Corps of Engineers, Beach Erosion Board, Washington, D.C., Nov. 1951.

HELLSTROM, B., "Wind Effects on Lakes and Rivers," Nr. 158, Handlingar, Ingeniors Vetenskaps Akademien, Stockholm, 1941.

HIDAKA, K., "A Theory of Shelf Seiches, and Seiches in a Channel," *Memoirs of the Imperial Marine Observatory*, Kobe, Japan, 1934-35.

HIDY, G.M., and PLATE, E.J., "Wind Action on Water Standing in a Laboratory Channel," *Journal of Fluid Mechanics*, Vol. 25, 1966, pp. 651-687.

HONDA, K., et al., "Secondary Undulations of Oceanic Tides," *Journal, College of Science*, Imperial University, Tokyo, Japan, Vol. 24, 1908.

HUNT, I.A., "Design of Seawalls and Breakwaters," *Proceedings, American Society of Civil Engineers*, ASCE, Waterways and Harbors Division, Vol. 85, No, WW3, Sept. 1959.

HWANG, L., and DIVOKY, D., "Breaking Wave Setup and Decay on Gentle Slopes," *Proceedings of the 12th Coastal Engineering Conference*, ASCE, Vol. 1, 1970.

IJIMA, T., and TANG, F.L.W., "Numerical Calculation of Wind Waves in Shallow Water," *Proceedings of 10th Conference on Coastal Engineering*, ASCE, Tokyo, Vol. 2, 1966, pp. 38-45.

INOUE, T., "On the Growth of the Spectrum of a Wind Generated Sea According to a Modified Miles-Phillips Mechanism," Geophysical Sciences Laboratory Report No. TR-66-6, Department of Meteorology and Oceanography, New York University, N.Y., 1966.

INOUE, T., "On the Growth of the Spectrum of a Wind Generated Sea According to a Modified Miles-Phillips Mechanism and its Application to Wave Forecasting," Geophysical Sciences Laboratory Report No. TR-67-5, Department of Meteorology and Oceanography, New York University, N.Y., 1967.

IPPEN, A.T., "Estuary and Coastline Hydrodynamics," *Engineering Societies Monographs*, McGraw-Hill, New York, 1966.

IRISH, S.M., "The Prediction of Surges in the Southern Basin of Lake Michigan," Part II," A Case Study of the Surge of August 3, 1960," *Monthly Weather Review*, Vol. 93, 1965, pp. 282-291.

IRISH, S.M., and PLATZMAN, G.W., "An Investigation of the Meteorological Conditions Associated with Extreme Wind Tides on Lake Erie," *Monthly Weather Review*, Vol. 90, 1962, pp. 39-47.

ISAACS, J.D., and SAVILLE, T. JR., "A Comparison Between Recorded and Forecast Waves on the Pacific Coast," *Annals of the New York Academy of Sciences*, Vol. 51, Art. 3, "Ocean Surface Waves," 1949, pp. 502-510.

JACOBS, S.L., "Wave Hindcasts vs. Recorded Waves," Final Report 06768, Department of Meterology and Oceanography, University of Michigan, Ann Arbor, Mich., 1965.

JELESNIANSKI, C.P., "The July 6, 1954 Water Wave on Lake Michigan Generated by a Pressure Jump Passage," Unpublished Master of Science Thesis, 1958.

JELESNIANSKI, C.P. "Numerical Computations of Storm Surges Without Bottom Stress," *Monthly Weather Review*, Vol. 94, No. 6, 1966, pp. 379-394.

JELESNIANSKI, C.P., "Numerical Computations of Storm Surges with Bottom Stress," *Monthly Weather Review*, Vol. 95, No. 11, 1967, pp. 740-756.

JELESNIANSKI, C.P., "Bottom Stress Time-History in Linearized Equations of Motion of Storm Surges," *Monthly Weather Review*, Vol. 98, No. 6, 1970, pp. 462-478.

JELESNIANSKI, C.P., "SPLASH-Special Program to List Amplitudes of Surges from Hurricanes," National Weather Service, Unpublished Manuscript, National Oceanic and Atmospheric Administration, Rockville, Md., 1972.

KAPLAN, K., "Analysis of Moving Fetches for Wave Forecasting," TM-35, U.S. Army, Corps of Engineers, Beach Erosion Board, Washington, D.C., Mar. 1953.

KAPLAN, K., and SAVILLE, T. JR., "Comparison of Hindcast and Observed Waves Along the Northern New Jersey Coast for the Storm of Nov. 6-7, 1953," *The Bulletin of the Beach Erosion Board*, Vol. 8, No. 3, July 1954, pp. 13-17.

KEULEGAN, G.H., "Wind Tides in Small Closed Channels," *Journal of Research*, National Bureau of Standards, RP2207, Vol. 46, No. 5, 1951.

KINSMAN, B., *Wind Waves*, Prentice-Hall, Englewood Cliffs, N.J., 1965.

KRECKER, F.H., "Periodic Oscillations in Lake Erie," Contribution No. 1, Franz Theodore Stone Laboratory, Ohio State University Press, Columbus, Ohio, 1928.

LAPLACE, P.S., "Recherches sur plusieurs points du systeme du monde," *Memoirs*, *Academy of Royal Sciences*, Vol. 88, 1775, pp. 75-185.

LEENDERTSE, J.J., "Aspects of a Computational Model for Long-Period Water Wave Propagation," Memorandum RM-5294-PR, prepared for U.S. Air Force, Project Rand, 1967.

LONGUET-HIGGINS, M.S., and STEWART, R.W., "Changes in the Form of Short-Gravity Waves on Long Waves and Tidal Currents," *Journal of Fluid Mechanics*, Vol. 8, No. 565, 1960.

LONGUET-HIGGINS, M.S., and STEWART, R.W., "Radiation Stress and Mass Transport in Gravity Waves, with Application to Surf Beat," *Journal of Fluid Mechanics*, Vol. 13, 1962, pp. 481-504.

LONGUET-HIGGINS, M.S., and STEWART, R.W., "A Note on Wave Setup," *Journal of Marine Research*, Vol. 21(1), 1963, pp. 4-10.

LONGUET-HIGGINS, M.S., and STEWART, R.W., "Radiation Stress in Water Waves; A Physical Discussion with Application," *Deep-Sea Research*, Vol. 11, 1964, pp. 529-562.

MARINOS, G., and WOODWARD, J.W., "Estimation of Hurricane Surge Hydrographs," *Journal of the Waterways and Harbors Division*, ASCE, Vol. 94, WW2, Proc. Paper 5945, 1968, pp. 189-216.

MARMER, H.A., *The Tide*, D. Appleton, New York, 1926, 282 pp.

MASCH, F.D., et al, "A Numerical Model for the Simulation of Tidal Hydro-
dynamics in Shallow Irregular Estuaries," Technical Report HYD 12,6901
Hydraulic Engineering Laboratory, University of Texas, Austin, Tex.,
1969.

MILES, J.W., "On the Generation of Surface Waves by Shear Flows," *Journal
of Fluid Mechanics*, Vol. 3, 1957, pp. 185-204.

MIYAZAKI, M., "A Numerical Computation of the Storm Surge of Hurricane
Carla 1961 in the Gulf of Mexico," Technical Report No. 10, Depart-
ment of Geophysical Sciences, University of Chicago, Chicago, Ill.,
1963.

MORTIMER, C.H., "Spectra of Long Surface Waves and Tides in Lake Michigan
and at Green Bay, Wisconsin," *Proceedings, Eight Conference on Great
Lakes Research*, 1965.

MOSKOWITZ, L., "Estimates of the Power Spectrums for Fully Developed Seas
for Wind Speeds of 20 to 40 Knots," *Journal of Geophysical Research*,
Vol. 69, No. 24, 1964, pp. 5161-5179.

MUNGALL, J.C.H., and MATTHEWS, J.B., "A Variable - Boundary Numerical
Tidal Model," Report No. R70-4, Office of Naval Research, Arlington,
Va., 1970.

MUNK, W.H., "Proposed Uniform Procedure for Observing Waves and Interpret-
ing Instrument Records," Wave Project, Scripps Institute of Oceanogra-
phy, LaJolla, Calif., 1944.

MYERS, V.A., "Characteristics of United States Hurricanes Pertinent to
Levee Design for Lake Okeechobee, Florida," Hydrometeorological Report
No. 32, U.S. Weather Bureau, Washington, D.C., 1954.

PATTERSON, M.M., "Hindcasting Hurricane Waves in the Gulf of Mexico,"
Offshore Technology Conference, Houston, Tex., Preprint, Vol. 1, 1971.

PETERSON, K.R., and GOODYEAR, H.V., "Criteria for a Standard Project North-
easter for New England North of Cape Cod," National Hurricane Research
Project, Report No. 68, U.S. Weather Bureau, Washington, D.C., 1964.

PHILLIPS, O.M., "On the Generation of Waves by Turbulent Wind," *Journal
of Fluid Mechanics*, Vol. 2, 1957, pp. 417-445.

PHILLIPS, O.M., "The Dynamics of the Upper Ocean," Cambridge University
Press, Cambridge, 1966.

PIERSON, W.J., JR., and MOSKOWITZ, L., "A Proposed Spectral Form for
Fully Developed Wind Seas Based on the Similarity Theory of S.A.
Kitaigorodskii," *Journal of Geophysical Research*, Vol. 69, No. 24,
1964, pp. 5181-5190.

PIERSON, W.J., JR., NEUMANN, G., and JAMES, R.W., "Practical Methods for
Observing and Forecasting Ocean Waves by Means of Wave Spectra and
Statistics," Publication No. 603, U.S. Navy Hydrographic Office,
Washington, D.C., 1955.

PLATZMAN, G.W., "A Numerical Computation of the Surge of 26 June 1954 on Lake Michigan," *Geophysics*, Vol. 6, 1958.

PLATZMAN, G.W., "The Dynamic Prediction of Wind Tides on Lake Erie," *Meteorological Monographs*, Vol. 4, No. 26, 1963, 44 pp.

PLATZMAN, G.W., "The Prediction of Surges in the Southern Basin of Lake Michigan," Part I, "The Dynamical Basis for Prediction," *Monthly Weather Review*, Vol. 93, 1965, pp. 275-281.

PLATZMAN, G.W., "A Procedure for Operational Prediction of Wind Setup on Lake Erie," Technical Report to Environmental Science Services Administration, U.S. Weather Bureau, 1967.

PLATZMAN, G.W., "Two-Dimensional Free Oscillations in National Basins," *Journal of Physical Oceanography*, Vol. 2, 1972, pp. 117-138.

PLATZMAN, G.W., and RAO, D.B., "Spectra of Lake Erie Water Levels," *Journal of Geophysical Research*, Vol. 69, Oct. 1963, pp. 2525-2535.

PLATZMAN, G.W., and RAO, D.B., "The Free Oscillations of Lake Erie," *Studies on Oceanography*, University of Washington Press, Seattle, Wash., 1965, pp. 359-382.

PORE, N.A., "Ocean Surface Waves Produced by Some Recent Hurricanes," *Monthly Weather Review*, Vol. 85, No. 12, Dec. 1957, pp. 385-392.

PORE, N.A., and CUMMINGS, R.A., "A Fortran Program for the Calculation of Hourly Values of Astronomical Tide and Time and Height of High and Low Water," Technical Memorandum WBTM TDL-6, U.S. Department of Commerce, Environmental Science Services Administration, Washington, D.C., 1967.

PORE, N.A., and RICHARDSON, W.S., "Interim Report on Sea and Swell Forecasting," Technical Memorandum TDL-13, U.S. Weather Bureau, 1967.

PORE, N.A., and RICHARDSON, W.S., "Second Interim Report on Sea and Swell Forecasting," Technical Memorandum TDL-17, U.S. Weather Bureau, 1969.

PREISENDORFER, R.W., "Recent Tsunami Theory," NOAA-JTRE-60, HIG-71-15, Hawaii Institute of Geophysics, University of Hawaii, Honolulu, Hawaii 1971.

PROUDMAN, J., and DOODSON, A.T., "Tides in Oceans Bounded by Meridians," *Philosophical Transactions of the Royal Society* (London), Parts I and II, Vol. 235, No. 753, 1936, pp. 273-342; Part III, Vol. 237, No. 779, 1938, pp. 311-373.

PUTNAM, J.A., "Loss of Wave Energy Due to Percolation in a Permeable Sea Bottom," *Transactions of the American Geophysical Union* Vol. 30, No. 3, 1949, pp. 349-357.

PUTNAM, J.A., and JOHNSON, J.W., "The Dissipation of Wave Energy by Bottom Friction," *Transactions of the American Geophysical Union*, Vol. 30, No. 1, 1949, pp. 67-74.

REID, R.O., "Short Course on Storm Surge," Summer Lectures, Texas A&M University, College Station, Tex., 1964.

REID, R.O., and BODINE, B.R., "Numerical Model for Storm Surges Galveston Bay," *Journal of the Waterways and Harbors Division*, ASCE, Vol. 94, No. WW1, Proc. Paper 5805, 1968, pp. 33-57.

RICHARDS, T.L., DRAGERT, H., and MacINTYRE, D.R., "Influence of Atmospheric Stability and Over-Water Fetch on Winds Over the Lower Great Lakes," *Monthly Weather Review*, Vol. 94, No. 1, 1966, pp. 448-453.

ROCKWELL, D.C., "Theoretical Free Oscillations of the Great Lakes," *Proceedings, Ninth Conference on Great Lakes Research*, 1966, pp. 352-368.

ROLL, H.U., and FISHER, F., "Eine Kritische Bemerkung zum Neumann-Spektrum des Seeganges," *Deut. Hydrograph. Z.*, Vol. 9, No. 9, 1956.

SAVAGE, R.P., "Model Tests of Wave Runup for the Hurricane Protection Project," *The Bulletin of the Beach Erosion Board*, Vol. 11, July 1957, pp. 1-12.

SAVILLE, T., JR., "Wind Setup and Waves in Shallow Water," TM-27, U.S. Army, Corps of Engineers, Beach Erosion Board, Washington, D.C., June 1952.

SAVILLE, T., JR., "The Effect of Fetch Width on Wave Generation," TM-70, U.S. Army, Corps of Engineers, Beach Erosion Board, Washington, D.C., Dec. 1954.

SAVILLE, T. JR., "Experimental Determination of Wave Setup," *Proceedings, Second Technical Conference on Hurricanes*, National Hurricane Research Project, Report No. 50, 1961, pp. 242-252.

SCHUREMAN, P., "Manual of Harmonic Analysis and Prediction of Tides," Special Publication No. 98, U.S. Department of Commerce, Coast and Geodetic Survey, Washington, D.C., 1941.

SENTER, P.K., "Design of Proposed Crescent City Harbor, California, Tsunami Model," Report H-71-2, U.S. Army, Corps of Engineers, Waterways Experiment Station, Vicksburg, Miss., 1971.

SHEMDIN, O.H., and HSU, E.T., "The Dynamics of Wind in the Vicinity of Progressive Water Waves," Technical Report No. 66, Department of Civil Engineering, Stanford University, Stanford, Calif., 1966.

SHIELDS, G.C., and BURDWELL, G.B., "Western Region Sea State and Surf Forecaster's Manual," Technical Memorandum WR-51, U.S. Weather Bureau, 1970.

SIBUL, O., "Laboratory Study of Wind Tides in Shallow Water," TM-61, U.S. Army, Corps of Engineers, Beach Erosion Board, Washington, D.C., Aug. 1955.

SILVESTER, R., and VONGVISESSOMJAI, S., "Computation of Storm Waves and Swell," *The Institution of Civil Engineers*, Vol. 48, 1971, pp. 259-283.

SIMPSON, R.B., and ANDERSON, D.V., "The Periods of the Longitudinal Surface Seiche of Lake Ontario," *Proceedings, Seventh Conference on Great Lakes Research*, 1964.

SVERDRUP, H.U., JOHNSON, M.W., and FLEMING, R.H., *The Oceans; Their Physics, Chemistry, and General Biology;* Prentice-Hall, New York, 1942.

SVERDRUP, H.U., and MUNK, W.H., "Wind, Sea, and Swell: Theory of Relations for Forecasting," Publication No. 601, U.S. Navy Hydrographic Office, Washington, D.C., Mar. 1947.

SYMONS, T.M., and ZELTER, B.D., "The Tsunami of May 22, 1960 as Recorded at Tide Stations, Preliminary Report," U.S. Dept. of Commerce, Coast and Geodetic Survey, Washington, D.C., 1960.

TICKNER, E.G., "Effect of Bottom Roughness on Wind Tide in Shallow Water," TM-95, U.S. Army, Corps of Engineers, Beach Erosion Board, Washington, D.C., May, 1957.

TUCKER, M.J., "Simple Measurement of Wave Records," *Proceedings of the Conference on Wave Recording for Civil Engineers*, National Institute of Oceanography, 1961.

U.S. ARMY, CORPS OF ENGINEERS, "Shore Protection, Planning and Design," Technical Report No. 4, 3rd ed., Coastal Engineering Research Center, Washington, D.C., 1966.

U.S. ARMY, CORPS OF ENGINEERS, "Waves and Wind Tides in Shallow Lakes and Reservoirs, Summary Report, Project CW-167," South Atlantic-Gulf Region, Engineer District, Jacksonville, Fla., 1955.

U.S. ARMY, CORPS OF ENGINEERS, "Hilo Harbor, Hawaii: Report on Survey for Tidal Wave Protection and Navigation," Hawaii Region, Engineer District, Honolulu, Hawaii, 1960.

U.S. ARMY, CORPS OF ENGINEERS, "Waves in Inland Reservoirs, (Summary Report on Civil Works Investigation Projects CW-164 & CW-165)," TM-132, Beach Erosion Board, Washington, D.C., Nov. 1962.

U.S. DEPARTMENT OF COMMERCE, COAST AND GEODETIC SURVEY, "Annotated Bibliography on Tsunamis," International Union of Geodesy and Geophysics, Paris, 1964.

U.S. DEPARTMENT OF COMMERCE, NATIONAL OCEANIC AND ATMOSPHERIC ADMINI-STRATION, *Tide Tables, East Coast, North and South America*, National Ocean Survey, Rockville, Md., 1973.

U.S. DEPARTMENT OF COMMERCE, NATIONAL OCEANIC AND ATMOSPHERIC ADMINISTRA-TION, *Tide Tables, West Coast, North and South America*, National Ocean Survey, Rockville, Md., 1973.

U.S. FLEET WEATHER FACILITY, "Forecasting Ocean Waves and Surf," U.S. Naval Air Station, Oceanographic Services Section, Operations Depart-ment, San Diego, Calif., 1966.

U.S. NAVAL WEATHER SERVICE COMMAND, "Summary of Synoptic Meteorological Observations, North American Coastal Marine Areas," Vols. 1-10, 1970.

U.S. WEATHER BUREAU, "Meteorological Characteristics of the Probable Maximum Hurricane, Atlantic and Gulf Coasts of the United States," Hurricane Research Interim Report, HUR 7-97 and HUR 7-97A, U.S. Weather Bureau, Washington, D.C., 1968.

U.S. WEATHER BUREAU, "Preliminary Analysis of Surface Wind Field and Sea-Level Pressures of Hurricane Camille (August 1969)," Hurricane Research Report, HUR 7-113, U.S. Weather Bureau, Washington, D.C., 1969.

U.S. WEATHER BUREAU, "Revised Surface Wind Field (30 ft) of Hurricane Camille in Gulf of Mexico (August 1969)," Hurricane Research Report, HUR 7-113A, U.S. Weather Bureau, Washington, D.C., 1970.

U.S. WEATHER BUREAU, "Synoptic Code," WB-242, U.S. Weather Bureau, Washington, D.C., 1949.

VAN DORN, W.C., "Wind Stress on an Artificial Pond, *Journal of Marine Research*, Vol. 12, 1953.

VERMA, A.P., and DEAN, R.G., "Numerical Modeling of Hydromechanics of Bay Systems," *Proceedings of the Conference on Civil Engineering in the Oceans II*, ASCE, 1969.

WELANDER, P., "Numerical Prediction of Storm Surges," *Advances in Geo-physics*, Vol. 8, 1961, pp. 316-379.

WIEGEL, R.L., *Oceanographical Engineering*, Prentis-Hall, Englewood Cliffs, N.J., 1964.

WILSON, B.W, "Graphical Approach to the Forecasting of Waves in Moving Fetches," TM-73, U.S. Army, Corps of Engineers, Beach Erosion Board, Washington, D.C., Apr. 1955.

WILSON, B.W., "Hurricane Wave Statistics for the Gulf of Mexico," TM-98, U.S. Army, Corps of Engineers, Beach Erosion Board, Washington, D.C., June, 1957.

WILSON, B.W., "Deep Water Wave Generations by Moving Wind Systems,"
Journal of the Waterways and Harbors Division, ASCE, Vol. 87,
No. WW2, Proc. Paper 2821, May, 1961, pp. 113-141.

WILSON, B.W., "Propagation and Run-up of Tsunami Waves," National Engi-
neering Science Co., Washington, D.C., 1964.

WILSON, B.W., "Design Sea and Wind Conditions for Offshore Structures,"
Proceedings of Offshore Exploration Conference, Long Beach, Calif.,
1966, pp. 665-708.

WILSON, B.W., WEB, L.M., and HENDRICKSON, J.A., "The Nature of Tsunamis,
Their Generation and Dispersion in Water of Finite Depth," National
Engineering Science Co., Washington, D.C., 1962.

CHAPTER 4

LITTORAL

PROCESSES

NORTH CAROLINA COAST – 13 February 1973

CHAPTER 4

LITTORAL PROCESSES

4.1 INTRODUCTION

Littoral processes result from the interactions among winds, waves, currents, tides, sediments, and other phenomena in the littoral zone. The purpose of this chapter is to discuss those littoral processes which involve sediment motion. Shores erode, accrete, or remain stable, depending on the rates at which sediment is supplied to and removed from the shore. Excessive erosion or accretion may endanger the structural integrity or functional usefulness of a beach, or other coastal structures. Therefore an understanding of littoral processes is needed to predict erosion or accretion rates. An aim of coastal engineering design is to maintain a stable shoreline where sediment supplied to the shore balances that which is removed. This chapter presents information needed for understanding the effects of littoral processes on coastal engineering design.

4.11 DEFINITIONS

In describing littoral processes, it is necessary to use clearly defined terms. Commonly used terms, such as "beach" and "shore," have specific meanings in the study of littoral processes, as shown in the Glossary. (See Appendix A.)

4.111 Beach Profile. Profiles perpendicular to the shoreline have characteristic features that reflect the action of littoral processes. (See Figure 1-1, Chapter 1, and Figures A-1 and A-2 of the Glossary for specific examples.) At any given time, a profile may exhibit only a few specific features, but usually a dune, berm and beach face can be identified.

Profiles across a beach adapt to imposed wave conditions in ways as illustrated in Figure 4-1 by a series of profiles taken between February 1963 and November 1964 at Westhampton Beach, N.Y. The figure shows how the berm built up gradually from February through August 1963, then was cut back in November through January, and was rebuilt in March through September 1964. This process is typical of a cyclical process of storm erosion in winter and progradation with the lower, and often longer, waves in summer.

4.112 Areal View. Figure 4-2 shows three generalized charts of different U.S. coastal areas, all to the same scale. Figure 4-2a shows a rocky coast, well-indented, where sand is restricted to local pocket beaches. Figure 4-2b shows a long straight coast with an uninterrupted sand beach. Figure 4-2c shows short barrier islands interrupted by inlets. These are some of the different coastal configurations which reflect differences in littoral processes and the local geology.

4.12 ENVIRONMENTAL FACTORS

4.121 Waves. Water waves are the principal cause of most shoreline changes. Without wave action on a coast, most of the coastal engineering
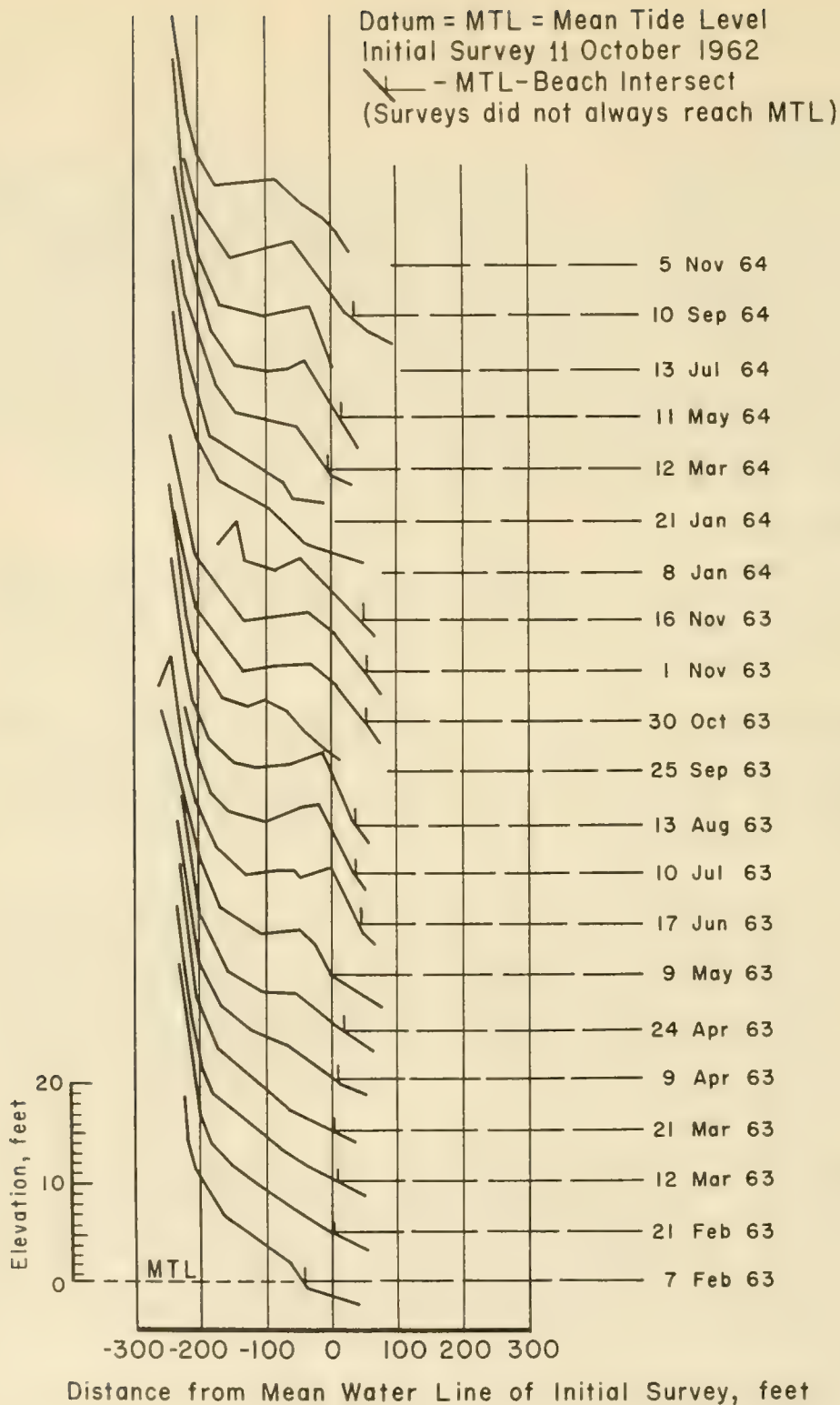
Figure 4-1.   Typical Profile Changes with Time, Westhampton
Beach, New York

Rhode Island
(See USC & GS Chart 1210)

OCEAN
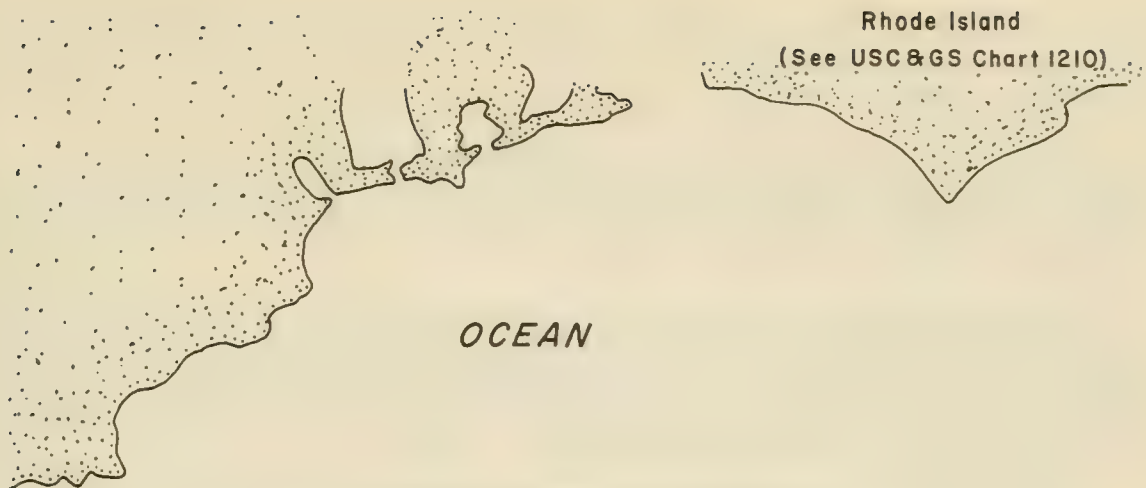
a. Rocky Coast with Limited Beaches

Northeastern Florida
(See USC & GS Chart 1246)

BAY

OCEAN
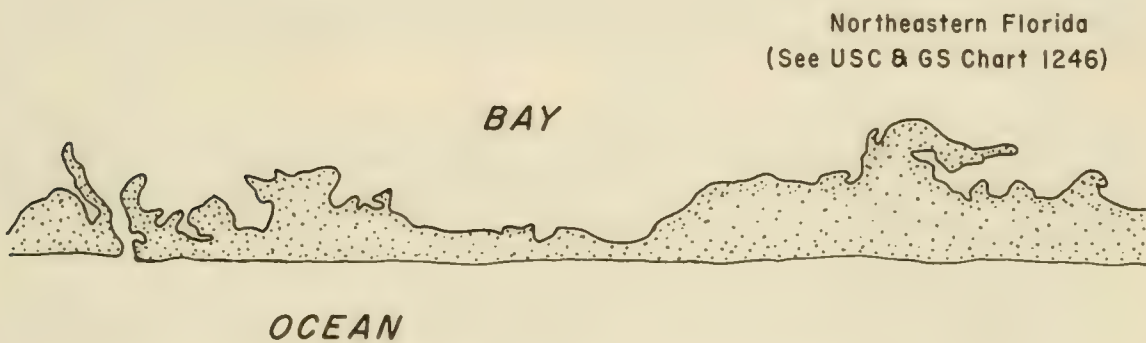
b. Straight Barrier Island Shoreline

Southern New Jersey
(See USC & GS Chart 1217)

BAY

OCEAN

Scale in Miles
0   1   2   3
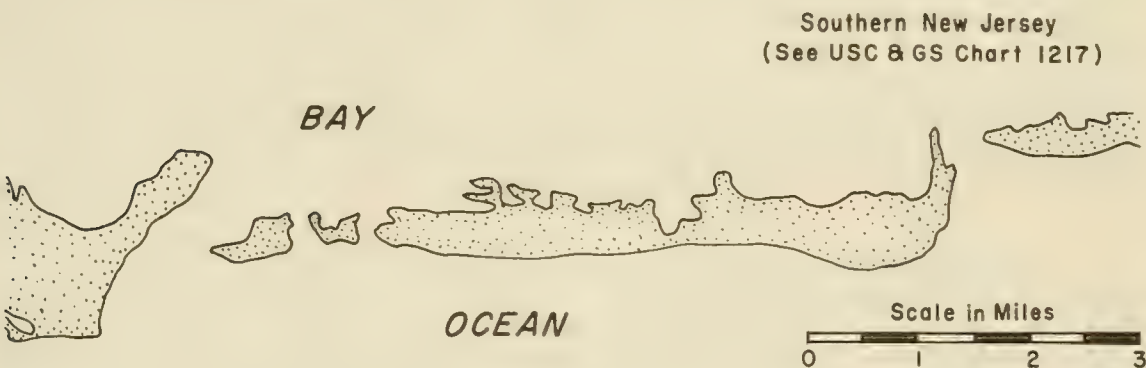
c. Short Barrier Island Shoreline

Figure 4-2.   Three Types of Shoreline

problems involving littoral processes would not occur. A knowledge of incident waves, or of surf, is essential for coastal engineering planning, design, and construction.

Three important aspects of a study of waves on beaches are: the theoretical description of wave motion; the climatological data for waves as they occur on a given segment of coast; and the description of how waves interact with the shore to move sand.

The theoretical approach can provide a useful description of water motion caused by waves when the limiting assumptions of the theory are satisfied. Surprisingly, the small-amplitude theory (Section 2.23) and aspects of solitary wave theory (Section 2.27) have proved useful beyond the limits assumed in their derivations.

The theoretical description of water-wave motion provides estimates of water motion, longshore force, and energy flux due to waves. These estimates are useful in understanding the effect of waves on sediment transport, but currently (1973) the prediction of wave-induced sediment motion for engineering purposes relies heavily on empirical coefficients and judgement rather than on theory.

Statistical distributions of wave characteristics along a given shore-line provide a basis for describing the wave climate of a coastal segment. Important wave characteristics affecting sediment transport near the beach are height, period, and direction of breaking waves. Breaker height is significant in determining the quantity of sand in motion; breaker direction is a major factor in determining longshore transport direction and rate. Waves affect sediment motion in the littoral zone in two ways: they initiate sediment movement, and they drive current systems that transport the sediment once motion is initiated.

4.122 Currents. Water waves induce an orbital motion in the fluid beneath them. (See Section 2.23.) These are not closed orbits, and the fluid experiences a slight wave-induced drift, or *mass transport*. Magnitude and direction of mass transport are functions of elevation above bottom and wave parameters (Equation 2-55), and are also influenced by wind and tem-perature gradients. The action of mass transport, extended over a long period, can be important in carrying sediment onshore or offshore, par-ticularly seaward of the breaker position.

As waves approach breaking, wave-induced bottom motion in the water becomes more intense, and its effect on sediment becomes more pronounced. Breaking waves create intense local currents (turbulence) that move sedi-ment. As waves cross the surf zone after breaking, the accompanying fluid motion is mostly uniform horizontal motion, except during the brief pass-age of the breaker front where significant turbulence occurs. Since wave crests at breaking are usually at a slight angle to the shoreline, there is usually a longshore component of momentum in the fluid composing the breaking waves. This longshore component of momentum entering the surf

4-4

zone is the principal cause of longshore currents - currents that flow parallel to the shoreline within the surf zone. These longshore currents are largely responsible for the longshore sediment transport.

There is some mean exchange between the water flowing in the surf zone and the water seaward of the breaker zone. The most easily seen of these exchange mechanisms are the rip currents (Shepard and Inman, 1950), which are concentrated jets of water flowing seaward through the breaker zone.

4.123 Tides and Surges. In addition to wave-induced currents, there are other currents affecting the shore that are caused by tides and storm surges. Tide-induced currents can be impressed upon the prevailing wave-induced circulations, especially near entrances to bays and lagoons and in regions of large tidal range. (Notices to Mariners and the Coastal Pilot often carry this information.) Tidal currents are particularly important in transporting sand in shoals and sand waves around entrances to bays and estuaries.

Currents induced by storm surges (Murray, 1970) are less well known because of the difficulty in measuring them, but their effects are un-doubtedly significant.

The change in water level by tides and surges is a significant factor in sediment transport, since, with a higher water level, waves can then attack a greater range of elevations on the beach profile. (See Figure 1-7.) The appropriate theory for predicting storm surge levels is discussed in Section 3.8.

4.124 Winds. Winds act directly on beaches by blowing sand off the beaches (deflation) and by depositing sand in dunes. (Savage and Wood-house, 1968.) Deflation usually removes the finer material, leaving behind coarser sediment and shell fragments. Sand blown seaward from the beach usually falls in the surf zone; thus it is not lost, but is introduced into the littoral transport system. Sand blown landward from the beach may form dunes, add to existing dunes, or be deposited in lagoons behind barrier islands.

For dunes to form, a significant quantity of sand must be available for transport by wind, as must features that act to trap the moving sand. Topographic irregularities, the dunes themselves, and vegetation are the principal features that trap sand.

The most important dunes in littoral processes are *foredunes* - the line of dunes immediately landward of the beach. They usually form because beachgrasses growing just landward of the beach will trap sand blown landward off the beach. Foredunes act as a barrier to prevent waves and high water from moving inland, and provide a reservoir of sand to replenish the nearshore regime during severe shore erosion.

The effect of winds in producing currents on the water surface is well documented, both in the laboratory and in the field. (Bretschneider,

1967; Keulegan, 1951; and van Dorn, 1953.) These surface currents drift in the direction of the wind at a speed equal to 2 to 3 percent of the wind speed. In hurricanes, winds generate surface currents of 2 to 8 feet per second. Such wind-induced surface currents toward the shore cause significant bottom return flows which may transport sediment seaward; similarly, strong offshore winds can result in an offshore surface current, and an onshore bottom current which can aid in transporting sediment landward.

4.125 Geologic Factors. The geology of a coastal region affects the supply of sediment on the beaches and the total coastal morphology. Thus, geology determines the initial conditions for littoral processes, but geologic factors are not usually active processes affecting coastal engineering.

One exception is the rate of change of sea level with respect to land which may be great enough to influence design, and should be examined if project life is 50 years or more. On U.S. coasts, typical rates of sea level rise average about 1 to 2 millimeters per year, but changes range from -13 to +9 millimeters per year. (Hicks, 1972.) (Plus means a rise in sea level with respect to local land level.)

4.126 Other Factors. Other principal factors affecting littoral processes are the works of man and activities of organisms native to the particular littoral zone. In engineering design, the effects on littoral processes of construction activities, the resulting structures, and structure maintenance must be considered. This consideration is particularly necessary for a project that may alter the sand budget of the area, such as jetty or groin construction. In addition biological activity may be important in producing carbonate sands, in reef development, or (through vegetation) in trapping sand on dunes.

4.13 CHANGES IN THE LITTORAL ZONE

Because most of the wave energy is dissipated in the littoral zone, this zone is where beach changes are most rapid. These changes may be short-term due to seasonal changes in wave conditions and to occurrence of intermittent storms separated by intervals of low waves, or long-term due to an overall imbalance between the added and eroded sand. Short-term changes are apparent in the temporary redistribution of sand across the profile (Fig. 4-1); long-term changes are apparent in the more nearly permanent shift of the shoreline. (See Figures 4-3, 4-4, and 4-5.)

Maximum seasonal or storm-induced changes across a profile, such as those shown in Figure 4-1, are typically on the order of a few feet vertically and from 10 to 100 feet horizontally. (See Table 4-1.) Only during extreme storms, or where the available sand supply is restricted, do unusual changes occur over a short period.

Typical seasonal changes on southern California beaches are shown in Table 4-1. (Shepard, 1950.) These data show greater changes on the beach
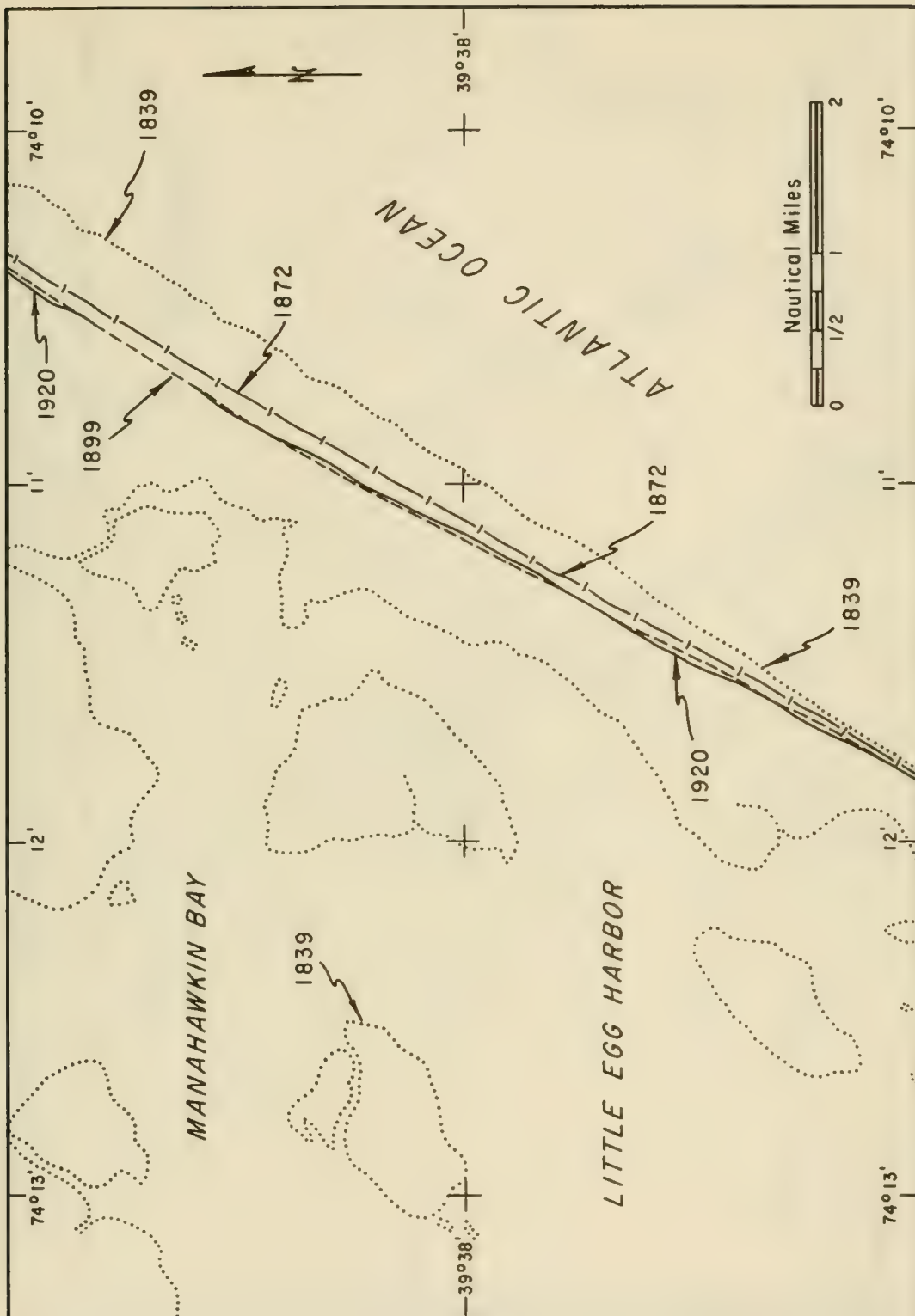
Figure 4-3. Shoreline Erosion Near Shipbottom, New Jersey

4-7
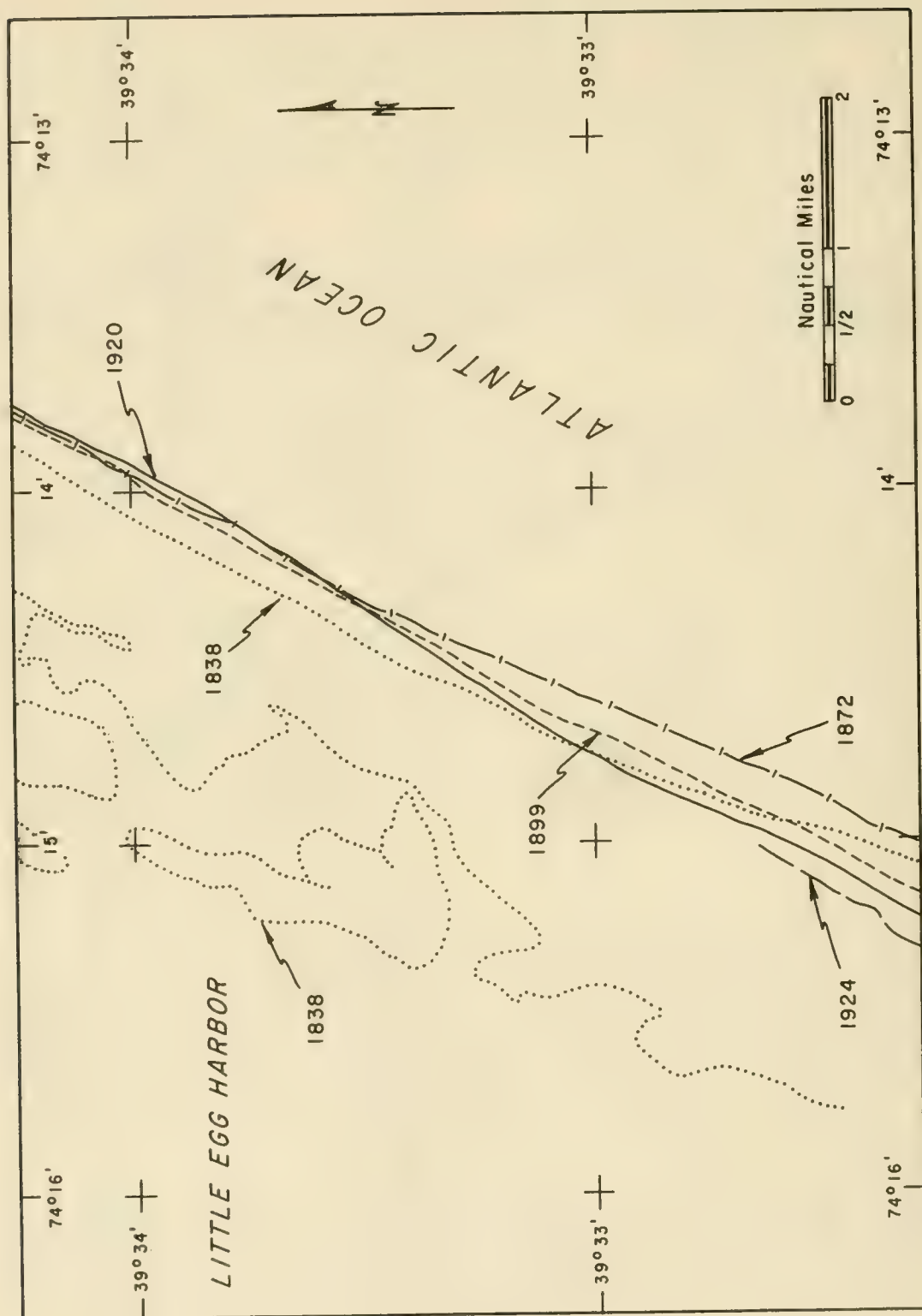
Figure 4-4. Shoreline Accretion and Erosion Near Beach Haven, New Jersey

4-8
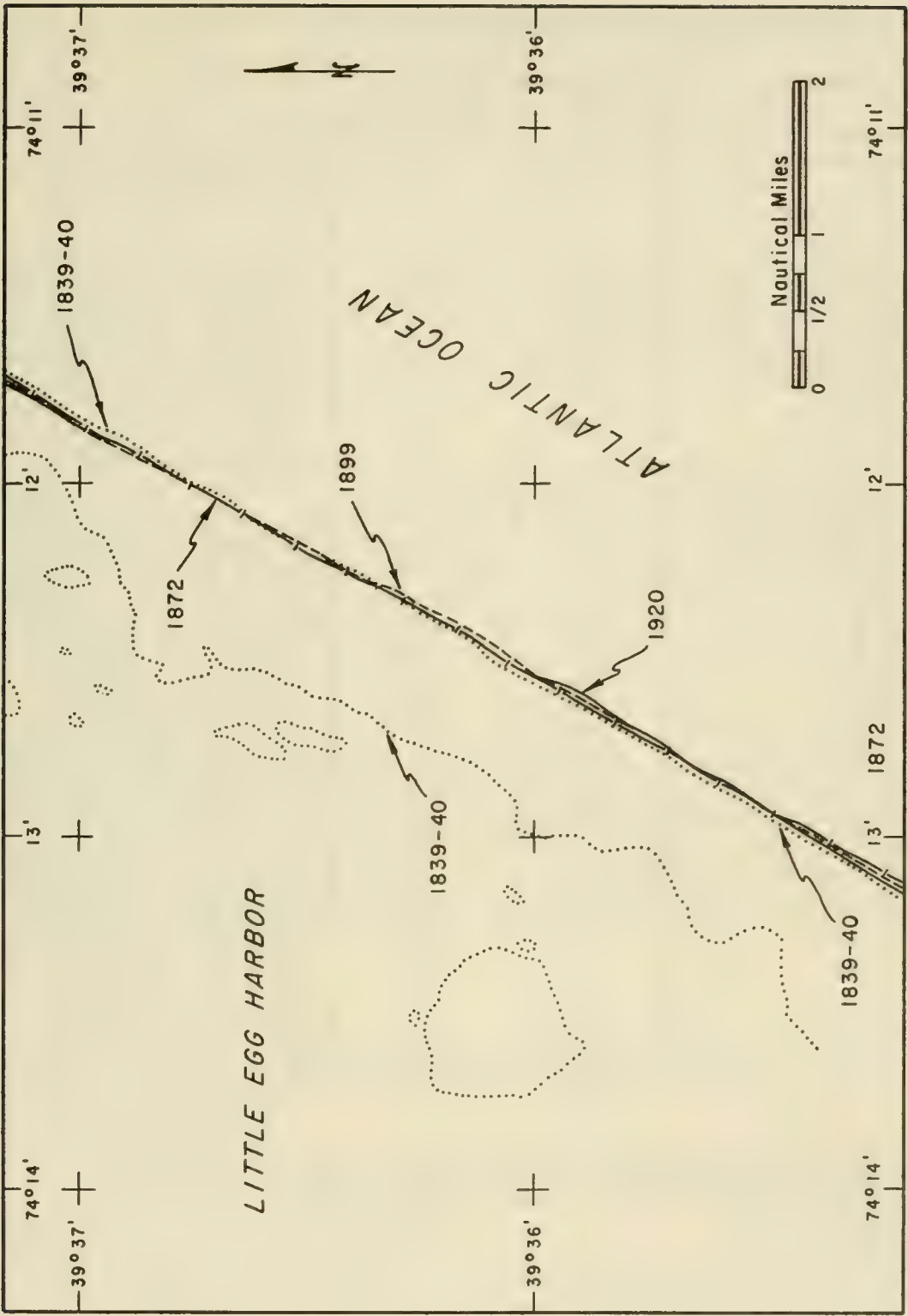
Figure 4-5. Stable Shoreline Near Peahala, New Jersey

Table 4-1. Seasonal Profile Changes on Southern California Beaches

| Locality | Erosion | | Date |
	Vertical* (ft.)	Horizontal at MWL (ft.)	
Marine Street	5.9	24	27 Nov 45— 5 Apr 46
Beacon Inn	8.2	117	2 Nov 45—19 Mar 46
South Oceanside	5.0	41	2 Nov 45—26 Apr 46
San Onofre			
Surf Beach	4.2	43	6 Nov 45—12 Apr 46
Fence Beach	10.8	87	6 Nov 45—12 Apr 46
Del Mar	3.4	-----	2 Nov 45—10 May 46
Santa Monica Mountains	6.2	-----	28 Aug 45—13 Mar 46
Point Mugu	6.0	-----	28 Aug 45—13 Mar 46
Rincon Beach	2.7	-----	22 Aug 45—13 Mar 46
Goleta Beach	0.5	-----	22 Aug 45—13 Mar 46
Point Sur			27 Aug 45—14 Mar 46
South Side	1.8	-----	
North Side	6.3	-----	
Carmel Beach (South)	6.7	-----	26 Aug 45—14 Mar 46
Point Reyes	5.1	-----	26 Aug 45—16 Mar 46
Scripps Beach			
Range A	1.6	88	19 Nov 45—29 Apr 46
Range B	3.2	240	7 Nov 45—10 Apr 46
Range C	5.6	260	7 Nov 45—10 Apr 46
Range D	5.3	250	7 Nov 45— 9 May 46
Range E	3.3	-----	7 Nov 45—24 Apr 46
Range F	1.5	67	7 Nov 45—10 May 46
Range G	0.7	15	19 Oct 45—10 Apr 46
Range H	1.6	44	7 Nov 45—24 Apr 46
Scripps Pier	3.8	33	13 Oct 37—26 Mar 38
,, ,,	3.6†	30†	26 Mar 38—30 Aug 38
,, ,,	4.3	38	30 Aug 38—13 Feb 39
,, ,,	3.2†	32†	13 Feb 39—22 Sep 39
,, ,,	2.5	28	22 Sep 39—24 Jan 40
,, ,,	3.4†	34†	24 Jan 40—18 Sep 40
,, ,,	1.2	12	18 Sep 40—16 Apr 41
,, ,,	1.2†	11†	16 Apr 41—17 Sep 41
,, ,,	2.9	30|	17 Sep 41—29 Apr 42
,, ,,	1.9†	16†	29 Apr 42—30 Sep 42

(from Shepard 1950)

* Vertical erosion measured at berm for all localities except Scripps Beach and Scripps Pier where the mean water line (MWL) was used.

† Accretion values.

than are typical of Atlantic coast beaches. (Urban and Galvin, 1969; Zeigler and Tuttle, 1961.) Available data indicate that the greatest changes on the profile are in the position of the beach face and of the longshore bar - two relatively mobile elements of the profile. Beaches change in plan view as well. Figure 4-6 shows the change in shoreline position at seven east coast localities as a function of time between autumn 1962 and spring 1967.

Comparison of beach profiles before and after storms suggests erosion of the beach above MSL from 10,000 to 50,000 cubic yards per mile of shoreline during storms expected to recur about once a year. (DeWall, et al., 1971; and Shuyskiy, 1970.) While impressive in aggregate, such sediment transport is minor compared to longshore transport of sediment. Longshore transport rates may be greater than 1 million cubic yards per year.

The long-term changes shown in Figures 4-3, 4-4, and 4-5 illustrate shorelines of erosion, accretion, and stability. Long-term erosion or accretion rates are rarely more than a few feet per year in horizontal motion of the shoreline, except in localities particularly exposed to erosion, such as near inlets or capes. Figure 4-5 indicates that shorelines can be stable for a long time. It should be noted that the eroding, accreting, and stable beaches shown in Figures 4-3, 4-4, and 4-5 are on the same barrier island within a few miles of each other.

Net longshore transport rates along ocean beaches range from near zero to 1 million cubic yards per year, but are typically 100,000 to 500,000 cubic yards per year. Such quantities, if removed from a 10- to 20-mile stretch of beach year after year, would result in severe erosion problems. The fact that many beaches have high rates of longshore transport without unusually severe erosion suggests that an equilibrium condition exists on these beaches, in which the material eroded is balanced by the material supplied; or in which seasonal reversals of littoral transport replace material previously removed.

4.2 LITTORAL MATERIALS

Littoral materials are the solid materials (mainly sedimentary) in the littoral zone on which the waves and currents act.

4.21 CLASSIFICATION

The characteristics of the littoral materials are a primary input to any coastal engineering design. Median grain size is the most frequently used design characteristic.

4.211 Size and Size Parameters. Littoral materials are classified by grain size into clay, silt, sand, gravel, cobble, and boulder. Several size classifications exist, of which two, the Unified Soil Classification, (based on the Casagrande Classification) and the Wentworth Classification, are most commonly used in coastal engineering. (See Figure 4-7.) The
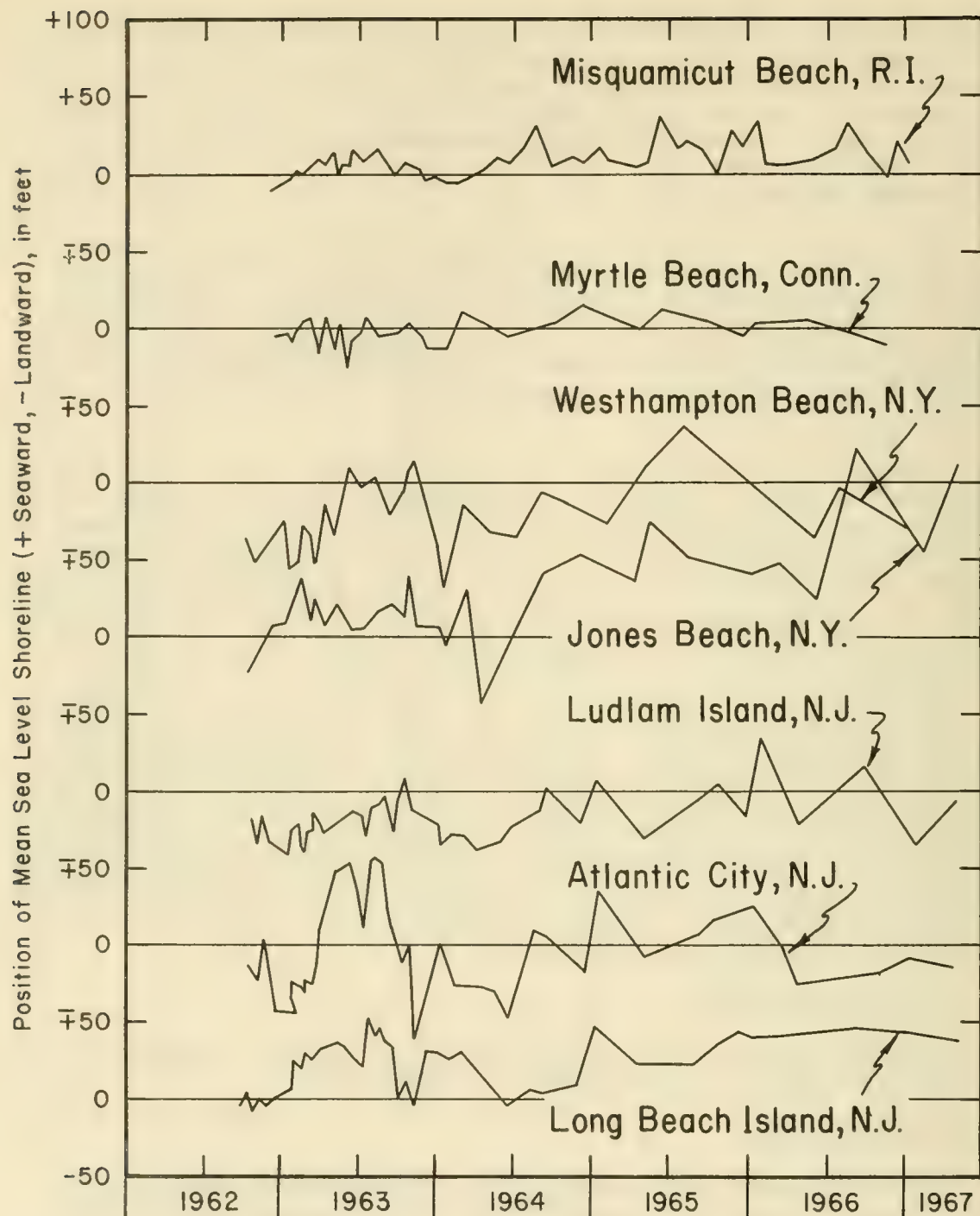
Figure 4-6. Fluctuations in Location of Mean Sealevel
Shoreline on Seven East Coast Beaches

Unified Soil Classification is the principal classification used by engineers. The Wentworth classification is the basis of a classification widely used by geologists, but is becoming more widely used by engineers designing beach fills.

For most shore protection design problems, typical littoral materials are sands with sizes between 0.1 and 1.0 millimeters or, in phi units, between 3.3 and 0 phi. According to the Wentworth classification, sand size is in the range between 0.0625 and 2.0 millimeters (4 and -1 phi); according to the Unified Soil Classification, it is between 0.074 and 4.76 millimeters (3.75 and -2.25 phi). Within these sand-size ranges, engineers commonly distinguish size classes by median grain size measured in millimeters, based on sieve analyses.

Samples of typical beach sediment usually have a few relatively large particles covering a wide range of diameters, and many small particles within a small range of diameters. Thus, to distinguish one sample from another, it is necessary to consider the small differences (in absolute magnitude) among the finer sizes more than the same differences among the larger sizes. For this reason, all sediment size classifications exaggerate absolute differences in the finer sizes compared to absolute differences in the coarser sizes.

As shown in Figure 4-7, limits of the size classes differ. The Unified Soil Classification boundaries correspond to U.S. Standard Sieve sizes. The Wentworth classification varies as powers of 2 millimeters; that is, the size classes have limits, in millimeters, determined by the relation 2^n, where n is any positive or negative whole number, including zero. For example, the limits on sand size in the Wentworth scale are 0.0625 millimeters and 2 millimeters, which correspond to 2^{-4} and 2^{+1} millimeters.

This property of having class limits defined in terms of whole number powers of 2 millimeters led Krumbein (1936) to propose a phi unit scale based on the definition:

$$\text{Phi units } (\phi) = -\log_2 \text{ (diameter in mm.)} \tag{4-1}$$

Phi unit scale is indicated by writing ϕ or phi after the numerical value. The phi unit scale is shown in Figure 4-7. Advantages of phi units are:

(a) Limits of Wentworth size classes are whole numbers in phi units. These phi limits are the negative value of the exponent, n, in the relation 2^n. For example, the sand size class ranges from +4 to -1, in phi units.

(b) Sand size distributions typically are near lognormal, so that a unit based on the logarithm of the size better emphasizes the small significant differences between the finer particles in the distribution.

4-13

Wentworth Scale (Size Description)		Phi Units ϕ*	Grain Diameter d (mm)	U.S. Standard Sieve Size	Unified Soil Classification (USC)	
Boulder		−8	256		Cobble	
Cobble			76.2	3 in.		
Pebble		−6	64.0		Coarse	Gravel
			19.0	¾ in.	Fine	
			4.76	No. 4		
Granule		−2	4.0		Coarse	Sand
Sand	Very Coarse	−1	2.0	No. 10		
		0	1.0		Medium	
	Coarse	1	0.5			
	Medium		0.42	No. 40		
		2	0.25		Fine	
	Fine	3	0.125			
	Very Fine		0.074	No. 200		
Silt		4	0.0625		Silt or Clay	
Clay		8	0.00391			
Colloid		12	0.00024			

* $\phi = -\log_2 d$ (mm)

Figure 4-7. Grain Size Scales (Soil Classification)

(c) The normal distribution is described by its mean and standard deviation. Since the distribution of sand size is approximately lognormal, then individual sand size distributions can be more easily described by units based on the logarithm of the diameter rather than the absolute diameter. Comparison with the theoretical lognormal distribution is also a convenient way of characterizing and comparing the size distribution of different samples.

Of these three advantages, only (a) is unique to the phi units. The other two, (b) and (c), would be valid for any unit based on the logarithm of size.

Disadvantages of phi units are:

(a) Phi units increase as absolute size in millimeters decreases.

(b) Physical appreciation of the size involved is easier when the units are millimeters rather than phi units.

(c) The median diameter can be easily obtained without phi units.

(d) Phi units are dimensionless, and are not usable in physically related quantities where grain size must have units of length such as grain-size, Reynolds number, or relative roughness.

Size distributions of samples of littoral materials vary widely. Qualitatively, the size distribution of a sample may be characterized by a diameter that is in some way typical of the sample, and by the way that the sizes coarser and finer than the typical size are distributed. (Note that size distributions are generally based on weight, rather than number of particles.)

A size distribution is described qualitatively as *well-sorted* if all particles have sizes that are close to the typical size. If all the particles have exactly the same size, then the sample is *perfectly sorted*. If the particle sizes are distributed evenly over a wide range of sizes, then the sample is said to be *well-graded*. A well-graded sample is poorly sorted; a well-sorted sample is poorly graded.

The *median* (M_d) and the *mean* (M) define typical sizes of a sample of littoral materials. The median size, M_d in millimeters, is the most common measure of sand size in engineering reports. It may be defined as

$$M_d = d_{50}$$ (4-2)

where d_{50} is the size in millimeters that divides the sample so that half the sample, by weight, has particles coarser than the d_{50} size. An equivalent definition holds for the median of the phi size distribution, using the symbol $M_{d\phi}$ instead of M_d.

Several formulas have been proposed to compute an approximate mean (M) from the cumulative size distribution of the sample. (Otto, 1939;

Inman, 1952; Folk and Ward, 1957, McCammon, 1962.) These formulas are averages of 2, 3, 5, or more symmetrically selected percentiles of the phi frequency distribution, such as the formula of Folk and Ward.

$$M_\phi = \frac{\phi_{16} + \phi_{50} + \phi_{84}}{3} \qquad (4\text{-}3)$$

where ϕ is the particle size in phi units from the distribution curve at the percentiles equivalent to the subscripts 16, 50 and 84 (Fig. 4-8); ϕ_x is the size in phi units that is exceeded by x percent (by dry weight) of the total sample. These definitions of percentile (after Griffiths, 1967, p. 105) are known as graphic measures. A more complex method - the method of moments - can yield more precise results when properly used.

To a good approximation, the median, M_d is interchangeable with the mean, (M), for most beach sediment. Since the median is easier to determine it is widely used in engineering studies. For example, in one CERC study of 465 sand samples from three New Jersey beaches, the mean computed by the method of moments averaged only 0.01 millimeter smaller than the median for sands whose average median was 0.30 millimeter (1.74 phi). (Ramsey and Galvin, 1971.)

The median and the mean describe the approximate center of the sediment size distribution. In the past, most coastal engineering projects have used only this size information. However, for more detailed design calculations of fill quantities required for beach restoration projects (Sections 5.3 and 6.3), it is necessary to know more about the size distribution.

Since the actual size distributions are such that the log of the size is approximately normally distributed, the approximate distribution can be described (in phi units) by the two parameters that describe a normal distribution - the mean and the standard deviation. In addition to these two parameters (mean and standard deviation), skewness and kurtosis describe how far the actual size distribution of the sample departs from this theoretical lognormal distribution.

Standard deviation is a measure of the degree to which the sample spreads out around the mean and may be approximated using Inman's (1952) definition, by

$$\sigma_\phi = \frac{\phi_{84} - \phi_{16}}{2} , \qquad (4\text{-}4)$$

where ϕ_{84} is the sediment size, in phi units, that is finer than 84 percent by weight, of the sample. If the sediment size in the sample actually has a lognormal distribution, then σ_ϕ is the standard deviation of the
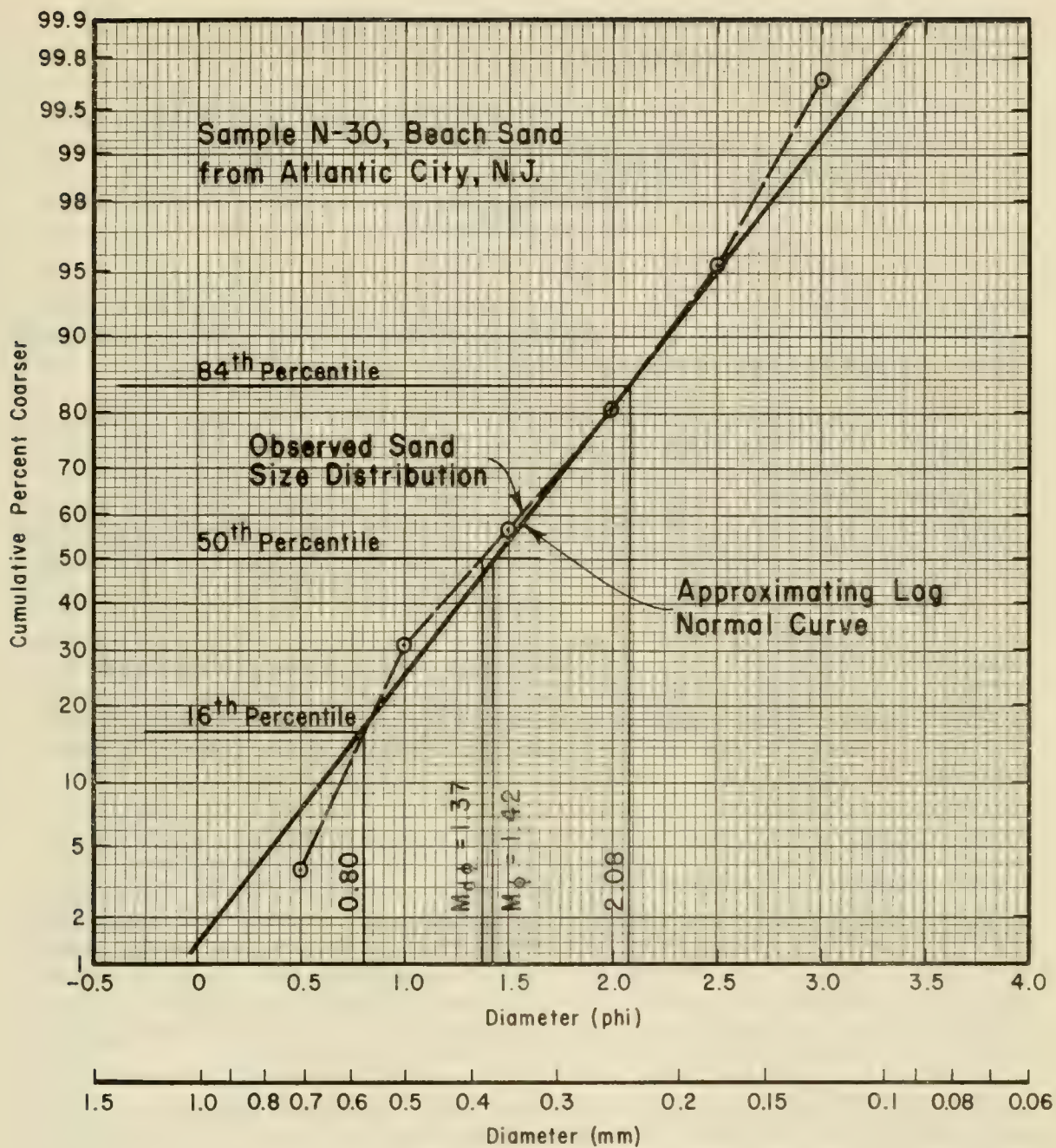
Figure 4-8. Example Size Distribution

sediment in phi units. For perfectly sorted sediment, $\sigma_\phi = 0$. For typical well-sorted sediments, $\sigma_\phi \approx 0.5$.

The degree by which the phi size distribution departs from symmetry is measured by the skewness (Inman, 1952), as

$$\alpha_\phi = \frac{M_\phi - M_{d\phi}}{\sigma\phi} , \qquad (4\text{-}5)$$

where M_ϕ is the mean, $M_{d\phi}$ is the median, and $\sigma\phi$ is the standard deviation in phi units. For a perfectly symmetric distribution, the mean equals the median, and the skewness is zero.

Extensive literature is available on the definition, use, and implication of σ, α, and other measures of the size distribution. (Inman, 1952; Folk and Ward, 1957; McCammon, 1962; Folk, 1965, 1966; and Griffiths, 1967), but despite a long history of investigation and a considerable background of data, applications of size distribution information "are still largely empirical, qualitative, and open to alternative interpretations." (Griffiths, 1967, p. 104.)

Currently, median grain size is the most commonly reported sand size characteristic, probably because there are only limited data to show the usefulness of other size distribution parameters in coastal engineering design. However, the standard deviation (Equation 4-4) must also be given as a parameter for use in beach fill design. (See Section 5.3; Krumbein and James, 1965; Vallianos, 1970; Berg and Duane, 1968.)

4.212 Composition. In addition to classification by size, littoral material may be classified by composition. For shore protection purposes, composition normally is not an important factor, since the dominant littoral materials are quartz sands which are durable and chemically inert for periods longer than typical project lifetimes. However, sediment composition is useful when the material departs from this expected condition. Other than quartz, littoral material may be composed of carbonates (usually shell, coral, and algal material), organics (most often peat), and clays and silts (marsh and tidal flat deposits).

4.213 Other Characteristics. In addition to size and composition, sediments have a number of other properties by which they may be classified. Table 4-2 lists some density-related properties. Radioactive properties of naturally occurring thorium minerals have been used as tracers in beach sands. (Kamel, 1962; Kamel and Johnson, 1962, p. 324.) Other properties more directly related to soil mechanics studies are found in soil mechanics manuals.

4.22 SAND AND GRAVEL

By definition the word sand refers to a size class of material, but sand also implies the particular composition, usually quartz (silica).

Table 4-2. Density of Littoral Materials

Specific Gravity (dimensionless)	
Quartz	2.65
Calcite	2.72
Heavy Minerals	> 2.87 (commonly 2.87 to 3.33)

Unit Weight* (lbs./ft.³)		
	Dry	Saturated
Uniform Sand		
loose	90	118
dense	109	130
Mixed Sand		
loose	99	124
dense	116	135
Clay		
stiff glacial	------	129
soft, very organic	-----	89

*From Terzaghi and Peck, 1967.

In tropical climates, calcium carbonate, especially shell material, is often the dominant material in beach sand. In temperate climates, quartz and feldspar grains are the most abundant, commonly accounting for about 90 percent of beach sand. (Krumbein and Sloss, 1963, p. 134.)

Because of its resistance to physical and chemical changes, and its common occurrence in terrestrial rocks, quartz is the most common mineral found in littoral materials. The relative abundance of non-quartz materials is a function of the relative importance of the sources supplying the littoral zone and the materials available to those sources. The small amount of heavy minerals (specific gravity greater than 2.87) usually found in sand samples may indicate the source area of the material (McMaster, 1954; Giles and Pilkey, 1965; Judge, 1970), and thus they may be used as natural tracers. Such heavy minerals may form black or reddish concentrations at the base of dune scarps, along the berm, and around inlets. Occasionally heavy minerals occur in concentrations great enough to justify mining them as a metal ore. (Everts, 1971; Martens, 1928.) Table 4-3 from Pettijohn (1957, p. 117) lists the 26 most common minerals found in beach sands.

Sand is by far the most important littoral material in coastal engineering design. However, in some localities, such as New England, Oregon, Washington, and countries bordering on the North Sea, gravel and shingle are locally important. Gravel-sized particles are often rock fragments, that is, a mixture of different minerals, whereas sand-sized particles usually consist of single mineral grains.

Table 4-3. Minerals Occurring in Beach Sand

Common Dominant Constituents*		
Quartz—may average about 70 percent in beach sand; varies from near 0 to over 99 percent.	Feldspar—typically only 10 to 20 percent in beach sands, but may be much more, particularly in regions of eroding igneous rock.	Calcite—includes shell, coral, algal fragments, and oolites; varies from 0 to nearly 100 percent; may include significant quantities of aragonite.
Common Accessory Minerals (Adopted from Pettijohn, 1957)		
Andalusite	Epidote	*Muscovite
Apatite	Garnet	Rutile
Aragonite	Hornblende	Sphene
Augite	Hypersthene-enstatite	Staurolite
Biotite	Ilmenite	Tourmaline
Chlorite	Kyanite	Zircon
Diopside	Leucoxene	Zoisite
*Dolomite	Magnetite	

* These are light minerals with specific gravity not exceeding 2.87. The remaining minerals are heavy minerals with specific gravity greater than 2.87. Heavy minerals make up less than 1 percent of most beach sands.

4.23 COHESIVE MATERIALS

The amount of fine-grained, cohesive materials, such as clay, silt, and peat, in the littoral zone depends on the wave climate, contributions of fine sediment from rivers and other sources, and recent geologic history. Fine-grain size material is common in the littoral zone wherever the annual mean breaker height is below about 1.0 foot. Fine material is found at or near the surface along the coasts of Georgia, western Florida between Tampa and Cape San Blas, and in large bays such as Chesapeake Bay and Long Island Sound. These are all areas of low mean breaker height. In contrast, fine sediment is seldom found along the Pacific coast of California, Oregon, and Washington, where annual mean breaker height usually exceeds 2.5 feet.

Where rivers bring large quantities of sediment to the sea, the amount of fine material remaining along the coast depends on the balance between wave action acting to erode the fines and river deposition acting to replenish the fines. (Wright and Coleman, 1972.) The effect of the Mississippi River delta deposits on the coast of Louisiana is a primary example.

Along eroding, low-lying coasts, the sea moves inland over areas formerly protected by beaches, so that the present shoreline often lies where tidal flats, lagoons and marshes used to be. The littoral materials on such coasts may include silt, clay and organic material at shallow depths. As the active sand beach is pushed back, these former tidal flats

and marshes then outcrop along the shore. (e.g. Kraft, 1971.) Many barrier islands along the Atlantic and Gulf coasts contain tidal and marsh deposits at or near the surface of the littoral zone. The fine material is often bound together by the roots of marsh plants to form a cohesive deposit that may function for a time as beach protection.

4.24 CONSOLIDATED MATERIAL

Along some coasts, the principal littoral materials are consolidated materials, such as rock, beach rock, and coral, rather than unconsolidated sand. Such consolidated materials protect a coast and resist shoreline changes.

4.241 <u>Rock</u>. Exposed rock along a shore indicates that the rate at which sand is supplied to the coast is less than the potential rate of sand transport by waves and currents. Reaction of a rocky shore to wave attack is determined by the structure, degree of lithification, and ground water characteristics of the exposed rock, and by the severity of the wave climate. Protection of eroding cliffs is a complex problem involving geology, rock mechanics, and coastal engineering. Two examples of these problems are the protection of the cliffs at Newport, Rhode Island (U.S. Army, Corps of Engineers, 1965) and at Gay Head, Martha's Vineyard, Massachusetts. (U.S. Army, Corps of Engineers, 1970.)

Most rocky shorelines are remarkably stable, with individual rock masses identified in photos taken 50 years apart. (Shepard and Grant, 1947.)

4.242 <u>Beach Rock</u>. A layer of friable to well-lithified rock often occurs at or near the surface of beaches in tropical and subtropical climates. This material consists of local beach sediment cemented with calcium carbonate, and it is commonly known as beach rock. Beach rock is important to coastal engineers because it provides added protection to the coast, greatly reducing the magnitude of beach changes (Tanner, 1960), and because beach rock may affect construction activities. (Gonzales, 1970.)

According to Bricker (1971), beach rock is formed when saline waters evaporate in beach sands, depositing calcium carbonate from solution. The present active formation of beach rock is limited to tropical coasts, such as the Florida Keys, but rock resembling beach rock is common at shallow depths along the east coast of Florida, on some Louisiana beaches, and related deposits have been reported as far north as the Fraser River Delta in Canada. Comprehensive discussion of the subject is given in Bricker (1971) and Russell (1970).

4.243 <u>Organic Reefs</u>. Organic reefs are wave-resistant structures reaching to about mean sea level that have been formed by calcium carbonate secreting organisms. The most common reef-building organisms are hermatypic corals and coralline algae. Reef-forming corals are usually restricted to areas having winter temperatures above about 18°C (Shepard, 1963, p. 351), but coralline algae have a wider range. On U.S.

coastlines, active coral reefs are restricted to southern Florida, Hawaii, Virgin Islands and Puerto Rico. On Some of the Florida coast, reeflike structures are produced by sabellariid worms. (Kirtley, 1971.) Organic reefs stabilize the shoreline and sometimes affect navigation.

4.25 OCCURRENCE OF LITTORAL MATERIALS ON U.S. COASTS

Littoral materials on U.S. coasts vary from consolidated rock to clays, but sand with median diameters between 0.1 and 1.0 millimeters (3.3 and 0 phi) is most abundant. General information on littoral materials is in the reports of the U.S. Army Corps of Engineers' National Shoreline Study; information on certain specific geological studies is available in Shepard and Wanless (1971); and information on specific engineering projects is published in Congressional documents and is available in reports of the Corps of Engineers.

4.251 **Atlantic Coast.** The New England coast is generally characterized by rock headlands separating short beaches of sand or gravel. Exceptions to this dominant condition are the sandy beaches in northeastern Massachusetts, and along Cape Cod, Martha's Vineyard, and Nantucket.

From the eastern tip of Long Island, New York, to the southern tip of Florida, the littoral materials are characteristically sand with median diameters in the range of 0.2 to 0.6 millimeter (2.3 to 0.7 phi). This material is mainly quartz sand. In Florida, the percentage of calcium carbonate in the sand tends to increase going south until, south of the Palm Beach area, the sand becomes predominantly calcium carbonate. Size distributions for the Atlantic coast, compiled from a number of sources, are shown in Figure 4-9. (Bash, 1972.) Fine sediments and organic sediments are common minor constituents of the littoral materials on these coasts, especially in South Carolina and Georgia. Beach rock and coquina are common at shallow depths along the Atlantic coast of Florida.

4.252 **Gulf Coast.** The Gulf of Mexico coasts of Florida, Alabama, and Mississippi are characterized by fine white sand beaches and by stretches of swamp. The swampy stretches are mainly in Florida, extending from Cape Sable to Cape Romano, and from Tarpon Springs to the Ochlockonee River. (Shepard and Wanless, 1971, p. 163.)

The Louisiana coast is dominated by the influence of the Mississippi River which has deposited large amounts of fine sediment around the delta from which wave action has winnowed small quantities of sand. This sand has been deposited along barrier beaches offshore of a deeply indented marshy coast. West of the delta is a 75-mile stretch of shelly sand beaches and beach ridges.

The Texas coast is a continuation of the Louisiana coastal plain extending about 80 miles to Galveston Bay; from there a series of long, wide barrier islands extends to the Mexican border. Littoral materials in this area are dominantly fine sand, with median diameters between 0.1 and 0.2 millimeter (3.3 and 2.3 phi).
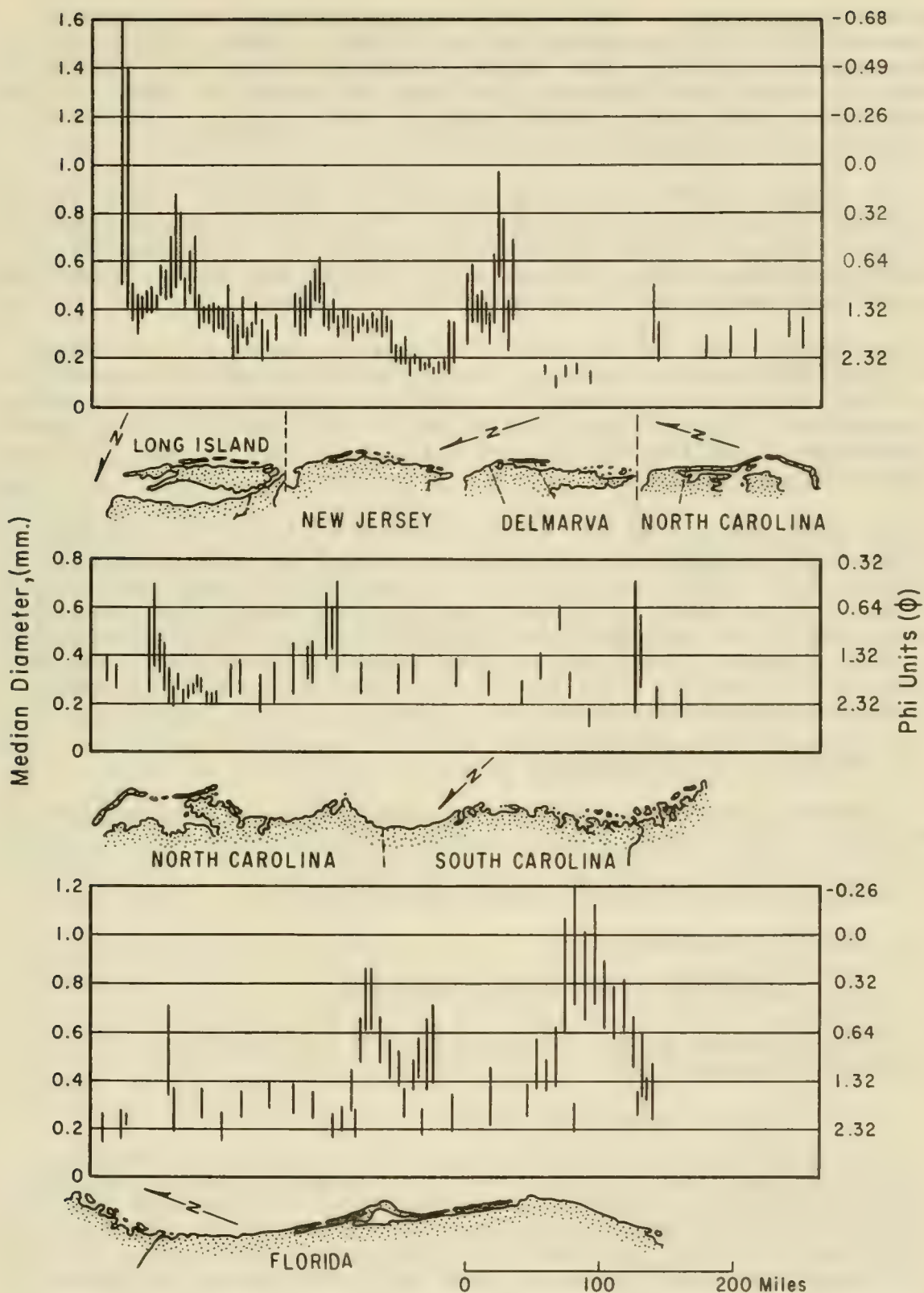
Figure 4-9. Sand Size Distribution Along the U.S. Atlantic Coast

4.253 Pacific Coast. Sands on the southern California coast range in size from 0.1 to 0.6 millimeter (3.3 to 0.7 phi). (Emery, 1960, p. 190.) The northern California coast becomes increasingly rocky, and coarser material becomes more abundant. The Oregon and Washington coasts include considerable sand (Bascom, 1964), with many rock outcrops. Sand-sized sediment is contributed by the Columbia River and other smaller rivers.

4.254 Alaska. Alaska has a long coastline (47,300 miles), and is correspondingly variable in littoral materials. However, beaches are generally narrow, steep, and coarse-grained; they commonly lie at the base of seacliffs. (Sellman, et al., 1971, p. D-10.) Quartz sand is less common and gravel more common here than on many other U.S. coasts.

4.255 Hawaii. Much of the Hawaiian islands is bounded by steep cliffs, but there are extensive beaches. Littoral materials consist primarily of bed rock, and white sand formed from calcium carbonate produced by marine invertebrates. Dark colored basaltic and olivine sands are common where river mouths reach the sea. (Shepard and Wanless, 1971, p. 497, U.S. Army, Corps of Engineers, 1971.)

4.256 Great Lakes. The U.S. coasts of the Great Lakes vary from high bluffs of clay, shale, and rock, through lower rocky shores and sandy beaches, to low marshy clay flats. (U.S. Army Corps of Engineers, National Shoreline Study, August 1971, North Central Division, p. 13.) The littoral materials are quite variable. Specific features are discussed, for example, by Bowman (1951); Hulsey (1962); Davis (1964-65); Bajorunas and Duane (1967); Berg and Duane (1968); Saylor and Upchurch (1970); Hands (1970); and Corps of Engineers (1953, 1971).

4.26 SAMPLING LITTORAL MATERIALS

Sampling programs are designed to provide information about littoral materials on one or more of the following characteristics:

(a) typical grain size (usually median size),

(b) size distribution,

(c) composition of the littoral materials,

(d) variation of (a), (b), and (c), with horizontal and vertical position on the site, and

(e) possible variation in (a), (b), (c), and (d) with time.

A sampling program will depend on the intended purpose of the samples, the time and money available for sampling, and an inspection of the site to be sampled. A brief inspection will often identify the principal variations in the sediment and suggest the best ways to sample these variations. Sampling programs usually involve beach and nearshore sands and potential borrow sources.

The extent of sampling depends on the importance of littoral materials as related to the total engineering problem. The sampling program should specify:

(a) horizontal location of sample,

(b) spacing between samples,

(c) volume of sample,

(d) vertical location and type of sampled volume (e.g. surface layer or vertical core),

(e) technique for sampling,

(f) method of storing and documenting the sample.

Beaches typically show more variation across the profile than along the shore, so sampling to determine variation in the littoral zone should usually be along a line perpendicular to the shoreline.

For reconnaissance sampling, a sample from both the wetted beach face and from the dunes is recommended. More extensive samples could be obtained at constant spacings across the beach or at different locations on the beach profile. Spacings between sampling lines are determined by the variation visible along the beach or by statistical techniques.

Many beaches have subsurface layers of peat or other fine material. If this material will affect the engineering problem, vertical holes or borings should be made to obtain samples at depth.

Sample volume should be adequate for analysis. For sieve analysis, about 50 grams are required; for settling tube analysis, smaller quantities will suffice, but at least 50 grams are needed if other studies are required later. A quarter of a cup is more than adequate for most uses.

Sand often occurs in fine laminae on beaches. However, for engineering applications it is rarely necessary to sample individual laminae of sand. It is easier and more representative to take an equidimensional sample that cuts across many laminae. Experience at CERC suggests that any method of obtaining an adequate volume of sample covering a few inches in depth usually gives satisfactory results. Cores should be taken where pile foundations are planned.

The sample is only as good as the information identifying it. The following minimum information should be recorded at the time of sampling: locality, date and time, position on beach, remarks, and initials of collector. This information must stay with the sample, which is best ensured by fixing it to the sample container or placing it inside the container. Unless precautions are taken, the sample label may deteriorate due to moisture, abrasion, or other causes. Improved labels result by using

ballpoint ink on plastic strip (plastic orange flagging commonly used by surveyors). Some information may be preprinted by rubber stamp on the plastic strip using indelible laundry ink. The advantage is that the label can be stored in the bag with the wet sample without the label deteriorating or the information washing or wearing off.

4.27 SIZE ANALYSES

Three common methods of analyzing a beach sediment for size are: visual comparison with a standard, sieve analysis, and settling tube analysis.

The mean size of a sand sample can be estimated qualitatively by visually comparing the sample with sands of known sizes. Standards can be easily prepared by sieving out selected diameters, or by selecting samples whose sizes are already known. The standards may be kept in labeled transparent vials, or glued on cards. If glued, care is necessary to ensure that the particles retained by the glue are truly representative of the standard.

Good, qualitative, visual estimates of mean size are possible with little previous experience. With experience, such visual estimates become semiquantitative. Visual comparison with a standard is a useful tool in reconnaisance, and in obtaining interim results pending a more complete laboratory size analysis.

4.271 Sieve Analysis. Sieves are graduated in size of opening according to the U.S. Standard series. These standard sieve openings vary by a factor of 1.19 from one opening to the next larger (by the fourth root of 2, or quarter phi intervals), e.g., 0.25, 0.30, 0.35, 0.42, and 0.50 millimeters (2.00, 1.75, 1.50, 1.25, 1.00 phi). The range of sieve sizes used, and the size interval between sieves selected can be varied as required. Typical beach sand can be analyzed adequately using sieves with openings ranging from 0.062 to 2.0 millimeters (4.0 to -1.0 phi), in size increments increasing by a factor of 1.41 (half-phi intervals).

Sediment is usually sieved dry. However, for field analysis or for size analysis of sediment with a high content of fine material, it may be useful to wet-sieve the sediment. Such wet-sieve analyses are described by (e.g., Lee, Yancy, and Wilde, 1970, p. 4).

Size analysis by sieves is relatively slow, but provides a widely accepted standard of reference.

4.272 Settling Tube. Spherical sedimentary particles settle through water at a speed that increases as the particle weight increases. Since most sand is approximately spherical quartz, or calcium carbonate with a specific gravity near quartz, particle size is proportional to particle weight. Thus fall velocity can be used to measure size. (e.g., Colby and Christensen, 1956; Zeigler and Gill, 1959; and Gibbs, 1972.) Figure 4-31 shows fall velocity for quartz spheres as a function of temperature.

There are numerous types of settling tubes; the most common is the visual accumulation tube (Colby and Christensen, 1956), of which there are also several types. The type now used at CERC (the rapid sediment analyzer or RSA) works in the following way:

A 3- to 6-gram sample of sand is dropped through a tube filled with distilled water at constant temperature. A pressure sensor near the bottom of the tube senses the added weight of the sediment supported by the column of water above the sensor. As the sediment falls past the sensor, the pressure decreases. The record of pressure versus time is empirically calibrated to give size distribution based on fall velocity. (Zeigler and Gill, 1959.)

The advantage of settling tube analysis is its speed. With modern settling tubes, average time for size analyses of bulk lots can be about one-fifth the time required by sieves.

It is often claimed that a settling tube also provides a physically more realistic size analysis than a sieve, since the fall velocity takes into account the hydrodynamic effects of shape and density. However, this claim has not been documented, and may be questioned in view of the limited knowledge concerning the fluid mechanics of a sand sample falling in a settling tube - the lead particles encounter effectively laminar flow, the trailing particles encounter turbulent flow, and all particles inter-act with each other.

Because of lack of an accepted standard settling tube, rapidly chang-ing technology, possible changes in tube calibration, and the uncertainty about fluid mechanics in settling tubes, it is recommended that all set-tling tubes be carefully calibrated by running a range of samples through both the settling tube and ASTM standard sieves. After thorough initial calibration, the calibration should be spot-checked periodically by running replicate sand samples of known size distribution through the tube.

4.3 LITTORAL WAVE CONDITIONS

4.31 EFFECT OF WAVE CONDITIONS ON SEDIMENT TRANSPORT

Waves arriving at the shore are the primary cause of sediment trans-port in the littoral zone. Higher waves break further offshore, widening the surf zone and setting more sand in motion. Changes in wave period or height result in moving sand onshore or offshore. The angle between the crest of the breaking wave and the shoreline determines the direction of the longshore component of water motion in the surf zone, and usually the longshore transport direction. For these reasons, knowledge about the wave climate - the combined distribution of height, period, and direction through the seasons - is required for an adequate understanding of the littoral processes of any specific area.

4.32 FACTORS DETERMINING LITTORAL WAVE CLIMATE

The wave climate at a shoreline depends on the offshore wave climate, caused by prevailing winds and storms, and on the bottom topography that modifies the waves as they travel shoreward.

4.321 Offshore Wave Climate. Wave climate is the distribution of wave conditions averaged over the years. A wave condition is the particular combination of wave heights, wave periods, and wave directions at a given time. A specific wave condition offshore is the result of local winds blowing at the time of the observation and the recent history of winds in the more distant parts of the same water body. For local winds, wave conditions offshore depend on the wind velocity, duration, and fetch. For waves reaching an observation point from distant parts of the sea, a decay factor is added which preferentially filters out the higher, shorter period waves with increasing distances. (Chapter 3 discusses wave generation and decay.)

4.322 Effect of Bottom Topography. As waves travel from deep water, they change height and direction because of refraction, shoaling, bottom friction, and percolation. Laboratory experiments indicate that height and apparent period are also changed by nonlinear deformation of the waves in shallow water.

Refraction is the bending of wave crests due to the slowing down of that part of the wave crest which is in shallower water. (See Section 2.32.) As a result, refraction tends to decrease the angle between the wave crest and the bottom contour. Thus, for most coasts, refraction reduces the breaker angle and spreads the wave energy over a longer crest length.

Shoaling is the change in wave height due to conservation of energy flux. (See Section 2.32). As a wave moves into shallow water the wave height first decreases slightly, and then increases continuously to the breaker position, assuming friction and refraction effects are negligible.

Bottom friction is important in reducing wave height where waves must travel long distances in shallow water. (Bretschneider, 1954.)

There has been only limited field study of nonlinear deformation in shallow water waves (Byrne, 1969), but because such deformation is common in laboratory experiments (Galvin, 1972), it is expected that such phenomena are also common in the field. An effect of nonlinear deformation is to split the incoming wave crest into two or more crests affecting both the resulting wave height and the apparent period.

Offshore islands, shoals, and other variations in hydrography also shelter parts of the shore. In general, bottom hydrography has the greatest influence on waves traveling long distances in shallow water. Because of the effects of bottom hydrography, nearshore waves generally have different characteristics than they had in deep water offshore.

Such differences are often visible on aerial photos. Photos may show two or more distinct wave trains in the nearshore area, with the wave train most apparent offshore decreasing in importance as the surf zone is approached. (e.g., Harris, 1972.) The difference appears to be caused by the effects of refraction and shoaling on waves of different periods. Longer period waves, which may be only slightly visible off-shore, may become the most prominent waves at breaking, because shoaling increases their height relative to the shorter period waves. Thus, the wave period measured from the dominant wave offshore may be less than the wave period measured from the dominant wave entering the surf zone when two wave trains of unequal period reach the shore at the same time.

4.323 **Winds and Storms.** The relation of a shoreline locality to the seasonal distribution of winds and to storm tracks is a major factor in determining the wave energy available for littoral transport. For example, strong winter winds in the northeastern United States usually are from the northwest, but because they blow from land to sea, they do not produce large waves at the shore. These northwest winds often imme-diately follow a northeaster - a low pressure system with strong north-east winds that generate high waves offshore.

A storm near the coastline will influence wave climate with storm surge and high seas; a storm offshore will influence wave climate only by swell. The relation between the meteorological severity of a storm and the resulting beach change is complicated. (See Section 4.35.) Storms are not uniformly distributed in time or space: storms vary seasonally and from year to year; storms originate more frequently in some areas than in others; and storms follow characteristic tracks deter-mined by prevailing global circulation and weather patterns.

An investigation of 170 damaging storms affecting the east coast of the U.S. from 1921-1962 (Mather, et al., 1964), classified the storms into eight types based on origin, structure, and path of movement. Of these eight types, although 33 percent were hurricanes, two types, comprising only 19 percent of the total, characterized by weather fronts east and south of the U.S. coasts produced more damage per storm because of long fetches. (Damage is defined by Mather, et al., as "at best some water damage," and includes "wave damage, coastal flooding, and tidal inunda-tion," but specifically excludes wind damage.)

The probability that a given section of coast will experience storm waves depends on its ocean exposure, its location in relation to storm tracks, and the shelf bathymetry.

4.33 **NEARSHORE WAVE CLIMATE**

4.331 **Mean Value Data on U.S. Littoral Wave Climates.** Wave height and period data for some localities of the U.S. are becoming increasingly available (e.g., Thompson and Harris, 1972), but most localities still lack such data. However, wave direction is difficult to measure, and consequently direction data are rarely available.

The quality and quantity of available data often do not justify elaborate statistical analysis. Even where adequate data are available, a simple characterization of wave climate meets many engineering needs. While mean values of height and, to a lesser degree, period are useful, data on wave direction are generally of insufficient quality for even mean value use. Table 4-4 compiles mean annual wave heights collected from a number of wave gages and by visual observers along the coasts of the United States. Visual observations were made from the beach of waves near breaking. The gages were fixed in depths of 10 to 28 feet.

Wave data treated in this section are limited to nearshore observations and measurements. Consequently waves were fully refracted and had been fully affected by bottom friction, percolation, and nonlinear changes in wave form by shoaling. Thus, these data differ from data that would be obtained by simple shoaling calculations based on the deepwater wave statistics. In addition, data are normally lacking for the rarer, high-wave events. For these reasons, the data should not be used for structural design, since they are only applicable to the particular site where they were obtained. Normal design practice is based on deepwater wave statistics which are then adjusted to the shallow-site conditions. However, the nearshore data are useful in littoral transport calculations.

Mean wave height and period from a number of visual observations by coastguardmen at shore stations are plotted by month in Figures 4-10 and 4-11, using the average values of stations within each of five coastal segments. Table 4-4 and Figures 4-10 and 4-11 show average values characteristic of the wave climate in exposed coastal localities. Visual height data represent an average value of the higher waves just before they first break. The data provide only approximate indications of the height distributions, but mean values of these distributions are useful.

In Figure 4-10 the *minimum* monthly mean littoral zone wave height averaged for the California, Oregon, and Washington coasts exceeds the *maximum* mean littoral zone wave height averaged for the other coasts. This difference greatly affects the potential for sediment transport in the respective littoral zones, and should be considered by engineers when applying experience gained in a locality with one nearshore wave climate to a problem at a locality with another wave climate.

4.332 Mean vs Extreme Conditions. Section 3.22 contains a discussion of wave height distributions and the relations between various wave height statistics, such as the mean, significant, and RMS heights, and extreme values. In general, a group of waves from the same record can be approximately described by a Rayleigh distribution. (See Section 3.22.) However, a different distribution appears necessary to describe the distribution of significant wave heights, where each significant wave height is from a different wave record at the locality. (See Figure 4-12.)

Visual analysis of waves recorded on chart paper is discussed in Section 3.22 and by Draper (1967), Tucker (1963), Harris (1970), and Magoon (1970). Spectrum analysis of wave records is discussed in
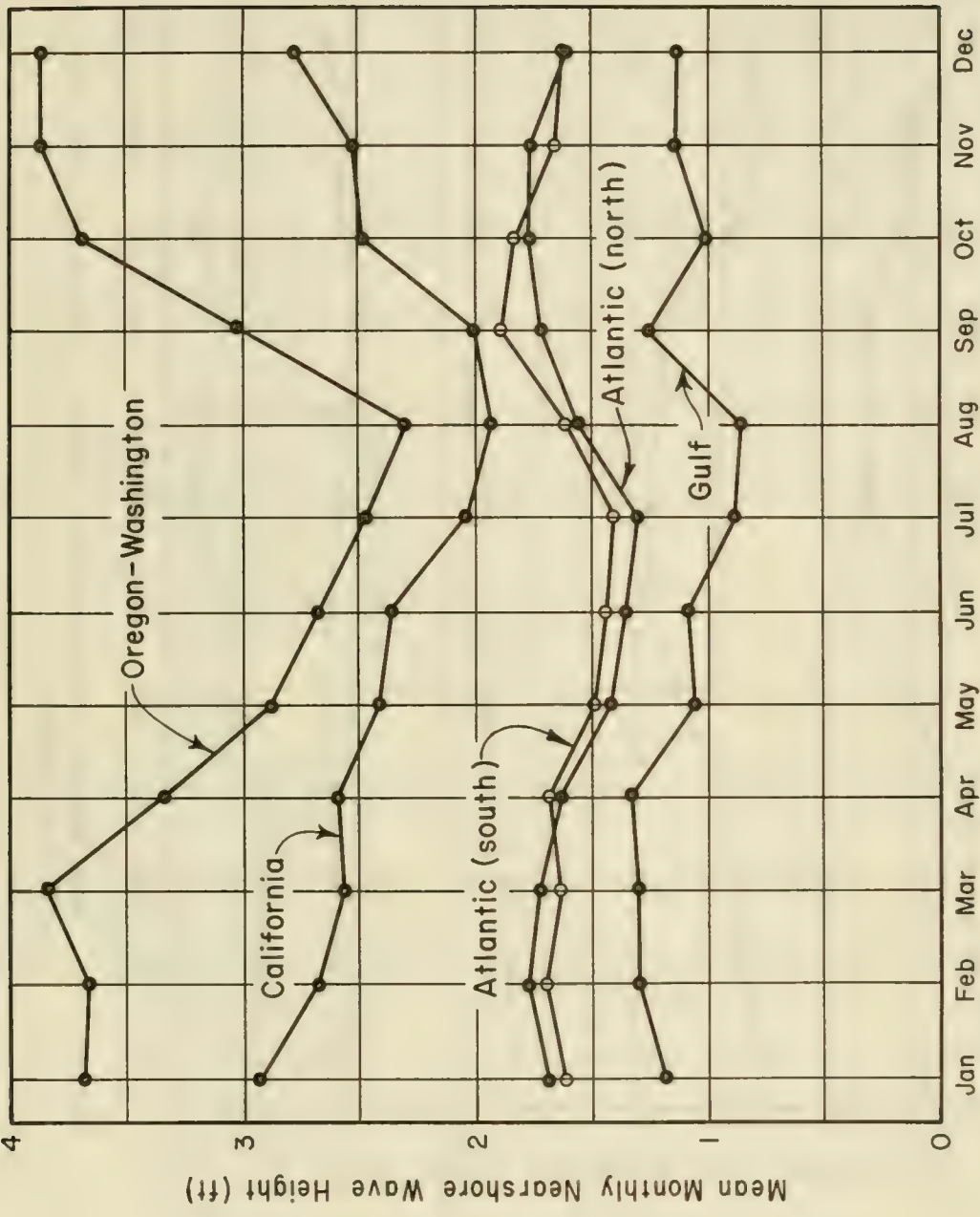
Figure 4-10. Mean Monthly Nearshore Wave Heights for Five Coastal Segments
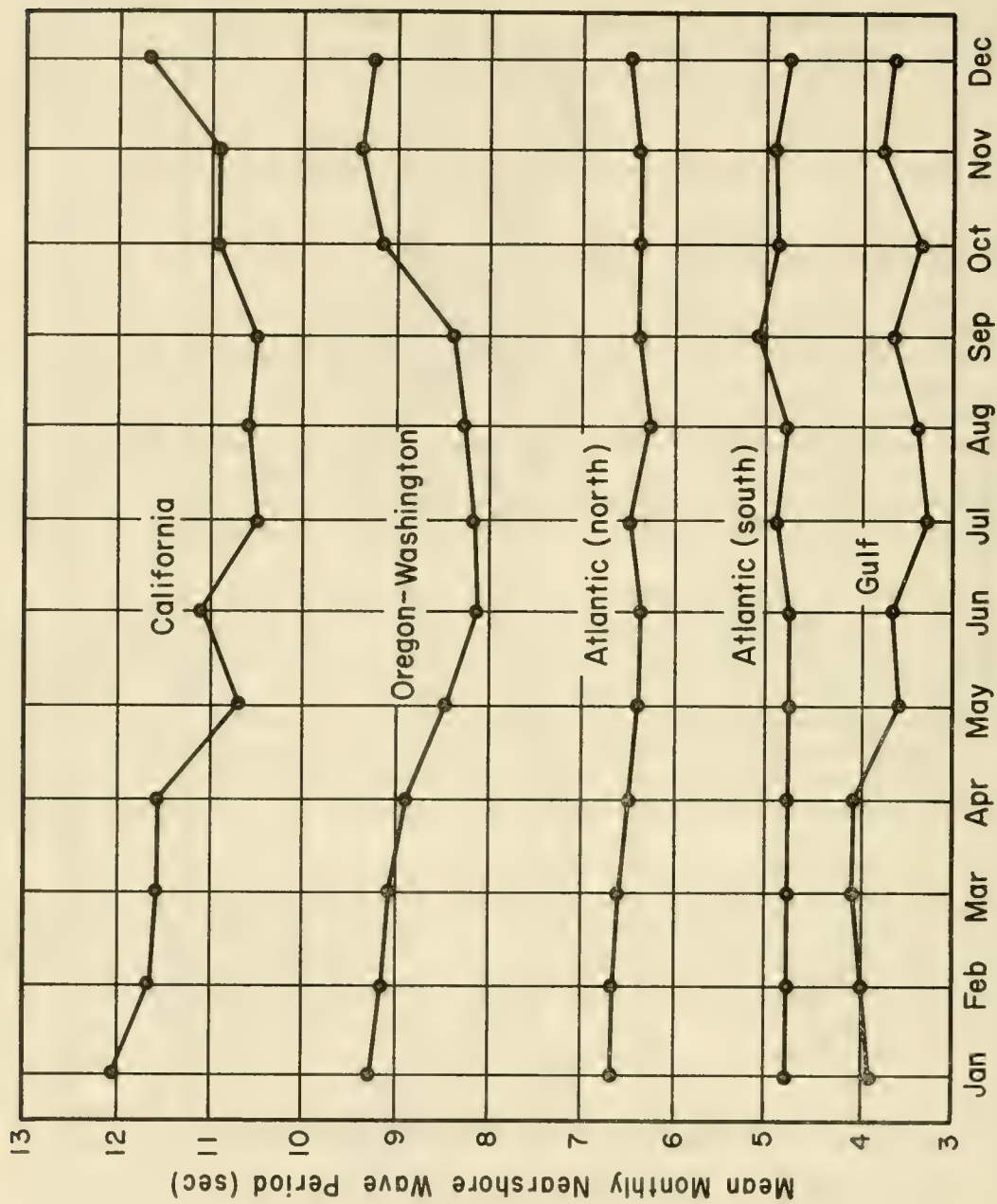
Figure 4-11. Mean Monthly Nearshore Wave Periods (Including Calms) for Five Coastal Segments

Table 4-4. Mean Wave Height at Coastal Localities of Conterminous United States

Location	Mean Annual Wave Height (ft.)	Location	Mean Annual Wave Height (ft.)
Atlantic Coast			
Maine		**New Jersey (cont.)**	
Moose Peak	1.5	† Ludlam Island	1.9
New Hampshire		**Maryland**	
Hampton Beach	1.4	Ocean City	1.8
Massachusetts		**Virginia**	
Nauset	1.8	† Assateague	2.6
† Cape Cod	2.5	*Virginia Beach	1.8
Rhode Island		Virginia Beach	2.0
Point Judith	1.8	**North Carolina**	
† Misquamicut	1.4	*Nags Head	3.0
New York		Nags Head	3.9
† Southampton	1.9	† Wrightsville	2.3
† Westhampton	2.6	Oak Island	1.2
† Jones Beach	2.6	† Holden Beach	1.7
Short Beach	1.7	**Georgia**	
New Jersey		St. Simon Island	0.4
Monmouth	1.7	**Florida**	
† Deal	2.3	*Daytona Beach	1.9
Toms River	2.0	Ponce deLeon	2.2
† Brigantine	2.2	*Lake Worth	2.3
*Atlantic City	2.8	*Palm Beach	2.3
Atlantic City (BEP)	1.3	† Boca Raton	1.9
† Atlantic City (CG)	1.9	Hillsboro	1.3
Gulf Coast			
Florida		**Florida (cont.)**	
*Naples	1.0	‡ Navarre Beach	2.3
Cape San Blas	0.7	Santa Rosa	1.4
‡ Panama City	1.7	**Louisania**	
‡ Greyton Beach	1.7	Grand Island	1.4
‡ Crystal Beach	1.7	**Texas**	
‡ Beasley Park	1.8	*Galveston	1.4
Pacific Coast			
California		**California (cont.)**	
Point Loma	2.1	Point Arguello	2.5
‡ South Carlsbad	2.7	‡ Natural Bridges	2.9
‡ Carlsbad	2.9	‡ Thornton	4.1
*Huntington Beach	1.7	‡ Goat Rock	4.6
‡ Huntington	2.6	Point Arena	2.6
‡ Bolsa Chica	2.2	‡ Prairie Creek	3.7
‡ Leo Carrillo	2.3	**Oregon**	
‡ PEG at Point Mugu	3.0	Umpqua River	3.3
*Point Mugu	2.7	Yaquina Bay	5.1
‡ McGrath	3.5	**Washington**	
‡ Carpinteria	1.8	Willapa Bay	1.8
Point Conception	2.8	Cape Flattery	1.7
‡ El Capitan	2.0		

*   CERC wave gage records.

The following mean wave heights are from visual (nearbreaker) observations.

  †   CERC Beach Evaluation Program.

  ‡   CERC Littoral Environment Observation Program.

Unmarked Coast Guard Observations.
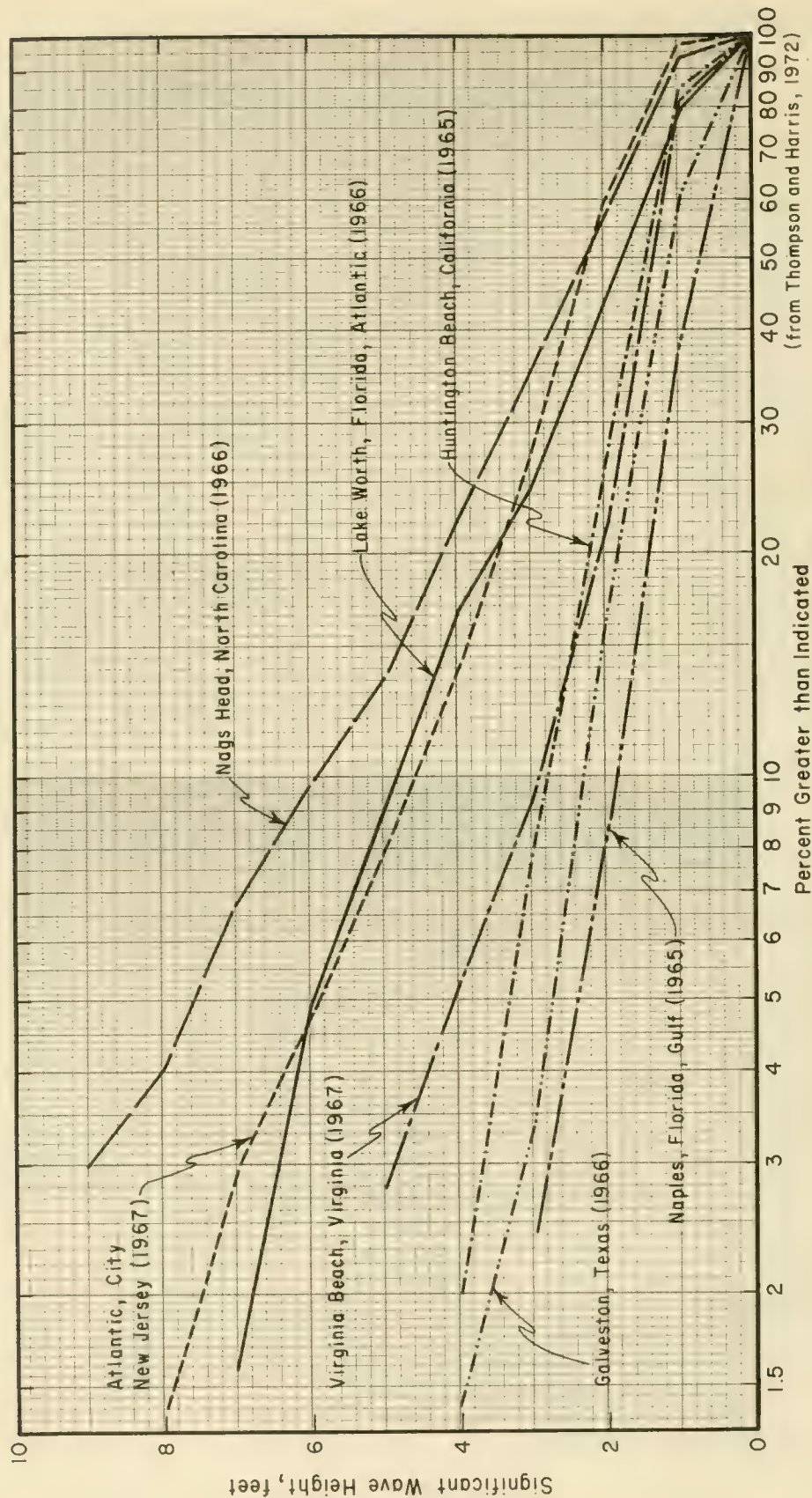
Figure 4-12. Distribution of Significant Wave Heights from Coastal Wave Gages for 1-Year Records

(from Thompson and Harris, 1972)

4-34

Section 3.23 and by Kinsman (1965), National Academy of Sciences (1963), and Neumann and Pierson (1966).

For the distribution of significant wave heights as defined by the data reduction procedures at CERC (Thompson and Harris, 1972), the data fit a modified exponential distribution of form

$$F\left(H_s > \widehat{H}_s\right) = e^{-\left[\dfrac{\widehat{H}_s - H_{s\,min}}{\sigma}\right]}, \qquad (4\text{-}6)$$

where H_s is the significant height, $\widehat{H}_s$ the significant height of interest, $H_{s\,min}$ is the approximate "minimum significant height," and σ is the significant wave height standard deviation. This equation depends on two parameters, $H_{s\,min}$ and σ which are related to the mean height,

$$\overline{H}_s = H_{s\,min} + \sigma . \qquad (4\text{-}7)$$

If $H_{s\,min}$ or σ are not available, but the mean significant height, $\overline{H}_s$ is known, then an approximation to the distribution of (4-6) can be obtained from the data of Thompson and Harris (1972, Table 1), which suggest

$$H_{s\,min} \approx 0.38\,\overline{H}_s . \qquad (4\text{-}8)$$

This approximation reduces Equation 4-6 to a one-parameter distribution depending only on mean significant wave height

$$F\left(H_s > \widehat{H}_s\right) \approx e^{-\left[\dfrac{1.61\,\widehat{H}_s - 0.61\,\overline{H}_s}{\overline{H}_s}\right]}. \qquad (4\text{-}9)$$

Equation 4-9 is not a substitute for the complete distribution function, but when used with the wave-gage data on Figure 4-12, it provides an estimate of higher waves with agreement within 20 percent. Greater scatter would be expected with visual observations.

4.34 OFFICE STUDY OF WAVE CLIMATE

Information on wave climate is necessary for understanding local littoral processes. Usually, time does not permit obtaining data from the field, and it is necessary to compile information in an office study. The primary variables of engineering interest for such a compilation are wave height and direction.

Shipboard observations covering conterminous U.S. coasts and other ocean areas are available as summaries (Summary of Synoptic Meterological Observations, SSMO) through the National Technical Information Service, Springfield, Va. 22151. See Harris (1972) for a preliminary evaluation of this data for coastal engineering use.

When data are not available for a specific beach, the wave climate can be estimated by extrapolating from another location, after correcting for differences in coastal exposure, winds, and storms.

On the east, gulf, and Great Lakes coasts, local winds are often highly correlated with the direction of longshore currents. Such wind data are available in "Local Climatological Data" sheets published monthly by the National Weather Service, National Oceanographic and Atmospheric Agency (NOAA) for about 300 U.S. weather stations. Other NOAA wind-data sources include annual summaries of the Local Climatological Data by station (Local Climatological Data with Comparative Data), and weekly summaries of the observed weather (Daily Weather Maps), all of which can be ordered from the Superintendent of Documents, U.S. Government Printing Office, Washington, D.C. 20402.

Local weather data are often affected by conditions in the neighborhood of the weather station, so care should be used in extrapolating weather records from inland stations to a coastal locality. However, statistics on frequency and severity of storm conditions do not change appreciably for long reaches of the coast. For example, in a study of Texas hurricanes, Bodine (1969) felt justified in assuming no difference in hurricane frequency along the Texas coast. In developing information on the Standard Project Hurricane, Graham and Nunn (1959) divided the Atlantic Coast into zones 200 miles long and the gulf coast into zones 400 miles long. Variation of most hurricane parameters within zones is not great along straight open stretches of coast.

The use of weather charts for wave hindcasting is discussed in Section 3.4. Computer methods for generating offshore wave climate are now (1973) under test and development. However, development of nearshore wave climate from hindcasting is usually a time-consuming job, and the estimate obtained may suffer in quality because of the inaccuracy of hindcast data, and the difficulty of assessing the effect of nearshore topography on wave statistics. At the present time, if available at the specific location, statistics based on wave-gage records are preferable to hindcast statistics when wave data for the shallow-water conditions are required.

Other possible sources of wave climate information for office studies include aerial photography, newspaper records, and comments from local residents.

Data of greater detail and reliability than that obtained in an office study can be obtained by recording the wave conditions at the shoreline locality for at least 1 year by the use of visual observers or wave gages. A study of year-to-year variation in wave height statistics collected at CERC wave gages (Thompson and Harris, 1972), indicates that six observations per day for 1 year gives a reliable wave height distribution function to the 1 percent level of occurrence. At the gage at Atlantic City, one observation a day for 1 year provided a useful height-distribution function.

Infrequent events of great magnitude, such as hurricanes, cause significant modification of the littoral zone, particularly to the profile of a beach. An *extreme* event could be defined as an event, great in terms of total energy expended or work done, that is not expected to occur at a particular location, on the average, more than once every 50 to 100 years. Hurricane Camille in 1969 and the East Coast Storm of March 1962 can be considered extreme events. Because large storms are infrequent, and because it does not necessarily follow that the magnitude of a storm determines the amount of geomorphic change, the relative importance of extreme events is difficult to establish.

Wolman and Miller (1960) suggested that the equilibrium profile of a beach is more related to moderately strong winds that generate moderate storm waves, rather than to winds that accompany infrequent catastrophic events. Saville (1950) showed that for laboratory tests with constant wave energy and angle of attack there is a particular critical wave steepness at which littoral transport is a maximum. Under field conditions, there is probably a similar critical value that produces transport out of proportion to its frequency of occurrence. The winds associated with this critical wave steepness may be winds generated by smaller storms, rather than the winds associated with extreme events.

A review of studies of beach changes caused by major storms indicates that no general conclusion that can be made concerning the significance of extreme events. Many variables affect the amount of damage a beach will sustain in a given storm.

Most storms move large amounts of sand from the beach offshore, but after the storm, the lower waves that follow tend to restore this sand to the face of the beach. Depending on the extent of restoration, the storm may result in little permanent change. Depending on the path of the storm and the angle of the waves, a significant amount of material can also be moved alongshore. If the direction of longshore transport caused by the storm is opposite to the net direction of transport, the sand will probably be returned in the months after the storm and permanent beach changes effected by the storm will be small. If the direction of transport before, during, and after the storm is the same, then large amounts of material could be moved by the storm with little possibility of restoration. Successive storms on the same beach may cause significant transport in opposite directions. (e.g. Everts, 1973.)

There are some unique events that are only accomplished by catastrophic storms. The combination of storm surge and high waves allows water to reach some areas not ordinarily attacked by waves. These extreme conditions may result in the overtopping of dunes and in the formation of washover fans and inlets. (Morgan, et al., 1958; Nichols and Marston, 1939.) Some inlets are periodically reopened by storms and then sealed by littoral drift transported by normal wave action.

The wave climate at a particular beach also determines the effect a storm will have. In a high-energy climate, storm waves are not much larger than ordinary waves, and their effects may not be significant. An example of this might be northeasters occurring at Cape Cod. In a low-energy wave climate, where transport volumes are usually low, storm waves can move significant amounts of sand, as do hurricanes on the gulf coast.

The type of beach sediment is also important in storm-induced changes. A storm can uncover sediments not ordinarily exposed to wave action, and thus alter the processes that follow the storm. (Morgan, et al., 1958.) In sand-deficient areas where the beach is underlain by mud, the effects of a storm can be severe and permanent.

The effects of particular storms on certain beaches are described in the following paragraphs. These examples illustrate how an extreme event may affect the beach.

In October 1963, the worst storm in the memory of the Eskimo people occurred over an ice-free part of the Arctic Ocean, and attacked the coast near Barrow, Alaska. (Hume and Schalk, 1967.) Detailed measurements of some of the key coastal areas had been made just before the storm. Freeze-up just after the storm preserved the changes to the beach until surveys could be made the following July. Most of the beaches accreted 1 to 2 feet, although Point Barrow was turned into an island. According to Hume and Schalk, "The storm of 1963 would appear to have added to the Point the sediment of at least 20 years of normal longshore transport." Because of the low-energy wave climate and the short season in which littoral processes can occur at Barrow, this storm significantly modified the beach.

A study of two hurricanes, Carla (1961) and Cindy (1963), was made by Hayes (1967). He concluded that "the importance of catastrophic storms as sediment movers cannot be over-emphasized," and observed that, in low-energy wave climates, most of the total energy is expended in the near-shore zone as a series of catastrophes. In this region, however, the rare "extreme" hurricane is probably not as significant in making net changes as the more frequent moderate hurricanes.

Surprisingly, Hurricane Camille, with maximum winds of 200 mph, did not cause significant changes to the beaches of Mississippi and Louisiana. Tanner (1970) estimated that the sand transport along the beach appeared to have been an amount equal to less than a year's amount under ordinary conditions, and theorized that "the particular configuration of beach, sea wall, and coastal ridge tended to suppress large scale transport."

Hurricane Audrey struck the western coast of Louisiana in June, 1957. The changes to the beach during the storm were not extreme nor permanent. However, the storm exposed marsh sediments in areas where sand was deficient, and "set the stage for a period of rapid shoreline retreat following the storm." (Morgan, et al., 1958.) Indirectly, then, the storm was responsible for significant geomorphic change.

A hurricane (unnamed) coincided with spring tide on the New England coast on 21 September 1938. Property damage and loss of life were both high. A storm of this magnitude was estimated to occur about once every 150 years. A study of the beach changes along a 12-mile section of the Rhode Island coast (Nichol and Marsten, 1939) showed that most of the changes in the beach profile were temporary. The net result was some cliff erosion and a slight retrogression of the beaches.

Beach changes from Hurricane Donna which hit Florida in September 1960 were more severe and permanent. In a study of the southwestern coast of Florida before and after the storm, Tanner (1961), concluded that "Hurricane Donna appears to have done 100 year's work, considering the typical energy level thought to prevail in the area."

On 1 April 1946, a tsunami struck the Hawaiian Islands with runup in places as high as 55 feet above sea level. (Shepard, et al., 1950.) The beach changes were similar to those inflicted by storm waves although "in only a few places were the changes greater than those produced during normal storm seasons or even by single severe storms." Because a tsunami is of short duration, extensive beach changes do not occur, although property damage can be quite high.

Several conclusions can be drawn from the above examples. If a beach has a sufficient sand supply and fairly high dunes, and if the dunes are not breached, little permanent modification will result from storms, except for a brief acceleration of the normal littoral processes. This acceleration will be more pronounced on a shore with low-energy wave conditions.

4.4 NEARSHORE CURRENTS

Nearshore currents in the littoral zone are predominantly wave-induced motions superimposed on the wave-induced oscillatory motion of the water. The net motions generally have low velocities, but because they transport whatever sand is set in motion by the wave-induced water motions, they are important in determining littoral transport.

There is only slight exchange of fluid between the offshore and the surf zone. Onshore-offshore flows take place in a number of ways, which at present are not fully understood.

4.41 WAVE-INDUCED WATER MOTION

In idealized deepwater waves, water particles have a circular motion in a vertical plane perpendicular to the wave crest (Fig. 2-4, Section 2.235), but this motion does not reach deep enough to affect sediment on the bottom. In depths where waves are affected by the bottom, the circular motion becomes elliptical, and the water at the bottom begins to move. In shallow water, the ellipses elongate into nearly straight lines. At breaking, particle motion becomes more complicated, but even in the surf zone, the water moves forward and backward in paths that are mostly horizontal, with brief, but intense, vertical motions produced by the passage

of the breaker crest. Since it is this wave-induced water particle motion that causes the sediment to move, it is useful to know the length of the elliptical path traveled by the water particles and the maximum velocity and acceleration attained during this orbit.

The basic equations for water-wave motion before breaking are discussed in Chapter 2. Quantitative estimates of water motion are possible from small-amplitude wave theory (Section 2.23), even near breaking where assumptions of the theory are not valid. (Dean, 1970; Eagleson, 1956.) Equations 2-13 and 2-14, in Section 2.234 give the fluid-particle velocity components u, w in a wave where small-amplitude theory is applicable. (See Figure 2-3 for relation to wave phase and water particle acceleration.)

For sediment transport, the conditions of most interest are those when the wave is in shallow water. For this condition, and making the small-amplitude assumption, the horizontal length 2A, of the path moved by the water particle as a wave passes in shallow water is approximately

$$2A = \frac{H\,T\sqrt{gd}}{2\pi d} \,, \qquad (4\text{-}10)$$

and the maximum horizontal water velocity is

$$u_{max} = \frac{H\sqrt{gd}}{2d} . \qquad (4\text{-}11)$$

The term under the radical is the wave speed in shallow water.

* * * * * * * * * * * * * EXAMPLE PROBLEM * * * * * * * * * * * * * * *

GIVEN: A wave 1 foot high with a period of 5 seconds is progressing shoreward in a depth of 2 feet.

FIND:

   (a) Calculate the maximum horizontal distance 2A the water particle moves during the passing of a wave.

   (b) Determine the maximum horizontal velocity u_{max} of a water particle.

   (c) Compare the maximum horizontal distance 2A with the wavelength in the 2-foot depth.

   (d) Compare the maximum horizontal velocity u_{max}, with the wave speed, C.

SOLUTION:

(a) Using Equation 4-10, the maximum horizontal distance is

$$2A = \frac{HT\sqrt{gd}}{2\pi d}$$

$$2A = \frac{1\,(5)\,\sqrt{32.2\,(2)}}{2\pi\,(2)} = 3.2 \text{ feet}.$$

(b) Using Equation 4-11, the maximum horizontal velocity is

$$u_{max} = \frac{H\sqrt{gd}}{2d}$$

$$u_{max} = \frac{1\sqrt{32.2\,(2)}}{2\,(2)} = 2.0 \text{ feet per second}.$$

(c) Using the relation $L = T\sqrt{gd}$ to determine the shallow-water wavelength,

$$L = 5\sqrt{32.2\,(2)} = 40.1 \text{ feet}.$$

From (a) above, the maximum horizontal distance $2A$ is 3.2 feet therefore the ratio $2A/L$ is

$$\frac{2A}{L} = \frac{3.2}{40.1} = 0.08.$$

(d) Using the relation $C = \sqrt{gd}$ (Equation 2-9) to determine the shallow-water wave speed

$$C = \sqrt{32.2\,(2)} = 8.0 \text{ feet per second}.$$

From (b) above the maximum horizontal velocity u_{max}, is 2.0 feet per second. Therefore the ratio u_{max}/C is

$$\frac{u_{max}}{C} = \frac{2.0}{8.0} = 0.25.$$

* *

Although small-amplitude theory gives a fair understanding of many wave-related phenomena, there are important phenomena that it does not predict. Observation and a more complete analysis of wave motion show that particle orbits are not closed. Instead, the water particles advance a little in the direction of the wave motion each time the wave

passes. The rate of this advance is the *mass transport velocity*; (Equation 2-55, Section 2.253). This velocity becomes important for sediment transport, especially for sediment suspended above ripples seaward of the breaker.

For conditions evaluated at the bottom (z = -d), the maximum bottom velocity, $u_{max(-d)}$, given by Equation 2-13 determines the average bottom mass transport velocity, $\overline{u}_{(-d)}$, obtained from Equation 2-55, according to the equation

$$\overline{u}_{(-d)} = \frac{\left(u_{max(-d)}\right)^2}{2C} , \qquad (4\text{-}12)$$

where C is the wave speed given by Equation 2-3. Equation 2-55, and thus Equation 4-12, does not include allowance for return flow which must be present to balance the mass transported in the direction of wave travel. In addition, the actual distribution of the time-averaged net velocity depends sensitively on such external factors as bottom characteristics, temperature distribution, and wind velocity. (Mei, Liu, and Carter, 1972.) Most observations show the time-averaged net velocity near the bottom is directed toward the breaker region from both sides. (See Inman and Quinn, (1952), for field measurements in surf zone; Galvin and Eagleson, (1965) for laboratory observations; and Mei, Liu and Carter (1972, p. 220), for comprehensive discussion.) However, both field and laboratory observations have shown that wind-induced bottom currents may be great enough to reverse the direction of the shoreward time-averaged wave-induced velocity at the bottom when there are strong onshore winds. (Cook and Gorsline, 1972; and Kraai, 1969.)

4.42 FLUID MOTION IN BREAKING WAVES.

During most of the wave cycle in shallow water, the particle velocity is approximately horizontal and constant over the depth, although right at breaking there are significant vertical velocities as the water is drawn up into the crest of the breaker. The maximum particle velocity under a breaking wave is approximated by solitary wave theory (Equation 2-66) to be

$$u_{b\ max} = C = \sqrt{g(H+d)} , \qquad (4\text{-}13)$$

where (H+d) is the distance measured from crest of the breaker to the bottom.

Fluid motions at breaking cause most of the sediment transport in the littoral zone, because the bottom velocities and turbulence at breaking suspend more bottom sediment. This suspended sediment can then be transported by currents in the surf zone whose velocities are normally too low to move sediment at rest on the bottom.

The mode of breaking may vary significantly from spilling to plunging to collapsing to surging, as the beach slope increases or the wave

steepness (height-to-length ratio) decreases. (Galvin, 1967.) Of the four breaker types, spilling breakers most closely resemble the solitary waves whose speed is described by Equation 4-13. (Galvin, 1972.) Spilling breakers differ little in fluid motion from unbroken waves (Divoky, LeMehaute, and Lin, 1970), and thus tend to be less effective in transporting sediment than plunging or collapsing breakers.

The most intense local fluid motions are produced by plunging breakers. As the wave moves into shallower depths, the front face begins to steepen. When the wave reaches a mean depth about equal to its height, it breaks by curling over at the crest. The crest of the wave acts as a free-falling jet that scours a trough into the bottom. At the same time, just seaward of the trough, the longshore bar is formed, in part by sediment scoured from the trough and in part by sediment transported in ripples moving from the offshore.

The effect of the tide on nearshore currents is not discussed, but tide-generated currents may be superimposed on wave-generated nearshore currents, especially near estuaries. In addition, the changing elevation of the water level as the tide rises and falls may change the area and the shape of the profile through the surf zone, and thus alter the nearshore currents.

4.43 ONSHORE-OFFSHORE CURRENTS

4.431 Onshore-Offshore Exchange. Field and laboratory data indicate that water in the nearshore zone is divided by the breaker line into two distinct water masses between which there is only a limited exchange of water.

The mechanisms for the exchange are: mass transport velocity in shoaling waves, wind-induced surface drift, wave-induced setup, currents induced by irregularities on the bottom, rip currents, and density currents. The resulting flows are significantly influenced by, and act on, the hydrography of the surf and nearshore zones. Figure 4-13 shows the nearshore current system measured for particular wave conditions on the southern California coast.

At first observation, there appears to be extensive exchange of water between the nearshore and the surf zone. However, the breaking wave itself is formed largely of water that has been withdrawn from the surf zone after breaking. (Galvin, 1967.) This water then reenters the surf zone as part of the new breaking wave, so that only a limited amount of water is actually transferred offshore. This inference is supported by the calculations of Longuet-Higgins (1970, p. 6788) which show that little mixing is needed to account for observed velocity distributions. Most of the exchange mechanisms indicated act with speeds much slower than the breaking-wave speed, which may be taken as an estimate of the maximum water particle speed in the littoral zone indicated by Equation 4.13.

2 December 1948
Wave Period 15 Seconds
Wave from WNW

→ 0 – .25
⇒ .25 – .50 KN
⇒ .50 – 1.0 KN
➡ >1 Knot
--→ Observed Current (not measured)
∘ Starting Position of Surface Float
H_b = Breaker Height
▨ Float Recovery Area

Scripps Canyon

Lost

Scripps Institution

H_b = 4.5'

H_b = 3.5'

H_b = 5.5'

H_b = 6'

H_b = 5'

H_b = 3.5'

H_b = 2.5'

H_b = 2'

H_b = 2'

H_b = 2.5'

Shelf

Lost

La Jolla Canyon

Lost

1130 PDT

1215 PDT

N

SCALE IN FEET
0   500   1000

(from Shepard and Inman, 1950)

Figure 4-13.   Nearshore Current System Near La Jolla Canyon, California

4-44

4.432 _Diffuse Return Flow._ Wind- and wave-induced water drift, pres-
sure gradients at the bottom due to setup, density differences due to
suspended sediment and temperature, and other mechanisms produce patterns
of motion in the surf zone that vary from highly organized rip currents
to broad diffuse flows that require continued observation to detect. Dif-
fuse return flows may be visible in aerial photos as fronts of turbid
water moving seaward from the surf zone. Such flows may be seen in the
photos reproduced in Sonu (1972, p. 3239).

4.433 _Rip Currents._ Most noticeable of the exchange mechanisms between
offshore and surf zone are rip currents. (See Figure 4-14, and Figure
A-7, Appendix A.) Rip currents are concentrated jets that carry water
seaward through the breaker zone. They appear most noticeable when long,
high waves produce wave setup on the beach. In addition to the classi-
cal rip currents, there are other localized currents directed seaward
from the shore. Some are due to concentrated flows down gullies in the
beach face, and others can be attributed to interacting waves and edge
wave phenomena. (Inman, Tait, and Nordstrom, 1971, p. 3493.) The origin
of rip currents is discussed by Arthur (1962), and Sonu (1972).

Three-dimensional circulation in the surf is documented by Shepard and
Inman (1950), and this complex flow needs to be considered, especially in
evaluating the results of laboratory tests for coastal engineering purposes.
However, at present, there is no proven way to predict the conditions that
produce rip currents or the spacing between rips. In addition, data are
lacking that would indicate quantitatively how important rip currents are
as sediment transporting agents.

4.44 LONGSHORE CURRENTS

4.441 _Velocity and Flow Rate._ Longshore currents flow parallel to the
shoreline, and are restricted mainly between the zone of breaking waves
and the shoreline. Most longshore currents are generated by the long-
shore component of motion in waves that obliquely approach the shoreline.

Longshore currents typically have mean values of 1 foot per second
or less. Figure 4-15 shows a histogram of 5,591 longshore current veloc-
ities measured at 36 sites in California during 1968. Despite frequent
reports of exceptional longshore current speeds, most data agree with
Figure 4-15 in showing that speeds above 3 feet per second are unusual.
A compilation of 352 longshore current observations, most of which appear
to be biased toward conditions producing high speed, showed that the maxi-
mum observed speed was 5.5 feet per second, and that the highest observa-
tions were reported to have been wind-aided. (Galvin and Nelson, 1967.)
Although longshore currents generally have low speeds, they are important
in littoral processes because they flow along the shore for extended peri-
ods of time, transporting sediment set in motion by the breaking waves.

The most important variable in determing the longshore current veloc-
ity is the angle between the wave crest and the shoreline. However, the
volume rate of flow of the current and the longshore transport rate depend

Figure 4-14. Typical Rip Currents, Ludlam
Island, New Jersey

mostly on breaker height. The outer edge of the surf zone is determined by the breaker position. Since waves break in water depths approximately proportional to wave height, the width of the surf zone on a beach increases with wave height. This increase in width increases the cross section of the surf zone.
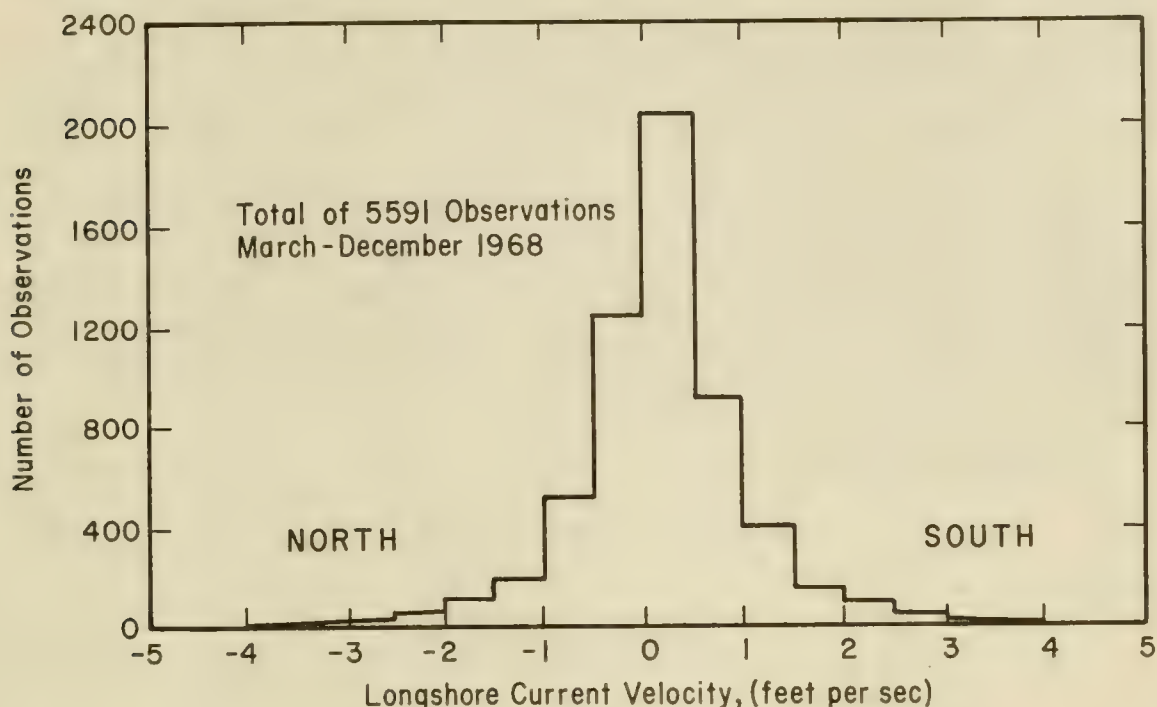
Figure 4-15. Distribution of Longshore Current Velocities. Data taken from CERC California LEO Study (See Szuwalski 1970).

If the surf zone cross section is approximated by a triangle, then an increase in height increases the area (and thus the volume of the flow) as the square of the height, which nearly offsets the increase in energy flux (which increases as the 5/2 power of height). Thus, the height is important in determining the width and volume rate of longshore current flow in the surf zone. (Galvin, 1972.)

Longshore current velocity varies both across the surf zone (Longuet-Higgins, 1970b) and in the longshore direction (Galvin and Eagleson, 1965). Where an obstacle to the flow, such as a groin, extends through the surf zone, the longshore current speed downdrift of the obstacle is low, but it increases with distance downdrift. Laboratory data suggest that the current takes a longshore distance of about 10 surf widths to become fully developed. These same experiments (Galvin and Eagleson, 1965) suggest that the velocity profile varies more across the surf zone at the start of the flow than it does downdrift where the flow has fully developed. The ratio of longshore current speed at the breaker position to longshore current speed averaged across the surf zone varied from about 0.4 where the flow started to about 0.8 or 1.0 where the flow was fully developed.

4.442 Velocity Prediction. The variation in longshore current velocity
across the surf zone and along the shore, and the uncertainties in vari-
ables such as the surf zone hydrography, make prediction of longshore
current velocity uncertain. There are three equations of possible use
in predicting longshore currents: Longuet-Higgins (1970); an adaptation
from Bruun (1963); and Galvin (1963). All three equations require co-
efficients identified by comparing measured and computed velocities, and
all three show about the same degree of agreement with data. Two sets of
data (Putnam, et al., 1949, field data; Galvin and Eagleson, 1965, labora-
tory data) appear to be the most appropriate for checking predictions.

The radiation stress theory of Longuet-Higgins (1970a, Equation 62),
as modified by fitting it to the data, is the one recommended for use
based on its theoretical foundation. The other two semiempirical equa-
tions may provide a check on the Longuet-Higgins prediction. Written
in common symbols (m is beach slope; g is acceleration of gravity; H_b
is breaker height; T is wave period; and α_b is angle between breaker
crest and shoreline), these equations are:

   a. Longuet-Higgins.

$$v_b = M_1 \ m \left(gH_b\right)^{\frac{1}{2}} \sin 2\alpha_b \ , \tag{4-14}$$

where

$$M_1 = \frac{0.694 \ \Gamma (2\beta)^{-\frac{1}{2}}}{f_f} \tag{4-15}$$

According to Longuet-Higgins (1970a, p. 6788), v_b is the longshore cur-
rent speed at the breaker position, Γ is a mixing coefficient which
ranges between 0.17 (little mixing) and 0.5 (complete mixing), but is
commonly about 0.2; β is the depth-to-height ratio of breaking waves
in shallow water taken to be 1.2 and f_f is the friction coefficient,
taken to be 0.01. Using these values, $M_1 = 9.0$.

Applying equation 4-14 to the two sets of data yields predictions
that average about 0.43 of the measured values. In part, these predicted
speeds are lower because v_b, as given in Equation 4-14 is for the speed
at the breaker line, whereas the measured velocities are mostly from the
faster zone of flow shoreward of the breaker line. (Galvin and Eagleson,
1965.) Therefore, Equation 4-14 multiplied by 2.3 leads to the modified
Longuet-Higgins equation for longshore current velocity:

$$v = 20.7 \ m \left(gH_b\right)^{\frac{1}{2}} \sin 2\alpha_b \ , \tag{4-16}$$

used in Figure 4-16. Further developments in the Longuet-Higgins' (1970b
and 1971) theory permit calculation of velocity distribution, but there
is no experience with these predictions for longshore currents flowing
on erodible sand beds.

4-48
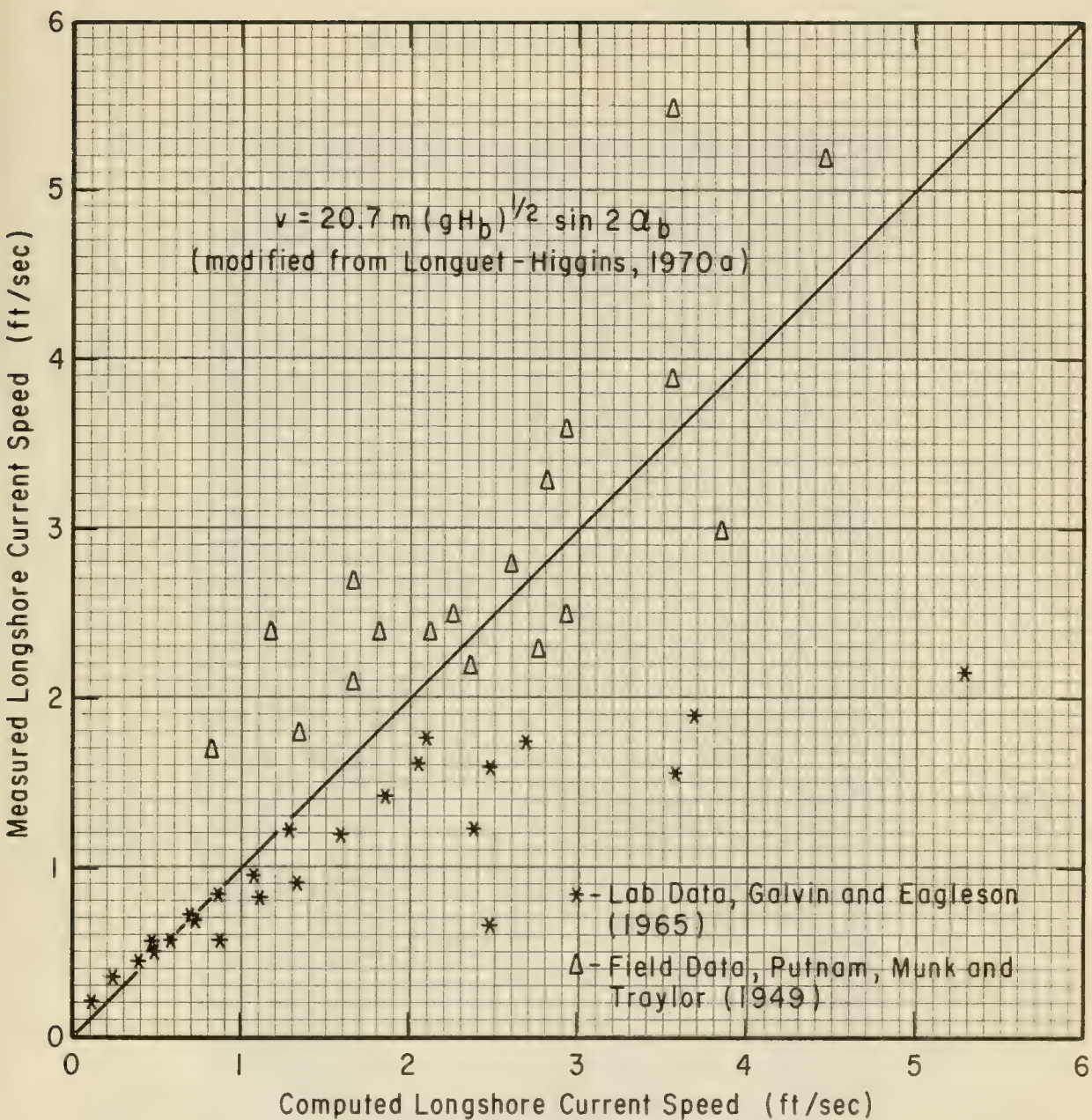
Figure 4-16. Measured Versus Predicted Longshore Current Speed

b. **Bruun (1963 as Modified).**

$$v_b = M_2 \left(gH_b\right)^{\frac{1}{4}} \left[mH_b \left(\sin 2\alpha_b\right)/T\right]^{\frac{1}{2}} , \qquad (4\text{-}17)$$

where v_b is the mean velocity in the surf zone where the flow is fully developed, and M_2 involves a friction factor of the Chezy kind (see Galvin, 1967, p. 297.)

c. **Galvin (1963).**

$$v_b = K g m T \sin 2\alpha_b , \qquad (4\text{-}18)$$

where v_b is the mean velocity in the surf zone where the flow is fully developed, and K is a coefficient depending on breaker height-to-depth ratio and the ratio of trough depression on breaker height. To a good approximation, K may be taken as 1.0. (Galvin and Eagleson, 1965.)

4.45 SUMMARY

The major currents in the littoral zone are wave-induced motions superimposed on the wave-induced oscillatory motion of the water. The net motions generally have low velocities, but because they transport whatever sand is set in motion by the wave-induced water motions, they are important in determining littoral transport.

Evidence indicates that there is only slight exchange of fluid between the offshore and the surf zone.

Longshore current velocities are most sensitive to changes in breaker angle, and to a lesser degree, to changes in breaker height. However, the volume rate of flow of the longshore current is most sensitive to breaker height, probably proportional to H^2. The modified Longuet-Higgins equation (4-16) is recommended for predicting mean longshore current velocity of fully developed flows, and the two semiempirical equations (4-17 and 4-18) are available as checks on the Longuet-Higgins equation.

4.5 LITTORAL TRANSPORT

4.51 INTRODUCTION

4.511 **Importance of Littoral Transport.** Sediment motions indicated by the shoreline configuration in Figure 4-17 are aspects of *littoral transport*. If the coast is examined on satellite imagery as shown in Figure 4-17, only its general characteristics are visible. At this elevation, the shore consists of bright segments that are straight or slightly curved. The brightness is evidence of sand, the most common material along the shore. The straightness often is evidence of sediment transport.

In places, the straight segments of shoreline cut across preexisting topography. Elsewhere, the shoreline segments are separated by wide lagoons from the irregular mainland. The fact that the shore is nearly straight across both mainland and irregular bays is evidence of headland
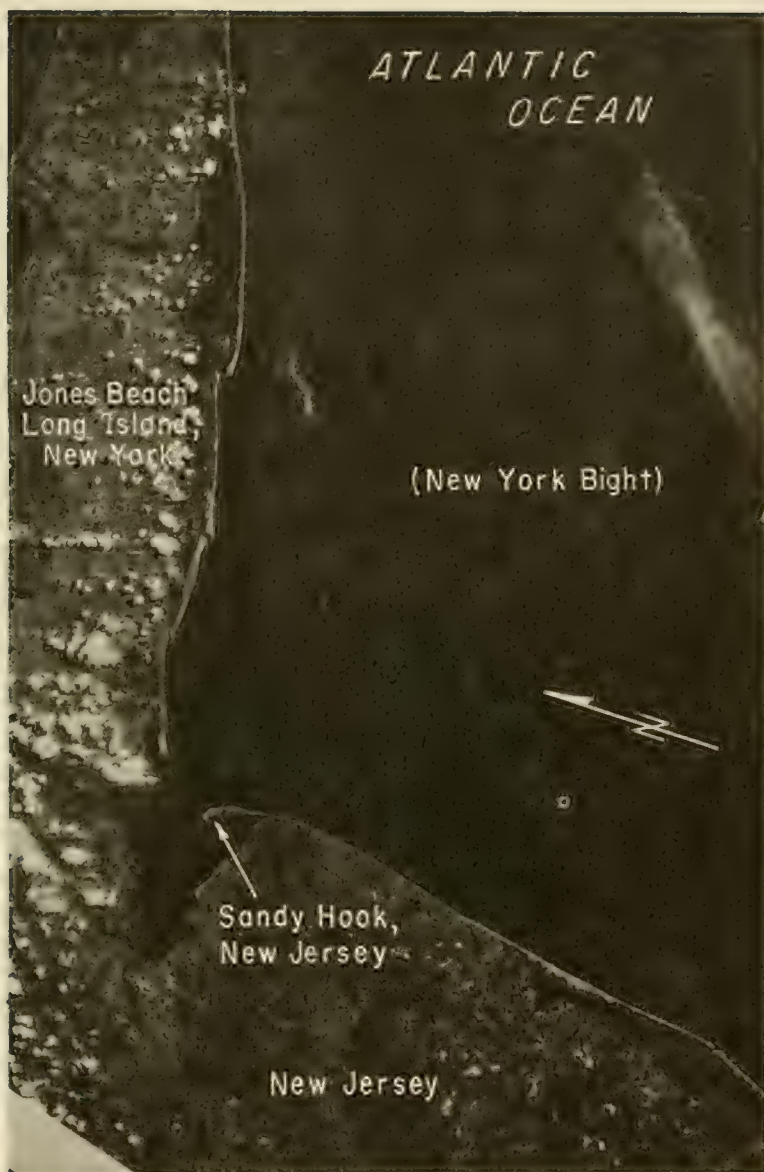
Figure 4-17. Coasts in Vicinity of New York Bight

erosion, accompanied by longshore transport which has carried sand along the coast to supply the barriers and spits extending across the bays. The primary agent producing this erosion and transport is the action of waves impinging on the shore.

Littoral transport is the movement of sedimentary material in the littoral zone by waves and currents. The littoral zone extends from the shoreline to just beyond the most seaward breakers.

Littoral transport is classified as *onshore-offshore transport* or as *longshore transport*. Onshore-offshore transport has an average net direction perpendicular to the shoreline; longshore transport has an average net direction parallel to the shoreline. The instantaneous motion of sedimentary particles has both an onshore-offshore and a longshore component. Onshore-offshore transport is usually the most significant type of transport in the offshore zone, except in regions of strong tidal currents. Both longshore and onshore-offshore transport are significant in the surf zone.

Engineering problems involving littoral transport generally require answers to one or more of the following questions:

(a) What are the longshore transport conditions at the site? (Needed for the design of groins, jetties, navigation channels, and inlets.)

(b) What is the trend of shoreline migration over short and long time intervals? (Needed for design of coastal structures, including navigation channels.)

(c) How far seaward is sand actively moving? (Needed in the design of sewage outfalls and water intakes.)

(d) What is the direction and rate of onshore-offshore sediment motion? (Needed for sediment budget studies and beach fill design.)

(e) What is the average shape, and the expected range of shapes, for a given beach profile? (Needed for design of groins, beach fills, navigation structures and flood protection.)

(f) What effect will a postulated structure or project have on adjacent beaches and on littoral transport? (Needed for design of all coastal works.)

This section presents recommended methods for answering these and related questions. The section indicates accepted practice based on field observations and research results. Section 4.52 deals with onshore-offshore transport, presenting material pertinent to answering questions (b) through (f). Section 4.53 deals with longshore transport, presenting material pertinent to questions (a), (b), and (f).

4.512 Zones of Transport. Littoral transport occurs in two modes: *bed-load transport*, the motion of grains rolled over the bottom by the shear of water moving above the sediment bed; and *suspended-load transport*, the transport of grains by currents after the grains have been lifted from the bed by turbulence.

Both modes of transport are usually present at the same time, but it is hard to distinguish where bedload transport ends and suspended-load transport begins. It is more useful to identify two zones of transport based on the type of fluid motion initiating sediment motion: the offshore zone where transport is initiated by wave-induced motion over ripples, and the surf zone where transport is initiated by the passing breaker. In either zone, net sediment transport is the product of two processes: the periodic wave-induced fluid motion that initiates sediment motion, and the superimposed currents (usually weak) which transport the sediment set in motion.

a. Offshore Zone. Waves traveling toward shallow water eventually reach a depth where the water motion near the bottom begins to affect the sediment on the bottom. At first, only low-density material (such as seaweed and other organic matter) moves. This material oscillates back and forth with the waves, often in ripple-like ridges parallel to the wave crests. For a given wave condition, as the depth decreases, water motion immediately above the sediment bed increases until it exerts enough shear to move sand particles. The sand then forms ripples with crests parallel to the wave crests. These ripples are typically uniform and periodic, and sand moves from one side of the crest to the other with the passage of each wave.

As depth decreases to a value several times the wave height, the velocity distribution with time changes from approximately sinusoidal to a distribution that has a high shoreward component associated with the brief passage of the wave crest, and lower seaward velocities associated with the longer time interval occupied by the passage of the trough. As the shoreward water velocity associated with the passing crest decreases and begins to reverse direction over a ripple, a cloud of sand erupts upward from the lee (landward) side of the ripple crest. This cloud of sand drifts seaward with the seaward flow under the trough. At these shallow depths, the distance traveled by the cloud of suspended sediment is two or more ripple wavelengths, so that the sand concentration at a point above the ripples usually exhibits at least two maximums during the passage of the wave trough. These maximums are the suspension clouds shed by the two nearest upstream ripples. The approach of the next wave crest reverses the direction of the sand remaining suspended in the cloud. The landward flow also drags material shoreward as bedload.

For the nearshore profile to be in equilibrium with no net erosion or accretion, the average rate at which sand is carried away from a point on the bottom must be balanced by the average rate at which sand is added. Any net change will be determined by the net residual currents near the bottom which transport sediment set in motion by the waves. These currents,

the subject of Section 4.4, include longshore currents and mass-transport currents in the onshore-offshore direction. It is possible to have ripple forms moving shoreward while residual currents above the ripples carry suspended sediment clouds in a net offshore direction. Information on the transport of sediment above ripples is given in Bijker (1970), Kennedy and Locher (1972), and Mogridge and Kamphuis (1972).

b. Surf Zone. The stress of the water on the bottom due to turbulence and wave-induced velocity gradients moves sediment in the surf zone with each passing breaker crest. This sediment motion is both bedload and suspended-load transport. Sediment in motion oscillates back and forth with each passing wave, and moves alongshore with the longshore current. On the beach face, the landward termination of the surf zone, the broken wave advances up the slope as a bore of gradually decreasing height, and then drains seaward in a gradually thinning sheet of water. Frequently, the draining return flows in gullies and carries sediment to the base of the beach face.

In the surf zone, ripples cause significant sediment suspension, but here there are additional eddies caused by the breaking wave. These eddies have more energy and are larger than the ripple eddies. The greater energy suspends more sand in the surf zone than offshore. The greater eddy size mixes the suspended sand over a larger vertical distance. Since the size is about equal to the local depth, significant quantities of sand are suspended over most of the depth in the surf zone.

Since breaking waves suspend the sediment, the amount suspended is partly determined by breaker type. Data from Fairchild (1972, Figure 5), show that spilling breakers usually produce noticeably lower suspended sediment concentrations than do plunging breakers. See Fairchild (1972) and Watts (1953) for field data; Fairchild (1956 and 1959) for lab data. Typical suspended concentrations of fine sand range between 20 parts per million and 2 parts per thousand by weight in the surf zone, and are about the same near the ripple crests in the offshore zone.

Studies of suspended sediment concentrations in the surf zone by Watts (1953) and Fairchild (1972) indicate that sediment in suspension in the surf zone may form a significant portion of the material in longshore transport. However, present understanding of sediment suspension, and the practical difficulty of obtaining and processing sufficient suspended sediment samples have limited this approach to predicting longshore transport.

4.513 Profiles. Profiles are two-dimensional vertical sections showing how elevation varies with distance. Coastal profiles (See Figs. 4-1 and 4-18) are usually measured perpendicular to the shoreline, and may be shelf profiles, nearshore profiles, or beach profiles. Changes on nearshore and beach profiles are interrelated, and are highly important in the interpretation of littoral processes. The measurement and analysis of combined beach and nearshore profiles is a major part of most engineering studies of littoral processes.
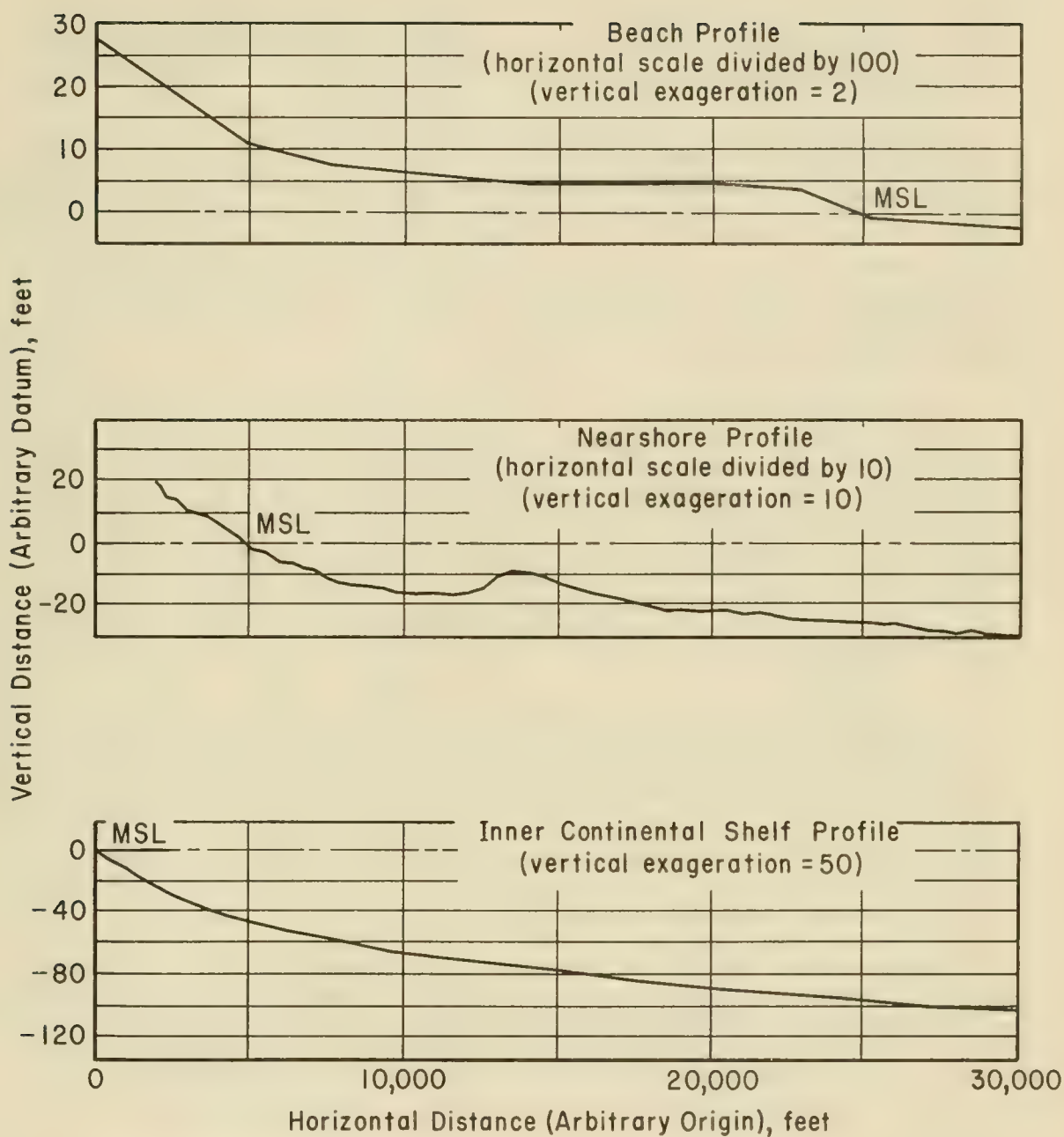
Figure 4-18. Three Scales of Profiles, Westhampton, Long Island

a. Shelf Profiles. The shelf profile is typically a smooth, concave-up curve showing depth to increase seaward at a rate that decreases with distance from shore. (bottom profile in Figure 4-18.) The smoothness of the profile may be interrupted by other superposed geomorphic features, such as linear shoals. (Duane, et al., 1972.) Data for shelf profiles are usually obtained from charts of the National Ocean Survey (formerly, U.S. Coast and Geodetic Survey).

The measurable influence of the shelf profile on littoral processes is largely its effect on waves. To an unknown degree, the shelf may also serve as a source or sink for beach sand. Geologic studies show that much of the outer edge of a typical shelf profile is underlain by relatively coarse sediment, indicating a winnowing of fine sizes. (Dietz, 1963; Milliman, 1972; and Duane, et al., 1972.) Landward from this residual sediment, sediment often becomes finer before grading into the relatively coarser beach sands.

b. Nearshore Profiles. The nearshore profile extends seaward from the beach to depths of about 30 feet. Prominent features of most nearshore profiles are longshore bars; see middle profile of Figure 4-18 and Section 4.525. In combination with beach profiles, repetitive nearshore profiles are used in coastal engineering to estimate erosion and accretion along the shore, particularly the behavior of beach fill, groins, and other coastal engineering structures. Data from nearshore profiles must be used cautiously. (see Section 4.514.) Under favorable conditions nearshore profiles have been used in measuring longshore transport rates. (Caldwell, 1956.)

c. Beach Profiles. Beach profiles extend from the foredunes, cliffs, or mainland out to mean low water. Terminology applicable to features of the beach profile is in Appendix A (especially Figures A-1 and A-2). The backshore extends seaward to the foreshore, and consists of one or more berms at elevations above the reach of all but storm waves. Berm surfaces are nearly flat and often slope landward at a slight downward angle. (See Figure 4-1.) Berms are often bounded on the seaward side by a break in slope known as the berm crest.

The foreshore is that part of the beach extending from the highest elevation reached by waves at normal high tide seaward to the ordinary low water line. The foreshore is usually the steepest part of the beach profile. The boundary between the backshore and the foreshore may be the crest of the most seaward berm, if a berm is well developed. The seaward edge of the foreshore is often marked by an abrupt step at low tide level.

Seaward from the foreshore, there is usually a low-tide terrace which is a nearly horizontal surface at about mean low tide level. (Shepard, 1950; and Hayes, 1971.) The low-tide terrace is commonly covered with sand ripples and other minor bed forms, and may contain a large bar-and-trough system, which is a landward-migrating sandbar (generally parallel to the shore) common in the nearshore following storms. Seaward from the low-tide

terrace (seaward from the foreshore, if the low-tide terrace is absent) are the longshore troughs and longshore bars.

4.514 Profile Accuracy. Beach and nearshore profiles are the major source of data for engineering studies of beach changes; sometimes littoral transport can be estimated from these profiles. Usually, beach and nearshore profiles are measured at about the same time, but different techniques are needed for their measurement. The nearshore profile is usually measured from a boat or amphibious craft, using an echo sounder or leadline. or from a sea sled. (Kolessar and Reynolds, 1965-66; and Reimnitz and Ross, 1971.) Beach profiles are usually surveyed by standard leveling and taping techniques.

The accuracy of profile data is affected by four types of error: sounding error, spacing error, closure error, and error due to temporal fluctuations in the sea bottom. These errors are more significant for nearshore profiles than for beach profiles.

Saville and Caldwell (1953) discuss sounding and spacing errors. Sounding error is the difference between the measured depth and the actual depth. Under ideal conditions, average sonic sounding error may be as little as 0.1 foot, and average leadline sounding error may be about twice the sonic sounding error. (Saville and Caldwell, 1953.) (This suggests that sonic sounding error may actually be less than elevation changes caused by transient features like ripples. Experience with successive soundings in the nearshore zone indicates that errors in practice may approach 0.5 foot.) Sounding errors are usually random and tend to average out when used in volume computations, unless a systematic error due to the echo sounder or tide correction is involved. Long-period water level fluctuations affect sounding accuracy by changing the water level during the survey. At Santa Cruz, California, the accuracy of hydrographic surveys was ±1.5 feet due to this effect. (Magoon, 1970.)

Spacing error is the difference between the actual volume of a segment of shore and the volume estimated from a single profile across that segment. Spacing error is potentially more important than sounding error, since survey costs of long reaches usually dictate spacings between nearshore profiles of thousands of feet. For example, if a 2-mile segment of shore 4,000 feet wide is surveyed by profiles on 1,000-foot spacings, then the spacing error is about 9 cubic yards per foot of beach front per survey, according to the data of Saville and Caldwell (1953, Figure 5). This error equals a major part of the littoral budget in many localities.

Closure error arises from the assumption that the outer ends of nearshore profiles have experienced no change in elevation between two successive surveys. Such an assumption is often made in practice, and may result in significant error. An uncompensated closure error of 0.1 foot, spread over 1,000 feet at the seaward end of a profile, implies a change of 3.7 cubic yards per time interval per foot of beach front where

the time interval is the time between successive surveys. Such a volume change may be an important quantity in the sediment budget of the littoral zone.

A fourth source of error comes from assuming that the measured beach profiles (which are only an instantaneous picture), represent a long-term condition. Actually, beach and nearshore profiles change rapidly in response to changing wave conditions, so that differences between successive surveys of a profile may merely reflect temporary differences in bottom elevation caused by storms and seasonal changes in wave climate. Such fluctuations obliterate long-term trends during the relatively short time available to most engineering studies. This fact is illustrated for nearshore profiles by the work of Taney (1961a, Appendix B) who identified and tabulated 128 profile lines on the south shore of Long Island that had been surveyed more than once from 1927 to 1956. Of these, 47 are on straight shorelines away from apparent influence by inlets, and extend from Mean Low Water (MLW) to about -30 feet MLW. Most of these 47 profiles were surveyed three or more times, so that 86 separate volume changes are available. These data lead to the following conclusions:

(a) The net volume change appears to be independent of the time between surveys, even though the interval ranged from 2 months to 16 years. (See Figure 4-19.)

(b) Gross volume changes (the absolute sums of the 86 volume changes) are far greater than net volume changes (the algebraic sums of the 86 volume changes). The gross volume change for all 86 measured changes is 8,113 cubic yards per foot; the net change is -559 cubic yards per foot (loss in volume).

(c) The mean net change between surveys, averaged over all pairs of surveys, is -559/86 or -6.5 cubic yards per foot of beach. The median time between surveys is 7 years, giving a nominal rate of volume change of about -1 cubic yard per year per foot.

These results point out that temporary changes in successive surveys of nearshore profiles are usually much larger than net changes, even when the interval between surveys is several years. These data show that care is needed in measuring nearshore profiles if results are to be used in engineering studies. The data also suggest the need for caution in interpreting differences obtained in two surveys of the same profiles.

The positions of beach profiles must be marked so that they can be recovered during the life of the project. The profile monuments should be tied in by survey to local permanent references. If there is a longterm use for data at the profile positions, the monuments should be referenced by survey to a state coordinate system or other reference system, so that the exact position of the profile may be recovered in the future. Even if there is no anticipated long-term need, future studies in any coastal region are likely, and will benefit greatly from accurately surveyed, retrievable benchmarks.
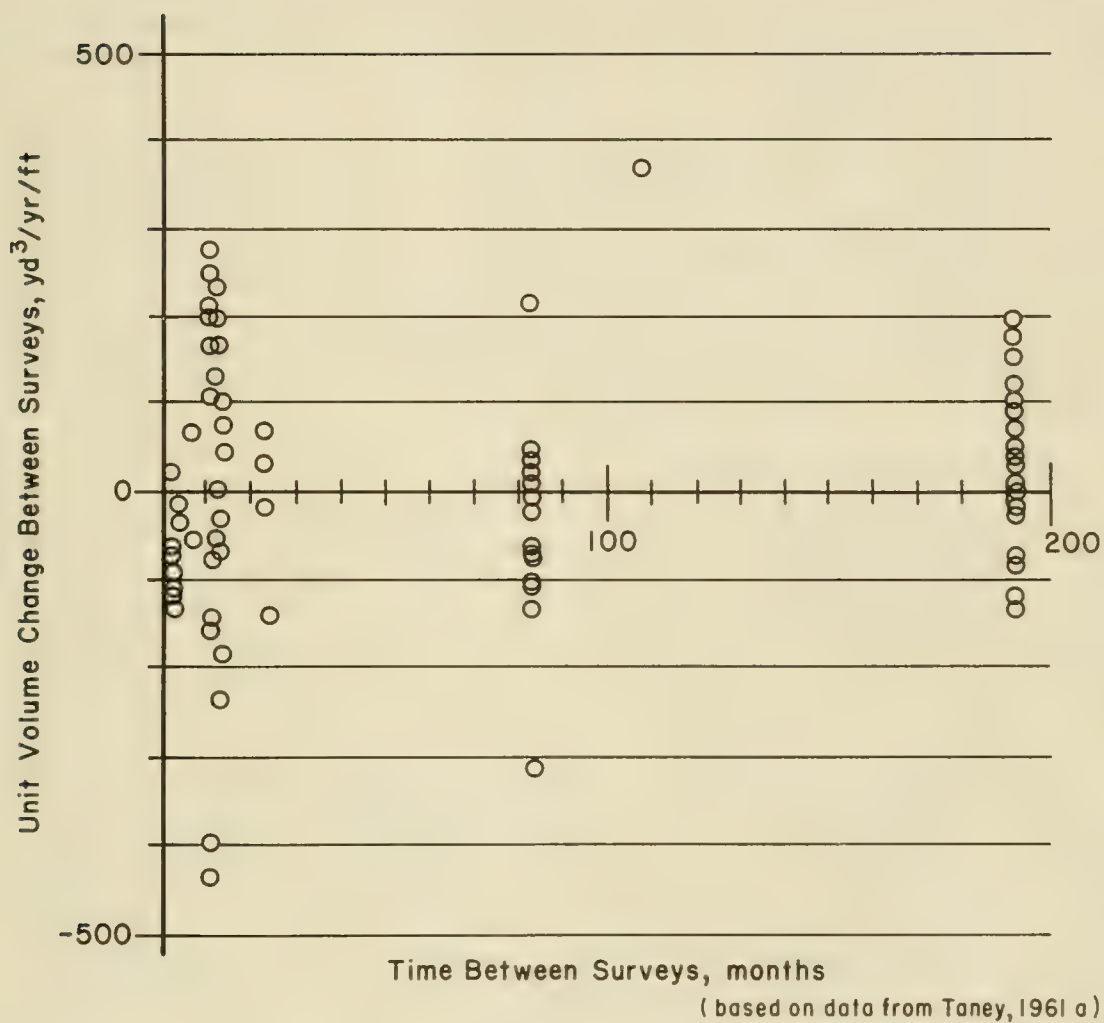
Figure 4-19. Unit Volume Change Versus Time Between Surveys for Profiles on South Shore of Long Island. Data from Profiles Extending from MSL to about the -30 depth Contour.

For coastal engineering, the accuracy of shelf profiles is usually less critical than the accuracy of beach and nearshore profiles. Generally, observed depth changes between successive surveys of the shelf do not exceed the error inherent in the measurement. However, soundings separated by decades suggest that the linear shoals superposed on the profile do show small but real shifts in position. (Moody, 1964, p. 143.) Charts giving depths on the continental shelves may include soundings that differ by decades in date.

Plotted profiles usually use vertical exaggeration or distorted scales to bring out characteristic features. This exaggeration may lead to a false impression of the actual slopes. As plotted, the three profiles in Figure 4-18 have roughly the same shape, but this sameness has been obtained by vertical exaggerations of 2x, 10x, and 50x.

Sand level changes in the beach and nearshore zone may be measured quite accurately from pipes imbedded in the sand. (Inman and Rusnak, 1956; Urban and Galvin, 1969; and Gonzales, 1970.)

4.52 ONSHORE-OFFSHORE TRANSPORT

4.521 Sediment Effects. Properties of individual particles which have been considered important in littoral transport include: size, shape, immersed specific gravity, and durability. Collections of particles have the additional properties of size distribution, permeability, and porosity. These properties determine the forces necessary to initiate and maintain sediment motion.

For typical beach sediment, size is the only property that varies greatly. However, quantitative evaluation of the size effect is usually lacking. A gross indication of a size effect is the accumulation of coarse sediment in zones of maximum wave energy dissipation, and deposition of fine sediment in areas sheltered from wave action. (e.g. King, 1972, pp. 302, 307, 426.) Sorting by size is common over ripples (Inman, 1957) and large longshore bars (Saylor and Hands, 1970). Field work on size effects in littoral transport does not permit definite conclusions. (King, 1972, p. 483; Inman, Komar, and Bowen, 1969; Castanho, 1970; Ingle, 1966, Figure 112; Yasso, 1962; and Zenkovich, 1967a.)

The shape of most littoral materials is approximately spherical; departures from spherical are usually too slight to affect littoral transport.

Immersed specific gravity (specific gravity of sediment minus specific gravity of fluid) is theoretically an important physical property of the sediment particle. (Bagnold, 1963.) However, the variation in immersed specific gravity for typical littoral materials in water is small since most beach sediments are quartz (immersed specific gravity = 1.65), and most of the remainder are calcium carbonate (immersed specific gravity = 1.9). Thus, little variation in littoral transport is expected from variation in immersed specific gravity.

4-60

Durability (resistance to abrasion, crushing, and solution) is usu-
ally not a factor within the lifetime of an engineering project. (Kuenen,
1956; Rusnak, Stockman, and Hofmann, 1966; and Thiel, 1940.) Possible
exceptions may include basaltic sands on Hawaiian beaches (Moberly, 1968),
some fragile carbonate sands which may be crushed to finer sizes when sub-
ject to traffic, (Duane and Meisburger, 1969, p. 44), and carbonate sands
which may be soluble under some conditions. (Bricker, 1971.) In general,
recent information lends further support to the conclusion of Mason (1942)
that, "On sandy beaches the loss of material ascribable to abrasion . . .
occurs at rates so low as to be of no practical importance in shore pro-
tection problems."

Size distribution and its relation to sediment sorting may be impor-
tant for design of beach fills. (See Sections 5.3 and 6.3.) Permeability
and porosity affect energy dissipation (Bretschneider and Reid, 1954; Bret-
schneider, 1954) and wave runup. (See Section 7.21; and Savage, 1958.)

Sediment properties are physically most important in determining fall
velocity and the hydraulic roughness of the sediment boundary. Fall velo-
city effects are important in onshore-offshore transport. Hydraulic rough-
ness effects have been insufficiently studied, but they appear to affect
initiation of sediment transport and energy dissipation. This may be par-
ticularly true for flow of the swash on the plane surface of the foreshore.
(Everts, 1972.)

4.522 Initiation of Sediment Motion. Considerable hydraulic and coastal
engineering research has been devoted to the initiation of sediment motion
under moving water. From this research has come general agreement (Graf,
1971, Chapter 6; Hjulstrom, 1939; and Everts, 1972) that the initiation of
motion on a level bed of fine or medium sand requires less shear (lower
velocities) than the initiation of motion on a level bed of silt or gravel;
(Figure 4-7 for size classes). It is also generally agreed that critical
entraining velocities for sand are usually less than 1 foot per second.

Velocities of wave-induced water motion in the offshore zone can be
estimated fairly well from the equation of small-amplitude theory. (See
Chapter 2.) This theory leads to Equation 2-13 which can be transformed
into a dimensionless expression for velocity at the sand surface (z = -d)

$$\frac{u_{max\,(-d)}\,T}{H} = \frac{\pi}{\sinh \frac{2\pi d}{L}} \,, \tag{4-19}$$

which is plotted in dimensionless form in Figure 4-20 and for common values
of wave period in Figure 4-21. Figures 4-20 and 4-21 give maximum bottom
particle velocity, $u_{max(-d)}$, as a function of depth, wave period, and
local wave height. This prediction by linear theory for the offshore zone,
and the related results from solitary-wave theory for the zone near break-
ing, agree fairly well with measurement in the field. (Inman and Nasu,
1956; and Cook and Gorsline, 1972, Figures 5 and 6.).
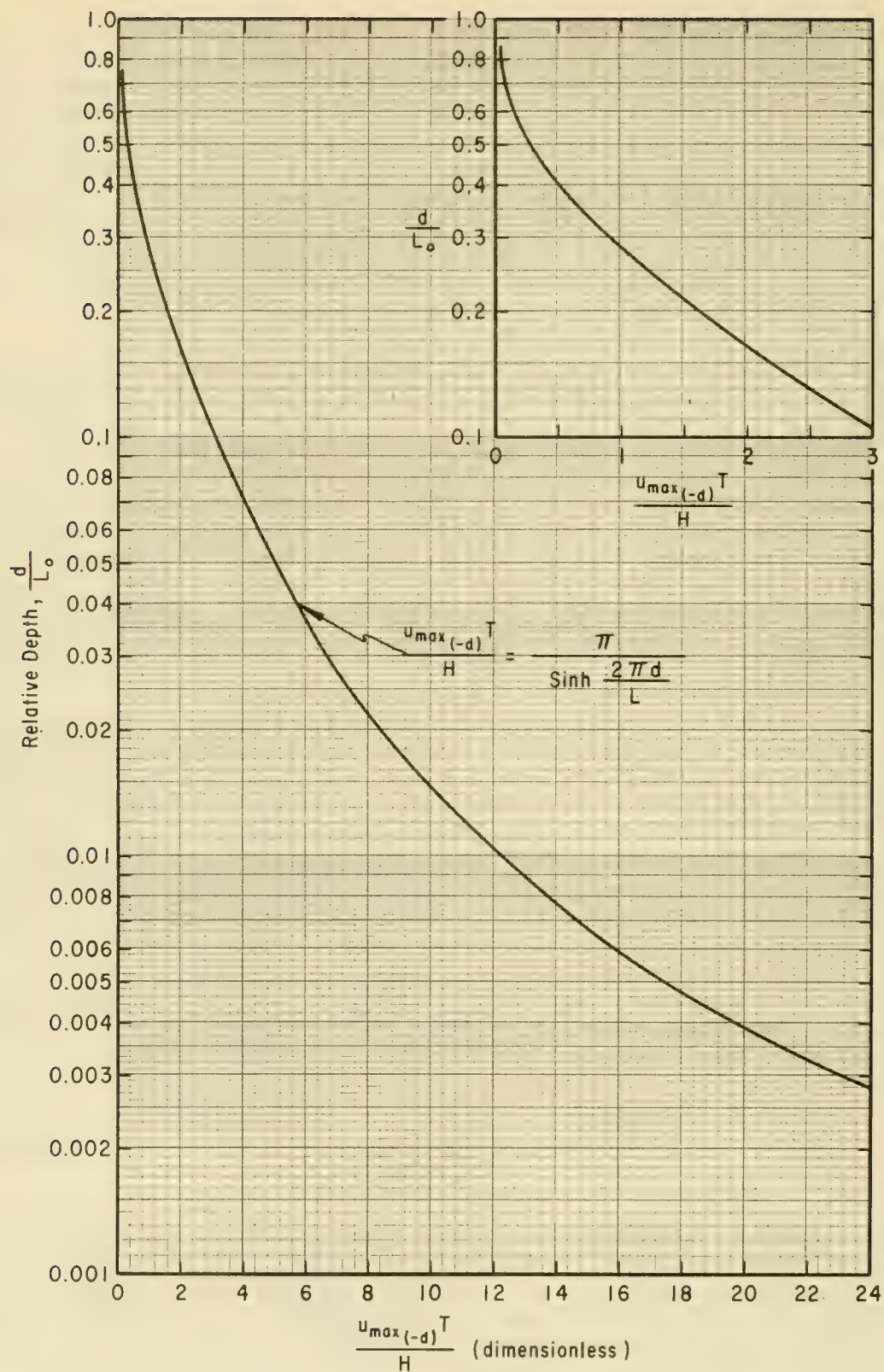
Figure 4-20. Maximum Wave Induced Bottom Velocity as a Function of Relative Depth

4-62
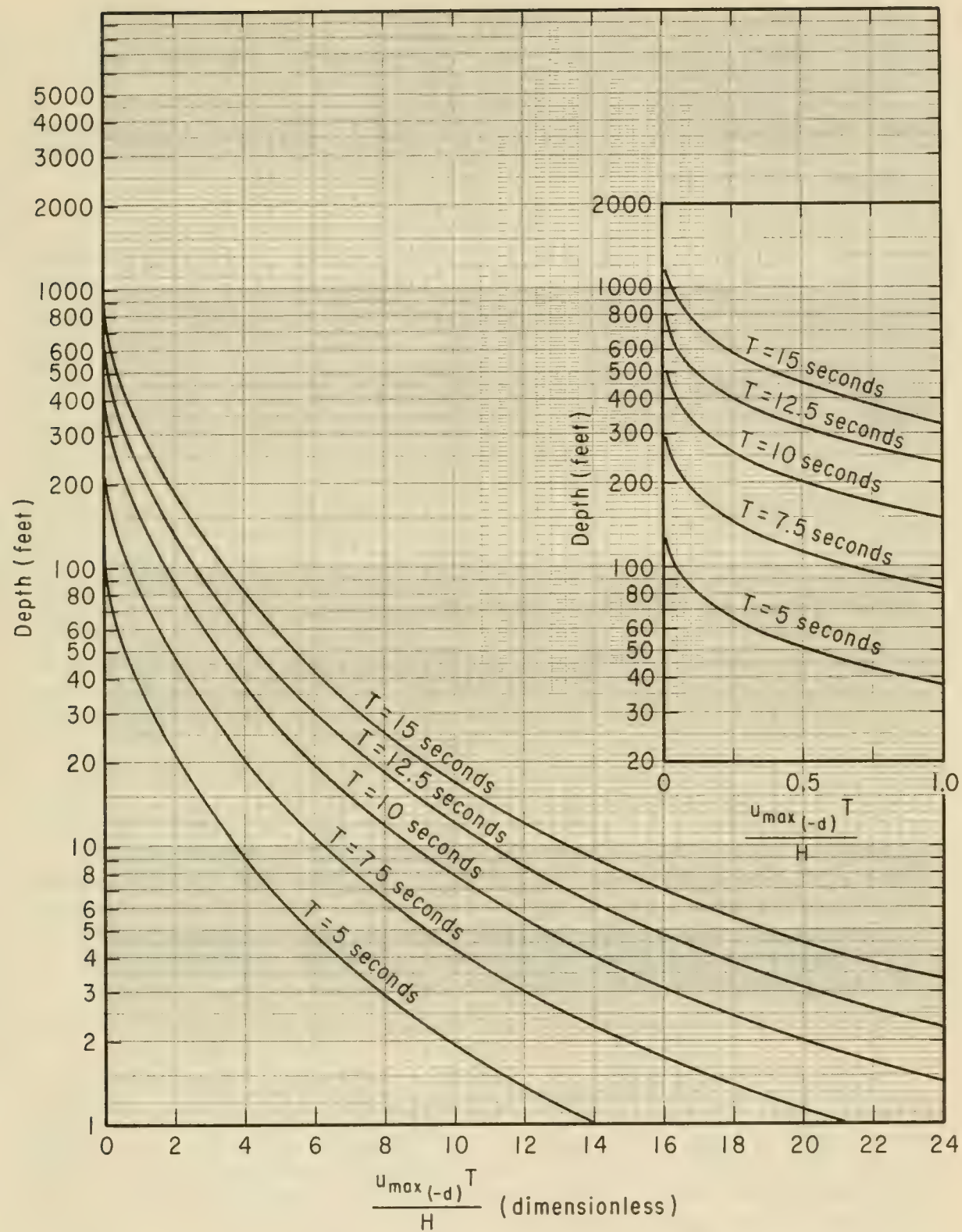
Figure 4-21. Maximum Bottom Velocity from Small Amplitude Theory

* * * * * * * * * * * * * EXAMPLE PROBLEM * * * * * * * * * * * * * * * * *

GIVEN: A wave in depth d = 200 feet, with period T = 9 seconds, and a maximum bottom velocity $u_{max(-d)} \geq 1.0$ foot per second.

FIND: The minimum wave height that will create the given bottom velocity.

SOLUTION: Calculate

$$L_o = \frac{gT^2}{2\pi}$$

$$= 5.12\,(9)^2$$

$$= 415 \text{ feet} .$$

and

$$\frac{d}{L_o} = \frac{200}{415}$$

$$= 0.482$$

Entering Figure 4-20 with $d/L_O = 0.482$, determine

$$\frac{u_{max(-d)} T}{H} = 0.30 ,$$

$$H = \frac{u_{max(-d)} T}{0.30} ,$$

$$H = \frac{(1)\,(9)}{0.30} = 30 \text{ feet.}$$

Thus a 30-foot minimum wave height with a 9-second wave period is needed to create a bottom velocity equal to or greater than 1 foot per second in 200 feet of water. Alternatively, a curve for a 9-second period can be interpolated in Figure 4-21 and $u_{max(-d)} T/H$ can be read from the curve's intersection with the 200-foot depth.

* *

    As a wave moves into shallower water, both bottom velocity and size of water-particle orbit increase. For some low velocities where the horizontal orbit is small, sand moves as individual grains rolling across the surface, but for most conditions, once quartz sand begins to move, ripples form (Kennedy and Falcon, 1965; Carstens, et al., 1969; Cook, 1970). Thus, the initiation of sediment motion is usually indicated by the formation of sediment ripples.

Figure 4-22, from Inman (1957) and including data from two earlier studies, shows the velocity needed to start motion in a sediment bed of a given grain size. These results are in general agreement with other studies relating critical velocity to grain size. Also shown in this figure are maximum velocities above which ripples tend to be smoothed off, in qualitative agreement with conditions for bed forms in unidirectional flows. (Southard, 1972.)

From Figure 4-22, it appears that maximum wave-induced bottom velocities between 0.4 and 1.0 foot per second are sufficient to initiate sand motion under waves. In field studies, Inman (1957) found that ripples are always present whenever computed maximum velocities exceed 0.33 foot per second, and Cook and Gorsline (1972) report ripples above a velocity range of 0.5 to 0.6 foot per second. Equation 4-19 can be used to determine the combination of wave conditions and depth that produces any given critical value of u_{max} at the bottom. Figure 4-23 shows the relation between depth and wave height, for given wave periods, for a critical velocity, u_{max} = 0.5 foot per second.

4.523 Seaward Limit of Significant Transport. Figures 4-20 through 4-23 and a knowledge of offshore wave climate suggest that waves can move bottom sediments over most of the Continental Shelf (to depths of 100 to 400 feet or more) during some time of the year. Geologic studies indicate that fine material has been winnowed from the surficial sediments over much of the shelf. (Shepard, 1963; and Dietz, 1963.) The question is, what is the maximum depth to which the rate of sand movement is significant in coastal engineering? This section discusses field data that supply partial answers to this question.

a. Bathymetry. Dietz (1963) and others point out that waves rework nearshore sands, smoothing out irregularities by longshore and onshore-offshore transport. This smoothing produces a quasi-equilibrium surface in the nearshore zone which forms relatively straight contours, nearly parallel to the shoreline.

Most bathymetric charts with closely spaced contours as illustrated by Figures 4-24 and 4-25 show that isobaths near the shore run parallel to the shoreline; further offshore, the contours may indicate linear shoals (Duane, et al., 1972), or other irregular submarine features.

Following the idea of Dietz (1963), the depth below which shore-parallel contours give way to irregular contours is assumed to mark the local transition between the nearshore zone where sands are moved by the waves in significant quantities and the offshore zone where sand is moved in lesser quantities. Possible exceptions to this shore-parallel contour rule are the contours around river deltas and inlets, or where reefs and ledges occur in the nearshore zone.
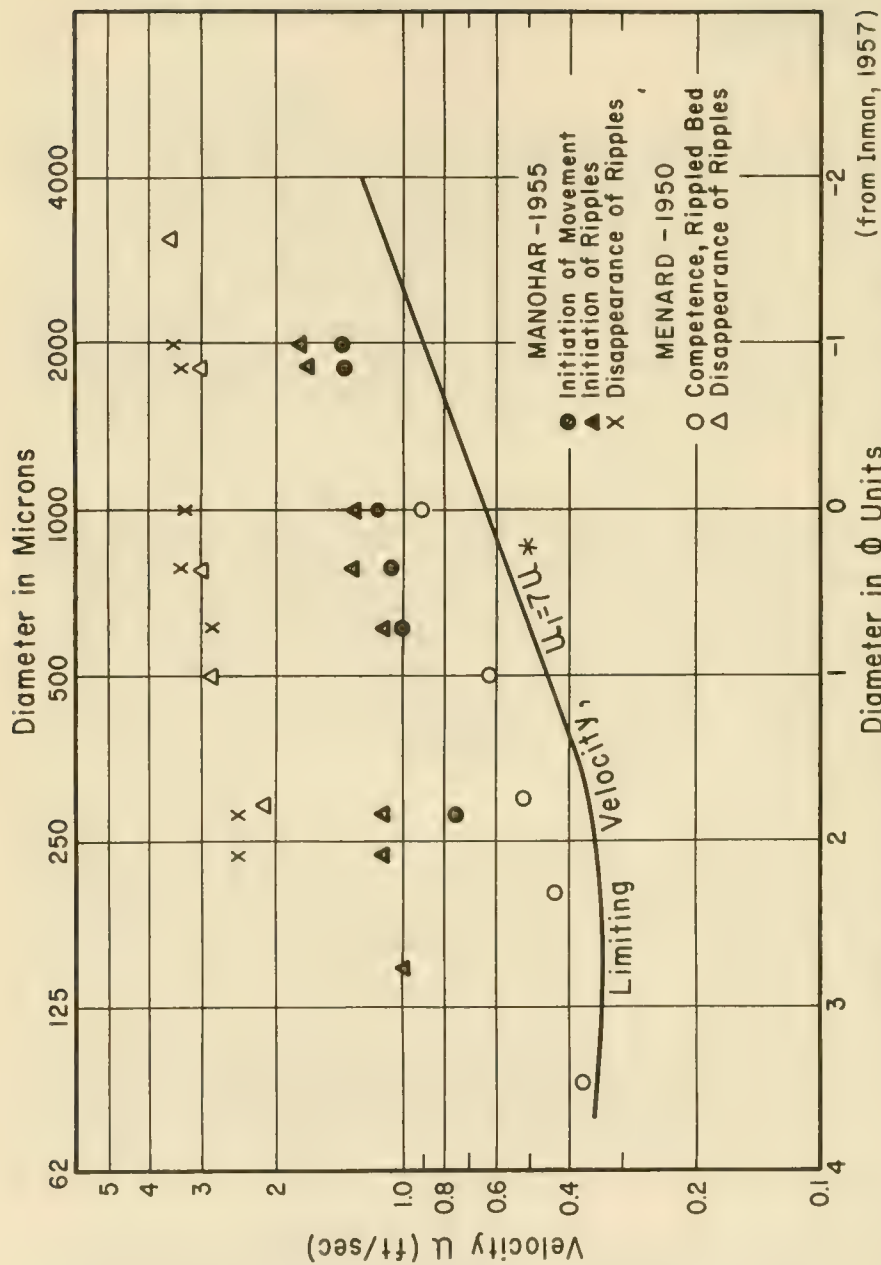
4-65

Figure 4-22. Initiation of Ripple Motion

Limiting velocity, arbitrarily defined as equal to $7u_*$, where u_* is the threshold or critical friction velocity. (Inman, 1949.) For unidirectional flow this relation would give a limiting velocity equivalent, for example, to the mean velocity measured 1 foot above a bottom which has a roughness length of 2 cm. Field observations near the surf zone indicate that planation and disappearance of ripples does not occur unless the maximum velocity associated with the wave crest somewhat exceeds that listed by Menard and Manohar.

4-66

Figure 4-23. Wave Conditions Producing Maximum Bottom Velocity
of 0.5 Ft/Sec (Based on Linear Theory)
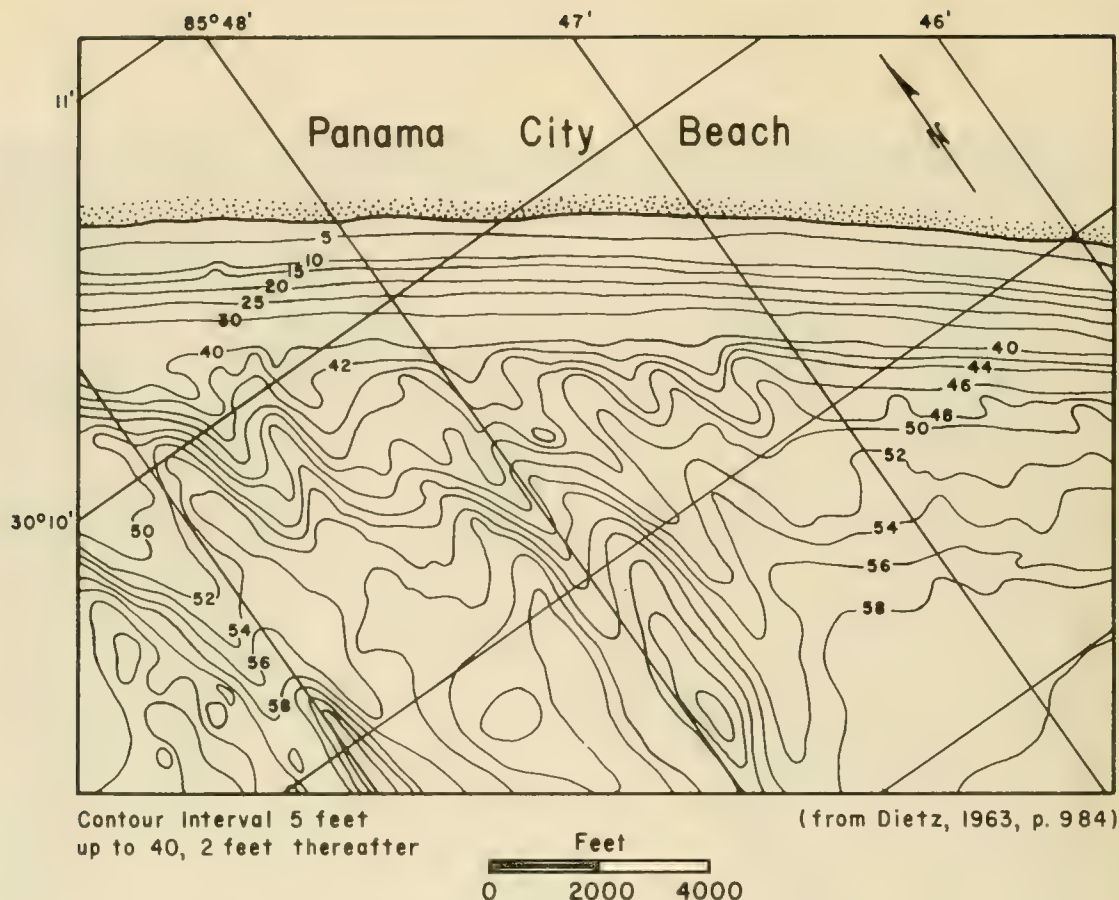
Figure 4-24.   Nearshore Bathymetry with Shore-Parallel
Contours off Panama City, Florida

Bathymetry, such as that in Figures 4-24 and 4-25, suggests that the depth to the deepest shore-parallel contour is usually constant along the shore for distances of several miles, but that this depth may vary with longshore distances of about 10 miles. (See Figure 4-25.) The depth to the deepest shore-parallel contour may depend on the contour spacing, but this is not important if contour intervals are small relative to the total depths involved. In general, the deepest shore-parallel contour is between 15 and 60 feet. In most localities, this depth is somewhat deeper than that at which nearshore profiles are presumed to close-out. These near-shore contours probably reflect longer term adjustment to extreme storms that occur rarely during the typical time interval between repetitive nearshore profile surveys.

b. Size Distribution. Geologic studies (Milliman, 1972; and Curray, 1965) suggest that littoral sands grade seaward into finer materials before the relatively coarse sands of the shelf are reached. In some places the boundary between the coarser shelf sediment and this finer material is quite sharp. (Pilkey and Frankenberg, 1964.) The finer material is currently
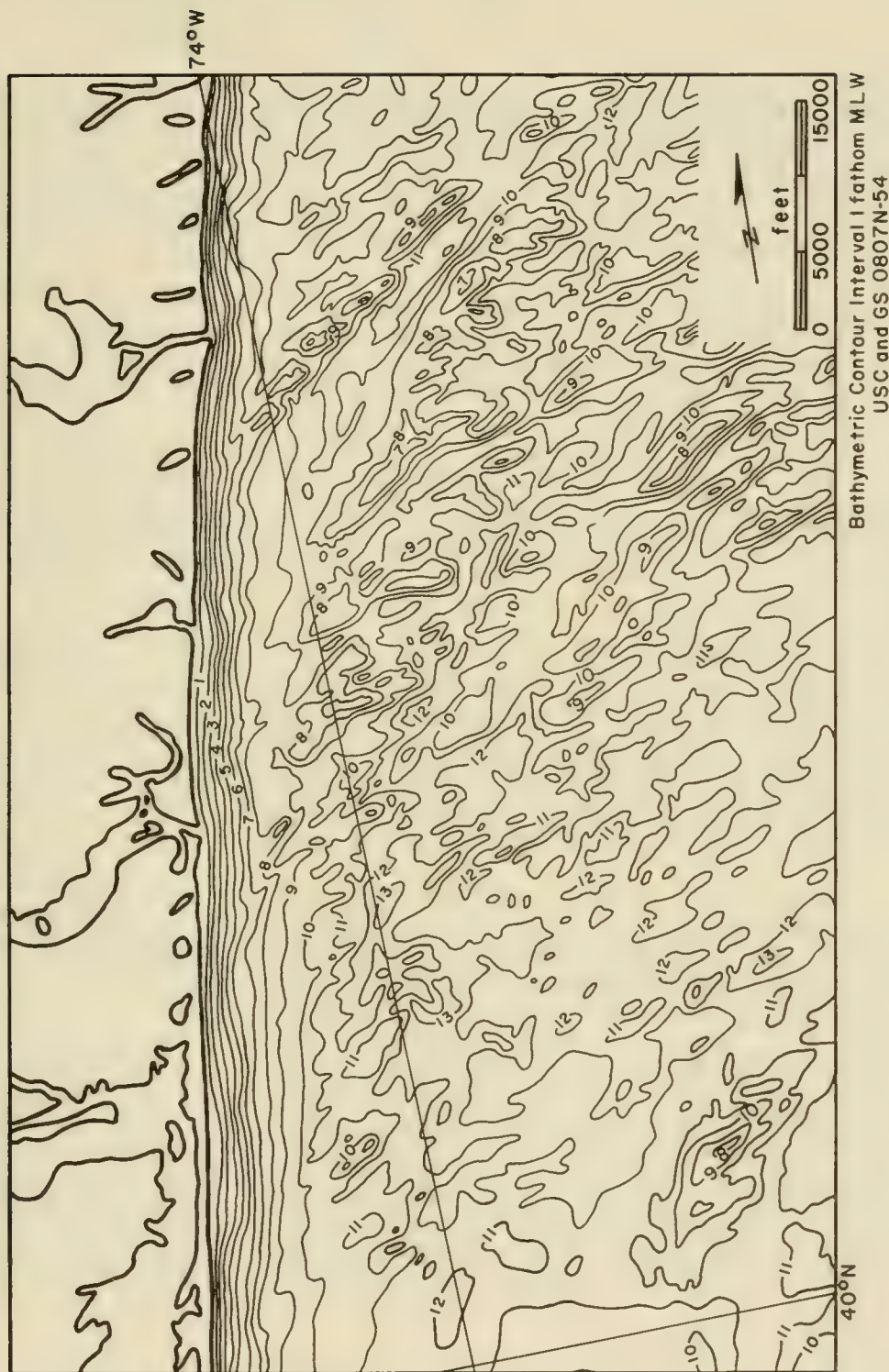
Figure 4-25. Nearshore Bathymetry with Shore-Parallel Contours and Linear Bars off Manasquan, New Jersey

Bathymetric Contour Interval 1 fathom MLW
USC and GS 0807N-54

4-69

interpreted as bounding the seaward edge of sediment moved by waves in significant quantities. This band of finer material suggests that there is little exchange between littoral and shelf sands in most places.

c. Sand Budget Balancing. Onshore sand transport has been suggested as a source of sand for several coastal localities that lack other obvious sand sources. (Shepard, 1963, pp. 176-177; and Pierce, 1969.) For example, Pierce suggests that the offshore must supply 440,000 cubic yards per year of sand to the southern segment of the Outer Banks of North Carolina because other known sources do not balance the budget.

d. Transport in Nearshore Zone. Although theoretical, experimental, and field data show that waves move sand some of the time over most of the Continental Shelf, most of the data suggest that sand from the shelf is not a significant contributor to the sediment budget of the littoral zone.

Sand transport from the nearshore zone is more likely. Surveys show that sand in the nearshore zone does move, although it is difficult to measure direction of motion. The presence of shore-parallel contours along most open shores is evidence that the waves actively mold the sand bottom in the nearshore zone. However, the time scale of transport in the nearshore zone may be relatively slow.

In tests at Santa Barbara, California, and at Atlantic City and Long Branch, New Jersey, dredged sands were dumped offshore in depths ranging from 15 to 40 feet, but no measurable onshore migration of the sand resulted for times of about 1 year. (Hall and Herron, 1950.) Radioactive tracers have shown that gravel moves slowly landward in 30 feet of water at a rate of about 0.5 cubic yard per year per foot of beach. (Crickmore and Waters, 1972.)

At shallower depths in the nearshore zone, onshore sand transport following storms is well documented. Transport of sediment suspended over ripples by the mass transport velocity is more than adequate to return sand eroded from the beach or to transport sand eroded from the nearshore bottom to the beach.

e. Summary on Seaward Limit. The deepest shore-parallel contour appears to be a usable estimate of the maximum depth where significant sand transport can be expected. This depth varies from 15 feet to perhaps 60 feet or more along U.S. coasts. This choice may be modified for specific wave conditions using Figure 4-23 to find the depth where maximum wave-induced velocity first exceeds 0.5 foot per second. If this depth is less than the depth of the deepest shore-parallel contour, it should be used as the seaward limit for the given wave conditions.

4.524 Beach Erosion and Recovery.

a. Beach Erosion. Beach profiles change frequently in response to winds, waves, and tides. Profiles are also affected by events in the longshore direction that influence the longshore transport of sand. The most

notable rapid rearrangement of a profile is by storm waves, especially during storm surge (Section 3.8) which enables the waves to attack at higher elevations on the beach. (see Figure 1-7.)

The part of the beach washed by runup and runback is the beach face. Under normal conditions, the beach face is contained within the foreshore, but during storms, the beach face is moved shoreward by the cutting action of the waves on the profile. The waves during storms are steeper, and the runback of each wave on the beach face carries away more sand than is brought to the beach by the runup of the next wave. Thus the beach face migrates landward, cutting a scarp into the berm. (See Figure 1-7.)

In moderate storms, the storm surge and accompanying steep waves will subside before the berm has been significantly eroded. In severe storms, or after a series of moderate storms, the backshore may be completely eroded, after which the waves will begin to erode the coastal dunes, cliffs, or mainland behind the beach.

The extent of storm erosion depends on wave conditions, storm surge, the stage of the tide and storm duration.

Potential damage to property behind the beach depends on all these factors and on the volume of sand stored in the beach-dune system when a storm occurs.

For planning and design purposes, it is useful to know the magnitude of beach erosion to be expected during severe storms. Table 4-5 tabulates the effect of four notable extratropical storms along the Atlantic coast of the U.S. This table provides information on typical observed order-of-magnitude values for beach erosion above mean sea level (MSL) from single storms.

For the storm of 17 December 1970, information is available from seven localities (Column 2 of Table 4-5). (DeWall, et al., 1971.) The three other storms include two closely spaced storms affecting Jones Beach, New York, in February 1972 (Everts, 1972), and a storm that affected the northern New Jersey coast in November 1953. (Caldwell, 1959.) Characteristics that distinguish one storm from another are duration and storm surge. (See Columns 9 and 10, Table 4-5.) Storm waves lasted about 1 day for the 17 December 1970 storm, and about 2 days for the other three storms. (See Column 9.) Storm surge elevation varied from a low of 2.8 feet to a high of 6 feet in the New York Bight area. The November 1953 storm combined longer duration and high storm surge; the 17 December 1970 storm had short duration and moderate storm surge; and the February 1972 storms both had longer duration, one with moderate storm surge and the other with low storm surge.

Duration and storm surge (Columns 9 and 10) are consistent with storm damage data (Columns 11 through 16, although the effect is influenced by the choice of profiles included in each study. The December 1970 storm

Table 4-5. Storm-Induced Beach Changes

	Identification			Beach Data				Storm Data		
	(1) Storm Date	(2) Locality	(3) Survey Date	(4) Profiles	(5) Beach Length (ft.)	(6) Normal Berm Elevation (ft. above MSL)	(7) Sand Size (See Figure 4-7)	(8) Recurrence Interval	(9) Wind Wave Duration (hr.)	(10) Storm Surge (ft.)
A	17 Dec 70	Cape Cod, Mass.*	10-18 Dec 70	10	54,900	10.5	medium/coarse	1/year	24	2.0*
B	17 Dec 70	Misquamicut, R.I.*	9-23 Dec 70	7	15,950	7.0	medium	1/year	24	2.8†
C	17 Dec 70	Westhampton, N.Y.*	1-18 Dec 70	11	49,300	8.1	medium/fine	1/year	24	3.6‡
D	17 Dec 70	Jones Beach, N.Y.*	12-20 Dec 70	15	71,750	9.1	medium/fine	1/year	24	3.6‡
E	17 Dec 70	Long Beach Is., N.J.*	7-18 Dec 70	20	99,300	7.8	medium	1/year	24	3.6‡
F	17 Dec 70	Atlantic City, N.J.*	9-18 Dec 70	7	14,750	6.9	fine	1/year	24	3.6‡
G	17 Dec 70	Ludlam Island, N.J.*	10-18 Dec 70	20	38,550	6.4	fine/very fine	1/year	24	3.6‡
H	17 Dec 70	All Localities*	—	90	344,500 (65.2 mi.)	—	—	1/year	—	—
I	4 Feb 72	Jones Beach, N.Y.†	2-6 Feb 72	10	45,500	9.1	medium	NA	48	2.8§
J	19 Feb 72	Jones Beach, N.Y.†	6-24 Feb 72	10	45,500	9.1	medium	NA	48	4.0§
K	6-7 Nov 53	Sandy Hook to Barnegat Light, N.J.‡	Summer to Nov. 1953	19	198,000 (37.5 mi.)	9.0	NA	NA	NA	NA

Footnotes by Column

(2) * Dewall, et al., 1971
   † Everts, 1972
   ‡ Caldwell, 1959, and U.S.C.E., 1954

(7) (8) (9) (10) NA = Not Available

(10) * Boston
   † Newport
   ‡ Sandy Hook
   § The Battery

Table 4-5. Storm-Induced Beach Changes—Continued

	Storm Damage Data						
	(11) Profiles with Net Erosion Above MSL	(12) Profiles with Net Accretion Above MSL	(13) Profiles with Seaward Movement of MSL Contour	(14) Profiles with Landward Movement of MSL Contour	(15) Average Erosion * All Profiles (cu.yd./ft. of beach)	(16) Extreme Erosion * Single Profile (cu.yd./ft. of beach)	(17) Ratio of Erosion Extreme/Average
A	8	2	5	5	5.5	21.7	3.9
B	6	1	5	2	4.0	8.0	2.0
C	8	3	4	5	4.1	16.9	4.1
D	13	2	11	3	7.4	19.4	2.6
E	15	5	4	10	3.5	20.8	5.9
F	4	3	2	3	0.3 † / 4.4 ‡	24.4 † / 10.2	34.0 † / 2.3 ‡
G	16	3	15	4	2.6	16.3	6.3
H	70	19	46	32	4.0 †	21.7	5.4
I	10	9	1	7	9.9	17.3	1.7
J	0	1	3	5	5.8	17.2	3.0
K	18	1	2	12	40.5 §	88.9	2.2

Footnotes by Column

(15) * Above MSL
  † All Profiles
  ‡ Omitting profile near jetty
  § Caldwell, 1959, average plot

(16) * Above MSL
  † Accretion

(17) † All 7 profiles
  ‡ 6 profiles

includes all profiles surveyed. The two February 1972 storms at Jones
Beach include all profiles away from the influence of inlets, reducing
the number of profiles from 15 in the December 1970 storm to 10 in the
February 1972 storms. The November 1953 storm gives relatively high
storm damage which may partly result from the long time interval between
pre-storm survey and the storm. (See Columns 1 and 3.) These results
are also affected by the fact that they omit some profiles "believed to
be influenced by the presence of a seawall or a bulkhead." (Caldwell,
1959, p. 4.)

Although the data in Table 4-5 are not completely comparable, the
results do suggest that the average volume of sand eroded above mean sea
level from beaches about 5 or more miles long has a certain range of val-
ues. A moderate storm may remove 4 to 10 cubic yards per foot of beach
front above MSL; an extreme storm (or a moderate storm that persists for
a long time) may remove 10 to 20 cubic yards per foot; rare storms that
are most destructive in beach erosion due to a combination of intensity,
duration, and orientation may remove 20 to 50 cubic yards per foot. These
values are average for beaches 5 to 10 miles or more long, and they are
compatible with other, less complete, data for notable storms. (Caldwell,
1959; Shuyskiy, 1970; and Harrison and Wagner, 1964.) For comparative
purposes, a berm 100 feet wide at an elevation of 10 feet MSL contains 37
cubic yards per foot of beach front, a quantity that would be adequate
except for extreme storms.

In terms of horizontal changes rather than the volume changes in
Table 4-5, a moderate storm can erode a typical beach 75 to 100 feet or
more, and leave it exposed to greater erosion if a second storm follows
before the beach has recovered. This possibility should be considered
in design and placement of beach fills and other protective measures.

Extreme values of erosion may be more useful than mean values for
design. Column 17 of Table 4-5 suggests that the ratio of the most ero-
ded above-MSL-profile to the average profile for east coast beaches ranges
from about 1.5 to 6. If the average erosion per profile is based only on
those profiles showing net erosion, then this ratio is probably between
1.5 and 3.

Although the dominant result of storms on the above MSL part of
beaches is erosion, most post-storm surveys show that the storm produces
local accretion as well. Of the 90 profiles from Cape Cod, Massachusetts,
to Cape May, New Jersey, surveyed immediately after the December 1970
storm, 16 showed net accretion above mean sea level. (Compare Columns 4,
11, and 12 in Table 4-5.) Similar results are indicated for a number of
more severe storms. (Caldwell, 1959.)

The storm surveys also show that the shoreline on many beaches may
prograde seaward even though the profile as a whole loses volume, or
vice versa. This possibility suggests caution in interpreting aerial
photos of storm damage. (Everts, 1973.)

b. Beach Recovery. The typical beach profile left by a severe storm is a simple, concave-upward curve extending seaward to low tide level or below. (See top of Figure 4-26.) The sand that has been eroded from the beach is deposited mostly as a ramp or bar in the surf zone that exists at the time of the storm. Immediately after the storm, beach repair begins by a process that has been documented in detail. (e.g., Hayes, 1971; Davis, et al., 1972; Davis and Fox, 1972; and Sonu and van Beek, 1971.) Sand that has been deposited seaward of the shoreline during the storm begins moving landward as a sandbar with a gently sloping seaward face and a steeper landward face. (See Figure 4-26.) These bars have associated lows (runnels) on the landward side and occasional drainage gullies across them. (King, 1972, p. 339.) These systems are characteristic of post-storm beach accretion under a wide range of wave, tide, and sediment conditions. (Davis, et al., 1972.) They are sometimes called ridge-and-runnel systems.

The processes of accretion occur as follows. Sand is transported landward over the nearly flat seaward face of the bar by the waves. At the bar crest, the sand avalanches down the landward slip face. If the process continues long enough, the bar reaches the landward limit of storm erosion where it is "welded" onto the beach. (e.g. Davis, et al., 1972.) Further accretion continues by adding layers of sand to the top of the bar which, by then, is a part of the beach. (See Figure 4-27.)

Berms may form immediately on a post-storm profile without an intervening bar-and-trough, but the mode of berm accretion is quite similar to the mode of bar-and-trough growth. Accretion occurs both by addition of sand laminae to the beach face (analogous to accretion on the seaward-dipping top of the bar in the bar-and-trough) and by addition of sand on the slight landward slope of the berm surface when waves carrying sediment overtop the berm crest (analogous to accretion on the landward dipping slip face of the bar). This process of berm accretion is also illustrated in Figure 4-1.

The rate at which the berm builds up or the bar migrates landward to weld onto the beach varies greatly, apparently in response to: wave conditions, beach slope, grain size, and the length of time the waves work on the bars. (Hayes, 1971.) Compare the slow rate of accretion at Crane Beach in Figure 4-26 (mean tidal range 9 feet, spring range 13 feet) with the rapid accretion on the Lake Michigan shore in Figure 4-27 (tidal range less than 0.25 foot).

Post-storm studies by CERC show that the rate of post-storm replenishment by bar migration and berm building is usually rapid immediately after the storm. This rapid buildup is important in evaluating the effect of severe storms because (unless surveys are made within hours after the storm) the true extent of erosion during the storm is likely to be obscured by the post-storm recovery. Lack of surveys before the start of post-storm recovery may explain some survey data that show MSL accretion on profiles that have lost volume.
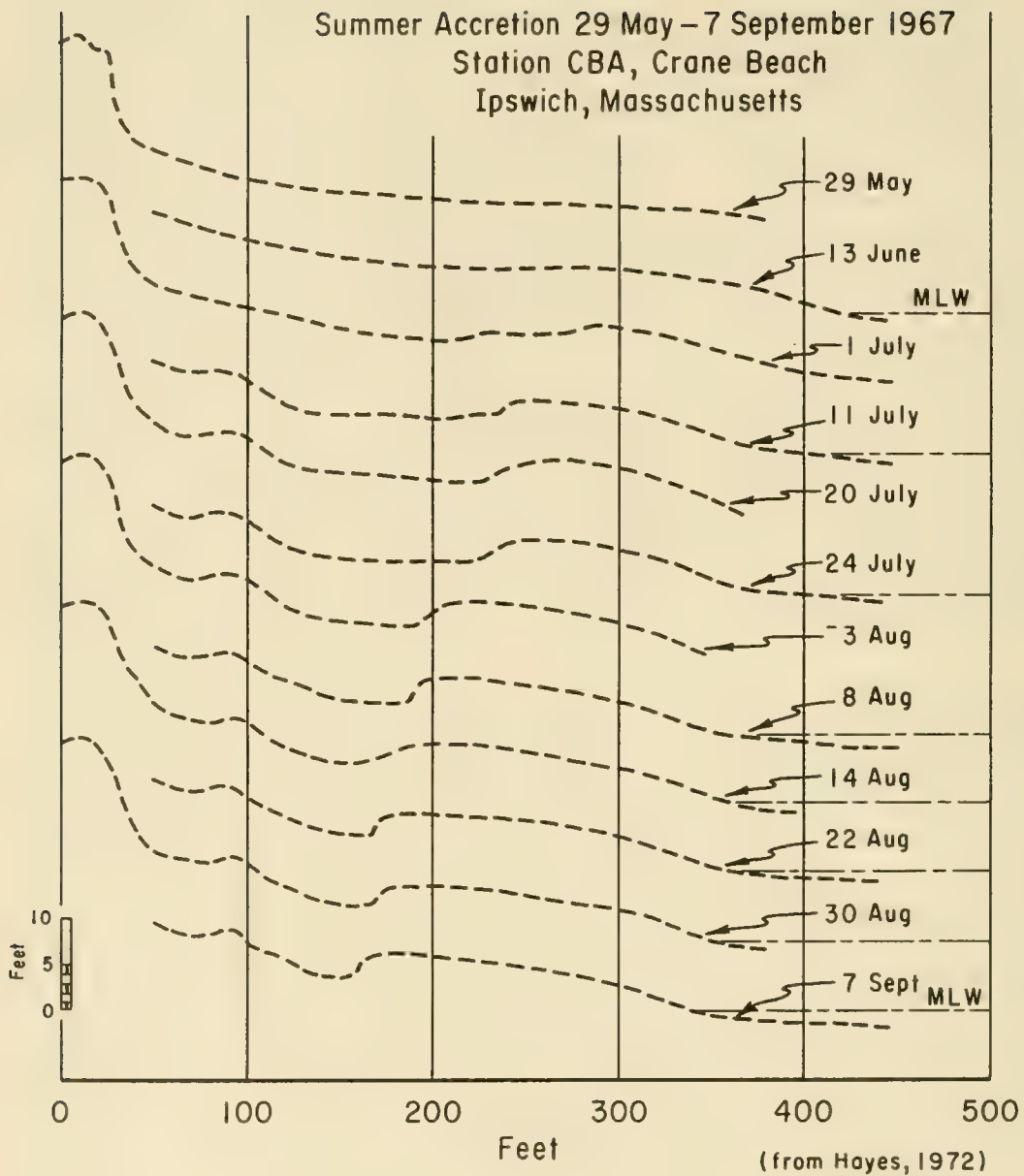
Figure 4-26. Slow Accretion of Ridge-and-Runnel at Crane Beach, Massachusetts
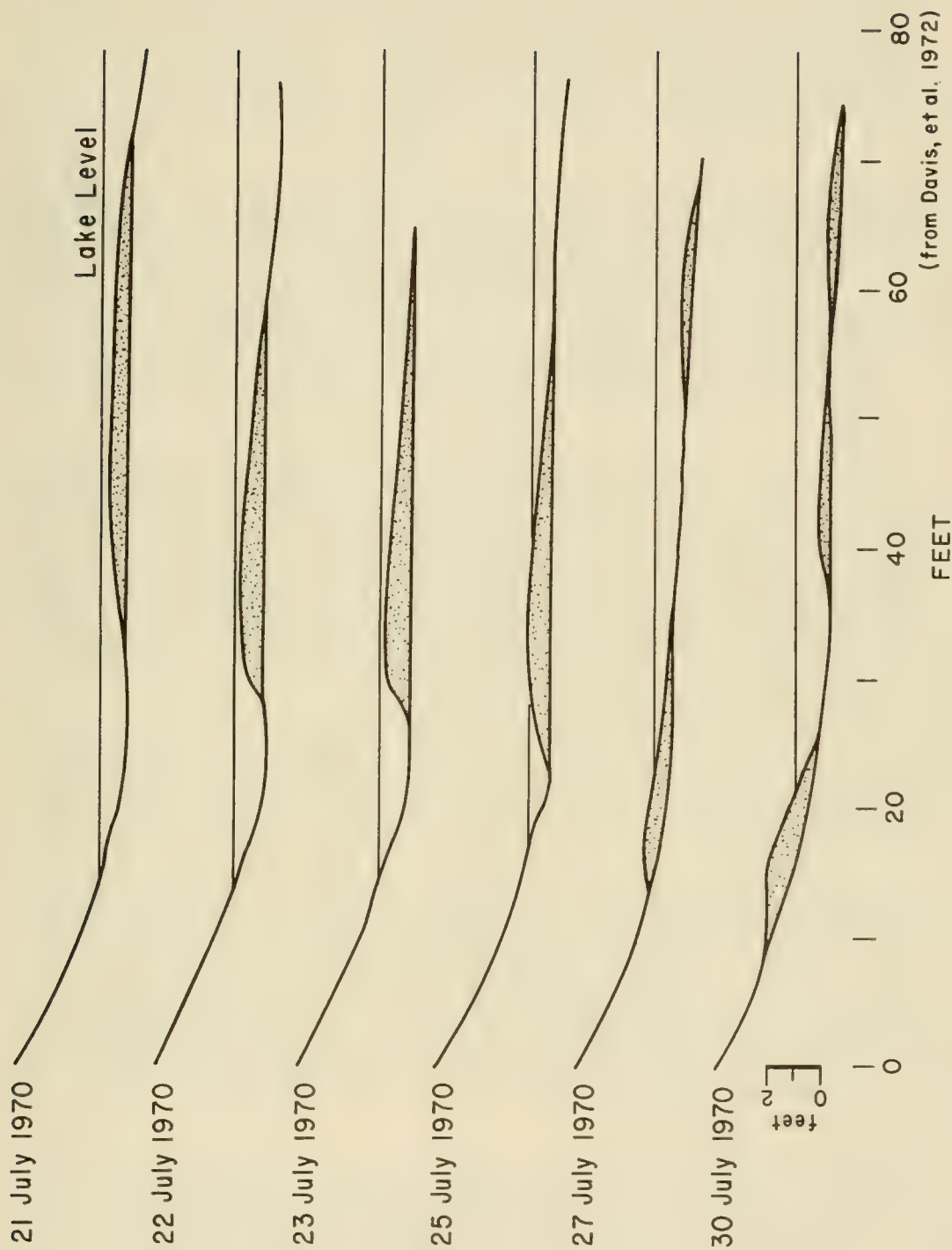
Figure 4-27. Rapid Accretion of Ridge-and-Runnel - Lake Michigan (Holland, Michigan)

(from Davis, et al. 1972)

4-77

The ideal result of post-storm beach recovery is a wide backshore that will protect the shore from the next storm. Beach recovery may be prevented when the period between successive storms is too short. Maintenance of coastal protection requires knowledge of the necessary width and elevation of the backshore appropriate to local conditions, and adequate surveillance to determine when this natural sand reservoir is diminished to a point where it may not protect the backshore during the next storm.

4.525 Bar-Berm Prediction. High, steep waves scour the beach, eroding the foreshore into a simple concave-upwards profile. The material eroded from the beach is deposited offshore as a longshore bar. Waves of low steepness tend to push sand onto the beach, usually as migrating longshore-bar systems which eventually become part of the beach. In contrast to the concave-up eroded profile discussed previously, the accreted profile is concave-downward. Idealized eroded and accreted profiles (measured in a prototype-scale wave tank) across the beach and nearshore zone are shown in Figure 4-28.

To design a beach that contains a reservoir of sand in the backshore sufficient to survive a design storm, a minimum requirement is the ability to distinguish wave conditions that cause eroded profiles from those that cause accretion. Usually, it is assumed that a berm characterizes an accreted profile and that a bar characterizes an eroded profile. (See Figure 4-28.) This picture is somewhat idealized. A sharp berm crest between backshore and foreshore is often lacking, and on some beaches the berm is absent, so that the top of the foreshore reaches the dune or cliff line. Berms are illustrated in Figures 4-1 and 4-27.

Similarly, the idealized longshore bar seaward of an eroded beach, (middle profile of Figure 4-18) is often absent, and in its place there may be several subdued bars or a platform extending to the breaker line at nearly constant depth.

a. Longshore Bars. The term *bar* has been applied to a number of quite different coastal features, including barrier islands (the "off-shore bar" of Johnson, 1919), ridge-and-runnel systems, and linear shoals. (Duane, et al., 1972.) Longshore bars are unrelated to any of these features. They appear to most nearly resemble a ridge-and-runnel system, but differ in that longshore bars are located at the breaker position and, at least in part, are eroded out of the bottom by the falling breaker, whereas the ridge-and-runnel system is an accretionary feature migrating landward across the surf zone.

The typical longshore bar, as described from the observations of Shepard (1950) and the experiments of Keulegan (1948), is a ridge of sand parallel to the shore and formed at the breaking position of large plunging breakers. Longshore bars seem most directly related to the height of larger breakers (not necessarily of maximum height). The depth to the seaward bar increases with the height of the larger breakers along the Pacific coast. (Shepard, 1950.) Bars form readily in tidal seas, but seem better
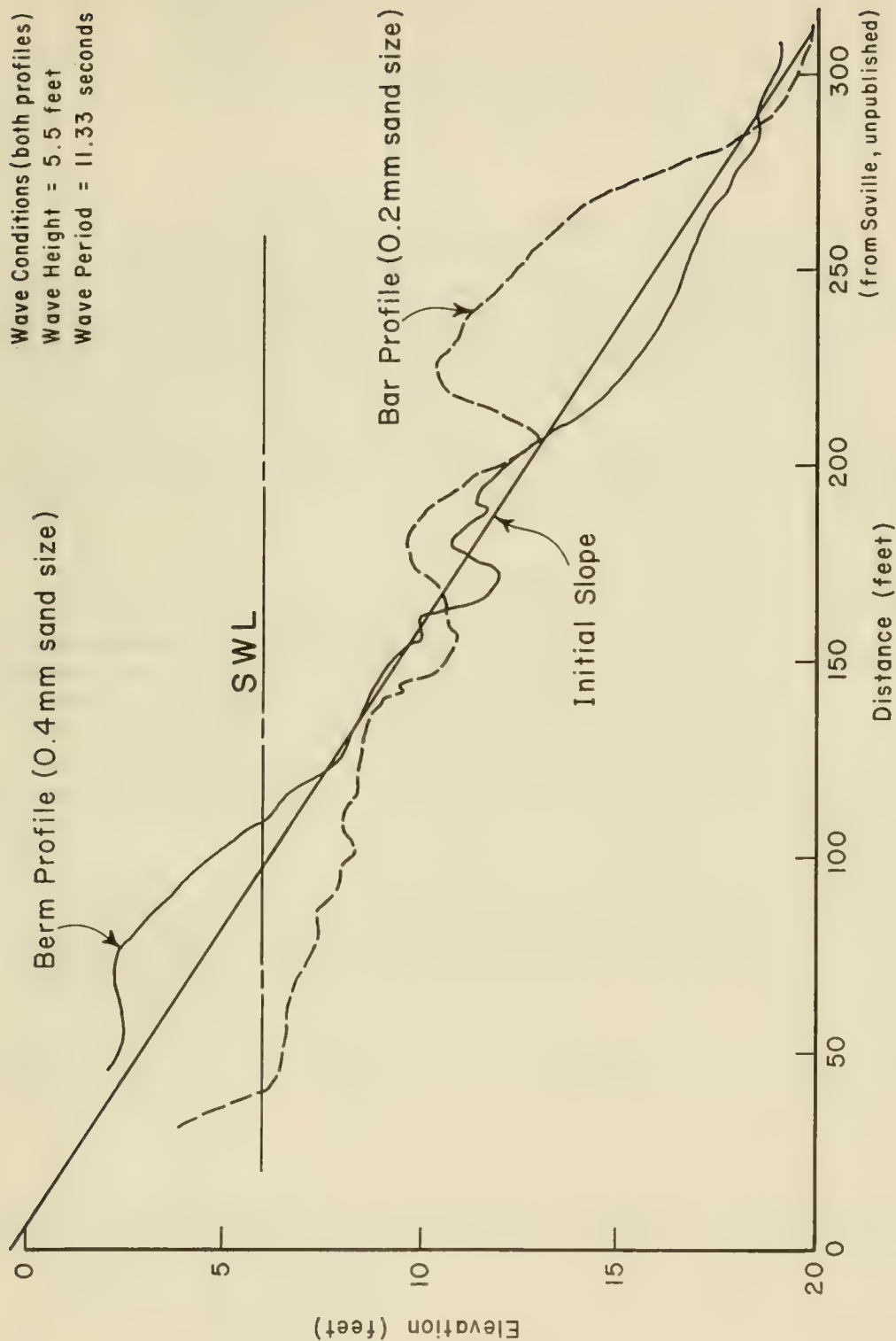
Figure 4-28. Typical Berm and Bar Profiles from Prototype Size Laboratory Wave Tank

developed in tideless seas such as Lake Michigan (Fig. 4-27). (Saylor and Hands, 1970.) Keulegan (1948) found that the ratio of depth of longshore trough to depth of bar was approximately 1.69 in laboratory experiments, but most field measurements showed less depth difference, averaging about 1.23 (based on MLLW) for 276 measurements from the Scripps pier. (Shepard, 1950.) According to Shepard, bars are not significant on slopes steeper than 4° (1 on 14).

There is evidence that longshore bars, as described, are formed by a transient condition when waves of a given height and period plunge on a relatively plane sand slope. Shepard found that steep storm waves eliminate the bars rather than build them, and that bars form after the largest storm wave subsided. Such a relation is consistent with plunging breaker conditions predicted by the breaker type parameter (Galvin, 1972). Because bars are formed by high waves, they may persist through long intervals of low waves. Once formed, bars may trigger the breaking of higher waves, dissipating the wave energy and thus reducing beach erosion. (Davis and Fox, 1972; and Zwamborn, Fromme, and Fitzpatrick, 1970.)

Laboratory observations show that longshore bars form when waves plunge, and that these bars are absent when waves spill. With constant wave conditions, a wave may plunge initially on a steep sand slope and form a bar. The beach then erodes forming a flatter slope, which changes the breaker type to spilling, which eliminates the pronounced longshore bar. For other constant wave conditions, a wave may spill initially on a gentle sand slope, and no pronounced bar forms. Later in the test, the breaker position migrates closer to the steeper foreshore, the breaker begins to plunge, and a longshore bar forms.

b. Steepness Effect. The distinction between profiles with pronounced berms (usually without bars) and profiles with eroded foreshores (often with longshore bars) is well known. (Nayak, 1970, and Johnson, 1956.) Early laboratory results suggested that the shape of the profile depends on deepwater steepness, H_O/L_O, of the waves reaching the beach. Between 1936 and 1956, laboratory experiments were made which led to the assumption that beach profiles generally eroded if H_O/L_O exceeded 0.025 and accreted if H_O/L_O was less than about 0.02.

However, neither field data nor prototype-size laboratory experiments support this widely used criterion. (Saville, 1957.) Field and prototype-size laboratory data of Saville showed that beaches eroded at significantly lower deepwater steepness than the value of 0.025 derived from model laboratory experiments. Saville (1957) concluded that the absolute size of wave height was probably as important as steepness in determining the profile.

c. <u>Dimensionless Fall Time</u>. Prediction of accreted (berm) or erod-
ed (bar) profiles is possible using a dimensionless fall-time parameter

$$F_o = \frac{H_o}{V_f T} , \qquad (4\text{-}20)$$

where H_o is deepwater wave height, T is wave period, and V_f is the
fall velocity of the beach sediment. (Dean, 1973.)

The fall-time parameter F_o, is plotted against deepwater steep-
ness, H_o/L_o, in Figure 4-29 using the profile data of Rector (1954, Table
1, Column 25) and Saville (1957, unpublished). These data include wave
heights ranging from about 0.05 foot to 5.0 feet, a range compatible with
field conditions. They also include a range of initial slopes.

In Figure 4-29, the line of demarcation between deposition offshore
and deposition onshore is approximately at the value $F_o = 1$. More com-
plete separation is possible when F_o is plotted against H_o/M_d. (See
Figure 4-30.)

Values of $F_o > 1$ indicate that the time required by the particle
to fall a distance about equal to the maximum depth in the surf zone is
greater than the time available between arriving wave crests. Thus,
values of F_o significantly greater than 1 suggest significant concen-
trations of suspended sediment, which are expected to diffuse seaward
and deposit offshore.

Since values of V_f range from about 0.066 foot per second (2 centi-
meters per second) for fine sand to 0.49 foot per second (15 centimeters
per second) for coarse sand (Fig. 4-31), F_o ranges from about 0.25 for
low swell on coarse sand beaches to 10 or more for storm waves on fine
sand beaches. Such values suggest that typical field and laboratory con-
ditions define a range of conditions within which the importance of sus-
pended sediment in the surf zone may vary from significant to negligible.

The effect of temperature on fall velocity (Fig. 4-31) is important
enough to be critical under some conditions. It appears that temperature
by itself, in its effect on fall velocity, can change a profile from erod-
ing to accreting.

To summarize results on berm-bar criteria, the dimensionless fall
time, $F_o = H_o/(V_f T)$, Equation 4-20 provides an estimate of the separa-
tion between berm and bar-type profiles. A value of F_o between 1 and 2
appears to be the critical value, with $F_o = 2$ being more appropriate for
prototype-size waves. For F_o less than the critical value, the beach
accretes above MLW. The effect of fall velocity is important. Deepwater
wave steepness by itself is an unreliable criterion for prototype condi-
tions.
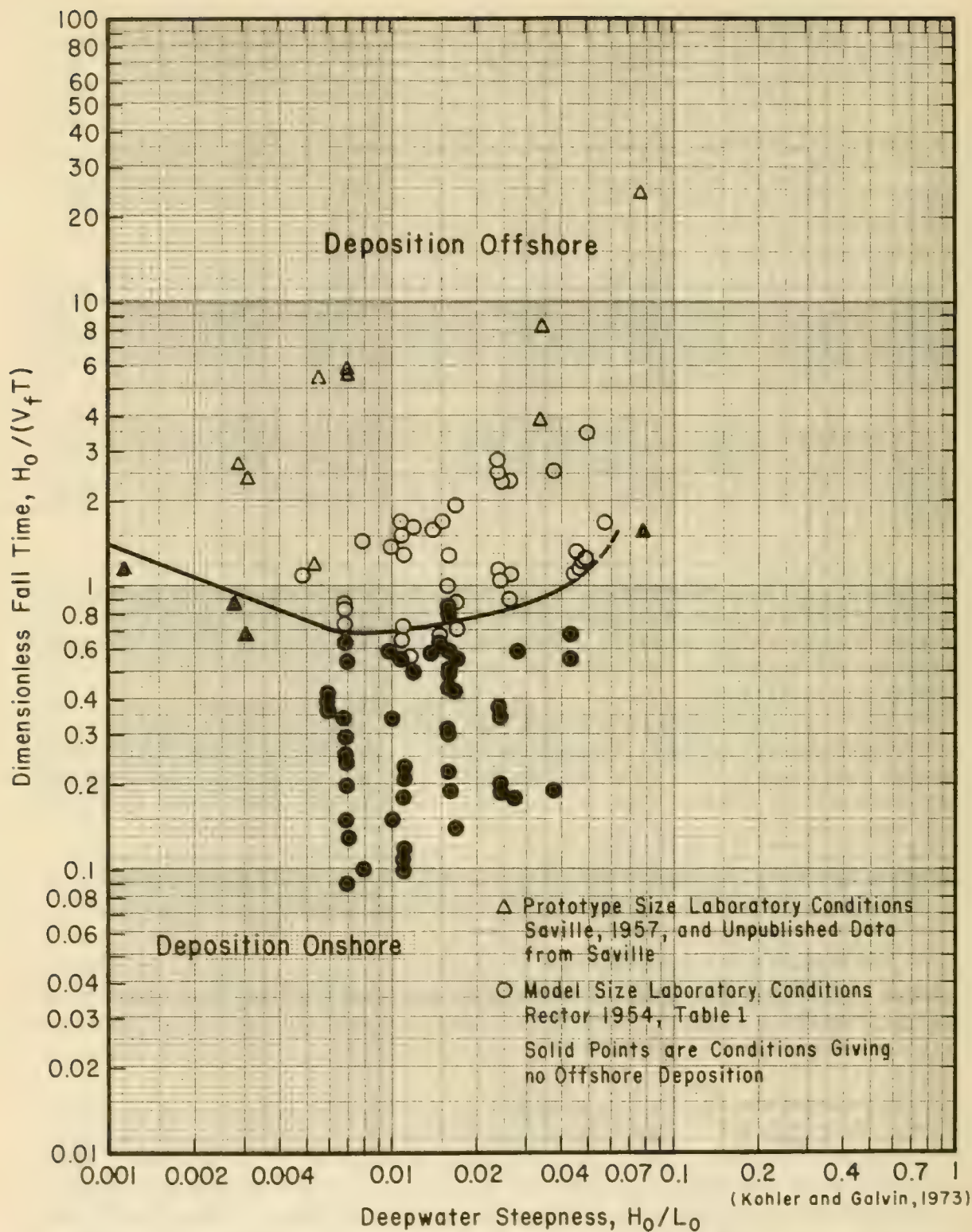
Figure 4-29.   Berm-Bar Criterion Based on Dimensionless Fall
Time and Deep Water Steepness
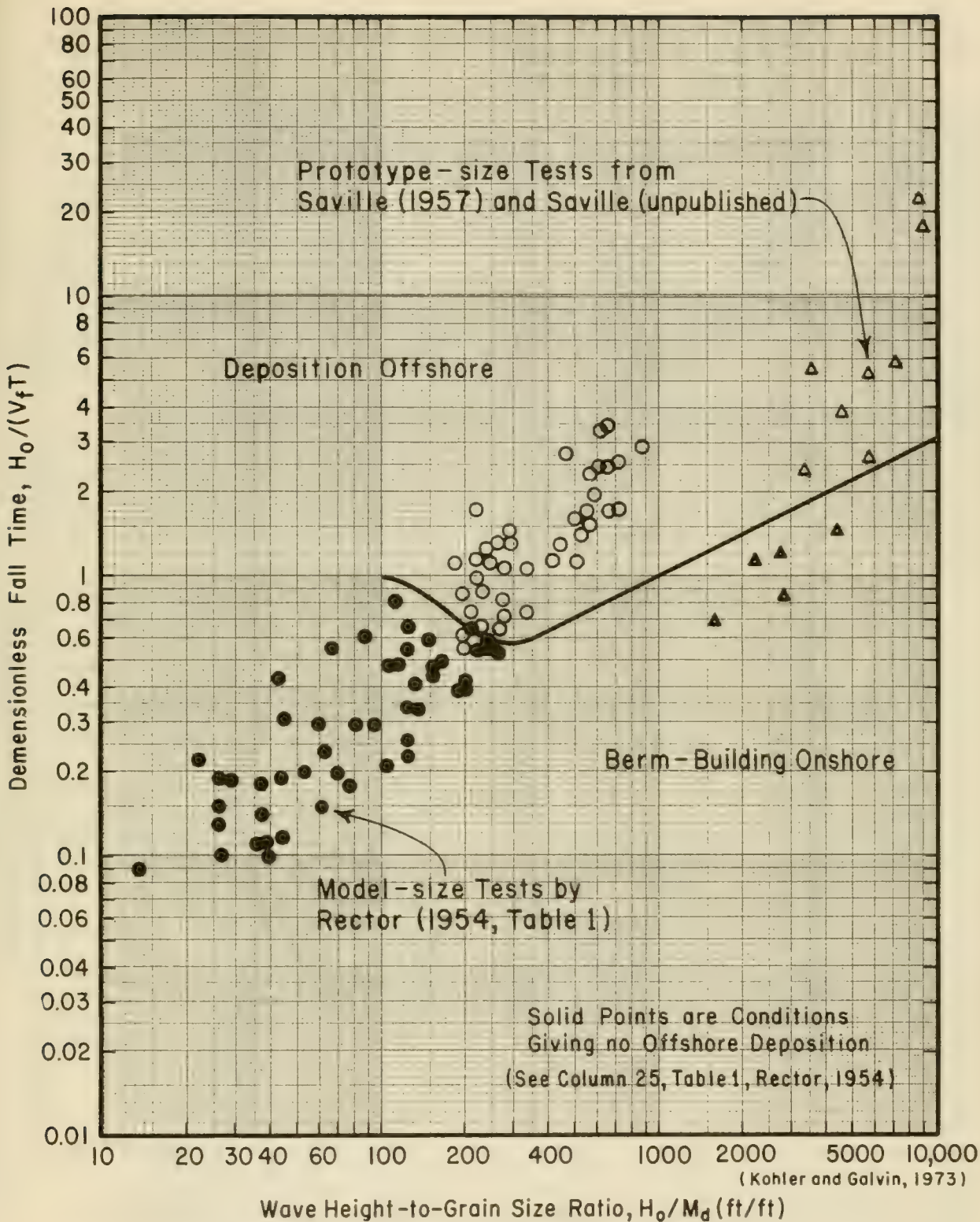
Figure 4-30. Berm-Bar Criterion Based on Dimensionless Fall
Time and Height-to-Grain Size Ratio

4-83
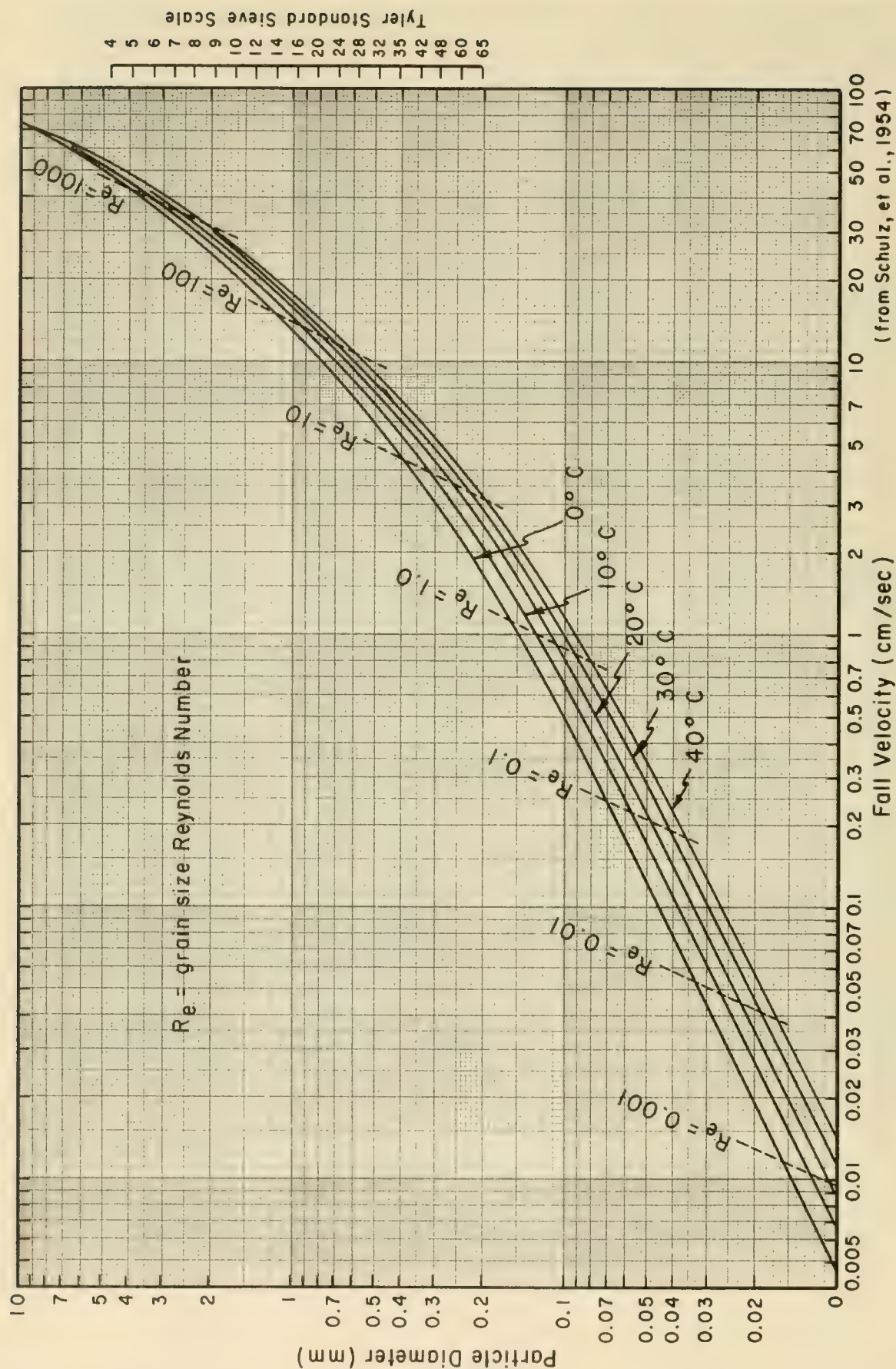
Figure 4-31. Fall Velocity of Quartz Spheres in Water as a Function of Diameter and Temperature

4.526 Slope of the Foreshore. The foreshore is the steepest part of the
beach profile. The equilibrium slope of the foreshore is a useful design
parameter, since this slope, along with the berm elevation, determines
minimum beach width.

The slope of the foreshore tends to increase as the grain size in-
creases. (U.S. Army, Beach Erosion Board, 1933; Bascom, 1951; and King,
1972, p. 324.) This relationship between size and slope is modified by
exposure to different wave conditions (Bascom, 1951; and Johnson, 1956);
by specific gravity of beach materials (Nayak, 1970; and Dubois, 1972);
by porosity and permeability of beach material (Savage, 1958); and prob-
ably by the tidal range at the beach. Analysis by King (1972, p. 330)
suggests that slope depends dominantly on sand size, and also signifi-
cantly on an unspecified measure of wave energy.

Figure 4-32 shows trends relating slope of the foreshore to grain
size along the Florida Panhandle, New Jersey-North Carolina, and the
U.S. Pacific coasts. Trends shown on the figure are simplifications of
actual data, which are plotted in Figure 4-33. The trends show that,
for constant sand size, slope of the foreshore usually has a low value
on Pacific beaches, intermediate value on Atlantic beaches, and high
value on Gulf beaches.

This variation in foreshore slope from one region to another appears
to be related to the mean nearshore wave heights. (See Figures 4-10, 4-11,
and Table 4-4.) The gentler slopes occur on coasts with higher waves. An
increase in slope with decrease in wave activity is illustrated by data
from Half Moon Bay (Bascom, 1951), and is indicated by the results of King
(1972, p. 332).

The inverse relation between slope and wave height is partly caused
by the relative frequency of steep or high eroding waves which produce
gentle foreshore slopes and low accretionary post-storm waves which pro-
duce steeper beaches. (See Figures 4-1, 4-26, and 4-27.)

The relation between foreshore slope and grain size shows greater
scatter in the laboratory than in the field. However, the tendency for
slope of the foreshore to increase with decreasing mean wave height is
supported by laboratory data of Rector (1954, Table 1). In this labora-
tory data, there is an even stronger inverse relation between deepwater
steepness, H_O/L_O, and slope of the foreshore than between H_O and the
slope.

To summarize the results on foreshore slope for design purposes, the
following statements are supported by available data:

(a) Slope of the foreshore on open sand beaches depends principally
on grain size, and (to a lesser extend) on nearshore wave height.

(b) Slope of the foreshore tends to increase with increasing median
grain size, but there is significant scatter in the data.
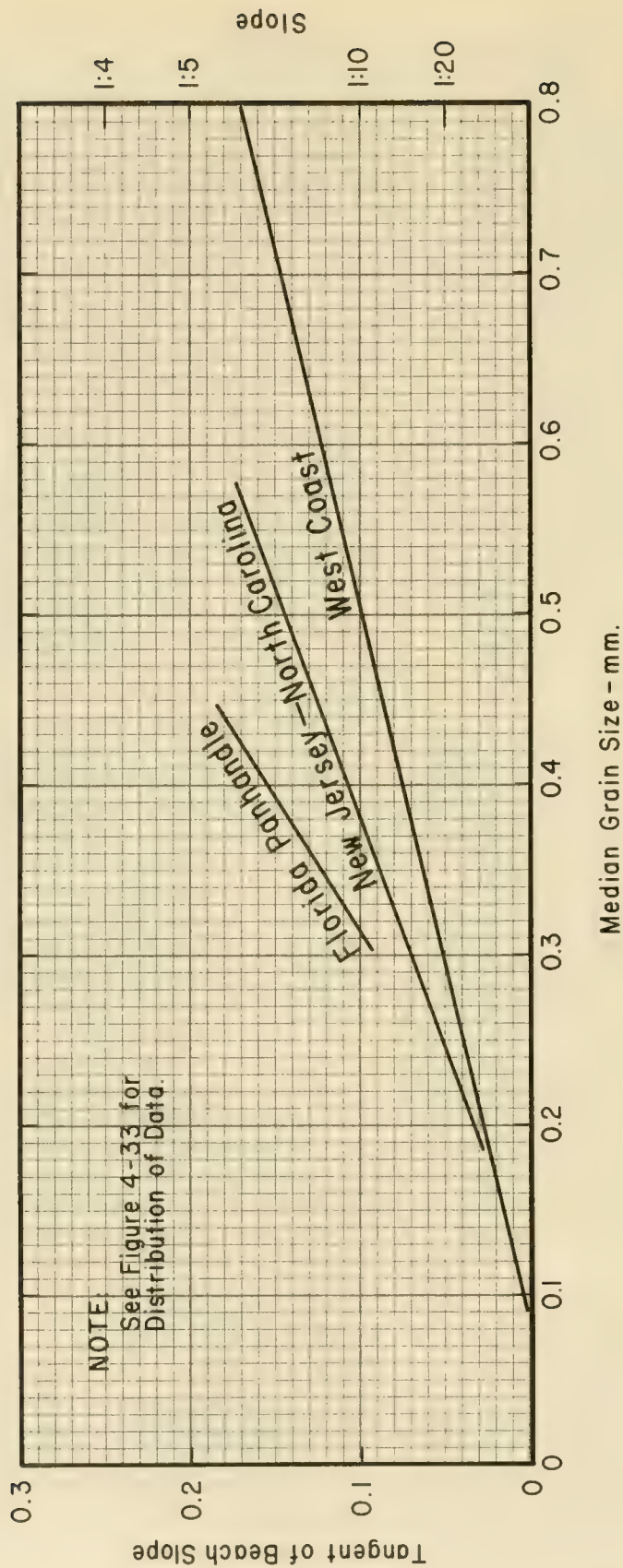
Figure 4-32. Data Trends - Median Grain Size Versus Foreshore Slope
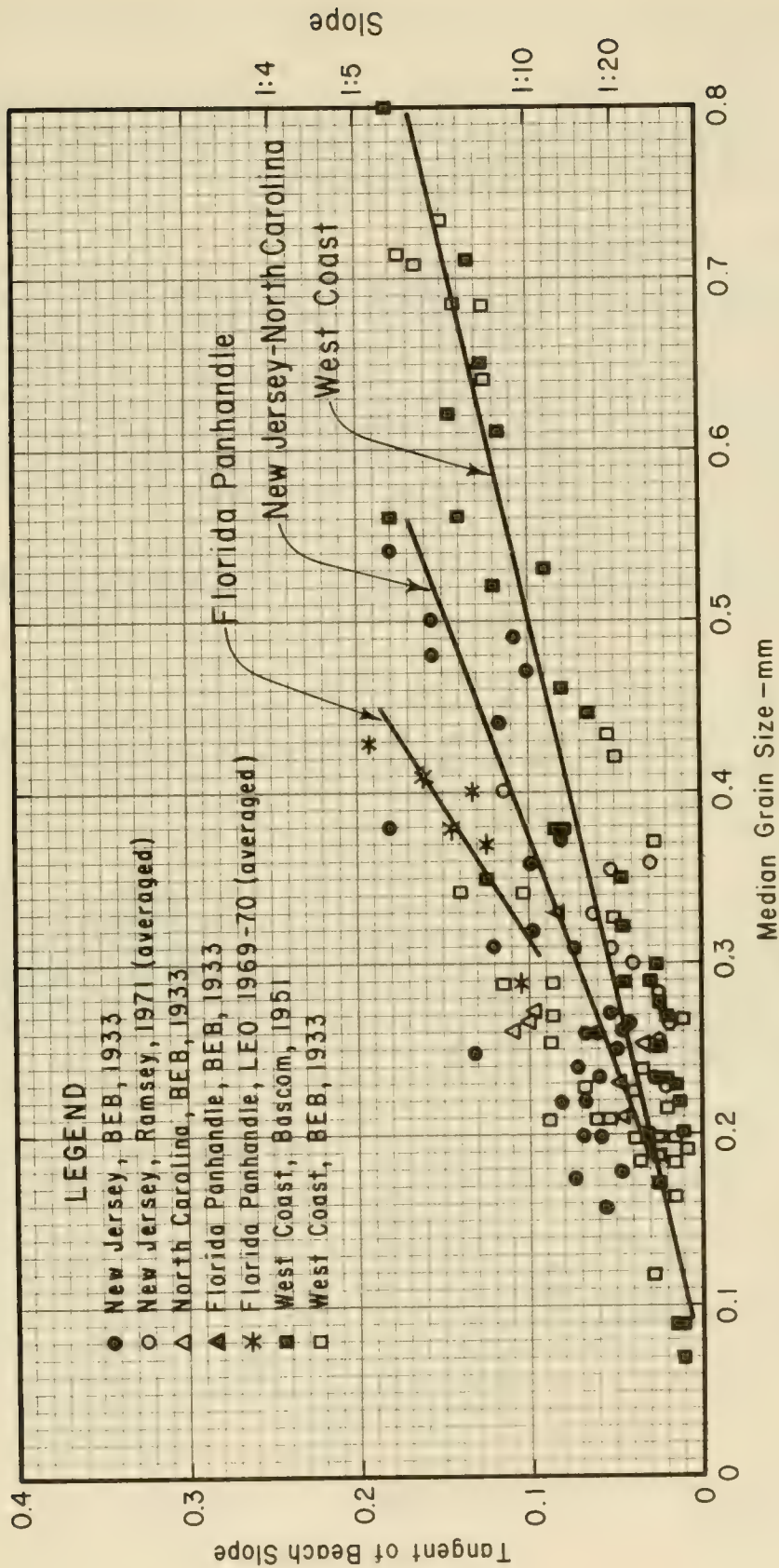
Figure 4-33. Data - Median Grain Size Versus Foreshore Slope

(c) Slope of the foreshore tends to decrease with increasing wave height, again with scatter.

(d) For design of beach profiles on ocean or gulf beaches, use Figure 4-32, keeping in mind the large scatter in the basic data on Figure 4-33, much of which is caused by the need to adjust the data to account for differences in nearshore wave climate.

4.53 LONGSHORE TRANSPORT RATE

4.531 Definitions and Methods. *Littoral drift* is the sediment (usually sand) moved in the littoral zone under action of waves and currents. The rate, Q, at which littoral drift is moved parallel to the shoreline is the *longshore transport rate*. Since this movement is parallel to the shoreline, there are two possible directions of motion, right and left, relative to an observer standing on the shore looking out to sea. Movement from the observer's right to his left is motion toward the left, indicated by the subscript ℓt. Movement toward the observer's right is indicated by the subscript rt.

Gross longshore transport rate, Q_g, is the sum of the amounts of littoral drift transported to the right and to the left, past a point on the shoreline in a given time period.

$$Q_g = Q_{rt} + Q_{\ell t} \, , \tag{4-21}$$

Similarly, *net longshore transport rate*, Q_n, is defined as the difference between the amounts of littoral drift transported to the right and to the left past a point on the shoreline in a given time period.

$$Q_n = Q_{rt} - Q_{\ell t} \, . \tag{4-22}$$

The quantities Q_{rt}, $Q_{\ell t}$, Q_n and Q_g have engineering uses: for example, Q_g is used to predict shoaling rates in uncontrolled inlets; Q_n is used for design of protected inlets and for predicting beach erosion on an open coast; Q_{rt} and $Q_{\ell t}$ are used for design of jetties and impoundment basins behind weir jetties. In addition, Q_g provides an upper limit on other quantities.

Occasionally, the ratio

$$\gamma = \frac{Q_{\ell t}}{Q_{rt}} \, , \tag{4-23}$$

is known, rather than the separate values $Q_{\ell t}$ and Q_{rt}. Then Q_g is related to Q_n in terms of γ by

$$Q_g = Q_n \frac{(1 + \gamma)}{(1 - \gamma)} \, . \tag{4-24}$$

This equation is not very useful when γ approaches 1.

4-88

Longshore transport rates are usually given in units of volume per time (cubic yards per year in the U.S.). Typical rates for oceanfront beaches range from 10^5 to 10^6 cubic yards per year. (See Table 4-6.) These volume rates typically include about 40 percent voids and 60 percent solids.

At present, there are four basic methods to use for the prediction of longshore transport rate:

1. The best way to predict longshore transport at a site is to adopt the best known rate from a nearby site, with modifictions based on local conditions.

2. If rates from nearby sites are unknown, the next best way to predict transport rates at a site is to compute them from data showing historical changes in the topography of the littoral zone (charts, surveys, and dredging records are primary sources).

3. If neither Method 1 nor Method 2 is practical, then it is accepted practice to use either measured or calculated wave conditions to compute a longshore component of "wave energy flux" which is related through an empirical curve to longshore transport rate. (Das, 1972.)

4. A recently developed empirical method (Galvin, 1972) is available to estimate gross longshore transport rate from mean annual nearshore breaker height. The gross rate, so obtained, can be used as an upper limit on net longshore transport rate.

Method 1 depends largely on engineering judgement and local data. Method 2 is an application of historical data, which gives usable answers if the basic data are reliable and available at reasonable cost, and the interpretation is based on a thorough knowledge of the locality. By choosing only a few representative wave conditions, Method 3 can usually supply an answer with less work than Method 2, but with correspondingly less certainty. Because calculation of wave statistics in Method 3 follows an established routine, it is often easier to use than researching the hydrographic records and computing the changes necessary for Method 2. Method 4 requires mean nearshore breaker height data. Section 4.532 utilizes Methods 3 and 4. Methods 1 and 2 are discussed in Section 4.8.

4.532 Energy Flux Method. Method 3 is based on the assumption that longshore transport rate, Q, depends on the longshore component of energy flux in the surf zone. The longshore energy flux in the surf zone is approximated by assuming conservation of energy flux in shoaling waves, using small-amplitude theory, and then evaluating the energy flux relation at the breaker position. The energy flux per unit length of wave crest, or, equivalently, the rate at which wave energy is transmitted across a plane of unit width perpendicular to the direction of wave advance is (from Section 2.238, combining Equations 2-39 and 2-40):

$$\overline{P} = \overline{E} \, C_g = \frac{\rho g}{8} H^2 \, C_g \, . \qquad (4\text{-}25)$$

Table 4-6. Longshore Transport Rates from U.S. Coasts

Location	Predominant Direction of Transport	Longshore* Transport (cu.yd./yr.)	Date of Record	Reference
Atlantic Coast				
Suffolk County, N.Y.	W	200,000	1946–55	U.S. Army (1955a)
Sandy Hook, N.J.	N	493,000	1885–1933	U.S. Army (1954b)
Sandy Hook, N.J.	N	436,000	1933–51	U.S. Army (1954b)
Asbury Park, N.J.	N	200,000	1922–25	U.S. Army (1954b)
Shark River, N.J.	N	300,000	1947–53	U.S. Army (1954b)
Manasquan, N.J.	N	360,000	1930–31	U.S. Army (1954b)
Barneget Inlet, N.J.	S	250,000	1939–41	U.S. Army (1954b)
Absecon Inlet, N.J. †	S	400,000	1935–46	U.S. Army (1954b)
Ocean City, N.J. †	S	400,000	1935–46	U.S. Congress (1953a)
Cold Spring Inlet, N.J.	S	200,000	————	U.S. Congress (1953b)
Ocean City, Md.	S	150,000	1934–36	U.S. Army (1948a)
Atlantic Beach, N.C.	E	29,500	1850–1908	U.S. Congress (1948)
Hillsboro Inlet, Fla.	S	75,000	1850–1908	U.S. Army (1955b)
Palm Beach, Fla.	S	150,000 to 225,000	1925–30	U.S. Army (1947)
Gulf of Mexico				
Pinellas County, Fla.	S	50,000	1922–50	U.S. Congress (1954a)
Perdido Pass, Ala.	W	200,000	1934–53	U.S. Army (1954c)
Pacific Coast				
Santa Barbara, Calif.	E	280,000	1932–51	Johnson (1953)
Oxnard Plain Shore, Calif.	S	1,000,000	1938–48	U.S. Congress (1953d)
Port Hueneme, Calif.	S	500,000	————	U.S. Congress (1954b)
Santa Monica, Calif.	S	270,000	1936–40	U.S. Army (1948b)
El Segundo, Calif.	S	162,000	1936–40	U.S. Army (1948b)
Redondo Beach, Calif.	S	30,000	————	U.S. Army (1948b)
Anaheim Bay, Calif. †	E	150,000	1937–48	U.S. Congress (1954c)
Camp Pendleton, Calif.	S	100,000	1950–52	U.S. Army (1953a)
Great Lakes				
Milwaukee County, Wis.	S	8,000	1894–1912	U.S. Congress (1946)
Racine County, Wis.	S	40,000	1912–49	U.S. Congress (1953e)
Kenosha, Wis.	S	15,000	1872–1909	U.S. Army (1953b)
Ill. State Line to Waukegan	S	90,000	————	U.S. Congress (1953f)
Waukegan to Evanston, Ill.	S	57,000	————	U.S. Congress (1953f)
South of Evanston, Ill.	S	40,000	————	U.S. Congress (1953f)
Hawaii				
Waikiki Beach †	--	10,000	————	U.S. Congress (1953g)

(from Wiegel, 1964; Johnson, 1957)

* Transport rates are estimated net transport rates, Q_n. In some cases, these approximate the gross transport rates, Q_g.

† Method of measurement is by Accretion except for Absecon Inlet, and Ocean City, New Jersey, and Anaheim Bay, California, by Erosion, and Waikiki Beach, Hawaii, by Suspended Load Samples.

If the wave crests make an angle, α with the shoreline, the energy flux in the direction of wave advance *per unit length of beach* is

$$\overline{P} \cos \alpha = \frac{\rho g H^2}{8} C_g \cos \alpha , \qquad (4\text{-}26)$$

and the longshore component is given by

$$P_\ell = \overline{P} \cos \alpha \sin \alpha = \frac{\rho g}{8} H^2 C_g \cos \alpha \sin \alpha ,$$

or since $\cos \alpha \sin \alpha = 1/2 \sin 2\alpha$

$$P_\ell = \frac{\rho g}{16} H^2 C_g \sin 2\alpha . \qquad (4\text{-}27)$$

The surf-zone approximation of P_ℓ is written as $P_{\ell s}$.

$$P_{\ell s} = \frac{\rho g}{16} H_b^2 C_g \sin 2\alpha_b . \qquad (4\text{-}28)$$

Usable formulations of this surf-zone approximation can be obtained by several methods. The principal approximation is in evaluating C_g and H at the breaker position. It is standard practice to approximate the group velocity, C_g, by the phase velocity, C, at breaking. The phase velocity may then be approximated by either linear wave theory (Equation 2-3) or by solitary wave theory (Equation 4-13).

Figure 4-34 presents the longshore component of wave energy flux in a dimensionless form, $P_\ell/\rho g^2 H_b^2 T$, as a function of breaker steepness, H_b/gT^2, and the angle the wave crest makes with the shoreline in either deep water α_o, or at the breaker line, α_b. Figure 4-34 is based on Equation 4-28 using linear wave theory to determine C_g and assuming that refraction is by straight parallel bottom contours. Figure 4-35 can be used to determine the longshore component of wave energy flux when breaker height, H_b, period, T, and angle, α_b, are known--for example, for surf observation data. The use of Figure 4-34 is illustrated by an example problem below.

For linear theory, in shallow water, $C_g \approx C$ and

$$P_{\ell s} = \frac{\rho g}{16} H_b^2 C \sin 2\alpha_b , \qquad (4\text{-}29)$$

where H_b and α_b are the wave height and direction at breaking and C is the wave speed from Equation 2-3, evaluated in a depth equal to 1.28 H_b.
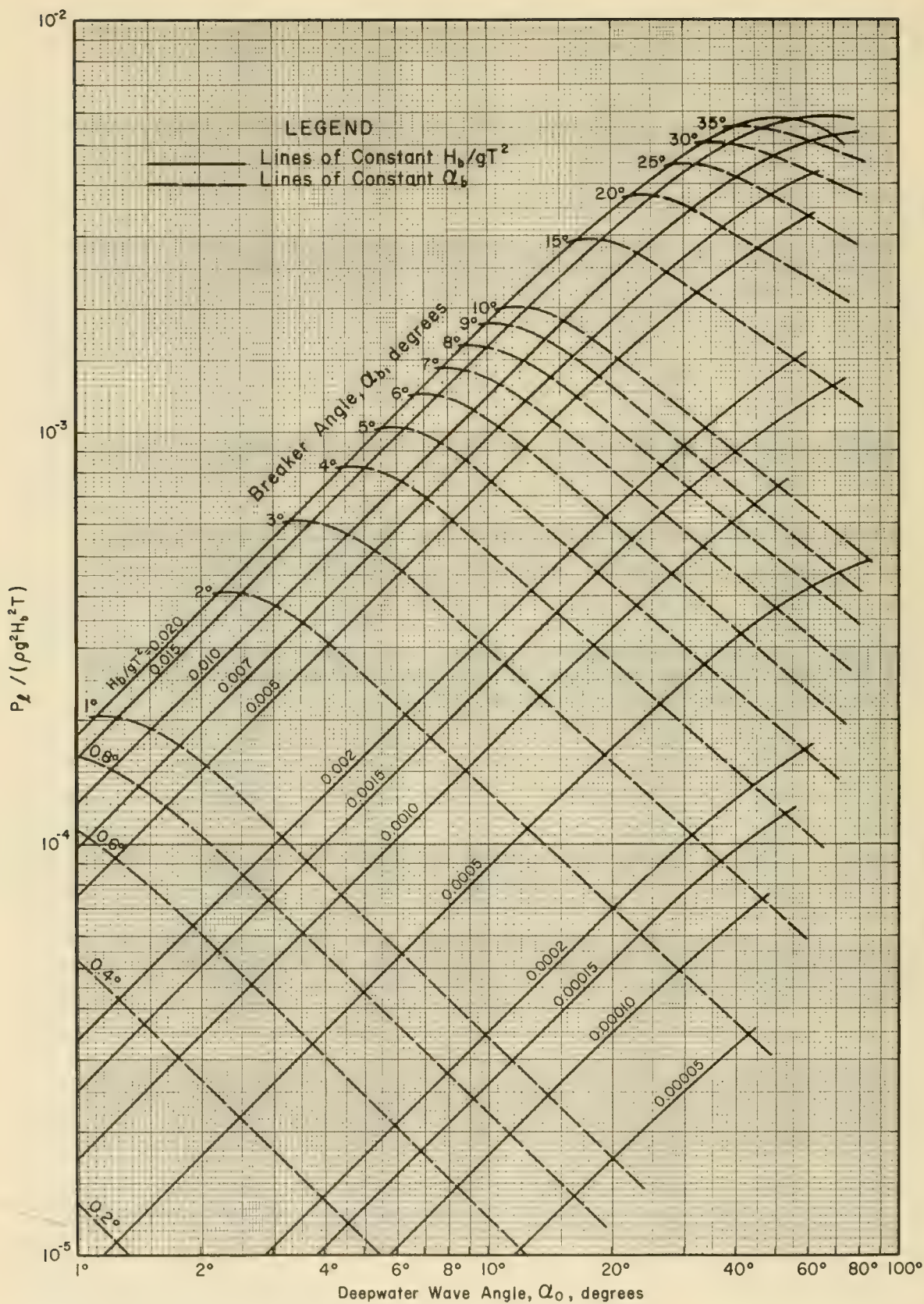
Figure 4-34. Longshore Component of Wave Energy Flux in Dimensionless Form
as a Function of Breaker Conditions

* * * * * * * * * * * * * * EXAMPLE PROBLEM * * * * * * * * * * * * * * * * *

GIVEN: A breaking wave with height, H_b = 4 feet; period T = 7 seconds. Surf observations indicate that the wave crest at breaking makes an angle, α_b = 6° with the shoreline.

FIND:

(a) The longshore component of wave energy flux.

(b) The angle the wave made with the shoreline when it was in deep water, α_o.

SOLUTION: Calculate

$$\frac{H_b}{gT^2} = \frac{4.0}{32.2\,(7.0)^2} = 0.00254 \ .$$

Enter Figure 4-34 to the point where the line labeled α_b = 6° crosses H_b/gT^2 = 0.00254 and read $P_\ell/\rho g^2\,H_b^2\,T$ = 6.7 x 10^{-4} from the left axis and α_o = 18° from the bottom axis.

The longshore energy flux can then be calculated as,

$$P_\ell \ = \ 0.00067\ \rho g^2\ H_b^2\ T \ ,$$

$$P_\ell \ = \ 0.00067\ (2)\ (32.2)^2\ (4.0)^2\ (7.0) \ .$$

$$P_\ell \ = \ 155.6 \ , \text{ say } 160 \text{ ft.-lb./ft.-sec. } ,$$

and

$$\alpha_o \ = \ 18° \ .$$

* *

For offshore conditions, the group velocity is equal to one-half the deepwater wave speed C_o, where C_o is given by Equation 2-7, and the refraction coefficient, K_R, can be determined by the methods of Section 2.32. Hence,

$$P_{\ell s} \ = \ \frac{\rho g^2}{64\pi} \ T\,(H_o\ K_R)^2 \ \sin 2\alpha_b \ . \tag{4-30}$$

Figure 4-35 also presents the longshore component of wave energy flux in a dimensionless form, $P_\ell/(\rho g^2\ H_o^2\ T)$, as a function of deepwater wave steepness, H_o/gT^2, and the angle the wave crest makes with the shoreline in either deep water, α_o, or at the breaker line, α_b. Refraction by straight parallel bottom contours is again assumed. As illustrated by

4-93
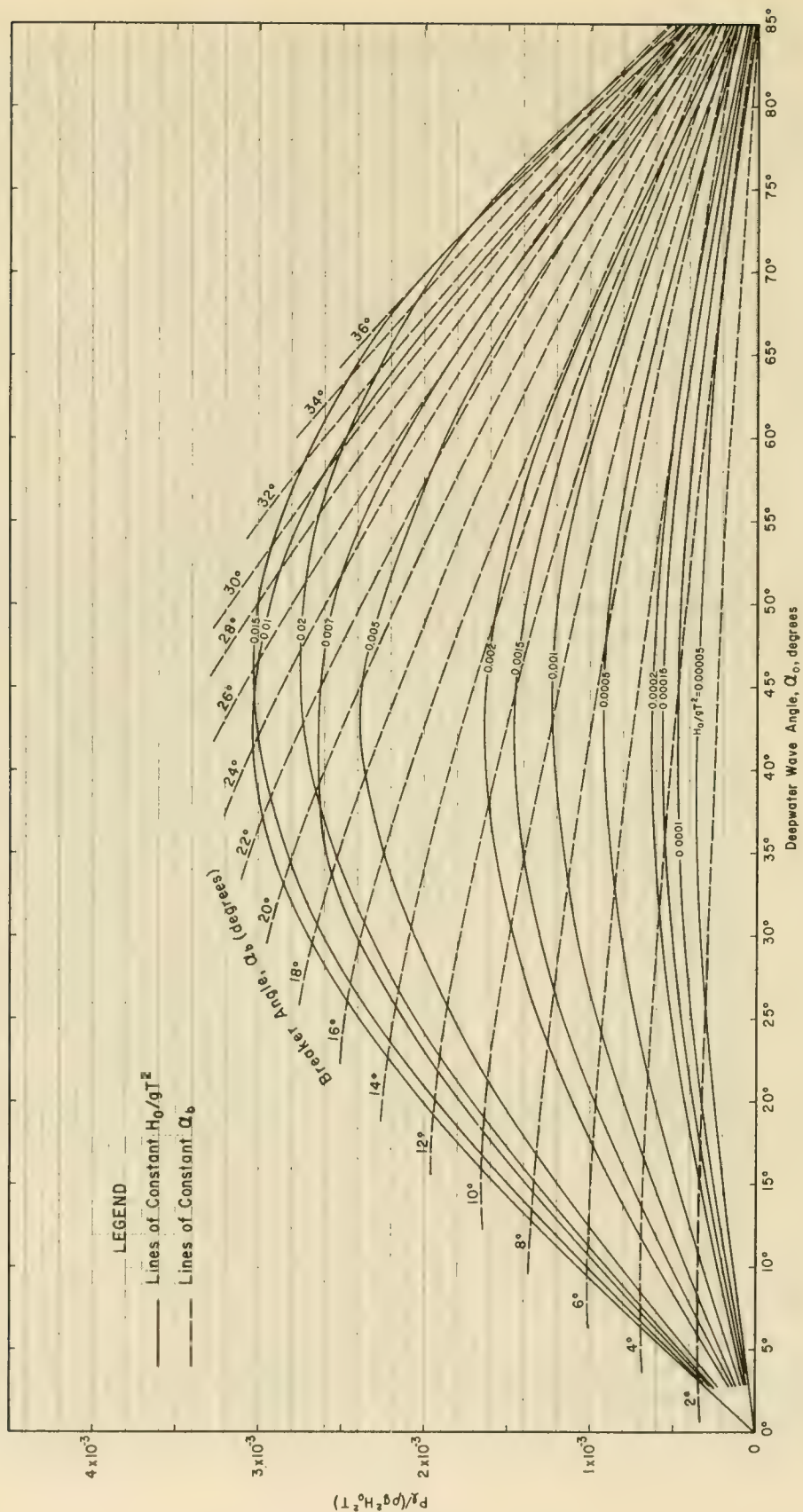
Figure 4-35 Longshore Component of Wave Energy Flux as a Function of Deepwater Wave Conditions

the example problem below, Figure 4-35 can be used to determine the longshore component of wave energy flux when deepwater wave height, H_O, period, T, and deepwater wave angle, α_O, are known.

* * * * * * * * * * * * * * EXAMPLE PROBLEM * * * * * * * * * * * * * * * *

GIVEN: A wave in deep water has a height, H_O = 5 feet and a period, T = 7 seconds. While in deep water, the wave crest makes an angle, α_O = 25° with the shoreline.

FIND:

(a) The longshore component of wave energy flux.

(b) The angle the wave makes with the shoreline when it breaks (assuming refraction is by straight, parallel bottom contours).

SOLUTION: Calculate,

$$\frac{H_o}{gT^2} = \frac{5.0}{32.2\,(7.0)^2} = 0.0032 \; .$$

Enter Figure 4-35 with α_O = 25° and H_o/gT^2 = 0.0032, read $P_\ell/\rho g^2 H_o^2\, T$ = 1.5 x 10^{-3}. This corresponds with a breaker angle α_b = 9.5° which is obtained by interpolation between the dashed curves of constant α_b. Therefore,

$$P_\ell \;=\; (0.0015)\,\rho g^2\, H_o^2\, T \; ,$$

$$P_\ell \;=\; (0.0015)\,(2)\,(32.2)^2\,(5)^2\,(7.0) \; ,$$

$$P_\ell \;=\; 544.3\,, \; \text{say } 540 \text{ ft.-lb./ft.-sec.} \; ,$$

and

$$\alpha_b \;=\; 9.5° \; .$$

* *

Equations 4-25 and 4-28 are valid only if there is a single wave train with one period and one height. However, most ocean wave conditions are characterized by a variety of heights with a distribution usually described by a Rayleigh distribution. (See Section 3.22.) For a Rayleigh distribution, the correct height to use in Equation 4-28 or in the formulas shown in Table 4-8 is the root-mean-square amplitude. However, most wave data are available as significant heights, and coastal engineers are used to dealing with significant heights.

Significant height is implied in all equations for $P_{\ell s}$. The value of $P_{\ell s}$ computed using significant height is approximately twice the

value of the exact energy flux for sinusoidal wave heights with a Rayleigh distribution. Since this means that $P_{\ell s}$ is proportional to energy flux and not equal to it, $P_{\ell s}$ is referred to as the *longshore energy flux factor* in Table 4-8 and the following sections.

Longshore energy flux in this general case (P_ℓ) is given by equation 4-27. This is an exact equation for the longshore component of energy flux in a single small-amplitude, periodic wave. This equation is good for any specified depth, but because the wave refracts, P_ℓ will have different values as the wave moves into shallower water. The value of P_ℓ in Equation 4-27 can be manipulated through use of small-amplitude wave theory to obtain the four equivalent formulas for P_ℓ shown in Table 4-7.

In order to use P_ℓ for longshore transport computations in the surf zone, it is necessary to approximate P_ℓ for conditions at the breaker position. These approximations are shown as $P_{\ell s}$ in Table 4-8, evaluated in foot-pound per second units. The bases for these approximations are shown in Table 4-9. Measurements show that the longshore transport rate depends on $P_{\ell s}$. (See Figures 4-36 and 4-37.)

As implied by the definition of $P_{\ell s}$, the energy flux factors in Figures 4-36 and 4-37 are based on significant wave heights. The plotted $P_{\ell s}$ values were obtained in the following manner. For the field data of Watts (1953) and Caldwell (1956), the original references give energy flux factors based on significant height, and these original data (after unit conversion) are plotted as $P_{\ell s}$ in Figures 4-36 and 4-37. Similarly, the one field point of Moore and Cole (1960), as adopted by Saville (1962), is assumed to be based on significant height. (See Figure 4-37.) Finally, the field data of Komar (1969), are given in terms of root-mean-square energy flux. This energy flux is multiplied by a factor of 2 (Das, 1972), converted to consistent units, and then plotted in Figure 4-36 and 4-37.

For laboratory conditions (Fig. 4-36 only), waves of constant height are assumed. When these heights are used in the equations of Table 4-8, the result is an approximation of the *exact* longshore energy flux. In order to plot the laboratory data in terms of an energy-flux factor consistent with the plotted field data, this energy flux is multiplied by 2 before plotting in Figure 4-36.

For the purpose of this section, it is assumed that the shoaling coefficient, K_s, for nearshore breaking waves is equivalent to the breaker height index, H_b/H_o', found from observation. (See Figure 2-65.)

The choice of equations to determine $P_{\ell s}$ depends on the data available. The right hand columns of Tables 4-7 and 4-8 tabulate the data required to use each of the formulas. An example using the second $P_{\ell s}$ formula is given in Section 4.533.

Possible changes in wave height due to energy losses as waves travel over the Continental Shelf are not considered in these equations. Such

Table 4-7. Longshore Energy Flux, P_ℓ, for a Single Periodic Wave in Any Specified Depth. (Four Equivalent Expressions from Small-Amplitude Theory)

Equation	P_ℓ (energy/time/distance)	Data Required (any consistent units)
4–31	$2C_g \left(\frac{1}{4} \overline{E} \sin 2\alpha\right)$	d, T, H, α_o
4–32	$C \left(\frac{1}{4} \overline{E}_o \sin 2\alpha_o\right)$	d, T, H_o, α_o
4–33	$K_R^2 C_o \left(\frac{1}{4} \overline{E}_o \sin 2\alpha\right)$	T, H_o, α_o, α
4–34	$(2C)(K_R^2 C_o)^{-1} C_g \left(\frac{1}{4} \overline{E} \sin 2\alpha_o\right)$	$d, T, H, \alpha_o, \alpha$

no subscript indicates a variable at the specified depth where small-amplitude theory is valid

C_g = group velocity (see assumption 1b, Table 4-9)
C_o = deepwater
d = water depth
H = significant wave height
T = wave period
α = angle between wave crest and shoreline

K_R = refraction coefficient $\sqrt{\dfrac{\cos \alpha_o}{\cos \alpha}}$

Table 4-8. Approximate Formulas for Computing Longshore Energy Flux Factor, $P_{\ell s}$, Entering the Surf Zone

Equation	$P_{\ell s}$ (ft.-lbs./sec./ft. of beach front)	Data Required (ft.-sec. units)
4–35	$32.1 \, H_b^{5/2} \sin 2\alpha_b$	H_b, α_b
4–36	$18.3 \, H_o^{5/2} (\cos \alpha_o)^{1/4} \sin 2\alpha_o$	H_o, α_o
4–37	$20.5 \, T \, H_b^2 \sin \alpha_b \cos \alpha_o$	$T, H_o, \alpha_o, \alpha_b$
4–38	$100.6 \, (H_b^3/T) \sin \alpha_o$	T, H_b, α_o

H_o = deepwater
H_b = breaker position
H = significant wave height
T = wave period
α = angle between wave crest and shoreline

See Table 4-7 for equivalent small amplitude equations and Table 4-9 for assumptions used in deriving $P_{\ell s}$ from P_ℓ.

Table 4-9. Assumptions for P_{ℓ_s} Formulas in Table 4-8.

1. Formula 1 — Equation 4-35

   a. Energy density at breaking is given by linear theory,

   $$\bar{E} = \left(\rho\, g\, H_b^2\right)/8 \approx 8\, H_b^2$$

   b. Group velocity equals wave speed at breaking, and breaking speed is given by solitary wave theory according to the approximation. (Galvin, 1967, Equation 11.)

   $$C_g = C \approx \left(2g\, H_b\right)^{\frac{1}{2}} = 8.02\, \left(H_b\right)^{\frac{1}{2}}$$

   c. α can be replaced by α_b

2. Formula 2 — Equation 4-36

   a. Same as 1b above

   b. H_b is related to H_o by refraction and shoaling coefficients, where the coefficients are evaluated at the breaker position

   $$H_b = K_R\, K_s\, H_o$$

   c. Refraction coefficient K_R given by small-amplitude theory; shoaling coefficient K_s assumed constant, so that

   d. $\left(H_b\right)^{\frac{1}{2}} = 1.14\, \left(\cos\alpha_o\right)^{\frac{1}{4}}\, H_o^{\frac{1}{2}}$

   if $\left(\cos\alpha_b\right)^{\frac{1}{4}} = 1.0$

   and $\left(K_s\right)^{\frac{1}{2}} = 1.14$

3. Formula 3 — Equation 4-37

   a. Refraction coefficient at breaking is given by small-amplitude theory.

4. Formula 4 — Equation 4-38

   a. Same as 1a above
   b. Same as 1b above
   c. Same as 3a above
   d. $\cos\alpha_b = 1.0$

NOTE: Constants evaluated for foot-pound-second units. Small-amplitude theory is assumed valid in deep water. Nearshore contours are assumed to be straight and parallel to the shoreline.
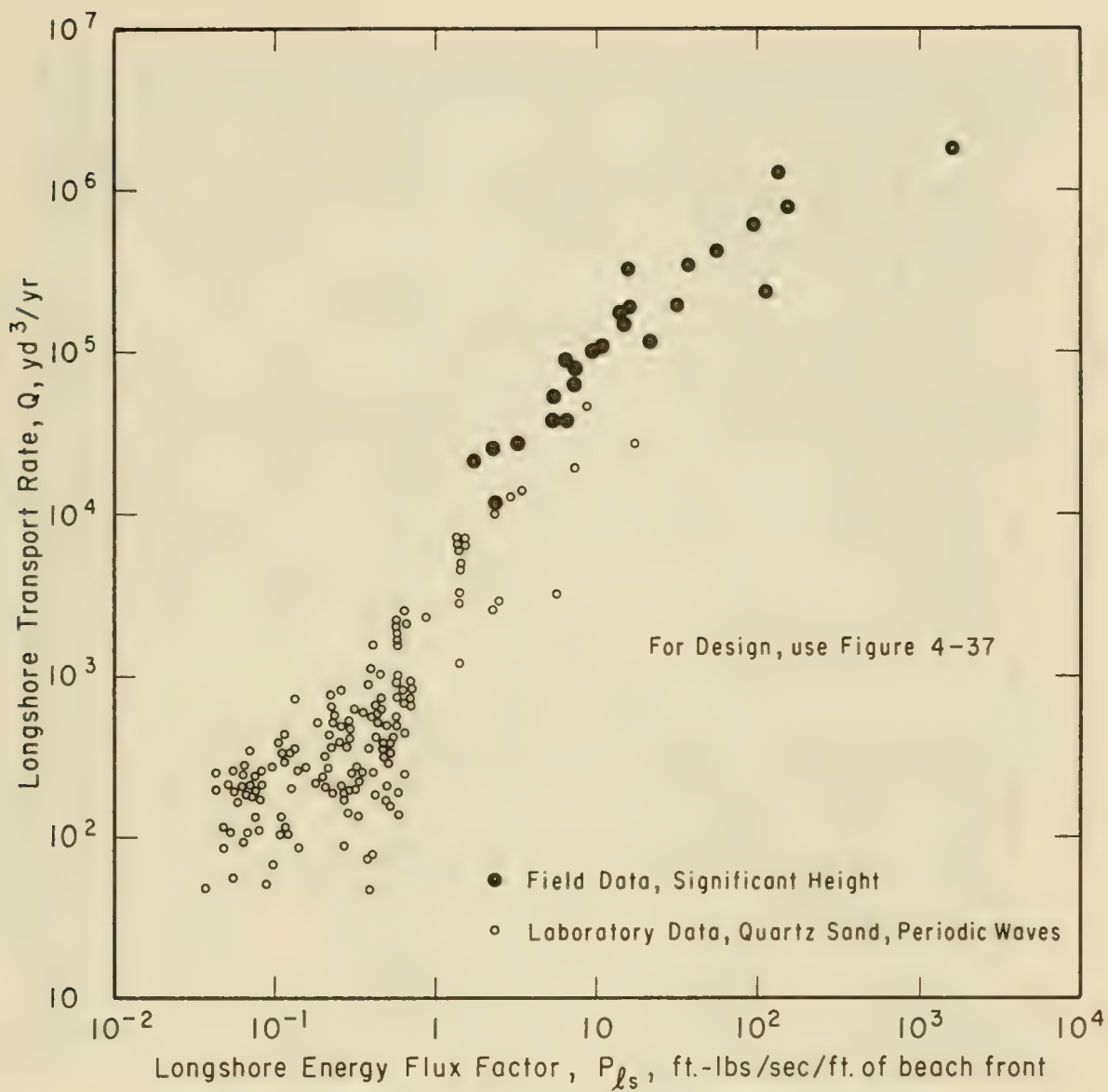
Figure 4-36.   Longshore Transport Rate Versus Energy Flux Factor for Field and Lab Conditions
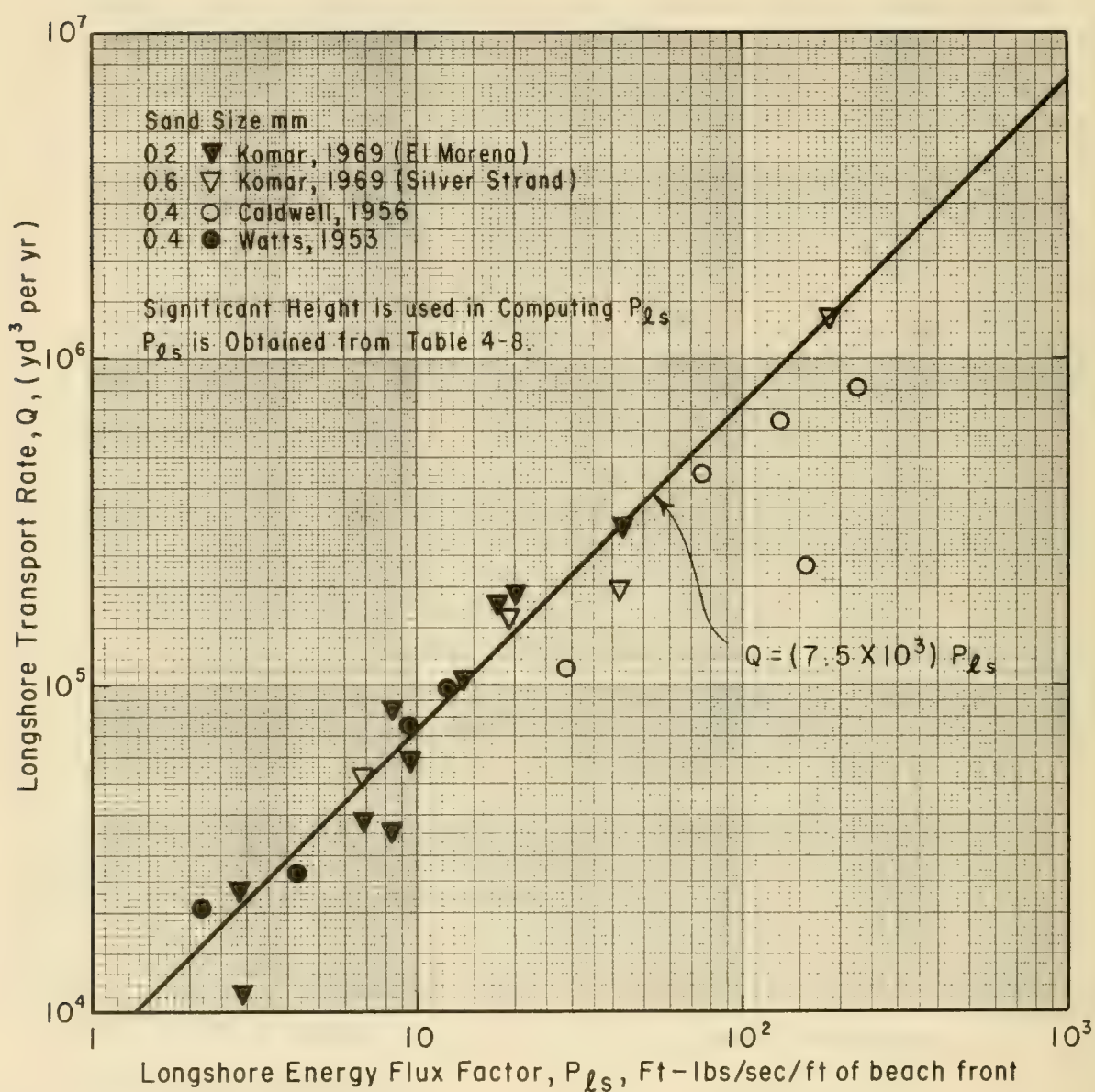
Figure 4-37.   Design Curve for Longshore Transport Rate versus Energy
Flux Factor.   Only field data are included.

changes may reduce the value of $P_{\ell s}$ when deepwater wave height statistics are used as a starting point for computing $P_{\ell s}$. (Walton, 1972; Bretschneider and Reid, 1954; and Bretschneider, 1954.)

The Equations 4-35 through 4-38 in Table 4-8 are related to the Equation for E_a previously recommended for use with this method (Caldwell, 1956, Equations 5 and 6; or the equations in Figure 2-22, page 175, CERC Technical Report No. 4, 1966 edition) by a constant

$$E_a = (8.64 \times 10^4) P_{\ell s} \qquad (4-39)$$

where E_a is in units of foot-pounds per foot per day and $P_{\ell s}$ is in units of foot-pounds per foot per second.

The term in parenthesis for Equation 4-32 in Table 4-7 is identical to the longshore force of Longuet-Higgins (1970a). This longshore force also correlates well with the longshore transport rate.

The relation between Q and $P_{\ell s}$ in Figures 4-36 and 4-37 can be approximated by

$$Q = (7.5 \times 10^3) P_{\ell s} \qquad (4-40)$$

Equation 4-40 tends to overestimate Q at the higher values of $P_{\ell s}$ for the plotted field data, but it falls below the estimated rates computed from the data of Johnson (1952). (See Das, 1972, Figure 6.) The value of 7.5×10^3 in Equation 4-40 is approximately twice the equivalent value from the design curve of CERC Technical Report No. 4, 1966 edition, and is about 5 percent greater than the value estimated by Komar and Inman (1970).

Judgement is required in applying Equation 4-40. Although the data in Figures 4-36 and 4-37 appear to follow a smooth trend, the log-log scale compresses the data scatter. For example, the average difference between the plotted points from field data and the prediction given by Equation 4-40 is at least 28 percent of the value of prediction (average difference derived by Das (1972) is 42 percent). In addition, some incomplete measurements suggest transport rates ranging from two orders of magnitude below the line (Thornton, 1969) to one order of magnitude above the line. (Johnson, 1952.) These additional data are plotted by Das (1972).

As an aid to computation, Figures 4-38 and 4-39 give lines of constant Q based on Equation 4-40 and Equations 4-35 and 4-36 for $P_{\ell s}$ given in Table 4-8. To use Figures 4-38 and 4-39 to obtain the longshore

transport rate, only the (H_b, α_b) data and Figure 4-38, or the (H_o, α_o) data and Figure 4-39 are needed. If the shoaling coefficient is significantly different from 1.3, multiply the Q obtained from Figure 4-39 by the factor 0.88 $\sqrt{K_s}$. (See Table 4-9, Assumption 2d.)

Figure 4-39 applies accurately only if α_o is a point value. If α_o is a range of values, for example a 45° sector implied by the direction NE, then the transport evaluated from Figure 4-39 using a single value of α_o for NE may be 12 percent higher than the value obtained by averaging over the 45° sector implied by NE. The more accurate approach is given in the example problem of the next section.

The unit for Q is a volume of deposited quartz sand (including voids in the volume) per year. Bagnold (1963) suggests using immersed weight instead of volume in the unit for longshore transport rate (Section 4.521), since immersed weight is the pertinent physical variable related to the wave action causing the sediment transport. Use of an immersed weight unit does eliminate the difference between lightweight material and quartz that occurs if volume units are used. (Das, 1972.) However, in coastal engineering design, it is the volume and not the immersed weight of eroded or deposited sand that is important, and since beach sand is predominantly quartz (specific gravity 2.65), volume is directly proportional to immersed weight. On some beaches the sand may be calcium carbonate which has a specific gravity ranging from 2.87 (calcite) to 2.98 (aragonite) in pure form. Naturally occurring oolitic aragonite sand with a specific gravity of 2.88 (Monroe, 1969), has an immersed weight 14 percent greater than pure quartz sand. Since the longshore transport Equation 4-40, with one exception (Watts, 1953; and Das, 1971, p. 14), is based on quartz sand, then oolitic sand beaches may have slightly lower longshore transport rates than is suggested by comparison with data from quartz sand beaches. However, the scatter in the data (Fig. 4-36) makes such a specific gravity effect difficult to detect.

4.533 _Energy Flux Example (Method 3)._ Assume that an estimate of the longshore transport rate is required for a locality on the north-south coastline along the west edge of an inland sea. The locality is in an area where stronger winds blow out of the northwest and north, resulting in a deepwater distribution of height and direction as listed in Table 4-10. Assume the statistics were obtained from visual observations collected over a 2-year interval at a point 2 miles offshore by seamen aboard vessels entering and leaving a port in the vicinity. This type of problem, based on SSMO wave statistics (Section 4.34), is discussed in detail by Walton, (1972), and Walton and Dean (1973). Shipboard data are subject to uncertainty in their applicability to littoral transport, but often they are the only data available. It is assumed that shipboard visual observations are equivalent to significant heights. (Cartwright, 1972; and Walton, 1972.)

Plotted from Equation 4-40 ($Q = 7.5 \times 10^3\, P_{\ell s}$) and

Equation 4-35 ($P_{\ell s} = 32.1\, H_b^{5/2} \sin 2\, \alpha_b$)

Q in cu. yds./yr

100×10^5

50×10^5

25×10^5
15×10^5
10×10^5
7.5×10^5
5.0×10^5
2.5×10^5
2.0×10^5
0.5×10^5

Breaker Angle, α_b (degrees)

Significant Wave Breaker Height, H_b, (feet)
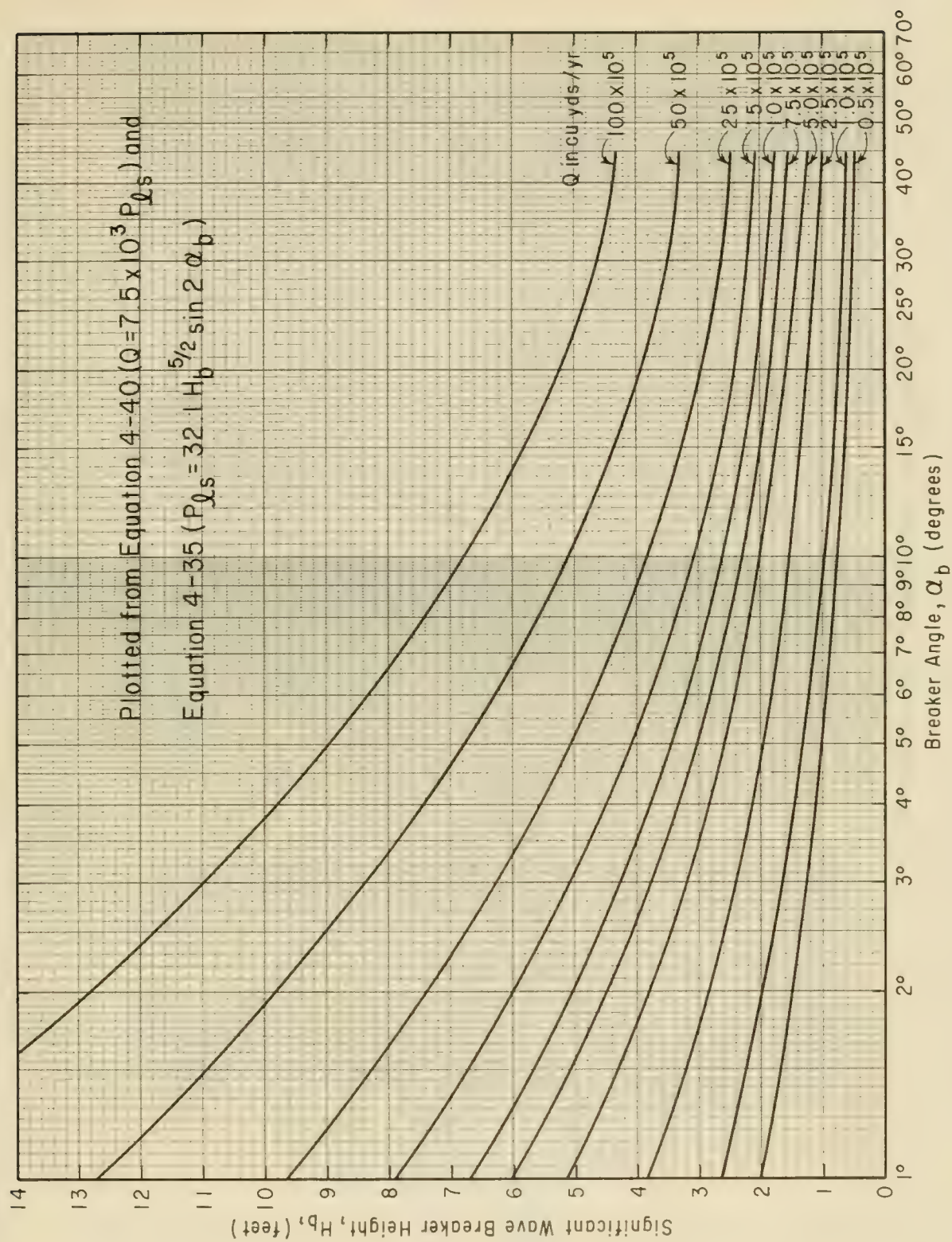
Figure 4-38. Longshore Transport Rate as a Function of Breaker Height and Breaker Angle

4-103
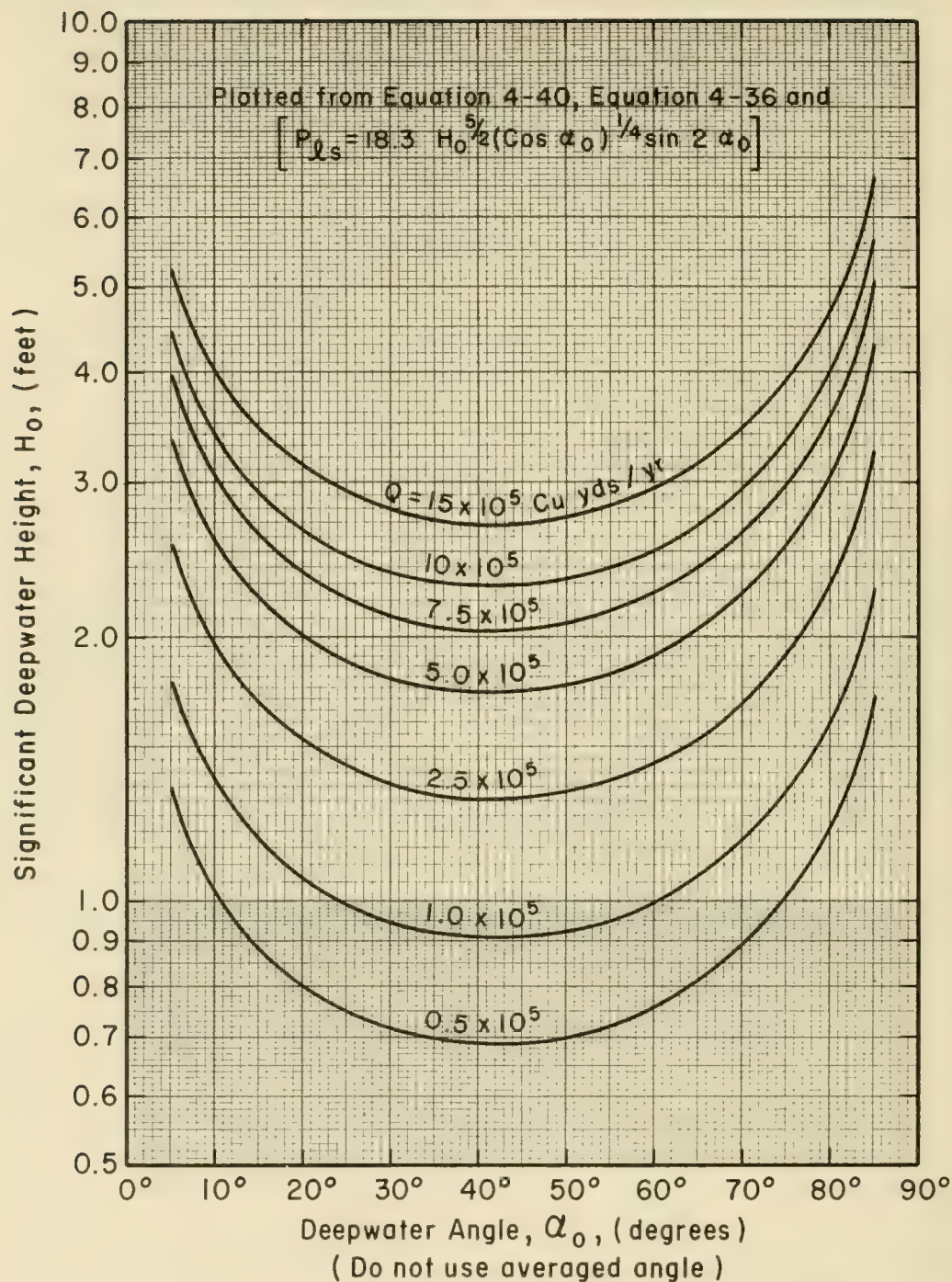
Figure 4-39. Longshore Transport Rate as a Function of Deepwater Height and Deepwater Angle

4-104

Table 4-10. Deepwater Wave Heights, in Percent by Direction, off East-Facing Coast of Inland Sea

Compass Direction α_o	N 90°	NE 45°	E 0°	SE −45°	S −90°	Other*
H_o† (ft.)						
1	9	10	6	5	5	
2	5	5	2	2	2	
3	4	3	1	1	1	
4	2	1				
5	1					
8	1					
Total	22	19	9	8	8	34

*Calm conditions, or waves from SW, W, or NW.

†Shipboard visual observations assumed equivalent to significant height (See Walton, 1972.)

This problem could be solved using Figure 4-39, but for illustration, and because of a slightly higher degree of accuracy from the direction data given, the problem is illustrated in detail.

In this example, the available data are the joint frequency distribution of H_o and α_o. For each combination of α_o and H_o, the corresponding Q_{α_o, H_o} is calculated for Table 4-11 in the following manner. The basic equation is a form of Equation 4-40 written

$$Q_{\alpha_o, H_o} = \left\{f A P_{\ell s}\right\}_{\alpha_o, H_o}, \qquad (4\text{-}41)$$

where f is the decimal frequency, which is the percent frequency in Table 4-10, divided by 100. The constant, A, is of the type used in Equation 4-40.

Since the available data are α_o and H_o, the appropriate equation for $P_{\ell s}$ is given in Table 4-8. If A = 7.5 x 10³ as in Equation 4-40 and Equation 4-36 in Table 4-8 are used,

$$Q_{\alpha_o, H_o} = 1.373 \times 10^5 \, f H_o^{5/2} \, F(\alpha_o), \qquad (4\text{-}42)$$

where

$$F(\alpha_o) = \left\{(\cos \alpha_o)^{1/4} \sin 2\alpha_o\right\}. \qquad (4\text{-}43)$$

This direction term, $F(\alpha_o)$, requires careful consideration. A compass point direction for the given data (Table 4-10) represents a 45°

sector of wave directions. If $F(\alpha_O)$ is evaluated at $\alpha_O = 45°$ (NE or SE in the example problem), it will have a value 12 percent higher than the average value for $F(\alpha_O)$ over 45° sector bisected by the NE or SE directions. Thus, if the data warrant a high degree of accuracy, Equation 4-43 should be averaged by integrating over the sector of directions involved.

Table 4-11. Computed Longshore Transport for East-Facing Coast of Inland Sea

H_O	$Q\alpha_O$, H_O in cu.yd./yr. from Equation 4-42
	N*	NE	E	SE	S*
1	1.61 X 10^3†	11.26 X 10^3	±1.52 X 10^3	− 5.63 X 10^3	− 0.89 X 10^3
2	5.05 X 10^3	31.84 X 10^3	± 2.87 X 10^3	− 12.74 X 10^3	− 2.02 X 10^3
3	11.13 X 10^3	52.42 X 10^3	± 3.96 X 10^3	− 17.55 X 10^3	− 2.78 X 10^3
4	11.42 X 10^3	36.03 X 10^3			
5	9.98 X 10^3				
8	32.31 X 10^3				
Totals	71.50 X 10^3	131.78 X 10^3	(±8.35 X 10^3) 16.70 X 10^3	− 35.92 X 10^3	− 5.69 X 10^3

Q_{rt} = (71.50 + 131.78 + 8.35) X 10^3 = 212 X 10^3 or 212,000 cu.yd./yr.

$Q_{\ell t}$ = (8.35 + 35.92 + 5.69) X 10^3 = 50 X 10^3 or 50,000 cu.yd./yr.

Q_n = Q_{rt} − $Q_{\ell t}$ = 212 X 10^3 − 50 X 10^3 = 162 X 10^3 or 162,000 cu.yd./yr.

Q_g = Q_{rt} + $Q_{\ell t}$ = 212 X 10^3 + 50 X 10^3 = 262 X 10^3 or 262,000 cu.yd./yr.

*Coast runs N-S so frequencies of waves from N and S are halved.

†Calculation of this number is shown in detail in the text.

If $F(\alpha_O)$ is evaluated at $\alpha_O = 0$ (waves from the E in the example problem), then $F(\alpha_O) = 0$. Actually, $\alpha_O = 0°$ is only the center of a 45° sector which can be expected to produce transport in both directions. Therefore, $F(\alpha_O)$ should be averaged over 0° to 22.5° and 0° to -22.5°, giving $F(\alpha_O) = \pm 0.370$ rather than 0. The + or − sign comes out of the $\sin 2\alpha_O$ term in $F(\alpha_O)$ (Equation 4-43), which is defined such that transport to the right is positive, as implied by Equation 4-22.

A further complication in direction data is that waves from the north and south sectors include waves traveling in the offshore direction. It is assumed that, for such sectors, frequency must be multiplied by the fraction of the sector including landward traveling waves. For example the frequencies from N and S in Table 4-10 are multiplied by 0.5 to obtain the transport values listed in Table 4-11.

To illustrate how values of Q_{α_O}, H_O listed in Table 4-11 were calculated, the value of Q_{α_O}, H_O is here calculated for $H_O = 1$ and the north direction, the top value in the first column on Table 4-11. The direction term, $F(\alpha_O)$, is averaged over the sector from $\alpha = 67.5°$ to $\alpha = 90°$, i.e., from NNE to N in the example. The average value of $F(\alpha_O)$ is found to be 0.261. H_O to the 5/2 power is simply 1 for this case. The frequency given in Table 4-10 for $H_O = 1$ and direction = north (NW to NE) is 9 percent or in decimal terms, 0.09. This is multiplied by 0.5 to obtain the part of shoreward directed waves from the north sector (i.e., N to NE) resulting in f = 0.09 (0.5) = 0.045. Putting all these values into Equation 4-42 gives

$$Q_{N,1} = 1.373 \times 10^5 \ (0.045) \ (1)^{5/2} \ (0.261)$$

$$= 1,610 \ \text{yd.}^3/\text{yr.} \hspace{2cm} \text{(See Table 4-11)}$$

Table 4-11 indicates the importance of rare high waves in determining the longshore transport rate. In the example, shoreward moving 8-foot waves occur only 0.5 percent of the time, but they account for 12 percent of the gross longshore transport rate. (See Table 4-11.)

Any calculation of longshore transport rate is an estimate of *potential* longshore transport rate. If sand on the beach is limited in quantity, then calculated rates may indicate more sand transport than there is sand available. Similarly, if sand is abundant, but the shore is covered with ice for 2 months of the year, then calculated transport rates must be adjusted accordingly.

The procedure used in this example problem is approximate and limited by the data available. Equation 4-42, and the other approximations listed in Table 4-11, can be refined if better data are available. An extensive discussion of this type of calculation is given by Walton (1972).

Although this example is based on shipboard visual observations of the SSMO type (Section 4.34), the same approach can be followed with deepwater data from other sources, if the joint distribution of height and direction is known. At this level of approximation, the wave period has little effect on the calculation, and the need for it is bypassed as long as the shoaling coefficient (or breaker height index) reasonably satisfies the relation $(K_S)^{1/2} = 1.14$. (See Assumption 2d, Table 4-9.) For waves on sandy coasts, this relation is reasonably satisfied. (e.g., Bigelow and Edmondson, 1947, Table 33; and Goda, 1970, Figure 7.)

4.534 Empirical Prediction of Gross Longshore Transport Rate (Method 4). Longshore transport rate depends partly on breaker height, since as breaker height increases, more energy is delivered to the surf zone. At the same time, as breaker height increases, breaker position moves offshore widening the surf zone and increasing the cross-section area through which sediment moves.

Galvin (1972) showed that when field values of longshore transport rate are plotted against mean annual breaker height from the same locality, a curve

$$Q = 2 \times 10^5 H_b^2 ,\qquad(4\text{-}44)$$

forms an envelope above almost all known pairs of (Q, H_b), as shown in Figure 4-40. Here, as before, Q is given in units of cubic yards per year; H_b in feet.

Figure 4-40 includes all known (Q, H_b) pairs for which both Q and H_b are based on at least 1 year of data, and for which Q is considered to be the gross longshore transport rate, Q_g, defined by Equation 4-21. Since all other known (Q, H_b) pairs plot below the line given by Equation 4-41, the line provides an upper limit on the estimate of longshore transport rate. From the defining equations for Q_g and Q_n, any line that forms an upper limit to longshore transport rate must be the gross transport rate, since the quantities Q_{rt}, $Q_{\ell t}$, and Q_n, as defined in Section 4.531, are always less than or equal to Q_g.

In Equation 4-44, wave height is the only independent variable, and the physical explanation assumes that waves are the predominant cause of transport. (Galvin, 1972.) Therefore, where tide-induced currents or other processes contribute significantly to longshore transport, Equation 4-44 would not be the appropriate approximation. The corrections due to currents may either add or subtract from the estimate of Equation 4-44, depending on whether currents act with or against prevailing wave-induced transport.

4.535 Method 4 Example (Empirical Prediction of Gross Longshore Transport Rate. Near the site of the problem outlined in Section 4.533, it is desired to build a small craft harbor. The plans call for an unprotected harbor entrance, and it is required to estimate costs of maintenance dredging in the harbor entrance. The gross transport rate is a first estimate of the maintenance dredging required, since transport from either direction could be trapped in the dredged channel. Wave height statistics were obtained from a wave gage in 12 feet of water at the end of a pier. (See Columns (1) and (2) of Table 4-12.) Heights are available as empirically determined significant heights. (Thompson and Harris, 1972.) (To facilitate comparison, the frequencies are identical to the deepwater frequencies of onshore waves in Table 4-10 for the problem of Section 4.533. That is, the frequency associated with each H_g in Table 4-12 is the sum of the frequencies of the shoreward H_o on the corresponding line of Table 4-10.)

The breaker height, H_b, in the empirical Equation 4-44 is related to the gage height, H_g, by a shoaling-coefficient ratio, $(K_s)_b/(K_s)_g$, where $(K_s)_b$ is the shoaling coefficient (Equation 2-44), $(H/H_o'$ in
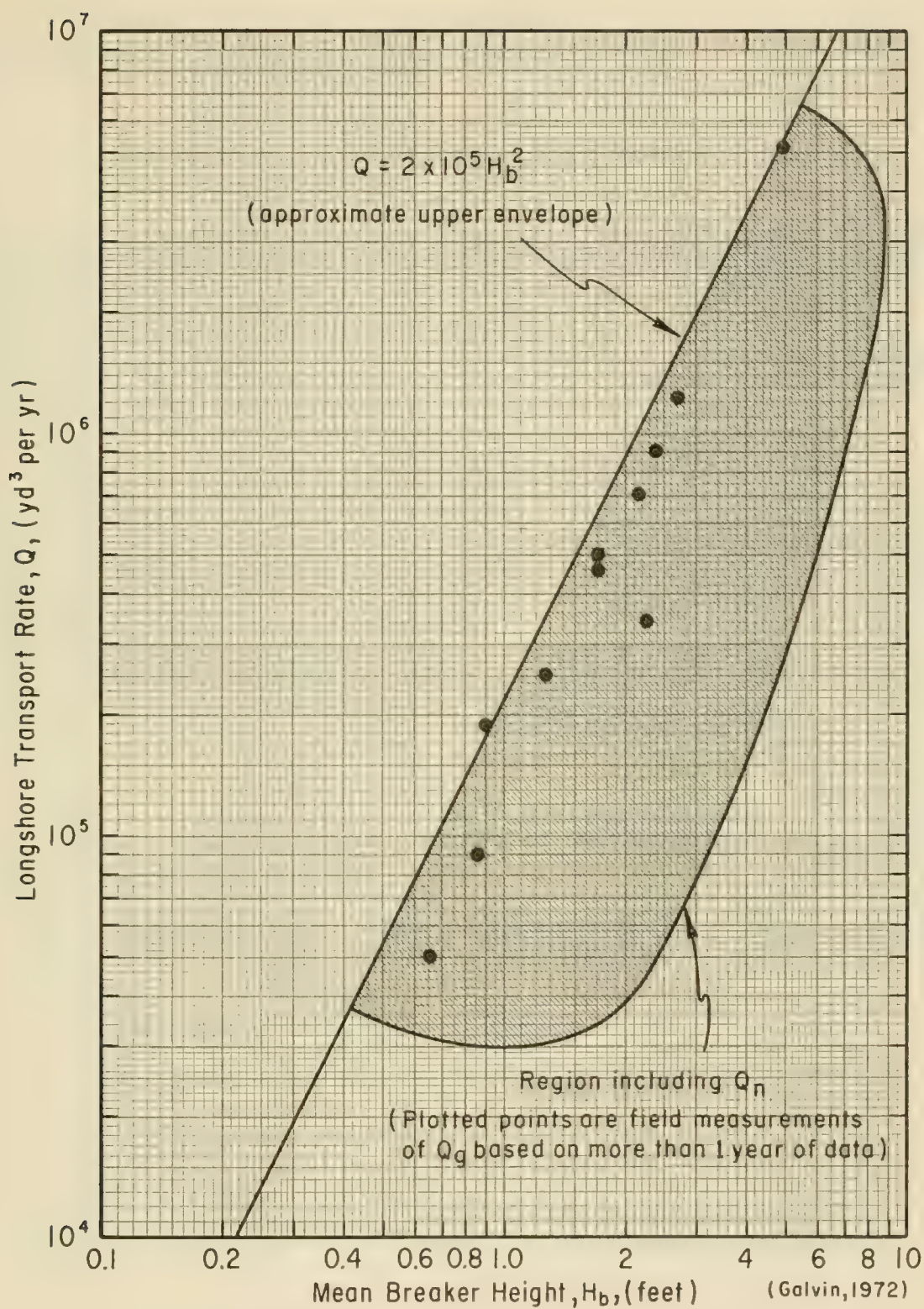
Figure 4-40. Upper Limit on Longshore Transport Rates

Table 4-12. Example Estimate of Gross Longshore Transport Rate for Shore of Inland Sea

(1) H_g (ft.)	(2) f	(3) fH_g (ft.)	(4) $(K_s)_b/(K_s)_g$	(5) (3) × (4) (ft.)
1	0.28	0.28	1.2	0.336
2	0.125	0.25	1.2	0.300
3	0.075	0.225	1.2	0.270
4	0.02	0.08	1.1	0.088
5	0.005	0.025	1.1	0.028
8	0.005	0.04	1.0	0.040
			H_b =	1.062

(1) H_g = significant height reduced from gage records, assumed to correspond to the height obtained by visual observers

(2) f = decimal frequency of wave heights

(4) $\dfrac{(K_s)_b}{(K_s)_g}$ = assumed shoaling-coefficient ratio.

(5) $H_b = \Sigma \dfrac{(K_s)_b}{(K_s)_g} fH_g = 1.062$ ft.

$Q = 2 \times 10^5\ H_b^2 = 2.26 \times 10^5$ cu.yd./yr. from Equation 4-44

Note that shoreward-moving waves exist only 51 percent of the time.

Table C-1 Appendix C) evaluated at the breaker position and $(K_s)_g$ is the shoaling coefficient evaluated at the wave gage:

$$H_b = H_g \ \frac{(K_s)_b}{(K_s)_g} \ , \tag{4-45}$$

K_s or H/H_o' can be evaluated from small-amplitude theory, if wave-period information is available from the wave gage statistics. For simplicity, assume shoaling-coefficient ratios as listed in Column 4 of Table 4-12. Such shoaling coefficient ratios are consistent with the shoaling coefficient of $K_s=1.3$ (between deepwater and breaker conditions) assumed in deriving $P_{\ell s}$ (Table 4-9), and with the fact that waves on the inland sea of the problem would usually be steep, locally generated waves.

Column 5 of the table is the product $fH_g \ (K_s)_b/(K_s)_g$. The sum (1.06 feet) of entries in this column is assumed equivalent to the average of visually observed breaker heights. Substituting this value in Equation 4-44, the estimated gross longshore transport rate is 226,000 cubic yards per year. It is instructive to compare this value with the value of 262,000 cubic yards per year obtained from the deepwater example. (See Table 4-11.) The two estimates are not expected to be the same, since the same wave statistics have been used for deep water in the first problem and for a 12-foot depth in the second problem. However, the numerical values do not differ greatly. It should be noted that the empirical estimate just obtained is completely independent of the longshore energy flux estimate of the deepwater example.

In this example, wave gage statistics have been used for illustrative purposes. However, visual observations of breakers, such as those listed in Table 4-4, would be even more appropriate since Equation 4-44 has been "calibrated" for such observations. On the other hand, hindcast statistics would be less satisfactory than gage statistics due to the uncertain effect of nearshore topography on the transformation of deepwater statistics to breaker conditions.

4.6 ROLE OF FOREDUNES IN SHORE PROCESSES

4.61 BACKGROUND

The cross section of a barrier island shaped solely by marine hydraulic forces has three distinct subaerial features: beach, crest of island, and deflation plain. (See Figure 4-41.) The dimensions and shape of the beach change in response to varying wave and tidal conditions (Section 4.524), but usually the beach face slopes upward to the island crest - the highest point on the barrier island cross section. From the island crest, the back of the island slopes gently across the deflation plain to the edge of the lagoon separating the barrier island from the mainland. These three features are usually present on duneless barrier island cross sections; however, their dimensions may vary.
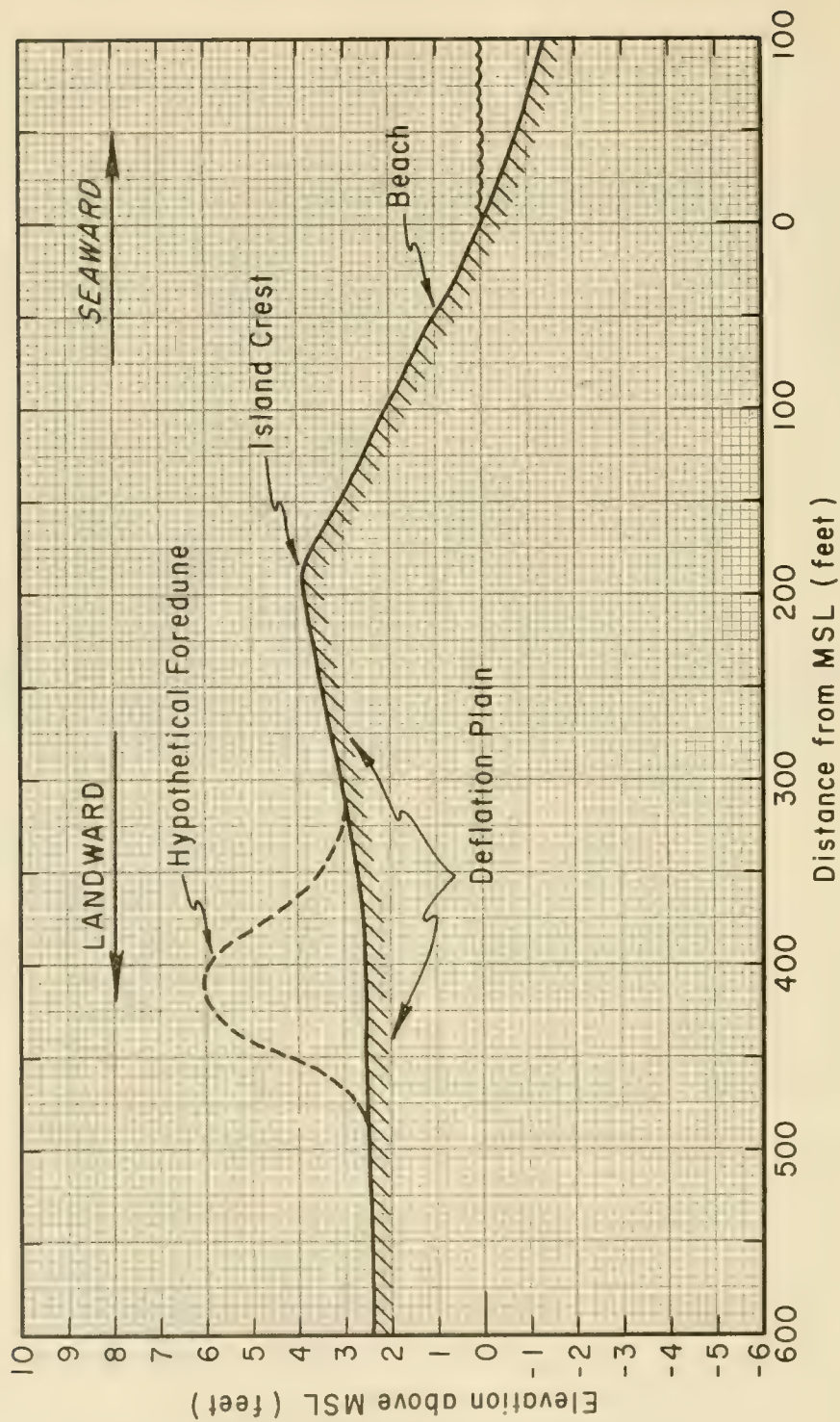
Figure 4-41. Typical Barrier Island Profile Shape (Approximation of Padre Island, Texas)

Island crest elevation is determined by the nature of the sand form-
ing the beach, and by the waves and water levels of the ocean. The beach
and waves interact to determine the elevation of the limit of wave runup -
the primary factor in determining island crest elevation. Normally the
island crest elevation is almost constant over long sections of beach.
However, duneless barrier island crest elevations vary with geographical
area. For example, the crest elevation typical of Core Banks, North
Carolina, is about +6 feet MSL; +4 feet MSL is typical for Padre Island,
Texas; +11 feet MSL is typical for Nauset Beach, Massachusetts.

Landward of the upper limit of wave uprush or berm crest are the back-
shore and the deflation plain. This area is shaped by the wind, and in-
frequently by the flow of water down the plain when the island crest is
overtopped by waves. (e.g., Godfrey, 1972.) Obstructions which trap
wind-transported sand cause the formation of dunes in this area. (See
discussion in Section 6.4 Sand Dunes.) Beachgrasses which trap wind-
transported sand from the beach and the deflation plain are the major
agent in creating and maintaining foredunes.

4.62 ROLE OF FOREDUNES

Foredunes, the line of dunes just behind a beach, have two primary
functions in shore processes. First, they prevent overtopping of the
island during some abnormal sea conditions. Second, they serve as a
reservoir for beach sand.

4.621 Prevention of Overtopping. By preventing water from overtopping,
foredunes prevent wave and water damage to installations landward of the
dune. They also block the water transport of sand from the beach area to
the back of the island and the flow (overwash) of overtopping sea water.

Large reductions in water overtopping are effected by small increases
in foredune crest elevations. For example, the hypothetical 4-foot dune
shown in Figure 4-41 raises the maximum island elevation about 3 feet to
an elevation of 6 feet. On this beach of Padre Island, Texas, the water
levels and wave runup maintain an island crest elevation of +4 feet MSL
(about 2 feet above MHW). This would imply that the limit of wave runup
in this area is 2 feet (the island crest elevation of 4 feet minus the
MHW of 2 feet). Assuming the wave runup to be the same for all water
levels, the 4-foot dune would prevent significant overtopping at water
levels up to 4 ft MSL (the 6-foot effective island height at the dune
crest minus 2 feet for wave runup). This water level occurs on the aver-
age once each 5 years along this section of coast. (See Figure 4-42.)
Thus, even a low dune, one which can be built with vegetation and sand
fences in this area in 1 year (Woodard et al., 1971) provides consider-
able protection against wave overtopping. (See Section 5.3 and 6.3.)

Foredunes or other continuous obstructions on barrier islands may
cause unacceptable ponding from the land side of the island when the la-
goon between the island and mainland is large enough to support the needed
wind setup. (See Section 3.8.) There is little danger of flooding from
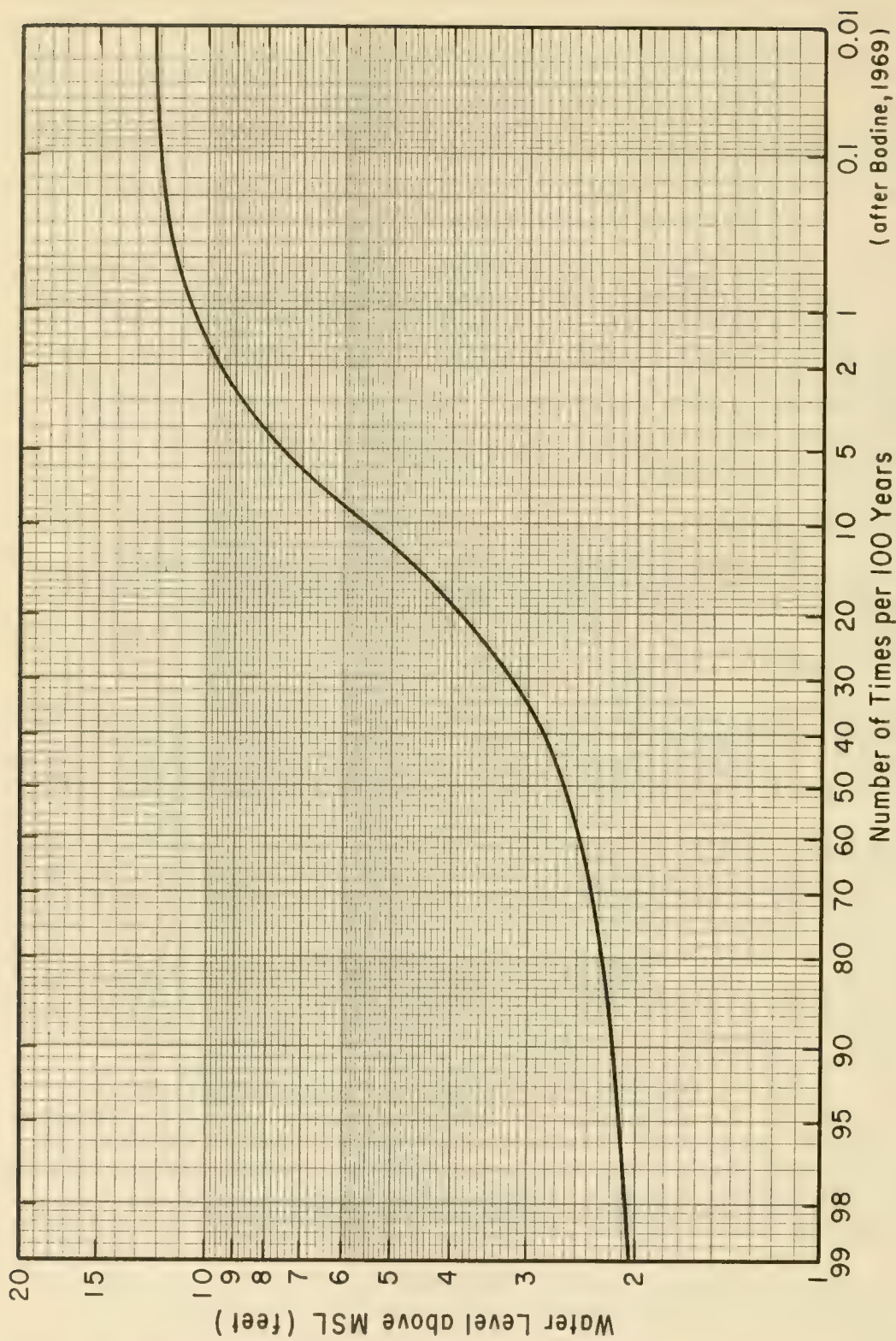
Figure 4-42. Frequency Per 100 Years the Stated Water Level is Equalled or Exceeded on the Open Coast, South Padre Island, Texas

4-114

this source if the lagoon is less than 5 miles wide. Where the lagoon
is wider (especially 10 miles or greater) flooding from the lagoon side by
wind setup should be investigated before large dune construction projects
are undertaken.

4.622 Reservoir of Beach Sand. During storms, erosion of the beach occurs
and the shoreline recedes. If the storm is severe, waves attack and erode
the foredunes and supply sand to the beach; in later erosion stages, sand
is supplied to the back of the island by overwash. (Godfrey, 1972.)

Volumes of sand eroded from beaches during storms have been estimated
in recent beach investigations. Everts (1973) reported on two storms dur-
ing February 1972 which affected Jones Beach, New York. The first storm
eroded an average of 27,000 cubic yards per mile above mean sea level for
the 9-mile study area; the second storm (2 weeks later) eroded an average
of 35,000 cubic yards of sand per mile above mean sea level at the same
site. Losses at individual profiles ranged up to 120,000 cubic yards per
mile. Davis (1972) reported a beach erosion rate on Mustang Island, Texas,
following Hurricane Fern (September 1971), of 12.3 cubic yards per linear
foot of beach for a 1,500-foot stretch of beach (about 65,000 cubic yards
per mile of beach). On Lake Michigan in July 1969, a storm eroded an aver-
age of 3.6 cubic yards per linear foot of beach (about 29,000 cubic yards
per mile) from an 800-foot beach near Stevensville, Michigan. (Fox, 1970.)
Because much of the eroded sand is usually returned to the beach by wave
action soon after the storm, these volumes are probably representative of
temporary storm losses.

Volumes equivalent to those eroded during storms have been trapped
and stored in foredunes adjacent to the beach. Foredunes constructed
along Padre Island, Texas, and Core Banks, North Carolina, (Section 6.43
and 6.447) contain from 30,000 to 80,000 cubic yards of sand per mile of
beach. Assuming the present rate of entrapment of sand continues for the
next 3 years at these sites, sand volumes ranging from 50,000 to 160,000
cubic yards per mile of beach will be available to nourish eroding beaches
during a major storm. Sand volumes trapped during a 30-year period by
European beachgrass at Clatsop Spit, Oregon, averaged about 800,000 cubic
yards per mile of beach. Thus, within a few years, foredunes can trap and
store a volume of sand equivalent to the volumes eroded from beaches dur-
ing storms of moderate intensity.

4.623 Long-Term Effects. Dolan, (1972-73) advances the concept that a
massive, unbroken foredune line restricts the landward edge of the surf
zone during storms causing narrower beaches and thus increased turbulence
in the surf zone. The increased turbulence causes higher sand grain attri-
tion and winnowing rates and leads to accelerated losses of fine sand, an
erosive process that may be detrimental to the long-range stability of bar-
rier islands. However, as discussed in Section 4.521, the effects of sedi-
ment size are usually of secondary importance in littoral transport pro-
cesses - processes which are important in barrier island stability. In
addition, geographical location is probably more important in determining
beach sand size than dune effects, since both fine and coarse sand beaches

front major foredune systems in different geographical locations. For example, fine sand beaches front a massive foredune system on Mustang Island, Texas, and coarse sand beaches front dunes on the Cape Cod spits.

Godfrey (1972) discusses the effect of a foredune system on the long term stability of the barrier islands of the Cape Hatteras and Cape Lookout National Seashores, North Carolina. Important implicit assumptions of the discussion are that no new supply or inadequate new supplies of sand are available to the barrier island system, and that rising sea level is, in effect, creating a sand deficit by drowning some of the available island volume. The point of the geomorphic discussion is that under such conditions the islands must migrate landward to survive. A process called "oceanic overwash" (the washing of sand from low foredunes or from the beach over the island crest onto the deflation plain by overtopping waves) is described as an important process in the landward migration of the islands. Since a foredune system blocks overtopping and prevents oceanic overwash, foredunes are viewed as a threat to barrier island stability.

Granted the implicit assumptions and a geologic time frame, the geomorphic concept presented has convincing logic and probably has merit. However, the assumptions are not valid on all barrier islands or at all locations in most barrier islands or at all locations in most barrier island systems. Too, most coastal engineering projects are based on a useful life of 100 years or less. In such a short period, geologic processes, such as sea-level rise, have a minor effect in comparison with the rapid changes caused by wind and waves. Therefore, the island crest elevation and foredune system will maintain their elevation relative to the mean water level on stable or accreting shores over the life of most projects. On eroding shores, the foredunes will eventually be eroded and overwash will result in shoreward migration of the island profile; sand burial and wave and water damage will occur behind the original duneline. Therefore, planning for and evaluation of the probable success of a foredune system must consider the general level of the area of the deflation plain to be protected, the rate of sea level rise, and the rate of beach recession.

4.7 SEDIMENT BUDGET

4.71 INTRODUCTION

4.711 Sediment Budget. A sediment budget is based on sediment removal, transportation and deposition, and the resulting excesses or deficiencies of material quantities. Usually, the sediment quantities are listed according to the sources, sinks, and processes causing the additions and subtractions. In this chapter, the sediment is usually sand, and the processes are either littoral processes or the changes made by man.

The purpose of a sediment budget is to assist the coastal engineer by: identifying relevant processes; estimating volume rates required for design purposes; singling out significant processes for special attention; and, on occasion, through balancing sand gains against losses, checking the accuracy and completeness of the design budget.

Sediment budget studies have been presented by Johnson (1959), Bowen and Inman (1966), Vallianos (1970), Pierce (1969), and Caldwell (1966).

4.712 <u>Elements of Sediment Budget</u>. Any process that increases the quantity of sand in a defined control volume is called a *source*. Any process that decreases the quantity of sand in the control volume is called a *sink*. Usually, sources are identified as positive and sinks as negative. Some processes (longshore transport is the most important) function both as source and sink for the control volume, and these are called *convecting processes*.

Point sources or point sinks are sources or sinks that add or sub-tract sand across a limited part of a control volume boundary. A tidal inlet often functions as a point sink. Point sources or sinks are gener-ally measured in units of volume per year.

Line sources or line sinks are sources or sinks that add or subtract sand across an extended segment of a control volume boundary. Wind trans-port landward from the beaches of a low barrier island is a line sink for the ocean beach. Line sources or sinks are generally measured in units of volume per year per unit length of shoreline. To compute the total effect of a line source or sink, it is necessary to multiply this quantity by the total length of shoreline over which the line source or sink operates.

The following conventions are used for elements of the sediment budget:

$$Q_i^+ \quad \text{is a point source}$$

$$Q_i^- \quad \text{is a point sink}$$

$$q_i^+ \quad \text{is a line source}$$

$$q_i^- \quad \text{is a line sink}$$

These subscripted elements of the sediment budget are identified by name in Table 4-13 according to whether the element makes a point or line con-tribution to the littoral zone, and according to the boundary across which the contribution enters or leaves. Each of the elements is discussed in following sections.

The length of shoreline over which a line source is active is in-dicated by b_i and the total contribution of the line source or line sink by Q_i^{*+} or Q_i^{*-}, so that in general

$$Q_i^* = b_i \, q_i \, . \tag{4-46}$$

Table 4-13. Classification of Elements in the Littoral Zone Sediment Budget

Location of Source or Sink	Offshore Side of Littoral Zone	Onshore Side of Littoral Zone	Within Littoral Zone	Longshore Ends of Littoral Zone
Point Source (cu.yd./yr.)	Q_1^+ Offshore shoal or island	Q_2^+ Rivers, streams*	Q_3^+ Replenishment	Q_4^+ Longshore transport in*
Point Sink (cu.yd./yr.)	Q_1^- Submarine canyon	Q_2^- Inlets*	Q_3^- Mining, extractive dredging	Q_4^- Longshore transport out*
Line Source (cu.yd./yr./ft. of beach)	q_1^+ Sand transport from the offshore	q_2^+ Coastal erosion including erosion of dunes and cliffs*	q_3^+ Beach erosion* $CaCO_3$ production	
Line Sink (cu.yd./yr./ft. of beach)	q_1^- Sand transport to the offshore	q_2^- Overwash Coastal land and dune storage	q_3^- Beach storage* $CaCO_3$ losses	

*Naturally occurring sources and sinks that usually are major elements in the sediment budget.

It is often useful to specify a source or sink as a fraction, k_i, of the gross longshore transport rate:

$$Q_i = k_i Q_g \ . \tag{4-47}$$

In a complete sediment budget, the difference between the sand added by all sources and the sand removed by all sinks should be zero. In the usual case, a sand budget calculation is made to estimate an unknown erosion or deposition rate. This estimated rate will be the difference resulting from equating known sources and sinks. The total budget is shown schematically as follows:

Sum of Sources - Sum of Sinks = 0, or

Sum of Known Sources - Sum of Known Sinks = Unknown (Sought) Source or Sink

$$\sum_{i=1}^{4} Q_i^+ + \sum_{i=1}^{4} Q_i^{*+} - \left(\sum_{i=1}^{3} Q_i^- + \sum_{i=1}^{3} Q_i^{*-} \right) = 0 \ . \tag{4-48}$$

The Q_i^* are obtained using Equation 4-46 and the appropriate q_i and b_i. The subscript, i, equals 1, 2, 3, or 4 and corresponds to the subscripts in Table 4-13.

4.713   Sediment Budget Boundaries.   A sediment budget is used to identify and quantify the sources and sinks that are active in a specified area. By so doing, erosion or deposition rates are determined as the balance of known sinks and sources.   Boundaries for the sediment budget are determined by the area under study, the time scale of interest, and study purposes.   In a given study area, adjacent sand budget compartments (control volumes) may be needed with shore-perpendicular boundaries at significant changes in the littoral system.   For example, compartment boundaries may be needed at inlets, between eroding and stable beach segments, and between stable and accreting beach segments.   Shore-parallel boundaries are needed on both the seaward and landward sides of the control volumes.   They may be established wherever needed, but the seaward boundary is usually established at or beyond the limit of active sediment movement, and the landward boundary beyond the erosion limit anticipated for the life of the study.   The bottom surface of a control volume should pass below the sediment layer that is actively moving, and the top boundary should include the highest surface elevation in the control volume.   Thus, the budget of a particular beach and nearshore zone would have shore parallel boundaries landward of the line of expected erosion and at or beyond the seaward limit of significant transport.   A budget for barrier island sand dunes might have a boundary at the bay side of the island and the landward edge of the backshore.

A sediment budget example and analysis are shown in Figure 4-43. This example considers a shoreline segment along which the incident wave climate can transport more material entering from updrift.   Therefore the longshore transport in the segment is being fed by a continuously eroding sea cliff.   The cliff is composed of 50 percent sand and 50 percent clay.   The clay fraction is assumed to be lost offshore while the sand fraction feeds into the longshore transport.   The budget balances the sources and sinks using the following continuity equation:

Sum of Known Sources - Sum of Known Sinks = Difference

An example calculation is shown in Figure 4-43.

4.72 SOURCES OF LITTORAL MATERIAL

4.721   Rivers.   It is estimated that rivers of the world bring about 3.4 cubic miles or 18.5 billion cubic yards of sediment to the coast each year (volume of solids without voids).   (Stoddard, 1969; from Strakhov, 1967.) Only a small percentage of this sediment is in the sand size range that is common on beaches.   The large rivers which account for most of the volume of sediment carry relatively little sand.   For example, it is estimated (Scruton, 1960) that the sediment load brought to the Gulf of Mexico each year by the Mississippi River consists of 50 percent clay, 48 percent silt, and only 2 percent sand.   Even lower percentages of sand seem probable for other large river discharges.   (See Gibbs, 1967, p. 1218, for information on the Amazon River.)   But smaller rivers flowing through sandy drainage areas may carry 50 percent or more of sand.   (Chow, 1964, p. 17-20.)   In southern California, sand brought to the coast by the floods of small rivers is a significant source of littoral material.   (Handin, 1951; and Norris, 1964.)
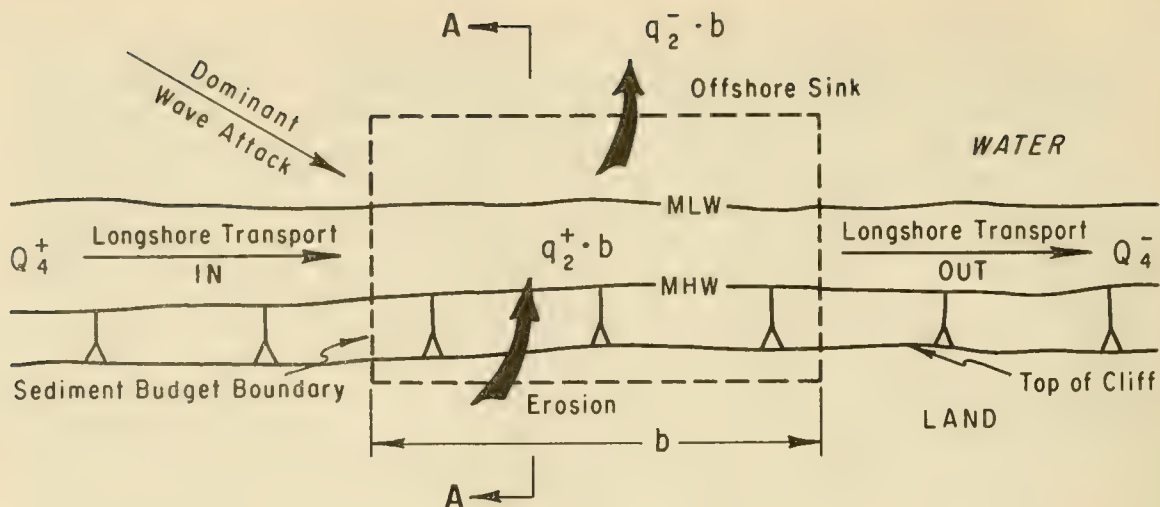
ERODING SHORELINE – PLAN VIEW
(Not to Scale)
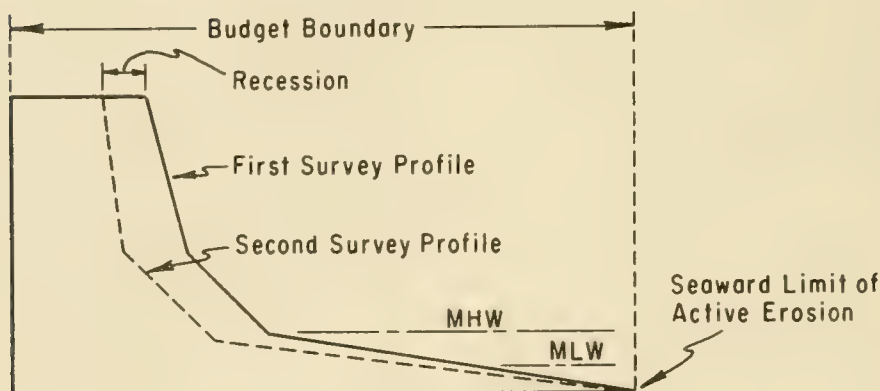
SECTION A-A
(Not to Scale)

Assumptions	Budget Calculations

$Q_4^+ = 100{,}000$ yd.^{3}/yr.

$q_2^+ = 1$ yd.^{3}/yr./ft.

$q_2^- = 0.5$ yd.^{3}/yr./ft.

$b = 10{,}000$ ft.

Sum of Sources — Sum of Sinks = Difference

Find Q_4^-

$$\left(Q_4^+ + q_2^+ b\right) - \left(Q_4^- + q_2^- b\right) = 0$$

$$\left(10^5 + 1.0 \times 10^4\right) - \left(Q_4^- + 0.5 \times 10^4\right) = 0$$

$$Q_4^- = 110{,}000 - 5{,}000$$

$$Q_4^- = \underline{\underline{105{,}000 \text{ yd.}^3/\text{yr.}}}$$

Figure 4-43. Basic Example of Sediment Budget

Most of the sediment carried to the coast by rivers is deposited in comparatively small areas, often in estuaries where the sediment is trapped before it reaches the coast. (Strakhov, 1967.) The small fraction of sand in the total material brought to the coast and the local estuarine and deltaic depositional sites of this sediment suggest that rivers are not the immediate source of sediment on beaches for much of the world's coastline. Many sources of evidence indicate that sand-sized sediment is not supplied to the coasts by rivers on most segments of the U.S. Atlantic and Gulf coasts. Therefore, other sediment sources must be important.

4.722 <u>Erosion of Shores and Cliffs</u>. Erosion of the nearshore bottom, the beach, and the seaward edge of dunes, cliffs, and mainland (Fig. 4-44) results in a sand loss. In many areas, erosion from cliffs of one area is the principal source of sand for downdrift beaches. Kuenen (1950) estimates that beach and cliff erosion along all coasts of the world totals about 0.03 cubic mile or 160 million cubic yards per year. Although this amount is only about 1 percent of the total solid material carried by rivers, it is a major source in terms of sand delivered to the beaches, since the sand fraction in the river sediments is usually small, and is usually trapped before it reaches the littoral zone. Shore erosion is an especially significant source where older coastal deposits are being eroded, since these usually contain a large fraction of sand.

If an eroding shore maintains approximately the same profile above the seaward limit of significant transport while it erodes, then the erosion volume per foot of beach front is the vertical distance from dune base or berm crest to the depth of the seaward limit (h), multiplied by the horizontal retreat of the profile, Δx. (See Figure 4-44.)

Figure 4-44 shows three equivalent volumes, all indicating a net erosion of $h\Delta x$. To the right in Figure 4-44 is a typical beach profile. The dashed line profile below it is the same as the solid line profile. The horizontal distance between solid and dashed profiles is Δx, the horizontal retreat of the profile due to (assumed) uniform erosion. The unit volume loss, $h\Delta x$, between dune base and depth to seaward limit is equivalent to the unit volume indicated by the slanted parallelogram on the middle of Figure 4-44. The unit volume of this parallelogram, $h\Delta x$, is equivalent to the shaded rectangle on the left of Figure 4-44. If the vertical distance, h is 40 feet, and $\Delta x = 1$ foot of horizontal erosion, then the unit volume lost is 40/27, or 1.5 cubic yards per foot of beach front.

4.723 <u>Transport from Offshore Slope</u>. An uncertain and potentially significant source in the sediment budget is the contribution from the offshore slope. However, hydrography, sediment size distribution, and related evidence discussed in Section 4.523 indicate that contributions from the continental shelf to the littoral zone are probably negligible in many areas. Most shoreward moving sediment appears to originate in areas fairly close to shore. Significant onshore-offshore transport takes place within the littoral zone due to seasonal and storm-induced profile changes and to
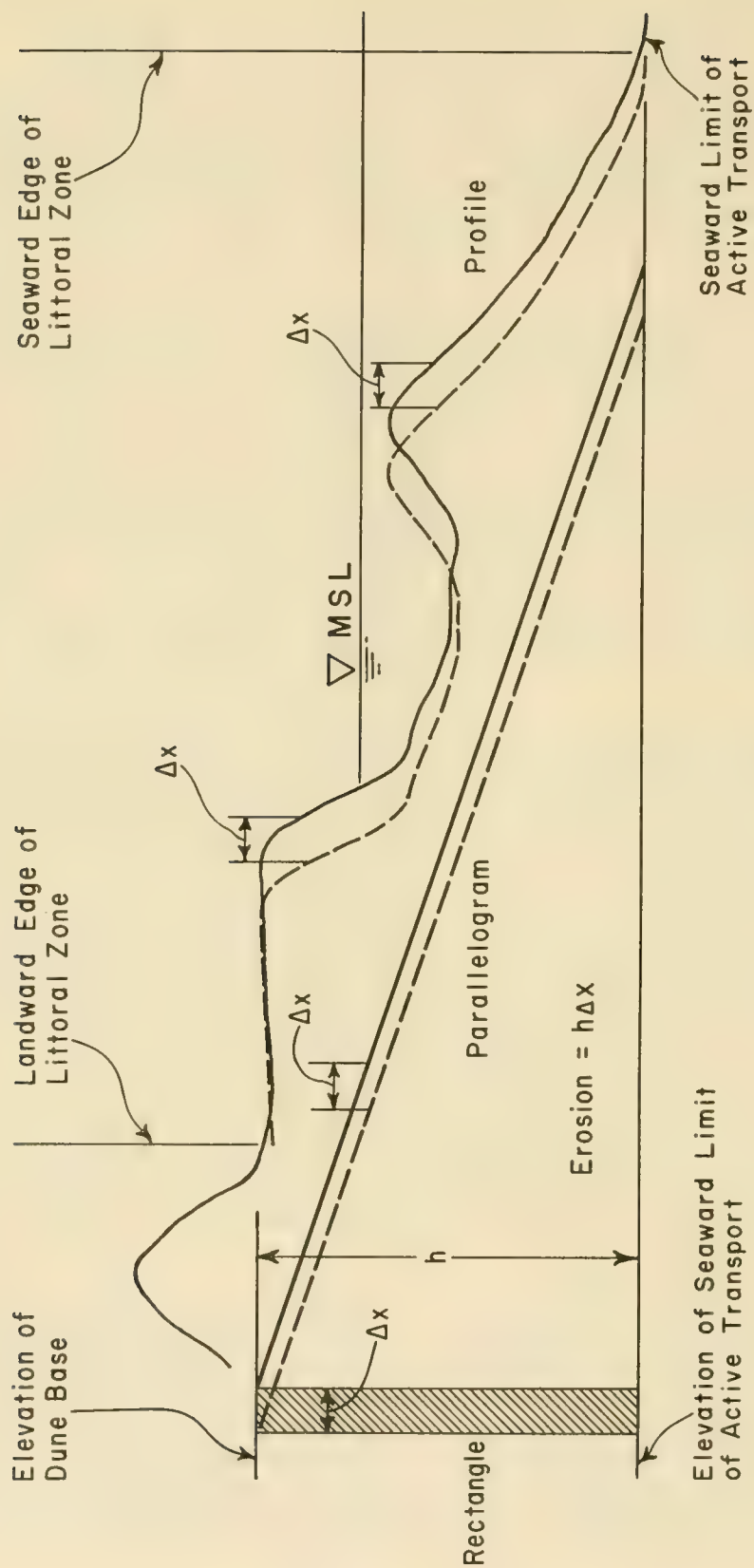
Figure 4-44. Erosion Within Littoral Zone During Uniform Retreat of an Idealized Profile

erosion of the nearshore bottom and beaches, but in the control volume defined, this transport takes place within the control volume. Transport from the offshore has been treated as a line source.

In some places, offshore islands or shoals may act as point sources of material for the littoral zone. For example, the drumlin islands and shoals in Boston Harbor and vicinity may be point sources for the nearby mainland.

4.724 Windblown Sediment Sources. To make a net contribution to the littoral zone in the time frame being considered, windblown sand must come from a land source whose sand is not derived by intermediate steps from the same littoral zone. On U.S. ocean coasts, such windblown sand is not a significant source of littoral materials. Where wind is important in the sediment budget of the ocean shore, wind acts to take away sand rather than to add it, although local exceptions probably occur.

However, windblown sand can be an important source, if the control volume being considered is a beach on the lagoon side of a barrier island. Such shores may receive large amounts of windblown sand.

4.725 Carbonate Production. Dissolved calcium carbonate concentration in the ocean is near saturation, and it may be precipitated under favorable conditions. In tropical areas, many beaches consist of calcium carbonate sands; in temperate zones, calcium carbonate may be a significant part of the littoral material. These calcium carbonate materials are generally fragments of shell material whose rate of production appears to increase with high temperature and with excessive evaporation. (See Hayes, 1967.) Oolitic sands are a nonbiogenic chemical precipitate of calcium carbonate on many low latitude beaches.

Quantitative estimates of the production of calcium carbonate sediment are lacking, but maximum rates might be calculated from the density and rate of growth of the principal carbonate-producing organisms in an area. For example, following northeasters along the Atlantic coast of the U.S., the foreshore is occasionally covered with living clams thrown up by the storm from the nearshore zone. One estimate of the annual contribution to the littoral zone from such a source would assume an average shell thickness of about 0.04 foot completely covering a strip of beach 100 feet wide all along the coast. On an annual basis, this would be about 0.15-cubic yard per year per foot of beach front. Such a quantity is negligible under almost all conditions. However, the dominance of carbonate sands in tropical littoral zones suggests that the rate of production can be much higher.

4.726 Beach Replenishment. Beach protection projects often require placing sand on beaches. The quantity of sand placed on the beach in such beach-fill operations may be a major element in the local sediment budget. Data on beach-fill quantities may be available in Corps of Engineer District offices, in records of local government engineers, and in dredging company records. The exact computation of the quantity of a

beach fill is subject to uncertainties: the source of the dredged sand
often contains significant but variable quantities of finer materials that
are soon lost to the littoral zone; the surveys of both the borrow area
and the replenished area are subject to uncertainty because sediment trans-
port occurs during the dredging activities; and in practice only limited
efforts are made to obtain estimates of the size distribution of fill
placed on the beach. Thus, the resulting estimate of the quantity of
suitable fill placed on the beach is uncertain. More frequent sampling
and surveys could help identify this significant element in many sedi-
ment budgets.

4.73 SINKS FOR LITTORAL MATERIALS

4.731 Inlets and Lagoons. Barrier islands are interrupted locally by
inlets which may be kept open by tidal flow. A part of the sediment moved
alongshore by wave action is moved into these inlets by tidal flow. Once
inside the inlet, the sediment may deposit where it cannot be moved sea-
ward by the ebb flow. (Brown, 1928.) The middleground shoals common to
many inlets are such depositional features. Such deposition may be reduced
when the ebb currents are stronger than the flood currents. (Johnson,
1956.)

It is evident from aerial photography (e.g., of Drum Inlet, N.C.,
Fig. 4-45) that inlets do trap significant quantities of sand. Caldwell's
(1966) estimate of the sand budget for New Jersey, calculates that 23
percent of the local gross longshore transport is trapped by the seven
inlets in southern New Jersey, or about 250,000 cubic yards per year for
each inlet. In a study of the south shore of Long Island, McCormick (1971)
estimated from the growth of the floodtide delta of Shinnecock Inlet (shown
by aerial photos taken in 1955 and 1969) that this inlet trapped 60,000
cubic yards per year. This amounts to about 20 percent of the net long-
shore transport (Taney, 1961a, p. 46), and probably less than 10 percent
of the gross transport. (Shinnecock Inlet is a relatively small inlet.)
It appears that the rate at which an inlet traps sediment is higher imme-
diately after the inlet opens than it is later in its history.

4.732 Overwash. On low barrier islands, sand may be removed from the
beach and dune area by overwashing during storms. Such rates may average
locally up to 1 cubic yard per year per foot. Data presented by Pierce
(1969) suggest that for over half of the shoreline between Cape Hatteras
and Cape Lookout, North Carolina, the short term loss due to overwash was
0.6 cubic yard per year per foot of beach front. Figure 4-46 is an aerial
view of overwash in the region studied by Pierce (1969). Overwash does
not occur on all barrier islands, but if it does, it may function as a
source for the beach on the lagoon side.

4.733 Backshore and Dune Storage. Sand can be temporarily withdrawn
from transport in the littoral zone as backshore deposits and dune areas
along the shore. Depending on the frequency of severe storms, such sand
may remain in storage for intervals ranging from months to years. Back-
shore deposition can occur in hours or days by the action of waves after

Figure 4-45.   Sediment Trapped Inside Old Drum Inlet,
North Carolina

(1 November 1971)

Figure 4-46. Overwash on Portsmouth Island, North
Carolina

storms. Dune deposits require longer to form - months or years - because wind transport usually moves material at a lesser rate than wave transport. If the immediate beach area is the control volume of interest, and budget calculations are made based on data taken just after a severe storm, allowance should be made in budget calculations for sand that will be stored in berms through natural wave action. (See Table 4-5.)

4.734 Offshore Slopes. The offshore area is potentially an important sink for littoral material. Transport to the offshore is favored by: storm waves which stir up sand, particularly when onshore winds create a seaward return flow; turbulent mixing along the sediment concentration gradient which exists between the sediment-water mixture of the surf zone and the clear water offshore; and the slight offshore component of gravity which acts on both the individual sediment particles and on the sediment-water mixture.

It is often assumed that the *sediment sorting loss* that commonly reduces the volume of newly placed beach fill is lost to the offshore slopes. (Corps of Engineers, Wilmington District, 1970; and Watts, 1956.) A major loss to the offshore zone occurs where spits build into deep water in the longshore direction. Sandy Hook, New Jersey, is an example. (See Figure 4-47.) It has been suggested (Bruun and Gerritsen, 1959) that ebb flows from inlets may sometimes cause a loss of sand by jetting sediment seaward into the offshore zone.

The calculation of quantities lost to the offshore zone is difficult, since it requires extensive, accurate, and costly surveys. Some data on offshore changes can be obtained by studies of sand level changes on rods imbedded in the sea floor (Inman and Rusnak, 1956), but without extending the survey beyond the boundary of the moving sand bed, it is difficult to determine net changes.

4.735 Submarine Canyons. Probably the most frequently mentioned sinks for littoral materials are submarine canyons. Shepard (1963) and Shepard and Dill (1966) provide extensive description and discussion of the origin of submarine canyons. The relative importance of submarine canyons in sediment budgets is still largely unknown.

Of 93 canyons tabulated by Shepard and Dill (1966), 34 appear to be receiving sediment from the coast, either by longshore transport or by transport from river mouths. Submarine canyons are thought to be especially important as sinks off southern California. Herron and Harris (1966, p. 654) suggest that Mugu Canyon, California, traps about 1 million cubic yards per year of the local littoral drift.

The exact mechanism of transport into these canyons is not clear, even for the La Jolla Canyon (California) which is stated to be the most extensively studied submarine feature in the world. (Shepard and Buffington, 1968.) Once inside the canyons, the sediment travels down the floors of the heads of the canyons, and is permanently lost to the littoral zone.

Sandy Hook,
New Jersey

ATLANTIC OCEAN

(14 September 1969)

Figure 4-47. Growth of a Spit into Deep Water, Sandy
Hook, New Jersey

4-128

4.736 __Deflation__. The loose sand that forms beaches is available to be transported by wind. After a storm, shells and other objects are often found perched on pedestals of sand left standing after the wind eroded less protected sand in the neighborhood. Such erosion over the total beach surface can amount to significant quantities. Unstabilized dunes may form and migrate landward, resulting in an important net loss to the littoral zone. Examples include some dunes along the Oregon coast (Cooper, 1958), between Pismo Beach and Point Arguello, California (Bowen and Inman, 1966); central Padre Island (Watson, 1971); and near Cape Henlopen, Delaware (Kraft, 1971). Typical rates of transport due to wind range from 1 to 10 cubic yards per year per foot of beach front where wind transport is noticeable. (Cooper, 1958; Bowen and Inman, 1966; Savage and Woodhouse, 1968; and Gage, 1970.) However average rates probably range from 1 to 3 cubic yards per year per foot.

The largest wind-transported losses are usually associated with accreting beaches that provide a broad area of loose sand over a period of years. Sand migrating inland from Ten Mile River Beach in the vicinity of Laguna Point, California, is shown in Figure 4-48.

Study of aerial photographs and field reconnaissance can easily establish whether or not important losses or gains from wind transport occur in a study area. However, detailed studies are usually required to establish the importance of wind transport in the sediment budget.

4.737 __Carbonate Loss__. The abrasion resistance of carbonate materials is much lower than quartz, and the solubility of carbonate materials is usually much greater than quartz. However, there is insufficient evidence to show that significant quantities of carbonate sands are lost from the littoral zone in the time scale of engineering interest through either abrasion or solution.

4.738 __Mining and Dredging__. From ancient times, sand and gravel have been mined along coasts. In some countries, for example Denmark and England, mining has occasionally had undesirable effects on coastal settlements in the vicinity. Sand mining in most places has been discouraged by legislation and the rising cost of coastal land, but it still is locally important. (Magoon, et al., 1972.) It is expected that mining will become more important in the offshore area in the future. (Duane, 1968, and Fisher, 1969.)

Such mining must be conducted far enough offshore so the mined pit will not act as a sink for littoral materials, or refract waves adversely, or substantially reduce the wave damping by bottom friction and percolation.

Material is also lost to the littoral zone when dredged from navigable waters (channels and entrances) within the littoral zone, and the dredged material is dumped in some area outside of the littoral zone. These dump areas can be for land fill, or in deep water offshore. This action has been a common practice, because the first costs for some dredging operations are cheaper when done this way.

PACIFIC

OCEAN

Migrating Sand
Dunes

(24 May 1972)

Figure 4-48. Dunes Migrating Inland Near Laguna Point, California

4-130

4.74 CONVECTION OF LITTORAL MATERIALS

Sources and sinks of littoral materials are those processes that result in net additions or net subtractions of material to the selected control volume. However, some processes may subtract at the same rate that they add material, resulting in no net change in the volume of littoral material of the control volume.

The most important convecting process is longshore sediment transport. It is possible for straight exposed coastlines to have gross longshore transport rates of more than 1 million cubic yards per year. On a coast without structures, such a large Q_g can occur, and yet not be apparent because it causes no obvious beach changes. Other convecting processes that may produce large rates of sediment transport with little noticeable change include tidal flows, especially around inlets, wind transport in the longshore direction, and wave-induced currents in the offshore zone.

Since any structure that interrupts the equilibrium convection of littoral materials will normally result in erosion or accretion, it is necessary that the sediment budget quantitatively identify all processes convecting sediment through the study area. This is most important on shores with high waves.

4.75 RELATIVE CHANGE IN SEA LEVEL

Relative changes in sea level may be caused by changes in sea level and changes in land level. Sea levels of the world are now generally rising. The level of inland seas may either rise or fall, generally depending on hydrologic influences. Land level may rise or fall due to tectonic forces, and land level may fall due to subsidence. It is often difficult to distinguish whether apparent changes in sea level are due to change in sea level, change in land level, or both. For this reason, the general process is referred to as relative change in sea level.

While relative changes in sea level do not directly enter the sediment budget process, the net effect of these elevation changes is to move the shoreline either landward (relative rise in sea level) or seaward (relative fall in sea level). It thus can result in the appearance of a gain or loss of sediment volume.

The importance of relative change in sea level on coastal engineering design depends on the time scale and the locality involved. Its effect should be determined on a case-by-case basis.

4.76 SUMMARY OF SEDIMENT BUDGET

Sources, sinks, and convective processes are summarized diagrammatically in Figure 4-49 and listed in Table 4-14. The range of contributions or losses from each of these elements is described in Table 4-14 measured as a fraction of the gross longshore transport rate, or as a rate given in cubic yards per year per foot of beach front. The relative importance

of elements in the sand budget varies with locality and with the bound-
aries of the particular littoral control volume. (These elements are
classified as point or line sources or sinks in Table 4-13, and the budget
is summarized in Equation 4-48.)
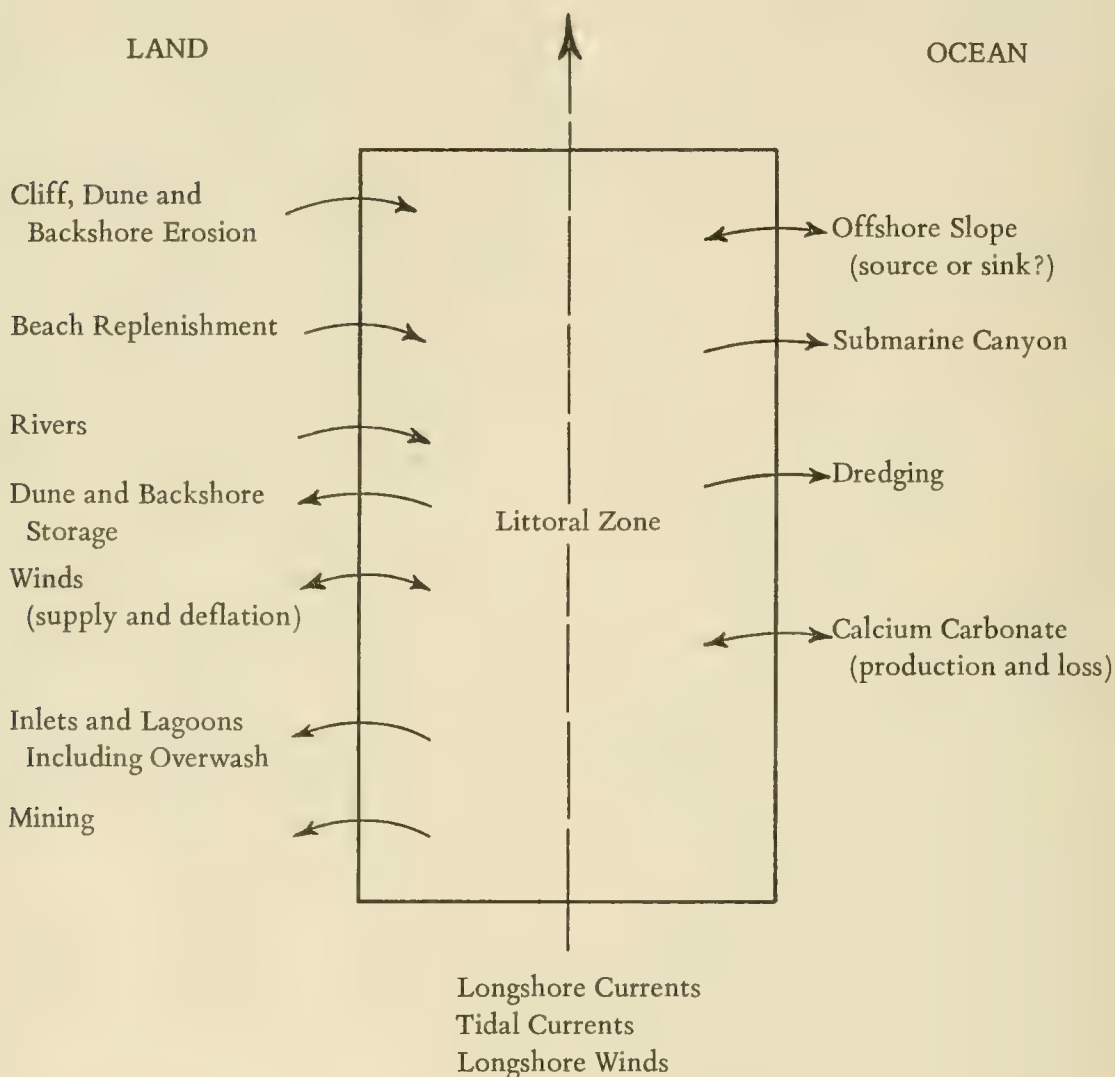
Figure 4-49. Materials Budget for the Littoral Zone

In most localities, the gross longshore transport rate significantly
exceeds other volume rates in the sediment budget, but if the beach is
approximately in equilibrium, this may not be easily noticed.

The erosion of beaches and cliffs and river contributions are the
principal known natural sources of beach sand in most localities. Inlets,

Table 4-14. Sand Budget of the Littoral Zone

Sources	
Rivers and streams	The major source in the limited areas where rivers carry sand to the littoral zone. In affected areas notable floods may contribute several times Q_g.
Cliff, dune and backshore erosion	Generally the major source where rivers are absent. 1 to 4 cu.yd./yr./ft.
Transport from offshore	Quantity uncertain.
Wind transport	Not generally important as a source.
$CaCO_3$ production	Significant in tropical climate. The value of 0.25 cu.yd./yr./ft. seems reasonable upper limit on temperate beach.
Beach replenishment	Varies from 0 to greater than Q_g.

Sinks	
Inlets and lagoons	May remove from 5 to 25 percent of Q_g per inlet. Depends on number of inlets, inlet size, tidal flow characteristics, and inlet age.
Overwash	Less than 1 cu.yd./yr./ft. at most, and limited to low barrier islands.
Beach storage	Temporary, but possibly large, depending on beach condition when budget is made. (See Table 4-5, pages 4-72, 4-73.)
Offshore slopes	Uncertain quantity. May receive much fine material, some coarse material.
Submarine canyons	Where present, may intercept up to 80 percent of Q_g.
Deflation	Usually less than 2 cu.yd./yr./ft. of beach front, but may range up to 10 cu.yd./yr./ft.
$CaCO_3$ loss	Not known to be important.
Mining and dredging	May equal or exceed Q_g in some localities.

Convective Processes	
Longshore transport (waves)	May result in accretion of Q_g, erosion of Q_n, or no change depending on conditions of equilibrium.
Tidal Currents	May be important at mouth of inlet and vicinity, and on irregular coasts with high tidal range.
Winds	Longshore winds are probably not important, except in limited regions.

lagoons and deep water in the longshore direction comprise the principal known natural sinks for beach sand. Of potential, but usually unknown, importance as either a source or a sink is the offshore zone seaward of the beach.

The works of man in beach replenishment and in mining or dredging may provide major sources or sinks in local areas. In a few U.S. localities, submarine canyons or wind may provide major sinks, and calcium carbonate production by organisms may be a major source.

* * * * * * * * * * * * * * EXAMPLE PROBLEM * * * * * * * * * * * * * * * *

GIVEN:

(a) An eroding beach 4.4 miles long at root of spit that is 10 miles long. Beaches on the remainder of the spit are stable. (See Figure 4-50a.)

(b) A uniform recession rate of 3 feet per year along the eroding 4.4 miles.

(c) Depth of lowest shore parallel contour is -30 feet MSL, and average dune crest elevation is 15 feet MSL.

(d) Sand is accumulating at the tip of the spit at an average rate of 400,000 cubic yards per year.

(e) The variation of γ along the beaches of the spit is shown in Figure 4-51. ($\gamma = Q_{\ell t}/Q_{rt}$; Equation 4-23.)

(f) No sand accumulates to the right of the erosion area; no sand is lost to the offshore.

(g) A medium-width jettied inlet is proposed which will breach the spit as shown in Figure 4-50a.

(h) The proposed inlet is assumed to trap about 15 percent of the gross transport, Q_g.

(i) The 1.3-mile long beach to the right of the jettied inlet will stabilize (no erosion) and realign with γ changing to 3.5.

(j) The accumulation at the end of the spit will continue to grow at an average annual rate of 400,000 cubic yards per year after the proposed inlet is constructed.

(a) Site Sketch

Reach 4 | Reach 3 | Reach 2 | Reach 1

5 mi. — 3.1 mi. — 1.3 mi.

Ocean

Bay

Proposed Inlet
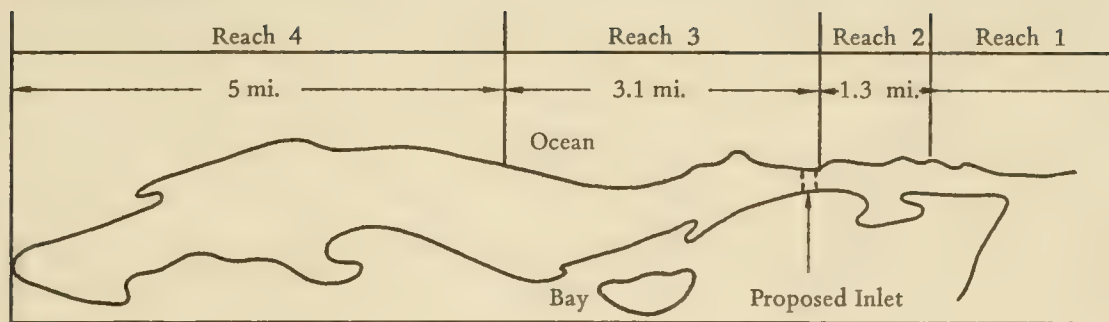
(b) Before Inlet

Reach 4	Reach 3	Reach 2	Reach 1
$Q_{g(4)} = 400{,}000$	$Q_{g(3,4)} = 490{,}000$	$Q_{g(2,3)} = 530{,}000$	$Q_{g(1,2)} = 474{,}000$
$Q_{n(4)} = 400{,}000$	$Q_{n(3,4)} = 400{,}000$	$Q_{n(2,3)} = 318{,}000$	$Q_{n(1,2)} = 284{,}000$
	$Q_{rt(3,4)} = 45{,}000$	$Q_{rt(2,3)} = 105{,}000$	$Q_{rt(1,2)} = 95{,}000$
$Q_{\ell t(4)} = 400{,}000$	$Q_{\ell t(3,4)} = 445{,}000$	$Q_{\ell t(2,3)} = 425{,}000$	$Q_{\ell t(1,2)} = 379{,}000$

$b_{(3)}q_{3(3)}^{+} = 82{,}000 \qquad b_{(2)}q_{3(2)}^{+} = 34{,}000$

(c) After Inlet

Reach 4	Reach 3	Reach 2	Reach 1
$Q_{g(4)} = 400{,}000$	$Q_{g(3,4)} = 490{,}000$	$Q_{g(2,3)} = 512{,}000$	$Q_{g(1,2)} = 474{,}000$
$Q_{n(4)} = 400{,}000$	$Q_{n(3,4)} = 400{,}000$	$Q_{n(2,3)} = 284{,}000$	$Q_{n(1,2)} = 284{,}000$
	$Q_{rt(3,4)} = 45{,}000$	$Q_{rt(2,3)} = 114{,}000$	$Q_{rt(1,2)} = 95{,}000$
$Q_{\ell t(4)} = 400{,}000$	$Q_{\ell t(3,4)} = 445{,}000$	$Q_{\ell t(2,3)} = 398{,}000$	$Q_{\ell t(1,2)} = 379{,}000$

$b_{(3)}q_{3(3)}^{+} = 193{,}000 \qquad Q_{2}^{-} = 77{,}000$

LEGEND

Q_g Gross Volume

Q_n Net Volume

Q_{rt} Volume to Right

$Q_{\ell t}$ Volume to Left

Q_2^- Inlet Sink Volume

bq_3^+ Erosion Source Volume

Figure 4-50. Summary of Example Problem Conditions and Results

4-135
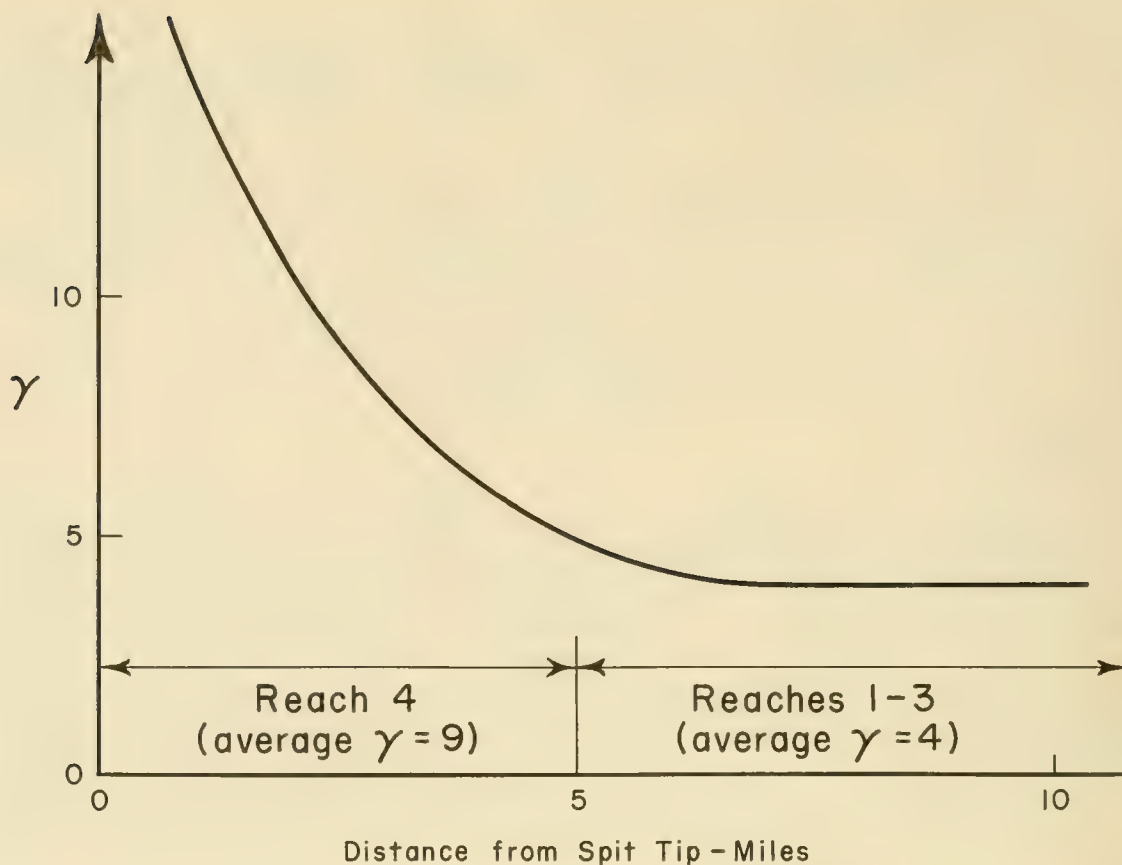
Figure 4-51. Variation of γ with Distance Along the Spit, before Inlet Condition

FIND:

(a) Annual littoral drift trapped by inlet.

(b) After-inlet erosion rate of the beach to the left of the inlet.

(c) After-inlet nourishment needed to maintain the historic erosion rate on the beach to the left of the inlet.

(d) After-inlet nourishment needed to eliminate erosion left of the inlet.

SOLUTION: Divide the beach under study into four sand budget compartments (control volumes called reaches) as shown in Figure 4-50a. Shore perpendicular boundaries are established where important changes in the littoral system occur. To identify and quantify the *before-inlet* system, the continuity of the net transport rate along the spit must be established. The terminology of Figure 4-43 and Table 4-13 is used

4-136

for the sand budget calculation. The average annual volume of material contributed to the littoral system per foot of eroding beach reaches 2 and 3 is:

$$q^+_{3(2)} = q^+_{3(3)} = h\Delta x = \frac{(15 + 30)\,(3)}{27}$$

$$= 5.0 \text{ yd}^3/\text{yr./ft. .}$$

Then, from Equation 4-46 the total annual contribution of the eroding beaches to the system can be determined as:

$$Q^{*+}_{i(2)} + Q^{*+}_{i(3)} = (1.3 \text{ mi.} + 3.1 \text{ mi.})\,(5280 \text{ ft./mi.})\,(5 \text{ yd}^3/\text{yr./ft.})$$

$$= 1.16 \times 10^5 \text{ yd}^3/\text{yr.}$$

Since there is no evidence of sand accumulation or erosion to the right of the eroding area, the eroding beach material effectively moves to the left becoming a component of the net transport volume (Q_n) toward the end of the spit. Contiuity requires the erosion volume and Reach 1 Q_n must combine to equal the acretion at the end of the spit (400,000 cubic yards per year). Thus, Q_n at the root of the spit is

$$Q_{n(1,2)} = 400,000 \text{ yd}^3/\text{yr.} - 116,000 \text{ yd}^3/\text{yr.}$$

$$Q_{n(1,2)} = 284,000 \text{ yd}^3/\text{yr.}$$

Q_n across the boundary between Reaches 2 and 3 $(Q_{n(2,3)})$ is:

$$Q_{n(2,3)} = Q_{n(1,2)} + b_{(2)}\left(q^+_{3(2)}\right)$$

$$= 284,000 \text{ yd}^3/\text{yr.} + (1.3 \text{ mi.})\left(5,280 \,\frac{\text{ft.}}{\text{mi.}}\right)(5 \text{ yd}^3/\text{yr./ft.})$$

$$= 318,000 \text{ yd}^3/\text{yr.}$$

Q_n across the boundary between Reaches 3 and 4 is:

$$Q_{n(3,4)} = Q_{n(2,3)} + b_{(3)}\left(q^+_{3(3)}\right)$$

$$= 318,000 \text{ yd}^3/\text{yr.} + (3.1 \text{ mi.})\left(5,280 \,\frac{\text{ft.}}{\text{mi.}}\right)(5 \text{ yd}^3/\text{yr./ft.})$$

$$= 4000,000 \text{ yd}^3/\text{yr.}$$

This $Q_{n(3,4)}$ moves left across reach 4 with no additions or subtractions, and since the accretion rate at the end of the spit is 400,000 cubic yards per year, the budget balances. Knowing Q_n and γ for each reach, gross transport, Q_g, transport to the right Q_{rt} and transport to the left Q_{lt} can be computed using the following equations:

4-137

From Equation 4-24

$$Q_g = Q_n \left(\frac{1+\gamma}{1-\gamma}\right),$$

then

$$Q_{rt} = \frac{Q_g}{1+\gamma} \; ,$$

and

$$Q_{\ell t} = Q_g - Q_{rt} \; .$$

Q_g, Q_{rt}, $Q_{\ell t}$, and Q_n for each reach are shown in Figure 4-50b.

Now the *after-inlet* condition can be analyzed.

$$Q_{n(1,2)} = 284,000 \text{ yd.}^3/\text{yr. (same as ``before inlet'')} \; ,$$

$$Q_{n(2,3)} = Q_{n(1,2)} = 284,000 \text{ yd.}^3/\text{yr. (reach 2 is stable)} \; .$$

The gross transport rate across the inlet with the new $\gamma = 3.5$ using Equation 4-24, is:

$$Q_{g(2,3)} = \frac{Q_{n(2,3)} \, (1+\gamma)}{(1-\gamma)} \; ,$$

$$Q_{g(2,3)} = (284,000 \text{ yd.}^3/\text{yr.}) \left(\frac{4.5}{2.5}\right) \; ,$$

$$Q_{g(2,3)} = 512,000 \text{ yd.}^3/\text{yr. } .$$

The inlet sink (Q_2^-) = 15 percent of $Q_{g(2,3)}$

$$Q_2^- = 512,000 \text{ yd.}^3/\text{yr. } \times 0.15 \; ,$$

$$Q_2^- = 77,000 \text{ yd.}^3/\text{yr.}$$

The erosion value from Reach 3 now becomes:

Reach 3 erosion = spit accretion + inlet sink - net littoral drift right of inlet.

$$b_{(3)} \left(q_{3(3)}^+\right) = Q_{n(3,4)} + Q_2^- - Q_{n(2,3)} \; ,$$

$$b_{(3)} \left(q_{3(3)}^+\right) = 400,000 \text{ yd.}^3/\text{yr. } + 77,000 \text{ yd.}^3/\text{yr. } - 284,000 \text{ yd.}^3/\text{yr. } ,$$

$$b_{(3)} \left(q_{3(3)}^+\right) = 193,000 \text{ yd.}^3/\text{yr. } .$$

4-138

Nourishment needed to maintain historic erosion rate on Reach 3 beach is:

Reach 3 nourishment = Reach 3 erosion "after inlet" - Reach 3 erosion "before inlet".

$$Q_{3(3)}^{+} = b_{(3)} \left(q_{3(3)}^{+} \right) \text{ after inlet } - b_{(3)} \left(q_{3(3)}^{+} \right) \text{ before inlet .}$$

$$Q_{3(3)}^{+} = 193{,}000 \text{ yd}^3\text{/yr.} - 82{,}000 \text{ yd}^3\text{/yr. ,}$$

$$Q_{3(3)}^{+} = 111{,}000 \text{ yd}^3\text{/yr. .}$$

If reach 3 erosion is to be eliminated, it will be necessary to provide nourishment of 193,000 cubic yards per year.

Q_g, $Q_{\ell t}$, and Q_{rt} for the *after-inlet* condition are computed using Equation 4-24 and related equations. The after-inlet sand budget is shown in Figure 4-50c.

* *

4.8 ENGINEERING STUDY OF LITTORAL PROCESSES

This section demonstrates the use of Chapter 4 in the engineering study of littoral processes.

4.81 OFFICE STUDY

The first step in the office phase of an engineering study of littoral processes is to define the problem in terms of littoral processes. The problem may consist of several parts, especially if the interests of local groups are in conflict. An ordering of the relative importance of the different parts may be necessary, and a complete solution may not be feasible. Usually, the problem will be stated in terms of the requirements of the owner or local interests. For example, local interests may require a recreational beach in an area of limited sand, making it necessary to estimate the potential rates of longshore and onshore-offshore sand transport. Or a fishing community may desire a deeper channel in an inlet through a barrier island, making it necessary to study those littoral processes that will affect the stability and long-term navigability of the inlet, as well as the effect of the improved inlet on neighboring shores and the lagoon.

4.811 Sources of Data. The next step is to collect pertinent data. If the problem area is located on a U.S. coastline, the *National Shoreline Study* may be consulted. This study can provide a general description of the area, and may give some indication of the littoral processes occurring in the vicinity of the problem area.

Historical records of shoreline changes are usually in the form of charts, surveyed profiles, dredging reports, beach replenishment reports and aerial photos. As an example of such historical data, Figure 4-52 shows the positions of the shoreline at Sandy Hook, New Jersey, during six surveys from 1835 to 1932. Such shoreline changes are useful for computing longshore transport rates. The Corps of Engineers maintains, in its District and Division offices, survey, dredging, and other reports relating to Corps projects. Charts may be obtained from various federal agencies including the Defense Mapping Agency Hydrographic Center, Geological Survey, National Ocean Survey, and Defense Mapping Agency Topographic Center. A map called "Status of Aerial Photography," which may be obtained from the Map Information Office, Geological Survey, Washington, D.C. 20242, shows the locations and types of aerial photos available for the U.S., and lists the sources from which the photos may be requested. A description of a coastal imagery data bank can be found in the interim report by Szuwalski (1972).

Other kinds of data usually available are wave, tide, and meteorological data. Chapter 3 discusses wave and water level predictions; Section 4.3 discusses the effects of waves on the littoral zone; and Subsection 4.34 presents methods of estimating wave climate and gives possible sources of data. These referenced sections indicate the wave, tide, and storm data necessary to evaluate coastal engineering problems.

Additional information can be obtained from local newspapers, courthouse records, and from area residents. Local people can often identify factors that outsiders may not be aware of, and can also provide qualititive information on previous coastal engineering efforts in the area and their effects.

4.812 Interpretation of Shoreline Position. Preliminary interpretation of littoral processes is possible from the position of the shoreline on aerial photos and charts. Stafford (1971) describes a procedure for utilizing periodic aerial photographs to estimate coastal erosion. Used in conjunction with charts and topographic maps, this technique may provide quick and fairly accurate estimates of shoreline movement, although the results can be biased by the short-term effects of storms.

Charts show the coastal exposure of a study site, and since exposure determines the possible directions from which waves reach the coast, exposure also determines the most likely direction of longshore transport.

Direction of longshore transport may also be indicated by the position of sand accumulation and beach erosion around littoral barriers. A coastal structure in the surf zone may limit or prevent the movement of sand, and the buildup of sediment on one side of the littoral barrier serves as an indicator of the net direction of transport. This buildup can be determined from dredging or sand bypassing records or aerial photos. Figure 4-53 shows the accumulation of sand on one side of a jetty. But wave direction and nearshore currents at the time of the photo indicate that transport then was in the opposite direction. Thus, an erroneous conclusion
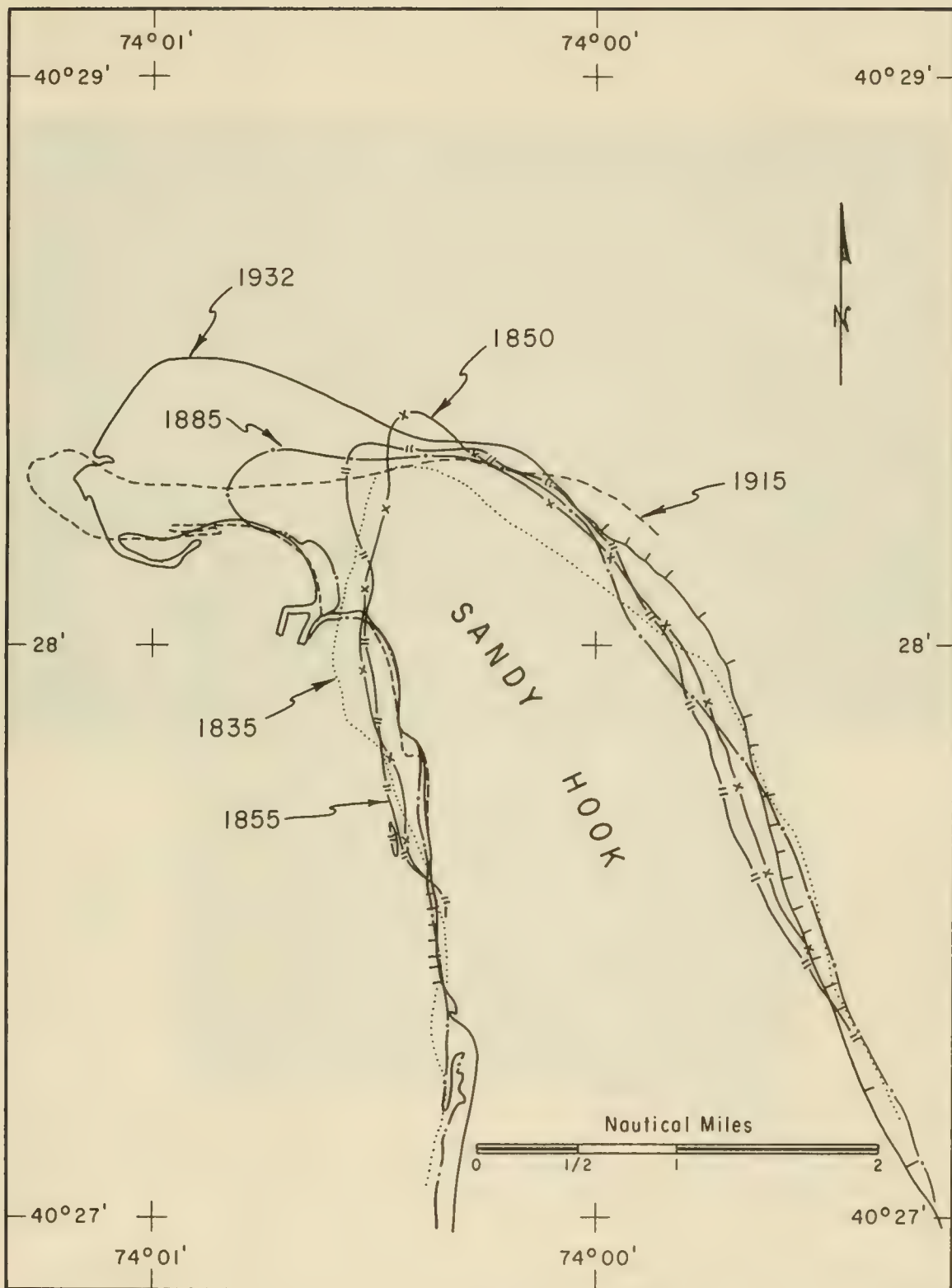
Figure 4-52. Growth of Sandy Hook, New Jersey, 1835-1932

about the net transport might be made, if only wave patterns of this photo are analyzed. The possibility of seasonal or storm-induced reversals in sediment transport direction should be investigated by periodic inspections or aerial photos of the sand accumulation at groins and jetties.

(4 December 1967)

Figure 4-53. Transport Directions at New Buffalo Harbor Jetty on Lake Michigan

The accumulation of sand on the updrift side of a headland is illustrated by the beach north of Point Mugu in Figure 4-54. The tombolo in Figure 4-55 was created by deposition behind an offshore barrier (Greyhound Rock, California). Where a beach is fixed at one end by a structure or natural rock formation, the updrift shore tends to align perpendicular to the direction of dominant wave approach. (See Figures 4-55, and 4-56.) This alignment is less complete along shores with significant rates of longshore transport.

Sand accumulation at barriers to longshore transport may also be used to identify nodal zones. There are two types of nodal zones: divergent and convergent. A divergent nodal zone is a segment of shore characterized by net longshore transport directed away from both ends of the zone. A convergent nodal zone is a segment of shore characterized by net longshore transport directed into both ends of the zone.

Figure 4-56 shows a nodal zone of divergence centered around the fourth groin from the bridge on the south coast of Staten Island, Outer New York Harbor. Central Padre Island, Texas, is thought to be an example

4-142

PACIFIC

OCEAN

Point
Mugu

(21 May 1972)
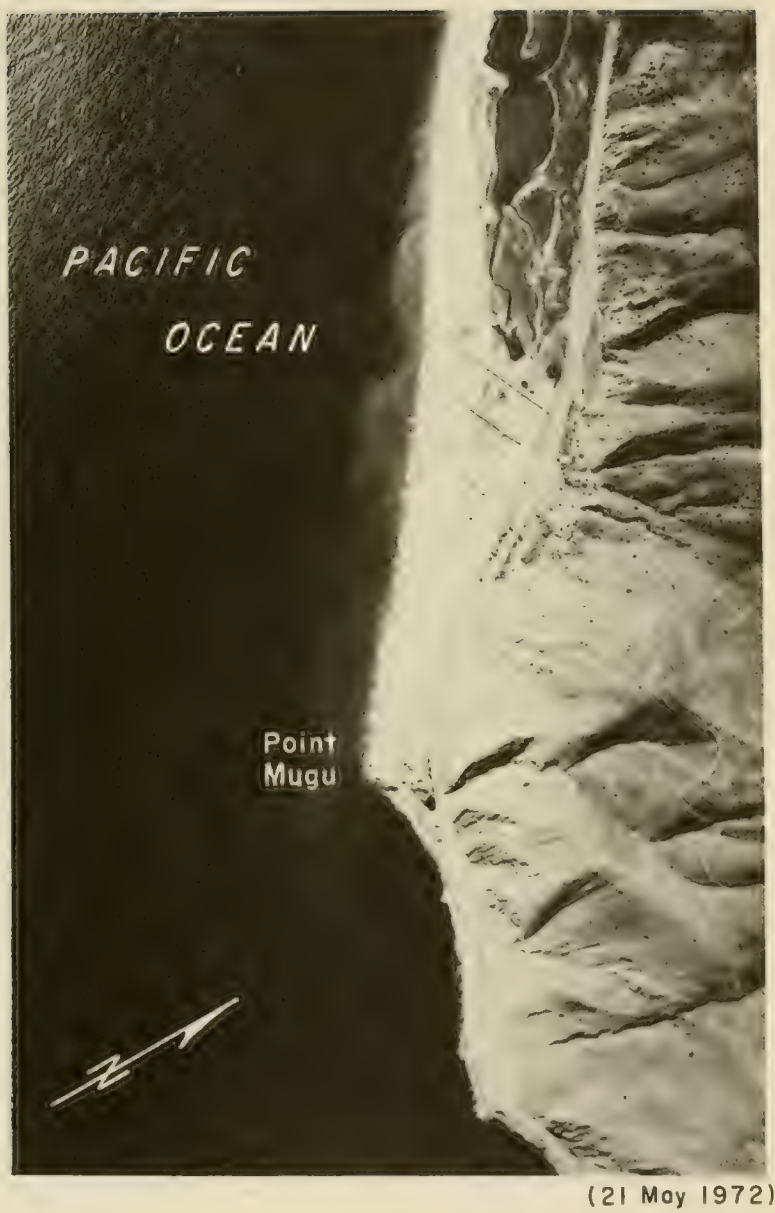
Figure 4-54.   Sand Accumulation at Point Mugu, California

(29 August 1972)

Figure 4-55.   Tombolo and Pocket Beach at Greyhound
Rock, California

(14 September 1969)

Figure 4-56. A Nodal Zone of Divergence Illustrated
by Sand Accumulation at Groins, South
Shore, Staten Island, New York

4-145

of a convergent nodal zone. (Watson, 1971.) Nodal zones of divergence are more common than nodal zones of convergence, because longshore transport commonly diverges at exposed shores and converges toward major gaps in the ocean shore, such as the openings of New York Harbor, Delaware Bay, and Chesapeake Bay.

Nodal zones are usually defined by long-term average transport directions, but because of insufficient data, the location of the mid-point of the nodal zone may be uncertain by up to 10's of miles. In addition, the short-term nodal zone most probably shifts along the coast with changes in wave climate.

The existence, location, and planform of inlets can be used to interpret the littoral processes of the region. Inlets occur where tidal flow is sufficient to maintain the openings against longshore transport which acts to close them. (e.g., Bruun and Gerritsen, 1959.) The size of the inlet opening depends on the tidal prism available to maintain it. (O'Brien, 1969.) The dependence of inlet size on tidal prism is illustrated by Figure 4-57, which shows three bodies of water bordering the beach on the south shore of Long Island, New York. The smallest of these (Sagaponack Pond) is sealed off by longshore transport; the middle one (Mecox Bay) is partly open; and the largest (Shinnecock Bay) is connected to the sea by Shinnecock Inlet, which is navigable.

(14 September 1969)

Figure 4-57. South Shore of Long Island, N.Y., Showing Closed, Partially Closed, and Open Inlets

4-146

Detailed study of inlets through barrier islands on the U.S. Atlantic and gulf coasts shows that the shape of the shoreline at an inlet can be classified in one of four characteristic planforms. (See Figure 4-58, adapted from Galvin, 1971.) Inlets with overlapping offset (Fig. 4-59) occur only where waves from the updrift side dominate longshore transport. Where waves from the updrift side are less dominant, the updrift offset (Fig. 4-59) is common. Where waves approach equally from both sides, inlets typically have negligible offset. (See Figure 4-60.) Where the supply of littoral drift on the updrift side is limited, and the coast is fairly well exposed, a noticeable downdrift offset is common as, for example, in southern New Jersey and southern Delmarva. (See Hayes, et al., (1970.) These planform relations to littoral processes have been found for inlets through sandy barrier islands, but they do not necessarily hold at inlets with rocky boundaries. The relations hold regionally, but temporary local departures due to inlet migration may occur.

4.82 FIELD STUDY

A field study of the problem area is usually necessary to obtain types of data not found in the office study, to supplement incomplete data, and to serve as a check on the preliminary interpretation and correlations made from the office data. Information on coastal processes may be obtained from wave gage data and visual observations, sediment sampling, topographic and bathymetric surveys, tracer programs, and effects of natural and manmade structures.

4.821 Wave Data Collection. A wave-gaging program yields height and period data. However, visual observations may currently be the best source of breaker direction data. Thompson and Harris (1972) determined that 1 year of wave-gage records provides a reliable estimate of the wave height frequency distribution. It is reasonable to assume that the same is true for wave direction.

A visual observation program is inexpensive, and may be used for breaker direction and for regional coverage when few wave-gage records are available. The observer should be provided with instructions, so that all data collected will be uniform, and contact between observer and engineer should be maintained.

4.822 Sediment Sampling. Sediment sampling programs are described in Section 4.26. Samples are usually surface samples taken along a line perpendicular to the shoreline. These are supplemented by borings or cores as necessary. Complete and permanent identification of the sample is important.

4.823 Surveys. Most engineering studies of littoral processes require surveying the beach and nearshore slope. Successive surveys provide data on changes in the beach due to storms, or long-term erosion or accretion. If beach length is also considered, an approximate volume of sand eroded or accreted can be obtained which provides information for the sediment budget of the beach. The envelope of a profile defines
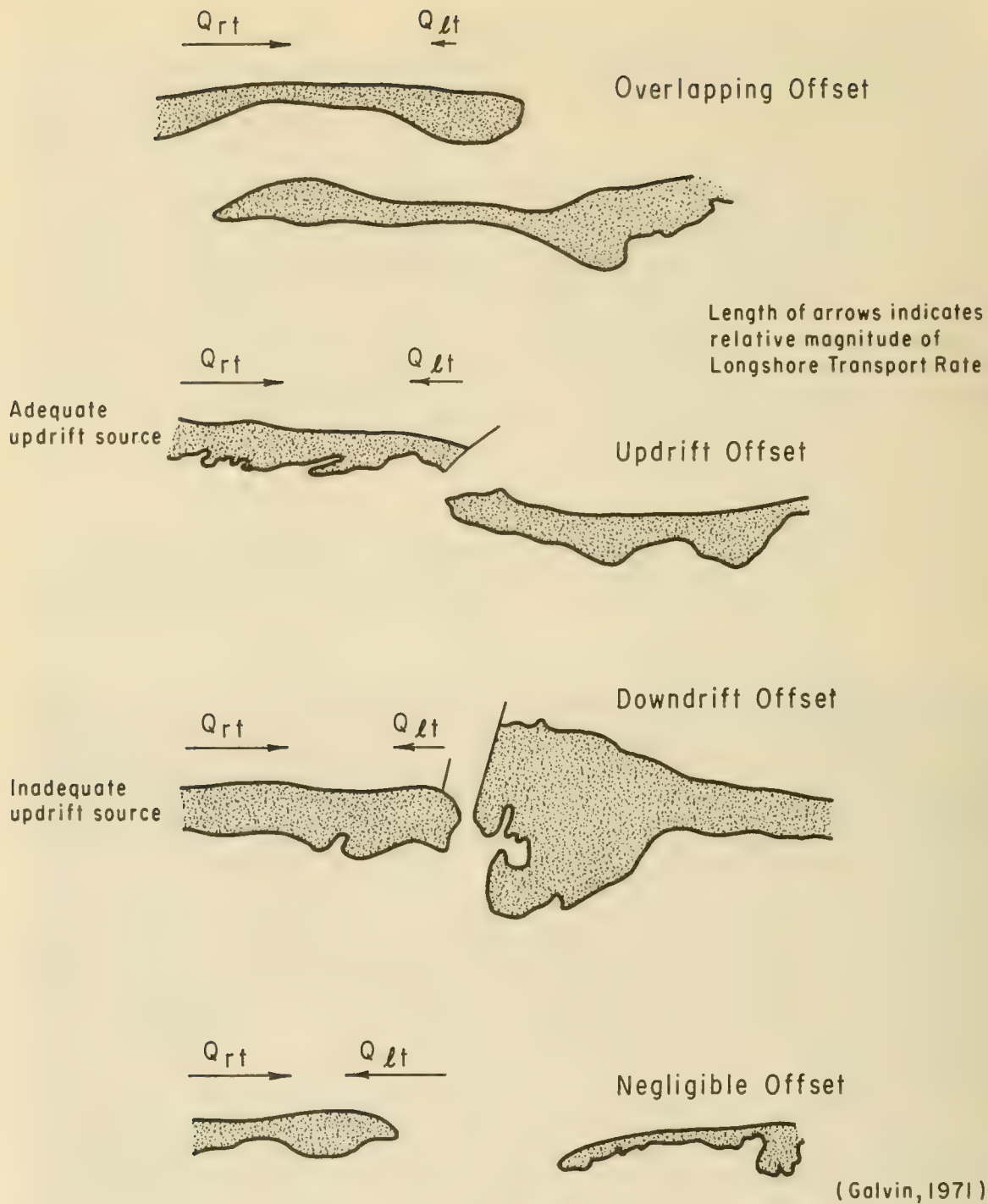
Figure 4-58. Four Types of Barrier Island Offset

BAY

ATLANTIC   OCEAN

(14 September 1969)

Figure 4-59.   Fire Island Inlet, New York - Overlapping Offset

BAY

ATLANTIC   OCEAN

(13 March 1963)

Figure 4-60.   Old Drum Inlet, North Carolina - Negligible Offset

4-149

fluctuations of sand level at a site (Everts, 1973), and thus provides data useful in beach fill and groin design.

Methods for obtaining beach and nearshore profiles, and the accuracy of the resulting profiles are discussed in Section 4.514.

4.824 <u>Tracers</u>. It is often possible to obtain evidence on the direction of sediment movement and the origins of sediment deposits by the use of tracer materials which move with the sediment. Fluorescent tracers were used to study sand migration in and around South Lake Worth Inlet, Florida. (Stuiver and Purpura, 1968.) Radioactive sediment tracer tests were conducted to determine whether potential shoaling material passes through or around the north and south jetties of Galveston Harbor. (Ingram, Cummins, and Simmons, 1965.)

Tracers are particles which react to fluid forces in the same manner as particles in the sediment whose motion is being traced, yet which are physically identifiable when mixed with this sediment. Ideally, tracers must have the same size distribution, density, shape, surface chemistry, and strength as the surrounding sediment, and in addition have a physical property that easily distinguishes them from their neighbors.

Three physical properties have been used to distinguish tracers: radioactivity, color, and composition. Tracers may be either naturally present or introduced by man. There is considerable literature on recent investigations using or evaluating tracers including reviews and bibliography: (Duane and Judge, 1969; Bruun, 1966; Galvin, 1964; and Huston, 1963); models of tracer motion: (James, 1970; Galvin, 1964; Hubbell and Sayre, 1965; and Duane, 1970); and use in engineering problems: (Hart, 1969; Cherry, 1965; Cummins, 1964; and Duane, 1970).

a. <u>Natural Tracers</u>. Natural tracers are used primarily for background information about sediment origin and transport directions, i.e., for studies which involve an understanding of sediment patterns over a long period of time.

Studies using stable, nonradioactive natural tracers may be based on the presence or absence of a unique mineral species, the relative abundance of a particular group of minerals within a series of samples, or the relative abundance and ratios of many mineral types in a series of samples. Although the last technique is the most complex, it is often used, because of the large variety of mineral types normally present in sediments and the usual absence of singularly unique grains. The most suitable natural tracers are grains of a specific rock type originating from a localized specific area.

Occasionally, characteristics other than mineralogy are useful for deducing source and movement patterns. Krinsley, et al., (1964) developed a technique for the study of surface textures of sand grains with electron microscopy, and applied the technique to the study of sand transport along the Atlantic shore of Long Island. Naturally occurring radioactive materials in beach sands have also been used as tracers. (Kamel, 1962.)

One advantage of natural tracers is their tendency to "average" out short-term trends and provide qualitatively accurate historical background information on transport. Their use requires a minimum amount of field work and a minimum number of technical personnel. Disadvantages include the irregularity of their occurrence, the difficulty in distinguishing the tracer from the sediment itself, and a lack of quantitative control on rates of injection. In addition, natural tracers are unable to reveal short-term changes in the direction of transport and changes in material sources.

Judge (1970) found that heavy mineral studies were unsatisfactory as indicators of the direction of longshore transport for beaches between Point Conception and Ventura, California, because of the lack of unique mineral species and the lack of distinct longshore trends which could be used to identify source areas. North of Point Conception, grain size and heavy mineral distribution indicated a net southward movement. Cherry (1965) concluded that the use of heavy minerals as an indicator of the direction of coastal sand movement north of Drakes Bay, California was generally successful.

b. Artificial Tracers. Artificial tracers may be grouped into two general categories: radioactive or nonradioactive. In either case, the tracers represent particles that are placed in an environment selected for study, and are used for relatively short-term studies of sediment dispersion.

While particular experiments employ specific sampling methods and operational characteristics, there are basic elements in all tracing studies. These are: selection of a suitable tracer material, tagging the particle, placing the particle in the environment, and detection of the particle.

Colored glass, brick fragments and oolitic grains are a few examples of nonradioactive particles that have been used as tracers. The most commonly used stable tracer is made by coating indigenous grains with bright colored paint or flourescent dye. (Yasso, 1962; Ingle, 1966; Stuvier and Purpura, 1968; Kidson and Carr, 1962; and Teleki, 1966.) The dyes make the grains readily distinguishable among large sample quantities, but do not significantly alter the physical properties of the grains. The dyes must be durable enough to withstand short-term abrasion. The use of paints and dyes as tracer materials offers advantages over radioactive methods in that they require less sophisticated equipment to tag and detect the grains, and do not require licensing or the same degree of safety precautions. However, less information is obtained for the same costs, and generally in a less timely matter.

When using nonradioactive tracers, samples must be collected and removed from the environment to be analyzed later by physically counting the grains. For fluorescent dyes and paints, the collected samples are viewed under an ultraviolet lamp and the coated grains counted.

For radioactive tracer methods, the tracer may be radioactive at the time of injection or it may be a stable isotope capable of being detected by activation after sampling. The tracer in the grains may be introduced

by a number of methods. Radioactive material has been placed in holes drilled in a large pebble. It has been incorporated in molten glass which, when hardened, is crushed and resized (Sato, et al., 1962; and Taney, 1963). Radioactive material has been plated on the surface of natural sediments. (Stephens, et al., 1968.) Radioactive gas (krypton 85 and xenon 133) has been absorbed into quartz sand. (Chleck, et al., 1963; and Acree, et al., 1969.)

In 1966, the Coastal Engineering Research Center, in cooperation with the Atomic Energy Commission, initiated a multiagency program to create a workable radioisotopic sand tracing (RIST) program, for use in the littoral zone. (Duane and Judge, 1969.) Tagging procedures (by surface plating with gold 198-199), instrumentation, field surveys and data handling techniques were developed which permit collection and analysis of over 12,000 bits of information per hour over a survey track about 18,000 feet long.

These recent developments in radioactive tracing permit *in situ* observations and faster data collection over much larger areas (Duane, 1970) than has been possible using fluorescent or stable isotope tracers. However, operational and equipment costs of radionuclide tracer programs can be high.

Accurate determination of long-term sediment transport volume is not yet possible from a tracer study, but qualitative data on sediment movement useful for engineering purposes can be obtained.

Experience has shown that tracer tests can give information on direction of movement, dispersion, shoaling sources, relative velocity and movement in various areas of the littoral zone, means of natural bypassing, and structure efficiency. Reasonably quantitative data on movement or shoaling rates can be obtained for short-time intervals. It should be emphasized that this type of information must be interpreted with care, since the data are generally determined by short-term littoral transport phenomena. However, tracer studies conducted repeatedly over several years at the same location could result in estimates of longer term littoral transport.

4.83 SEDIMENT TRANSPORT CALCULATIONS

4.831 Longshore Transport Rate. The example calculation of a sediment budget in Section 4.76 is typical in that the magnitude of the longshore transport rate exceeds by a considerable margin any other element in the budget. For this reason, it is essential to have a good estimate of the longshore transport rate in an engineering study of littoral processes.

A complete description of the longshore transport rate requires knowledge of two of the five variables

$$\left(Q_{rt}, Q_{\ell t}, Q_g, Q_n, \gamma\right),$$

defined by Equations 4-21, 4-22, and 4-23. If any two are known, the remaining three can be obtained from the three equations.

Section 4.531 describes four methods for estimating longshore transport rate, and Sections 4.532 through 4.535 describe in detail how to use two of these four methods. (See Methods 3 and 4.)

One approach to estimating longshore transport rate is to adopt a proven estimate from a nearby locality, after making allowances for local conditions. (See Method 1.) It requires considerable engineering judgement to determine whether the rate given for the nearby locality is a reliable estimate, and, if reliable, how the rate needs to be adjusted to meet the changed conditions at the new locality.

Method 2 is an analysis of historical data. Such data may be found in charts, maps, aerial photography, dredging records, beach fill records, and related information. Section 4.811 describes some of these sources.

To apply Method 2, it is necessary to know or assume the transport rate across one end of the littoral zone being considered. The most successful applications of Method 2 have been where the littoral zone is bounded on one end by a littoral barrier which is assumed to completely block all longshore transport. The existence of such a complete littoral barrier implies that the longshore transport rate is zero across the barrier, and this satisfies the requirement that the rate be known across the end of the littoral zone being considered. Examples of complete littoral barriers include large jetties immediately after construction, or spits building into deep quiet water.

Data on shoreline changes permit estimates of rates of erosion and accretion that may give limits to the longshore transport rate. Figure 4-50 is a shoreline change map which was used to obtain the rate of transport at Sandy Hook, New Jersey. (Caldwell, 1966.)

Method 3 (the energy flux method) is described in Section 4.532 with a worked example in Section 4.533. Method 4 (the empirical prediction of gross longshore transport rate) is described in Section 4.534 with a worked example in Section 4.535. The essential factor in Methods 3 and 4, and often in Method 1, is the availability of wave data. Wave data applicable to studies of littoral processes are discussed in detail in Section 4.3.

4.832 <u>Onshore-Offshore Motion</u>. Typical problems requiring knowledge of onshore-offshore sediment transport are described in Section 4.511. Four classes of problems are treated:

(1) The seaward limit of significant sediment transport. Available field data and theory suggest that waves are able to move sand during some days of the year over most of the Continental Shelf. However, field evidence from bathymetry and sediment size distribution suggest that the zone of significant sediment transport is confined close to shore where bathymetric contours approximately parallel the shoreline. The depth to the deepest shore-parallel contour tends to increase with average wave height, and typically varies from 15 to 60 feet.

(2) Sediment transport in the nearshore zone. Seaward of the breakers, sand is set in motion by waves moving over ripples, either rolling the sand as bed load, or carrying it up in vortices as suspended load. The sand, once in motion, is transported by mean tidal and wind-induced currents and by the mass transport velocity due to waves. The magnitude and direction of the resulting sediment transport are uncertain under normal circumstances, although mass transport due to waves is more than adequate to return sand lost from the beach during storms. It appears that bottom mass transport acts to keep the sand close to the shore, but that some material, probably finer sand, escapes offshore as the result of the combined wind- and wave-induced bottom currents.

(3) The shape and expectable changes in shape of nearshore and beach profiles. Storms erode beaches to produce a simple concave-up beach profile with deposition of the eroded material offshore. Rates of erosion due to individual storms vary from a few cubic yards per foot to 10's of cubic yards per foot of beach front. The destructiveness of the storm in producing erosion depends on its intensity, duration, and orientation, especially as these factors affect the elevation of storm surge and the wave height and direction. Immediately after a storm, waves begin to return sediment to the eroded beach, either through the motion of bar-and-trough (ridge-and-runnel) systems, or by berm building. The parameter, $F_O = H_O/(V_f T)$, given by Equation 4-20 determines whether the beach erodes or accretes under given conditions. If F_O is above critical value between 1 and 2 the beach erodes. (See Figures 4-29, and 4-30.)

(4) The slope of the foreshore. There is a tendency for the foreshore to become steeper as grain size increases, and to become flatter as mean wave height increases. Data for this relation exhibit much scatter and quantitative relationships are difficult to predict.

4.833 Sediment Budget. Section 4.76 summarizes material on the sediment budget. Table 4-14 tabulates the elements of the sediment budget and indicates the importance of each element. Table 4-13 classifies the elements of the sediment budget.

A sediment budget carefully defines the littoral control volume, identifies all elements transferring sediment to or from the littoral control volume, ranks the elements by their magnitude, and provides an estimate of unknown rates by the balancing of additions against losses (Equation 4-46).

If prepared with sufficient data and experience, the budget permits an estimate of how proposed improvements will affect neighboring segments of the littoral zone.

ACREE, E.H., et al., "Radioisotopic Sand Tracer Study (RIST), Status Report for May 1966-April 1968," OkNL-4341, Contract No. W-7405-eng-26, Oak Ridge National Laboratory (operated by Union Carbide Corp., for the U.S. Atomic Energy Commission), 1969.

AKYUREK, M., "Sediment Suspension by Wave Action Over a Horizontal Bed," Unpublished Thesis, University of Iowa, Iowa City, Iowa, July 1972.

ARTHUR, R.S., "A Note on the Dynamics of Rip Currents," *Journal of Geophysical Research*, Vol. 67, No. 7, July 1962.

AYERTON, H, "The Origin and Growth of Ripple Marks," *Philosophical Transactions of the Royal Society of London*, Ser. A, Vol. 84, 1910, pp. 285-310.

BAGNOLD, R.A., "Mechanics of Marine Sedimentation," *The Sea*, Vol. 3, Wiley, New York, 1963, pp. 507-528.

BAJORUNAS, L., and DUANE, D.B., "Shifting Offshore Bars and Harbor Shoaling," *Journal of Geophysical Research*, Vol. 72, 1967, pp. 6195-6205.

BASCOM, W.N., "The Relationship Between Sand Size and Beach-Face Slope," *Transactions of the American Geophysical Union*, Vol. 32, No. 6, 1951.

BASCOM, W.N., *Manual of Amphibious Oceanography*, Vol. 2, Sec. VI, University of California, Berkeley, Calif., 1952.

BASCOM, W.N., "Waves and Beaches," *Beaches*, Ch. IX, Doubleday, New York, 1964, pp. 184-212.

BASH, B.F., "Project Transition; 26 April to 1 June 1972," Unpublished Research Notes, U.S. Army, Corps of Engineers, Coastal Engineering Research Center, Washington, D.C., 1972.

BERG, D.W., "Systematic Collection of Beach Data," *Proceedings of the 11th Conference on Coastal Engineering*, London, Sept. 1968.

BERG, D.W., and DUANE, D.B., "Effect of Particle Size and Distribution on Stability of Artificially Filled Beach, Presque Isle Penninsula, Pennsylvania," *Proceedings of the 11th Conference Great Lakes Research*, April 1968.

BERTMAN, D.Y., SHUYSKIY, Y.D., and SHKARUPO I.V., "Experimental Study of Beach Dynamics as a Function of the Prevailing Wind Direction and Speed," Oceanology, Translation of the Russian Journal, *Okeanologiia* (Academy of Sciences of the U.S.S.R.), Vol. 12, Feb. 1972.

BIGELOW, H.B., and EDMONDSON, W.T., "Wind Waves at Sea Breakers and Surf," H.O. 602, U.S. Navy Hydrographic Office, Washington, D.C., 1947.

BIJKER, E.W., "Bed Roughness Influence on Computation of Littoral Drift," *Abstracts of the 12th Coastal Engineering Conference*, Washington, D.C., 1970.

BODINE, B.R., "Hurricane Surge Frequency Estimated for the Gulf Coast of Texas," TM-26, U.S. Army, Corps of Engineers, Coastal Engineering Research Center, Washington, D.C., Feb. 1969.

BOWEN, A.J., and INMAN, D.L., "Budget of Littoral Sands in the Vicinity of Point Arguello, California," TM-19, U.S. Army, Corps of Engineers, Coastal Engineering Research Center, Washington, D.C., Dec. 1966.

BOWMAN, R.S., "Sedimentary Processes Along Lake Erie Shore: Sandusky Bay, Vicinity of Willow Point," in "Investigations of Lake Erie Shore Erosion," Survey 18, Ohio Geological Survey, 1951.

BRETSCHNEIDER, C.L., "Fundamentals of Ocean Engineering - Part 1 - Estimating Wind Driven Currents Over the Continental Shelf," *Ocean Industry*, Vol. 2, No. 6, June 1967, pp. 45-48.

BRETSCHNEIDER, C.L., "Field Investigations of Wave Energy Loss in Shallow Water Ocean Waves," TM-46, U.S. Army, Corps of Engineers, Beach Erosion Board, Washington, D.C., Sept. 1954.

BRETSCHNEIDER, C.L., and REID, R.O., "Modification of Wave Height Due to Bottom Friction, Percolation, and Refraction," TM-45, U.S. Army, Corps of Engineers, Beach Erosion Board, Washington, D.C., Oct. 1954.

BRICKER, O.P., ed., *Carbonate Sediments*, No. 19, The Johns Hopkins University Studies in Geology, 1971, 376 pp.

BROWN, E.I., "Inlets on Sandy Coasts," *Proceedings of the American Society of Civil Engineers*, ASCE, Vol. 54, 1928, pp. 505-553.

BRUUN, P., "Sea-Level Rise as a Cause of Shore Erosion," *Journal of the Waterways and Harbors Division*, ASCE, Vol. 88, WW1, Feb. 1962, pp. 117-130.

BRUUN, P., "Longshore Currents and Longshore Troughs," *Journal of Geophysical Research*, Vol. 68, 1963, pp. 1065-1078.

BRUUN, P., "Use of Tracers in Coastal Engineering," *Shore and Beach*, No. 34, pp. 13-17, Nuclear Science Abstract, 20:33541, 1966.

BRUUN, P. and GERRITSEN, F., "Natural Bypassing of Sand at Inlets," *Journal of the Waterways and Harbors Division*, ASCE, Dec. 1959.

BUMPUS, D.F., "Residual Drift Along the Bottom on the Continental Shelf in the Middle Atlantic Bight," *Limnology and Oceanography*, 75th Anniversary Vol., Supplement to Vol. X, 1965.

BYRNE, R.J., "Field Occurrences of Induced Multiple Gravity Waves," *Journal of Geophysical Research*, Vol. 74, No. 10, May 1969, pp. 2590-2596.

CALDWELL, J.M., "Wave Action and Sand Movement Near Anaheim Bay, California," TM-68, U.S. Army, Corps of Engineers, Beach Erosion Board, Washington, D.C., Feb. 1956.

CALDWELL, J.M., "Shore Erosion by Storm Waves," MP 1-59, U.S. Army, Corps of Engineers, Beach Erosion Board, Washington, D.C., Apr. 1959.

CALDWELL, J.M., "Coastal Processes and Beach Erosion," *Journal of the Boston Society of Civil Engineers*, Vol. 53, No. 2, Apr. 1966, pp. 142-157.

CARSTENS, M.K., NEILSON, M., and ALTINBILEK, H.D., "Bed Forms Generated in the Laboratory Under an Oscillatory Flow: Analytical and Experimental Study," TM-28, U.S. Army, Corps of Engineers, Coastal Engineering Research Center, Washington, D.C., June 1969.

CARTWRIGHT, D.E., "A Comparison of Instrumental and Visually Estimated Wave Heights and Periods Recorded on Ocean Weather Ships," National Institute of Oceanography, Oct. 1972.

CASTANHO, J., "Influence of Grain Size on Littoral Drift," *Abstracts of the 12th Coastal Engineering Conference*, Washington, D.C., 1970.

CHERRY, J., "Sand Movement along a Portion of the Northern California Coast," TM-14, U.S. Army, Corps of Engineers, Coastal Engineering Research Center, Oct. 1965.

CHLECK, D., et al., "Radioactive Kryptomates," *International Journal of Applied Radiation and Isotopes*, Vol. 14, 1963, pp. 581-610.

CHOW, V.T., ed., *Handbook of Applied Hydrology*, McGraw-Hill, New York, 1964.

COLBY, B.C., and CHRISTENSEN, R.P., "Visual Accumulation Tube for Size Analysis of Sands," *Journal of the Hydraulics Division*, ASCE, Vol. 82, No. 3, June 1956.

COLONY, R.J., "Source of the Sands on South Shore of Long Island and the Coast of New Jersey," *Journal of Sedimentary Petrology*, Vol. 2, 1932, pp. 150-159.

COOK, D.O., "Sand Transport by Shoaling Waves," Ph.D. Thesis, University of Southern California, University Microfilms, Ann Arbor, Mich., 1970.

COOK, D.O., and GORSLINE, D.S., "Field Observations of Sand Transport by Shoaling Waves," *Marine Geology*, Vol. 13, No. 1, 1972.

COOPER, W.S., "Coastal Sand Dunes of Oregon and Washington," Memoir No. 72, Geological Society of America, June 1958.

COOPERATIVE FEDERAL INTER-AGENCY PROJECT, "Methods of Analyzing Sediment Samples," Report No. 4, St. Paul U.S. Engineer District Sub-Office, Hydraulic Laboratory, University of Iowa, Iowa City, 1941.

CRICKMORE, J.M., and WATERS, C.B., "The Measurement of Offshore Shingle Movement," *13th International Conference on Coastal Engineering*, Vancouver, B.C., Canada, July 1972.

CUMMINS, R.S., Jr., "Radioactive Sediment Tracer Tests, Cape Fear River, North Carolina," MP No. 2-649, Waterways Experiment Station, U.S. Army, Corps of Engineers, Vicksburg, Miss., May 1964.

CURRAY, J.R., "Late Quarternary History, Continental Shelves of the United States," *The Quarternary of the U.S.*, Princeton University Press, Princeton, N.J., 1965, pp. 723-735.

DABOLL, J.M., "Holocene Sediments of the Parker River Estuary, Massachusetts," Contribution No. 3-CRG, Department of Geology, University of Massachusetts, June 1969.

DARLING, J.M., "Surf Observations Along the United States Coasts," *Journal of the Waterways and Harbors Division*, ASCE, WW1, Feb. 1968, pp. 11-21.

DARLING, J.M., and DUMM, D.G., "The Wave Record Program at CERC," MP 1-67, U.S. Army, Corps of Engineers, Coastal Engineering Research Center, Washington, D.C., Jan. 1967.

DAS, M.M., "Longshore Sediment Transport Rates: A Compilation of Data," MP 1-71, U.S. Army, Corps of Engineers, Coastal Engineering Research Center, Washington, D.C., Sept. 1971.

DAS, M.M., "Suspended Sediment and Longshore Sediment Transport Data Review," *13th International Conference on Coastal Engineering*, Vancouver, B.C., Canada, July 1972.

DAVIS, R.A., Jr., "Sedimentation in the Nearshore Environment, Southeastern Lake Michigan," Thesis, University of Illinois, Urbana, Illinois, 1964.

DAVIS, R.A., Jr., "Beach Changes on the Central Texas Coast Associated with Hurricane Fern, September 1971," Vol. 16, Contributions in Marine Science, University of Texas, Marine Science Institute, Port Aransas, Tex., 1972.

DAVIS, R.A., Jr., and FOX, W.T., "Beach and Nearshore Dynamics in Eastern Lake Michigan," TR No. 4, ONR Task No. 388-092/10-18-68, (414), Office of Naval Research, Washington, D.C., June 1971.

DAVIS, R.A., Jr., and FOX, W.T., "Coastal Processes and Nearshore Sand Bars," *Journal of Sedimentary Petrology*, Vol. 42, No. 2, June 1972, pp. 401-412.

DAVIS, R.A., Jr., and FOX, W.T., "Four-Dimensional Model for Beach and Inner Nearshore Sedimentation," *The Journal of Geology*, Vol. 80, No. 4, July 1972.

DAVIS, R.A., Jr., et al., "Comparison of Ridge and Runnel Systems in Tidal and Non-Tidal Environments," *Journal of Seidmentary Petrology*, Vol. 42, No. 2, June 1972, pp. 413-421.

DAVIS, R.A., Jr., and MCGEARY, D.F.R., "Stability in Nearshore Bottom Topography and Sedimentary Distribution, Southeastern Lake Michigan," *Proceedings of the Eighth Conference on Great Lakes Research*, Pub. No. 13, Great Lakes Research Division, University of Michigan, Ann Arbor, Mich., 1965.

DEAN, R.G., "Relative Validities of Water Wave Theories," *Journal of the Waterways and Harbors Division*, ASCE, Vol. 96, WW1, 1970, pp. 105-119.

DEAN, R.G., "Storm Characteristics and Effects," *Proceedings of Seminar on Planning and Engineering in the Coastal Zone*, published by Coastal Plains Center for Marine Development Services, Wilmington, N.C., 1972.

DEAN, R.G., "Heuristic Models of Sand Transport in the Surf Zone," *Conference on Engineering Dynamics in the Coastal Zone*, 1973.

DEWALL, A.E., "The 17 December 1970 East Coast Storm Beach Changes," Unpublished Manuscript, U.S. Army, Corps of Engineers, Coastal Engineering Research Center, Washington, D.C., 1972.

DEWALL, A.E., PRITCHETT, P.C., and GALVIN, C.J., Jr., "Beach Changes Caused by a Northeaster Along the Atlantic Coast," *Abstracts from the Annual Meeting of the Geological Society of America*, Washington, D.C., 1971.

DEWALL, A.E., and RICHTER, J.J., "Beach Changes at Boca Raton, Florida," Annual Meeting of the American Shore and Beach Preservation Association, (presentation only) Fort Lauderdale, Fla., Aug. 1972.

DIETZ, R.S., "Wave Base, Marine Profile of Equilibrium, and Wave-Built Terraces: A Critical Appraisal," *The Geological Society of America Bulletin*, Vol. 74, No. 8, Aug. 1963, pp. 971-990.

DILL, R.F., "Sedimentation and Erosion in Scripps Submarine Canyon Head," *Papers in Marine Geology*, Shepard Commemorative Volume, Macmillan, New York, 1964.

DIVOKY, D., LeMEHAUTE, B., and LIN, A., "Breaking Waves on Gentle Slopes," *Journal of Geophysical Research*, Vol. 75, No. 9, 1970.

DOLAN, R., "Barrier Dune System Along the Outer Banks of North Carolina: A Reappraisal," *Science*, 1972, pp. 286-288.

DOLAN, R., "Barrier Islands: Natural and Controlled," in "Coastal Geomorphology," *Proceedings of the Third Annual Geomorphology Symposia Series*, 1973, pp. 263-278.

DOLAN, R., FERM, J.C., and McARTHUR, L.S., "Measurements of Beach Process Variables, Outer Banks, North Carolina," TR No. 64, Coastal Studies Institute, Louisiana State University, Baton Rouge, La., Jan. 1969.

DRAPER, L., "Wave Activity at the Sea Bed Around Northwestern Europe," *Marine Geology*, Vol. 5, 1967, pp. 133-140.

DUANE, D.B., "Sand Deposits on the Continental Shelf: A Presently Exploitable Resource," *Transactions of National Symposium on Ocean Sciences and Engineering of the Atlantic Shelf*, Marine Technology Society, Mar. 1968.

DUANE, D.B., "Synoptic Observations of Sand Movement," *Proceedings of the 12th Coastal Engineering Conference*, Washington, D.C. September 1970.

DUANE, D.B., "Tracing Sand Movement in the Littoral Zone: Progress in the Radioisotopic Sand Tracer (RIST) Study, July 1968- February 1969," MP 4-70, U.S. Army, Corps of Engineers, Coastal Engineering Research Center, Washington, D.C., Aug. 1970.

DUANE, D.B., et al., "Linear Shoals on the Atlantic Inner Continental Shelf, Florida to Long Island," *Shelf Sediment Transport*, edited by Swift, Duane, and Pilkey; Dowden, Hutchinson, and Ross, Stroudsburg, Pa. 1972.

DUANE, D.B., and JUDGE, C.W., "Radioisotopic Sand Tracer Study, Point Conception, California," MP 2-69, U.S. Army, Corps of Engineers, Coastal Engineering Research Center, Washington, D.C., May 1969.

DUANE, D.B., and MEISBURGER, E.P., "Geomorphology and Sediments of the Nearshore Continental Shelf, Miami to Palm Beach, Florida," TM-29, U.S. Army, Corps of Engineers, Coastal Engineering Research Center, Washington, D.C., Nov. 1969.

DUBOIS, R.N., "Inverse Relation Between Foreshore Slope and Mean Grain Size as a Function of the Heavy Mineral Content," *Geological Society of America Bulletin*, Vol. 83, Mar. 1972, pp. 871-876.

DUNN, G.E., and MILLER, B.I., *Atlantic Hurricanes*, Louisiana State University Press, Baton Rouge, 1964, pp. 204, 257-258.

EAGLESON, P.S., "Properties of Shoaling Waves by Theory and Experiment," *Transactions of the American Geophysical Union*, Vol. 37, 1956, pp. 565-572.

EAGLESON, P.S., and DEAN, R.G., "Wave-Induced Motion of Discrete Bottom Sediment Particles," *Proceedings of the American Society of Civil Engineers*, Vol. 85, No. HY10, 1959.

EAGLESON, P.S., and DEAN, R.G., "A Discussion of 'The Supply and Loss of Sand to the Coast' by J.W. Johnson," *Journal of the Waterways and Harbors Division*, ASCE, Vol. 86, No. WW2, June 1960.

EATON, R.O., "Littoral Processes on Sandy Coasts," *Proceedings of the First Conference on Coastal Engineering,* Council on Wave Research, Engineering Foundation, Oct. 1950.

EMERY, K.O., "The Sea off Southern California," *Sediments,* Ch. 6, Wiley, New York, 1960, pp. 180-295.

EMERY, K.O., "A Simple Method of Measuring Beach Profiles," *Limnology and Oceanography,* Vol. 6, No. 1, 1961, pp. 90-93.

EVANS, O.F., "The Classification of Wave-Formed Ripple-Marks," *Journal of Sedimentary Petrology,* Vol. 11, No. 1, Apr. 1941, pp. 37-41.

EVERTS, C.H., "A Rational Approach to Marine Placers," Unpublished Ph.D. Thesis, University of Wisconsin, Madison, Wis., 1971.

EVERTS, C.H., "Geometry of Profiles Across Some Inner Continental Shelves of the United States," Unpublished Research Paper, U.S. Army, Corps of Engineers, Coastal Engineering Research Center, Washington, D.C., 1972.

EVERTS, C.H., "Particle By-Passing on Loose, Flat Granular Boundaries," *Transactions of the American Geophysical Union,* Vol. 53, No. 4, Apr. 1972.

EVERTS, C.H., "Beach Profile Changes in Western Long Island," in "Coastal Geomorphology," *Proceedings of the Third Annual Geomorphology Symposia Series,* 1973, pp. 279-301.

FAIRCHILD, J.C., "Development of a Suspended Sediment Sampler for Laboratory Use Under Wave Action," *Bulletin of the Beach Erosion Board,* Vol. 10, No. 1, July 1956.

FAIRCHILD, J.C., "Suspended Sediment Sampling in Laboratory Wave Action," TM-115, U.S. Army, Corps of Engineers, Beach Erosion Board, Washington, D.C., June 1959.

FAIRCHILD, J.C., "Laboratory Tests of Longshore Transport," *Proceedings of the 12th Conference on Coastal Engineering,* ASCE, 1970.

FAIRCHILD, J.C., "Longshore Transport of Suspended Sediment," *Proceedings of the 13th Coastal Engineering Conference,* Vancouver, B.C., Canada, July 1972.

FISHER, C.H., "Mining the Ocean for Beach Sand," *Proceedings of Civil Engineering in the Oceans II,* ASCE, Dec. 1969.

FOLK, R.L., *Petrology of Sedimentary Rocks,* Hemphill's, Austin Tex., 1965.

FOLK, R.L., "A Review of Grain Size Parameters," *Sedimentology,* Vol. 6, 1966, pp. 73-93.

FOLK, R.L., and WARD, W.C., "Brazos River Bar. A Study in the Signifi-
    cances of Grain Size Parameters," *Journal of Sedimentary Petrology*,
    Vol. 27, 1957, pp. 3-26.

FOX, W.T., "Anatomy of a Storm on the Lake Michigan Coast," Unpublished
    Paper, *Conference on Effects of Extreme Conditions on Coastal Environ-
    ments*, Western Michigan University, Nov. 1970.

GAGE, B.O., "Experimental Dunes of the Texas Coast," MP 1-70, U.S. Army,
    Corps of Engineers, Coastal Engineering Research Center, Washington,
    D.C., Jan. 1970.

GALVIN, C.J., Jr., "Experimental and Theoretical Study of Longshore Cur-
    rents on a Plane Beach," Unpublished Ph.D. Thesis, Department of Geolo-
    gy and Geophysics, Massachusetts Institute of Technology, Cambridge,
    Mass., 1963.

GALVIN, C.J., Jr., "A Theoretical Distribution of Waiting Times for Tracer
    Particles on Sand Bed," Vol. I, Bulletin and Summary of Research Pro-
    gress, Fiscal Year 1964, U.S. Army, Corps of Engineers, Coastal
    Engineering Research Center, Washington, D.C., 1964.

GALVIN, C.J. Jr., "A Selected Bibliography and Review of the Theory and
    Use of Tracers in Sediment Transport Studies," Vol. I, Bulletin and
    Summary Report of Research Progress, Fiscal Year 1964, U.S. Army,
    Corps of Engineers, Coastal Engineering Research Center, Washington,
    D.C., 1964.

GALVIN, C.J., Jr., "Longshore Current Velocity: A Review of Theory and
    Data," *Reviews of Geophysics*, Vol. 5, No. 3, Aug. 1967.

GALVIN, C.J., Jr., "A Gross Longshore Transport Rate Formula," *Proceedings
    of the 13th Coastal Engineering Conference*, Vancouver, B.C., Canada,
    July 1972.

GALVIN, C.J., Jr., "Wave Breaking in Shallow Water," *Waves on Beaches and
    Resulting Sediment Transport*, Academic Press, March 1972.

GALVIN, C.J., Jr., "Finite-Amplitude, Shallow Water-Waves of Periodically
    Recurring Form," *Proceedings of the Symposium on Long Waves*, University
    of Delaware, Sept. 1970.

GALVIN, C.J., "Wave Climate and Coastal Processes," *Water Environments and
    Human Needs*, A.T. Ippen, Ed., M.I.T. Parsons Laboratory for Water
    Resources and Hydrodynamics, Cambridge, Mass., 1971., pp. 48-78.

GALVIN C.J., Jr., and EAGLESON, P.S., "Experimental Study of Longshore
    Currents on a Plane Beach," TM-10, U.S. Army, Corps of Engineers,
    Coastal Engineering Research Center, Washington, D.C., Jan. 1965.

GALVIN, C.J., and NELSON, R.A., "A Compilation of Longshore Current Data,"
    MP 2-67, U.S. Army, Corps of Engineers, Coastal Engineering Research
    Center, Washington, D.C., Mar. 1967.

GALVIN, C.J., and SEELIG, W.N., "Surf on U.S. Coastline," Unpublished Research Paper, U.S. Army, Corps of Engineers, Coastal Engineering Research Center, Washington, D.C., Aug. 1969.

GALVIN, C.J., and SEELIG, W.N., "Nearshore Wave Direction from Visual Observation," *Transactions of the American Geophysical Union*, Vol. 52, No. 4, Apr. 1971.

GIBBS, R.J., "The Geochemistry of the Amazon River System: Part I. The Factors that Control the Salinity and the Composition and Concentration of the Suspended Solids," *Geological Society of America Bulletin*, Vol. 78, Oct. 1967, pp. 1203-1232.

GIBBS, R.J., "The Accuracy of Particle-Size Analysis Utilizing Settling Tubes," *Journal of Sedimentary Petrology*, Vol. 42, No. 1, Mar. 1972.

GILES, R.T., and PILKEY, O.H., "Atlantic Beach and Dune Sediments of the Southern United States," *Journal of Sedimentary Petrology*, Vol. 35, No. 4, Dec. 1965, pp. 900-910.

GODA, Y., "A Synthesis of Breaker Indices," *Proceedings of the Japan Society of Civil Engineers*, No. 180, Aug. 1970.

GODFREY, P.J., and GODFREY, M.M., "Comparison of Ecological and Geomorphic Interactions Between Altered and Unaltered Barrier Island Systems in North Carolina," in "Coastal Geomorphology," *Proceedings of the Third Annual Geomorphology Symposia Series*, 1972, pp. 239-258.

GOLDSMITH, V., COLONELL, J.M., and TURBIDE, P.W., "Forms of Erosion and Accretion on Cape Cod Beaches," *Proceedings of the 13th International Conference on Coastal Engineering*, Vancouver, B.C., July 1972.

GONZALES, W.R., "A Method for Driving Pipe in Beach Rock," Vol. III, Bulletin and Summary of Research Progress, Fiscal Years 1967-69, U.S. Army, Corps of Engineers, Coastal Engineering Research Center, Washington, D.C., July 1970.

GRAF, W.H., *Hydraulics of Sediment Transport*, McGraw-Hill, New York, 1971.

GRAHAM, H.E., and NUNN, D.E., "Meteorological Considerations Pertinent to Standard Project Hurricane, Atlantic and Gulf Coasts of the United States," National Hurricane Research Project Report No. 33, U.S. Department of Commerce, Weather Bureau, Washington, D.C., Nov., 1959.

GRIFFITHS, J.C., *"Scientific Method in Analysis of Sediments,"* McGraw-Hill, New York, 1967.

HALL, J.V., and HERRON, W.J., "Test of Nourishment of the Shore by Offshore Deposition of Sand," TM-17, U.S. Army, Corps of Engineers, Beach Erosion Board, Washington, D.C., June 1950.

HALLERMEIER, R.J., and GALVIN, C.J., "Wave Height Variation Around Vertical Cylinders," *Transactions of the American Geophysical Union*, 53rd Annual Meeting, 1972, p. 397.

HANDIN, J.W., "The Source, Transportation, and Deposition of Beach Sediment in Southern California," TM-22, U.S. Army, Corps of Engineers, Beach Erosion Board, Washington, D.C., Mar. 1951.

HANDS, E.B., "A Geomorphic Map of Lake Michigan Shoreline," *Proceedings of the 13th Conference on Great Lakes Research*, International Association Great Lakes Research, 1970, pp. 250-265.

HANDS, E.B., "Anomalous Sand Size-Swash Slope Relationship," Unpublished MFR, U.S. Army, Corps of Engineers, Coastal Engineering Research Center, Washington, D.C., Apr. 1972.

HARRIS, D.L., "The Analysis of Wave Records," *Proceedings of the Conference on Coastal Engineering*, Washington, D.C., 1970, pp. 85-100.

HARRIS, D.L., "Characteristics of Wave Records in the Coastal Zone," *Waves on Beaches and Resulting Sediment Transport*, Academic Press, 1972.

HARRIS, D.L., "Wave Estimates for Coastal Regions," *Shelf Sediment Transport*, edited by Swift, Duane, and Pilkey. Dowden, Hutchinson, and Ross, Stroudsburg, Pa., 1972.

HARRISON, W., et al., "Circulation of Shelf Waters off the Chesapeake Bight," ESSA Professional Paper 3, U.S. Dept. of Commerce, Washington, D.C., June 1967.

HARRISON, W., and WAGNER, K.A., "Beach Changes at Virginia Beach, Virginia," MP 6-64, U.S. Army, Corps of Engineers, Coastal Engineering Research Center, Washington, D.C., Nov. 1964.

HART, E.D., "Radioactive Sediment Tracer Tests, Houston Ship Channel, Houston, Texas," H-69-2, U.S. Army Engineer Waterways Experiment Station, Vicksburg, Miss., 1969.

HAYES, M.O., "Hurricanes as Geological Agents: Case Studies of Hurricanes Carla, 1961, and Cindy, 1963," Report 61, Bureau of Economic Geology, University of Texas, Austin, Tex., 1967.

HAYES, M.O., "Relationship between Coastal Climate and Bottom Sediment on the Inner Continental Shelf," *Marine Geology*, 1967, pp. 111-132.

HAYES, M.O., "Forms of Sediment Accumulation in the Beach Zone," *Waves on Beaches and Resulting Sediment Transport*, Academic Press, New York, Oct. 1971.

HAYES, M.O., GOLDSMITH, V., and HOBBS, C.H. III, "Offset Coastal Inlets," *Proceedings of the 12th Coastal Engineering Conference*, Sept. 1970, pp. 1187-1200.

HERRON, W.J., and HARRIS, R.L., "Littoral Bypassing and Beach Restoration in the Vicinity of Port Hueneme, California," *Proceedings of the 10th Conference on Coastal Engineering,* Tokyo, 1966, ASCE, United Engineering Center, New York, 1967.

HICKS, S.D., "On Classifications and Trends of Long Period Sea Level Series," *Shore and Beach,* Apr. 1972.

HJULSTROM, F., "Transportation of Detritus by Moving Water," *Recent Marine Sediments,* American Association of Petroleum Geologists, 1939.

HODGES, T.K., "Sand Bypassing at Hillsboro Inlet, Florida," *Bulletin of the Beach Erosion Board,* Vol. 9, No. 2, Apr. 1955.

HOUBOLT, J.J.H.C., "Recent Sediment in the Southern Bight of the North Sea," *Geologie en Mijnbouw,* Vol. 47 (4), 1968, pp. 245-273.

HSU, S. "Coastal Air-Circulation System: Observations and Empirical Model," *Monthly Weather Review,* Vol. 98, No. 7, July 1970.

HUBBELL, D.W., and SAYRE, W.W., "Sand Transport Studies with Radioactive Tracers," *Journal of the Hydraulics Division,* ASCE, Vol. 90, No. HY3, 1965, pp. 39-68.

HULSEY, J.D., "Beach Sediments of Eastern Lake Michigan," Ph.D. Dissertation, University Microfilming 62-6164, University of Illinois, Urbana, Ill., 1962.

HUME, J.D., and SCHALK, M., "Shoreline Processes Near Barrow, Alaska: A Comparison of the Normal and the Catastrophic," *Arctic,* Vol. 20, No. 2, June 1967, pp. 86-103.

HUSTON, K.H., "A Critical Appraisal of the Technique of Using Naturally Occurring Radioactive Materials as Littoral Tracers," HEL-4-1, Hydraulic Engineering Institute, University of California, Berkeley, Calif., 1963.

INGLE, J.C., "The Movement of Beach Sand," *Devel. Sediment,* Vol. 5, Elsevier, Amsterdam, 1966.

INGRAM, L.F., CUMMINS, R.S., and SIMMONS, H.B., "Radioactive Sediment Tracer Tests Near the North and South Jetties, Galveston Harbor Entrance," MP 2-472, U.S. Army Engineer Waterways Experiment Station, Vicksburg, Miss., Nov. 1965.

INMAN, D.L., "Sorting of Sediments in the Light of Fluid Mechanics," *Journal of Sedimentary Petrology,* Vol. 19, 1949, pp. 51-70.

INMAN, D.L., "Measures for Describing the Size Distribution of Sediments," *Journal of Sedimentary Petrology,* Vol. 22, No. 3, Sept. 1952, pp. 125-145.

INMAN, D.L., "Wave-Generated Ripples in Nearshore Sands," TM-100, U.S. Army, Corps of Engineers, Beach Erosion Board, Washington, D.C., Oct. 1957.

INMAN, D.L., "Sediments: Physical Properties and Mechanics of Sedimentation," *Submarine Geology*, F.P. Shepard, 2nd ed., Harper and Row, New York, 1963.

INMAN, D.L., and Quinn, W.H., "Currents in the Surf Zone," *Proceedings of the Second Conference on Coastal Engineering*, ASCE, Council on Wave Research, Berkeley, Calif., 1952, pp. 24-36.

INMAN, D.L., and NASU, N., "Orbital Velocity Associated with Wave Action Near the Breaker Zone," TM-79, U.S. Army, Corps of Engineers, Beach Erosion Board, Washington, D.C., Mar. 1956.

INMAN, D.L., and RUSNAK, G.S., "Changes in Sand Level on the Beach and Shelf at La Jolla, California," TM-82, U.S. Army, Corps of Engineers, Beach Erosion Board, Washington, D.C., July 1956.

INMAN, D.L., and BOWEN, A.J., "Flume Experiments on Sand Transport by Waves and Currents," *Proceedings of the Eighth Conference on Coastal Engineering*, ASCE, Council on Wave Research, 1963, pp. 137-150.

INMAN, D.L., and FRAUTSCHY, J.D., "Littoral Processes and the Development of Shorelines," *Proceedings of the Coastal Engineering Specialty Conference (Santa Barbara)*, ASCE, 1966, pp. 511-536.

INMAN, D.L., KOMAR, P.D., and BOWEN, A.J., "Longshore Transport of Sand," *Proceedings of the 11th Conference on Coastal Engineering*, ASCE, London, 1969.

INMAN, D.L., TAIT, R.J., and NORDSTROM, C.E., "Mixing in the Surf Zone," *Journal of Geophysical Research*, Vol. 76, No. 15, May 1971, p. 3493.

IVERSEN, H.W., "Waves and Breakers in Shoaling Water," *Proceedings of the Third Conference on Coastal Engineering*, Council on Wave Research, ASCE, 1952, pp. 1-12.

IWAGAKI, Y, and NODA, H., "Laboratory Study of Scale Effect in Two Dimensional Beach Processes," *Proceedings of the Eighth Conference on Coastal Engineering*, Ch. 14, ASCE, 1962.

JAMES, W.R., "A Class of Probability Models for Littoral Drift," *Proceedings of the 12th Coastal Engineering Conference*, Washington, D.C., Sept. 1970.

JOHNSON, D.W., *Shore Processes and Shoreline Development*, Hafner Publishing, New York, 1919.

JOHNSON, J.W., "Sand Transport by Littoral Currents," IER, Technical Report Series 3, Issue 338, Wave Research Laboratory, University of California, Berkeley, Calif., June 1952.

JOHNSON, J.W., "Sand Transport by Littoral Currents," *Proceedings of the Fifth Hydraulics Conference*, Bulletin 34, State University of Iowa, Studies in Engineering, 1953, pp. 89-109.

JOHNSON, J.W., "Dynamics of Nearshore Sediment Movement," *American Association of Petroleum Geology Bulletin*, Vol. 40, No. 9, 1956, pp. 2211-2232.

JOHNSON, J.W., "The Littoral Drift Problem at Shoreline Harbors," *Journal of the Waterways and Harbors Division*, ASCE, 83, WW1, Paper 1211, Apr. 1957.

JOHNSON, J.W., "The Supply and Loss of Sand to the Coast," *ASCE Journal*, Vol. 85, No. WW3, Sept. 1959, pp. 227-251.

JUDGE, C.W., "Heavy Minerals in Beach and Stream Sediments as Indicators of Shore Processes between Monterey and Los Angeles, California," TM-33, U.S. Army, Corps of Engineers, Coastal Engineering Research Center, Washington, D.C., Nov. 1970.

JUDSON, S., "Erosion of the Land or What's Happening to Our Continents," *American Scientist*, Vol. 56, No. 4, 1968, pp. 356-374.

KAMEL, A.M., "Littoral Studies near San Francisco Using Tracer Techniques," TM-131, U.S. Army, Corps of Engineers, Beach Erosion Board, Washington, D.C., Nov. 1962.

KAMEL, A.M., and JOHNSON, J.W., "Tracing Coastal Sediment Movement by Naturally Radioactive Minerals," *Proceedings of the Eighth Coastal Engineering Conference*, ASCE, 1962, p. 324.

KAMPHUIS, J.W., "The Breaking of Waves at an Angle to the Shoreline and the Generation of Longshore Currents (A Laboratory Investigation)," Unpublished Thesis, Queens University, Kingston, Ontario, Apr. 1963.

KENNEDY, J.F., and FALCON, M., "Wave-Generated Sediment Ripples," Hydrodynamics Laboratory Report 86, Department of Civil Engineering, Massachusetts Institute of Technology, Cambridge, Mass., 1965.

KENNEDY, J.F., and LOCHER, F.A., "Sediment Suspension by Water Waves," *Waves on Beaches and Resulting Sediment Transport*, Academic Press, New York, 1972.

KENNEDY, V.C., and KOUBA, D.L., "Fluorescent Sand as a Tracer of Fluvial Sediment," Open-File Report, U.S. Geological Survey, Washington, D.C., 1968.

KEULEGAN, G.H., "An Experimental Study of Submarine Sand Bars," TR-3, U.S. Army, Corps of Engineers, Beach Erosion Board, Washington, D.C., Aug. 1948.

KEULEGAN, G.H., "Wind Tides in Small Closed Channels," Research Paper No. 2207, National Bureau of Standards, Washington, D.C., 1951.

KIDSON, C., and CARR, A.P., "Marking Beach Materials for Tracing Experiments," *Journal of the Hydraulics Division*, ASCE, Vol. 88, July 1962.

KING, C.A.M., *Beaches and Coasts*, Edward Arnold, Ltd., 1972.

KINSMAN, BLAIR, *Wind Waves, Their Generation and Propagation on The Ocean Surface*, Prentice-Hall, Englewood Cliffs, N.J., 1965.

KIRTLEY, D.W., "Reef-Building Worms," *Sea Frontiers*, Vol. 17, No. 2, 1971.

KOHLER, R.R., and GALVIN, C.J., "Berm-Bar Criterion," Unpublished CERC Laboratory Report, Aug. 1973, 70 p.

KOLESSAR, M.A., and REYNOLDS, J.L., "The Sears Sea Sled for Surveying in the Surf Zone," Vol. II, Bulletin and Summary Report of Research Progress, Fiscal years 1965-66, U.S. Army, Corps of Engineers, Coastal Engineering Research Center, Washington, D.C., 1966.

KOMAR, P.D., "The Longshore Transport of Sand on Beaches," Unpublished Ph.D. Thesis, University of California, San Diego, Calif., 1969.

KOMAR, P.D., "The Mechanics of Sand Transport on Beaches," *Journal of Geophysical Research*, Vol. 76, No. 3, Jan. 1971.

KOMAR, PAUL D., and INMAN, DOUGLAS L., "Longshore Sand Transport on Beaches, *Journal of Geophysical Research*, V. 75, No. 30, Oct 20, 1970, pp. 5914-5927.

KRAAI, P.T., "Comparison of Wind Wave and Uniform Wave Effects on a Beach," HEL 1-13, Hydraulic Engineering Laboratory, College of Engineering, University of California, Berkley, Calif., Aug. 1969.

KRAFT, J.C., "A Guide to the Geology of Delaware's Coastal Environments," Publication 2GL039, College of Marine Studies, University of Delaware, Newark, Del., 1971.

KRINSLEY, D., et al., "Transportation of Sand Grains Along the Atlantic Shore of Long Island, New York: An Application of Electron Microscopy," *Marine Geology*, Vol. 2, 1964, pp. 100-121.

KRUMBEIN, W.C., "Application of Logarithmic Moments to Size Frequency Distribution of Sediments," *Journal of Sedimentary Petrology*, Vol. 6, No. 1, 1936, pp. 35-47.

KRUMBEIN, W.C., "Shore Currents and Sand Movement on a Model Beach," TM-7, U.S. Army, Corps of Engineers, Beach Erosion Board, Washington, D.C., Sept. 1944.

KRUMBEIN, W.C., "A Method for Specification of Sand for Beach Fills," TM-102, U.S. Army, Corps of Engineers, Beach Erosion Board, Washington, D.C., Oct. 1957.

KRUMBEIN, W.C., and JAMES, W.R., "A Lognormal Size Distribution Model for Estimating Stability of Beach Fill Material," TM-16, U.S. Army, Corps of Engineers, Coastal Engineering Research Center, Washington, D.C., Nov. 1965.

KRUMBEIN, W.C., and SLOSS, L.L., "Stratigraphy and Sedimentation," Ch. 4, *Properties of Sedimentary Rocks,* W.H. Freeman & Company, 1963, pp. 93-149.

KUENEN, P.H., *Marine Geology,* Wiley, New York, 1950.

KUENEN, P.H., "Experimental Abrasion of Pebbles, Rolling by Current," *Journal of Geology,* Vol. 64, 1956, pp. 336-368.

LEE, J., YANCY, T., and WILDE, P., "Recent Sedimentation of the Central California Continental Shelf," Part A: Introduction and Grain Size Data, HEL 2-28, College of Engineers, University of California, Berkeley, Calif., Oct. 1970.

LeMEHAUTE, D., and LIN, "Internal Characteristics of Explosion-Generated Waves on the Continental Shelf," Tetra Technical Report No. TC - 116, 1968.

LONGUET-HIGGINS, M.S., "Longshore Currents Generated by Obliquely Incident Sea Waves, 1", *Journal of Geophysical Research,* Vol. 75, No. 33, Nov. 1970a, pp. 6788-6801.

LONGUET-HIGGINS, M.S., "Longshore Currents Generated by Obliquely Incident Sea Waves, 2," *Journal of Geophysical Research,* Vol. 75, No. 33, Nov. 1970b, pp. 6790-6801.

LONGUET-HIGGINS, M.S., "Recent Progress in the Study of Longshore Currents," *Waves on Beaches and Resulting Sediment Transport,* Academic Press, New York, Oct. 1971.

McCAMMON, R.B., "Efficiencies of Percentile Measures for Describing the Mean Size and Sorting of Sedimentary Particles," *Journal of Geology,* Vol. 70, 1962, pp. 453-465.

McCORMICK, C.L., "A Probable Cause for Some Changes in the Beach Erosion Rates on Eastern Long Island," Unpublished Paper, Southampton College, Long Island University, New York, 1971.

McMASTER, R.L., "Petrography and Genesis of the N.J. Beach Sands," Geology Series, Vol. 63, New Jersey Department of Conservation & Economic Development, 1954.

MAGOON, O.T., and SARLIN, W.O., "Effect of Long-Period Waves on Hydrographic Surveys," *Proceedings of the 12th Coastal Engineering Conference,* Washington, D.C., September 1970.

MAGOON, O.T., HAUGEN, J.C., and SLOAN, R.L., "Coastal Sand Mining in Northern California, U.S.A.," *Proceedings of the 13th Coastal Engineering Research Conference,* Vancouver, B.C., Canada, July 1972.

MANOHAR, M., "Mechanics of Bottom Sediment Movement Due to Wave Action," TM-75, U.S. Army, Corps of Engineers, Beach Erosion Board, Washington, D.C., June 1955.

MARTENS, J.H.C., "Beaches of Florida," Annual Report (21st-22nd), Florida State Geological Survey, 1928-1930.

MASON, M.A., "Abrasion of Beach Sands," TM-2, U.S. Army, Corps of Engineers, Beach Erosion Board, Washington, D.C., Feb. 1942.

MATHER, J.R., ADAMS, H., and YOSHIOKA, G.A., "Coastal Storms of the Eastern United States," *Journal of Applied Meteorology,* Vol. 3, 1964, pp. 693-706.

MEADE, R., "Landward Transport of Bottom Sediments in Estuaries of the Atlantic Coastal Plain, *Journal of Sedimentary Petrology,* Vol. 39, No. 1, pp. 222-234, 1969.

MEI, C.C., LIU, P., and CARTER, T.G., "Mass Transport in Water Waves, Part I: Theory - Part II: Experiments," Report No. 146, Ralph M. Parsons Laboratory for Water Resources and Hydrodynamics, Massachusetts Institute of Technology, Apr. 1972.

MENARD, H.W., "Sediment Movement in Relation to Current Velocity," *Journal of Sediment Petrology,* Vol. 20, 1950, pp. 148-160.

MILLIMAN, J.D., "Atlantic Continental Shelf and Slope of the United States-Petrology of the Sand Friction of Sediments, Northern New Jersey to Southern Florida," Geological Survey Professional Paper 529-J, U.S. Government Printing Office, Washington, D.C., 1972.

MOBERLEY, R., "Loss of Hawaiian Sand," *Journal of Sedimentary Petrology,* Vol. 38, 1968, pp. 17-34.

MOGRIDGE, G.R., and KAMPHUIS, J.W., "Experiments on Bed Form Generation by Wave Action," *Proceedings of the 13th Conference on Coastal Engineering,* July 1972.

MONROE, F.F., "Oolitic Aragonite and Quartz Sand: Laboratory Comparison Under Wave Action," MP 1-69, U.S. Army, Corps of Engineers, Coastal Engineering Research Center, Washington, D.C., Apr. 1969.

MOODY, D.W., "Coastal Morphology and Processes in Relation to the Development of Submarine Sand Ridges off Bethany Beach, Del.," Unpublished Ph.D. Dissertation, The John Hopkins University, Baltimore, Md., 1964.

MOORE, G.W., and COLE, A.Y., "Coastal Processes, Vicinity of Cape Thompson, Alaska," in "Geologic Investigations of Cape Thompson, NW Alaska - Preliminary Report," Trace Element Investigation Report 753, U.S. Geological Survey, Washington, D.C., 1960.

MORGAN, J.P., NICHOLS, L.G., and WRIGHT, M., "Morphological Effects of Hurricane Audrey on the Louisiana Coast (Advance Summary and Conclusions)," TR 10A, Coastal Studies Institute, Louisiana State University, Baton Rouge, La., 1958.

MORSE, B., and GROSS, M.G., and BARNES, C.A., "Movement of Seabed Drifters Near the Columbia River," *Journal of the Waterways and Harbors Division*, ASCE, Vol. 94, No. WW1, Paper No. 5817, Feb. 1968, pp. 93-103.

MURRAY, S.P., "Bottom Currents Near the Coast During Hurricane Camille," *Journal of Geophysical Research*, Vol. 75, No. 24, Aug. 1970.

NAKAMICHI, M., and SHIRAISHI, N., "Recent Researches on Sand Drift in Japan," *Proceedings of the 20th International Navigation Congress*, Baltimore, 1961, pp. 101-124.

NATIONAL ACADEMY OF SCIENCES, "Ocean Wave Spectra," *Proceedings of National Research Council Conference*, Easton, Md., May 1-4, 1961, Prentice-Hall, Englewood Cliffs, N.J., 1963.

NATIONAL MARINE CONSULTANTS, INC., "Wave Statistics for Seven Deep Water Stations Along the California Coast," prepared for Department of the Army, U.S. Army, Corps of Engineers Districts, Los Angeles and San Francisco, Calif., Dec. 1960a.

NATIONAL MARINE CONSULTANTS, INC., "Wave Statistics for Ten Most Severe Storms Affecting Three Selected Stations off the Coast of Northern California, During the Period 1951-1960," prepared for U.S. Army Engineer District, San Francisco, Calif., Dec. 1960b.

NAYAK, I.V., "Equilibrium Profiles of Model Beaches," Report HEL 2-25, University of California, Berkeley, Calif., May 1970.

NICHOLS, R.L., and MARSTON, A.F., "Shoreline Changes in Rhode Island Produced by Hurricane of Sept. 21, 1938," *Bulletin of the Geological Society of America*, Vol. 50, Sep. 1939, pp. 1357-1370.

NORRIS, R.M., "Dams and Beach-Sand Supply in Southern California," *Papers in Marine Geology*, Shepard Commemorative Volume, MacMillan, New York, 1964.

O'BRIEN, M.P., "Equilibrium Flow Areas of Inlets on Sandy Coasts," *Journal of the Waterways and Harbors Division*, ASCE, No. WW1, Feb. 1969, pp. 43-52.

OTTO, G.H., "A Modified Logarithmic Probability Graph for the Interpretation of Mechanical Analyses of Sediments," *Journal of Sedimentary Petrology*, Vol. 9, 1939, pp. 62-76.

PETTIJOHN, F.J., *Sedimentary Rocks*, Harper and Brothers, New York, 1957, p. 117.

PIERCE, J.W., "Sediment Budget Along a Barrier Island Chain," *Sedimentary Geology*, Vol. 3, No. 1, 1969, pp. 5-16.

PIERCE, J.W., "Holocene Evolution of Portions of the Carolina Coast," *Bulletin of the Geologic Society of America*, Vol. 81, Dec. 1970.

PIERSON, WILLARD J., JR., and NEUMANN, GERHARD, *Principles of Physical Oceanography*, Prentice-Hall, Englewood Cliffs, N.J., 1966.

PILKEY, O.H., and FIELD, M.E., "Onshore Transportation of Continental Shelf Sediment: Atlantic Southeastern United States," *Shelf Sediment Transport*, edited by Swift, Duane, and Pilkey; Dowden, Hutchinson, and Ross, Inc., Stroudsburg, Pa., 1972.

PILKEY, O.H., and FRANKENBERG, D., "The Relict-Recent Sediment Boundary on the Georgia Continental Shelf," *The Bulletin of the Georgia Academy of Science*, Vol. XXII, No. 1, Jan. 1964.

PRICE, W.A., "Reduction of Maintenance by Proper Orientation of Ship Channels Through Tidal Inlets," *Proceedings of the Second Conference on Coastal Engineering*, Council on Wave Research, University of California, Berkeley, Calif., 1952, pp. 243-255.

PUTNAM, J.A., MUNK W.H., and TRAYLOR, M.A., "The Prediction of Longshore Currents," *Transactions of the American Geophysical Union*, Vol. 30, 1949, pp. 337-345.

RAMSEY, M.D., "The Relationship Between Mean Sand Size vs Local Foreshore Slope for 166 New Jersey Sand Samples," Unpublished MFR, U.S. Army, Corps of Engineers, Coastal Engineering Research Center, Washington, D.C., Sept. 1971.

RAMSEY, M.D., and GALVIN, C.J., "Size Analysis of Sand Samples from Three S. New Jersey Beaches," Unpublished Paper, U.S. Army, Corps of Engineers, Coastal Engineering Research Center, Washington, D.C., Sept. 1971.

RAUDKIVI, A.J., *Loose Boundary Hydraulics*, Pergamon Press, New York, Jan. 1965.

RECTOR, R.L., "Laboratory Study of Equilibrium Profiles of Beaches," TM-41, U.S. Army, Corps of Engineers, Beach Erosion Board, Washington, D.C., Aug. 1954.

REIMNITZ, E., and ROSS, D.A., "The Sea Sled - A Device for Measuring Bottom Profiles in the Surf Zone," *Marine Geology*, Vol. 11, 1971.

ROSS, D.A., "Atlantic Continental Shelf and Slope of the United States - Heavy Minerals of the Continental Margin from Southern Nova Scotia to Northern New Jersey," Professional Paper 529-G, U.S. Geological Survey, U.S. Government Printing Office, Washington, D.C., 1970.

RUSNAK, G.A., STOCKMAN, R.W., and HOFMANN, H.A., "The Role of Shell Material in the Natural Sand Replenishment Cycle of the Beach and Nearshore Area Between Lake Worth Inlet and the Miami Ship Channel," CERC Contract Report (DA-49-055-CIV-ENG-63-12), Institute of Marine Sciences, University of Miami, Coral Gables, Fla., 1966.

RUSSELL, R.J., "Florida Beaches and Cemented Water-Table Rocks," Technical Report No. 88, Coastal Studies Institute, Louisiana State University, Baton Rouge, La., Oct. 1970.

SATO, S., IJIMA, T., and TANAKA, N., "A Study of Critical Depth and Mode of Sand Movement Using Radioactive Glass Sand," *Proceedings of the Eighth Conference on Engineering*, Mexico City, 1962, pp. 304-323.

SAUVAGE, M.G., and VINCENT, M.G., "Transport and Littoral Formation de Flecheset de Tombolos," *Proceedings of the Fifth Conference on Coastal Engineering*, 1955, pp. 296-328.

SAVAGE, R.P., "Wave Run-up on Roughened and Permeable Slopes," *Journal of the ASCE*, Vol. 84, No. WW3, May 1958.

SAVAGE, R.P., "Notes on the Formation of Beach Ridges," *Bulletin of the Beach Erosion Board*, Vol. 13, July 1959, pp. 31-35.

SAVAGE, R.P., "Laboratory Determination of Littoral Transport Rates," *Journal of the Waterways and Harbors Division*, ASCE, No. WW2, May 1962, pp. 69-92.

SAVAGE, R.P., and WOODHOUSE, W.W., "Creation and Stabilization of Coastal Barrier Dunes," *Proceedings of the 11th Coastal Engineering Conference*, London, Sept. 1968.

SAVILLE, T., Jr., "Model Study of Sand Transport Along an Infinitely Long Straight Beach," *Transactions of the American Geophysical Union*, Vol. 31, 1950.

SAVILLE, T., Jr., "Scale Effects in Two Dimensional Beach Studies," *Proceedings of the Seventh General Meeting*, International Association for Hydraulic Research, 1957.

SAVILLE, T., Jr., and CALDWELL, J.M., "Accuracy of Hydrographic Surveying In and Near the Surf Zone," TM-32, U.S. Army, Corps of Engineers, Beach Erosion Board, Washington, D.C., Mar. 1953.

SAVILLE, T., JR., and SAVAGE, R.P., "Laboratory Determination of Littoral Transport Rates," *Journal of the Waterways and Harbors Division*, ASCE, V. 88, No. WW2, May 1962, pp. 69-92. Discussion: Nov. 1962, Feb. 1963, Discussion by Thorndike Saville, Jr., Nov. 1962.

SAYLOR, J.H., and HANDS, E.B., "Properties of Longshore Bars in the Great Lakes," *Proceedings of the 12th Conference on Coastal Engineering*, Vol. 2, 1970, pp. 839-853.

SAYLOR, J.H., and UPCHURCH, S., "Bottom Stability and Sedimentary Processes at Little Lake Harbors, Lake Superior," U.S. Army, Corps of Engineers, Lake Survey District Detroit, Mich., 1970.

SCHULZ, E.F., WILDE, R.H., and ALBERTSON, M.L., "Influence of Shape on the Fall Velocity of Sedimentary Particles," U.S. Army, Corps of Engineers, Missouri River Division, 1954.

SCRUTON, P.C., "Delta Building and the Deltaic Sequence," *Recent Sediments, Northwest Gulf of Mexico*, American Association of Petroleum Geologists, 1960, pp. 82-102.

SEELIG, W.N., "Beach Evaluation Program, Visual Wave Observation Program," Unpublished Paper, U.S. Army, Corps of Engineers, Coastal Engineering Research Center, Washington, D.C., Mar. 1972.

SELLMAN, PAUL V., et al., "Investigations of Terrain and Coastal Conditions on the Arctic Alaskan Coastal Plain," Draft of Special Report, U.S. Army Cold Regions Research and Engineering Laboratories, Aug. 1971.

SHAY, E.A., and JOHNSON, J.W., "Model Studies on the Movement on Sand Transported by Wave Action Along a Straight Beach," Issue 7, Ser. 14, Institute of Engineering Research, University of California, Berkeley, Calif., 1951.

SHEPARD, F.P., "Beach Cycles in Southern California," TM-20, U.S. Army, Corps of Engineers, Beach Erosion Board, Washington, D.C., July 1950.

SHEPARD, F.P., "Gulf Coast Barriers," *Recent Sediments, Northwest Gulf of Mexico*, American Association of Petroleum Geologists, 1960a, pp. 197-220.

SHEPARD, F.P., "Rise of Sea Level Along Northwest Gulf of Mexico," *Recent Sediments, Northwest Gulf of Mexico*, American Association of Petroleum Geologists, 1960b, pp. 338-344.

SHEPARD, F.P., "Submarine Geology," *Physical Properties of Sediments*, Ch. V, and *Beaches and Related Shore Processes*, Ch VII, Harper and Row, New York, 1963, pp. 167-205.

SHEPARD, F.P., and BUFFINGTON, E.C., "La Jolla Submarine Fan Valley," *Marine Geology*, Vol. 6, 1968, pp. 107-143.

SHEPARD, F.P., and DILL, R.F., *"Submarine Canyons and Other Sea Valleys,"* Rand McNally, Chicago, 1966.

SHEPARD, F.P., and GRANT, U.S., IV, "Wave Erosion Along the Southern California Coast," *Bulletin of the Geologic Society of America*, Vol. 58, 1947, pp. 919-926.

SHEPARD, F.P., and INMAN, D.L., "Nearshore Water Circulation Related to Bottom Topography and Wave Refraction," *Transactions of the American Geophysical Union*, Vol. 31, No. 2, 1950, pp. 196-212.

SHEPARD, F.P., MacDONALD, G.A., and COX, D.C., "The Tsunami of April 1, 1946," *Bulletin of the Scripps Institute of Oceanography*, Vol. 5, No. 6, 1950, pp. 391-528.

SHEPARD, F.P., and WANLESS, H.R., *Our Changing Coastlines*, McGraw-Hill, New York, 1971.

SHUYSKIY, Y.D., "The Effect of Strong Storms on Sand Beaches of the Baltic Eastern Shore," *Oceanology*, Vol. 9, No. 3, 1970, p. 388.

SONU, C.J., "Field Observation of Nearshore Circulation and Meandering Currents," *Journal of Geophysical Research, Oceans and Atmospheres*, Vol. 77, No. 18, 1972.

SONU, C.J., and VAN BEEK, J.L., "Systemic Beach Changes on the Outer Banks, North Carolina," *Journal of Geology*, Vol. 79, 1971, pp. 416-425.

SOUTHARD, J.B., "Representation of Bed Configurations in Depth-Velocity-Size Diagrams," *Journal of Sedimentary Petrology*, Vol. 41, No. 4, Dec. 1972.

STAFFORD, D.B., "An Aerial Photographic Technique for Beach Erosion Surveys in North Carolina," TM-36, U.S. Army, Corps of Engineers, Coastal Engineering Research Center, Washington, D.C., Oct. 1971.

STEPHENS, N.H., et al., "Evaluation of Four Methods Using Gold-198 for Surface Labeling Sand and a New Technique for Simuluating Mass Labeling," ORNL-4338, Oak Ridge National Laboratory, 1968.

STODDARD, D.R., "World Erosion and Sedimentation," *Water, Earth, and Man*, Barnes and Noble, 1969.

STONE, R.O., and SUMMERS, H.J., "Final Report, Study of Subaqueous and Subaerial Sand Ripples," ONR Project No. N00014-67-A-0269-0002, Task No. NR-388-085, Report No. USG Geology 72-1, 1972.

STRAKHOV, N.M., *"Principles of Lithogenesis,"* Vol. 1, (Translation from 1962 Russian Edition by J.P. Fitzsimmons, Oliver, and Boyd), Edinburgh and London, 1967, p. 245.

STUIVER, M., and PURPURA, J.A., "Application of Fluorescent Coastal Sand in Littoral Drift and Inlet Studies," *Proceedings of the 11th Conference on Coastal Engineering*, ASCE, 1968, pp. 307-321.

SVENDSEN, S., "Munch-Petersen's Littoral Drift Formula," *Bulletin of the Beach Erosion Board*, Vol. 4, No. 4, Oct. 1950.

SWIFT, D.J.P., "Quarternary Shelves and the Return to Grade," *Marine Geology*, Elsevier Publishing, Amsterdam, 1970.

SZUWALSKI, A., "Littoral Environment Observation Program in California Preliminary Report," MP 2-70, U.S. Army, Corps of Engineers, Coastal Engineering Research Center, Washington, D.C., Feb. 1970.

SZULWALSKI, A., "Coastal Imagery Data Bank: Interim Report," MP-3-72, U.S. Army, Corps of Engineers, Coastal Engineering Research Center, Washington, D.C., Nov. 1972.

TANEY, N.E., "Geomorphology of the South Shore of Long Island, New York," TM-128, U.S. Army, Corps of Engineers, Beach Erosion Board, Washington, D.C., Sept. 1961a.

TANEY, N.E., "Littoral Materials of the South Shore of Long Island, New York," TM-129, U.S. Army, Corps of Engineers Beach Erosion Board, Washington, D.C., Nov. 1961b.

TANEY, N.E., "Laboratory Applications of Radioisotopic Tracers to Follow Beach Sediments," *Proceedings of the Eighth Conference on Coastal Engineering*, Council on Wave Research, ASCE, University of California, Berkeley, Calif., 1963, pp. 279-303.

TANNER, W.F., "Florida Coastal Classification," *Transactions of the Gulf Coast Association of Geological Societies*, Vol. X, 1960, pp. 259-266.

TANNER, W.F., "Mainland Beach Changes Due to Hurricane Donna," *Journal of Geophysical Research*, Vol. 66, No. 7, July 1961.

TANNER, W.F., "Significance of Camille," *Southeastern Geology*, Vol. 12, No. 2, 1970, pp. 95-104.

TELEKI, P., "Fluorescent Sand Tracers," *Journal of Sedimentary Petrology*, Vol. 36, June 1966.

TELEKI, P., "Automatic Analysis of Tracer Sand," *Journal of Sedimentary Petrology*, Vol. 37, Sept. 1967, pp. 749-759.

TERZAGHI, K., and PECK, R.B., *Soil Mechanics in Engineering Practice*, Wiley, New York, 1967, p. 28.

THIEL, G.A., "The Relative Resistance to Abrasion of Mineral Grains of Sand Size," *Journal of Sedimentary Petrology*, Vol. 10, 1940, pp. 102-124.

THOMPSON, E.F., and HARRIS, D.L., "A Wave Climatology for U.S. Coastal Waters," *Proceedings of Offshore Technology Conference*, Dallas, Texas, May, 1972.

THOREAU, H.D., *Cape Cod*, Thicknor and Fields, Boston, Mass., 1865.

THORNTON, E.B., "Longshore Current and Sediment Transport," TR-5, Department of Coastal and Oceanographic Engineering, University of Florida, Gainesville, Fla., Dec. 1969.

TRASK, PARKER D., "Movement of Sand around Southern California Promontories," TM-76, U.S. Army, Corps of Engineers, Beach Erosion Board, Washington, D.C., June 1955.

TUCKER, M.J., "Recent Measurement and Analysis Techniques Developed at The National Institute of Oceanography," *National Institute of Oceanography*, Collected Reprints, V. 11, No. 465, 1963. Reprinted from *Ocean Wave Spectra*; Proceedings of Conference on Ocean Wave Spectra, 1961, pp. 219-226.

URBAN, H.D., and GALVIN, C.J., "Pipe Profile Data and Wave Observations from the CERC Beach Evaluation Program, January - March, 1968," MP 3-69, U.S. Army, Corps of Engineers, Coastal Engineering Research Center, Washington, D.C., Sept. 1969.

U.S. ARMY, CORPS OF ENGINEERS, "Relation Between Sand Size and Slope of the Foreshore," Interim Report, Beach Erosion Board, Washington, D.C. 1933.

U.S. ARMY, CORPS OF ENGINEERS, "Beach Erosion Report on Cooperative Study at Palm Beach, Florida," Beach Erosion Board, Washington, D.C., 1947, (Unpublished).

U.S. ARMY, CORPS OF ENGINEERS, "Shoreline Effects, Harbor at Playa Del Rey, Calif.," Enclosure 20, Engineer District, Los Angeles, Calif., 1948a, (Unpublished).

U.S. ARMY, CORPS OF ENGINEERS, "Survey of Ocean City Harbor and Inlet and Sinepuxent Bay, Maryland," Engineer District, Baltimore, Md., 1948b, (Unpublished).

U.S. ARMY, CORPS OF ENGINEERS, "Illinois Shore of Lake Michigan - Beach Erosion Control Study," House Document 28, 83rd Congress, 1953a.

U.S. ARMY, CORPS OF ENGINEERS, "Ohio Shoreline of Lake Erie, (Sandusky to Vermillieni) Beach Erosion Control Study," House Document 32, 83rd Congress, 1953b.

U.S. ARMY, CORPS OF ENGINEERS, "Interim Report on Harbor Entrance Improve-Camp Pendleton, California," Engineer District, Los Angeles, Calif., 1953c, (Unpublished).

U.S. ARMY, CORPS OF ENGINEERS, "Preliminary Analysis of Cooperative Beach Erosion Study, City of Kenosha, Wisconsin, Engineer District, Milwaukee, Wis., 1953d, (Unpublished).

U.S. ARMY, CORPS OF ENGINEERS, "Beach Erosion Control Report, Cooperative Study of Perdido Pass, Alabama," Engineer District, Mobile, Ala., 1954a, (Unpublished).

U.S. ARMY, CORPS OF ENGINEERS, "Atlantic Coast of New Jersey, Sandy Hook to Barnegat Inlet, Beach Erosion Control Report on Cooperative Study," Engineer District, New York, N.Y., 1954b, (Unpublished).

U.S. ARMY, CORPS OF ENGINEERS, "Study of Monrovia Harbor, Liberia, and Adjoining Shore Line," Beach Erosion Board, Washington, D.C., 1955, (Unpublished).

U.S. ARMY, CORPS OF ENGINEERS, "Cliff Walk, Newport, Rhode Island, Beach Erosion Control Study," Letter from Secretary of the Army, U.S. Government Printing Office, Washington, 1965.

U.S. ARMY, CORPS OF ENGINEERS, "Shore Protection, Planning, and Design," TR No. 4, Coastal Engineering Research Center, Washington, D.C., 1966.

U.S. ARMY, CORPS OF ENGINEERS, "Littoral Environment Observations, Florida Panhandle, 1969-1970," Coastal Engineering Research Center, Washington, D.C.

U.S. ARMY, CORPS OF ENGINEERS, "A Study of Methods to Preserve Gay Head Cliffs, Martha's Vineyard, Massachusetts," Report prepared by Woodard-Moorhouse and Associates, Inc., for the Engineer, New England Division, Oct. 1970.

U.S. ARMY, CORPS OF ENGINEERS, "Investigation of Erosion, Carolina Beach, N.C.," Rpt. 1-69, Engineer District, Wilmington, N.C., 1970.

U.S. ARMY, CORPS OF ENGINEERS, "National Shoreline Study," Great Lakes Region-Inventory Report, Aug. 1971.

U.S. CONGRESS, "Beach Erosion Study, Lake Michigan Shore Line of Milwaukee County, Wisconsin," House Document 526, 79th Congress, 2nd Session, p. 16, 1946.

U.S. CONGRESS, "North Carolina Shore Line, Beach Erosion Study," House Document 763, 80th Congress, 2nd Session, 1948.

U.S. CONGRESS, "Ocean City, New Jersey, Beach Erosion Control Study," House Document 184, 83d Congress, 1st Session, 1953a.

U.S. CONGRESS, "Cold Spring Inlet (Cape May Harbor), New Jersey," House Document 206, 83d Congress, 1st Session, 1953b.

U.S. CONGRESS, "Gulf Shore of Galveston Island, Texas, Beach Erosion Control Study," House Document 218, 8d Congress, 1st Session, 1953c.

U.S. CONGRESS, "Coast of California, Carpinteria to Point Mugu," House Document 29, 83d Congress, 1st Session, 1953d.

U.S. CONGRESS, "Racine County, Wisconsin," House Document 88, 83d Congress, 1st Session, 1953e.

U.S. CONGRESS, "Illinois Shore of Lake Michigan," House Document 28, 83d Congress, 1st Session 1953f.

U.S. CONGRESS, "Waikiki Beach, Island of Oahu, T.H., Beach Erosion Study," House Document No. 227, 83d Congress, 1st Session, 1953g.

U.S. CONGRESS, "Pinellas County, Florida," House Document 380, 83d, Congress, 2d Session, 1954a.

U.S. CONGRESS, "Port Hueneme, California," House Document 362, 83d, Congress, 2d Session, 1954b.

U.S. CONGRESS, "Anaheim Bay Harbor, California," House Document 349, 83d Congress, 2d Session, 1954c.

VALLIANOS, F., "Recent History of Erosion at Carolina Beach, N.C.," *Proceedings of the 12th Conference on Coastal Engineering*, ASCE, Vol. 2, 1970.

VAN DORN, W.G., "Wind Stress on an Artificial Pond," *Journal of Marine Research*, Vol. 12, 1953, pp. 249-276.

VOLLBRECHT, K., "The Relationship Between Wind Records, Energy of Long-shore Drift, and the Energy Balance off the Coast of a Restricted Water Body, as Applied to the Baltic," *Marine Geology*, Vol. 4, No. 2, Apr. 1966, pp. 119-148.

WALTON, T.L., Jr., "Littoral Drift Computations Along the Coast of Florida by Use of Ship Wave Observations," Unpublished Thesis, University of Florida, Gainesville, Fla., 1972.

WALTON, T.L. and DEAN, R.G., "Application of Littoral Drift Roses to Coastal Engineering Problems," *Proceedings of the Conference on Engineering Dynamics in the Coastal Zone*, 1973.

WATSON, R.L., "Origin of Shell Beaches, Padre Island, Texas," *Journal of Sedimentary Petrology*, Vol. 41, No. 4, Dec. 1971.

WATSON, R.L., "Influence of Mean Grain Diameter on the Relationship Between Littoral Drift Rate and the Alongshore Component of Wave Energy Flux," EOS 53, No. 11, p. 1028, Nov. 1972.

WATTS, G.M., "Development and Field Tests of a Sampler for Suspended Sediment in Wave Action," TM-34, U.S. Army, Corps of Engineers, Beach Erosion Board, Washington, D.C., Mar. 1953a.

WATTS, G.M., "A Study of Sand Movement at South Lake Worth Inlet, Florida," TM-42, U.S. Army, Corps of Engineers, Beach Erosion Board, Washington, D.C., Oct. 1953b.

WATTS, G.M., "Laboratory Study of the Effect of Varying Wave Periods on Beach Profiles," TM-53, U.S. Army, Corps of Engineers, Beach Erosion Board, Washington, D.C., Sept. 1954.

WATTS, G.M., "Behavior of Beach Fill at Ocean City, New Jersey," TM-77 U.S. Army, Corps of Engineers, Beach Erosion Board, Washington, D.C., Feb. 1956.

WATTS, G.M., and DEARDUFF, R.F., "Laboratory Study of Effect of Tidal Action on Wave-Formed Beach Profiles," TM-52, U.S. Army, Corps of Engineers, Beach Erosion Board, Washington, D.C., Dec. 1954.

WIEGEL, R.L., *Oceanographic Engineering*, Prentice-Hall, Englewood Cliffs, N.J., 1964.

WOLMAN, G.M., and MILLER, J.P., "Magnitude and Frequency of Forces in Geomorphic Processes," *The Journal of Geology*, Vol. 68, No. 1, 1960, pp. 54-74.

WOODARD, D.W., et al., "The Use of Grasses for Dune Stabilization Along the Gulf Coast with Initial Emphasis on the Texas Coast," Report No. 114, Gulf Universities Research Corporation, Galveston, Tex., 1971.

WRIGHT, F., and COLEMAN, Jr., "River Delta Morphology: Wave Climate and the Role of the Subaqueous Profile," *Science*, Vol. 176, 1972, pp. 282-284.

YASSO, W.E., "Fluorescent Coatings on Coast Sediment: An Integrated System," TR-16, Columbia University, Department of Geology, New York, N.Y., 1962.

ZEIGLER, J.M., and GILL, B., "Tables and Graphs for the Settling Velocity of Quartz in Water Above the Range of Stokes Law," Ref. No. 59-36, Woods Hole Oceanographic Institution, Woods Hole, Mass., July 1959.

ZEIGLER, J.M., and TUTTLE, S.D., "Beach Changes Based on Daily Measurements of Four Cape Cod Beaches," *Journal of Geology*, Vol. 69, No. 5, 1961, pp. 583-599.

ZEIGLER, J.M., et al., "Residence Time of Sand Composing the Beaches and Bars of Outer Cape Cod," *Proceedings of the Ninth Conference on Coastal Engineering*, ASCE, Vol. 26, 1964, pp. 403-416.

ZENKOVICH, V.P., "Applications of Luminescent Substances for Sand Drift Investigation in the Nearshore Zones of the Sea," *Die Ingenieur*, Vol. 13, 1967a, pp. 81-89.

ZENKOVICH, V.P., *Processes of Coastal Development*, Interscience Publishers, New York, 1967b.

ZWAMBORN, J.A., FROMME, G.A.W., and FITZPATRICK, J.B., "Underwater Mound for the Protection of Durban's Beaches," *Proceedings of the 12th Conference on Coastal Engineering*, ASCE, 1970.

ZWAMBORN, J.A., et al., "Coastal Engineering Measurements," *Proceedings of the 13th International Conference on Coastal Engineering*, Canada, 1972.